

Chapter 14: Safety Analysis

Table of Contents

Section	Title	Page
14.0.1	Safety Analysis Overview	14.0-1
14.0.2	Safety Analysis Assumptions	14.0-7
14.0.3	Operating Parameters	14.0-7
14.0.3.1	Hot Channel Factors	14.0-8
14.0.4	Reactor Protection System	14.0-8
14.0.4.1	Steam Generator Safety Valves	14.0-10
14.0.4.2	Calorimetric Error Instrumentation Accuracy	14.0-10
14.0.4.3	Fuel/Reload Transition	14.0-11
14.0.5	Safety Analysis and Core Reload Methodology	14.0-13
14.0	References	14.0-16
14.1	CORE AND COOLANT BOUNDARY PROTECTION ANALYSIS	14.1-1
14.1.1	Uncontrolled RCCA Withdrawal from a Subcritical Condition	14.1-1
14.1.1.1	Accident Description	14.1-1
14.1.1.2	Method of Analysis	14.1-3
14.1.1.3	Results	14.1-4
14.1.1.4	Conclusions	14.1-5
14.1.2	Uncontrolled RCCA Withdrawal at Power	14.1-5
14.1.2.1	Accident Description	14.1-5
14.1.2.2	Method of Analysis	14.1-6
14.1.2.3	Results	14.1-7
14.1.2.4	Conclusions	14.1-9
14.1.3	RCCA Misalignment	14.1-9
14.1.3.1	Accident Description	14.1-9
14.1.3.2	Method of Analysis	14.1-10
14.1.3.3	Results	14.1-11
14.1.3.4	Conclusions	14.1-12
14.1.4	Chemical and Volume Control System Malfunction	14.1-13
14.1.4.1	Accident Description	14.1-13
14.1.4.2	Method of Analysis	14.1-13
14.1.4.3	Results	14.1-16
14.1.4.4	Conclusion	14.1-16
14.1.5	Startup of an Inactive Reactor Coolant Loop	14.1-17

Chapter 14: Safety Analysis

Table of Contents

Section	Title	Page
14.1.6	Excessive Heat Removal Due to Feedwater System Malfunctions	14.1-17
14.1.6.1	Accident Description	14.1-18
14.1.6.2	Method of Analysis	14.1-19
14.1.6.3	Results	14.1-20
14.1.6.4	Conclusions	14.1-22
14.1.7	Excessive Load Increase Incident	14.1-22
14.1.7.1	Accident Description	14.1-22
14.1.7.2	Method of Analysis	14.1-23
14.1.7.3	Conclusions	14.1-23
14.1.7.4	Historical Method of Analysis	14.1-23
14.1.7.5	Historical Results	14.1-24
14.1.7.6	Historical Conclusions	14.1-24
14.1.8	Loss of Reactor Coolant Flow	14.1-24
14.1.8.1	Partial Loss of Reactor Coolant Flow	14.1-25
14.1.8.2	Complete Loss of Forced Reactor Coolant Flow	14.1-27
14.1.8.3	Locked-Rotor Accident	14.1-30
14.1.8.4	Method of Analysis-Radiological Consequences	14.1-33
14.1.9	Loss of External Electrical Load	14.1-35
14.1.9.1	Accident Description	14.1-35
14.1.9.2	Method of Analysis	14.1-35
14.1.9.3	Results	14.1-37
14.1.9.4	Conclusions	14.1-38
14.1.10	Loss of Normal Feedwater	14.1-38
14.1.10.1	Accident Description	14.1-38
14.1.10.2	Method of Analysis	14.1-40
14.1.10.3	Results	14.1-41
14.1.11	Loss of Normal Feedwater - Operation at 100.6 Percent of 1772 MWt Reactor Power	14.1-41
14.1.11.1	Accident Description	14.1-41
14.1.11.2	Method of Analysis	14.1-42
14.1.11.3	Results	14.1-43
14.1.11.4	Conclusions	14.1-44
14.1.12	Anticipated Transients Without Scram	14.1-44

Chapter 14: Safety Analysis

Table of Contents

Section	Title	Page
14.1.13	Loss of AC Power to the Plant Auxiliaries	14.1-45
14.1.13.1	Accident Description	14.1-45
14.1.13.2	Method of Analysis	14.1-46
14.1.13.3	Results	14.1-47
14.1.13.4	Conclusions	14.1-48
14.1	References	14.1-48
14.2	STANDBY SAFETY FEATURES ANALYSIS	14.2-1
14.2.1	Fuel Handling Accidents	14.2-1
14.2.1.1	Causes and Assumptions	14.2-1
14.2.1.2	Activity Release Characteristics	14.2-4
14.2.1.3	Method of Analysis	14.2-4
14.2.2	Accidental Release-Recycle of Waste Liquid	14.2-5
14.2.3	Accidental Release-waste Gas	14.2-7
14.2.3.1	Gas Decay Tank Rupture	14.2-7
14.2.3.2	Volume Control Tank Rupture	14.2-8
14.2.4	Steam Generator Tube Rupture	14.2-10
14.2.4.1	Accident Description	14.2-10
14.2.4.2	Results	14.2-11
14.2.4.3	Environmental Consequences of a Tube Rupture	14.2-12
14.2.4.4	Summary of Calculated Doses	14.2-13
14.2.4.5	Recovery Procedure	14.2-14
14.2.5	Steam Line Break	14.2-15
14.2.5.1	Accident Description	14.2-15
14.2.5.2	Method of Analysis – Core Response	14.2-17
14.2.5.3	Results – Core Response	14.2-19
14.2.5.4	Double-Ended Rupture With Off-Site Power Available	14.2-19
14.2.5.5	Double-Ended Rupture Without Off-Site Power Available	14.2-20
14.2.5.6	Conclusions – Core Response	14.2-20
14.2.5.7	Method of Analysis - Containment Integrity	14.2-20
14.2.5.8	Results – Containment Integrity	14.2-24
14.2.5.9	Method of Analysis – Radiological Consequences	14.2-24
14.2.5.10	Results – Radiological Consequences	14.2-25

Chapter 14: Safety Analysis

Table of Contents

Section	Title	Page
	14.2.5.11 Conclusions	14.2-26
14.2.6	Rupture of a Control Rod Drive Mechanism Housing (RCCA Ejection) 14.2-26	
	14.2.6.1 Accident Description	14.2-26
	14.2.6.2 Method of Analysis	14.2-29
	14.2.6.3 Results	14.2-30
	14.2.6.4 Conclusions	14.2-30
	14.2.6.5 Analysis – Radiological Consequences	14.2-31
	14.2.6.6 Results – Radiological Consequences	14.2-31
	14.2.6.7 Conclusions – Radiological Consequences	14.2-32
14.2.7	Turbine Missile Damage to Spent Fuel Pool	14.2-32
14.2	References	14.2-32
14.3	REACTOR COOLANT SYSTEM PIPE RUPTURES (LOCA)	14.3-1
14.3.1	General	14.3-1
	14.3.1.1 Condition III - Infrequent Faults	14.3-1
	14.3.1.2 Condition IV - Limiting Faults	14.3-1
	14.3.1.3 Loss of Reactor Coolant From Small Ruptured Pipes or From Cracks In Large Pipes Which Actuates Emergency Core Cooling System	14.3-1
	14.3.1.4 Identification of Causes and Accident Description	14.3-1
	14.3.1.5 Analysis of Effects and Consequences	14.3-2
	14.3.1.6 Small-Break LOCA Analysis Using NOTRUMP	14.3-3
	14.3.1.7 Results	14.3-4
	14.3.1.8 Conclusions	14.3-5
	14.3.1.9 Additional Break Sizes	14.3-5
14.3.2	Major Reactor Coolant System Pipe Ruptures (LOCA)	14.3-6
	14.3.2.1 Performance Criteria for Emergency Core Cooling System	14.3-7
	14.3.2.2 Large-Break LOCA Analytical Model	14.3-8
	14.3.2.3 Large-Break LOCA Analysis Results	14.3-13
	14.3.2.4 Global Model Sensitivity Studies	14.3-17
	14.3.2.5 Evaluations	14.3-18
	14.3.2.6 Large-Break LOCA Conclusions	14.3-18
14.3.3	Core and Internals Integrity Analysis	14.3-19

Chapter 14: Safety Analysis

Table of Contents

Section	Title	Page
14.3.3.1	Reactor Internals Response Under Blowdown and Seismic Excitation.	14.3-20
14.3.3.2	Acceptance Criteria for Results of Analyses	14.3-20
14.3.3.3	Allowable Deflection and Stability Criteria.	14.3-21
14.3.3.4	Allowable Stress Criteria	14.3-21
14.3.3.5	Method of Analysis	14.3-22
14.3.4	Containment Integrity Evaluation	14.3-27
14.3.4.1	Long Term LOCA Mass and Energy Releases	14.3-27
14.3.4.2	Long-Term LOCA Containment Response Analysis	14.3-39
14.3.4.3	Conclusions	14.3-42
14.3.5	Off-Site Dose Consequences.	14.3-42
14.3.5.1	Introduction	14.3-42
14.3.5.2	Conservatism Between Analysis and Physical Situation	14.3-46
14.3.6	Charcoal Filter Ignition Hazard Due to Iodine Absorption.	14.3-47
14.3.7	Generation and Disposition of Hydrogen	14.3-48
14.3.7.1	General.	14.3-48
14.3.7.2	Summary of Reanalysis Based on Safety Guide 7.	14.3-49
14.3.7.3	Methods of Control	14.3-50
14.3.7.4	Venting to the Shield Building Annulus	14.3-50
14.3.7.5	Dilution by Containment Pressure Raise	14.3-50
14.3.7.6	Hydrogen Recombination	14.3-51
14.3.7.7	Analysis of Materials of Construction and Protective Coatings	14.3-51
14.3.7.8	Description of Materials.	14.3-51
14.3.7.9	Zinc-Bearing Surfaces	14.3-52
14.3.7.10	Aluminum Surfaces	14.3-54
14.3.7.11	Net Effect of Spray Additive	14.3-54
14.3.7.12	Analysis of Methods of Hydrogen Control	14.3-54
14.3.7.13	Analysis of Venting Through Shield Building Annulus	14.3-55
14.3.7.14	Analysis of Effects of Pressure Increase	14.3-56
14.3.7.15	Provisions for Mixing, Sampling, and Venting of Containment Gases	14.3-59
14.3.7.16	Venting to Shield Building Annulus	14.3-59

Chapter 14: Safety Analysis

Table of Contents

Section	Title	Page
	14.3.7.17 Provisions for Sampling.....	14.3-60
	14.3.8 Steam Generator Tube Plugging.....	14.3-61
	14.3.9 Steam Generator Tube Fatigue Analysis.....	14.3-61
	14.3.10 Steam Generator Tube Removal.....	14.3-61
14.3.1	References.....	14.3-62
14.3.2	References.....	14.3-62
14.3.3	References.....	14.3-63
14.3.4	References.....	14.3-64
14.3.5	References.....	14.3-65
14.3.9	References.....	14.3-65
Appendix 14A	Heat Transfer Coefficients Used in LOCTA-R2.....	14A-3
14A	References.....	14A-5
Appendix 14B	Westinghouse Heat Transfer Research and Development Programs.....	14B-3
14B	References.....	14B-4
Appendix 14C	Containment Pressure Response to LOCA.....	14C-3
14C.1	Steam Generators as an Active Heat Source.....	14C-3
14C.2	Sensitivity Studies.....	14C-12
14C.3	References.....	14C-13

Chapter 14: Safety Analysis

List of Tables

Table	Title	Page
14.0-1	Instrumentation Drift and Calorimetric Errors Nuclear Overpower Trip Channel	14.0-18
14.1.1-1	Assumptions and Results Uncontrolled RCCA Withdrawal From a Subcritical Condition	14.1-50
14.1.1-2	Sequence of Events Uncontrolled RCCA Withdrawal from a Subcritical Condition.	14.1-51
14.1.2-1	Time Sequence of Events for Uncontrolled RCCA Withdrawal at Power (Maximum Nominal RCS Tavg; Minimum Feedback).	14.1-52
14.1.2-2	Limiting Results for RCCA Bank Withdrawal at Power Transient	14.1-53
14.1.4-1	Sequence of Events – Chemical and Volume Control System Malfunctions	14.1-54
14.1.6-1	Sequence of Events for Feedwater System Malfunction Event at Full Power.	14.1-55
14.1.6-2	Sequence of Events for Feedwater System Malfunction Event at Zero Power	14.1-56
14.1.8-1	Sequence of Events – Partial Loss of Reactor Coolant Flow	14.1-57
14.1.8-2	Sequence of Events – Complete Loss of Reactor Coolant Flow	14.1-58
14.1.8-3	Sequence of Events – Reactor Coolant Pump Locked Rotor	14.1-59
14.1.9-1	Sequence of Events and Transient Results – Loss of External Electrical Load – With Pressurizer Pressure Control (for Minimum DNB).	14.1-60
14.1.9-2	Sequence of Events and Transient Results – Loss of External Electrical Load – Without Pressurizer Pressure Control (for Primary RCS Overpressure)	14.1-61
14.1.9-3	Sequence of Events and Transient Results – Loss of External Electrical Load – With Pressurizer Pressure Control (for MSS Overpressure)	14.1-62
14.1.10-1	Sequence of Events – Loss of Normal Feedwater	14.1-63
14.1.12-1	Sequence of Events – Loss of AC Power to the Plant Auxiliaries	14.1-64
14.2.5-1	Steam Line Break Analysis Assumptions and Sequence Of Events	14.2-34
14.2.6-1	Assumptions and Results – RCCA Ejection.	14.2-35
14.2.6-2	Sequence of Events – RCCA Ejection	14.2-36
14.3-1	Small-Break LOCA Time Sequence of Events	14.3-66
14.3-2	Small-Break LOCA Fuel Cladding Results	14.3-67
14.3.3-1	Large Break Local Containment Data Used for Calculation of Containment Pressure	14.3-68

Chapter 14: Safety Analysis

List of Tables

Table	Title	Page
14.3.3-2	Fan Cooler Heat Removal Data Used for Calculation of Containment Pressure.	14.3-69
14.3.3-3	Large Break Structural Heat Sink Data Used for Calculation of Containment Pressure.	14.3-70
14.3.3-4	Key LOCA Parameters and Reference Transient Assumptions.	14.3-72
14.3.3-5	KNPP Confirmatory Calculation PCT Results Summary	14.3-76
14.3.3-6	Large-Break LOCA Mass and Energy Releases Used for COCO Calculation	14.3-77
14.3.3-7	KNPP Break Size and Type Sensitivity PCT Results Summary	14.3-79
14.3.3-8	KNPP Best-Estimate Large-Break LOCA Results	14.3-80
14.3.3-9	KNPP Conditions Analyzed with <u>W</u> COBRA/TRAC Compared to be UPI Test Conditions.	14.3-81
14.3.3-10	Plant Operating Range Allowed by the Best-Estimate Large-Break LOCA Analysis (KNPP).	14.3-82
14.3-3	Components Nomenclature.	14.3-84
14.3-4	Maximum Deflections Under Blowdown (Inches)(1-millisecond Double-Ended Break)	14.3-85
14.3-5	Summary of Maximum Stress Intensities (PSI)(1-millisecond Pipe Break and Seismics)	14.3-86
14.3-6	Internal Energy Balance	14.3-87
14.3-7	Major Assumptions for Design Basis LOCA Analysis	14.3-88
14.3-8	Containment, Shield Building and Auxiliary Building Modeling Used for LBLOCA	14.3-90
14.3-9	Doses for Design Basis Loss-of-Coolant Accident	14.3-92
14.3-10	Exposed Zinc and Aluminum Bearing Surfaces Within Kewaunee Containment Vessel	14.3-93
14.3-11	Hydrogen Gas Production in Acidic and Basic Solutions	14.3-94
14.3-12	Sources and Assumptions for Hydrogen Calculations	14.3-95
14.3-13	Venting Requirements and Venting Doses without Pressure Increase.	14.3-96
14.3-14	Effects of Pressure Increase on Venting Doses	14.3-97
14.3.4-1	System Parameters Initial Conditions.	14.3-98
14.3.4-2	SI Flow Minimum Safeguards	14.3-99
14.3.4-3	SI Flow Maximum Safeguards	14.3-100
14.3.4-4	Containment Response Analysis Parameters	14.3-101
14.3.4-5	Kewaunee Structural Heat Sinks for Containment Integrity Analysis ^{1,2,3}	14.3-103
14.3.4-6	Thermo-Physical Properties of Containment Heat Sinks	14.3-105

Chapter 14: Safety Analysis

List of Tables

Table	Title	Page
14.3.4-7	Containment Fan Coil Unit Performance (CFCU)	14.3-106
14.3.4-8	LOCA Containment Response Results (Loss-of-Offsite Power Assumed)	14.3-107
14C-1	Summary of Heat Transfer Correlations Used to Calculate Steam Generator Heat Flow in the SATAN Code	14.C-14
14C-2	Sensitivity of Core Stored Energy to Power Level # Nodes in the Pellet and Fuel Densification	14.C-15
14C-3	Available Core Energy During Blowdown.	14.C-16
14C-4	Resistances Used in Reflood Analysis	14.C-17
14C-5	Summary of Results	14.C-18
14C-6	Reflood Energy Release (E+6 Btu)	14.C-19
14C-7	Structural Heat Sinks	14.C-21
14C-8	Post Reflood Mass and Energy Release	14.C-22
14C-9	Concrete As Passive Heat Sink.	14.C-24

Chapter 14: Safety Analysis

List of Figures

Figure	Title	Page
14.0-1	Scram Reactivity Insertion Rate Negative Reactivity vs. Time	14.0-19
14.0-2	Illustration of Overtemperature and Overpower DT Protection.	14.0-20
14.1.1-1	Uncontrolled RCCA Withdrawal from a Subcritical Condition Reactor Power vs. Time	14.1-65
14.1.1-2	Uncontrolled RCCA Withdrawal From a Subcritical Condition Heat Flux vs. Time	14.1-66
14.1.1-3	Uncontrolled RCCA Withdrawal from a Subcritical Condition Hot-Spot Fuel Centerline Temperature vs. Time	14.1-67
14.1.1-4	Uncontrolled RCCA Withdrawal from a Subcritical Condition Hot-Spot Fuel Average Temperature vs. Time.	14.1-68
14.1.1-5	Uncontrolled RCCA Withdrawal from a Subcritical Condition Hot-Spot Cladding Temperature vs. Time	14.1-69
14.1.2-1	Uncontrolled RCCA Bank Withdrawal at Power (100pcm/sec - Full Power) Power-Range High Neutron Flux Trip Maximum Nominal RCS Vessel T_{avg} , Minimum Feedback.	14.1-70
14.1.2-2	Uncontrolled RCCA Bank Withdrawal at Power (3 pcm/sec - 100 Percent Power) OTΔT Trip Maximum Nominal RCS Vessel T_{avg} , Minimum Feedback	14.1-74
14.1.2-3	Uncontrolled RCCA Bank Withdrawal at Power, 100 Percent Power (Sheet 1 of 3)	14.1-78
14.1.3-1	Representative Transient Response to Dropped RCCA Nuclear Power vs. Time	14.1-81
14.1.3-2	Representative Transient Response to Dropped RCCA Core Heat Flux vs. Time	14.1-82
14.1.3-3	Representative Transient Response to Dropped RCCA Pressurizer Pressure vs. Time	14.1-83
14.1.3-4	Representative Transient Response to Dropped RCCA Vessel Average Temperature vs. Time	14.1-84
14.1.4-1	CVCS Malfunction - Dilution at Power - Manual Control - High Pressure Reactor Power vs. Time	14.1-85
14.1.4-2	CVCS Malfunction - Dilution at Power - Manual Control - High Pressure Pressurizer Pressure vs. Time.	14.1-86
14.1.4-3	CVCS Malfunction - Dilution at Power - Manual Control High Pressure T_{ave} vs. Time	14.1-87
14.1.4-4	CVCS Malfunction - Dilution at Power - Manual Control High Pressure Heat Flux vs. Time.	14.1-88
14.1.4-5	CVCS Malfunction - Dilution at Power - Manual Control High Pressure Minimum DNBR vs. Time.	14.1-89

Chapter 14: Safety Analysis

List of Figures

Figure	Title	Page
14.1.5-1	Startup of an Inactive Reactor Coolant Loop T_{inlet} vs. Time	14.1-90
14.1.5-2	Startup of an Inactive Reactor Coolant Loop T_{ave} vs. Time.	14.1-91
14.1.5-3	Startup of an Inactive Reactor Coolant Loop Reactor Power vs. Time	14.1-92
14.1.5-4	Startup of an Inactive Reactor Coolant Loop Pressurizer Pressure vs. Time	14.1-93
14.1.5-5	Startup of an Inactive Reactor Coolant Loop Heat Flux vs. Time	14.1-94
14.1.6-1	Feedwater Malfunction Event at Full Power with Manual Rod Control Reactor Power vs. Time.	14.1-95
14.1.6-2	Feedwater Malfunction Event at Full Power with Manual Rod Control Pressurizer Pressure vs. Time	14.1-96
14.1.6-3	Feedwater Malfunction Event at Full Power with Manual Rod Control Core Average Temperature vs. Time	14.1-97
14.1.6-4	Feedwater Malfunction Event at Full Power with Manual Rod Control Vessel Outlet and Inlet Temperatures vs. Time	14.1-98
14.1.6-5	Feedwater Malfunction Event at Full Power with Manual Rod Control Minimum DNBR vs. Time	14.1-99
14.1.6-6	Feedwater Malfunction Event at Full Power with Automatic Rod Control Reactor Power vs. Time.	14.1-100
14.1.6-7	Feedwater Malfunction Event at Full Power with Automatic Rod Control Pressurizer Pressure vs. Time	14.1-101
14.1.6-8	Feedwater Malfunction Event at Full Power with Automatic Rod Control Core Average Temperature vs. Time.	14.1-102
14.1.6-9	Feedwater Malfunction Event at Full Power with Automatic Rod Control Vessel Outlet and Inlet Temperature vs. Time	14.1-103
14.1.6-10	Feedwater Malfunction Event at Full Power with Automatic Rod Control Minimum DNBR vs. Time	14.1-104
14.1.7-1	Excessive Load Increase - BOC Manual Control Reactor Power vs. Time	14.1-105
14.1.7-2	Excessive Load Increase - BOC Manual Control Pressurizer Pressure vs. Time	14.1-106
14.1.7-3	Excessive Load Increase - BOC Manual Control ΔT Loop vs. Time.	14.1-107
14.1.7-4	Excessive Load Increase - BOC Manual Control Minimum DNBR vs. Time	14.1-108
14.1.7-5	Excessive Load Increase - EOC Manual Control Reactor Power vs. Time	14.1-109

Chapter 14: Safety Analysis

List of Figures

Figure	Title	Page
14.1.7-6	Excessive Load Increase - EOC Manual Control Pressurizer Pressure vs. Time	14.1-110
14.1.7-7	Excessive Load Increase - EOC Manual Control ΔT Loop vs. Time.	14.1-111
14.1.7-8	Excessive Load Increase - EOC Manual Control Minimum DNBR vs. Time	14.1-112
14.1.7-9	Excessive Load Increase - BOC Auto Control Reactor Power vs. Time	14.1-113
14.1.7-10	Excessive Load Increase - BOC Auto Control Pressurizer Pressure vs. Time	14.1-114
14.1.7-11	Excessive Load Increase - BOC Auto Control ΔT Loop vs. Time.	14.1-115
14.1.7-12	Excessive Load Increase - BOC Auto Control T_{ave} vs. Time.	14.1-116
14.1.7-13	Excessive Load Increase - BOC Auto Control Minimum DNBR vs. Time	14.1-117
14.1.7-14	Excessive Load Increase - EOC Auto Control Reactor Power vs. Time	14.1-118
14.1.7-15	Excessive Load Increase - EOC Auto Control Pressurizer Pressure vs. Time	14.1-119
14.1.7-16	Excessive Load Increase - EOC Auto Control ΔT Loop vs. Time.	14.1-120
14.1.7-17	Excessive Load Increase - EOC Auto Control T_{ave} vs. Time.	14.1-121
14.1.7-18	Excessive Load Increase -EOC Auto Control Minimum DNBR vs. Time	14.1-122
14.1.8-1	Partial Loss of Flow, One Pump Coasting Down (PLOF) Total Core Inlet Flow vs. Time.	14.1-123
14.1.8-2	Partial Loss of Flow, One Pump Coasting Down (PLOF) RCS Faulted Loop Flow vs. Time	14.1-124
14.1.8-3	Partial Loss of Flow, One Pump Coasting Down (PLOF) Nuclear Power vs. Time	14.1-125
14.1.8-4	Partial Loss of Flow, One Pump Coasting Down (PLOF) Core Average Heat Flux vs. Time	14.1-126
14.1.8-5	Partial Loss of Flow, One Pump Coasting Down (PLOF) Pressurizer Pressure vs. Time	14.1-127
14.1.8-6	Partial Loss of Flow, One Pump Coasting Down (PLOF) RCS Faulted Loop Temperature vs. Time	14.1-128
14.1.8-7	Partial Loss of Flow, One Pump Coasting Down (PLOF) Hot Channel Heat Flux vs. Time	14.1-129
14.1.8-8	Partial Loss of Flow, One Pump Coasting Down (PLOF) DNBR vs. Time	14.1-130

Chapter 14: Safety Analysis

List of Figures

Figure	Title	Page
14.1.8-9	Complete Loss of Flow, Two Pump Coasting Down (CLOF) Total Core Inlet Flow vs. Time	14.1-131
14.1.8-10	Complete Loss of Flow, Two Pumps Coasting Down (CLOF) RCS Loop Flow vs. Time	14.1-132
14.1.8-11	Complete Loss of Flow, Two Pumps Coasting Down (CLOF) Nuclear Power vs. Time	14.1-133
14.1.8-12	Complete Loss of Flow, Two Pumps Coasting Down (CLOF) Core Average Heat Flux vs. Time	14.1-134
14.1.8-13	Complete Loss of Flow, Two Pumps Coasting Down (CLOF) Pressurizer Pressure vs. Time	14.1-135
14.1.8-14	Complete Loss of Flow, Two Pumps Coasting Down (CLOF) RCS Faulted Loop Temperature vs. Time	14.1-136
14.1.8-15	Complete Loss of Flow, Two Pumps Coasting Down (CLOF) Hot Channel Heat Flux vs. Time	14.1-137
14.1.8-16	Complete Loss of Flow, Two Pumps Coasting Down (CLOF) DNBR vs. Time	14.1-138
14.1.8-17	Complete Loss of Flow, Frequency Decay in Two Pumps (CLOF-UF) Total Core Inlet Flow vs. Time	14.1-139
14.1.8-18	Complete Loss of Flow, Frequency Decay in Two Pumps (CLOF-UF) RCS Loop Flow vs. Time	14.1-140
14.1.8-19	Complete Loss of Flow, Frequency Decay in Two Pumps (CLOF-UF) Nuclear Power vs. Time	14.1-141
14.1.8-20	Complete Loss of Flow, Frequency Decay in Two Pumps (CLOF-UF) Core Average Heat Flux vs. Time	14.1-142
14.1.8-21	Complete Loss of Flow, Frequency Decay in Two Pumps (CLOF-UF) Pressurizer Pressure vs. Time	14.1-143
14.1.8-22	Complete Loss of Flow, Frequency Decay in Two Pumps (CLOF-UF) RCS Loop Temperature vs. Time	14.1-144
14.1.8-23	Complete Loss of Flow, Frequency Decay in Two Pumps (CLOF-UF) Hot Channel Heat Flux vs. Time	14.1-145
14.1.8-24	Complete Loss of Flow, Frequency Decay in Two Pumps (CLOF-UF) DNBR vs. Time	14.1-146
14.1.8-25	Locked Rotor/Shaft Break - RCS Pressure/Peak Cladding Temperature Case Total Core Inlet Flow vs. Time	14.1-147
14.1.8-26	Locked Rotor/Shaft Break - RCS Pressure/Peak Cladding Temperature Case RCS Loop Flow vs. Time	14.1-148
14.1.8-27	Locked Rotor/Shaft Break - RCS Pressure/Peak Cladding Temperature Case Nuclear Power vs. Time	14.1-149

Chapter 14: Safety Analysis

List of Figures

Figure	Title	Page
14.1.8-28	Locked Rotor/Shaft Break - RCS Pressure/Peak Cladding Temperature Case Core Average Heat Flux vs. Time	14.1-150
14.1.8-29	Locked Rotor/Shaft Break - RCS Pressure/Peak Cladding Temperature Case Pressurizer Pressure vs. Time	14.1-151
14.1.8-30	Locked Rotor/Shaft Break - RCS Pressure/Peak Cladding Temperature Case Vessel Lower Plenum Pressure vs. Time	14.1-152
14.1.8-31	Locked Rotor/Shaft Break - RCS Pressure/Peak Cladding Temperature Case RCS Loop Temperature vs. Time	14.1-153
14.1.8-32	Locked Rotor/Shaft Break - RCS Pressure/Peak Cladding Temperature Case Hot Channel Heat Flux vs. Time	14.1-154
14.1.8-33	Locked Rotor/Shaft Break - RCS Pressure/Peak Cladding Temperature Case Hot-Spot Cladding Inner Temperature vs. Time	14.1-155
14.1.9-1	Loss of External Electrical Load With Automatic Pressure Control (DNB Case) Nuclear Power vs. Time	14.1-156
14.1.9-2	Loss of External Electrical Load With Automatic Pressure Control (DNB Case) Vessel Average and Core Inlet Temperatures vs. Time	14.1-157
14.1.9-3	Loss of External Electrical Load With Automatic Pressure Control (DNB Case) Pressurizer and RCP Exit Pressures vs. Time	14.1-158
14.1.9-4	Loss of External Electrical Load With Automatic Pressure Control (DNB Case) Pressurizer Water Volume vs. Time	14.1-159
14.1.9-5	Loss of External Electrical Load With Automatic Pressure Control (DNB Case) Steam Generator Pressure vs. Time	14.1-160
14.1.9-6	Loss of External Electrical Load With Automatic Pressure Control (DNB Case) DNBR vs. Time	14.1-161
14.1.9-7	Loss of External Electrical Load Without Automatic Pressure Control (RCS Overpressure Case) Nuclear Power vs. Time	14.1-162
14.1.9-8	Loss of External Electrical Load Without Automatic Pressure Control (RCS Overpressure Case) Vessel Average and Core Inlet Temperatures vs. Time	14.1-163
14.1.9-9	Loss of External Electrical Load Without Automatic Pressure Control (RCS Overpressure Case) Pressurizer and RCP Exit Pressures vs. Time	14.1-164
14.1.9-10	Loss of External Electrical Load Without Automatic Pressure Control (RCS Overpressure Case) Pressurizer Water Volume vs. Time	14.1-165

Chapter 14: Safety Analysis

List of Figures

Figure	Title	Page
14.1.9-11	Loss of External Electrical Load Without Automatic Pressure Control (RCS Overpressure Case) Steam Generator Pressure vs. Time	14.1-166
14.1.9-12	Loss of External Electrical Load With Automatic Pressure Control (MSS Overpressure Case) Nuclear Power vs. Time	14.1-167
14.1.9-13	Loss of External Electrical Load With Automatic Pressure Control (MSS Overpressure Case) Vessel Average and Core Inlet Temperatures vs. Time	14.1-168
14.1.9-14	Loss of External Electrical Load With Automatic Pressure Control (MSS Overpressure Case) Pressurizer and RCP Exit Pressures vs. Time	14.1-169
14.1.9-15	Loss of External Electrical Load With Automatic Pressure Control (MSS Overpressure Case) Pressurizer Water Volume vs. Time.	14.1-170
14.1.9-16	Loss of External Electrical Load With Automatic Pressure Control (MSS Overpressure Case) Steam Generator Pressure vs. Time	14.1-171
14.1.10-1	Loss of Normal Feedwater - High Pressure T_{ave} Volume vs. Time	14.1-172
14.1.10-2	Loss of Normal Feedwater - High Pressure Pressurizer Liquid Volume vs. Time.	14.1-173
14.1.10-3	Loss of Normal Feedwater - High Pressure SG A Wide Range Level vs. Time	14.1-174
14.1.10-4	Loss of Normal Feedwater - High Pressure SG B Wide Range Level vs. Time	14.1-175
14.1.10-5	Loss of Normal Feedwater - High Pressure Pressurizer Pressure vs. Time	14.1-176
14.1.10-6	Loss of Normal Feedwater Nuclear Power vs. Time	14.1-177
14.1.10-7	Loss of Normal Feedwater Vessel Average Temperature vs. Time	14.1-178
14.1.10-8	Loss of Normal Feedwater Pressurizer Pressure vs. Time	14.1-179
14.1.10-9	Loss of Normal Feedwater Pressurizer Water Volume vs. Time	14.1-180
14.1.10-10	Loss of Normal Feedwater Steam Generator Pressure vs. Time	14.1-181
14.1.10-11	Loss of Normal Feedwater Steam Generator Mass vs. Time	14.1-182
14.1.12-1	Loss of AC Power to the Plant Auxiliaries* Nuclear Power vs. Time	14.1-183
14.1.12-2	Loss of AC Power to the Plant Auxiliaries* Vessel Average Temperature vs. Time	14.1-184
14.1.12-3	Loss of AC Power to the Plant Auxiliaries Pressurizer Pressure vs. Time	14.1-185

Chapter 14: Safety Analysis

List of Figures

Figure	Title	Page
14.1.12-4	Loss of AC Power to the Plant Auxiliaries* Pressurizer Water Volume vs. Time	14.1-186
14.1.12-5	Loss of AC Power to the Plant Auxiliaries* Steam Generator Pressure vs. Time	14.1-187
14.1.12-6	Loss of AC Power to the Plant Auxiliaries* Steam Generator Mass vs. Time	14.1-188
14.2.4-1	Break Flow and SI Flow (Two Pumps) vs. Reactor Coolant Pressure	14.2-38
14.2.5-1	Variation of K_{eff} with Core Temperature	14.2-39
14.2.5-2	SI Curve	14.2-40
14.2.5-3	MSLB With Offsite Power Steam Generator Steam Pressure vs. Time	14.2-41
14.2.5-4	MSLB With Offsite Power Steam Generator Outlet Nozzle Mass Flow Rate vs. Time	14.2-42
14.2.5-5	MSLB With Offsite Power Pressurizer Pressure vs. Time	14.2-43
14.2.5-6	MSLB With Offsite Power Pressurizer Water Volume vs. Time	14.2-44
14.2.5-7	MSLB With Offsite Power Reactor Vessel Inlet Temperature vs. Time	14.2-45
14.2.5-8	MSLB With Offsite Power Core Heat Flux vs. Time	14.2-46
14.2.5-9	MSLB With Offsite Power Core Averaged Boron Concentration vs. Time	14.2-47
14.2.5-10	MSLB With Offsite Power Reactivity vs. Time	14.2-48
14.2.5-11	MSLB Without Offsite Power Steam Pressure vs. Time	14.2-49
14.2.5-12	MSLB Without Offsite Power Steam Generator Outlet Nozzle Mass Flow Rate vs. Time	14.2-50
14.2.5-13	MSLB Without Offsite Power Pressurizer Pressure vs. Time	14.2-51
14.2.5-14	MSLB Without Offsite Power Pressurizer Water Volume vs. Time	14.2-52
14.2.5-15	MSLB Without Offsite Power Reactor Vessel Inlet Temperature vs. Time	14.2-53
14.2.5-16	MSLB Without Offsite Power Core Heat Flux vs. Time	14.2-54
14.2.5-17	MSLB Without Offsite Power Core Averaged Boron Concentration vs. Time	14.2-55
14.2.5-18	MSLB Without Offsite Power Reactivity vs. Time	14.2-56
14.2.5-21	Limiting MSLB - Containment Pressure Response	14.2-57
14.2.5-22	Limiting MSLB - Containment Temperature Response	14.2-58
14.2.6-1	RCCA Ejection Accident from Full Power Beginning of Cycle Reactor Power vs. Time	14.2-59

Chapter 14: Safety Analysis

List of Figures

Figure	Title	Page
14.2.6-2	RCCA Ejection Accident from Full Power Beginning of Cycle Fuel and Cladding Temperatures vs. Time	14.2-60
14.2.6-3	RCCA Ejection Accident from Zero Power Beginning of Cycle Reactor Power vs. Time	14.2-61
14.2.6-4	RCCA Ejection Accident from Zero Power Beginning of Cycle Fuel and Cladding Temperatures vs. Time	14.2-62
14.2.6-5	RCCA Ejection Accident from Full Power End of Cycle Reactor Power vs. Time	14.2-63
14.2.6-6	RCCA Ejection Accident from Full Power End of Cycle Fuel and Cladding Temperatures vs. Time	14.2-64
14.2.6-7	RCCA Ejection Accident from Zero Power End of Cycle Reactor Power vs. Time	14.2-65
14.2.6-8	RCCA Ejection Accident from Zero Power End of Cycle Fuel and Cladding Temperatures vs. Time	14.2-66
14.3-1	SI Flow, Spill to RCS	14.3-108
14.3-2	SI Flow, Spill to Containment	14.3-109
14.3-3	Pressurizer Pressure 3-Inch Break High T_{avg}	14.3-110
14.3-4	Core Mixture Level 3-Inch Break High T_{avg}	14.3-111
14.3-5	Core Exit Stem Flow 3-Inch Break High T_{avg}	14.3-112
14.3-6	BL & IL Pumped SI Flow Rate 3-Inch Break High T_{avg}	14.3-113
14.3-7	Peak Clad Temp at PCT Elevation 3-Inch Break High T_{avg}	14.3-114
14.3-8	Hot Spot Fluid Temp at PCT Elevation 3-Inch Break High T_{avg}	14.3-115
14.3-9	Hot Rod HCT at PCT Elevation 3-Inch Break High T_{avg}	14.3-116
14.3-10	Pressurizer Pressure 2-Inch Break High T_{avg}	14.3-117
14.3-11	Core Mixture Level 2-Inch Break High T_{avg}	14.3-118
14.3-12	Peak Clad Temp at PCT Elevation 2-Inch Break High T_{avg}	14.3-119
14.3-13	Pressurizer Pressure 4-Inch Break High T_{avg}	14.3-120
14.3-14	Core Mixture Level 4-Inch Break High T_{avg}	14.3-121
14.3-15	Peak Clad Temp at PCT Elevation 4-Inch Break High T_{avg}	14.3-122
14.3-16	Pressurizer Pressure 3-Inch Break Low T_{avg}	14.3-123
14.3-17	Core Mixture Level 3-Inch Break Low T_{avg}	14.3-124
14.3-18	Peak Clad Temp at PCT Elevation 3-Inch Break Low T_{avg}	14.3-125
14.3-19	Loop Reactor Mathematical Model for Vertical Response	14.3-126
14.3-20	Reactor Internals Allowable Stress Criteria	14.3-127
14.3-21	Notes for Figure 14.3-20.	14.3-128

Chapter 14: Safety Analysis

List of Figures

Figure	Title	Page
14.3-22	Containment Fan Cooler Heat Removal Rate vs. Containment Pressure	14.3-130
14.3-23	Shield Building Ventilation System	14.3-131
14.3-24	Shield Building Ventilation Performance Test Curve and Shield Building Performance Curve	14.3-132
14.3-25	Annulus Pressure with Steel Shell Expansion Design Basis Transient	14.3-133
14.3-26	Flow Out of the SBVS with Steel Shell Expansion Design Basis Transient	14.3-134
14.3-27	[Deleted]	14.3-135
14.3-28	Hydrogen Control By Purging and Venting Through Shield Building Vent System Without Pressure Increase	14.3-136
14.3-29	Effects of Pressure Increase on Venting Requirements	14.3-137
14.3-30	Containment Leakage and Venting Requirements as Affected by Pressure Increase.	14.3-138
14.3-31	Provisions for Mixing, Sampling and Venting of Containment Gases.	14.3-139
14.3-32	Reactor Building Ventilation System Post LOCA-H ₂ Control Flow Diagram	14.3-141
14.3.2-1	Typical Time Sequence of Events for the KNPP BELOCA Analysis	14.3-143
14.3.2-2	Containment Pressure Curve Used in the KNPP BELOCA Analysis	14.3-144
14.3.2-3	KNPP Reference Transient-Peak Clad Temperature	14.3-145
14.3.2-4	KNPP Reference Transient-Split Break Flow	14.3-146
14.3.2-5	KNPP Reference Transient-Total Core at Midplane	14.3-147
14.3.2-6	KNPP Reference Transient-Accumulator Flow	14.3-148
14.3.2-7	KNPP Reference Transient-HHSI Flow	14.3-149
14.3.2-8	KNPP Reference Transient-LHSI Flow	14.3-150
14.3.2-9	KNPP Reference Transient-Average Liquid Levels in the Downcomer Channels.	14.3-151
14.3.2-10	KNPP Reference Transient-Lower Plenum Liquid Level	14.3-152
14.3.2-11	KNPP Reference Transient-Core Channel Liquid Level	14.3-153
14.3.2-12	KNPP P _{BOT} /P _{MID} Limits Superimposed on a Plot of All Possible Power Shapes	14.3-154
14.3.2-13	KNPP LHSI Flow (One 10% Degraded LHSI Pump)	14.3-155
14.3.2-14	KNPP HHSI Flow (One 15% Degraded HHSI Pump).	14.3-156

Chapter 14: Safety Analysis

List of Figures

Figure	Title	Page
14.3.4-1	Double-Ended Hot Leg Break - Containment Pressure	14.3-157
14.3.4-2	Double-Ended Hot Leg Break - Containment Atmosphere Temperature	14.3-158
14.3.4-3	Double-Ended Hot Leg Break - Containment Sump Temperature.	14.3-159
14.3.4-4	Double-Ended Pump Suction Break with Minimum Safeguards - Containment Pressure	14.3-160
14.3.4-5	Double-Ended Pump Suction Break with Minimum Safeguards - Containment Atmosphere Temperature.	14.3-161
14.3.4-6	Double-Ended Pump Suction Break with Minimum Safeguards - Containment Sump Temperature.	14.3-162
14.3.4-7	Double-Ended Pump Suction Break with Maximum Containment Safeguards - 1 Spray Pump Failure Containment Pressure	14.3-163
14.3.4-8	Double-Ended Pump Suction Break with Maximum Containment Safeguards - 1 Spray Pump Failure Containment Atmosphere Temperature	14.3-164
14.3.4-9	Double-Ended Pump Suction Break with Maximum Containment Safeguards - 1 Spray Pump Failure Containment Sump Temperature. . .	14.3-165
14.3.4-10	Double-Ended Pump Suction Break with Maximum Containment Safeguards - 1 Fan Cooler Failure Containment Pressure	14.3-166
14.3.4-11	Double-Ended Pump Suction Break with Maximum Containment Safeguards - 1 Fan Cooler Failure Containment Atmosphere Temperature	14.3-167
14.3.4-12	Double-Ended Pump Suction Break with Maximum Containment Safeguards - 1 Fan Cooler Failure Containment Sump Temperature. . .	14.3-168
14C-1	3.0 Ft ² Pump Suction Break (Split)	14.C-25
14C-2	3.0 Ft ² Pump Suction Break (Split)	14.C-26
14C-3	Hydraulic Model for Pump Suction Break	14.C-27
14C-4	Energy Balance Model	14.C-28
14C-5	3.0 Ft ² Pump Suction Break (Split) Mass and Energy Released During Blowdown.	14.C-29
14C-6	3.0 Ft ² Pump Suction Break (Split) Mass and Energy Released During Reflood	14.C-30
14C-7	3.0 Ft ² Pump Suction Break (Split) Accumulator Flow Rate.	14.C-31
14C-8	3.0 Ft ² Pump Suction Break (Split) Accumulator Flow Rate.	14.C-32
14C-9	3.0 Ft ² Pump Suction Break	14.C-33
14C-10	3.0 Ft ² Pump Suction Break	14.C-34
14C-11	Double Ended Pump Suction Break	14.C-35

Chapter 14: Safety Analysis

List of Figures

Figure	Title	Page
14C-12	0.6 Double Ended Pump Suction Break	14.C-36
14C-13	4.0 Ft ² Pump Suction Break	14.C-37
14C-14	2.0 Ft ² Pump Suction Break	14.C-38
14C-15	Double-Ended Cold Leg	14.C-39
14C-16	Double-Ended Hot Leg Break	14.C-40
14C-17	0.6 Double-Ended Hot Leg Break	14.C-41
14C-18	3.0 Ft ² Break (Split) Mass and Energy Released	14.C-42
14C-19	Containment Peak Pressures Sensitivity Study (Calculation No. SSFI-23-1, Revision 0, 02/03/89)	14.C-43

CHAPTER 14

SAFETY ANALYSIS

14.0.1 Safety Analysis Overview

In this section the safety aspects of the plant are evaluated to demonstrate that the plant can be operated safely and that radiological consequences from postulated accidents do not exceed the guidelines of 10 CFR 50.67.

The American Nuclear Society (ANS), Reference 1, has classified plant conditions into four categories in accordance with the anticipated frequency of occurrence and potential radiological consequences to the public. The four categories are as follows:

- Condition I: Normal Operation and Operational Transients
- Condition II: Incidents of Moderate Frequency
- Condition III: Infrequent Incidents
- Condition IV: Limiting Faults

A description of each category including design requirements, acceptance criteria, and the applicable design basis transient events is provided below:

Condition I: Normal Operation and Operational Transients

Definition

Condition I occurrences are operations that are expected frequently or regularly in the course of power operation, refueling, maintenance, or maneuvering of the plant.

Design Requirements

Condition I occurrences shall be accommodated with margin between any plant parameter and the value of that parameter which would require either automatic or manual protective action.

Events

Normal Operation (Base Load and Load Follow)

Acceptance Criteria

- No Clad Damage/Fuel Melting
- Reactor Coolant System (RCS) Pressure < Design Limits
- Main Steam System Pressure < Design Limits
- Containment Pressure and Temperature < Design Limits

Condition II: Incidents of Moderate Frequency**Definition**

Condition II occurrences include incidents, any one of which may occur during a calendar year for a particular plant.

Design Requirements

Condition II incidents shall be accommodated with, at most, a shutdown of the reactor with the plant capable of returning to operation after corrective action. Any release of radioactive materials in effluents to unrestricted areas shall be in conformance with Paragraph 20.1 of 10 CFR 20, "Standards for Protection Against Radiation."

By itself, a Condition II incident cannot generate a more serious incident of the Condition III or IV type without other incidents occurring independently. A single Condition II incident shall not cause consequential loss of function of any barrier to the escape of radioactive products. (No fuel rod failure or RCS overpressurization.)

Transient Events

- Uncontrolled Rod Control Cluster Assembly (RCCA) Withdrawal From Sub-critical
- Uncontrolled RCCA Withdrawal at Power
- RCCA Misalignment (Dropped/Static)
- Chemical and Volume Control System Malfunction
- Startup of Inactive Reactor Coolant Loop
- Feedwater System Malfunction
- Excessive Load Increase
- Partial Loss of Reactor Coolant Flow
- Loss of External Load
- Loss of Normal Feedwater
- Loss of AC Power to Plant Auxiliaries

Acceptance Criteria

- RCS Pressure < 110 percent of Design (2750 psia)
- MDNBR > MDNBR Limit
- Fuel Centerline Temp < 4700°F
- Dose Consequences < 10 CFR 20
- Main Steam System Pressure < 110 percent of Design (1210 psia)
- Containment Pressure and Temperature < Design Limits

Condition III: Infrequent Incidents**Definition**

Condition III occurrences include incidents, any one of which may occur during the lifetime of a particular plant.

Design Requirements

Condition III incidents shall not cause more than a small fraction of the fuel elements in the reactor to be damaged, although sufficient fuel element damage might occur to preclude resumption of operation for a considerable outage time.

The release of radioactive material due to Condition III incidents may exceed guidelines of 10 CFR 20, “Standards for Protection Against Radiation,” but shall not be sufficient to interrupt or restrict public use of those areas beyond the exclusion radius.

A Condition III incident shall not, by itself, generate a Condition IV fault or result in a consequential loss of function of the RCS or reactor containment barriers.

Transient Events

- Small Loss-of-Coolant Accident (LOCA)
- Small Steam Line Break
- Complete Loss of Reactor Coolant Flow
- Single RCCA Withdrawal at Power
- Fuel Assembly Misloading
- Volume Control Tank Rupture

Acceptance Criteria

Most incidents use Condition II criteria, which are more limiting than the Condition III criteria. If these are not satisfied, the following criteria are applied:

- MDNBR < MDNBR Limit - Small Fraction of Fuel Rods (<5 percent)
- Dose Consequences < Applicable Fraction of 10 CFR 50.67
- RCS Pressure < 2900 psia
- Containment Pressure and Temperature < Design Limits

Condition IV: Limiting Faults

Definition

Condition IV occurrences are faults that are not expected to occur but are postulated because their consequences would include the potential for the release of significant amounts of radioactive material. Condition IV faults are the most drastic, which must be designed against, and thus represent the limiting design cases.

Design Requirements

Condition IV faults shall not cause a release of radioactive material that results in an undue risk to public health and safety exceeding the guidelines of 10 CFR 50.67. A single Condition IV fault shall not cause a consequential loss of required functions of systems needed to cope with the fault including those of the RCS and the Reactor Containment System.

Events

- Large LOCA
- Steam Generator Tube Rupture
- Main Steam Line Break (MSLB)
- Locked Rotor
- RCCA Ejection
- Fuel Handling

Acceptance Criteria

- Dose Consequences < 10 CFR 50.67
- RCS Pressure < 2900 psia (emergency)
- RCS Pressure < 4000 psia (faulted)
- Containment Pressure < 46 psig
- Containment pressure at 24 hours <50 percent of the peak calculated containment pressure value
- Containment vessel shell temperature < 268°F

The following events have event specific limits that are more limiting than the Condition IV criteria:

- Steam Generator Tube Rupture
Dose Consequences <10 percent of 10 CFR 50.67 when an accident-initiated iodine spike is considered
- MSLB
MDNBR > MDNBR Limit (MSLB)
Dose Consequences <10 percent of 10 CFR 50.67 when an accident-initiated iodine spike is considered
- Locked Rotor
Peak Clad Temperature < 2700°F
Percentage of Fuel Rods Experiencing DNB <50 percent
Dose Consequences <10 percent of 10 CFR 50.67
- RCCA Ejection
Peak Clad Temperature < 2700°F
Average Fuel Enthalpy < 200 cal/g
Fuel Melt < Innermost 10 percent of the fuel pellet at the hot spot
Dose Consequence < 25 percent of 10 CFR 50.67
- Fuel Handling Accident
Dose Consequences < 25 percent of 10 CFR 50.67

The basic principle applied in relating design requirements to each of the conditions is that the most frequent occurrences must yield little or no radiological risk to the public and those extreme situations having the potential for the greatest risk to the public shall be those least likely to occur. Where applicable, Reactor Protection System (RPS) and Engineered Safeguards functioning is assumed to the extent allowed by considerations such as the single failure criterion in fulfilling this principle.

In the evaluation of the radiological consequences associated with initiation of a spectrum of accident conditions numerous assumptions must be postulated. In many instances, these assumptions are a product of extremely conservative judgments. This is due to the fact that many physical phenomena, in particular fission product transport under accident conditions, are not understood to the extent that accurate predictions can be made. Therefore, the set of assumptions postulated would predominantly determine the accident classification.

This section is divided into three subsections, dealing with various behavior categories:

- Core and Coolant Boundary Protection Analysis, Section 14.1
The abnormalities presented in Section 14.1 have no off-site radiation consequences.
- Standby Safety Features Analysis, Section 14.2
The accidents presented in Section 14.2 are more severe than those discussed in Section 14.1 and may cause release of radioactive material to the environment.
- Reactor Coolant System Pipe Ruptures (LOCA), Section 14.3
The accident presented in Section 14.3, the rupture of a reactor coolant pipe, is the worst-case accident analyzed and is the primary basis for the design of engineered safety features. It is shown that the consequences of even this accident are within the guidelines of 10 CFR 50.67.

Safety Analyses are analyses performed to satisfy regulatory requirements. The safety analyses are integral to the plant's design and licensing basis. The safety analyses demonstrate the integrity of the fission product barriers, the capability to shutdown the reactor and maintain it in a safe shutdown condition, and the capability to prevent or mitigate the consequences of accidents and transients. Systems, structures, and components (SSC's) that perform design basis functions are credited in the safety analyses for the purpose of mitigating the transient or accident. The design basis of the plant includes the bounding conditions under which SSC's must perform their design basis functions. These conditions are derived from accidents or events for which SSC's are required to function. Design basis parameter values or ranges of values chosen for controlling parameters as reference bounds are derived or confirmed by the safety analyses. SSC's are relied upon to remain functional during and following design basis events.

The safety analyses credit the design basis functions performed by the SSC's including engineered safeguards SSC's and the reactor protection system SSC's. The safety analyses also assume the worst single active failure of SSC's. Conservative inputs for the design basis parameters are assumed in the safety analyses, e.g. conservative timing, setpoints, flow rate, etc. Safety analyses assume that SSC's required to support the SSC's credited in the safety analyses are functioning and fulfilling their supporting design function.

Design basis safety analysis transients are described in Section 14.1. Design basis safety analysis accidents are described in Section 14.2 and Section 14.3. Each section within Section 14.1, Section 14.2, and Section 14.3 describes a design basis transient or accident event. The subsection includes both a description of the how the plant is designed to respond to the transient or accident (subsection entitled “accident description”) and how the safety analyses were performed (subsection entitled “method of analysis”). The intent of this presentation for each transient or accident is to show the conservativeness of the safety analyses when compared to the more realistic plant response.

14.0.2 Safety Analysis Assumptions

Parameters and assumptions that are common to the safety analyses are described below to avoid repetition in subsequent sections.

14.0.3 Operating Parameters

For most accidents that are DNB limited, nominal values of initial conditions are assumed. The allowances on power, temperature, and pressure are determined on a statistical basis and are included in the limit DNBR, as described in WCAP-11397 (Reference 7). This procedure is known as the “Revised Thermal Design Procedure.”

For accidents in which the Revised Thermal Design Procedure is not employed, the Standard Thermal Design Procedure (STDP) (Reference 13) is employed. In STDP analyses, the initial conditions are obtained by applying the maximum steady-state errors to the rated values in the direction that results in the least margin to the acceptance criterion under consideration. The following rated values and conservative steady-state errors were assumed in the analyses:

Core Power	1772 MWt	± 0.6% of 1772 MWt for calorimetric error
Avg RCS Temperature	556.3°F–573.0°F	± 6°F for deadband and measurement error
Pressurizer Pressure	2250 psia	± 50.1 psi for steady-state fluctuations and measurement error

Initial values for power, primary pressure, and core temperature are typically (but not always) selected to minimize the initial margin to the acceptance criteria under consideration.

The initial active core flow rate is conservatively set to account for increased core bypass flow due to thimble plug removal and increased steam generator tube plugging. Unless otherwise stated in the Method of Analysis section for a particular accident the RCS and core flow rates are set as follows:

	STDP	RTDP
RCS Flow	178,000 gal/min	186,000 gpm
Core Bypass Flow	7.0%	5.5%
Effective Core Flow	165,540 gpm	175,770 gpm

14.0.3.1 Hot Channel Factors

Unless otherwise stated in the sections describing specific accidents, the hot channel factors used are:

$$F_q^n \text{ (Nuclear Heat Flux Hot Channel Factor)} = 2.50 \text{ (2.35 for Framatome fuel)}$$

$$F_{\Delta H}^N \text{ (Nuclear Enthalpy Rise Hot Channel Factor)} = 1.70 \text{ STDP, } 1.64 \text{ RTDP}$$

The movable in-core instrumentation system is employed to verify that actual hot channel factors are, in fact, no higher than the limiting values of the Technical Specifications. These limits on hot channel factors are designed to ensure the assumptions used in the accident analyses conservatively bound the actual core hot channel factors.

14.0.4 Reactor Protection System

A reactor trip signal acts to open the two series trip breakers feeding power to the control rod drive mechanisms. The loss of power to the mechanism coils causes the mechanism to release the control rods, which then fall by gravity into the core. There are various instrumentation delays associated with each tripping function including delays in signal actuation, in opening the trip breakers and in the release of the rods by the mechanisms. The total delay to trip is defined as the time delay from the time that trip conditions are reached to the time the rods are free and begin to fall. The time delay and setpoint assumed for each tripping function used in the analysis are as follows:

Reactor Trip Function	Setpoint	Time Delay (sec)
Power Range Rate	N/M*	N/A
Power Range Low Setpoint	35%	0.65
Power Range High Setpoint	118%	0.65
Overpower ΔT	Variable, see Figure 14.0-2	6.0
Overtemperature ΔT	Variable, see Figure 14.0-2	6.0

Reactor Trip Function	Setpoint	Time Delay (sec)
RCS Low Flow	86.5% of loop flow	0.75
High Pressurizer Level	N/M*	N/A
Low Pressurizer Pressure	1860 psia**	2.0
High Pressurizer Pressure	2425 psia	1.0
Low-Low Steam Generator Level	0.0% of level span	1.5
RXCP Undervoltage	N/M*	N/A
RXCP Underfrequency	N/M*	N/A
Turbine Trip on High-High Steam Generator Level	100% NRS	3.0

* N/M - not explicitly modeled in safety analysis

** Does not represent an analytical limit for this function for Kewaunee Nuclear Power Plant.

The difference between the limiting trip setpoint assumed for the analysis and the actual trip setpoint represents a conservative allowance for instrumentation channel and setpoint errors. Results of surveillance tests demonstrate that actual instrument errors are equal to or less than the assumed values.

The instrumentation drift and calorimetric errors used in establishing the maximum overpower setpoint are presented in Table 14.0-1.

Reference is made above to Overpower and Overtemperature Delta T (ΔT) variable reactor trip setpoints illustrated in Figure 14.0-2. This figure presents the allowable reactor coolant loop average temperature and ΔT for the design flow and power distribution, as a function of primary coolant pressure. The boundaries of operation defined by the overpower ΔT trip and the overtemperature ΔT trip are represented as “Protection Lines” on this diagram. The protection lines are drawn to include all adverse instrumentation and setpoint errors so that under nominal conditions a trip would occur well within the area bounded by these lines. The utility of this diagram is in the fact that the limit imposed by any given DNBR can be represented as a line. The DNBR lines represent the locus of conditions for which the DNBR equals the limit value. All points below and to the left of a DNBR line for a given pressure have a DNBR greater than the limit value. The diagram shows that DNBR is prevented for all cases if the applicable DNBR line at any point does not traverse the area enclosed with the maximum protection lines. The area of permissible operation (power, pressure, and temperature) is bounded by the following combination of reactor trips: high neutron flux (fixed setpoint), high pressurizer pressure (fixed setpoint), low pressurizer pressure (fixed setpoint), overpower ΔT (variable setpoint) and overtemperature ΔT (variable setpoint).

Trip is defined for analytical purposes as the insertion of all full-length RCCAs except the most reactive RCCA, which is assumed to remain in the fully withdrawn position. This is to provide shutdown margin capability against the remote possibility of a stuck RCCA condition existing at a time when shutdown is required.

The negative reactivity insertion following a reactor trip is a function of the acceleration of the control rods and the variation in rod worth as a function of rod position. Control rod positions after trip have been determined experimentally as a function of time using an actual prototype assembly under simulated flow conditions. The resulting rod positions were combined with rod worths to define the negative reactivity insertion as a function of time, as shown in Figure 14.0-1.

In summary, reactor protection is designed to prevent cladding damage in all transients and abnormalities. The most probable modes of failure in each protection channel result in a signal calling for the protective trip. Coincidence of two-out-of-three (or two-out-of-four) signals is required where single channel malfunction could cause spurious trips while at power. A single component or channel failure in the protection system itself coincident with one stuck RCCA is always permissible as a contingent failure and does not cause violation of the protection criteria. The reactor protection systems are designed in accordance with Reference 2.

In the safety analyses there are transients and accidents that are limiting with respect to secondary side overpressure. The main steam safety valve setpoints assumed for these limiting overpressure events are provided below. The safety analysis MSSV setpoint includes appropriate allowance for: setpoint tolerance, accumulation and the pressure drop from the SG outlet to the MSSV.

MSSV #	Nominal MSSV Setpoint (psig)	Safety Analysis MSSV Setpoint (Pressure at the steam generator) (psia)
1	1074	1146
2	1090	1165
3	1105	1182
4	1120	1199
5	1127	1208

14.0.4.1 Calorimetric Error Instrumentation Accuracy

The calorimetric error is the error assumed in the determination of core thermal power as obtained from secondary plant measurements. The total ion chamber current (sum of the top and bottom sections) is calibrated (set equal) to this measured power on a periodic basis. The secondary power is obtained from measurement of feedwater flow, feedwater inlet temperature to the steam generator and steam pressure. High accuracy plant instrumentation is provided for these measurements with accuracy tolerances more restrictive than that which would be required to

only control the feedwater flow. Accuracy of the secondary power calorimetric using this instrumentation provides an assumed power measurement uncertainty of 2 percent.

Kewaunee Nuclear Power Plant (KNPP) has two methods to reduce the power measurement uncertainty, an installed CROSSFLOW Ultrasonic Flow Measurement Device (UFMD) and a full flow bypass loop with a precision flow measurement section.

The Crossflow UFMD derives feedwater flow and feedwater temperature correction factors. Use of the UFMD correction factors reduces the uncertainty of the power measurement to 0.6 percent. This uncertainty along with the relaxation of the 10 CFR 50, Appendix K rule regarding power measurement uncertainty, allows for operation at a power level consistent with the actual power measurement uncertainty (Reference 4). Operation with the Crossflow UFMD providing feedwater flow and feedwater temperature correction factors is the licensing basis for the KNPP measurement uncertainty recapture (MUR) power uprate utilizing the 0.6 percent power measurement uncertainty (Reference 4, Reference 5, and Reference 6). The power measurement uncertainties with the UFMD in and out of service are reported in Reference 5.

The KNPP feedwater bypass line (FBL) is a full flow main feedwater bypass loop designed to accurately measure total feedwater flow at KNPP when the UFMD is out of service. The FBL contains a flow section, which includes a flow straightener and a laboratory calibrated flow nozzle. The flow section is accurate to 0.25 percent. The total uncertainty of this feedwater measurement is a function of the uncertainty of the FBL calibration and the venturi repeatability. Correction factors for the feedwater venturis are derived by comparing the venturi flow to the total feedwater flow measured by the FBL flow element. The power measurement uncertainty associated with using feedwater flow correction factors from the FBL measurement is 1.55 percent. While this is less than the total flow uncertainty associated with using only the feedwater venturis, the uncertainty using the FBL correction factors does not support the requirements of the MUR uprate.

14.0.4.2 **Fuel/Reload Transition**

Kewaunee is transitioning from the Framatome-ANP fuel design to the Westinghouse 422V+ fuel design. This fuel/reload transition was documented and approved by the NRC (Reference 15).

The neutronic behavior of the Framatome-ANP fuel through the transition cores is accurately predicted by the standard nuclear design analytical models, codes (the ALPHA/PHOENIX/ANC code system) and methods of Westinghouse. The generic verification and validation basis for the Westinghouse models and methods is extensive and encompasses various Westinghouse fuel designs with different fuel rod diameters, cladding dimensions, assembly designs, core sizes, etc. The nature and magnitude of the differences between the various Westinghouse fuel designs in the qualification basis is significantly greater than the differences between the Westinghouse 422V+ fuel and the Framatome-ANP fuel (see table below). Moreover, the differences between the 422V+ fuel and the Framatome-ANP fuel that

impact neutronic behavior are even less significant and are dominated by the typical variations in the uranium loading, enrichments, and number and type of burnable poisons that are modeled. Finally, comparisons of the measured and predicted (i.e., predicted with Nuclear Management Company (NMC) standard methods) nuclear design data from previous KNPP cycles with the Westinghouse predicted data are used to verify that the Westinghouse models and methods accurately describe the Framatome-ANP fuel neutronic behavior.

Characteristic	Westinghouse 422V+	Framatome Heavy HTP
Fuel Rod O.D. (in)	0.422	0.424
Clad Thickness (in.)	0.0243	0.0250
Pellet Diameter (in.)	0.3659	0.3670
Fuel Rod Pitch (in.)	0.556	0.556

The transient and accident analysis results that are presented in USAR Section 14.1, Section 14.2 and Section 14.3 are for the limiting fuel design, the Westinghouse 422 V+ fuel design. The non-fuel related non-LOCA transient analysis results (e.g., RCS pressure, Main Steam System pressure, pressurizer water volume, etc.) are applicable to transition cores as well as full Westinghouse 422V+ cores. As such, these non-LOCA transient analysis results are bounding for Framatome-ANP fuel.

The fuel-related non-LOCA transient analyses which include the thermal-hydraulic analyses (e.g., DNBR, fuel centerline temperature, peak clad temperature, percent of rods in DNB, etc.) for Framatome-ANP fuel are generated with the approved methods of the NMC reload safety evaluation methods topical report for KNPP (Reference 3). The effects of the mixed core are evaluated. The thermal-hydraulic analyses for the Framatome-ANP fuel are generated during the reload safety evaluation process and are documented in the Reload Safety Evaluation Report.

The thermal hydraulic, transient analysis acceptance criteria for the Framatome-ANP fuel have been shown to be satisfied for the fuel transition. This is due to the fact that there is an increase in local fuel assembly flow for the Framatome-ANP fuel design due to the mixed core effects and there is a decrease in Framatome-ANP fuel design $F_{\Delta H}$ due to the once-burned status of the Framatome-ANP fuel.

The mechanical behavior of the Framatome-ANP fuel is evaluated by Framatome-ANP using the NRC approved models and methods of Framatome-ANP. The evaluation is performed for each cycle containing Framatome-ANP fuel and considers the transition core effects.

The thermal-hydraulic behavior of the Framatome-ANP fuel is evaluated by NMC using the approved models and methods (Reference 3) for KNPP. These models and methods consider the transition core effects and the power uprate. The presence of the 422V+ fuel improves the thermal

hydraulic analysis margins for the Framatome-ANP fuel due to the flow increase experienced by the Framatome-ANP fuel caused by the higher overall loss coefficient in the 422V+ fuel.

14.0.5 Safety Analysis and Core Reload Methodology

The core reload methodology is described in Reference 3 and Reference 13.

Summaries of some of the principal computer codes used in transient analyses are given below. Other codes, such as those used in the accident analysis of RCS pipe ruptures (Section 14.3), are summarized in the respective accident analysis sections.

FACTRAN (Reference 8)

FACTRAN calculates the transient temperature distribution in a cross-section of a metal clad UO_2 fuel rod and the transient heat flux at the surface of the cladding, using as input the nuclear power and the time-dependent coolant parameters of pressure, flow, temperature and density. The code uses a fuel model that simultaneously contains the following features:

1. A sufficiently large number of radial space increments to handle fast transients such as a rod ejection accident;
2. Material properties which are functions of temperature and a sophisticated fuel-to-cladding gap heat transfer calculation; and
3. The necessary calculations to handle post-DNB transients: film boiling heat transfer correlations, Zircaloy-water reaction, and partial melting of the fuel.

RETRAN (Reference 9)

RETRAN is used for studies of transient response of a pressurized water reactor (PWR) system to specified perturbations in process parameters. This code simulates a multi-loop system by a lumped parameter model containing the reactor vessel, hot and cold leg piping, reactor coolant pumps, steam generators (tube and shell sides), steam lines, and the pressurizer. The pressurizer heaters, spray, relief valves, and safety valves may also be modeled. RETRAN includes a point neutron kinetics model and reactivity effects of the moderator, fuel, boron, and control rods. The secondary side of the steam generator uses a detailed nodalization for the thermal transients. The RPS simulated in the code includes reactor trips on high neutron flux, overtemperature and overpower ΔT (OT ΔT /OP ΔT), low RCS flow, high and low pressurizer pressure, high pressurizer level, and lo-lo steam generator water level. Control systems are also simulated including rod control and pressurizer pressure control. Parts of the Safety Injection System (SIS), including the accumulators, may also be modeled. RETRAN approximates the transient value of departure from nucleate boiling ratio (DNBR) based on input from the core thermal safety limits. Detailed, stand-alone RETRAN models of the steam generator are used for entrainment calculations (Reference 3).

LOFTRAN (Reference 10)

Transient response studies of a pressurized water reactor (PWR) to specified perturbations in process parameters use the LOFTRAN computer code. This code simulates a multi-loop system by a model containing the reactor vessel, hot and cold leg piping, steam generators (tube and shell sides), the pressurizer and the pressurizer heaters, spray, relief valves, and safety valves. LOFTRAN also includes a point neutron kinetics model and reactivity effects of the moderator, fuel, boron, and rods. The secondary side of the steam generator uses a homogeneous, saturated mixture for the thermal transients. The code simulates the RPS, which includes reactor trips on high neutron flux, $OT\Delta T$, $OP\Delta T$, high and low pressurizer pressure, low RCS flow, lo-lo steam generator water level, and high pressurizer level. Control systems are also simulated including rod control, steam dump, and pressurizer pressure control. The SIS, including the accumulators, is also modeled. LOFTRAN also approximates the transient value of departure from nucleate boiling ratio (DNBR) based on the input from the core thermal safety limits.

TWINKLE (Reference 11)

TWINKLE is a multi-dimensional spatial neutron kinetics code. The code uses an implicit finite-difference method to solve the two-group transient neutron diffusion equations in one, two, and three dimensions. The code uses six delayed neutron groups and contains a detailed multi-region fuel-cladding-coolant heat transfer model for calculating pointwise Doppler and moderator feedback effects. The code handles up to 8000 spatial points and performs its own steady-state initialization. Aside from basic cross-section data and thermal-hydraulic parameters, the code accepts as input basic driving functions such as inlet temperature, pressure, flow, boron concentration, control rod motion, and others. The code provides various output, e.g., channelwise power, axial offset, enthalpy, volumetric surge, pointwise power and fuel temperatures. It also predicts the kinetic behavior of a reactor for transients that cause a major perturbation in the spatial neutron flux distribution.

VIPRE (Reference 12)

The VIPRE computer program performs thermal-hydraulic calculations. This code calculates coolant density, mass velocity, enthalpy, void fractions, static pressure and departure from nucleate boiling ratio (DNBR) distributions along flow channels within a reactor core.

DYNODE (Reference 3)

The DYNODE computer program performs transient calculations for the response of pressurized water reactor (PWR) nuclear steam supply systems (NSSS) process parameters for specified perturbations. This code simulates a multi loop system by a model containing the reactor vessel, hot and cold leg piping, steam generators (tube and shell sides), the pressurizer and the pressurizer heaters, spray, relief valves, and safety valves. DYNODE also includes a point neutron kinetics model and reactivity effects of the moderator, fuel, boron, and rods. The secondary side of the steam generator uses a homogeneous, saturated mixture for the thermal transients. The code simulates the RPS, which includes reactor trips on high neutron flux, $OT\Delta T$, $OP\Delta T$, high and low

pressurizer pressure, low RCS flow, lo-lo steam generator water level and high pressurizer level. Control systems are also simulated including rod control, steam dump and pressurizer pressure control. The SIS is also modeled. DYNODE is used for the MSLB mass and energy release calculation and the loss of normal feedwater (restricted power) calculation.

TOODEE (Reference 3)

TOODEE computer program performs similar functions as the FACTRAN and is used for fuel temperature analyses of Framatome-ANP fuel.

GOTHIC (Reference 14)

By application dated September 30, 2002, as supplemented by letters dated July 23 and September 26, 2003, the NMC requested changes to the KNPP analysis-licensing basis. Specifically, the proposed changes would revise the licensing basis from GOTHIC 6.0 (version 6.0a) to GOTHIC 7.0 (version 7.0p2).

The Nuclear Regulatory Commission (NRC) approved the use of the GOTHIC 6.0 computer code for the calculation of containment response to design-basis accidents, specifically, the LOCA and the MSLB (Reference 3). In the NMC September 30, 2002 application, NMC stated that GOTHIC 7.0 will be used for the same purposes that were noted in the GOTHIC 6.0 approval. NMC also stated that the principal difference between GOTHIC 6.0 and GOTHIC 7.0 is a mist diffusion layer model (MDLM), although several other changes were discussed.

The NRC authorized (Reference 14) the use of the upgraded computer code for design-basis accident containment integrity analyses called Generation of Thermal-Hydraulic Information for Containment (GOTHIC) version 7.0p2 (GOTHIC 7) with the following conditions:

1. The height effect scaling factor λ_h applied to the heat and mass transfer analogy shall not be used for the Kewaunee licensing calculations.
2. The Gido-Koestel (G-K) correlation shall not be used for Kewaunee licensing calculations.
3. The inclusion of mist in the mist diffusion layer model (MDLM) shall not be used for Kewaunee licensing calculations.

In addition,

4. It is not necessary to apply the proposed bias term to the mist diffusion layer model for Kewaunee licensing calculations.
5. It is not necessary to use a combination of Uchida and MDLM for the containment heat structures. MDLM may be used for heat transfer to all structures for Kewaunee licensing calculations.

14.0 References

1. ANSI N18.2-1973, "Nuclear Safety Criteria for the Design of Stationary Pressurized Water Reactor Plants"
2. IEEE 279, "Standard for Nuclear Plant Protection Systems," August 1968
3. Lamb J. B., (NRC) to M. E. Reddemann (NMC), transmitting the NRC SER approving WPSRSEM-NP, Revision 3, "Kewaunee Nuclear Power Plant - Review for Kewaunee Reload Safety Evaluation Methods Topical Report," Letter No. K-01-112, September 10, 2001
4. Lamb, J. B., (NRC) to T. Coutu (NMC) transmitting the NRC SER for Amendment No. 168 to the Operating License, approving the Measurement Uncertainty Recapture (MUR) Power Uprate (1.4%), Letter No. K-03-094, July 8, 2003
5. WCAP-15591, "Westinghouse Revised Thermal Design procedure Instrument Uncertainty Methodology-Kewaunee Nuclear Power Plant (Power Uprate to 1757 MWt-NSSS Power with Feedwater Venturis, or 1780 MWt-NSSS Power with Ultrasonic Flow Measurements, and 54F Replacement Steam Generators)," Revision 1, December 2002
6. CENPD-397-P-A, "Improved Flow Measurement Accuracy Using Crossflow Ultrasonic Flow Measurement Technology," Revision 1, May 2000
7. Friedland, A. J., S. Ray, "Revised Thermal Design Procedure," WCAP-11397-P-A (Proprietary), WCAP-11397-A (Non-Proprietary), April 1989
8. Hargrove, H. G., "FACTRAN-A FORTRAN-IV Code for Thermal Transients in a UO₂ Fuel Rod," WCAP-7908-A, December 1989
9. Huegel, D. S., et al., "RETRAN-02 Modeling and Qualification for Westinghouse Pressurized Water Reactor Non-LOCA Safety Analyses," WCAP-14882-P-A (Proprietary), April 1999
10. Burnett, T. W. T., et al., "LOFTRAN Code Description," WCAP-7907-P-A (Proprietary) and WCAP-7907-A (Non-Proprietary), April 1984
11. Risher, R. H., Jr., and R. F. Barry, "TWINKLE-A Multi-Dimensional Neutron Kinetics Computer Code," WCAP-7979-P-A (Proprietary) and WCAP-8028-A (Non-Proprietary), January 1975
12. Sung, Y. X., et al., "VIPRE-01 Modeling and Qualification for Pressurized Water Reactor Non-LOCA Thermal-Hydraulic Safety Analysis," WCAP-14565-P-A (Proprietary), October 1999
13. Bordelon, F. M., et al., "Westinghouse Reload Safety Evaluation Methodology," WCAP-9272-P-A (Proprietary), July 1985

14. Letter from A. C. McMurtray (NRC) to T. Coutu (NMC), “Kewaunee Nuclear Power Plant-Issuance of Amendment (TAC No. MB6408),” Letter No. K-03-136, September 29, 2003
15. NRC Safety Evaluation Report, Relating to Amendment 167 to Facility Operating License No. DPR-43, Nuclear Management Company, LLC, Kewaunee Nuclear Power Plant, April 4, 2003 approving KNPP LAR 187

Table 14.0-1
Instrumentation Drift and Calorimetric Errors
Nuclear Overpower Trip Channel

	Set Point and Error Allowances: (% of rated power)
Nominal set point	109
Calorimetric error	2 ^a
Axial power distribution effects on total ion chamber current	5
Instrumentation channel drift and set point reproducibility	2
Maximum overpower trip point assuming all individual errors are simultaneously in the most adverse direction	118

a. The 2.0% calorimetric error bounds the 0.6% UFMD calorimetric error with UFMDs in-service.

Figure 14.0-1
Scram Reactivity Insertion Rate
Negative Reactivity vs. Time

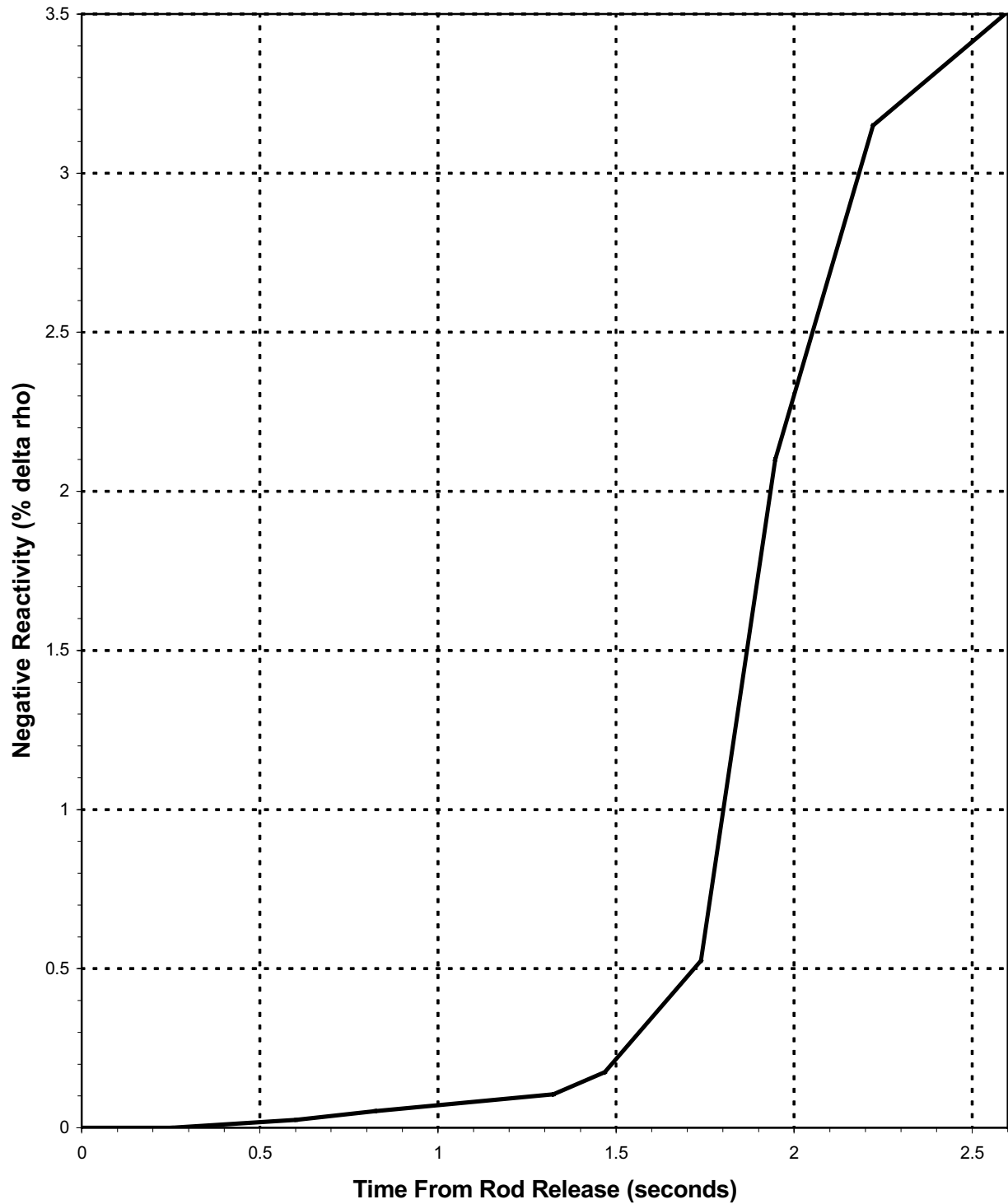
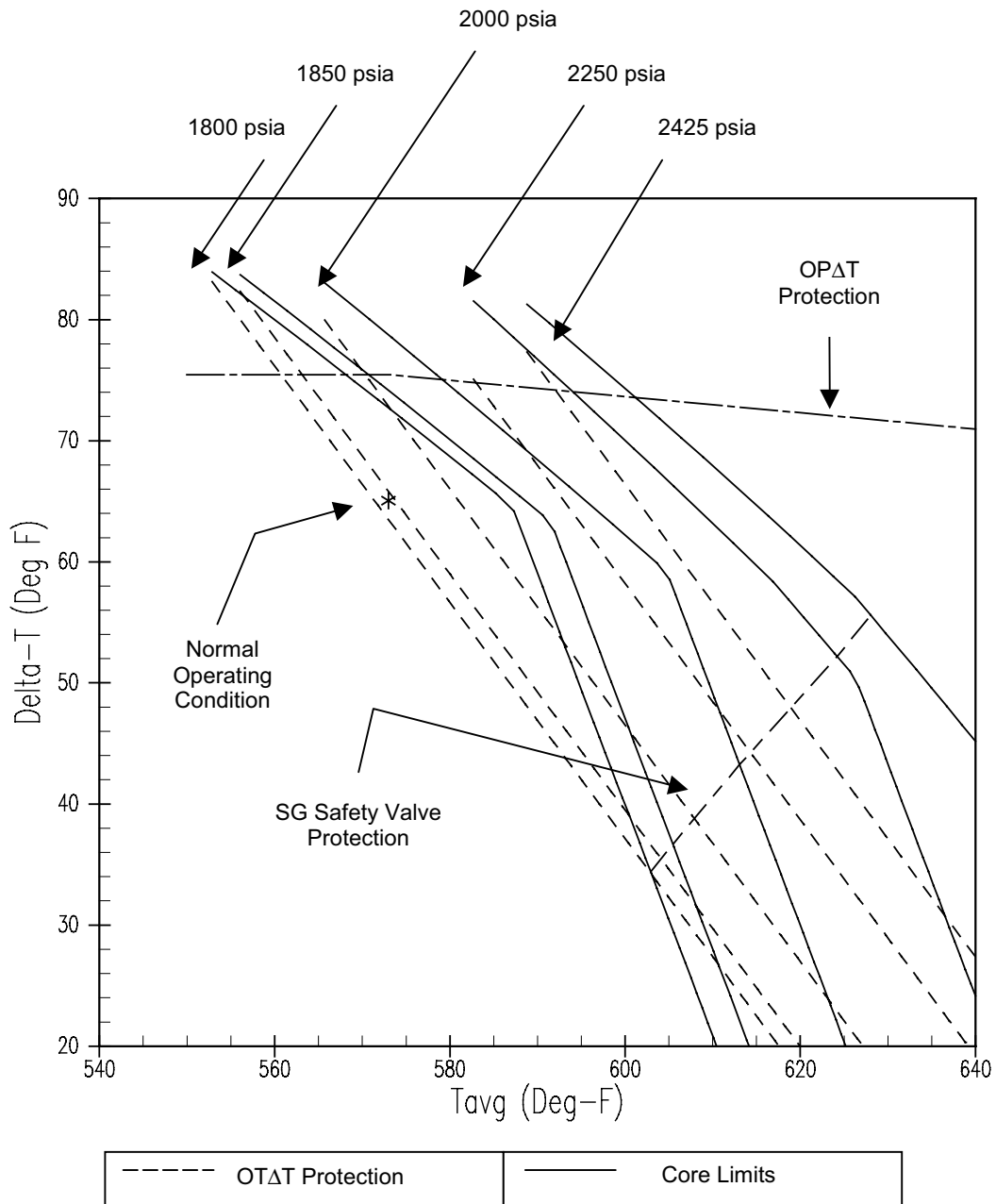


Figure 14.0-2
Illustration of Overtemperature and Overpower ΔT Protection



14.1 CORE AND COOLANT BOUNDARY PROTECTION ANALYSIS

The following anticipated events are abnormal operational transients resulting from component failure or operator error. They are anticipated to occur sometime in the design life of the plant.

In these events the reactor control and protection system and engineered safeguards are relied upon to protect the core and RCS boundary from damage.

- Uncontrolled RCCA Withdrawal from a Sub-critical Condition (Section 14.1.1)
- Uncontrolled RCCA Withdrawal at Power (Section 14.1.2)
- RCCA Misalignment (Section 14.1.3)
- Chemical and Volume Control System Malfunction (Section 14.1.4)
- Startup of an Inactive Reactor Coolant Loop (Section 14.1.5)
- Excessive Heat Removal Due to Feedwater System Malfunctions (Section 14.1.6)
- Excessive Load Increase Incident (Section 14.1.7)
- Loss of Reactor Coolant Flow (Section 14.1.8)
- Loss of External Electrical Load (Section 14.1.9)
- Loss of Normal Feedwater (Section 14.1.10)
- Loss of all AC Power to the Plant Auxiliaries (Section 14.1.13)

14.1.1 Uncontrolled RCCA Withdrawal from a Subcritical Condition

14.1.1.1 Accident Description

The RCCA withdrawal accident is defined as an uncontrolled addition of reactivity to the reactor core caused by withdrawal of RCCA banks resulting in a power excursion. While the occurrence of a transient of this type is unlikely, such a transient could be caused by a malfunction of the reactor control or the control rod drive system. This could occur with the reactor either subcritical, at hot zero power (HZP), or at power. The “at power” case is discussed in Section 14.1.2.

Withdrawal of an RCCA bank can add reactivity at a prescribed and controlled rate to bring the reactor from a subcritical condition to a low power level during startup. Initial startup procedure uses the method of boron dilution, subsequent startups can use RCCA bank withdrawal. An RCCA bank movement can cause much faster changes in reactivity than can be made by changing boron concentration (see Section 14.1.4, Chemical and Volume Control System Malfunction).

The RCCA drive mechanisms are wired into pre-selected bank configurations that are not altered during core life. These circuits prevent RCCAs from being withdrawn in other than their respective banks. Power supplied to the rod banks is controlled so that no more than two banks can be withdrawn at any time and in their proper withdrawal sequence. The RCCA drive mechanisms are the magnetic latch type; coil actuation is sequenced to provide variable speed travel. The analysis of the maximum reactivity insertion rate includes the assumption of the simultaneous withdrawal of the two sequential banks having the maximum combined worth at maximum speed.

The neutron flux response to a continuous reactivity insertion is characterized by a very fast flux increase terminated by the reactivity feedback effect of the negative Doppler coefficient. This self-limitation of the power burst is of primary importance since it limits the power to a tolerable level during the delay time for protective action. Should a continuous control rod assembly withdrawal event occur, the following automatic features of the RPS are available to terminate the transient:

- The source-range high neutron flux reactor trip is actuated when either of two independent source-range channels indicates a neutron flux level above a pre-selected manually adjustable setpoint and provides primary protection below the P6 permissive. This trip function may be manually bypassed when either intermediate range flux channel indicates a flux level above P6. It is automatically reinstated when both intermediate-range channels indicate a flux level below P6.
- The intermediate range high neutron flux reactor trip is actuated when either of two independent intermediate-range channels indicates a flux level above a pre-selected manually adjustable setpoint. This trip function may be manually bypassed when two-out-of-four power-range channels give readings above the P10 permissive (approximately 10 percent of full power) and is automatically reinstated when three-out-of-four channels indicate a power below P10.
- The power-range high neutron flux reactor trip (low setting) is actuated when two-out-of-four power-range channels indicate a power level above approximately 25 percent of full power. This trip function may be manually bypassed when two-out-of-four power-range channels indicate a power level above the P10 permissive and is automatically reinstated when three-out-of-four channels indicate a power level below P10.
- The power-range high neutron flux reactor trip (high setting) is actuated when two-out-of-four power-range channels indicate a power level above a preset setpoint (typically, 109 percent power). This trip function is always active while the reactor is at power.

In addition, control rod stops on high intermediate range flux (one-out-of-two) and high power-range flux (one-out-of-four) serve to cease rod withdrawal and prevent the need to actuate the intermediate-range flux trip and the power-range flux trip, respectively.

14.1.1.2 Method of Analysis

The analysis of the uncontrolled RCCA bank withdrawal from subcritical accident is performed in three stages. First, a spatial neutron kinetics computer code, TWINKLE, is used to calculate the core average nuclear power transient, including the various core feedback effects, that is, Doppler and moderator reactivity. FACTRAN uses the average nuclear power calculated by TWINKLE and performs a fuel rod transient heat transfer calculation to determine the average heat flux and temperature transients. Finally, the peak core-average heat flux calculated by FACTRAN is used in VIPRE for transient DNBR calculations.

In order to give conservative results for a startup accident, the following assumptions are made:

1. Since the magnitude of the power peak reached during the initial part of the transient for any given rate of reactivity insertion is strongly dependent on the DPC, a conservatively low (absolute magnitude) value for the DPC is used (corresponding to a DPD of 1100 pcm).
2. The contribution of the moderator reactivity coefficient is negligible during the initial part of the transient because the heat transfer time constant between the fuel and the moderator is much longer than the neutron flux response time constant. However, after the initial neutron flux peak, the moderator temperature coefficient (MTC) can affect the succeeding rate of power increase. The effect of moderator temperature changes on the rate of nuclear power increase is calculated in TWINKLE based on temperature-dependent moderator cross-sections. The MTC value used in this event analysis is +5 pcm/°F.
3. The analysis assumes the reactor to be at HZP nominal temperature of 547°F. This assumption is more conservative than that of a lower initial system temperature (that is, shutdown conditions). The higher initial system temperature yields a larger fuel-to-water heat transfer coefficient, a larger specific heat of the water and fuel, and a less negative (smaller absolute magnitude) DPC. The less negative DPC reduces the Doppler feedback effect, thereby increasing the neutron flux peak. The high neutron flux peak combined with a high fuel-specific heat and larger heat transfer coefficient yields a larger peak heat flux. The analysis assumes the initial effective multiplication factor (K_{eff}) to be 1.0 since this results in the maximum neutron flux peak.
4. Reactor trip is assumed to be initiated by power-range high neutron flux (low setting). The most adverse combination of instrumentation and setpoint errors is accounted for by assuming a 10 percent increase in the power-range flux trip setpoint (low setting), raising it from the nominal value of 25 percent to a value of 35 percent. Figure 14.1.1-1 shows that the rise in nuclear flux is so rapid that the effect of error in the trip setpoint on the actual time at which the rods are released is negligible. In addition, the total reactor trip reactivity is based on the assumption that the highest worth RCCA is stuck in its fully withdrawn position. Further, the delays for trip signal actuation and control rod assembly release are accounted for in the reactor trip delay time was shown in Section 14.0.4.

5. The maximum positive reactivity insertion rate assumed (100 pcm/in) is a plant-specific value confirmed for each reload cycle and is equal to that for the simultaneous withdrawal of the two sequential control banks having the greatest combined worth at a conservative speed (45 in/min., which corresponds to 72 steps/min.). It should be noted that the assumption of 72 steps/min. as the maximum rod withdrawal speed is contingent upon the performance of refueling interval surveillances as recommended in NSAL-01-001.
6. The DNB analysis assumes the most-limiting axial and radial power shapes possible during the fuel cycle associated with having the two highest combined worth banks in their high worth position.
7. The analysis assumes the initial power level to be below the power level expected for any shutdown condition (10^{-9} fraction of nominal power). The combination of highest reactivity insertion rate and low initial power produces the highest peak heat flux.
8. The analysis is performed at HZP conditions with one reactor coolant pump (RCP) in operation and bounds this accident in lower modes. This assumption also minimizes the resulting DNBR.
9. The accident analysis employs the STDP methodology. Use of the STDP stipulates that the RCS flow rate will be based on the Thermal Design Procedure (TDF) and that the RCS pressure is the nominal pressure minus the uncertainty. Since the event is analyzed from HZP, the steady-state STDP uncertainties on core power and RCS average temperature are not considered in defining the initial conditions.
10. A core flow reduction of 1.1 percent, which addresses the potential reactor coolant flow asymmetry associated with a maximum loop-to-loop steam generator tube plugging (SGTP) imbalance of 10 percent, has been applied.
11. The fuel rod heat transfer calculations performed to determine temperature transients during this event assume a total peaking factor or hot channel factor, F_Q , that is a function of the axial and radial power distributions. The conservatively high value used in this analysis is presented in Table 14.1.1-1.
12. Both Framatome Heavy and Westinghouse 422V+ fuel types, with up to 8 w/o Gadolinia content, were considered in the transient analysis and the most bounding transient results are reported here.

14.1.1.3 Results

Figure 14.1.1-1 through Figure 14.1.1-5 show the transient behavior for a reactivity insertion rate of 75 pcm/sec, with the accident terminated by the reactor trip at 35 percent of nominal power. The rate is greater than that calculated for the two highest worth sequential control banks, with both assumed to be in their highest incremental worth region.

Figure 14.1.1-1 shows the neutron flux transient. The neutron flux overshoots the full power nominal value for a very short period of time. Therefore, the energy release and fuel temperature increase are relatively small. The heat flux response of interest for the DNB considerations is shown in Figure 14.1.1-2. The beneficial effect of the inherent thermal lag in the fuel is evidenced by a peak heat flux of much less than the nominal full power value. Figure 14.1.1-3 through Figure 14.1.1-5 show the transient response of the hot spot fuel centerline, fuel average, and cladding temperatures, respectively. Transient DNBR calculations indicate that the minimum DNBR remains above the safety analysis limit value at all times.

Table 14.1.1-1 presents the assumptions and results of the analysis. Table 14.1.1-2 presents the calculated sequence of events. After reactor trip, the plant returns to a stable condition. The plant may subsequently be cooled down further by following normal shutdown procedures.

14.1.1.4 Conclusions

In the event of an RCCA withdrawal accident from the subcritical condition, the core and the RCS are not adversely affected since the combination of thermal power and coolant temperature result in a DNBR greater than the limit value. Therefore, no fuel or cladding damage is predicted as a result of this transient.

14.1.2 Uncontrolled RCCA Withdrawal at Power

14.1.2.1 Accident Description

The uncontrolled RCCA bank withdrawal at power event is defined as the inadvertent addition of reactivity to the core caused by the withdrawal of RCCA banks when the core is above the no-load condition. The reactivity insertion resulting from the bank (or banks) withdrawal will cause an increase in core nuclear power and subsequent increase in core heat flux. An RCCA bank withdrawal can occur with the reactor subcritical, at HZP, or at power. The uncontrolled RCCA bank at power event is analyzed for Mode 1 (power operation). The uncontrolled RCCA bank withdrawal from a subcritical or low-power condition is considered as an independent event in Section 14.1.1.

The event is simulated by modeling a constant rate of reactivity insertion starting at time zero and continuing until a reactor trip occurs. The analysis assumes a spectrum of possible reactivity insertion rates up to a maximum positive reactivity insertion rate greater than that occurring with the simultaneous withdrawal, at maximum speed, of two sequential RCCA banks having the maximum differential rod worth.

Unless the transient RCS response to the RCCA bank withdrawal event is terminated by manual or automatic action, the power mismatch and resultant temperature rise could eventually result in DNB and/or fuel centerline melt. Additionally, the increase in RCS temperature caused by this event will increase the RCS pressure, and if left unchecked, could challenge the integrity of the RCS pressure boundary or the main steam system (MSS) pressure boundary.

To avert the core damage that might otherwise result from this event, the RPS is designed to automatically terminate any such event before the DNBR falls below the limit value, the fuel rod kW/ft limit is reached, the peak pressures exceed their respective limits, or the pressurizer fills. Depending on the initial power level and the rate of reactivity insertion, the reactor may be tripped and the RCCA withdrawal terminated by any of the following trip signals:

- Power-range high neutron flux
- Positive flux rate
- OTΔT
- OPΔT
- High pressurizer pressure
- High pressurizer water level

In addition to the previously listed reactor trips, there are the following withdrawal blocks for the control rod assemblies:

- High nuclear power (one-out-of-four channels)
- High OPΔT (two-out-of-four channels)
- High OTΔT (two-out-of-four channels)

14.1.2.2 Method of Analysis

The uncontrolled RCCA bank withdrawal at power event is analyzed to show that:

1. the integrity of the core is maintained by the RPS because the DNBR and peak kW/ft remain within the safety analysis limit values and
2. the peak RCS and MS system pressures remain below 110 percent of the corresponding design limits. Of these, the primary concern for this event is assuring that the DNBR limit is met.

The RCCA bank withdrawal at power transient is analyzed with the RETRAN computer program (Reference 16). The program simulates the neutron kinetics, RCS, pressurizer, pressurizer relief and safety valves, pressurizer spray, steam generators, and steam generator relief and safety valves. The program computes pertinent plant variables including temperatures, pressures, and power level.

To obtain a conservative value for the minimum DNBR, the following analysis assumptions are made:

1. This accident is analyzed with the RTDP (Reference 13). Therefore, initial reactor power, pressure, and RCS temperatures are assumed to be at their nominal values. Uncertainties in initial conditions are included in the limit DNBR.
2. Reactivity coefficients - Two cases are analyzed:
 - a. Minimum reactivity feedback - A zero MTC of reactivity (0 pcm/°F) is assumed at full power. For power levels less than or equal to 60 percent power, a positive MTC of reactivity (+5 pcm/°F) is conservatively assumed, corresponding to the beginning of core life. A conservatively small (in absolute magnitude) DPC is used in the analysis.
 - b. Maximum reactivity feedback - A conservatively large positive moderator density coefficient and a large (in absolute magnitude) negative DPC are assumed.
3. The reactor trip on high neutron flux is actuated at a conservative value of 118 percent of nominal full power. The OTΔT trip includes all adverse instrumentation and setpoint errors. The delays for trip actuation are assumed to be the maximum values. No credit was taken for the other expected trip functions.
4. The RCCA trip insertion characteristic is based on the assumption that the highest worth assembly is stuck in its fully withdrawn position.
5. A range of reactivity insertion rates is examined. The maximum positive reactivity insertion rate is greater than that which would be obtained from the simultaneous withdrawal of the two control rod banks having the maximum combined differential rod worth at a conservative speed (45 inches/minute, which corresponds to 72 steps/minute).
6. Power levels of 10 percent, 60 percent and 100 percent of full power are considered.
7. The impact of a full-power RCS vessel T_{avg} window was considered for the uncontrolled RCCA bank withdrawal at power analysis. A conservative calculation modeling the high end of the RCS vessel T_{avg} window was explicitly analyzed.

The effect of RCCA movement on the axial core power distribution is accounted for by causing a decrease in the OTΔT trip setpoint proportional to a decrease in margin to DNB.

14.1.2.3 Results

The limiting results were calculated for the RCCA bank withdrawal at power transient analyzed for the FU/PU implementation. They are given in Table 14.1.2-2.

RCS pressures below the limit of 2750 psia are obtained for reactivity insertion rates less than or equal to 84 pcm/second. This reactivity insertion rate bounds that calculated for the simultaneous withdrawal, at maximum speed, of two sequential RCCA banks having the maximum differential rod worth.

Figure 14.1.2-1 shows the response of nuclear power, pressurizer pressure, RCS vessel T_{avg} , and DNBR to a rapid RCCA withdrawal incident starting from full power. Reactor trip on high neutron flux occurs shortly after the start of the accident. Since this is rapid with respect to the thermal time constants of the plant, small changes in reactor core T_{avg} and pressurizer pressure result, and a large margin to DNB is maintained.

The response of nuclear power, pressurizer pressure, RCS vessel T_{avg} , and DNBR for a slow control rod assembly withdrawal from 100 percent power is shown in Figure 14.1.2-2. Reactor trip on OT Δ T occurs after a longer period of time and the rise in temperature is consequently larger than for a rapid RCCA withdrawal. Again, the minimum DNBR is greater than the limit value.

Figure 14.1.2-3 shows the minimum DNBR as a function of the reactivity insertion rate for the three initial power levels (100 percent, 60 percent, and 10 percent) and for minimum and maximum reactivity feedback. It can be seen that the high neutron flux and OT Δ T trip channels provide protection over the whole range of reactivity insertion rates because the minimum DNBR is never less than the limit value.

In the referenced figures, the shape of the curves of minimum DNBR versus reactivity insertion rate is due both to the reactor core and coolant system transient response and to protection system action in initiating a reactor trip.

Referring to Figure 14.1.2-3 for example, it is noted that:

1. For high reactivity insertion rates (that is, between ~100 pcm/second and ~30 pcm/second) when modeling minimum reactivity feedback, reactor trip is initiated by the high neutron flux trip. The neutron flux level in the core rises rapidly for these insertion rates, while core heat flux and coolant temperature lag behind due to the thermal capacity of the fuel and coolant system fluid. Therefore, the reactor is tripped prior to a significant increase in the heat flux or core water temperature with resultant high minimum DNBRs during the transient. Within this range, as the reactivity insertion rate decreases, core heat flux and coolant temperatures can remain more nearly in equilibrium with the neutron flux. Therefore, minimum DNBR during the transient decreases with decreasing reactivity insertion rate.
2. With a further decrease in the reactivity insertion rate, the OT Δ T and high neutron flux trips become equally effective in terminating the transient (such as, at a reactivity insertion rate of approximately 30 pcm/second).

The OT Δ T reactor trip function initiates a reactor trip when the measured ΔT exceeds an OT Δ T setpoint that is based on the measured vessel T_{avg} and pressurizer pressure. It is important to note, however, that the contribution of RCS vessel T_{avg} to the OT Δ T trip function is lead-lag compensated to compensate for the effect of the thermal capacity of the RCS response to power increases.

For reactivity insertion rates between ~30 pcm/second and ~8 pcm/second, the effectiveness of the OTΔT trip increases (in terms of increased minimum DNBR). This is due to the fact that, with lower insertion rates, the power increase rate is slower, the rate of rise of RCS vessel T_{avg} is slower, and the system lags and delays become less significant.

3. For reactivity insertion rates of ~8 pcm/second and lower, the rise in RCS temperature is sufficiently high so that there is an increased steam relief through the steam generator safety valves prior to trip. This steam relief acts as an additional heat sink on the RCS and sharply slows the increase of the RCS vessel T_{avg} . This causes the OTΔT trip setpoint to be reached later with resulting lower minimum DNBRs.

14.1.2.4 Conclusions

The results for the uncontrolled RCCA bank withdrawal at power transient analyzed show that the high neutron flux and OTΔT trip channels provide adequate protection over the entire range of possible reactivity insertion rates; that is, the minimum calculated DNBR is always greater than the safety analysis limit value. In addition analysis results show that the peak kW/ft is less than the limit and the peak pressures in the RCS and secondary steam system do not exceed 110 percent of their respective design pressures.

Thus, all pertinent criteria are met for the uncontrolled RCCA bank withdrawal at power transient when assuming the FU/PU implementation.

14.1.3 RCCA Misalignment

14.1.3.1 Accident Description

The RCCA misalignment accidents include:

- Dropped full-length RCCAs
- Dropped full-length RCCA banks
- Statically misaligned full-length RCCAs

Each RCCA has a rod position indicator channel that displays the position of the assembly. The displays of assembly positions are grouped for operator convenience. Fully inserted assemblies are further indicated by rod bottom lights. The full-length assemblies are always moved in pre-selected banks and the banks are always moved in the same pre-selected sequence.

Dropped assemblies or assembly banks are detected by:

- Sudden drop in the core power level
- Asymmetric power distribution (as seen on out-of-core neutron detectors or core exit thermocouples)
- Rod bottom light(s)

- Rod deviation alarm (if the plant computer is in operation)
- Rod position indicators

Misaligned assemblies are detected by:

- Asymmetric power distribution (as seen on out-of-core neutron detectors or core exit thermocouples)
- Rod deviation alarm (if the plant computer is in operation)
- Rod position indicators

14.1.3.2 Method of Analysis

14.1.3.2.1 One or More Dropped RCCAs from the Same Group

The LOFTRAN computer code calculates transient system responses for the evaluation of a dropped RCCA event. The code simulates the neutron kinetics, RCS, pressurizer, pressurizer relief and safety valves, pressurizer spray, steam generator, and MSSVs. The code computes pertinent plant variables including temperatures, pressures, and power levels.

Transient RCS statepoints (temperature, pressure, and power) are calculated by LOFTRAN. Nuclear models are used to obtain a hot-channel factor consistent with the primary-system conditions and reactor power. By incorporating the primary conditions from the transient analysis and the hot-channel factor from the nuclear analysis, it is shown that the DNB design basis is met using the VIPRE code. The analysis does not take credit for the power-range negative flux rate reactor trip.

A generic statepoint analysis for this event, which was performed in 1986 to bound a number of two-loop PWRs, was evaluated and determined to be applicable to KNPP for the FU/PU Program. With the generic statepoints being applicable, the effects of the fuel transition and power uprate are accounted for in the DNB analysis, which is performed on a cycle-specific basis.

14.1.3.2.2 Dropped RCCA Bank

A dropped RCCA bank results in a symmetric power change in the core. Assumptions made in the methodology (Reference 17) for the dropped RCCA(s) analysis provide a bounding analysis for the dropped RCCA bank.

A generic statepoint analysis for this event, which was performed in 1986 to bound a number of two-loop PWRs, was evaluated and determined to be applicable to KNPP for the FU/PU Program. With the generic statepoints being applicable, the effects of the fuel transition and power uprate are accounted for in the DNB analysis, which is performed on a cycle-specific basis.

14.1.3.2.3 Statically Misaligned RCCA

Steady-state power distributions are analyzed using the appropriate nuclear physics computer codes. The peaking factors are then used as input to the VIPRE code to calculate the DNBR. The following cases are examined in the analysis assuming the reactor is initially at full power: the worst rod withdrawn with Bank D inserted at the insertion limit, the worst rod dropped with Bank D inserted at the insertion limit, and the worst rod dropped with all other rods out. It is assumed that the incident occurs at the time in the cycle at which the maximum all-rods-out $F_{\Delta H}$ occurs. This assures a conservative $F_{\Delta H}$ for the misaligned RCCA configuration.

14.1.3.3 Results

14.1.3.3.1 One or More Dropped RCCAs from the Same Group

Single or multiple dropped RCCAs within the same group result in a negative reactivity insertion. The core is not adversely affected during this period since power is decreasing rapidly. Either reactivity feedback or control bank withdrawal will re-establish power.

Following a dropped rod event in manual rod control, the plant will establish a new equilibrium condition. Without control system interaction, a new equilibrium is achieved at a reduced power level and reduced primary temperature. Therefore, the automatic rod control mode of operation is the limiting case.

For a dropped RCCA event in the automatic rod control mode, the rod control system detects the drop in power and initiates control bank withdrawal. Power overshoot may occur due to this action by the automatic rod controller, after which the control system will insert the control bank to restore nominal power. Figure 14.1.3-1 through Figure 14.1.3-4 show a typical transient response to a dropped RCCA (or RCCAs) event with the reactor in automatic rod control. In all cases, the minimum DNBR remains above the limit value.

Following plant stabilization, the operator may manually retrieve the RCCA(s) by following approved operating procedures.

14.1.3.3.2 Dropped RCCA Bank

A dropped RCCA bank results in a negative reactivity insertion greater than 500 pcm. The core is not adversely affected during the insertion period, since power is decreasing rapidly. The transient will proceed similar to that described in the previous “One or More Dropped RCCAs from the Same Group” section, but the return to power will be less due to the greater negative reactivity worth of an entire RCCA bank. The power transient for a dropped RCCA bank is symmetric. Following plant stabilization, normal procedures are followed.

14.1.3.3.3 Statically Misaligned RCCA

The most severe RCCA misalignment situations with respect to DNB at significant power levels are associated with cases in which one RCCA is fully inserted with either all rods out or Bank D at the insertion limit, or where Bank D is inserted to the insertion limit and one RCCA is fully withdrawn. Multiple independent alarms, including a bank insertion limit alarm, alert the operator well before the transient approaches the postulated conditions.

The insertion limits in the Technical Specifications may vary from time to time, depending on several limiting criteria. The full-power insertion limits on Control Bank D must be chosen to be above that position which meets the minimum DNBR and peaking factors. The full-power insertion limit is usually dictated by other criteria. Detailed results will vary from cycle to cycle depending on fuel arrangements.

For the RCCA misalignment case with one RCCA fully inserted (with either all rods out or Bank D at the insertion limit), the DNBR does not fall below the limit value. The analysis for this case assumes that the initial reactor power, RCS pressure, and RCS temperature are at nominal values with uncertainties included, and with the increased radial peaking factor associated with the misaligned RCCA.

For the RCCA misalignment case with Bank D inserted to the full-power insertion limit and one RCCA fully withdrawn, the DNBR does not fall below the limit value. The analysis for this case assumes that the initial reactor power, RCS pressure, and RCS temperature are at nominal values with uncertainties included, and with the increased radial peaking factor associated with the misaligned RCCA.

Departure from nucleate boiling does not occur for the RCCA misalignment incident. Therefore, there is no reduction in the ability of the primary coolant to remove heat from the fuel rod. The peak fuel temperature corresponds to a linear heat generation rate based on the radial peaking factor penalty associated with the misaligned RCCA and the design axial power distribution. The resulting linear heat generation rate is well below that which would cause fuel melting.

After identifying an RCCA group misalignment condition, the operator must take action as required by the plant Technical Specifications and operating procedures.

14.1.3.4 Conclusions

The evaluation of the generic statepoints that were obtained using the methodology in Reference 17, for cases of dropped RCCAs or dropped banks encompassing all possible dropped rod worths delineated in Reference 17, concluded that the minimum DNBR remains above the safety analysis limit value. For all cases of any single RCCA fully inserted, or Bank D inserted to the rod insertion limit and any single RCCA in that bank fully withdrawn (static misalignment), the minimum DNBR remains above the limit value. Therefore, the DNB design

criterion is met and the RCCA misalignments do not result in core damage given implementation of the FU/PU Program.

14.1.4 Chemical and Volume Control System Malfunction

14.1.4.1 Accident Description

Reactivity can be added to the core by feeding primary-grade water into the RCS via the reactor makeup portion of the chemical and volume control system. Boron dilution is a manual operation under strict administrative controls, with procedures calling for a limit on the rate and duration of dilution. A boric acid blend system is provided to permit the operator to match the boron concentration of reactor coolant makeup water during normal charging to that in the RCS. The chemical and volume control system is designed to limit, even under various postulated failure modes, the potential rate of dilution to a value which, after indication through alarms and instrumentation, provides the operator sufficient time to correct the situation in a safe and orderly manner.

The opening of the reactor makeup water control valve provides makeup water to the RCS that can dilute the reactor coolant. Inadvertent dilution from this source can be readily terminated by closing the control valve. For makeup water to be added to the RCS at pressure, the charging pumps must be running in addition to the reactor makeup water pumps.

The rate of addition of unborated makeup water to the RCS when it is not at pressure is limited by the capacity of the reactor makeup water pumps and the three charging pumps. Normally, two charging pumps are operated, one in manual and one in automatic control.

In order to dilute, two separate operations are required:

- The operator must switch from the automatic makeup mode to the dilute mode.
- The control switch must be activated.

Omitting either step prevents dilution.

Information on the status of the reactor coolant makeup is continuously available to the operator. Lights are provided on the control board to indicate the operating condition of the pumps in the chemical and volume control system. Alarms are actuated to warn the operator if boric acid or demineralized water flow rates deviate from preset values as a result of system malfunction.

14.1.4.2 Method of Analysis

Boron dilutions during refueling, startup, and power operation are considered in this analysis (boron dilutions during hot standby, hot shutdown, and cold shutdown are not part of the KPS licensing basis).

14.1.4.2.1 Dilution During Refueling

During refueling one residual heat removal pump is running to ensure continuous mixing in the reactor vessel.

The maximum flow rate of unborated water that can be delivered to the RCS during refueling is assumed to be 120 gpm. This value assumes a single failure such that two charging pumps are delivering maximum flow.

A minimum RCS water volume of 1762.0 ft³ is assumed, which is more conservative (that is, smaller) than the volume necessary to fill the reactor vessel up to the mid-plane of the nozzles plus the volume of one residual heat removal system (RHRS) train.

The ratio of the initial boron concentration to the maximum critical boron concentration during refueling is 1.34 (e.g., 2440 ppm / 1820 ppm). The boron concentration of the refueling water corresponding to a shutdown of at least 5 percent $\Delta k/k$ with all control rods in, is verified every reload cycle.

14.1.4.2.2 Dilution During Startup

In this mode, the plant is being taken from one long-term mode of operation, hot standby, to another, power. Typically, the plant is maintained in the startup mode only for the purpose of startup testing at the beginning of each cycle. During this mode of operation, rod control is in manual. All normal actions required to change power level, either up or down, require operator initiation. Conditions assumed for the analysis are:

- Dilution flow is the maximum capacity of two charging pumps, 120 gpm.
- A minimum RCS water volume of 5247.8 ft³ corresponding to the active RCS volume (such as, not including the pressurizer volume) and accounts for 10 percent SGTP.
- The ratio of initial boron concentration to maximum critical boron concentration during startup is 1.125 (e.g., 1800 ppm/1600 ppm). These are plant-specific values that are confirmed to be valid every cycle as part of the reload verification process.

This mode of operation is a transitory operational mode in which the operator intentionally dilutes and withdraws control rods to take the plant critical. During this mode, the plant is in manual rod control with the operator required to maintain a high awareness of the plant status. For a normal approach to criticality, the operator must manually initiate a limited dilution and subsequently manually withdraw the control rods. This process takes several hours. The Technical Specifications require that the operator determine the estimated critical position of the control rods prior to approaching criticality, thus assuring that the reactor does not go critical with the control rods below the insertion limits. Once critical, the power escalation must be sufficiently slow to allow the operator to manually block the source-range reactor trip. Failure to perform this manual action results in a reactor trip and an immediate shutdown of the reactor.

14.1.4.2.3 Dilution at Power

With the unit at power and the RCS at pressure, the dilution rate is limited by the capacity of the charging pumps. A dilution flow rate of 120 gpm is assumed.

A minimum RCS water volume of 5247.8 ft³ corresponding to the active RCS volume (such as, not including the pressurizer volume) accounts for 10 percent SGTP.

The ratio of initial boron concentration to maximum critical boron concentration during full power is 1.1125 (e.g., 1780 ppm/1600 ppm). These are plant-specific values that are confirmed to be valid every cycle as part of the reload verification process.

With the reactor in automatic control, indication to the operator of the postulated dilution accident is provided by the rod insertion limits alarms (low and lo-lo setpoints) as the control rods are automatically inserted to compensate for the reactivity increase. The operator isolates the reactor makeup water source and initiates reboration.

If the reactor is in the manual control mode, the initial indication of a dilution accident is provided to the operator via nuclear power and T_{avg} indicators. Since the plant is under manual control, the operator is expected to follow these parameters closely and to react properly by further inserting the rods. In this fashion, manual control resembles the case with automatic control, with the operator taking the necessary steps to borate no later than when the manual insertion of the rods reaches the rod insertion limits.

If, however, the operator fails to take note of this slow change in reactivity, the following three alarms alert the operator to the dilution accident:

- $T_{avg} - T_{ref}$ deviation alarm
- High flux, rod stop, and alarm
- OTΔT rod stop and turbine runback alarm

If the operator fails to take appropriate action on these alarms, the reactor trips on OTΔT. Dilution is indicated by constantly rising nuclear power and temperature and the absence of changes in rod position. Moreover, intermediate-range and source-range nuclear instrumentation system are available after the trip.

Once dilution has been identified, the operator terminates the flow of non-borated water. Following isolation of the reactor makeup water, the operator will re-borate the RCS. The manner in which the boration is performed has no impact on the USAR analysis.

14.1.4.2.4 Operator Action Time Requirements

Analyses to determine the extent of fuel cladding damage and the overpressurization of the RCS are not done for this event. Instead, a calculation is performed to determine the amount of time available for operator action prior to the loss of the plant shutdown margin due to the dilution. Fifteen minutes for the at-power and startup conditions and thirty minutes for the

refueling condition of plant operation from the initiation of the event are the criteria outlined in the earliest Standard Review Plan (SRP), Section 15.4.6 (September 1975). If these operator action times are met, it can be concluded that the fuel cladding damage and RCS overpressurization criteria are also satisfied.

14.1.4.3 Results

14.1.4.3.1 Dilution During Refueling

For dilution during refueling, the minimum time required for the shutdown margin to be lost and the reactor to become critical is 31.60 minutes.

14.1.4.3.2 For Dilution During Startup

For dilution during startup, the minimum time required for the shutdown margin to be lost and the reactor to become critical is 28.75 minutes.

14.1.4.3.3 For Dilution During Full-Power Operation

With the reactor in automatic control at full power, the power and temperature increase from boron dilution results in the insertion of the RCCAs and decrease in shutdown margin. Continuation of dilution and RCCA insertion would cause the assemblies to reach the minimum limit of the rod insertion monitor. Before reaching this point, however, two alarms are actuated to warn the operator of the accident condition. The first of these, the low insertion limit alarm, alerts the operator to initiate normal boration. The other, the lo-lo insertion limit alarm, alerts the operator to follow emergency boration procedures. The low alarm is set sufficiently above the lo-lo alarm to allow normal boration without the need for emergency procedures. If dilution continues after reaching the lo-lo alarm, it takes approximately 25.06 minutes before the total shutdown margin is lost due to dilution. Adequate time, therefore, is available following the alarms for the operator to determine the cause, isolate the reactor makeup water source, and initiate re-boration.

With the reactor in manual control, if no operator action is taken, the power and temperature rise causes the reactor to reach the OTΔT trip setpoint. The boron dilution accident in this case is essentially identical to an RCCA withdrawal accident at power. Prior to the OTΔT trip, an OTΔT alarm and turbine runback would be actuated. There is time available (~22.68 minutes) after a reactor trip for the operator to determine the cause of dilution, isolate the reactor makeup water source, and initiate re-boration before the reactor can return to criticality.

14.1.4.4 Conclusion

The time sequence of events is provided in Table 14.1.4-1. The boron dilution analyses at refueling, startup, and full-power conditions show the acceptability of the power uprating.

14.1.5 Startup of an Inactive Reactor Coolant Loop

If the plant were to operate with one reactor coolant pump (RCP) out-of-service, there would be reverse flow through the inactive loop due to the pressure difference across the reactor vessel and because there are no isolation valves or check valves in the reactor coolant loops. The cold-leg temperature in the inactive loop is identical to the cold-leg temperature of the active loop (the reactor core inlet temperature). If the reactor is operated at power with an inactive loop, and assuming that the secondary side of the steam generator in the inactive loop is not isolated, there is a temperature drop across the steam generator in the inactive loop. Therefore, with the reverse flow, the hot-leg temperature of the inactive loop would be lower than the reactor core inlet temperature.

The KPS TS limits the reactor power to < 2 percent rated thermal power when only one RCP is in operation. At this power level, the hot-leg temperature of the inactive loop would already be very close to the cold-leg inlet temperature. For this reason, no analysis is needed to show that the DNBR limit is satisfied for this event at KPS. The KPS TS will prevent unacceptable results from a potential transient due to startup of an inactive reactor coolant loop. Therefore, an analysis of this event is unnecessary.

Conclusions

The startup of an inactive reactor coolant loop event results in an increase in reactor vessel flow while the reactor is maintained at a power level that is non-limiting with respect to minimum DNBR (less than 2 percent of nominal). No analysis is required to show that the DNBR limit is satisfied for this event.

14.1.6 Excessive Heat Removal Due to Feedwater System Malfunctions

A change in steam generator feedwater conditions that results in an increase in feedwater flow or a decrease in feedwater temperature could result in excessive heat removal from the plant primary coolant system. Such changes in feedwater flow or feedwater temperature are a result of a failure of a feedwater control valve or feedwater bypass valve, failure in the feedwater control system, or operator error.

The occurrence of these failures that result in an excessive heat removal from the plant primary coolant system cause the primary-side temperature and pressure to decrease significantly. The existence of a negative moderator and fuel temperature reactivity coefficients, and the actions initiated by the reactor rod control system can cause core reactivity to rise, as the primary-side temperature decreases. In the absence of the RPS reactor trip or other protective action, this increase in core power, coupled with the decrease in primary-side pressure, can challenge the core thermal limits.

14.1.6.1 Accident Description

14.1.6.1.1 Feedwater Temperature Reduction

An extreme example of excessive heat removal from the RCS is the transient associated with the accidental opening of the feedwater bypass valve, which diverts flow around the low-pressure feedwater heaters. The function of this valve is to maintain net positive suction head on the main feedwater pump in the event that the heater drain pump flow is lost; such as, following a large-load reduction. In the event of an accidental opening of the feedwater bypass valve, there is a sudden reduction in feedwater inlet temperature to the steam generators. This increased subcooling would create a greater load demand on the RCS due to the increased heat transfer in the steam generator.

With the plant at no-load conditions, the addition of cold feedwater may cause a decrease in RCS temperature and thus a reactivity insertion due to the effects of the negative moderator temperature coefficient. However, the rate of energy change is reduced as load and feedwater flow decrease, so that the transient is less severe than the full-power case.

The net effect on the RCS due to a reduction in feedwater temperature is similar to the effect of increasing secondary steam flow; that is, the reactor will reach a new equilibrium condition at a power level corresponding to the new steam generator ΔT . The overpower/overtemperature protection (high neutron flux, OT ΔT , and OP ΔT trips) prevent any power increase that could lead to a DNBR lower than the safety analysis limit value.

14.1.6.1.2 Feedwater Flow Increase

Another example of excessive heat removal from the RCS is a common-mode failure in the feedwater control system that leads to the accidental opening of the feedwater regulating valves (FW-7A and FW-7B) to both steam generators. Valves FW-7A and FW-7B could fail open due to a high output signal to the feedwater control system.

This results in the valves stepping open 20 percent from their current position followed by a 20 percent step open every 5 minutes after that until full open. Accidental opening of the feedwater regulating valves results in an increase of feedwater flow to both steam generators, causing excessive heat removal from the RCS. At power, excess feedwater flow causes a greater load demand on the primary side due to increased subcooling in the steam generator. With the plant at zero-power conditions, the addition of relatively cold feedwater may cause a decrease in primary-side temperature, and, therefore, a reactivity insertion due to the effects of the negative moderator temperature coefficient. The resultant decrease in the average temperature of the core causes an increase in core power due to moderator and control system feedback. This transient is attenuated by the thermal capacity of the primary and secondary sides. If the increase in reactor power is large enough, the primary RPS trip functions (such as high neutron flux, OT ΔT , or OP ΔT) will prevent any power increase that can lead to a DNBR less than the safety analysis limit value. The RPS trip functions may not actuate if the increase in power is not large enough.

Continuous addition of cold feedwater after a reactor trip is prevented since the reduction of RCS temperature, pressure, and pressurizer level leads to the actuation of Safety Injection (SI) on low pressurizer pressure. The SI signal trips the main feedwater pumps, closes the feedwater pump discharge valves, and closes the main feedwater control valves.

14.1.6.2 Method of Analysis

14.1.6.2.1 Feedwater Temperature Reduction

The reduction in feedwater temperature is determined by computing conditions at the feedwater pump inlet following the opening of the heater bypass valve. These feedwater conditions are then used to recalculate a heat balance through the high-pressure heaters. This heat balance gives the new feedwater conditions at the steam generator inlet. The following assumptions are made:

1. Initial power level of 1780 MWt
2. Low-pressure heater bypass valve opens, resulting in condensate flow splitting between the bypass line and the low pressure heaters; the flow through each path is proportional to the pressure drops

An evaluation method was applied that demonstrates the decreased enthalpy caused by the feedwater temperature reduction is bounded by an equivalent enthalpy reduction that results from an excessive load increase incident (Section 14.1.7). No explicit analysis is performed.

14.1.6.2.2 Feedwater Flow Increase

The feedwater malfunction analysis is performed to demonstrate that the DNB design basis is satisfied. This is accomplished by showing that the calculated minimum DNBR is greater than the safety analysis limit DNBR. The overall analysis process is described as follows.

The feedwater system malfunction transient is analyzed using the RETRAN code. The RETRAN computer code is a flexible, transient thermal-hydraulic digital computer code, that has been reviewed and approved by the U.S. NRC for PWR licensing applications (Reference 16). The main features of the program include a point kinetics and one-dimensional kinetics model, one-dimensional homogeneous equilibrium mixture thermal-hydraulic model, control system models, and two-phase natural convection heat transfer correlations. The results from the RETRAN computer code are used to determine if the DNB safety analysis limits for the excessive heat removal due to feedwater malfunction event are met.

Feedwater system failures including the accidental opening of the feedwater regulating valves have the potential of allowing increased feedwater flow to each steam generator that will result in excessive heat removal from the RCS. Therefore, it is assumed that the feedwater control valves fail in the fully open position allowing the maximum feedwater flow to both steam generators. Cases with and without automatic rod control initiated at hot full-power (HFP)

conditions were considered. Also addressed is the initiation of a feedwater malfunction event from a HZP condition.

The following assumptions are made for the analysis of the feedwater malfunction event involving the accidental opening of the feedwater regulating valves:

1. The plant is operating at full-power (and no-load conditions for the HZP case) conditions with the initial reactor power, pressure, and RCS average temperatures assumed to be at the nominal values.
2. Uncertainties in initial conditions are included in the DNBR limit calculated using the RTDP methodology (Reference 13), where applicable (full-power cases).
3. The feedwater temperature of 437.1°F for the full-power cases is consistent with normal plant conditions. The no-load feedwater temperature of 198.0°F is assumed in the zero-power case.
4. The excessive feedwater flow event assumes accidental opening of the feedwater control valves with the reactor at full power with automatic and manual rod control, and zero power while modeling post reactor trip conditions with minimum shutdown margin. The feedwater flow malfunction results in a step increase to 150 percent of the nominal full-power feedwater flow to both steam generators.
5. Maximum (end of life) reactivity feedback conditions with a minimum Doppler-only power defect is conservatively assumed.
6. The heat capacity of the RCS metal and steam generator shell are ignored, thereby maximizing the temperature reduction of the RCS coolant.
7. The feedwater flow resulting from a fully open control valve is terminated by the steam generator hi-hi water level signal that closes all main feedwater control and feedwater control-bypass valves, trips the main feedwater pumps, closes all feedwater pump discharge valves, and trips the turbine generator.

The RPS features, including power-range high neutron flux, OPΔT, and turbine trip on hi-hi steam generator water level, are available to provide mitigation of the feedwater system malfunction transient.

14.1.6.3 Results

14.1.6.3.1 Feedwater Temperature Reduction

The opening of a low-pressure heater bypass valve causes a reduction in feedwater temperature that increases the thermal load on the primary system. The reduction in feedwater temperature is less than 33°F, resulting in an increase in heat load on the primary system of less than 10 percent of full power. The reduction in feedwater temperature due to a 10 percent step load increase is greater than 33°F. The increased thermal load, due to the opening of the low-pressure heater bypass valve, thus results in a transient very similar, but of reduced

magnitude, to the 10 percent step load increase incident described in Section 14.1.7. No transient results are presented, as no explicit analysis is performed.

14.1.6.3.2 Feedwater Flow Increase

The results of the analyses demonstrate that both the HFP cases and zero-power case meet the applicable DNBR acceptance criterion.

The most limiting case is the excessive feedwater flow from a full-power initial condition with automatic rod control. This case gives the largest reactivity feedback and results in the greatest power increase. A turbine trip, which results in a reactor trip, is actuated when the steam generator water level in either steam generator reaches the hi-hi water level setpoint. Assuming the reactor to be in manual rod control results in a slightly less severe transient. The rod control system is not required to function for this event. However, assuming that the rod control system is operable yields a slightly more limiting transient.

The excessive feedwater flow from a zero-power condition models a HZP post-trip condition (that is, HZP stuck rod coefficients, minimum shutdown margin) with maximum reactivity feedback conditions (end of life). The limiting HZP feedwater malfunction conditions were analyzed and confirmed that the calculated minimum DNBR is above the safety analysis DNBR limit. Therefore, the applicable DNBR acceptance criterion is met.

For each excessive feedwater flow case, continuous addition of cold feedwater is prevented by automatic closure of all feedwater control valves, closure of all feedwater bypass valves, a trip of the feedwater pumps, and a turbine trip on hi-hi steam generator water level. In addition, the feedwater discharge isolation valves will automatically close upon receipt of the feedwater pump trip signal.

Following turbine trip, the reactor will automatically be tripped, either directly due to the turbine trip or due to one of the reactor trip signals discussed in Section 14.1.9 (Loss of External Electrical Load). If the reactor was in automatic rod control, the control rods would be inserted at the maximum rate following the turbine trip, and the resulting transient would not be limiting in terms of peak RCS or MSS pressure.

Table 14.1.6-1 shows the time sequence of events for the HFP feedwater malfunction transients analyzed at full-power initial conditions assuming manual and automatic rod control. Table 14.1.6-2 shows the time sequence of events for the HZP feedwater malfunction transient. Figure 14.1.6-1 through Figure 14.1.6-5 show transient responses for various system parameters during a feedwater system malfunction initiated from HFP conditions without automatic rod control (manual control). Figure 14.1.6-6 through Figure 14.1.6-10 show transient responses for various system parameters during a feedwater system malfunction initiated from HFP conditions with automatic rod control.

14.1.6.4 Conclusions

Feedwater system malfunction transients involving a reduction in feedwater temperature or an increase in feedwater flow rate have been analyzed or evaluated. These transients show an increase in reactor power due to the excessive heat removal in the steam generators. With respect to the feedwater temperature reduction transient (accidental opening of the feedwater bypass valve), it was determined to be less severe than the excessive load increase incident (see USAR Section 14.1.7); no explicit analysis is performed. Based on results presented in Section 14.1.7, the applicable acceptance criteria for the feedwater temperature reduction transient have been met. Analyses of the accidental opening of the feedwater regulating valves were performed from a full-power initial condition with and without automatic rod control, and from a zero-power initial condition. It has been demonstrated that considerable margin to the safety analysis acceptance criteria exists throughout the transient. Therefore, the DNB design basis is satisfied. Hence, no fuel damage is predicted.

14.1.7 Excessive Load Increase Incident

14.1.7.1 Accident Description

An excessive load increase incident is defined as a rapid increase in steam generator steam flow that causes a power mismatch between the reactor core power and the steam generator load demand. The Reactor Control System is designed to accommodate a 10 percent step load increase or a 5 percent per minute ramp load increase (without a reactor trip) in the range of 15 to 95 percent of full power. Any loading rate in excess of these values may cause a reactor trip actuated by the RPS. If the load increase exceeds the capability of the Reactor Control System; the transient is terminated in sufficient time to prevent the DNBR from being reduced below the MDNBR limit. An excessive load increase incident could result from either an administrative violation such as excessive loading by the operator or an equipment malfunction in the steam dump control or turbine speed control.

For excessive loading by the operator or by system demand, the turbine load limiter keeps maximum turbine load from exceeding 100 percent rated load.

During power operation, steam dump to the condenser is controlled by reactor coolant condition signals; i.e., high reactor coolant temperature indicates a need for steam dump. A single controller malfunction does not cause steam dump; an interlock is provided which blocks the opening of the valves unless a large turbine load decrease or a turbine trip has occurred.

The possible consequence of this accident (assuming no protective functions) is DNB with subsequent fuel damage. Note that the accident is typically characterized by an approach of parameter values to the protections setpoints without the setpoints actually being reached.

Load increases caused by a hypothetical steam-line break are analyzed in Section 14.2.5.

14.1.7.2 Method of Analysis

The excessive load increase incident is analyzed to show that:

- The integrity of the core is maintained typically without the RPS being actuated (that is, the minimum DNBR remains above the safety analysis limit value).
- The peak RCS and MSS pressures remain below 110 percent of the design values.
- The pressurizer does not become water-solid.

Of these, the primary concerns are DNB and ensuring that the DNBR limit is met.

However, as discussed earlier, this transient does not typically result in the actuation of any RPS function (that is, no reactor trip). The effect of this transient on the minimum DNBR was evaluated by applying conservatively large deviations on the initial conditions for power, average coolant temperature, and pressurizer pressure at the normal full-power operating conditions in order to generate a limiting set of statepoints. These deviations bound the variations that could occur as a result of an excessive load increase incident and are only applied in the direction that had the most adverse impact on DNBR (increased power and coolant temperature, and decreased pressure). The reactor condition statepoints (power, temperature and pressure) were then compared to the conditions corresponding to operation at the DNB safety analysis limit (safety limit curves of Figure 14.0-2).

The results of the evaluation performed to support the KNPP FU/PU Program showed that the minimum DNBR would remain above the safety analysis limit value. Therefore, it was determined that a more detailed analysis using the RETRAN code was not necessary for implementation of the FU/PU Program.

14.1.7.3 Conclusions

In the event of an excessive load increase incident, (that is, a 10 percent step load increase), the minimum DNBR remains above the safety analysis limit value, thereby precluding fuel or cladding damage. Peak RCS and MSS pressures do not challenge applicable pressure limits.

The remaining discussion presented below pertains to analysis that no longer represents the current licensing basis for KNPP but is included for historical purposes.

14.1.7.4 Historical Method of Analysis

Four cases are analyzed to demonstrate the plant behavior for a 20 percent step increase from rated load. The first two cases are for a manually controlled reactor at beginning of cycle (BOC, $\alpha_m = \text{zero } \Delta k/k/^\circ\text{F}$) and end of cycle (EOC, $\alpha_m = -4.0\text{E}-4 \Delta k/k/^\circ\text{F}$) conditions (α_m is the moderator reactivity coefficient). Beginning of cycle represents a condition when the plant has the smallest moderator temperature coefficient of reactivity and, therefore, the least inherent transient capability. Two cases are analyzed for an automatic control situation at BOC and EOC conditions with control rods initially inserted to the power dependent insertion limits. A conservative limit on the turbine valve opening was assumed corresponding to 1.2 times nominal steam flow at nominal

steam pressure. Initial pressurizer pressure, reactor coolant average temperature and power are assumed at extreme values consistent with steady state, full-power operation, allowing for calibration and instrument errors. This results in the minimum margin to core DNB at the start of the transient. The analyses are performed using a detailed digital simulation of the plant including core kinetics, RCS, and the Steam and Feedwater Systems.

14.1.7.5 Historical Results

Figure 14.1.7-1 through Figure 14.1.7-8 illustrate the transient with the reactor in the manual control mode. As expected, the EOC case has a much larger increase in reactor power and ΔT due to the moderator feedback. Both of the manual control cases demonstrate adequate MDNBR margin.

Figure 14.1.7-9 through Figure 14.1.7-18 illustrate the transient assuming the reactor is in automatic control. In automatic control the reactor power transient is greater than for the corresponding case in manual control. The automatic control cases still show adequate margin to the MDNBR limit.

The following table shows the comparison of the important calculated safety parameters to their respective acceptance criteria (Calculated Value/Acceptance Criterion):

Excessive Load Increase	MDNBR	RCS Pressure (psia)	MSS Pressure (psia)
BOC Manual Control	1.704/1.14	2200/2750	763/1210
BOC Auto Control	1.527/1.14	2201/2750	763/1210
EOC Manual Control	1.544/1.14	2200/2750	763/1210
EOC Auto Control	1.502/1.14	2200/2750	884/1210

14.1.7.6 Historical Conclusions

The four cases analyzed show a considerable margin to the limiting MDNBR. It is concluded that reactor integrity is maintained throughout lifetime for the excessive load increase incident.

14.1.8 Loss of Reactor Coolant Flow

The loss of reactor coolant flow events are categorized as follows in the KPS USAR:

- Flow coastdown accidents
- Locked-rotor accident

The first category includes the partial and complete loss of reactor coolant flow, and the reactor coolant pump underfrequency events. The second category includes the hypothetical event that addresses an instantaneous seizure of an RCP rotor.

14.1.8.1 Partial Loss of Reactor Coolant Flow

14.1.8.1.1 Accident Description

The partial loss-of-coolant-flow accident can result from a mechanical or electrical failure in an RCP, or from a fault in the power supply to the RCP. If the reactor is at power at the time of the accident, the immediate effect of loss-of-coolant flow is a rapid increase in the coolant temperature. This increase could result in DNB with subsequent fuel damage if the reactor is not tripped promptly.

Normal power for the pumps is supplied through individual buses connected to the generator and the offsite power system. When a generator trip occurs, the buses continue to be supplied from external power lines, and the pumps continue to supply coolant to the core.

The necessary protection against a partial loss-of-coolant-flow accident is provided by the low primary coolant flow reactor trip signal, which is actuated in any reactor coolant loop by two-out-of-three low flow signals. Above 10-percent nuclear instrumentation system (NIS) power (Permissive 8), low flow in either loop will actuate a reactor trip. Above 10 percent NIS and 10 percent turbine power (Permissive 7), low flow in both loops will actuate a reactor trip.

14.1.8.1.2 Method of Analysis

The loss of an RCP with both loops in operation event is analyzed to show that: 1) the integrity of the core is maintained as the DNBR remains above the safety analysis limit value, and 2) the peak RCS and secondary system pressures remain below the design limits. Of these, the primary concerns are DNB and assuring that the DNBR limit is met.

The loss of an RCP event is analyzed with two computer codes. First, the RETRAN computer code is used to calculate the loop and core flow during the transient, the time of reactor trip based on the calculated flows, the nuclear power transient, and the primary-system pressure and temperature transients. The VIPRE computer code is then used to calculate the hot-channel heat flux transient and DNBR, based on the nuclear power and RCS temperature (enthalpy), pressure, and flow from RETRAN. The DNBR transients presented represent the minimum of the typical or thimble cell.

This event is analyzed with the RTDP. Initial reactor power, pressurizer pressure, and RCS temperature are assumed to be at their nominal values. Minimum measured flow is also assumed. A conservatively large absolute value of the Doppler-only power coefficient is used, along with the most-positive MTC limit for full-power operation (0 pcm/°F). These assumptions maximize the core power during the initial part of the transient when the minimum DNBR is reached.

A limiting EOC DNB axial power shape is assumed in VIPRE for the calculation of DNBR. This shape provides the most limiting minimum DNBR for the loss-of-flow events.

A conservatively low trip reactivity value (3.5-percent $\Delta\rho$) is used to minimize the effect of rod insertion following reactor trip and maximize the heat flux statepoint used in the DNBR evaluation for this event. This value is based on the assumption that the highest worth RCCA is stuck in its fully withdrawn position. A conservative trip reactivity worth versus rod position was modeled in addition to a conservative rod drop time (1.8 seconds to dashpot). The trip reactivity versus rod position curve is confirmed to be valid as part of the Reload Safety Analysis Checklist (RSAC) verification process.

The flow coastdown analysis is based on a momentum balance around each reactor coolant loop and across the reactor core. This momentum balance is combined with the continuity equation, a pump momentum balance, and the pump characteristics. Also, it is based on conservative estimates of system pressure losses.

A maximum, uniform, SGTP level of 10 percent was assumed in the RETRAN analysis. However, a core flow reduction of 1.1 percent, which addresses the potential reactor coolant flow asymmetry associated with a maximum loop-to-loop SGTP imbalance of 10 percent, was applied.

14.1.8.1.3 Results

Figure 14.1.8-1 through Figure 14.1.8-8 illustrate the transient response for the loss of an RCP with both loops in operation. The minimum DNBR is 1.646/1.666 (thimble/typical), which occurred at 3.5 seconds (DNBR limit: 1.34/1.34 (thimble/typical)).

The calculated sequence of events table is shown in Table 14.1.8-1. This transient trips on a low primary reactor coolant flow trip setpoint, which is assumed to be 86.5 percent of loop flow. Following reactor trip, the affected RCP will continue to coast down, and the core flow will reach a new equilibrium value corresponding to the remaining pump still in operation. With the reactor tripped, a stable plant condition will eventually be attained. Normal plant shutdown may then proceed.

14.1.8.1.4 Conclusions

The analysis performed has demonstrated that for the partial loss-of-coolant event, the DNBR does not decrease below the limit value at any time during the transient. Therefore, no fuel or cladding damage is predicted and all applicable acceptance criteria are met.

14.1.8.2 Complete Loss of Forced Reactor Coolant Flow

14.1.8.2.1 Accident Description

A complete loss of forced reactor coolant flow may result from a simultaneous loss of electrical supplies to all RCPs. If the reactor is at power at the time of the accident, the immediate effect of loss-of-coolant flow is a rapid increase in the coolant temperature. This increase could result in DNB with subsequent fuel damage if the reactor were not tripped promptly.

Normal power for the RCPs is supplied through buses from a transformer connected to the generator and the offsite power system. Each pump is on a separate bus. When a generator trip occurs, the buses continue to be supplied from external power lines and the pumps continue to supply coolant flow to the core.

The following signals provide the necessary protection against a complete loss-of-flow accident:

- Reactor coolant pump power supply undervoltage reactor trip
- Low reactor coolant loop flow reactor trip
- Pump circuit breaker opening, (RCP supply underfrequency opens pump circuit breaker, which trips the reactor).

The reactor trip on RCP undervoltage is provided to protect against conditions that can cause a loss of voltage to all RCPs; that is, station blackout. This function is blocked below approximately 10 percent NIS and 10 percent turbine power (Permissive 7).

The reactor trip on low primary coolant flow is provided to protect against loss-of-flow conditions that affect one or both reactor coolant loops. This function is generated by two-out-of-three low flow signals per reactor coolant loop. Above 10 percent NIS power (Permissive 8), low flow in either loop will actuate a reactor trip. Above 10 percent NIS and 10 percent turbine power (Permissive 7), low flow in both loops will actuate a reactor trip.

The reactor trip on RCP underfrequency (pump circuit breaker opening) is available to trip the reactor for an underfrequency condition, resulting from frequency disturbances on the power grid. However, the analysis conservatively assumes that this function is not available to provide a reactor trip. Therefore, the low primary coolant flow reactor trip function is assumed to provide primary protection against an underfrequency event.

This event is conservatively analyzed to the following acceptance criteria:

- Pressure in the RCS and MSS should be maintained below 110 percent of the design values.
- Fuel cladding integrity shall be maintained by ensuring that the minimum DNBR remains above the limit value.
- An incident of moderate frequency should not generate a more serious plant condition without other faults occurring independently.

14.1.8.2.2 Method of Analysis

The complete loss-of-flow transient is analyzed as a loss of both RCPs with both loops in operation. The event is analyzed to show that the integrity of the core is maintained as the DNBR remains above the safety analysis limit value. The loss-of-flow events do result in an increase in RCS and MSS pressures, but these pressure increases are generally not severe enough to challenge the integrity of the RCS and MSS. Since the maximum RCS and MSS pressures do not exceed 110 percent of their respective design pressures for the loss-of-load event, it is concluded that the maximum RCS and MSS pressures will also remain below 110 percent of their respective design pressures for the loss-of-flow events.

Two cases are analyzed:

- Complete loss-of-flow transient due to a loss of power to both pumps
- Complete loss-of-flow transient due to an underfrequency condition

The underfrequency case represents the worst credible coolant flow loss. A conservative, constant frequency decay rate of 5 Hz/sec is assumed. Reference 2 determined that this is the maximum credible frequency decay rate that could occur on a typical electrical grid. Analysis of the Wisconsin-Upper Michigan transmission system indicates that the worst-case frequency decay rate is to be approximately 2 Hz/sec. (See Reference 3.) Therefore, 5 Hz/sec is a very conservative decay rate. In addition, the assumption of a constant rate is conservative, since Reference 2 also shows that the expected grid frequency decay rate actually decreases during the transient.

Prior to the opening of the RXCP breaker, the RXCP speed is assumed to be directly proportional to the power supply frequency. As discussed in Reference 4, this is a conservative assumption, since the speed coastdown will lag the frequency coastdown due to the effects of pump inertia and induction motor slip. During steady state operation the pump motor speed is below the synchronous speed because of induction motor slip. After the frequency decay starts, the deceleration of the pump-motor-flywheel combination provides a positive driving torque to the pump so that the required electrical torque decreases. The reduction in electrical torque reduces the induction motor slip, thus resulting in a higher speed than that assumed in the analysis. The degree of conservatism varies directly with the assumed decay rate because the inertia torque increases directly with the decay rate. At 5 Hz/sec the expected speed is

approximately 1.2 percent higher than the analysis value. For this case, flow decreases due to a constant frequency decay rate of 5 Hz/sec. Reactor trip is then caused by a low-flow signal.

The transients are analyzed with two computer codes. First, the RETRAN computer code is used to calculate the loop and core flow during the transient, the time of reactor trip based on the calculated flows, the nuclear power transient, and the primary-system pressure and temperature transients. The VIPRE computer code is then used to calculate the heat flux and DNBR transients based on the nuclear power and RCS temperature (enthalpy), pressure, and flow from RETRAN. The DNBR transients presented represent the minimum of the typical or thimble cell for the fuel.

This event is analyzed with RTDP. Initial reactor power, pressurizer pressure and RCS temperature are assumed to be at their nominal values. Minimum measured flow is also assumed. A conservatively large absolute value of the Doppler-only power coefficient is used, along with the most-positive MTC limit for full-power operation (0 pcm/°F). These assumptions maximize the core power during the initial part of the transient when the minimum DNBR is reached.

A limiting EOC DNB axial power shape is assumed in VIPRE for the calculation of DNBR. This shape provides the most limiting minimum DNBR for the loss-of-flow events.

A conservatively low trip reactivity value (3.5 percent $\Delta\rho$) is used to minimize the effect of rod insertion following reactor trip and maximize the heat flux statepoint used in the DNBR evaluation for this event. This value is based on the assumption that the highest worth RCCA is stuck in its fully withdrawn position. A conservative trip reactivity worth versus rod position was modeled in addition to a conservative rod drop time (1.8 seconds to dashpot). The trip reactivity versus rod position curve is confirmed to be valid as part of the RSAC verification process.

The flow coastdown analysis is based on a momentum balance around each reactor coolant loop and across the reactor core. This momentum balance is combined with the continuity equation, a pump momentum balance, and the pump characteristics. Also, it is based on conservative estimates of system pressure losses.

A maximum, uniform, SGTP level of 10 percent was assumed in the RETRAN analysis. RCS loop flow asymmetry due to a loop-to-loop SGTP imbalance does not need to be considered for transients in which both reactor coolant pumps experience a coastdown.

14.1.8.2.3 Results

Figure 14.1.8-9 through Figure 14.1.8-16 illustrate the transient response for the complete loss of flow associated with a loss of power to both RCPs with both loops in operation. The minimum DNBR is 1.386/1.386 (thimble/typical) which occurred at 4.0 seconds (DNBR limit: 1.34/1.34 (thimble/typical)).

Figure 14.1.8-17 through Figure 14.1.8-24 illustrate the transient response for the complete loss-of-flow (underfrequency) case. Both RCPs decelerate at a constant rate until a reactor trip on low flow is initiated. The minimum DNBR is 1.423/1.420 (thimble/typical), which occurred

at 4.15 seconds (DNBR limit: 1.34/1.34 (thimble/typical)). These results are based on a cycle-specific worst-power shape that was utilized to obtain margin between the safety analysis DNBR limit and the design DNBR limit.

The calculated sequence of events for both complete loss-of-flow cases are shown on Table 14.1.8-2. Following reactor trip, the RCPs will continue to coast down, and natural circulation flow will eventually be established. With the reactor tripped, a stable plant condition will eventually be attained. Normal plant shutdown may then proceed.

14.1.8.2.4 Conclusions

The analysis performed has demonstrated that for the complete loss-of-flow event, the DNBR does not decrease below the limit value at any time during the transient. Therefore, no fuel or cladding damage is predicted and all applicable acceptance criteria are met.

14.1.8.3 Locked-Rotor Accident

14.1.8.3.1 Accident Description

The postulated locked-rotor accident is an instantaneous seizure of an RCP rotor. Flow through the affected reactor coolant loop is rapidly reduced, leading to an initiation of a reactor trip on a low-flow signal. The consequences of a postulated pump shaft break accident are similar to the locked-rotor event. With a broken shaft, the impeller is free to spin, as opposed to it being fixed in position during the locked-rotor event. Therefore, the initial rate of reduction in core flow is greater during a locked-rotor event than in a pump shaft break event because the fixed shaft causes greater resistance than a free-spinning impeller early in the transient, when flow through the affected loop is in the positive direction. As the transient continues, the flow direction through the affected loop is reversed. If the impeller is able to spin free, the flow to the core will be less than that available with a fixed-shaft during periods of reverse flow in the affected loop. Because peak pressure, cladding temperature, and DNB occur very early in the transient, the reduction in core flow during the period of forward flow in the affected loop dominates the severity of the results. Consequently, the bounding results for the locked-rotor transients also are applicable to the RCP shaft break.

After the locked rotor, reactor trip is initiated on an RCS low-flow signal. At the time of reactor trip, the unaffected RCP is assumed to lose power and coast down freely.

Following initiation of the reactor trip, heat stored in the fuel rods continues to be transferred to the coolant causing the coolant to expand. At the same time, heat transfer to the shell side of the steam generators is reduced. This is because, first, the reduced flow results in a decreased tube-side film coefficient; and then because the reactor coolant in the tubes cools down while the shell-side temperature increases (turbine steam flow is reduced to zero upon plant trip). The rapid expansion of the coolant in the reactor core, combined with reduced heat transfer in the steam generators, causes an insurge into the pressurizer and a pressure increase throughout the RCS. The insurge into the pressurizer compresses the steam volume, actuates the automatic spray

system, opens the PORVs, and opens the pressurizer safety valves, in that sequence. The two PORVs are designed for reliable operation and would be expected to function properly during the accident. However, for conservatism in the peak-pressure evaluation, their pressure-reducing effect and the pressure-reducing effect of the pressurizer sprays are not included in the analysis.

The locked-rotor event is analyzed to the following criteria:

- Pressure in the RCS should be maintained below the designated limit (see below).
- Coolable core geometry is ensured by showing that the peak cladding temperature and maximum oxidation level for the hot spot are below 2700°F and 16.0 percent by weight, respectively.
- Activity release is such that the calculated doses meet 10 CFR 50.67 guidelines.

For KPS, the locked-rotor RCS pressure limit is equal to 110 percent of the design value, or 2750 psia. For the secondary side, the locked-rotor pressure limit is also assumed to be equal to 110 percent of design pressure, or 1210 psia. Since the loss-of-load analysis bounds the locked rotor, a specific MSS overpressurization analysis is not performed.

A hot-spot evaluation is performed to calculate the peak cladding temperature and maximum oxidation level. Finally, a calculation of the “rods-in-DNB” is performed for input to the radiological dose analysis.

14.1.8.3.2 Method of Analysis

The locked-rotor transient is analyzed with three computer codes. First, the RETRAN computer code is used to calculate the loop and core flow during the transient, the time of reactor trip based on the calculated flows, the nuclear power transient, and the primary-system pressure and temperature transients. The FACTRAN computer code is then used to calculate the thermal behavior of the fuel located at the core hot spot based on the nuclear power and RCS flow from RETRAN. The FACTRAN computer code includes a film boiling heat transfer coefficient. Finally, the VIPRE code is used to calculate the rods-in DNB using the nuclear power and RCS temperature (enthalpy), pressure, and flow from RETRAN.

For the case analyzed to determine the maximum RCS pressure and peak cladding temperature, the plant is assumed to be in operation under the most adverse steady-state operating conditions; that is, a maximum steady-state thermal power, maximum steady-state pressure, and maximum steady-state coolant average temperature. The case analyzed to determine the rods-in-DNB utilizes the RTDP methodology. Initial reactor power, pressurizer pressure and RCS temperature are assumed to be at their nominal values. Minimum measured flow is also assumed.

A maximum, uniform, SGTP level of 10 percent was assumed in the RETRAN analysis. However, a core flow reduction of 1.1 percent, which addresses the potential reactor coolant flow asymmetry associated with a maximum loop-to-loop SGTP imbalance of 10 percent, was applied.

A conservatively large absolute value of the Doppler-only power coefficient is used, along with the most-positive MTC limit for full-power operation (0 pcm/°F). These assumptions maximize the core power during the initial part of the transient when the peak RCS pressures and hot-spot results are reached.

A conservatively low trip reactivity value (3.5 percent $\Delta\rho$) is used to minimize the effect of rod insertion following reactor trip and maximize the heat flux statepoint used in the DNBR evaluation for this event. This value is based on the assumption that the highest worth RCCA is stuck in its fully withdrawn position. A conservative trip reactivity worth versus rod position was modeled in addition to a conservative rod drop time (1.8 seconds from dashpot). The trip reactivity versus rod position curve is confirmed to be valid as part of the RSAC verification process.

A loss-of-offsite-power is assumed with the unaffected RCP losing power instantaneously at reactor trip.

For the peak RCS pressure evaluation, the initial pressure is conservatively estimated as 50.1 psi above the nominal pressure (2250 psia) to allow for errors in the pressurizer pressure measurement and control channels. This is done to obtain the highest possible rise in the coolant pressure during the transient. The peak RCS pressure occurs in the lower plenum of the vessel. The pressure transient in the lower plenum is shown in Figure 14.1.8-30.

For this accident, an evaluation of the consequences with respect to the fuel rod thermal transient is performed. The evaluation incorporates the assumption of rods going into DNB as a conservative initial condition to determine the cladding temperature and zirconium water reaction resulting from the locked rotor. Results obtained from the analysis of this hot-spot condition represent the upper limit with respect to cladding temperature and zirconium water reaction. In the evaluation, the rod power at the hot spot is assumed to be 2.5 times the average rod power (that is, $FQ = 2.5$) at the initial core power level.

14.1.8.3.2.1 *Film Boiling Coefficient* The film boiling coefficient is calculated in the FACTRAN code using the Bishop-Sandberg-Tong film boiling correlation. The fluid properties are evaluated at film temperature. The program calculates the film co-efficient at every time step based upon the actual heat transfer conditions at the time. The nuclear power, system pressure, bulk density, and RCS flow rate as a function of time are based on the RETRAN results.

14.1.8.3.2.2 *Fuel Cladding Gap Coefficient* The magnitude and time dependence of the heat transfer coefficient between fuel and cladding (gap co-efficient) has a pronounced influence on the thermal results. The larger the value of the gap co-efficient, the more heat is transferred between the pellet and cladding. Based on investigations on the effect of the gap co-efficient upon the maximum cladding temperature during the transient, the gap co-efficient was assumed to increase from a steady-state value consistent with initial fuel temperature to 10,000 BTU/hr-ft²-°F at the initiation of the transient. Therefore, the large amount of energy stored in the fuel because of the small initial value is released to the cladding at the initiation of the transient.

14.1.8.3.2.3 *Zirconium-Steam Reaction* The zirconium-steam reaction can become significant above 1800°F (cladding temperature). The Baker-Just parabolic rate equation is used to define the rate of zirconium-steam reaction. The effect of the zirconium-steam reaction is included in the calculation of the hot-spot cladding temperature transient.

14.1.8.3.3 Results

Figure 14.1.8-25 through Figure 14.1.8-33 illustrate the transient response for the locked-rotor event (peak RCS pressure/peak cladding temperature case). The peak RCS pressure is 2683 psia and is less than the acceptance criterion of 2750 psia. Also, the peak cladding temperature is 1900°F, which is considerably less than the limit of 2700°F. The zirconium-steam reaction at the hot spot is 0.61 percent by weight, which meets the criterion of less than 16 percent zirconium-steam water reaction. For the radiological dose evaluation, the total percentage of fuel rods calculated to experience DNB is less than 50 percent (rods-in-DNB case). The sequence of events for the peak RCS pressure/peak cladding temperature case is given in Table 14.1.8-3. This transient trips on a low primary reactor coolant flow trip setpoint, which is assumed to be 86.5 percent.

14.1.8.3.4 Conclusions

The analysis performed has demonstrated that for the locked-rotor event, the RCS pressure remains below 110 percent of the design pressure and the hot-spot cladding temperature and oxidation levels remain below the limit values. Therefore, all applicable acceptance criteria are met. In addition, the total percentage of rods calculated to experience DNB is less than 50 percent.

14.1.8.4 Method of Analysis-Radiological Consequences

Fuel-cladding damage may result from the locked rotor accident. Due to the pressure differential between the primary and secondary systems and assumed steam generator tube leakage, fission products transfer from the primary into the secondary system. A portion of this radioactivity is released to the outside atmosphere through either the atmospheric relief valves, or safety valves. In addition, iodine activity is contained in the secondary coolant prior to the accident, and some of this activity is released to the atmosphere as a result of steaming from the steam generators following the accident. The analysis of the locked rotor radiological consequences uses the analytical methods and assumptions outlined in Regulatory Guide 1.183.

14.1.8.4.1 Source Term

The analysis of the locked rotor radiological consequences assumes an iodine concentration-60 $\mu\text{Ci/gm}$ of dose-equivalent (DE) I-131 exists in the RCS at the time of the event.

The noble gas and alkali metal activity concentration in the primary coolant when the accident occurs is based on a fuel defect level of 1 percent. The iodine activity concentration of the secondary coolant when the locked rotor occurs is assumed to be 0.10 $\mu\text{Ci/gm}$ of dose equivalent (DE) I-131. The alkali metal activity concentration of the secondary coolant at the time the locked rotor occurs is assumed to be 10 percent of the primary side concentration.

As a result of the locked-rotor event, less than 50 percent of the fuel rods in the core undergo DNB. In the determination of the offsite and Control Room doses following the locked-rotor event, it is conservatively assumed that 100 percent of the fuel rods in the core suffer sufficient damage that all of their gap activity is released to the primary coolant. It is assumed that 8 percent of the total core activity of iodine, 5 percent of the total core activity for noble gases, and 12 percent of the total core activity for alkali metals are the fuel-cladding gap and are released into the primary coolant.

14.1.8.4.2 Release Pathway

Activity is released to the environment by way of primary to secondary leakage and steaming from the secondary side to the environment. The primary to secondary steam generator tube leakage rate is assumed to be at the Technical Specification limit of 150 gpd/SG.

The RHRS is assumed to remove all decay heat 8 hours into the accident, with no further releases to the environment after that time.

An iodine-partition factor in the steam generators of 0.01 (curies iodine/gm steam)/(curies iodine/gm water) is used. This partition factor is applied to alkali metals. Prior to reactor trip and concurrent loss of off-site power, an iodine-removal factor of 0.01 could be taken for steam released to the condenser, but this is conservatively ignored.

All noble gas activity carried over to the secondary side through steam generator tube leakage is assumed to be immediately released to the outside atmosphere.

14.1.8.4.3 Control Room Isolation

It is assumed that the Control Room HVAC system begins in normal-operation mode. The activity level in the air supply duct gradually increases as activity builds up in the Control Room, and the concentration of activity in the steam generators (and consequently in the steam being released) increases. This causes a high-radiation signal to be generated. It is conservatively assumed that the Control Room HVAC does not fully enter the accident mode of operation until 10 minutes after event initiation.

14.1.8.4.4 Results and Conclusions

The doses due to the locked rotor, including the 1.06 multiplier developed to bound variations in core average enrichment, core mass, and cycle length for this event, are:

Case	TEDE Dose (rem)	Acceptance Criteria (rem TEDE)
SB	0.50	2.5
LPZ	0.08	2.5
Control Room	1.40	5

The acceptance criteria are met. The SB dose reported is for the worst 2-hour period, determined to be from 6 to 8 hours.

14.1.9 Loss of External Electrical Load

14.1.9.1 Accident Description

The loss-of-external-electrical-load event is defined as a complete loss of steam load or a turbine trip from full power without a direct reactor trip. This anticipated transient is analyzed as a turbine trip from full power because it bounds both events: the loss of external electrical load and turbine trip. The turbine-trip event is more severe than the total loss-of-external-electrical-load event since it results in a more rapid reduction in steam flow.

For a turbine trip, the reactor would be tripped directly (unless below approximately 10 percent power) from a signal derived from either the turbine auto-stop oil pressure or a closure of the turbine stop valves. The automatic steam dump system accommodates the excess steam generation. Reactor coolant temperatures and pressures do not significantly increase if the steam dump system and pressurizer pressure control system are functioning properly. If the turbine condenser were not available, the excess steam generation would be dumped to the atmosphere. Additionally, main feedwater flow would be lost if the turbine condenser were not available. For this situation, steam generator level would be maintained by the auxiliary feedwater (AFW) system.

For a loss of external electrical load without subsequent turbine trip, no direct reactor trip signal would be generated. The plant would be expected to trip from the RPS. A continued steam load of approximately 5 percent would exist after a total loss of external electrical load because of the steam demand of plant auxiliaries.

In the event of a large loss of load in which the steam dump valves fail to open or a complete loss of load with the steam dump operating, the MSSVs may lift and the reactor may be tripped by any of the following signals: high pressurizer pressure, high pressurizer water level, OTΔT and OPΔT, or lo-lo steam generator water level. The steam generator shell-side pressure and reactor coolant temperatures will increase rapidly. However, the PSVs and MSSVs are sized to protect the RCS and steam generators against overpressure for all load losses without assuming the operation of the steam dump system. The steam dump valves will not be opened for load reductions of 10 percent or less, but may open for larger load reductions. The RCS and MSS steam relieving capacities were designed to ensure safety of the unit without requiring automatic rod control, pressurizer pressure control, steam bypass control systems, or a reactor trip on turbine trip.

14.1.9.2 Method of Analysis

The loss-of-load transients are analyzed using the RETRAN computer code. The code simulates the neutron kinetics, RCS, pressurizer, pressurizer relief and safety valves, pressurizer spray, steam generators, and MSSVs. The code computes pertinent plant variables including temperatures, pressures, and power levels.

The loss-of-load accident is analyzed for the following:

- To confirm that the PSVs and MSSVs are adequately sized to prevent overpressurization of the primary RCS and MSS, respectively
- To ensure that the increase in RCS temperature does not result in a DNB in the core

The RPS is designed to automatically terminate any such transient before the DNBR falls below the limit value.

In this analysis, the behavior of the unit is evaluated for a complete loss-of-steam load from full power with no credit taken for a direct reactor trip on turbine trip. This assumption will delay reactor trip until conditions in the RCS cause a trip on some other signal. Therefore, the analysis assumes a worst-case transient and demonstrates the adequacy of the pressure-relieving devices and plant-specific RPS setpoints assumed in the analysis for this event.

Of the three cases analyzed, one is performed to address DNB concerns, one ensures that the peak primary RCS pressure remains below the design limit (2750 psia), and the final case confirms that the peak MSS pressure remains below 110 percent of the steam generator shell design pressure (1210 psia). The major assumptions for these cases are summarized as follows:

1. [Deleted]
2. The loss-of-load event results in a primary-system heatup and, therefore, is conservatively analyzed assuming minimum reactivity feedback consistent with BOC conditions. This includes assuming an MTC value consistent with BOC HFP conditions (that is, zero MTC) and a least negative DPC. Maximum feedback (EOC) cases that were previously considered in the USAR are no longer analyzed since they have been determined (as part of the Westinghouse methodology for the analysis of this event) to be non-limiting with respect to the minimum DNBR, peak primary RCS pressure, and peak MSS pressure.
3. It is conservative to assume that the reactor is in manual control. If the reactor were in automatic control, the control rod banks would move prior to trip and reduce the severity of the transient.
4. No credit is taken for the operation of the steam dump system or steam generator power-operated relief valves (PORVs). The steam generator pressure rises to the safety valve setpoints, where steam release through the MSSV limits the secondary-side steam pressure to the setpoint values. The MSSVs are explicitly modeled in the loss-of-load licensing basis analysis assuming the conservative MSSV setpoints for secondary overpressure analysis. Note that by maximizing the pressure transient in the MSS, the saturation temperature in the steam generators is maximized, resulting in limiting pressure and temperature conditions in the RCS.

5. Three cases are analyzed:
 - a. For the case analyzed for DNB, automatic pressurizer pressure control is assumed. Therefore, full credit is taken for the effect of the pressurizer spray and PORVs in reducing or limiting the primary coolant pressure. Safety valves are also available and are modeled assuming a -1 percent setpoint tolerance.
 - b. For the case analyzed for primary RCS overpressure concerns, it is assumed that automatic pressurizer pressure control is not available. Therefore, no credit is taken for the effect of the pressurizer spray or PORVs in reducing or limiting the primary coolant pressure. Safety valves are assumed operable, but are modeled assuming a $+1$ percent setpoint tolerance. The effects of the PSV loop seals are also conservatively modeled in the analysis.
 - c. For the case analyzed for MSS overpressure concerns, it is assumed that automatic pressurizer pressure control is available. Credit is taken for the effect of the pressurizer spray and PORVs in reducing or limiting the primary coolant pressure, therefore conservatively delaying the actuation of the RPS until an OTAT reactor trip signal is generated. Delaying the reactor trip ensures that the energy input to the secondary system, and subsequently the MSS pressure, is maximized.
6. Main feedwater flow to the steam generators is assumed to be lost at the time of turbine trip. No credit is taken for AFW flow since a stabilized plant condition will be reached before AFW initiation is normally assumed to occur for full-power cases. However, the AFW pumps would be expected to start on a trip of the main feedwater pumps. The AFW flow would remove core decay heat following plant stabilization.
7. The analysis is performed for operation with 422V+ fuel and a maximum SGTP level (uniform) for KNPP of ≤ 10 percent.
8. A maximum SGTP level of 10 percent is modeled. SGTP imbalances do not adversely affect this transient.

14.1.9.3 Results

The transient responses for a total loss of load from full-power operation are shown in Figure 14.1.9-1 through Figure 14.1.9-16 for the 3 cases assuming BOC reactivity feedback conditions with and without automatic pressurizer pressure control (pressurizer spray and PORVs).

Figure 14.1.9-1 through Figure 14.1.9-6 show the transient responses for the total loss of steam load at BOC (minimum feedback reactivity coefficients) assuming full credit for the pressurizer spray and PORVs to calculate the transient DNBR response. Following event initiation, the pressurizer pressure and average RCS temperature increase due to the rapidly reduced steam flow and heat removal capacity of the secondary side. The peak pressurizer pressure and water volume and RCS average temperature are reached shortly after the reactor is

tripped by the OTΔT trip function. The DNBR initially increases slightly, then decreases until the reactor trip is tripped. Finally, following reactor trip, it increases rapidly. The minimum DNBR remains well above the safety analysis limit value. The MSSVs actuate to limit the MSS pressure below 110 percent of the steam generator shell design pressure. Table 14.1.9-1 summarizes the sequence of events and limiting conditions for this case.

The total loss-of-load event was also analyzed assuming the plant to be initially operating at full power at BOC with no credit taken for the pressurizer spray or PORVs to maximize the primary RCS pressure response. Figure 14.1.9-7 through Figure 14.1.9-11 show the transients for this case. The neutron flux remains relatively constant prior to reactor trip, while pressurizer pressure, pressurizer water volume, and RCS average temperature increase due to the sudden reduction in primary to secondary heat transfer. The reactor is tripped on the high pressurizer pressure trip signal. In this case, the PSVs are actuated and maintain the primary RCS pressure below 110 percent of the design value. The MSSVs actuate to limit the MSS pressure below 110 percent of the steam generator shell design pressure. Table 14.1.9-2 summarizes the sequence of events and limiting conditions for this case.

Figure 14.1.9-12 through Figure 14.1.9-16 show the transient responses for the total loss of steam load at BOC (minimum feedback reactivity coefficients) assuming full credit for the pressurizer spray and PORVs to maximize the MSS pressure response. Following event initiation, the pressurizer pressure and average RCS temperature increase due to the rapidly reduced steam flow and heat removal capacity of the secondary side. The peak pressurizer pressure and water volume and RCS average temperature are reached shortly after the reactor is tripped by the OTΔT trip function. The MSS pressure increases, resulting in the actuation of the first three MSSVs, and then decreases rapidly following reactor trip. The MSSVs actuate to limit the MSS pressure below 110 percent of the steam generator shell design pressure. Table 14.1.9-3 summarizes the sequence of events and limiting conditions for this case.

14.1.9.4 Conclusions

The results of the analyses show that the plant design is such that a total loss of external electrical load without a direct or immediate reactor trip presents no hazard to the integrity of the primary RCS or MSS. Pressure-relieving devices that have been incorporated into the plant design are adequate to limit the maximum pressures to within the safety analysis limits; that is, 2750 psia for the primary RCS and 1210 psia for the MSS.

The integrity of the core is maintained by operation of the RPS; that is, the minimum DNBR is maintained above the safety analysis limit value of 1.34.

14.1.10 Loss of Normal Feedwater

14.1.10.1 Accident Description

A loss of normal feedwater (from a pipe break, pump failure, valve malfunctions, or loss of off-site power) results in a reduction in capability of the secondary system to remove the heat

generated in the reactor core. If the reactor is not tripped during this accident, RCS damage could possibly occur from a sudden loss of heat sink. If an alternative supply of feedwater is not supplied to the plant, residual heat following reactor trip heats the coolant to the point where water relief from the pressurizer occurs. Significant loss of water from the RCS could conceivably lead to core damage. Since the reactor is tripped well before the steam generator heat transfer capability is reduced, the primary system never approaches a condition where the DNBR limit may be violated.

The following provides the necessary protection against a loss of normal feedwater:

1. Reactor trip on Low-Low water level in either steam generator.
2. Reactor trip on steam flow-feedwater flow mismatch in coincidence with low water level in either steam generator.
3. Two motor driven auxiliary feedwater pumps which are started automatically on:
 - a. Low-Low level in two-out-of-three level channels in either steam generator, or
 - b. Opening of both feedwater pump circuit breakers, or
 - c. SI signal, or
 - d. Loss of off-site power, or
 - e. Steam generator AMSAC low-low level, or
 - f. Manually
4. One turbine driven pump which is started automatically on:
 - a. Low-Low level in two-out-of-three level channels in both steam generators, or
 - b. Loss of voltage on both 4 kV buses, or
 - c. Steam generator AMSAC low-low level, or
 - d. Manually

The auxiliary feedwater (AFW) system is started automatically on the signals described above. Below 15 percent of rated thermal power, selected AFW valves (AFW-2A, AFW-2B, AFW-10A and AFW-10B) can be placed in the closed position, thereby precluding AFW flow to the steam generators. For this condition, manual operator action to re-initiate AFW after it has been isolated has been justified. The motor-driven auxiliary feedwater pumps are supplied power by the diesel generators if a loss of outside power occurs. The turbine-driven pump uses steam from the secondary system and exhausts the secondary steam to the atmosphere. The auxiliary feedwater pumps take suction directly from the condensate storage tank for delivery to the steam generators.

The analysis shows that following a loss of normal feedwater, the AFW system is capable of removing the stored energy, residual decay heat and RCP heat, thus preventing over-pressurization of the RCS and a loss of water from the reactor core.

Three auxiliary feedwater pumps are provided in the plant (two motor driven and one turbine driven). Necessary protection against the consequences of a loss of normal feedwater including that caused by loss of off-site power is therefore available. An active failure on one of the operable auxiliary feedwater pumps even when one of the pumps is out-of-service during a loss of normal feedwater event does not result in a violation of any acceptance criteria provided power is limited to 102 percent or less of 1650 MWt reactor power.

When all three pumps are operable there is considerable backup in equipment and control to insure that reactor trip and automatic auxiliary feedwater flow occur following loss of normal feedwater.

14.1.10.2 Method of Analysis

Operation at 102 percent or Less of 1650 MWt Reactor Power

The analysis was performed using a digital simulation of the plant to show that following a loss of normal feedwater, the Auxiliary Feedwater System is adequate to remove stored and residual heat.

The following assumptions are made:

1. The initial steam generator water level (in both steam generators) when the reactor trip occurs is assumed to be at 0 percent NRL. This is conservative, because this level would result in a reactor trip and automatic initiation of the auxiliary feedwater flow.
2. The plant is initially operating at 102 percent of 1650 MWt.
3. Off-Site power is not available, resulting in natural circulation flow in the RCS.
4. A conservative core residual heat generation based upon long-term operation at the initial power level preceding the trip.
5. Only one motor-driven auxiliary feedwater (AFW) pump is available 630 seconds after the accident is initiated.
6. Auxiliary feedwater is delivered to only one steam generator. The AFW is modeled as a function of steam generator pressure, and the AFW flow rate at a SG pressure of 1106 psig (pressure of the first (lowest setpoint) MSSV plus 3 percent for accumulation) is approximately 176 gpm. The AFW enthalpy is assumed to be 90.8 BTU/lbm (120°F and 1100 psia).
7. Secondary system steam relief is through the self-actuated safety valves. Steam relief through the steam generator power-operated relief valves (PORVs) or condenser dump valves is assumed to be unavailable.

14.1.10.3 Results

Figure 14.1.10-1 through Figure 14.1.10-5 show the plant parameters following a loss of normal feedwater accident with the assumptions listed above. Following the reactor and turbine trip from full load, the water level in the steam generators falls due to the reduction of steam generator void fraction and because steam flow through the safety valves continues to dissipate the stored and generated heat. The auxiliary feedwater pump is delivering flow 630 seconds following the initiation of the low-low level trip, thus reducing the rate of water level decrease. The capacity of the auxiliary feedwater pump is such that the water level in the steam generator being fed does not recede below the lowest level at which sufficient heat transfer area is available to dissipate core residual heat without water relief from the primary system relief or safety valves.

From Figure 14.1.10-1 through Figure 14.1.10-5, it can be seen that at no time is the tube sheet uncovered in the steam generator receiving auxiliary feedwater flow and at no time is there water relief from the pressurizer. If the auxiliary feed delivered is greater than that of one motor driven pump, the initial reactor power is <102 percent of 1650 MWt, or the steam generator water level in one or both steam generators is above 0 percent NRL at the time of trip, then the result is a steam generator minimum water level higher than shown and an increased margin to the point at which reactor coolant water relief occurs.

The following table shows the comparison of the important calculated safety parameters (Calculated Value/Acceptance Criterion):

	MDNBR	RCS Pressure (psia)	MS Pressure (psia)
Loss of Feedwater	1.704/1.14	2500/2750	1165/1210

14.1.11 Loss of Normal Feedwater - Operation at 100.6 Percent of 1772 MWt Reactor Power

14.1.11.1 Accident Description

With the Auxiliary Feedwater (AFW) system in its normal standby alignment, the AFW system is started automatically on the signals described above.

For operation at <15 percent of rated thermal power (RTP), KPS Technical Specifications (TS) allow operation with the automatic startup disabled. AFW-2A, AFW-2B, AFW-10A and AFW-10B may be closed, and the switches for the AFW pumps may be in the “pull out” position (per TS 3.4.b). Based on the 100 percent of RTP loss-of-normal feedwater analysis, in which an 800-second AFW delay has been assumed, operator action to manually establish AFW flow from at least two AFW pumps within 800 seconds (13.3 minutes) after a reactor trip has been determined to be acceptable when the event is initiated from <15 percent of RTP.

Following a loss of off-site power, the emergency diesel generators supply electrical power to the two motor-driven AFW pumps. The turbine-driven AFW pump is powered via steam flow

from the secondary system that exhausts to the atmosphere. All of the AFW pumps are normally aligned to take suction from the condensate storage tank (CST) for delivery to the steam generators.

The analysis shows that following a loss of normal feedwater, the AFW system is capable of removing the stored energy, residual decay heat and RCP heat following reactor trip. The pressurizer is prevented from becoming water-solid, which could lead to rising RCS pressure and a loss of water from the RCS via a pressurizer pressure-relief or safety valve.

14.1.11.2 Method of Analysis

Operation at 100.6 percent of 1772 MWt Reactor Power

The loss-of-normal-feedwater transient is analyzed using the RETRAN computer code. The RETRAN model simulates the RCS, neutron kinetics, pressurizer, pressurizer relief and safety valves, pressurizer heaters, pressurizer spray, steam generators, feedwater system and main steam safety valves (MSSVs). The code computes pertinent plant variables including steam generator mass, pressurizer water volume and reactor coolant average temperature.

The major assumptions are summarized below:

1. The plant is initially operating at 100.6 percent of 1780 MWt NSSS (includes 10 MWt of RCP heat).
2. Reactor trip occurs on steam generator lo-lo water level at 0 percent of narrow range span (NRS). Turbine trip occurs coincident with reactor trip.
3. A conservative core residual heat generation is assumed, based on the ANS 5.1-1979 decay heat model plus 2 sigma.
4. AFW flow from two motor-driven AFW pumps is initiated with flow split equally between the two steam generators (equal split is the limiting case) 800 seconds after the reactor trip on lo-lo steam generator water level. This AFW flow assumption accounts for the limiting single failure that is the loss of the turbine-driven AFW pump. The AFW is modeled as a function of steam generator pressure, and the flow with the first (lowest setpoint) MSSVs open is approximately 170 gpm. The AFW enthalpy is assumed to be 90.8 BTU/lbm (120°F and 1100 psia).
5. Secondary system steam relief is achieved through the MSSVs. The MSSVs are explicitly modeled assuming the conservative MSSV setpoints for secondary overpressure analyses. Steam relief through the steam generator power-operated relief valves (PORVs) or condenser dump valves is assumed to be unavailable.
6. The initial reactor coolant average temperature is assumed to be 6°F higher than the nominal full power value of 573.0°F because this results in a greater expansion of the RCS water during the transient, thus resulting in a higher pressurizer water level.

7. The initial pressurizer pressure is assumed to be 50 psi above the nominal value of 2250 psia. A sensitivity study was performed that demonstrated that a high initial pressurizer pressure is conservative. An additional 0.1 psi uncertainty has been determined to be negligible.
8. The initial pressurizer water level is assumed to be 5 percent of span above the nominal value of 48 percent of span, which corresponds to the high nominal full-power vessel average temperature of 573°F. A high initial pressurizer water level is conservative because it minimizes the initial margin to filling the pressurizer water-solid.
9. Normal reactor control systems are not assumed to function. However, the pressurizer PORVs, pressurizer heaters and pressurizer sprays are assumed to operate normally. This assumption results in a conservative transient with respect to the peak pressurizer water level. If these control systems did not operate, the pressurizer safety valves would maintain peak RCS pressure around the actuation setpoint throughout the transient, which would limit the peak pressurizer water volume.
10. The initial steam generator water level is assumed to be 7 percent of narrow range span (NRS) above the nominal value of 44 percent of NRS. A high initial steam generator water level is conservative because it maximizes the time to reach the steam generator lo-lo water level, thereby maximizing the RCS heatup.
11. Reactor trip on steam flow-feedwater flow mismatch coincident with low water level in either steam generator is not credited.

The loss-of-normal-feedwater analysis is performed to demonstrate the adequacy of the RPS to trip the reactor and the engineered safeguards features actuation system (AFW system) to remove long-term decay heat, stored energy and RCS heat following reactor trip. The actuation of the AFW system prevents excessive heatup or overpressurization of the RCS. As such, the assumptions used in the analysis are designed to maximize the time to reactor trip and to minimize the energy removal capability of the AFW system. These assumptions maximize the possibility of water relief from the RCS by maximizing the expansion of the RCS inventory, as noted in the assumptions listed above.

14.1.11.3 Results

Figure 14.1.10-6 through Figure 14.1.10-11 show the significant plant responses following a loss of normal feedwater. The calculated sequence of events is listed in Table 14.1.10-1.

Following the reactor and turbine trip from full load, the water level in each steam generator falls due to the reduction of the steam generator void fraction in the tube bundle region, and because the steam releases through the MSSVs, which open to dissipate the RCS stored and generated heat. Eight hundred seconds after the initiation of the lo-lo steam generator water level reactor trip, flow from the two motor-driven AFW pumps is credited, thus reducing the rate of water level decrease in the steam generators.

The capacity of two motor-driven AFW pumps is sufficient to dissipate core residual heat, stored energy and RCP heat without water relief through the pressurizer PORVs or safety valves. Figure 14.1.10-9 shows that at no time is there water relief from the pressurizer, as the peak pressurizer water volume is less than the limit of 1000.0 ft³. Plant emergency operating procedures may be followed to further cool down the plant. The peak main steam system (MSS) pressure is less than 110 percent of the steam generator design pressure. Also, the analysis shows that the RCS overpressurization limit is not challenged during this transient. However, note that the pressurizer sprays and PORVs are assumed to be operable so as to maximize the potential for pressurizer filling. This event is bounded by the loss of external electrical load with respect to peak RCS and MSS pressures.

14.1.11.4 Conclusions

The results of the loss-of-normal feedwater analysis show that all applicable acceptance criteria are satisfied. The AFW capacity is sufficient to dissipate core residual heat, stored energy and reactor coolant pump heat such that reactor coolant water is not relieved through the pressurizer relief or safety valves.

14.1.12 Anticipated Transients Without Scram

An Anticipated Transient Without Scram (ATWS) is a postulated anticipated operational occurrence (such as loss of feedwater, loss of condenser vacuum, or loss of off-site power) that is accompanied by a failure of the RPS to shut down the reactor.

The Kewaunee Nuclear Power Plant was originally licensed based on the results of a study of ATWS presented in WCAP-7486. (See Reference 6.) The conclusions of this study are that there is very little likelihood of failure to trip the reactor and that even in the hypothetical case of no protective reactor trip, there is no gross fuel damage. WCAP-8330 presented the results of generic ATWS analysis for 2, 3, and 4 loop Westinghouse plants. The results of these analyses showed that the consequences of an ATWS were acceptable as long as the turbine was tripped and AFW initiated in a timely fashion. Acceptable consequences are defined as RCS pressure remaining below 3200 psig and no fuel failure. The results of the analyses in WCAP-8330 also showed that the most severe ATWS transients were those which entailed a loss of main feedwater. Subsequent to the operational license at KNPP and based on the studies cited above, additional ATWS protection was required as described below.

The Code of Federal Regulations (CFR), Section 10 CFR 50.62 (Reference 7) specifies ATWS mitigation system requirements. The Westinghouse Owners Group developed a set of conceptual ATWS Mitigating System Actuation Circuitry (AMSAC) designs (Reference 8). The AMSAC actuation on low steam generator water level design has been implemented, with the exception that AMSAC is armed at all power levels (the “c-20 permissive” signal is not used). The logic of AMSAC is to trip the turbine and start all three auxiliary feedwater pumps when low-low steam generator water level signals are present on 3 of 4 channels for a specified time period. However, as discussed in Section 6.6, manual initiation of auxiliary feedwater may be required at

low power levels (< 15 percent). The level setpoint and time delay criteria are described in Reference 8.

The NRC Safety Evaluation Report (Reference 9) and a subsequent NRC Special Inspection Report (Reference 10) reviewed the Kewaunee design and installation against 14 key elements for compliance. The NRC concluded that the Kewaunee AMSAC is acceptable and in compliance with the ATWS rule, 10 CFR 50.62.

In 1998, in response to an engineering evaluation of the AFW system, a plant design change added a Diverse Scram System (DSS). The DSS is initiated on a signal from the existing AMSAC system and de-energizes the Rod Drive MG Set exciter field. Removing the Rod Drive MG set exciter field will interrupt power to the control rod grippers, allowing the control rods to free fall into the core, ending the ATWS event.

The DSS was installed to ensure the AFW pumps would continue to run throughout a loss of main feedwater ATWS. The DSS in conjunction with the AMSAC system will end the transient before the AFW flow to the steam generators increases to a point where AFW pump NPSH could be lost. The loss of main feedwater ATWS, mitigated by the DSS and AMSAC system, was analyzed using a similar methodology as the loss of main feedwater transient described in Section 14.1.10.

The original AMSAC submittal to the NRC was amended to include the DSS. The NRC Safety Evaluation Report (Reference 12) concluded that the Kewaunee DSS design was acceptable. The WPSC Safety Evaluation for the original AMSAC and the DSS included a review of the 14 key elements of ATWS compliance used by the NRC. This review concluded that the original AMSAC design reviewed by the NRC was unaffected by the addition of the DSS.

14.1.13 Loss of AC Power to the Plant Auxiliaries

14.1.13.1 Accident Description

A complete loss of non-emergency AC power results in the loss of all power to the plant auxiliaries, such as the RCPs or condensate pumps. The loss of power may be caused by a complete loss of the offsite grid accompanied by a turbine generator trip at the station, or by a loss of the onsite AC distribution system.

The events following a loss of AC power with turbine and reactor trip are described in the sequence as follows:

- Plant vital instruments are supplied from emergency power sources.
- Steam dump to the condenser and steam generator PORVs are unavailable. Therefore, the MSSVs lift to dissipate the sensible heat of the fuel and coolant plus the residual decay heat.

- As the no-load temperature is approached, the steam generator PORVs (or the safety valves, if the PORVs are not available) are used to dissipate the residual decay heat and maintain the plant at the hot shutdown condition.
- The standby diesel generators, started on loss of voltage on the plant emergency busses, begin to supply plant vital loads.

The AFW system is started automatically, as discussed in the loss-of-normal-feedwater analysis (Section 14.1.10). The TDAFWP utilizes steam from the secondary system and exhausts to the atmosphere. The motor-driven AFW pumps are supplied by power from the diesel generators. The pumps take suction directly from the condensate storage tank for delivery to the steam generators.

Upon the loss of power to the RCPs, coolant flow necessary for core cooling and the removal of residual heat is maintained by natural circulation in the reactor coolant loops. Following the RCP coastdown caused by the loss of AC power, the natural circulation capability of the RCS removes residual and decay heat from the core, aided by the AFW in the secondary system.

In response to Generic Letter 81-21, the ability to cooldown via natural circulation without voiding the upper head of the reactor vessel was reviewed. The NRC concluded in Reference 11 that Kewaunee has adequately demonstrated the ability to cooldown without voiding the reactor vessel head and determined that sufficient condensate supply exists to support its cooldown procedures.

14.1.13.2 Method of Analysis

The loss-of-all-AC-power-to-the-station-auxiliaries transient is analyzed using the RETRAN computer code. The code simulates the neutron kinetics, RCS including natural circulation, pressurizer, pressurizer relief and safety valves, pressurizer heaters, pressurizer spray, steam generators, feedwater system, and MSSVs. The code computes pertinent plant variables including steam generator mass, pressurizer water volume, and reactor coolant average temperature.

Major assumptions made in the loss of all auxiliary AC power analysis are the following:

1. The plant is initially operating at 102 percent of the 1780 MWt.
2. Reactor trip occurs on steam generator lo-lo level at 0 percent of narrow range span (NRS). Turbine trip occurs coincident with reactor trip.
3. A conservative core residual heat generation based on ANS 5.1-1979 decay heat plus 2 sigma is assumed (Reference 15).
4. The amount of heat transfer assumed to occur in the steam generators following the RCP coastdown is based on RCS natural circulation conditions.

5. One minute after the lo-lo steam generator water level setpoint is reached, the AFW system provides 176 gpm of flow split equally between the two steam generators (equal split is the limiting case). The AFW flow assumption is conservative with respect to the worst-case scenario for available AFW flow during a loss-of-all-auxiliary-AC-power event, as the TDAFWP (single failure) and the second MDAFWP are assumed to be unavailable. The AFW enthalpy is assumed to be 90.8 BTU/lbm (120°F and 1100 psia).
6. Secondary-system steam relief is achieved through the MSSVs. The MSSVs are explicitly modeled assuming the conservative MSSV setpoints for secondary overpressure analysis. Steam relief through the steam generator PORVs or condenser dump valves is assumed unavailable.
7. The initial reactor coolant average temperature is assumed to be 6°F lower than the nominal value of 573.0°F because this results in a greater expansion of the RCS water during the transient, thus, resulting in a higher pressurizer water level.
8. The initial pressurizer pressure is assumed to be 50 psi above its nominal value.
9. Nominal reactor control systems are not assumed to function. However, the pressurizer PORVs, pressurizer heaters, and pressurizer spray are assumed to operate normally. This assumption results in a conservative transient with respect to the peak pressurizer water level. If these control systems did not operate, the pressurizer safety valves would maintain peak RCS pressure around the actuation setpoint throughout the transient.

The assumptions used in the analysis are similar to the loss of normal feedwater (Section 14.1.10) except that power is assumed to be lost to the reactor coolant pumps due to the reactor trip.

14.1.13.3 Results

Figure 14.1.12-1 through Figure 14.1.12-6 show the significant plant responses following a loss-of-all-AC-power-to-the-station-auxiliaries event. The calculated sequence of events is listed in Table 14.1.12-1.

The first few seconds after the loss of power to the RCPs will closely resemble the simulation of the complete loss-of-flow accident (USAR Section 14.1.8), where core damage due to rapidly increasing core temperature is prevented by promptly tripping the reactor.

After the reactor trip, stored and residual decay heat must be removed to prevent damage to either the RCS or the core. The peak pressurizer water volume is 698 ft³, which is less than the limit of 1000.0 ft³. The maximum steam generator pressure calculated was less than 110 percent of the design pressure of 1085 psig. Also, the analysis shows that the RCS overpressurization limit is not challenged during this transient. However, note that the pressurizer PORVs are assumed to be operable so as to maximize the potential for pressurizer filling. This event is bounded by the loss of external electrical load (Section 14.1.9) with respect to peak RCS and MSS pressures.

The RETRAN code results show that the reactor coolant natural circulation flow available is sufficient to provide adequate core decay heat removal following reactor trip and RCP coastdown.

14.1.13.4 Conclusions

The results of the analysis show that a loss of all AC power to the station auxiliaries does not adversely affect the core, the RCS, or the MSS. The AFW capacity is sufficient to dissipate core residual heat. Consequently, reactor coolant is not relieved through the pressurizer relief or safety valves.

14.1 References

1. Letter WPS-90-160 from K. B. Chesko (Westinghouse) to M. L. Marchi (WPSC), May 10, 1990
2. Baldwin, M. S., et al., "An Evaluation of Loss of Flow Accidents Caused by Power System Frequency Transients in Westinghouse PWRs," WCAP-8424, Revision 1, June 1975
3. 1983 Islanding Study of the Wisconsin-Upper Michigan Systems, February 1985
4. Letter NS-CE-934 from C. Eicheldinger (Westinghouse) to D. B. Vassallo (NRC), Supplemental Information to WCAP-8424, Revision 1, February 3, 1976
5. Lamb, J. G., (NRC) to T. Coutu (NMC) transmitting the NRC SER for Amendment No. 166 to the Operating License, approving Implementation of Alternate Source Term, Letter No. K-03-040, March 17, 2003
6. Gangloff, W. C., "An Evaluation of Anticipated Operational Transients in Westinghouse Pressurized Water Reactors," WCAP-7486, May 1971
7. 10 CFR 50.62, Requirements for reduction of risk from anticipated transients without scram (ATWS) events for light-water-cooled nuclear power plants
8. Adler, M. R., "AMSAC Generic Design Package," WCAP-10858P-A, Revision 1, July 1987
9. NRC Safety Evaluation Report, J. G. Giitter (NRC) to D. C. Hintz (WPS) Letter No. K-88-202, August 25, 1988
10. NRC Special Inspection Report, R. W. Cooper II (NRC) to K. H. Evers (WPS), Letter No. K-89-209, October 25, 1989
11. NRC Safety Evaluation Report, S. A. Varga (NRC) to C. W. Giesler (WPS), Letter No. K-83-170, August 15, 1983
12. Letter from W. O. Long (NRC) to M. L. Marchi (WPSC), transmitting the NRC SER approving the AMSAC Modification, Letter No. K-98-101, July 19, 1998
13. Friedland, A. J. and S. Ray, "Revised Thermal Design Procedure," WCAP-11397-P-A, April 1989

14. [Deleted] |
15. “Decay Heat Power In Light Water Reactor,” ANSI/ANS-5.1-1979, August 29, 1979
16. Huegel, D. S., et al., “RETRAN-02 Modeling and Qualification for Westinghouse Pressurized Water Reactor Non-LOCA Safety Analyses,” WCAP-14882-P-A, April 1999
17. Haessler, R. L., et al., “Methodology for the Analysis of the Dropped Rod Event,” WCAP-11394-P-A, January 1990
18. [Deleted] |

Table 14.1.1-1
Assumptions and Results
Uncontrolled RCCA Withdrawal From a Subcritical Condition

Initial Power Level, %	0
Reactivity Insertion Rate, pcm/sec	75
Delayed Neutron Fraction	0.0072
Doppler Power Defect, pcm	1100
Trip Reactivity, % Δk	1.0
Hot Channel Factor	6.64
Number of RCPs Operating	1

Results

	Calculated Value	Limit
Peak Fuel Centerline Temperature, °F	2685	4746
Peak Fuel Average Temperature, °F	2159	4746
Minimum DNBR (thimble cell)	1.588	1.39
Minimum DNBR (typical cell)	1.733	1.39

Table 14.1.1-2
Sequence of Events Uncontrolled RCCA
Withdrawal from a Subcritical Condition

Event	Time (seconds)
Initiation of Uncontrolled RCCA Bank Withdrawal	0
Power-Range High Neutron Flux Low Setpoint Reached	10.0
Peak Nuclear Power Occurs	10.1
Rod Motion Begins	10.65
Peak Cladding Temperature Occurs	12.3
Peak Heat Flux Occurs	12.4
Minimum DNBR Occurs	12.4
Peak Fuel Average Temperature Occurs	13.1
Peak Fuel Centerline Temperature Occurs	15.2

Table 14.1.2-1
Time Sequence of Events for Uncontrolled RCCA Withdrawal at Power
(Maximum Nominal RCS T_{avg} ; Minimum Feedback)

Event	Time (Seconds)
Case A:	
Initiation of Uncontrolled RCCA Withdrawal at Full Power with Minimum Reactivity Feedback (100 pcm/sec)	0
Power-Range High Neutron Flux High Trip Point Reached	1.38
Rods Begin to Fall into Core	2.03
Minimum DNBR Occurs	2.75
Case B:	
Initiation of Uncontrolled RCCA Withdrawal at Full Power with Minimum Reactivity Feedback (3 pcm/sec)	0
OTΔT Reactor Trip Signal Initiated	45.28
Rods Begin to Fall into Core	47.28
Minimum DNBR occurs	47.63

Table 14.1.2-2
Limiting Results for RCCA Bank Withdrawal at Power Transient

Criterion	Limiting Value	Analysis Limit	Case
DNBR	1.46	1.34	Full power, minimum reactivity feedback, 4 pcm/second reactivity insertion rate
Core Heat Flux (FON)	1.17	1.18	Full power, maximum reactivity feedback 37 pcm/second reactivity insertion rate
MSS Pressure (psia)	1204	1210	60% of full power, maximum reactivity feedback, 5 pcm/second reactivity insertion rate

Table 14.1.4-1
Sequence of Events – Chemical and Volume Control System Malfunctions

	Event	Time (minutes)
Refueling	Dilution begins	0
	Shutdown margin is lost	> 30
Startup	Dilution begins	0
	Shutdown margin is lost	> 15
At Power		
Automatic Reactor Control	Dilution begins	0
	Shutdown margin is lost	> 15
Manual Reactor Control	Dilution begins	0
	OTΔT reactor trip signal reached	2.38
	Rod motion begins	2.41
	Shutdown margin is lost (if dilution continues after trip)	> 22.68

Table 14.1.6-1
Sequence of Events for Feedwater System Malfunction Event at Full Power

Event	Time (Seconds)	
	Without Automatic Rod Control	With Automatic Rod Control
Main Feedwater Control Valves Fail Full Open	0.0	0.0
Hi-Hi Steam Generator Water Level Trip Setpoint is Reached	80.8	81.5
Reactor Trip Occurs Due to Turbine Trip	83.7	84.4
Turbine Trip Occurs Due to Hi-Hi Steam Generator Level	81.9	82.6
Minimum DNBR Occurs	83.4	84.1
Feedwater Isolation Valves Fully Closed	166.0	166.7
Results		
Peak Nuclear Power, Fraction of Initial	1.164	1.169
Peak Core Heat Flux, Fraction of Initial	1.157	1.162
Minimum DNBR	1.730	1.709
Safety Analysis Limit DNBR (WRB-1 correlation limit)	1.34	1.34

Table 14.1.6-2
Sequence of Events for Feedwater System Malfunction Event at Zero Power

Event	Time (Seconds)
Main Feedwater Control Valves Fail Full Open	0.0
Hi-Hi Steam Generator Water Level Trip Setpoint is Reached	51.3
Feedwater Isolation Valves Fully Closed	125.4
Results	
Peak Nuclear Power, Fraction of Initial	0.207
Peak Core Heat Flux, Fraction of Initial	0.210
Minimum DNBR	2.837
Safety Analysis Limit DNBR (W-3 correlation limit)	1.472

Table 14.1.8-1
Sequence of Events – Partial Loss of Reactor Coolant Flow

Event	Time (seconds)
One Operating RCP Loses Power and Begins Coasting Down	0.0
Low Flow Reactor Trip Setpoint is Reached	1.62
Rods Begin to Drop	2.37
Minimum DNBR Occurs	3.50

Table 14.1.8-2
Sequence of Events – Complete Loss of Reactor Coolant Flow

Event	Time (seconds)
Complete Loss of Flow	
All Operating RCPs Lose Power and Coastdown Begins	0.0
Low Flow Reactor Trip Setpoint is Reached	1.82
Rods Begin to Drop	2.57
Minimum DNBR Occurs	4.00
Complete Loss of Flow - Underfrequency	
Frequency Decay Begins and All Operating RCPs Begin to Decelerate	0.0
Low Flow Reactor Trip Setpoint is Reached	1.88
Rods Begin to Drop	2.63
Minimum DNBR Occurs	4.15

Table 14.1.8-3
Sequence of Events – Reactor Coolant Pump Locked Rotor

Event	Time (seconds)
Rotor on One Pump Locks	0.00
Low Flow Reactor Trip Setpoint Reached	0.05
Rods Begin to Drop	0.80
Loss-of-Offsite-Power (remaining active pump begins to coastdown)	0.80
Maximum RCS Pressure Occurs	4.50
Maximum Cladding Temperature Occurs	5.00

Table 14.1.9-1
Sequence of Events and Transient Results – Loss of External Electrical Load –
With Pressurizer Pressure Control (for Minimum DNB)

Event	Time (seconds)
Turbine Trip	0.0
Reactor Trip on OTΔT	11.9
Rod Motion Begins	13.9
Time of Minimum DNBR	14.9
Time of Peak MSS Pressure	21.1
Minimum DNBR Value	1.74
DNBR Limit	1.34
Peak MSS Pressure	1194 psia
MSS Pressure Limit	1210 psia

Table 14.1.9-2
Sequence of Events and Transient Results – Loss of External Electrical Load – Without
Pressurizer Pressure Control (for Primary RCS Overpressure)

Event	Time (seconds)
Turbine Trip	0.0
Reactor Trip on High Pressurizer Pressure	7.9
Rod Motion Begins	8.9
Time of Peak RCS Pressure	11.1
Time of Peak MSS Pressure	16.9
Peak RCS Pressure	2697 psia
RCS Pressure Limit	2750 psia
Peak MSS Pressure	1182 psia
MSS Pressure Limit	1210 psia

Table 14.1.9-3

Sequence of Events and Transient Results – Loss of External Electrical Load – With Pressurizer Pressure Control (for MSS Overpressure)

Event	Time (seconds)
Turbine Trip	0.0
Reactor Trip on OTΔT	10.2
Rod Motion Begins	12.2
Time of Peak RCS Pressure	11.1
Time of Peak MSS Pressure	17.6
Peak RCS Pressure	2432 psia
RCS Pressure Limit	2750 psia
Peak MSS Pressure	1202 psia
MSS Pressure Limit	1210 psia

Table 14.1.10-1
Sequence of Events – Loss of Normal Feedwater

Event	Time (seconds)
Main Feedwater Flow Stops	20
Lo-Lo Steam Generator Water Level Trip Setpoint Reached	53.0
Rods Begin To Drop	54.5
Two Steam Generators Begin To Receive Auxiliary Feedwater	854.5
Peak Water Level In The Pressurizer Occurs	1157.5
Core Heat Decreases To Auxiliary Feedwater Heat Removal Capacity	~1300

Table 14.1.12-1
Sequence of Events – Loss of AC Power to the Plant Auxiliaries

Event	Time (seconds)
Main Feedwater Flow Stops	20
Lo-Lo Steam Generator Water Level Trip Setpoint Reached	54.7
Rods Begin to Drop	56.2
RCPs Begin to Coast Down	58.2
Two Steam Generators Begin to Receive Auxiliary Feedwater from One Motor-Driven AFW Pump	116.2
Peak Water Level in the Pressurizer Occurs	4235
Core Heat Decreases to Auxiliary Feedwater Heat Removal Capacity	~4300
Peak Pressurizer Water Volume	698 ft ³
Pressurizer Water Volume Limit	1000.0 ft ³

Figure 14.1.1-1
Uncontrolled RCCA Withdrawal from a Subcritical Condition
Reactor Power vs. Time

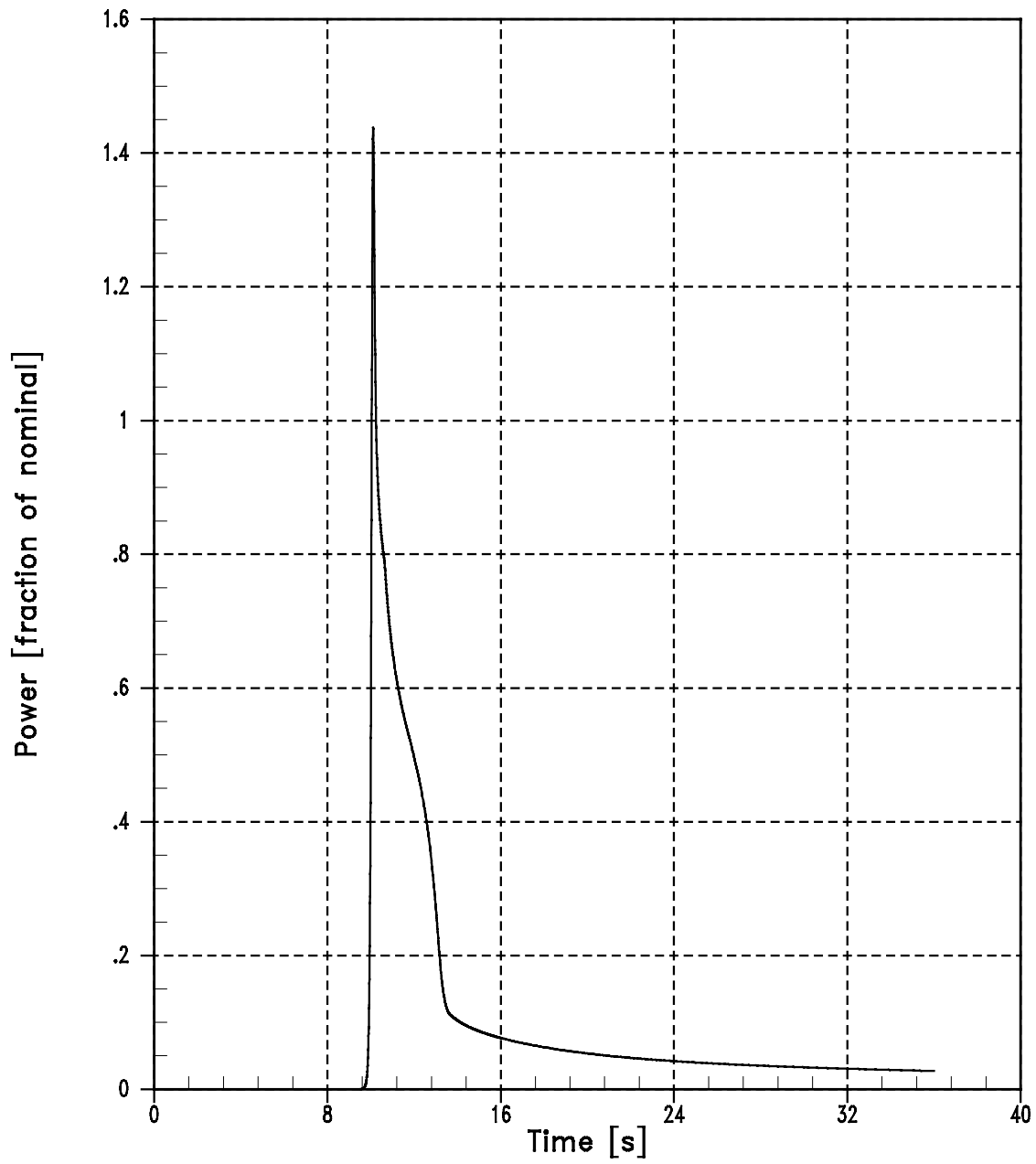


Figure 14.1.1-2
Uncontrolled RCCA Withdrawal From a Subcritical Condition Heat Flux vs. Time

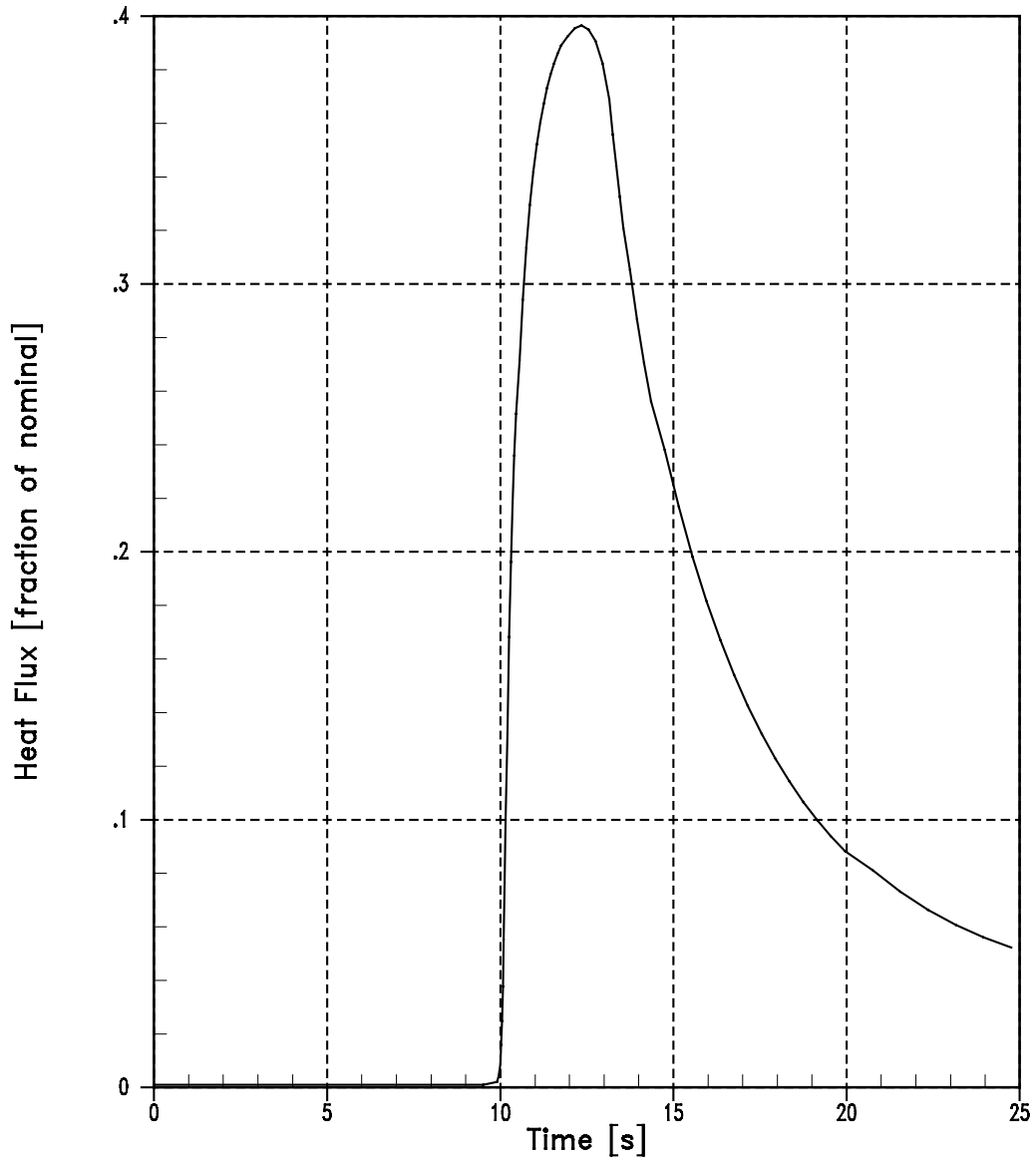


Figure 14.1.1-3
Uncontrolled RCCA Withdrawal from a Subcritical Condition
Hot-Spot Fuel Centerline Temperature vs. Time

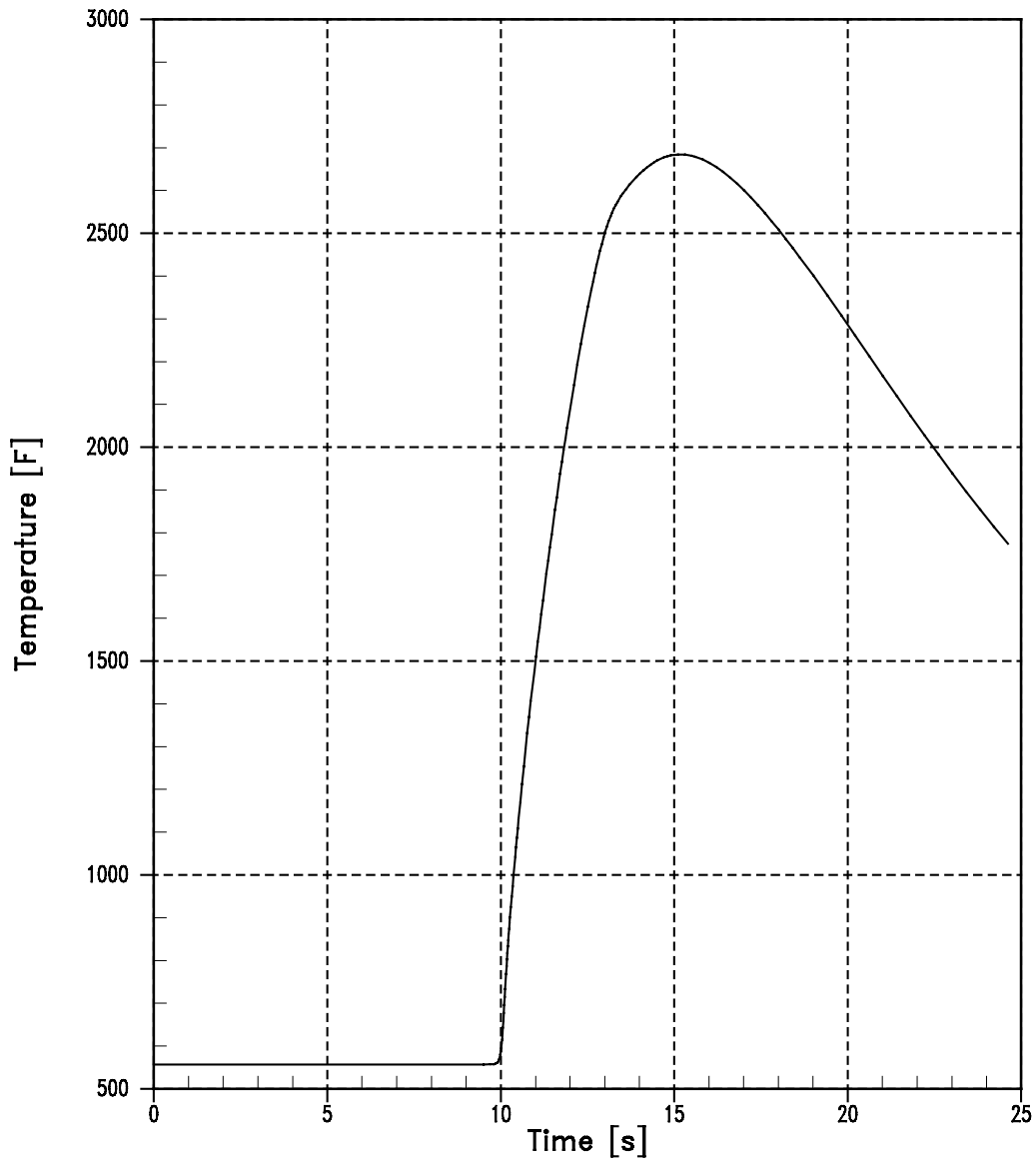


Figure 14.1.1-4
Uncontrolled RCCA Withdrawal from a Subcritical Condition
Hot-Spot Fuel Average Temperature vs. Time

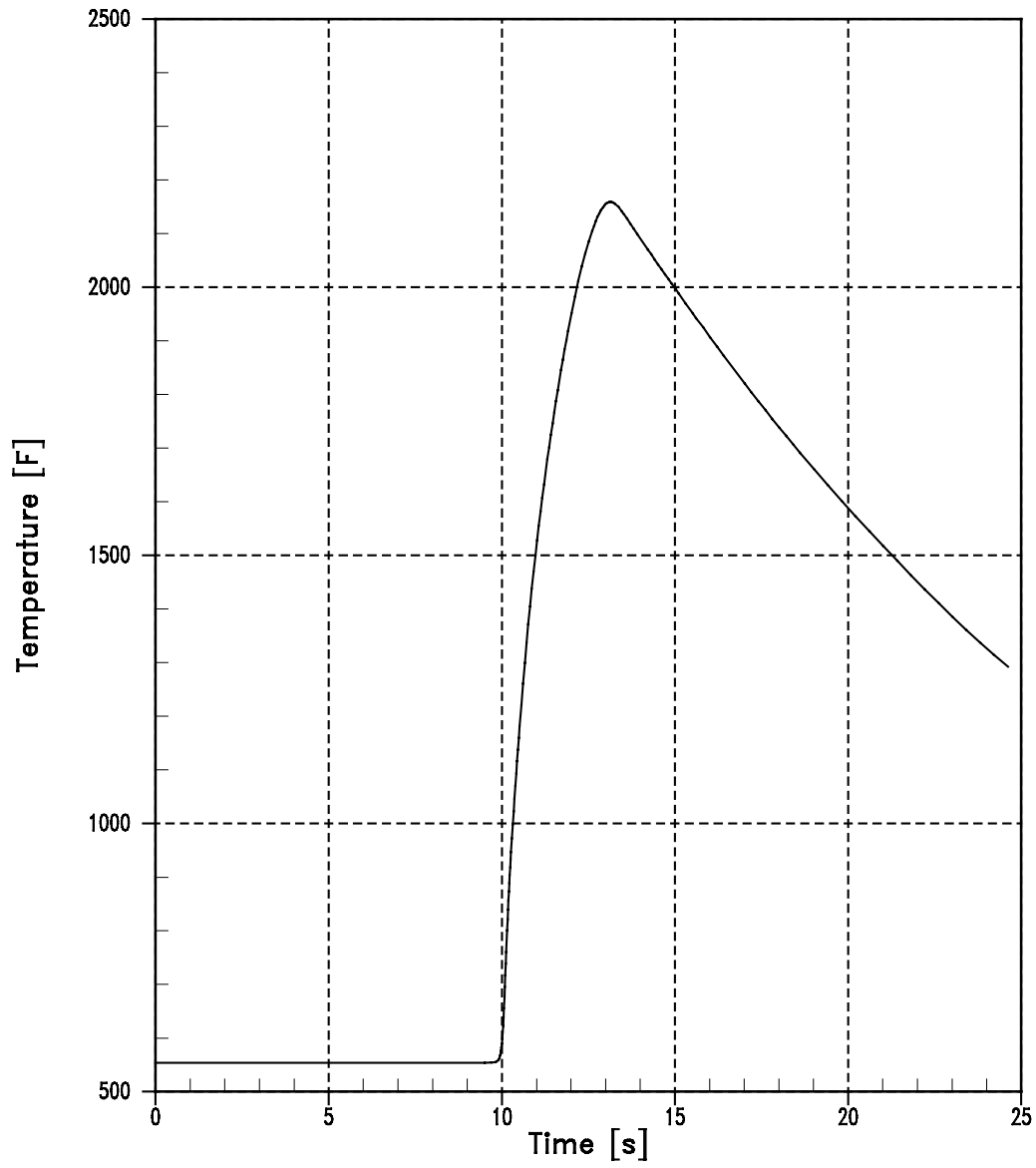


Figure 14.1.1-5
Uncontrolled RCCA Withdrawal from a Subcritical Condition
Hot-Spot Cladding Temperature vs. Time

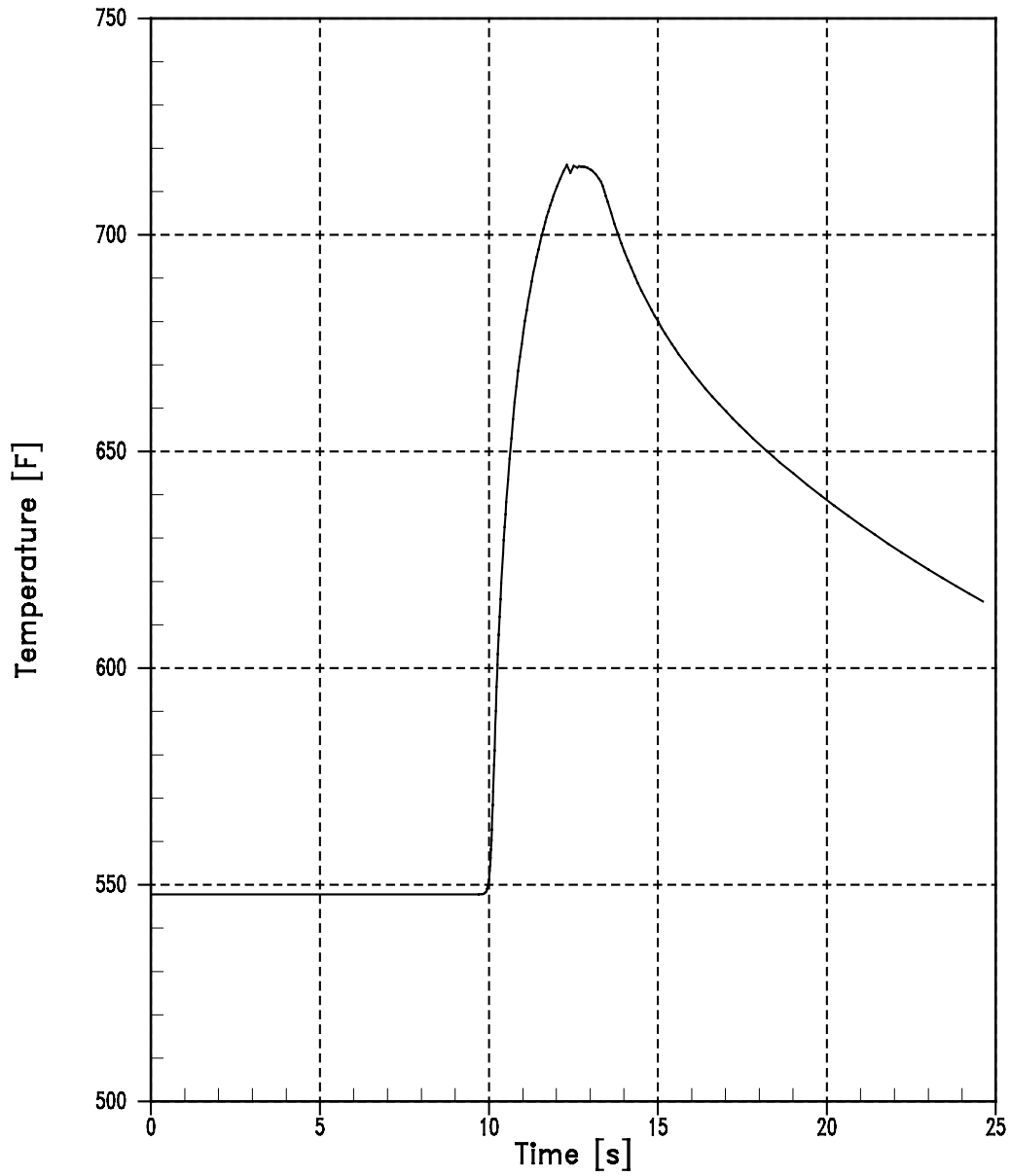


Figure 14.1.2-1 (Sheet 1 of 4)
Uncontrolled RCCA Bank Withdrawal at Power (100pcm/sec - Full Power)
Power-Range High Neutron Flux Trip
Maximum Nominal RCS Vessel T_{avg} , Minimum Feedback

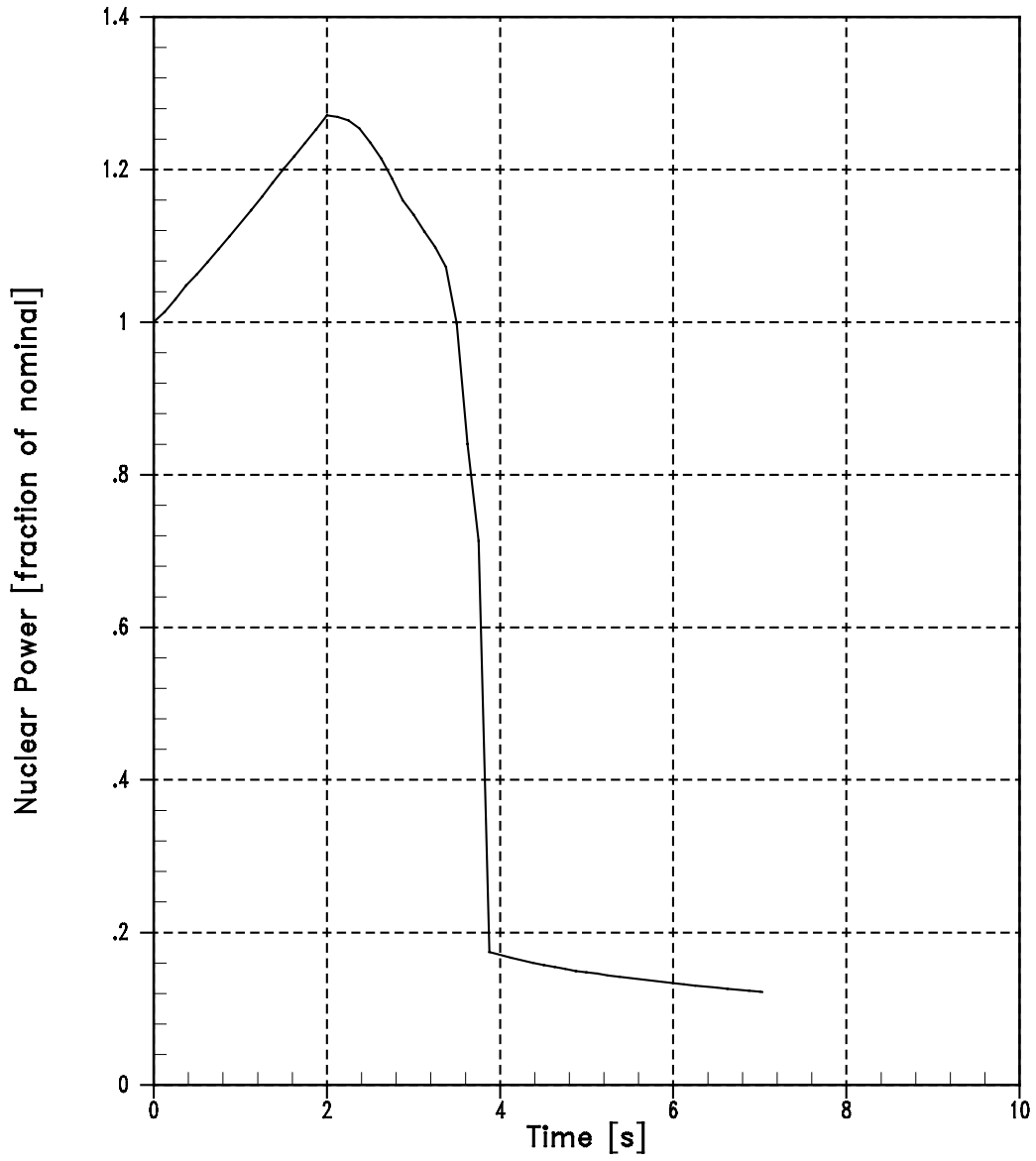


Figure 14.1.2-1 (Sheet 2 of 4)
Uncontrolled RCCA Bank Withdrawal at Power (100pcm/sec - Full Power)
Power-Range High Neutron Flux Trip
Maximum Nominal RCS Vessel T_{avg} , Minimum Feedback

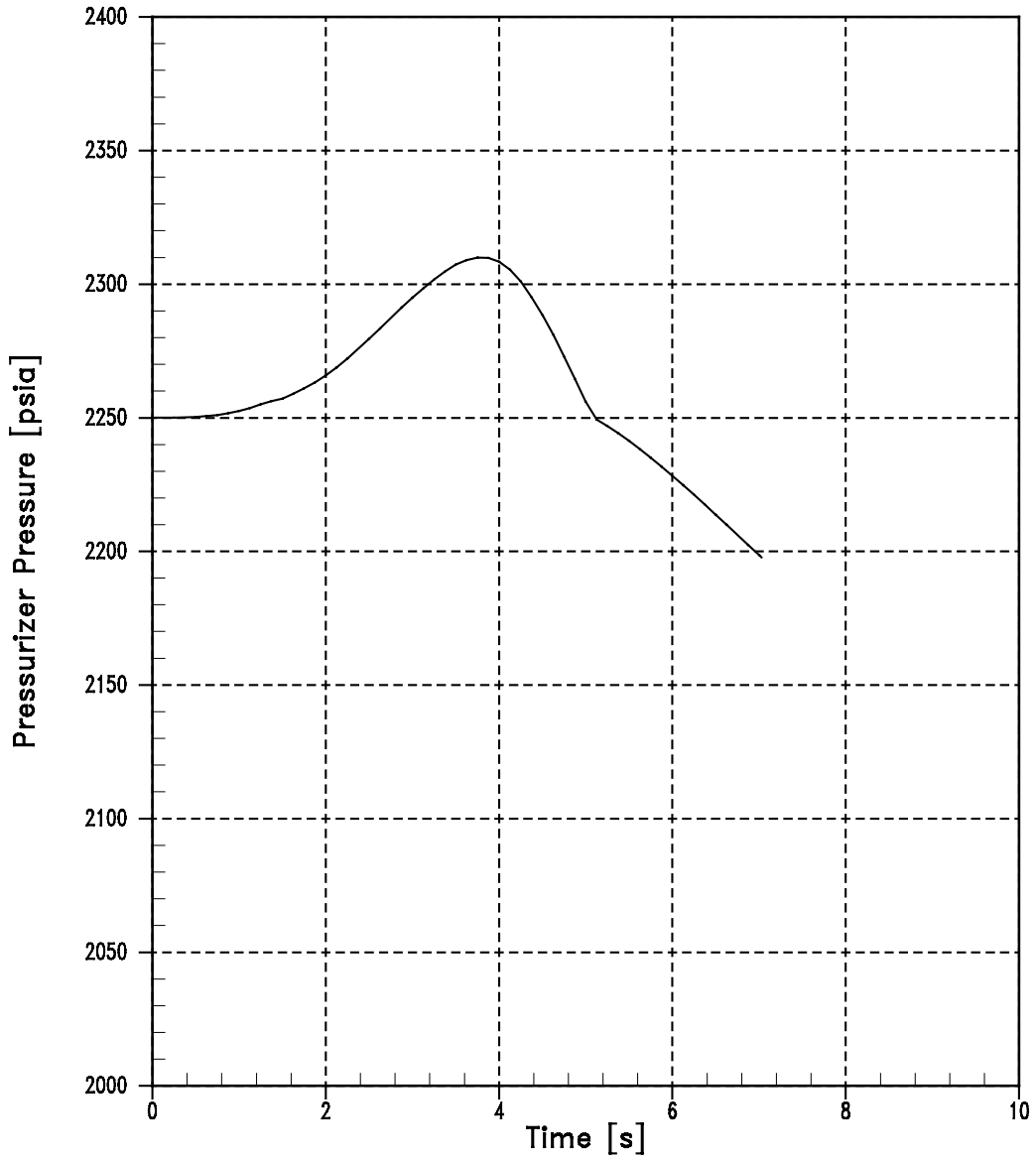


Figure 14.1.2-1 (Sheet 3 of 4)
Uncontrolled RCCA Bank Withdrawal at Power (100pcm/sec - Full Power)
Power-Range High Neutron Flux Trip
Maximum Nominal RCS Vessel T_{avg} , Minimum Feedback

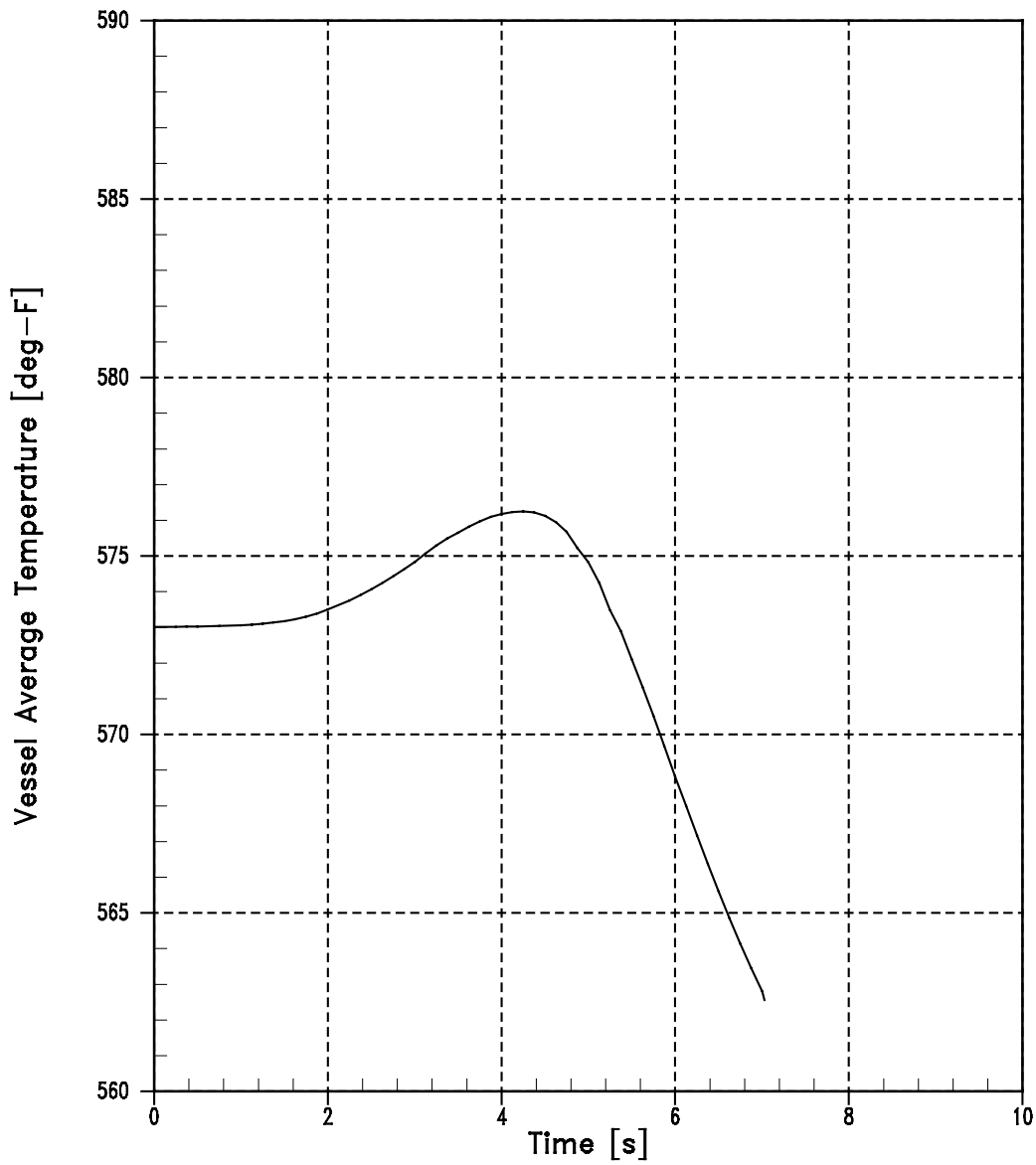


Figure 14.1.2-1 (Sheet 4 of 4)
Uncontrolled RCCA Bank Withdrawal at Power (100pcm/sec - Full Power)
Power-Range High Neutron Flux Trip
Maximum Nominal RCS Vessel T_{avg} , Minimum Feedback

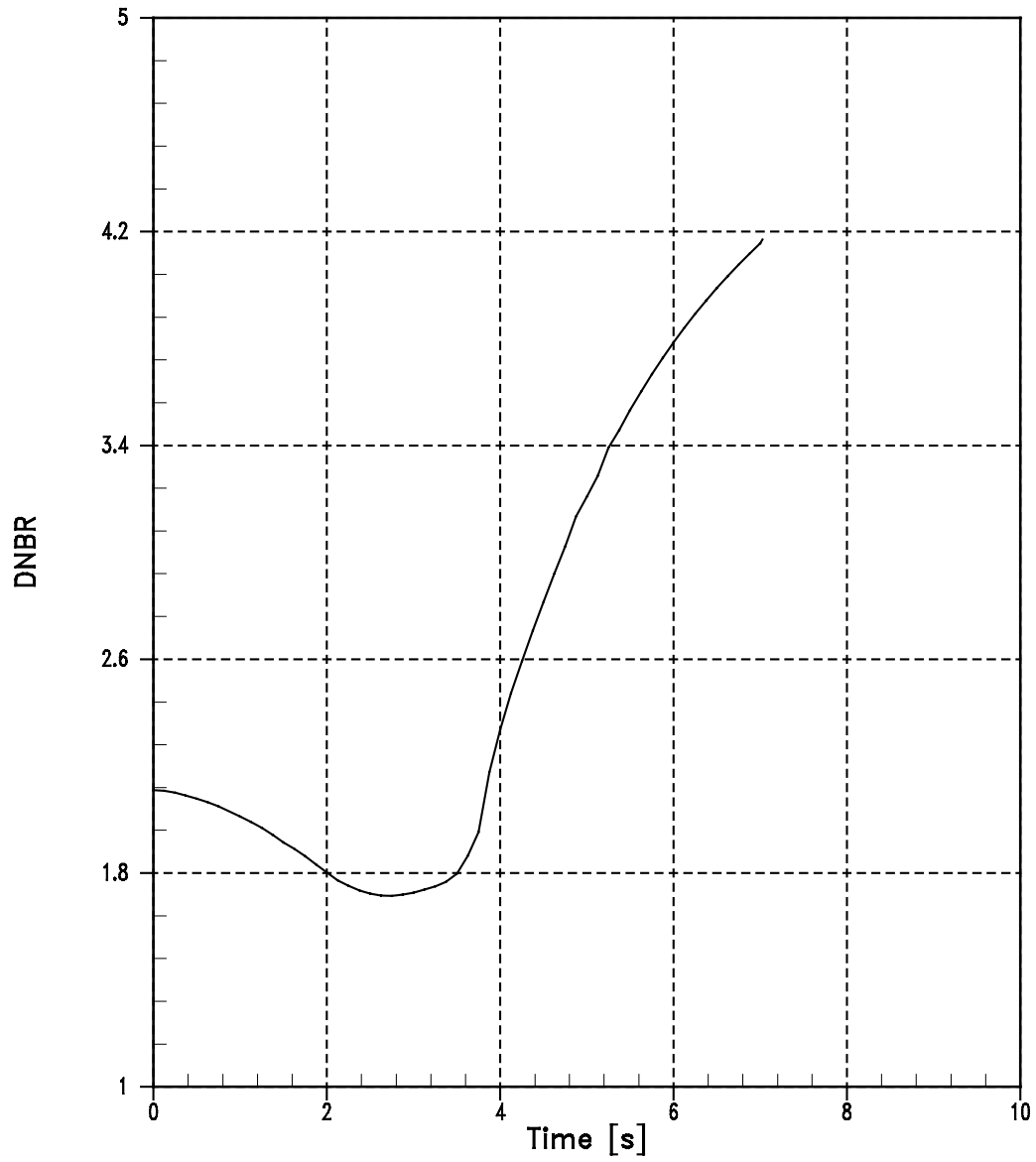


Figure 14.1.2-2 (Sheet 1 of 4)
Uncontrolled RCCA Bank Withdrawal at Power
(3 pcm/sec - 100 Percent Power) OTΔT Trip
Maximum Nominal RCS Vessel T_{avg} , Minimum Feedback

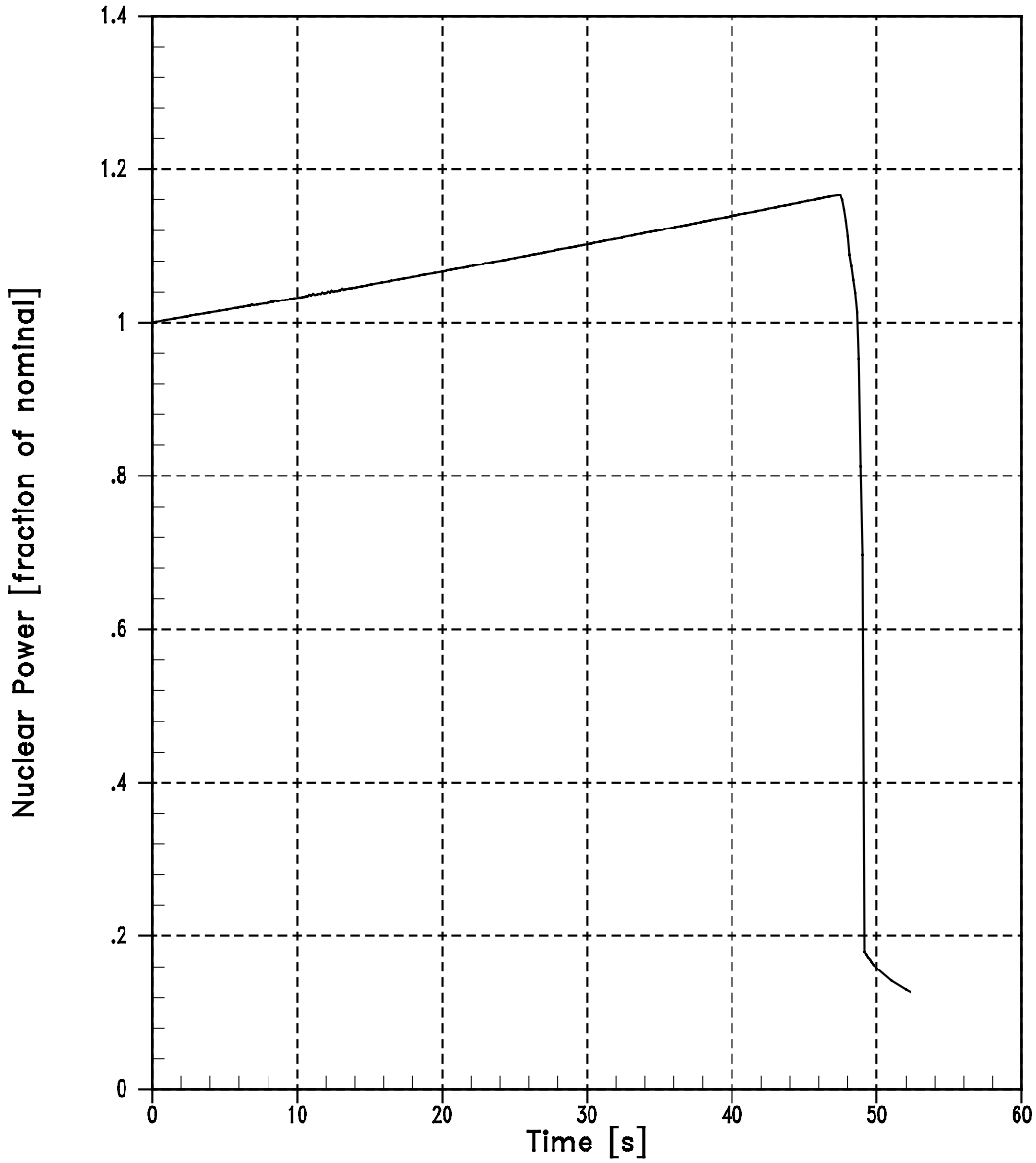


Figure 14.1.2-2 (Sheet 2 of 4)
Uncontrolled RCCA Bank Withdrawal at Power
(3 pcm/sec - 100 Percent Power) OTΔT Trip
Maximum Nominal RCS Vessel T_{avg} , Minimum Feedback

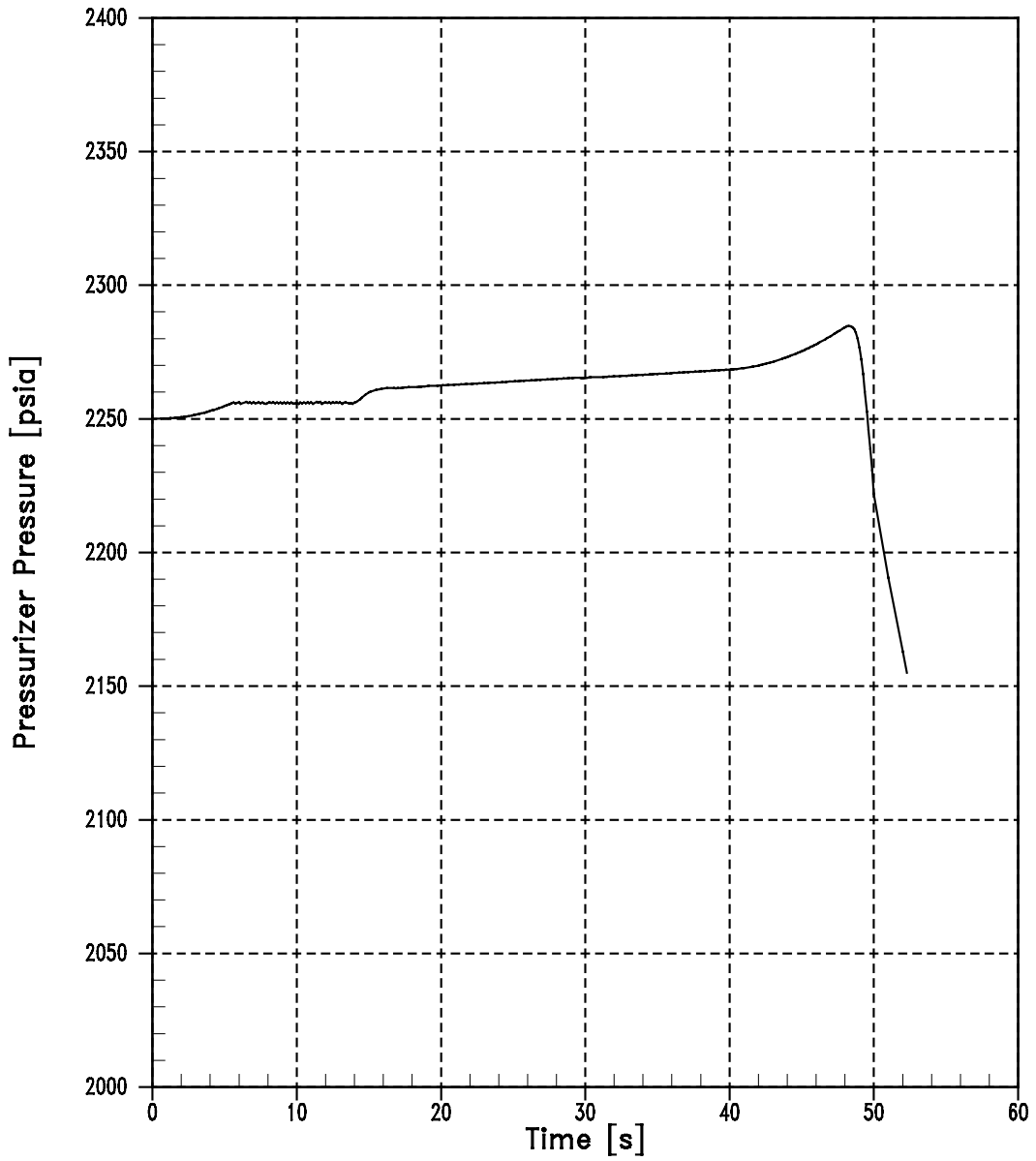


Figure 14.1.2-2 (Sheet 3 of 4)
Uncontrolled RCCA Bank Withdrawal at Power
(3 pcm/sec - 100 Percent Power) OTΔT Trip
Maximum Nominal RCS Vessel T_{avg} , Minimum Feedback

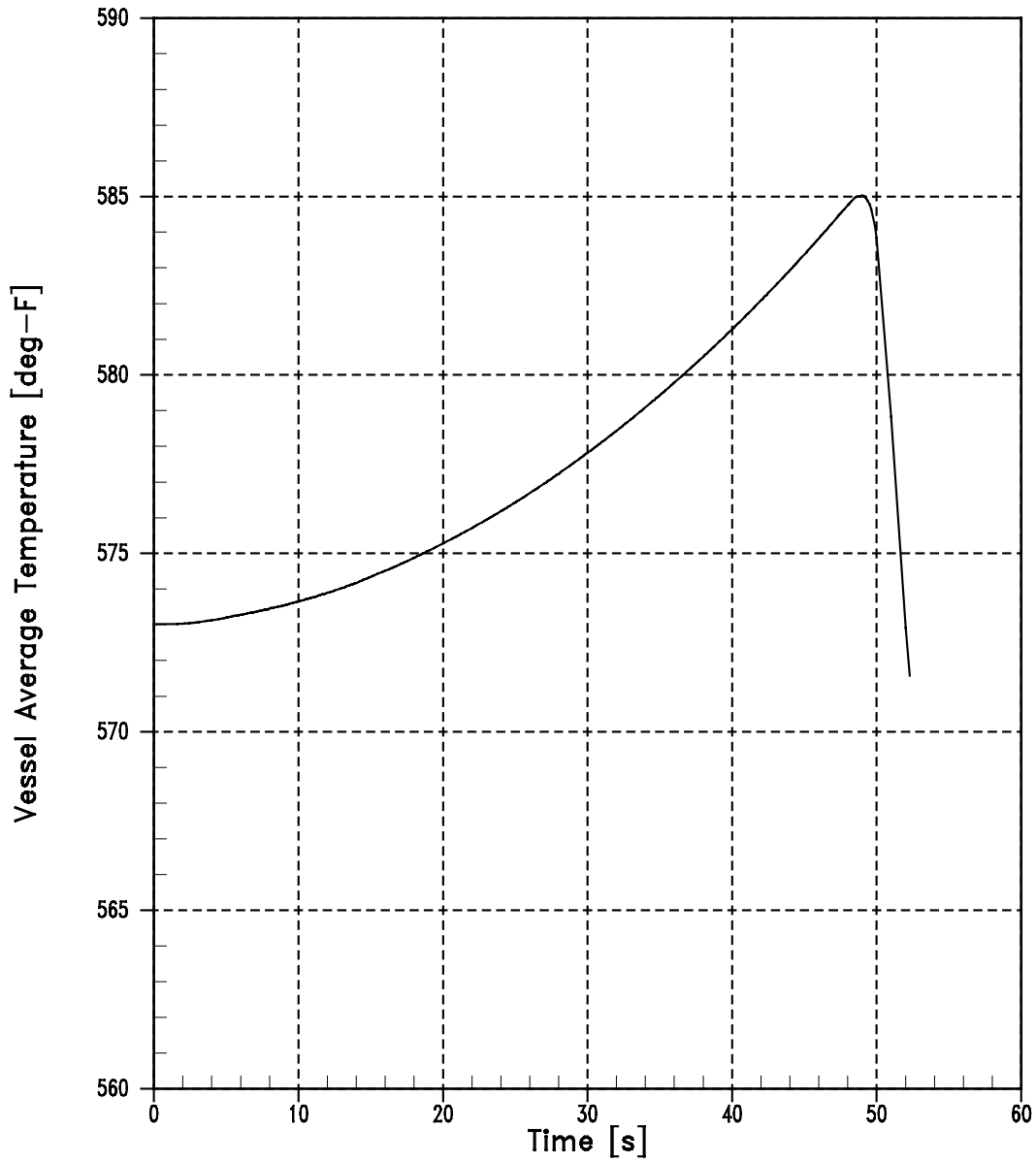


Figure 14.1.2-2 (Sheet 4 of 4)
Uncontrolled RCCA Bank Withdrawal at Power
(3 pcm/sec - 100 Percent Power) OTΔT Trip
Maximum Nominal RCS Vessel T_{avg} , Minimum Feedback

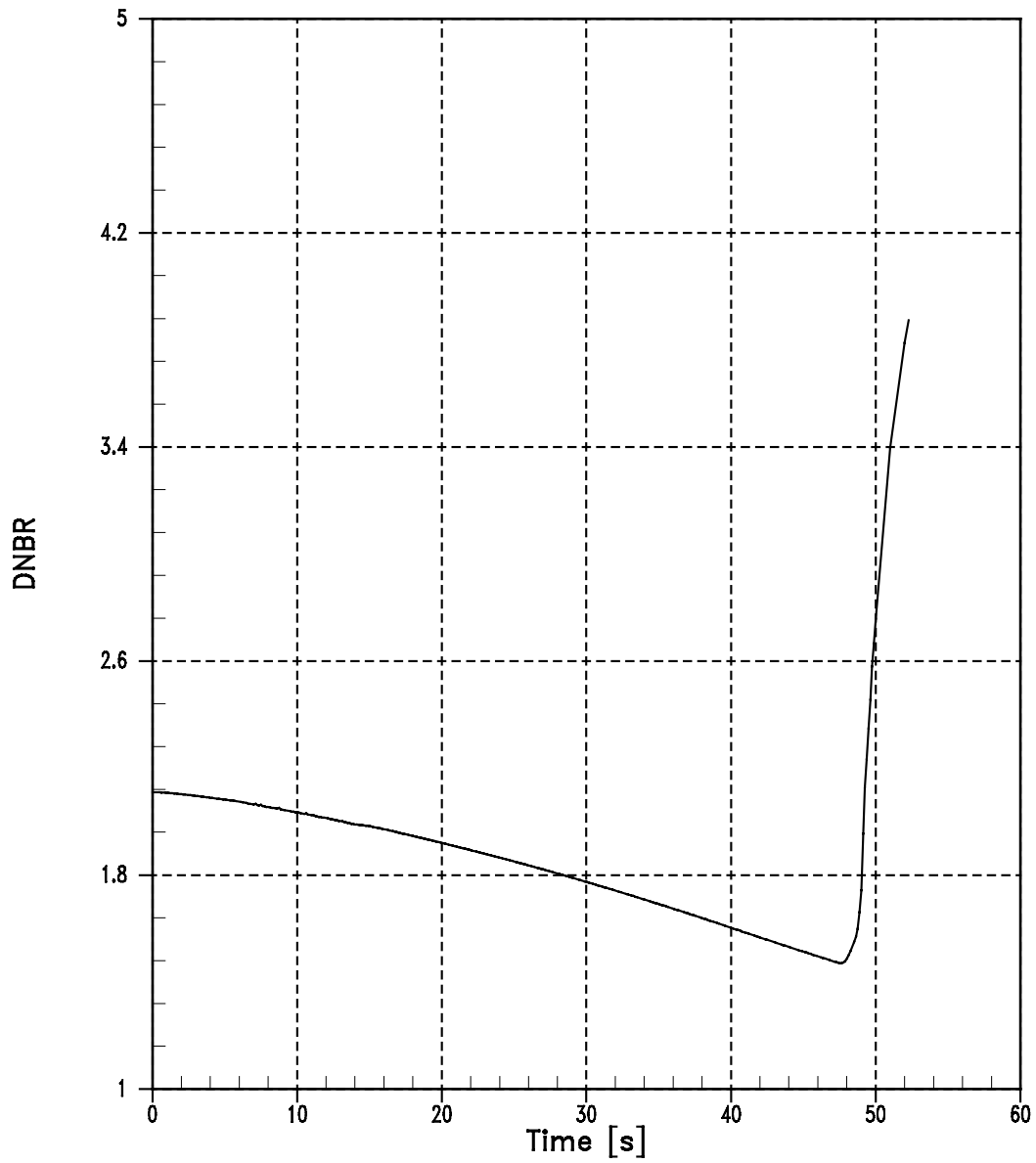


Figure 14.1.2-3
Uncontrolled RCCA Bank Withdrawal at Power, 100 Percent Power (Sheet 1 of 3)

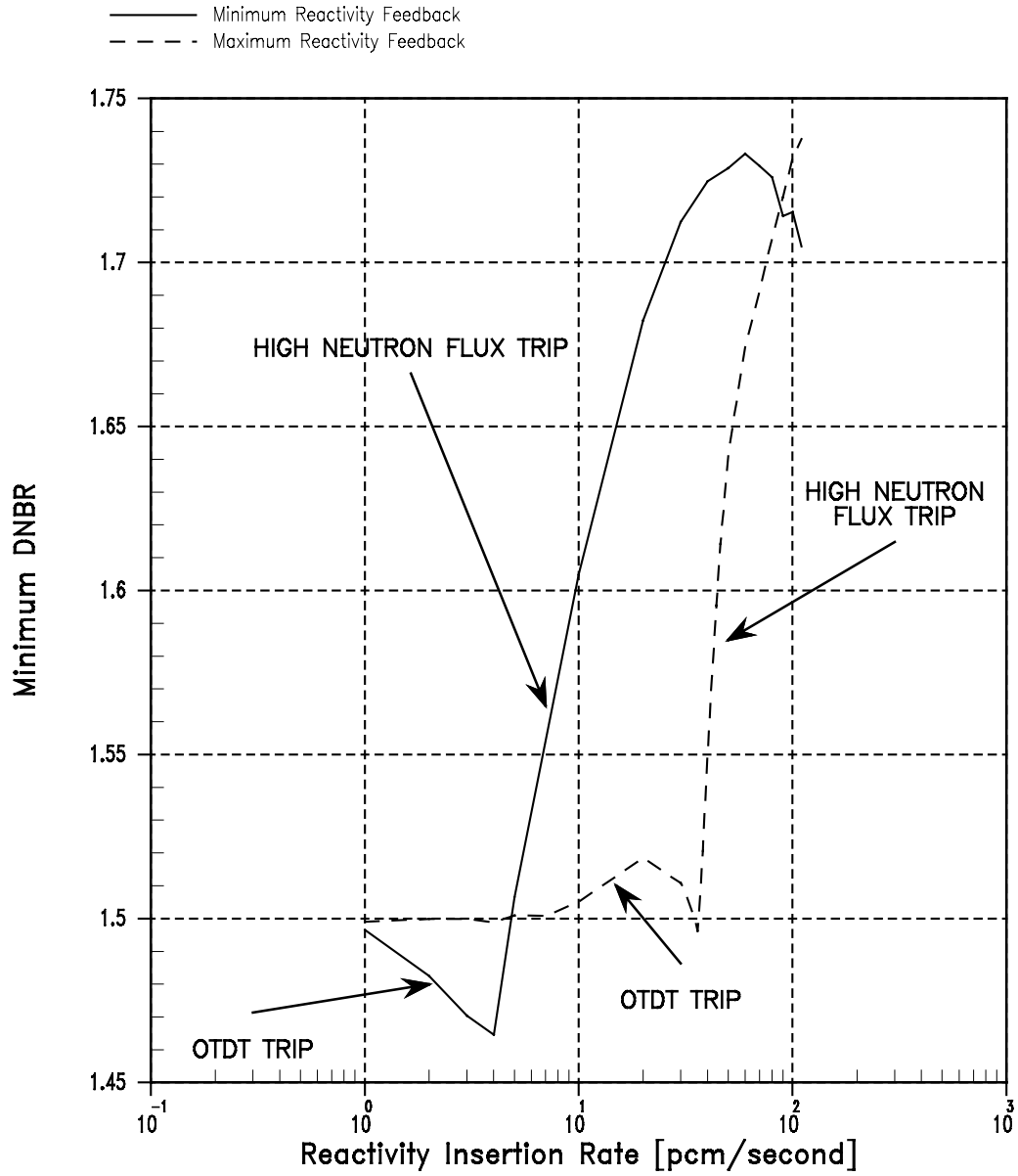


Figure 14.1.2-3 (Sheet 2 of 3)
Uncontrolled RCCA Bank Withdrawal at Power, 60 Percent Power

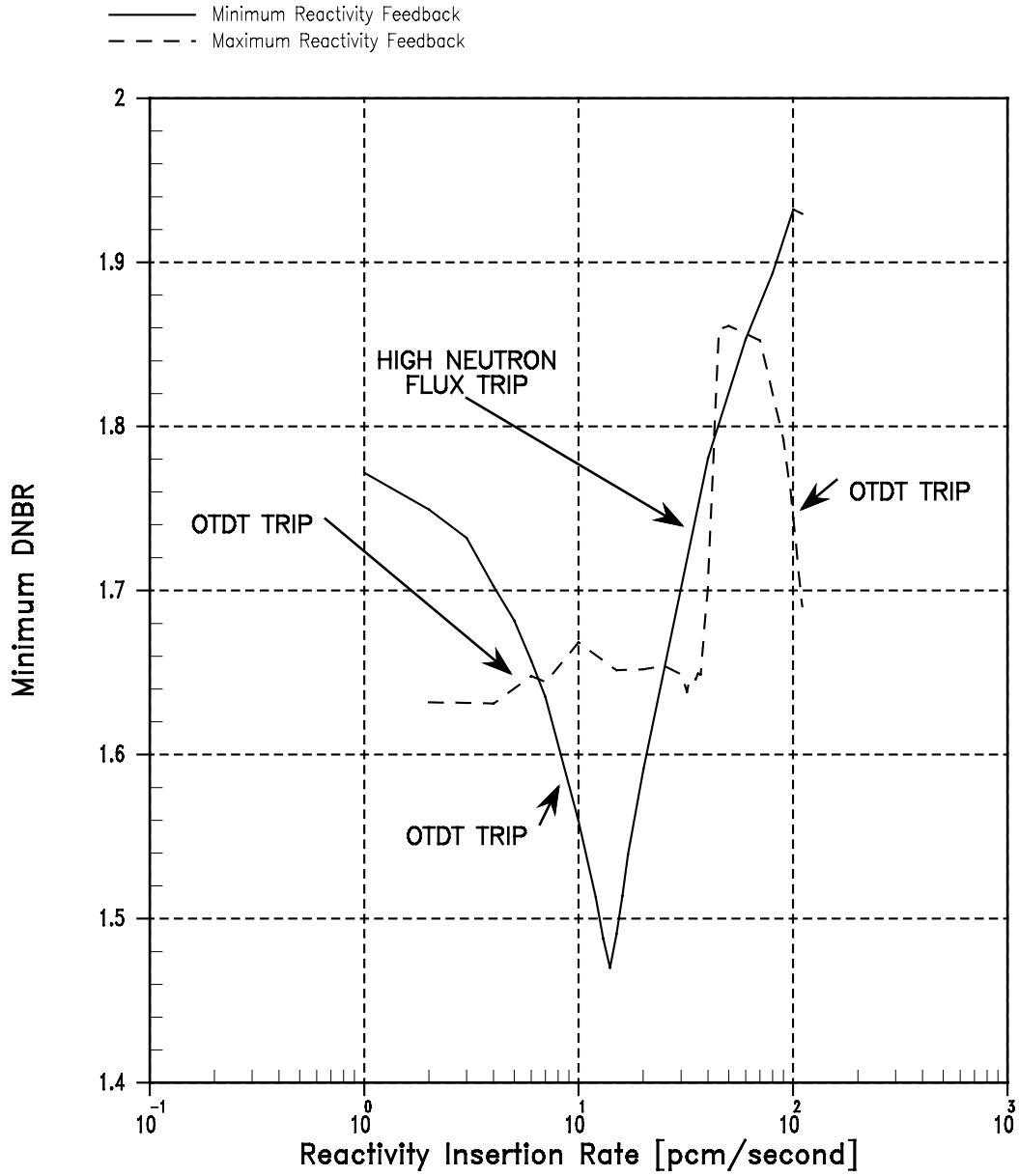


Figure 14.1.2-3 (Sheet 3 of 3)
Uncontrolled RCCA Bank Withdrawal at Power, 10 Percent Power

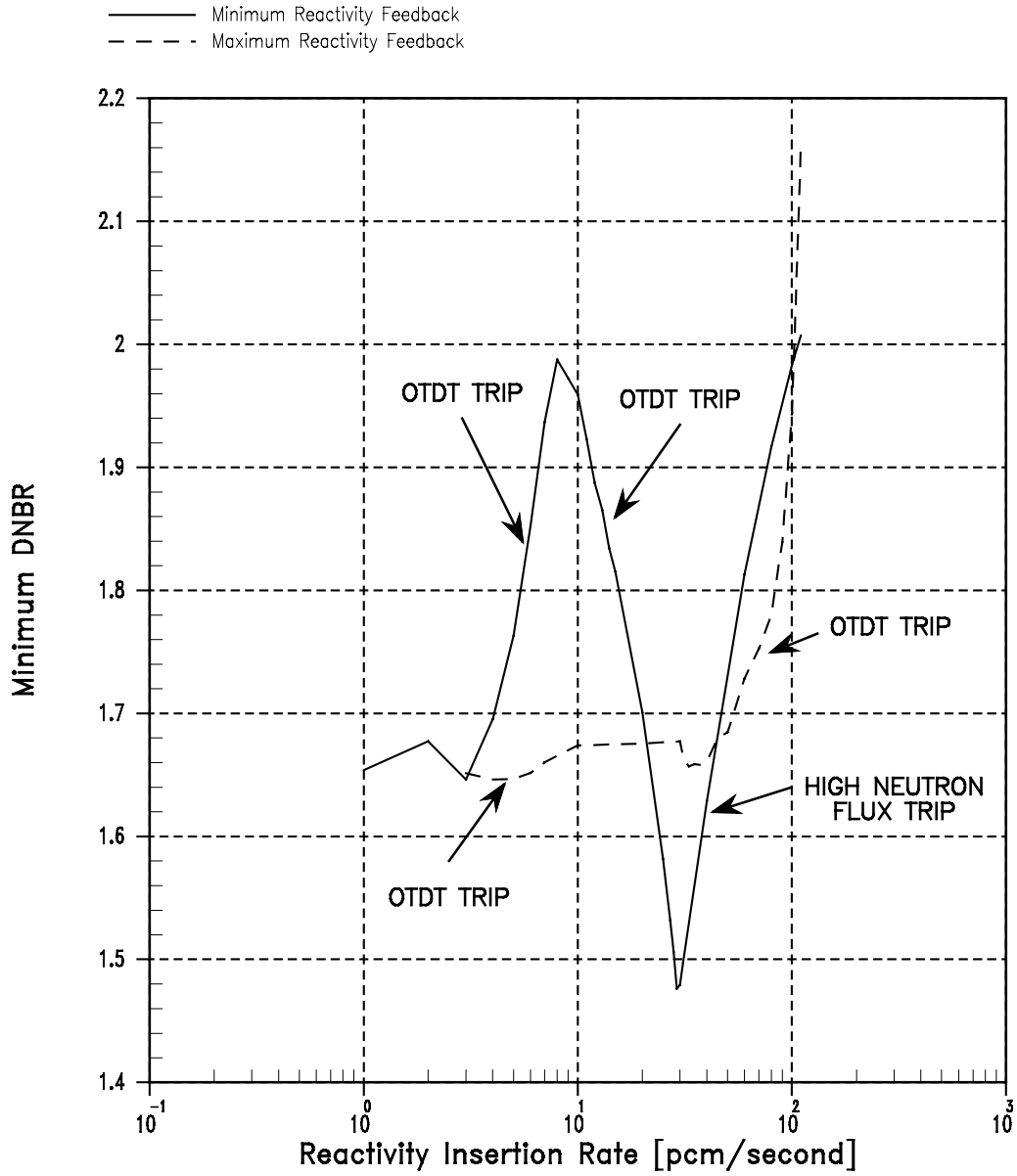


Figure 14.1.3-1
Representative Transient Response to Dropped RCCA
Nuclear Power vs. Time

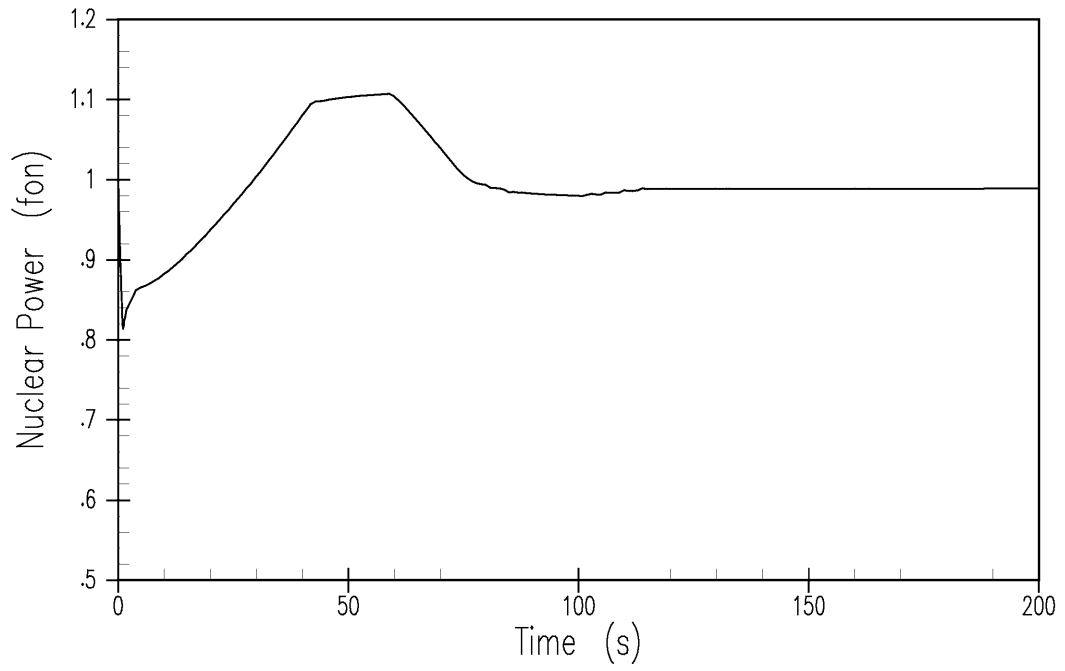


Figure 14.1.3-2
Representative Transient Response to Dropped RCCA
Core Heat Flux vs. Time

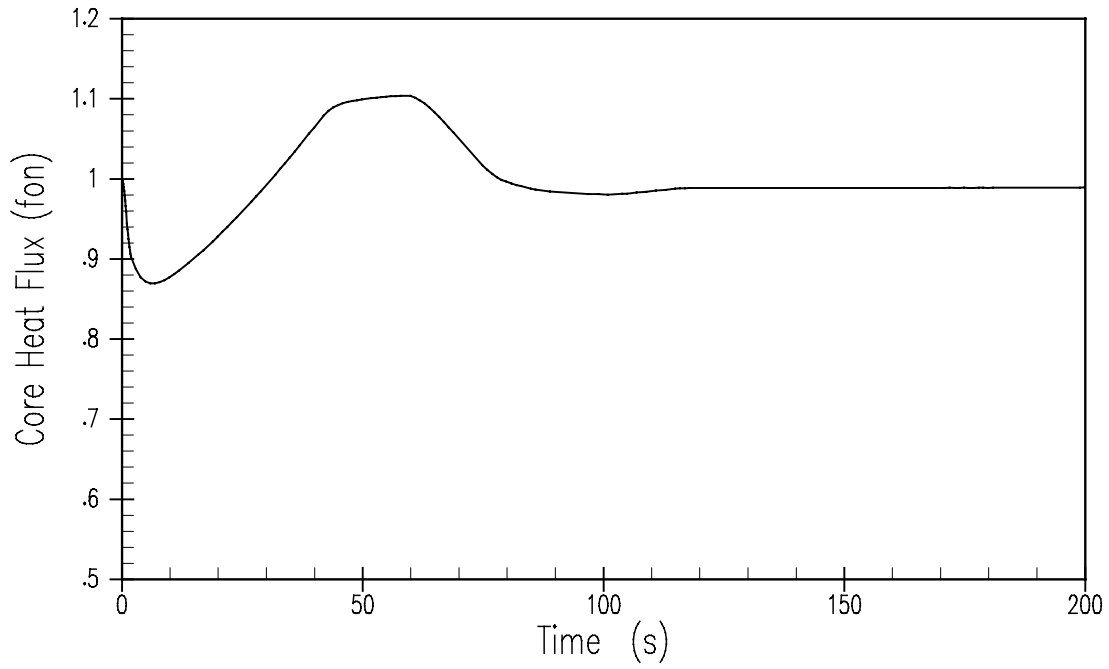


Figure 14.1.3-3
Representative Transient Response to Dropped RCCA
Pressurizer Pressure vs. Time

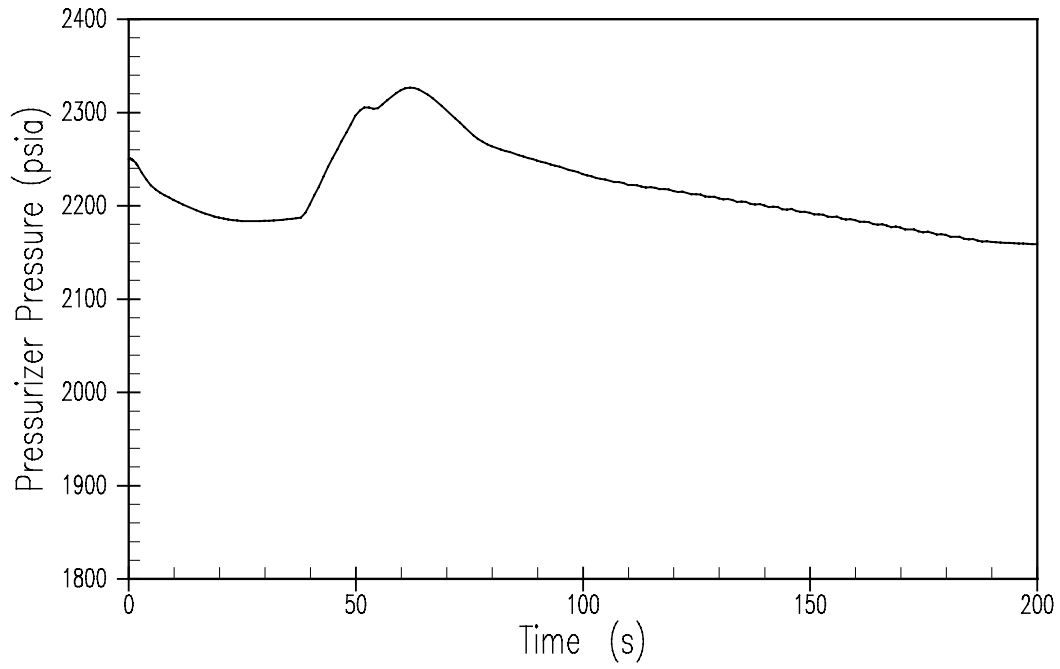


Figure 14.1.3-4
Representative Transient Response to Dropped RCCA
Vessel Average Temperature vs. Time

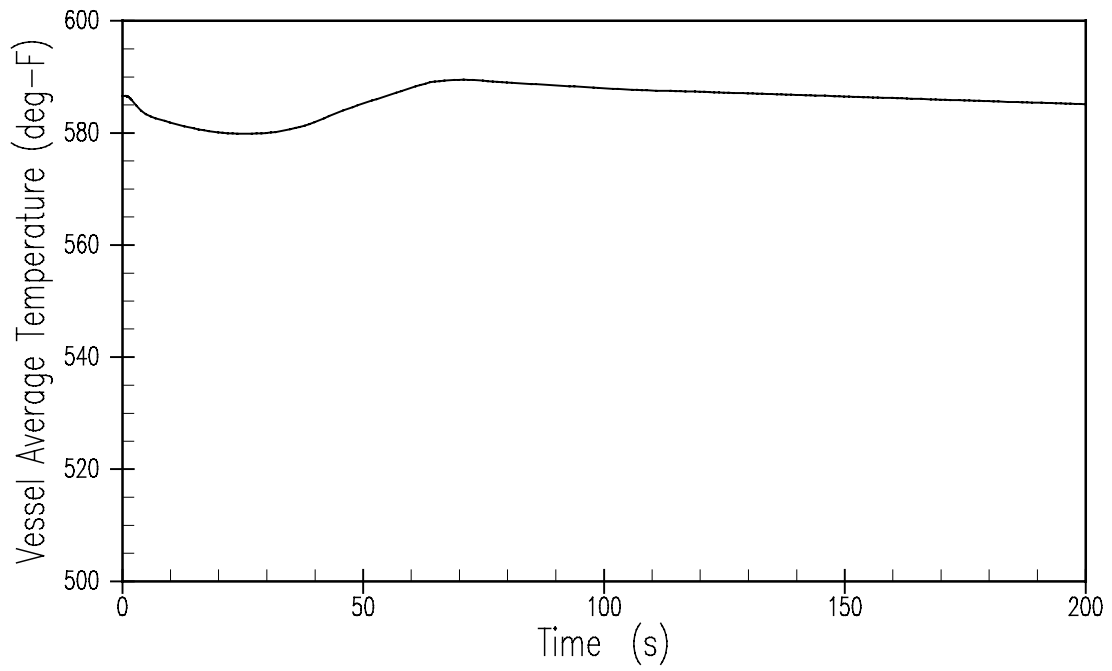


Figure 14.1.4-1
CVCS Malfunction - Dilution at Power - Manual Control - High Pressure
Reactor Power vs. Time

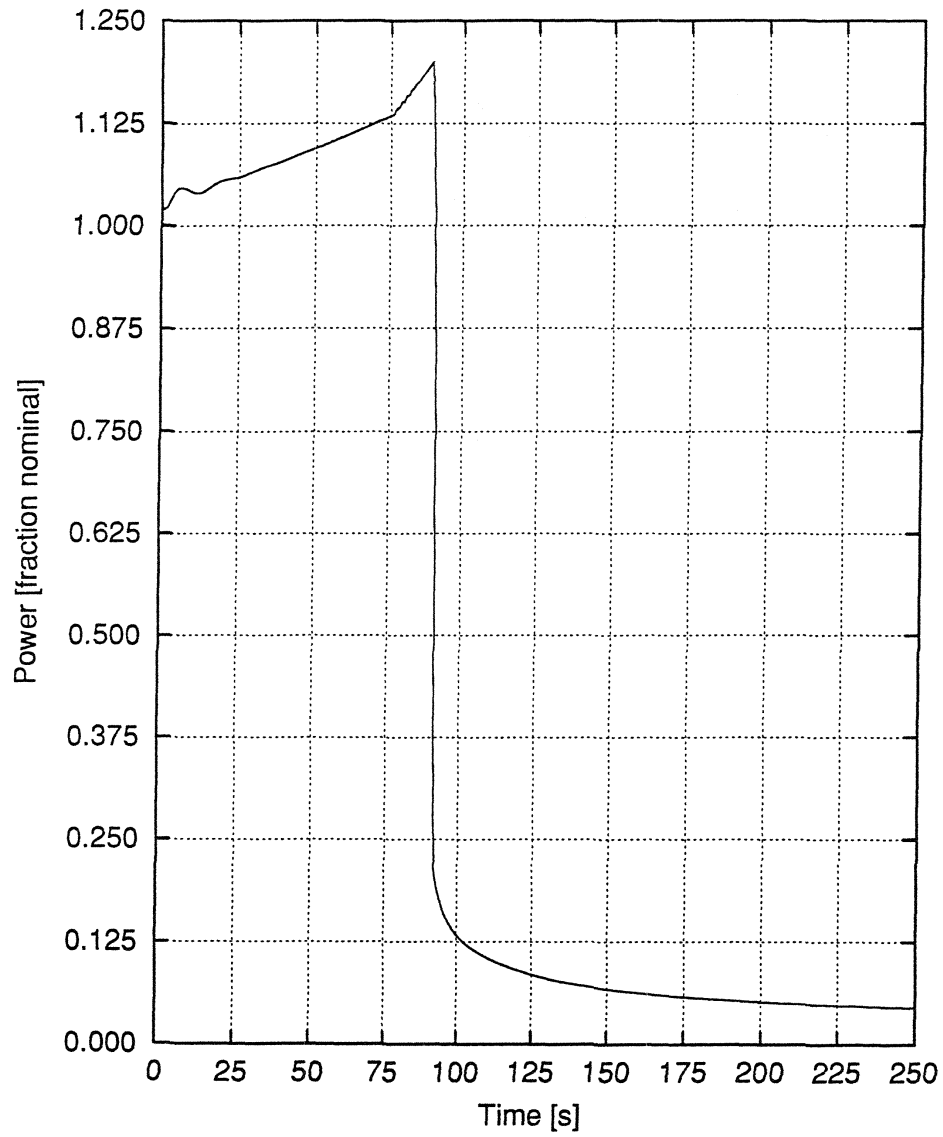


Figure 14.1.4-2
CVCS Malfunction - Dilution at Power - Manual Control - High Pressure
Pressurizer Pressure vs. Time

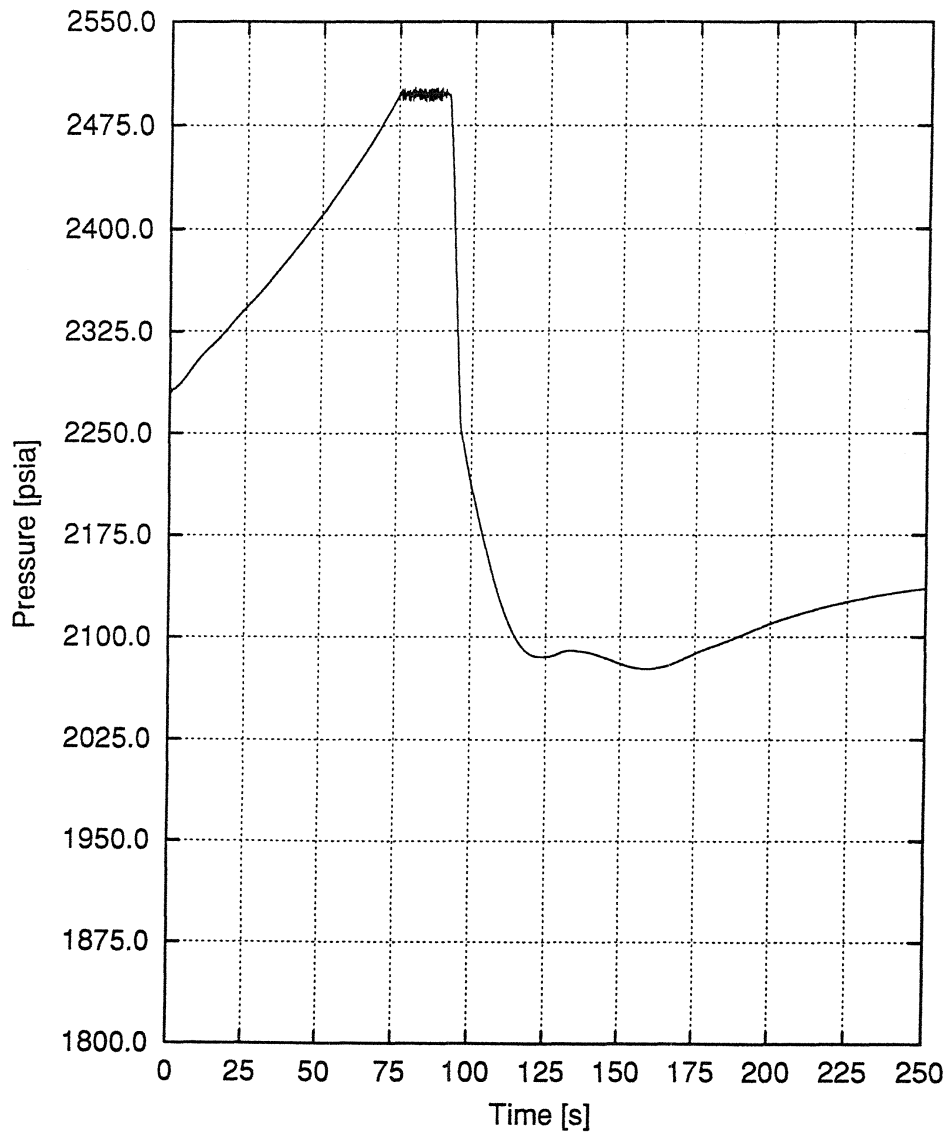


Figure 14.1.4-3
CVCS Malfunction - Dilution at Power - Manual Control
High Pressure T_{ave} vs. Time

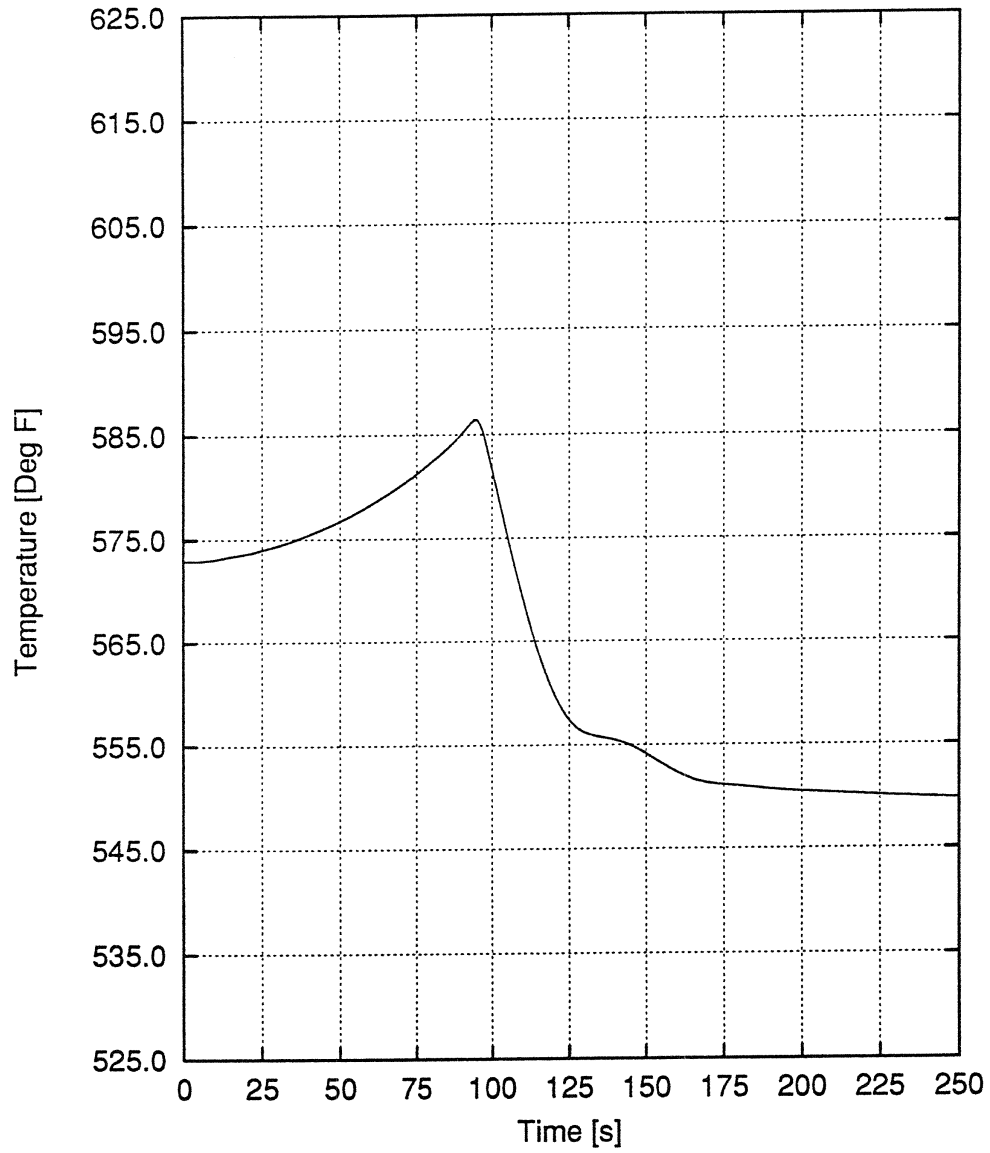


Figure 14.1.4-4
CVCS Malfunction - Dilution at Power - Manual Control
High Pressure Heat Flux vs. Time

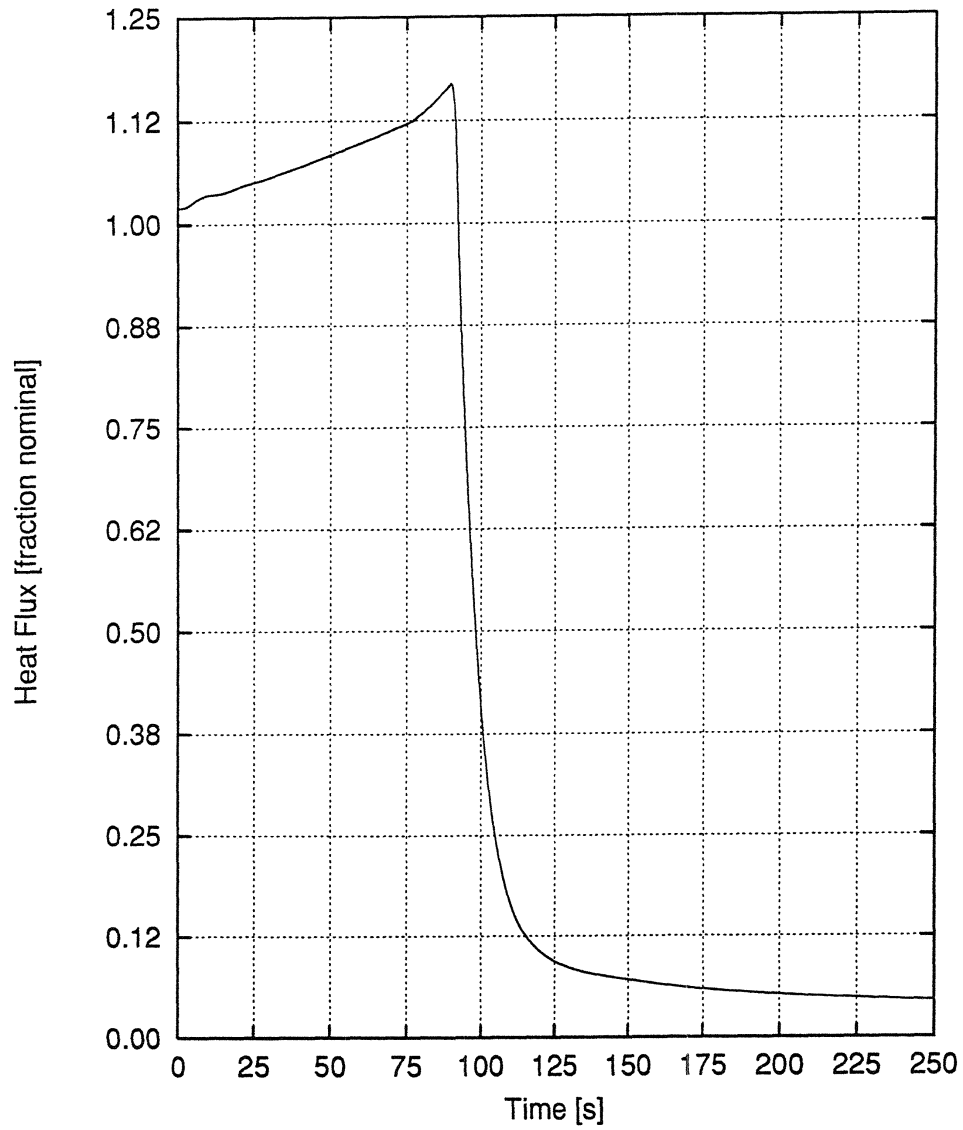


Figure 14.1.4-5
CVCS Malfunction - Dilution at Power - Manual Control
High Pressure Minimum DNBR vs. Time

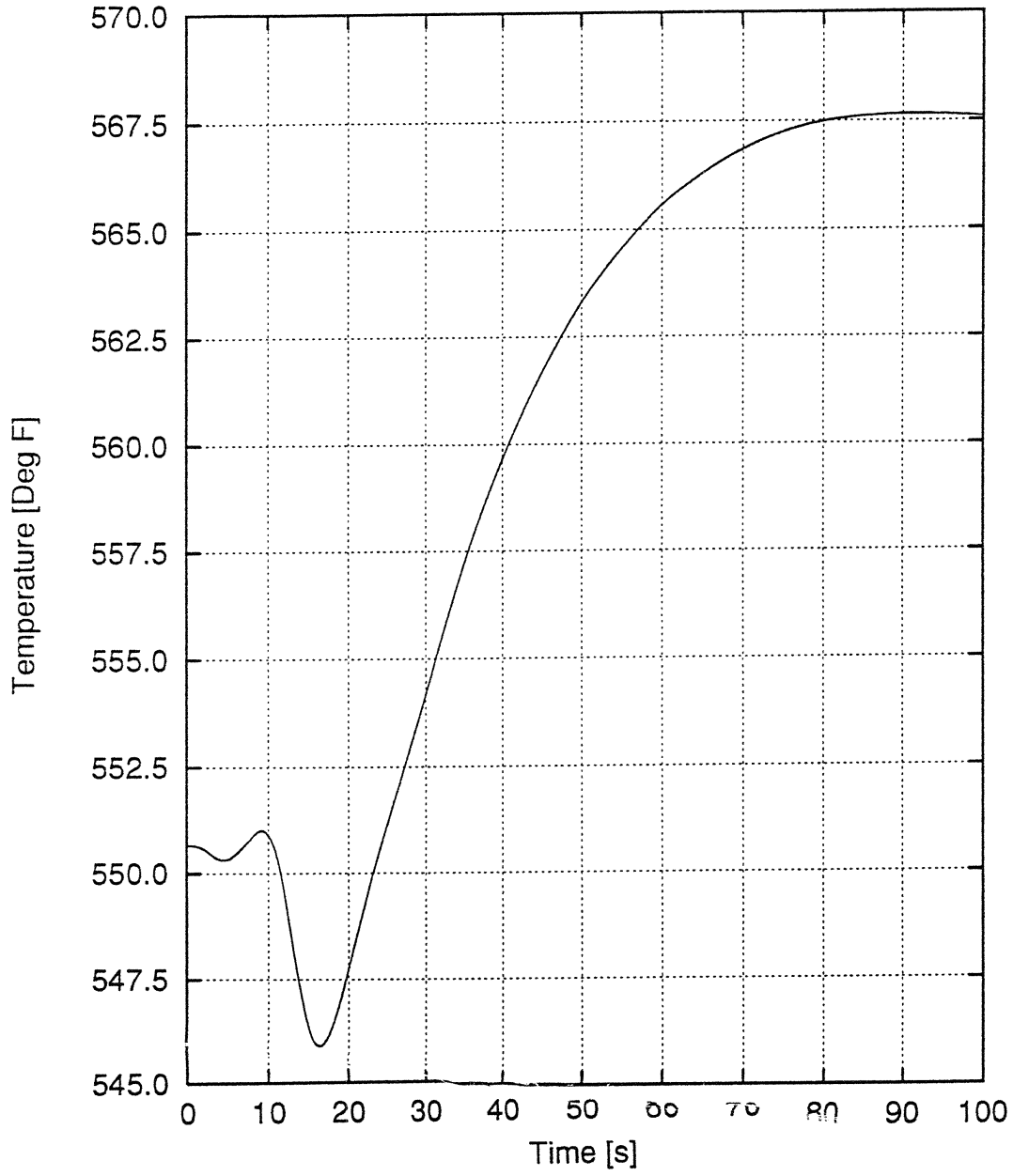


Figure 14.1.5-1
Startup of an Inactive Reactor Coolant Loop
 T_{inlet} vs. Time

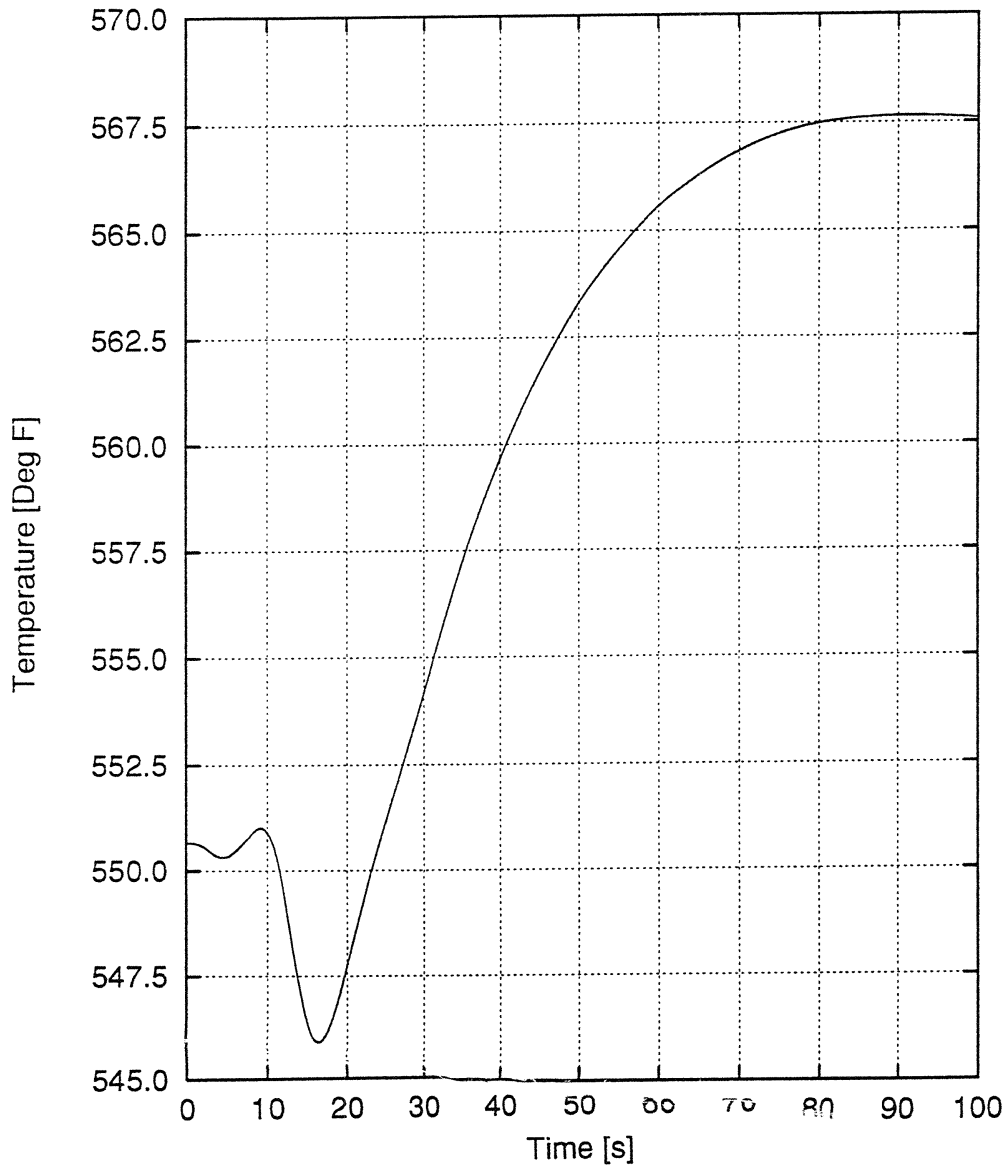


Figure 14.1.5-2
Startup of an Inactive Reactor Coolant Loop
 T_{ave} vs. Time

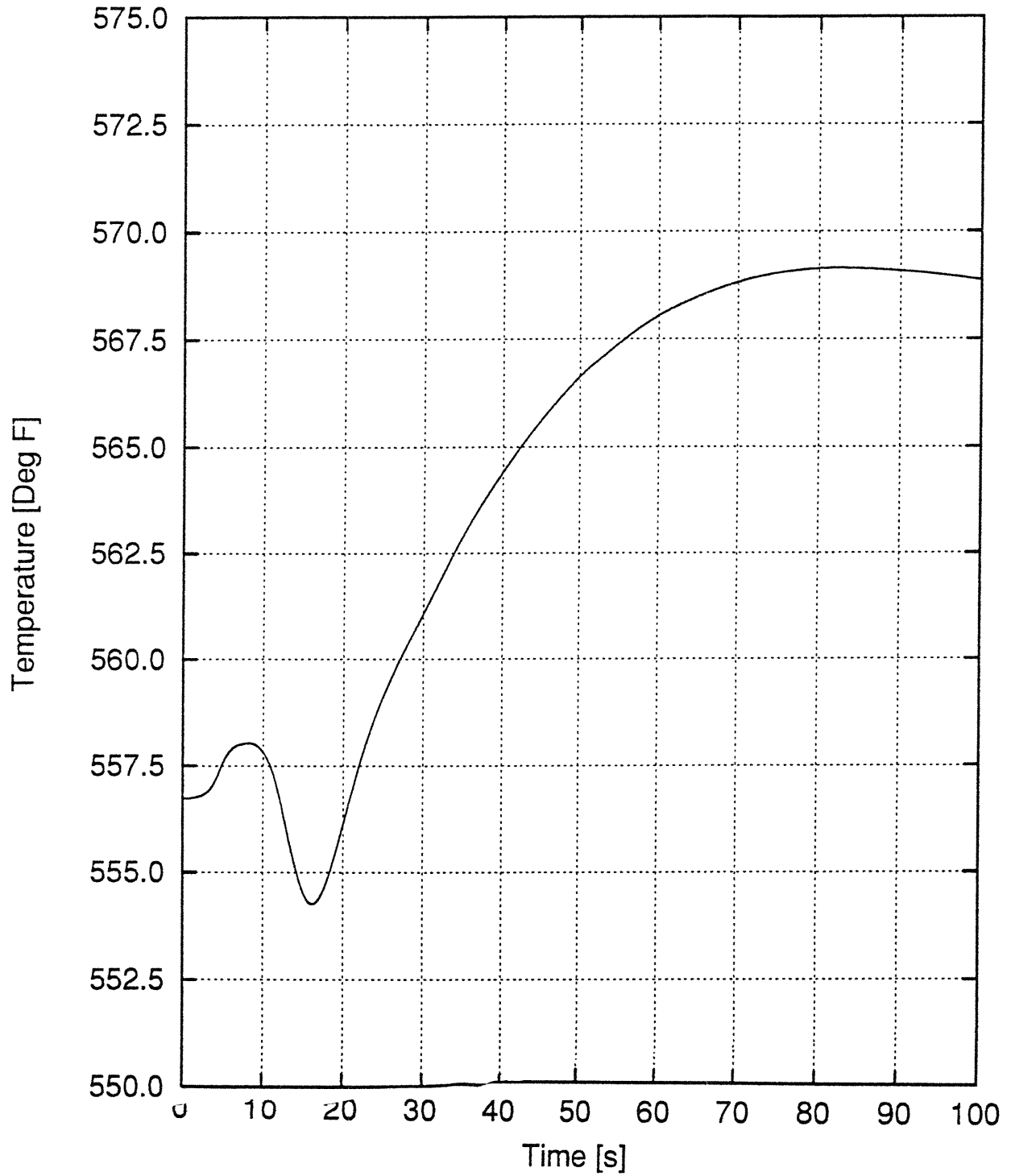


Figure 14.1.5-3
Startup of an Inactive Reactor Coolant Loop
Reactor Power vs. Time

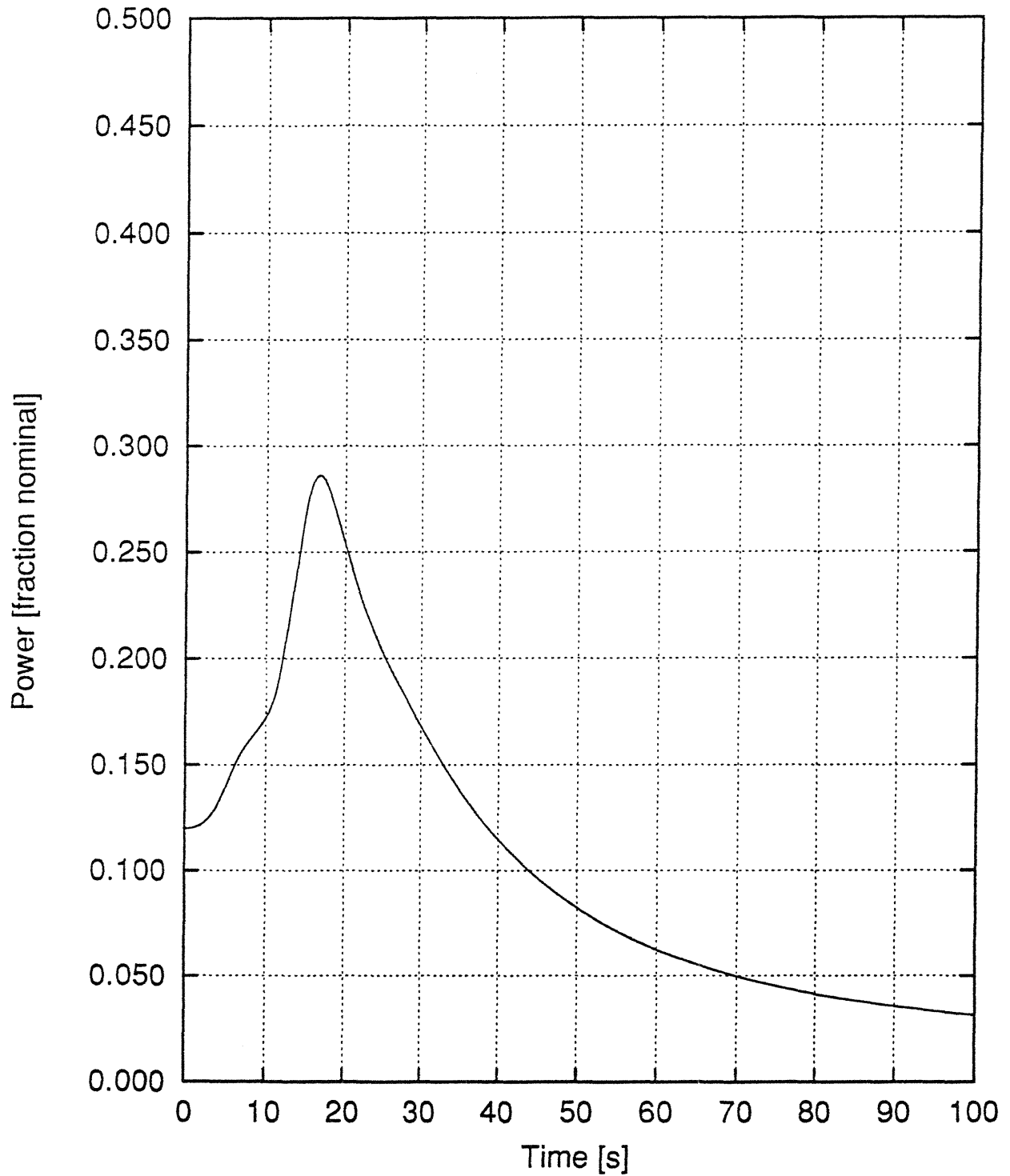


Figure 14.1.5-4
Startup of an Inactive Reactor Coolant Loop
Pressurizer Pressure vs. Time

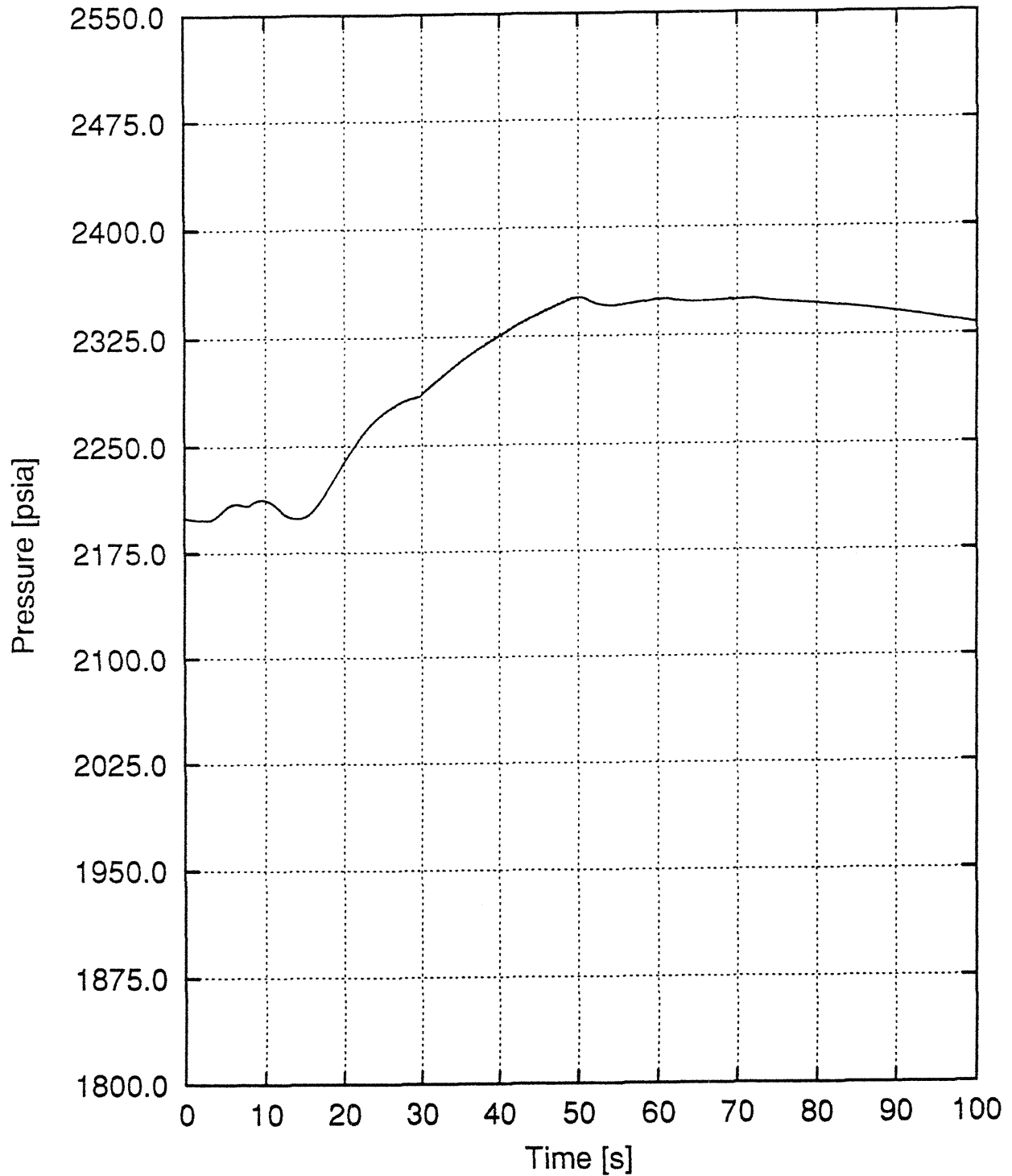


Figure 14.1.5-5
Startup of an Inactive Reactor Coolant Loop
Heat Flux vs. Time

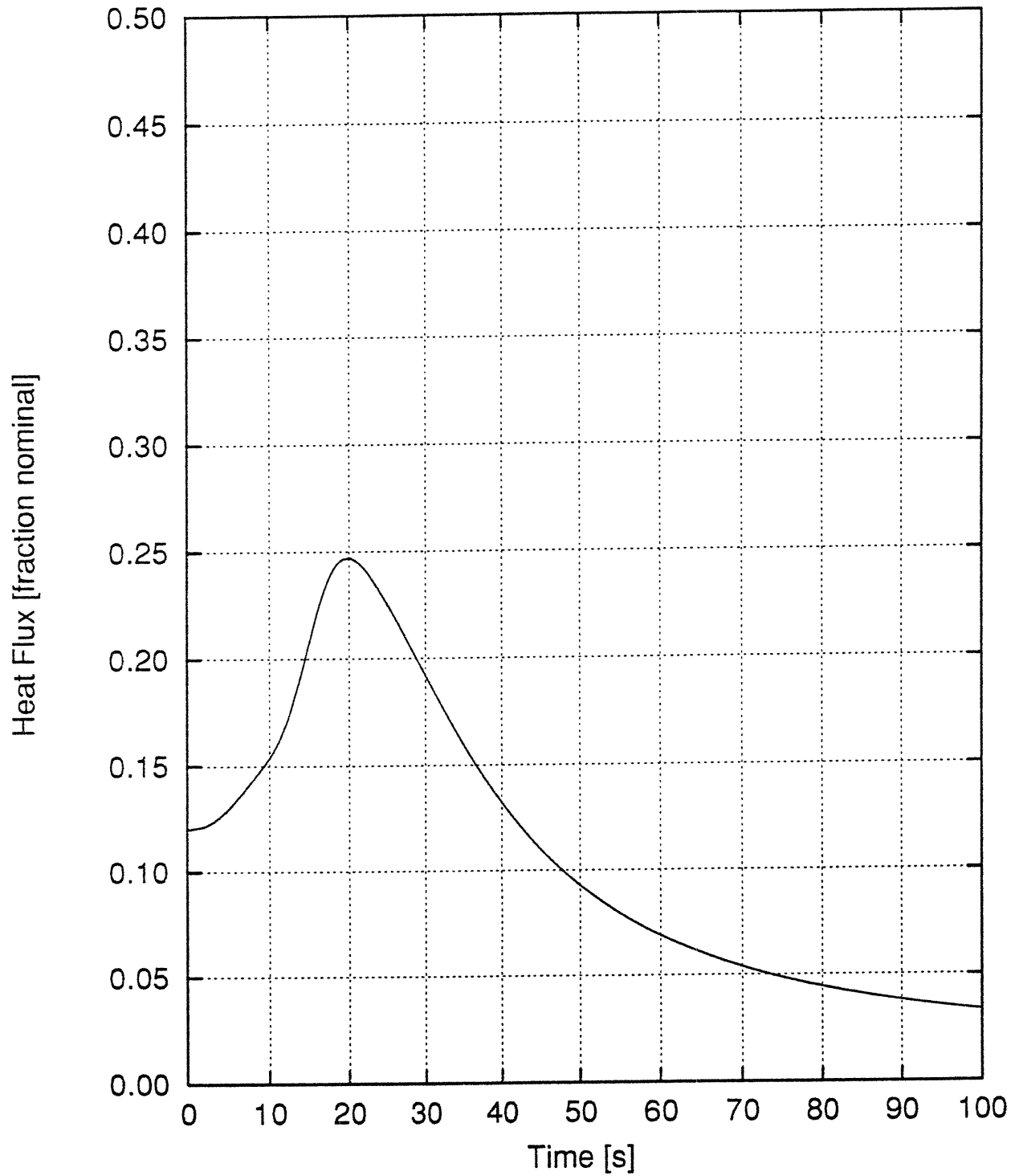


Figure 14.1.6-1
Feedwater Malfunction Event at Full Power with Manual Rod Control
Reactor Power vs. Time

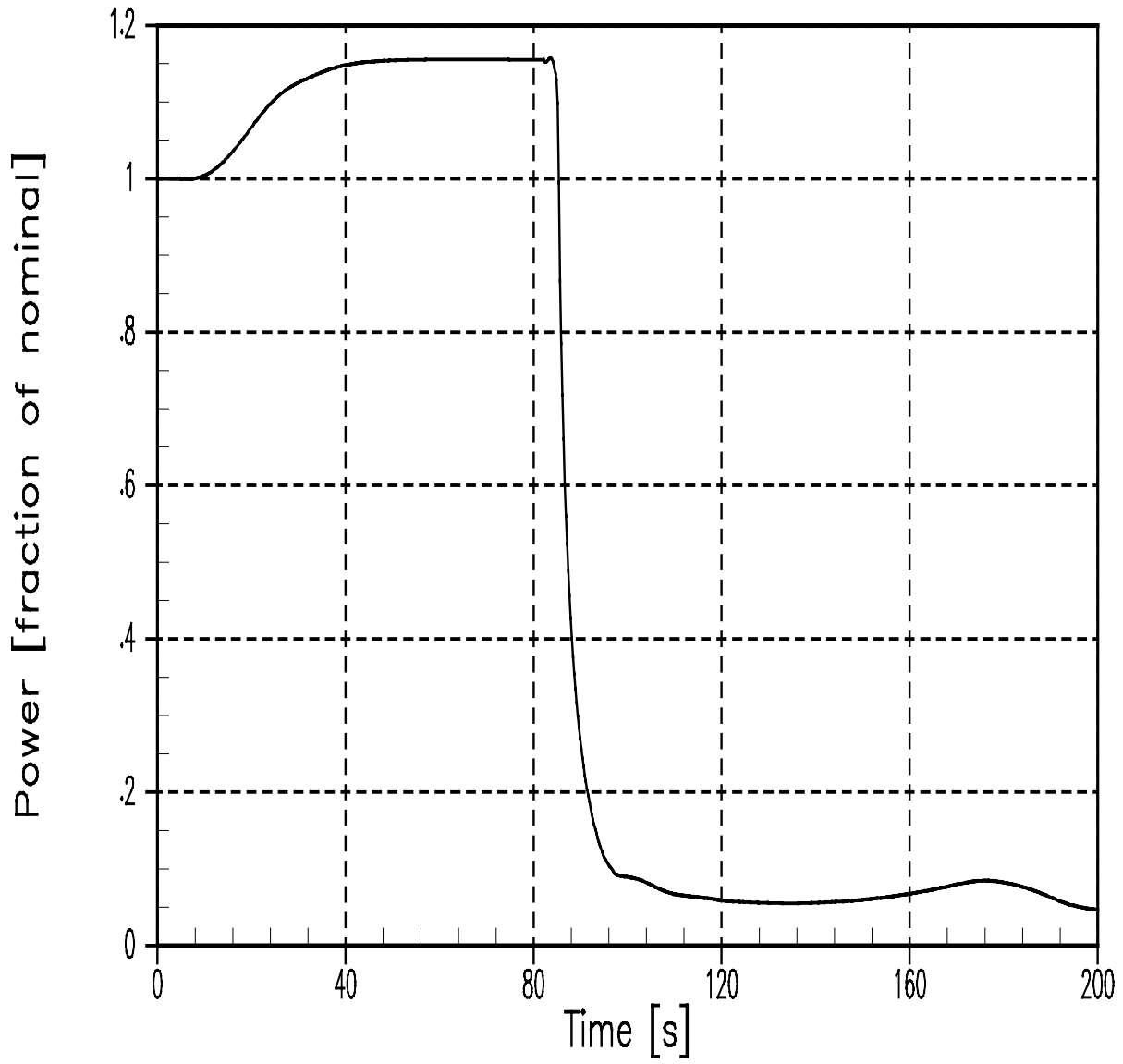


Figure 14.1.6-2
Feedwater Malfunction Event at Full Power with Manual Rod Control
Pressurizer Pressure vs. Time

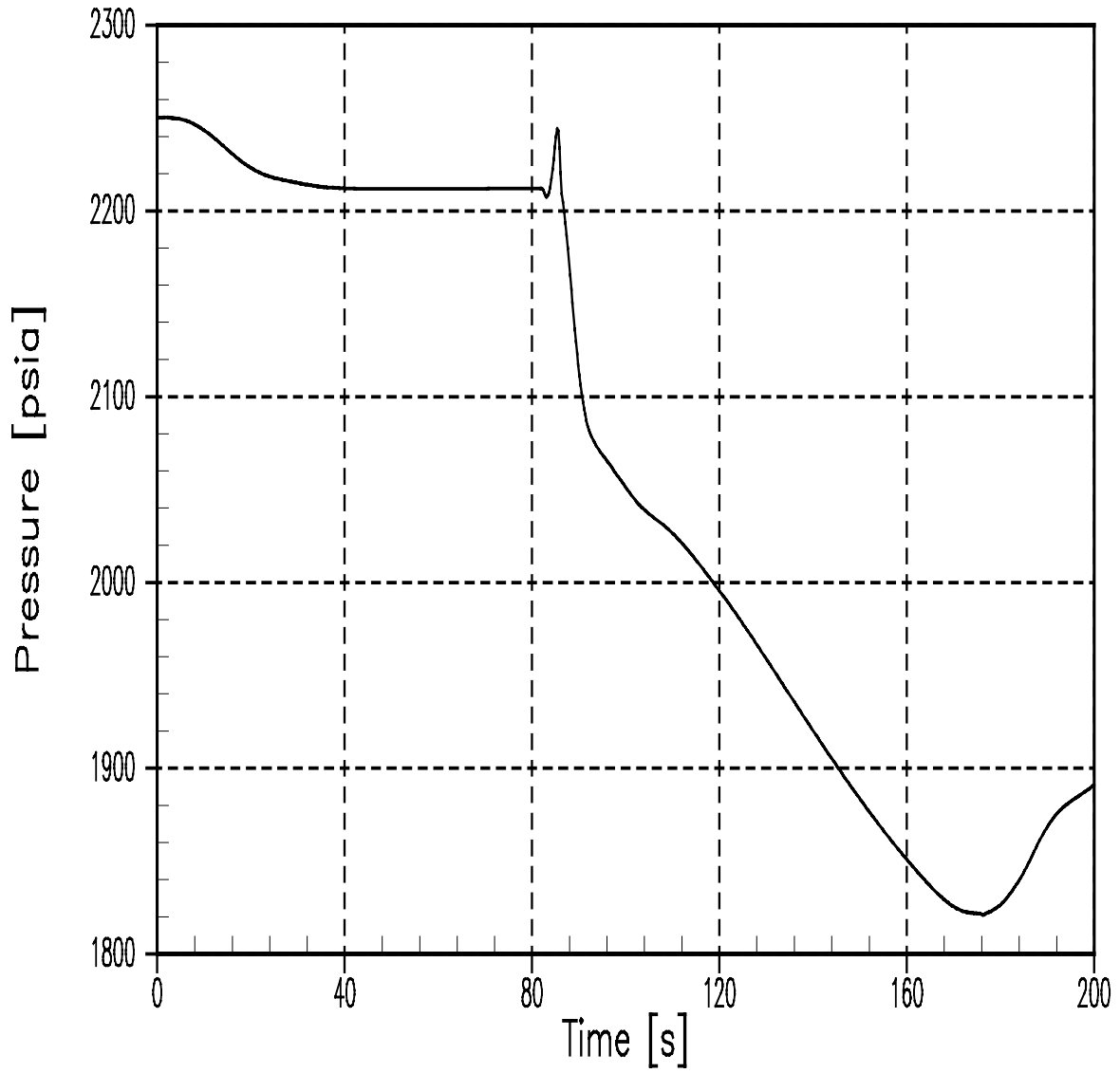


Figure 14.1.6-3
Feedwater Malfunction Event at Full Power with Manual Rod Control
Core Average Temperature vs. Time

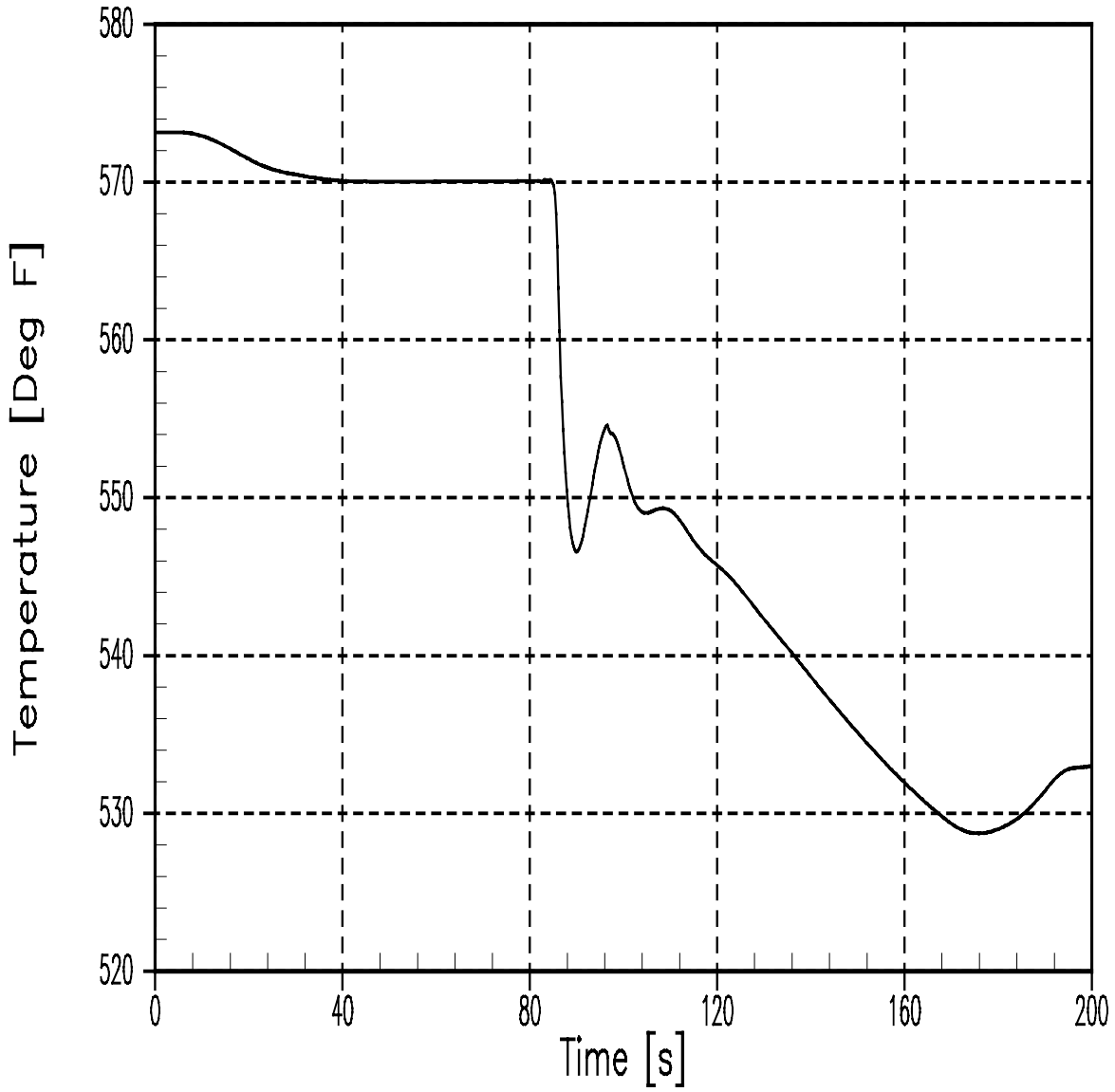


Figure 14.1.6-4
Feedwater Malfunction Event at Full Power with Manual Rod Control
Vessel Outlet and Inlet Temperatures vs. Time

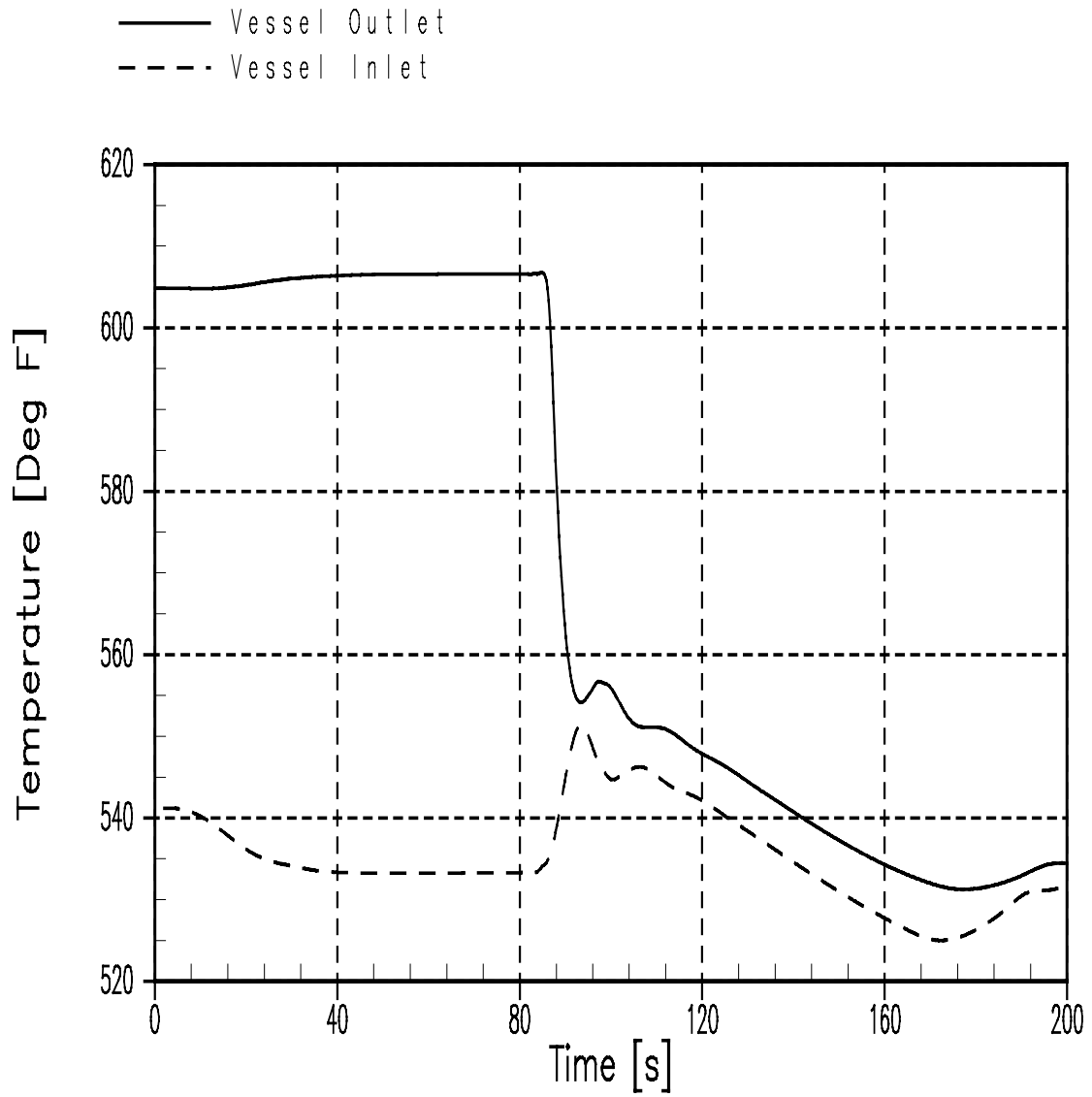


Figure 14.1.6-5
Feedwater Malfunction Event at Full Power with Manual Rod Control
Minimum DNBR vs. Time

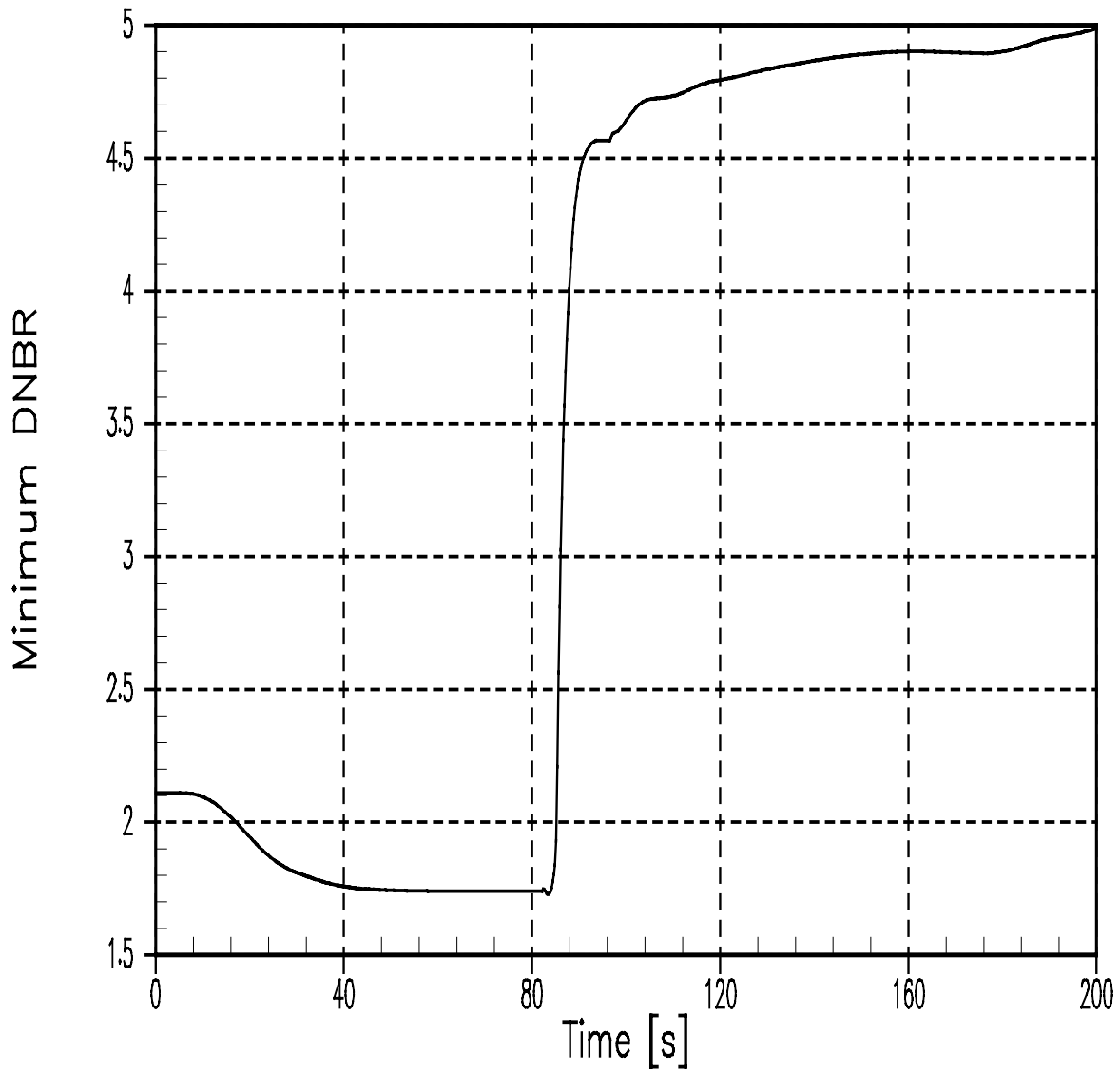


Figure 14.1.6-6
Feedwater Malfunction Event at Full Power with Automatic Rod Control
Reactor Power vs. Time

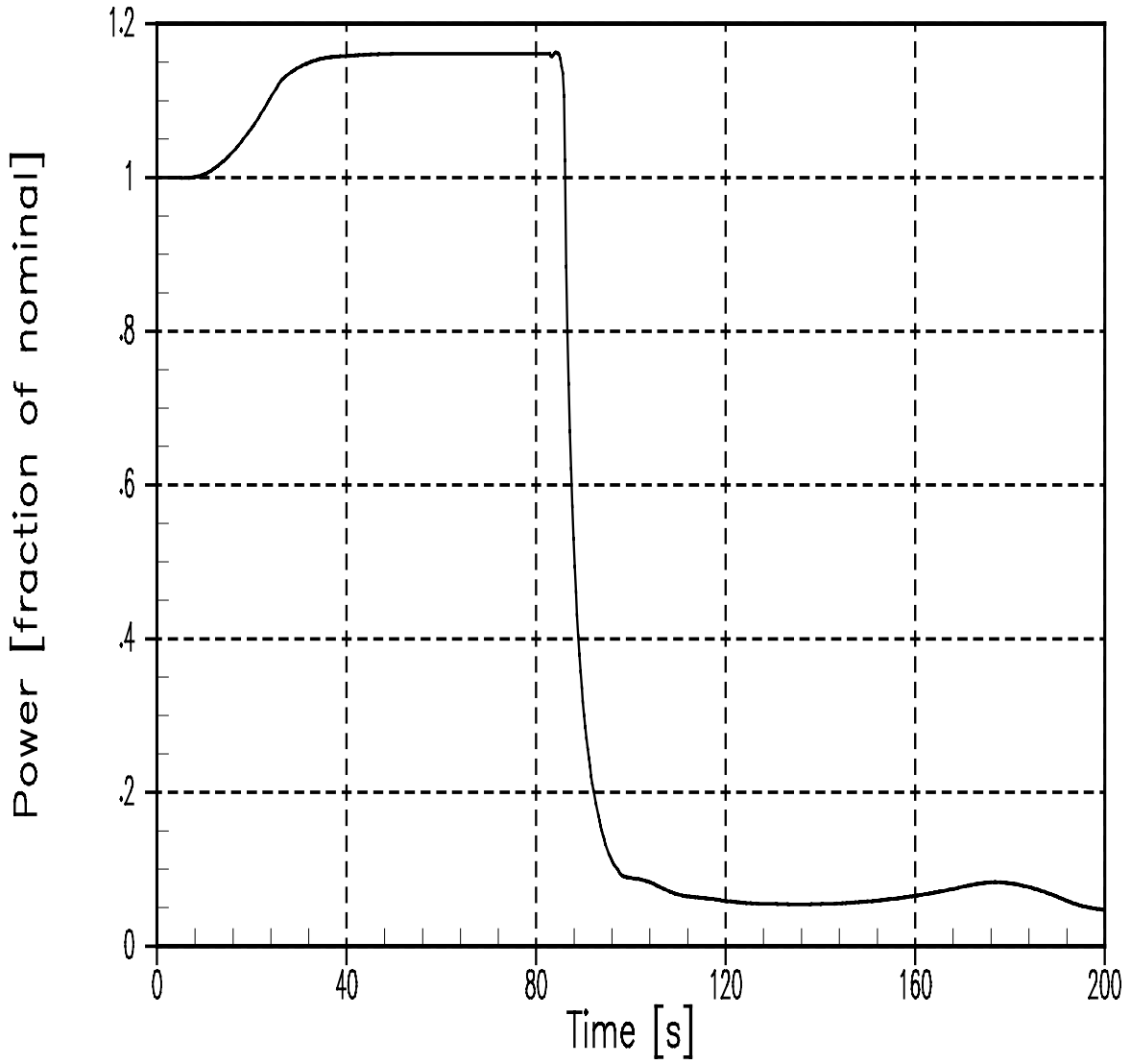


Figure 14.1.6-7
Feedwater Malfunction Event at Full Power with Automatic Rod Control
Pressurizer Pressure vs. Time

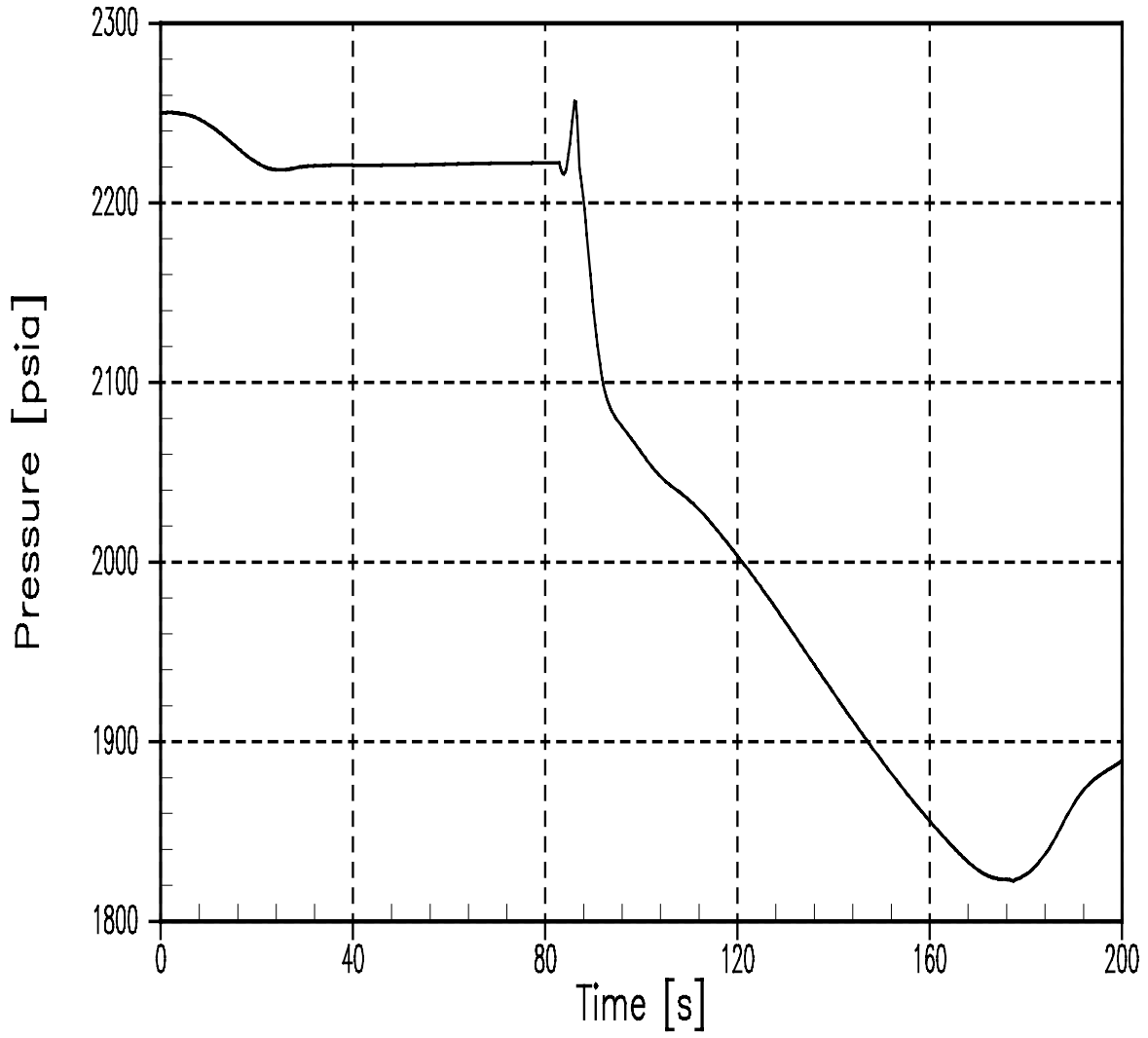


Figure 14.1.6-8
Feedwater Malfunction Event at Full Power with Automatic Rod Control
Core Average Temperature vs. Time

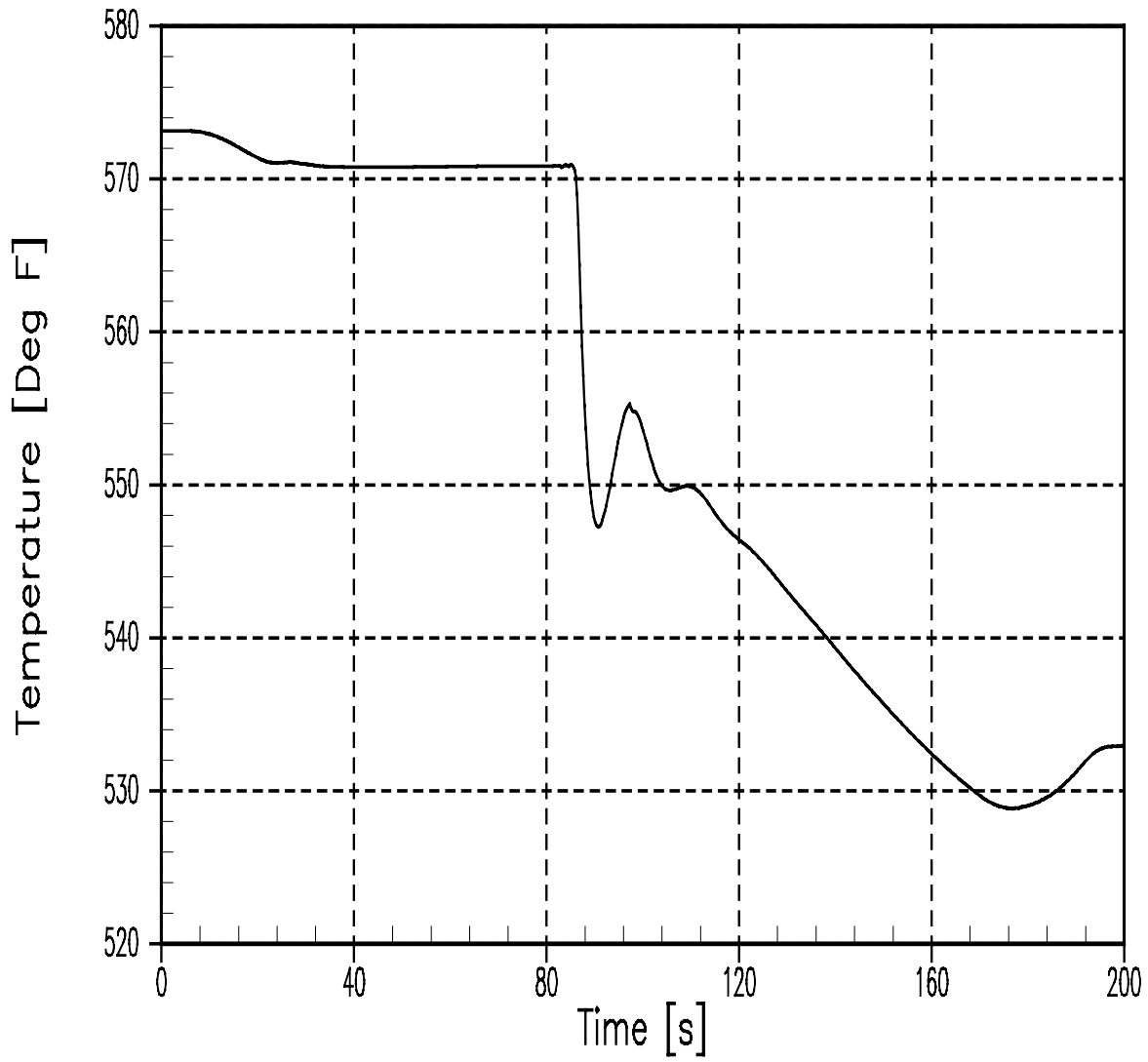


Figure 14.1.6-9
Feedwater Malfunction Event at Full Power with Automatic Rod Control
Vessel Outlet and Inlet Temperature vs. Time

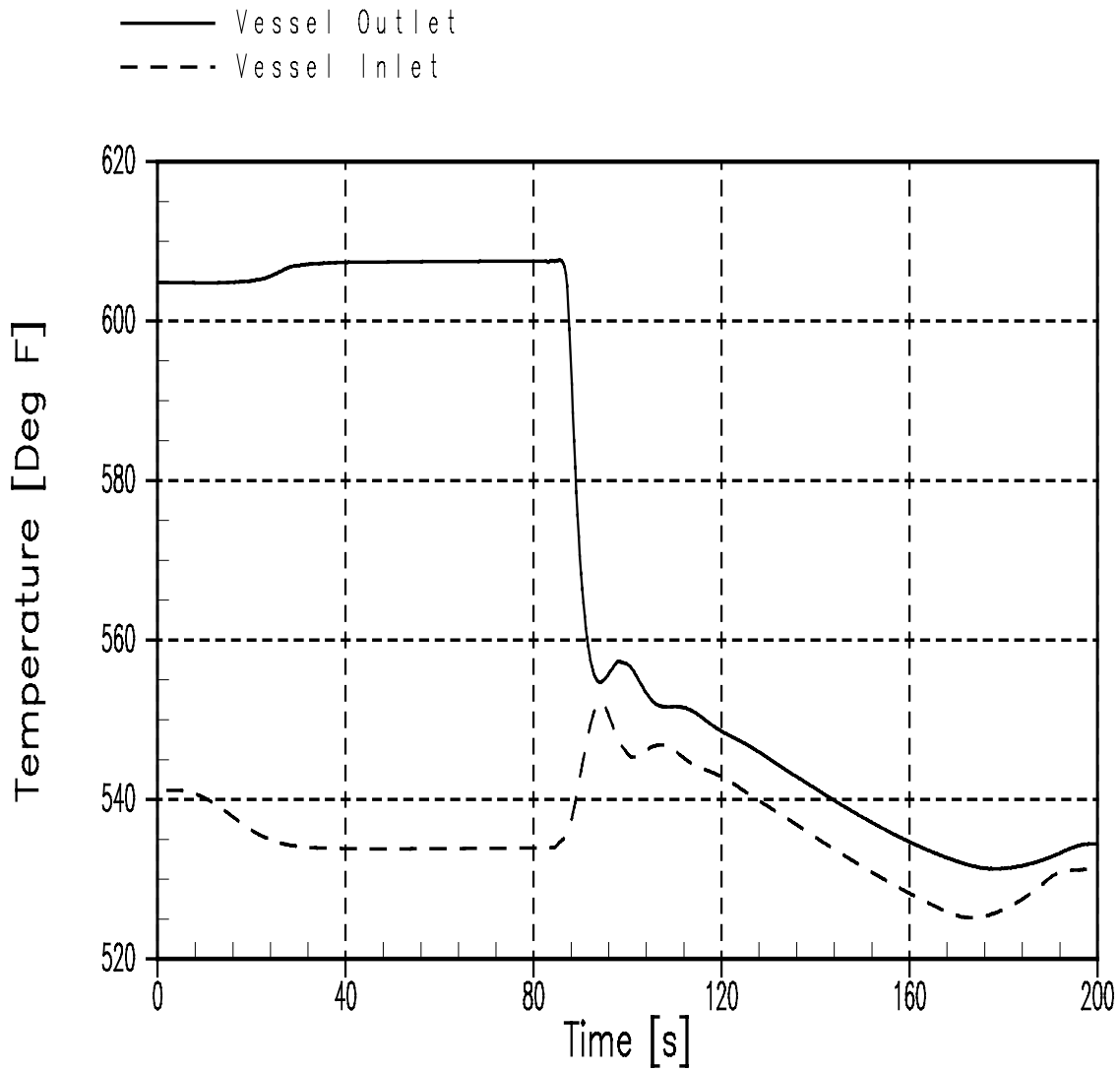


Figure 14.1.6-10
Feedwater Malfunction Event at Full Power with Automatic Rod Control
Minimum DNBR vs. Time

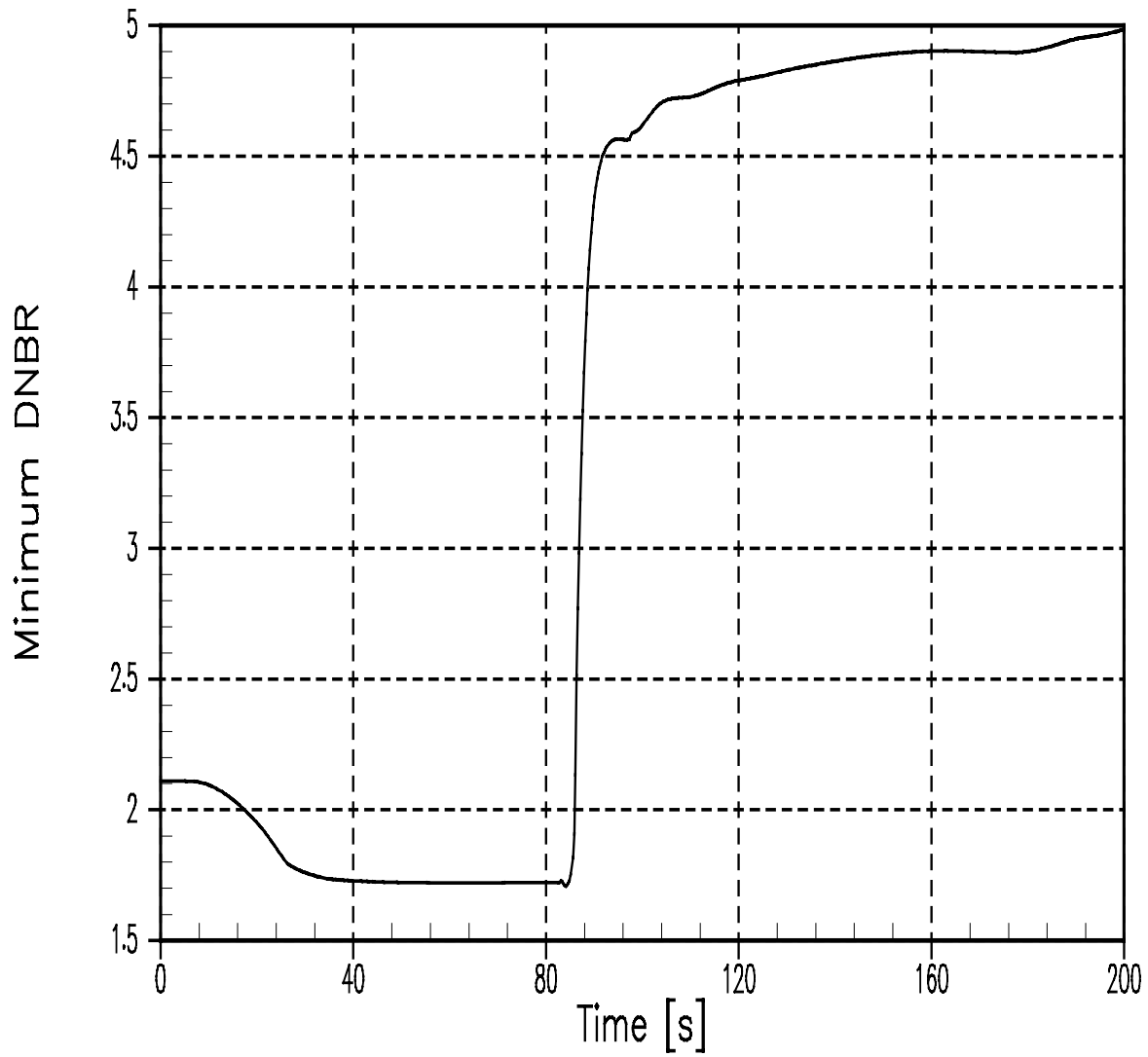


Figure 14.1.7-1
Excessive Load Increase - BOC Manual Control
Reactor Power vs. Time

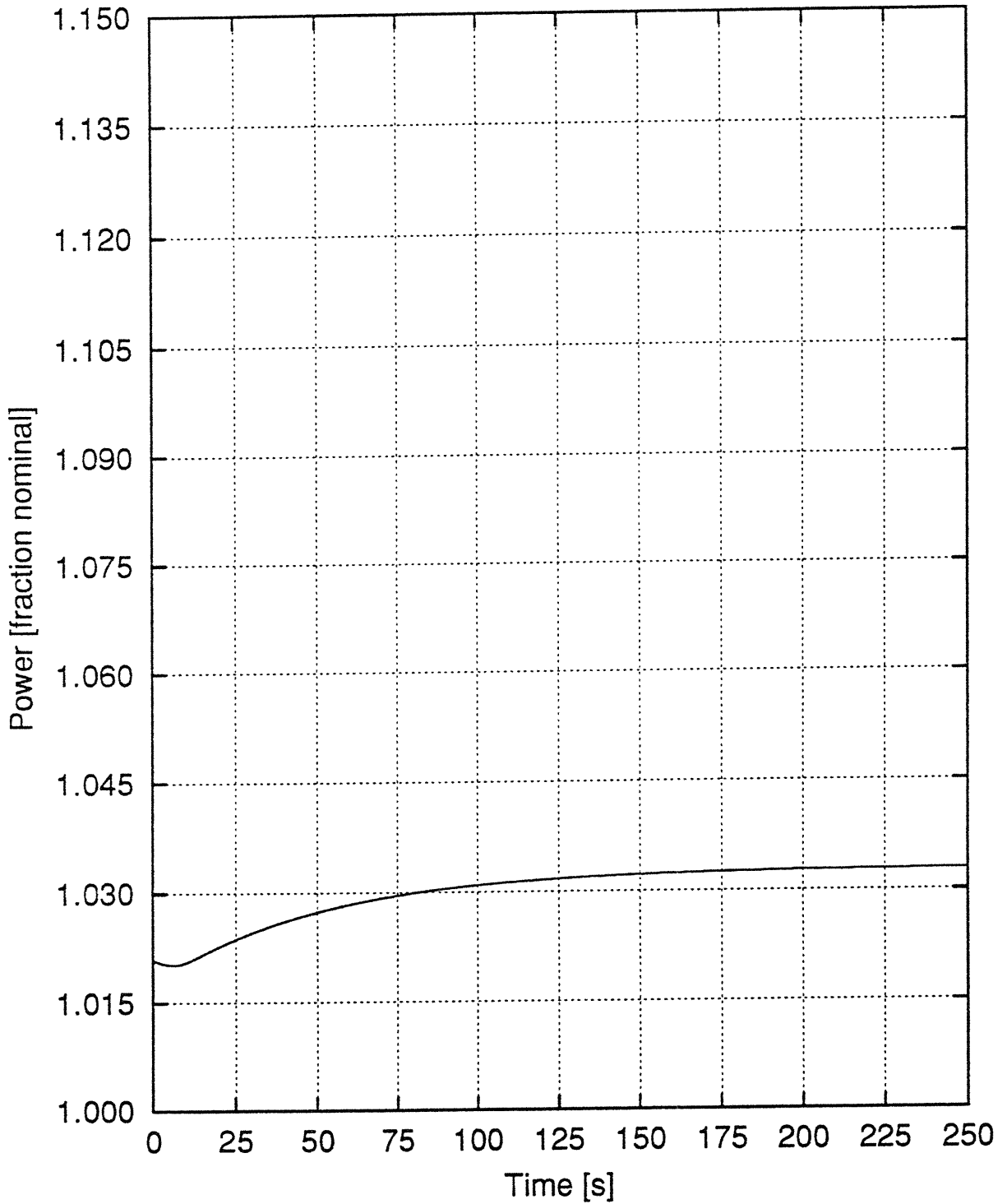


Figure 14.1.7-2
Excessive Load Increase - BOC Manual Control
Pressurizer Pressure vs. Time

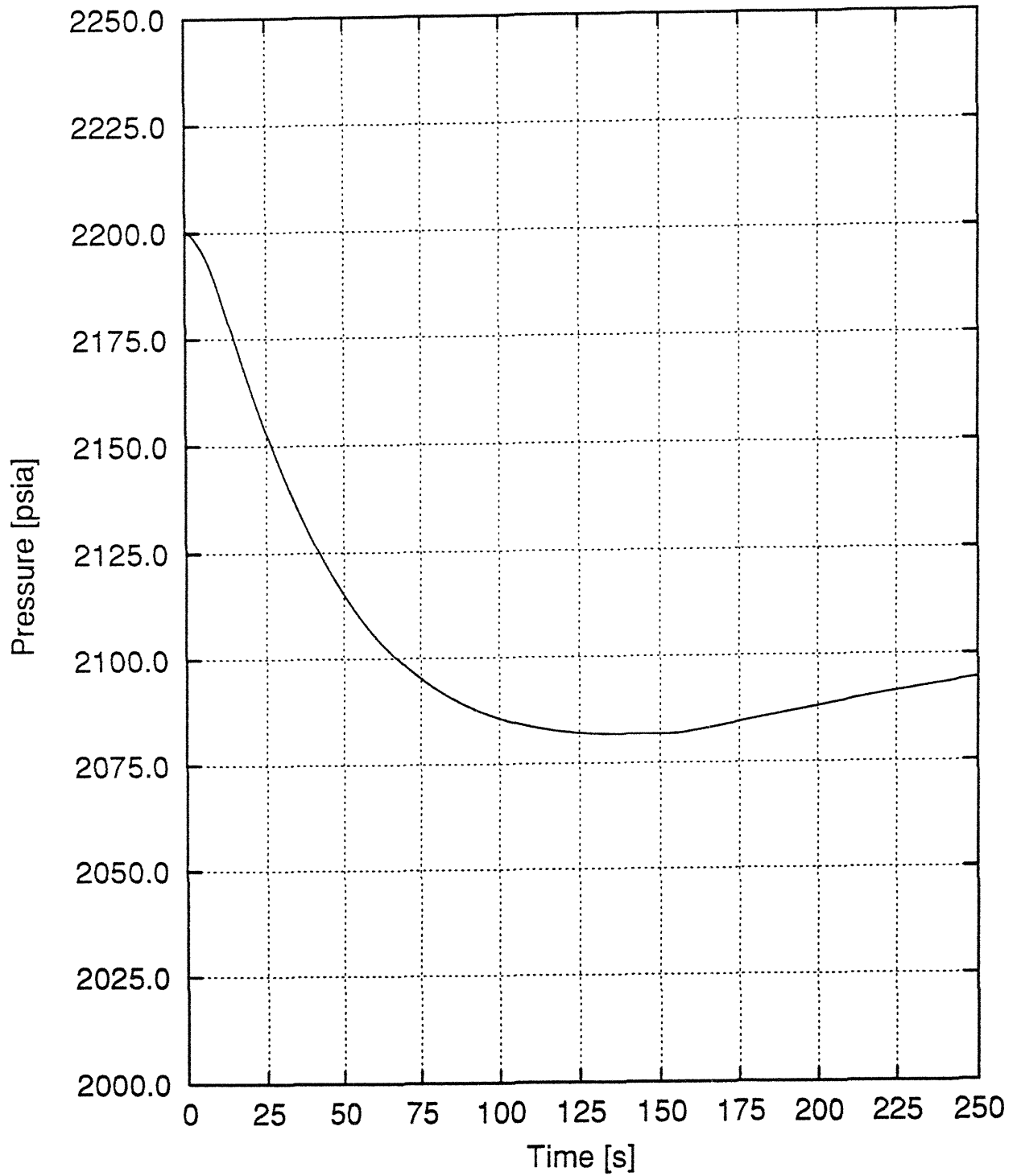


Figure 14.1.7-3
Excessive Load Increase - BOC Manual Control
 ΔT Loop vs. Time

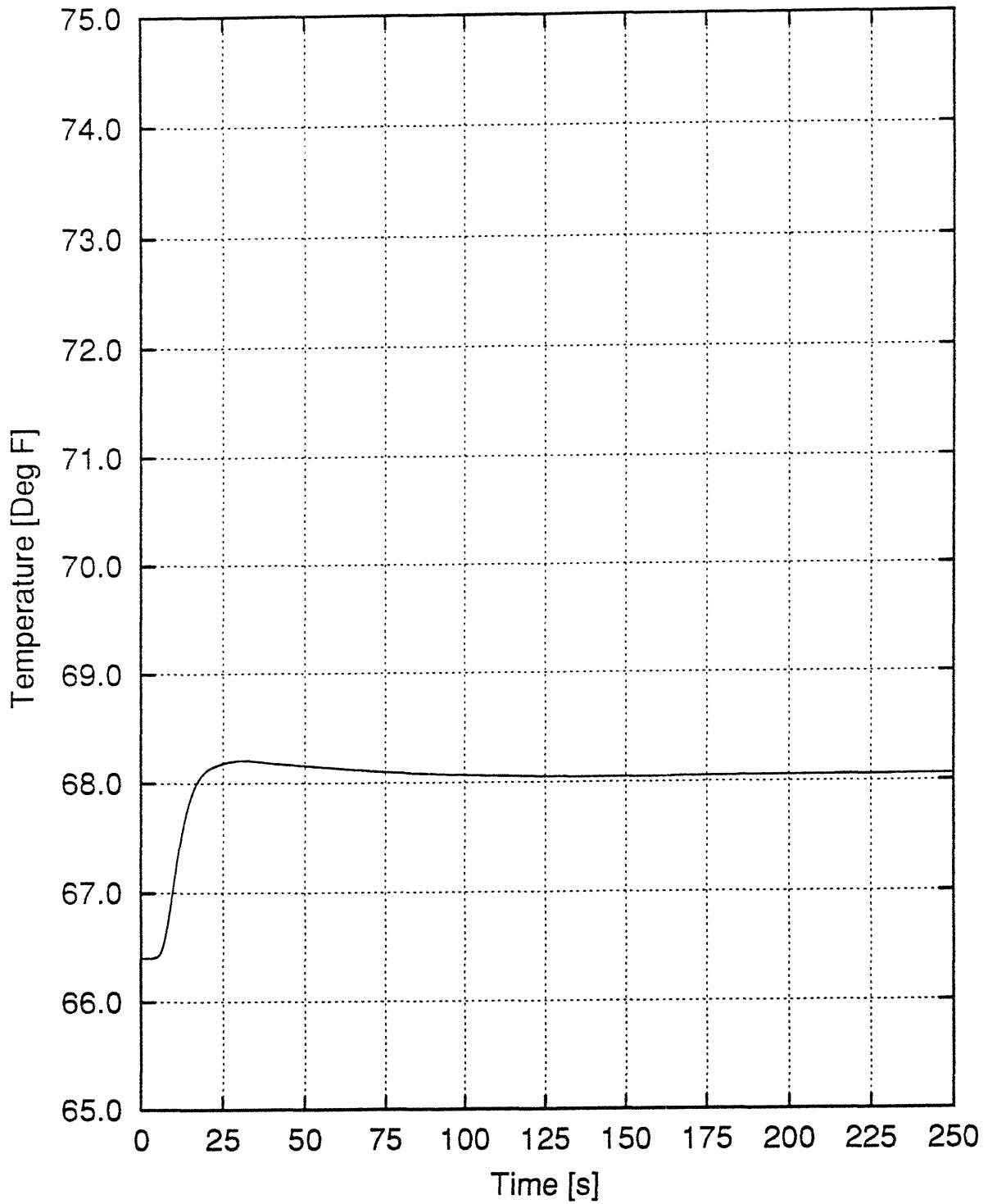


Figure 14.1.7-4
Excessive Load Increase - BOC Manual Control
Minimum DNBR vs. Time

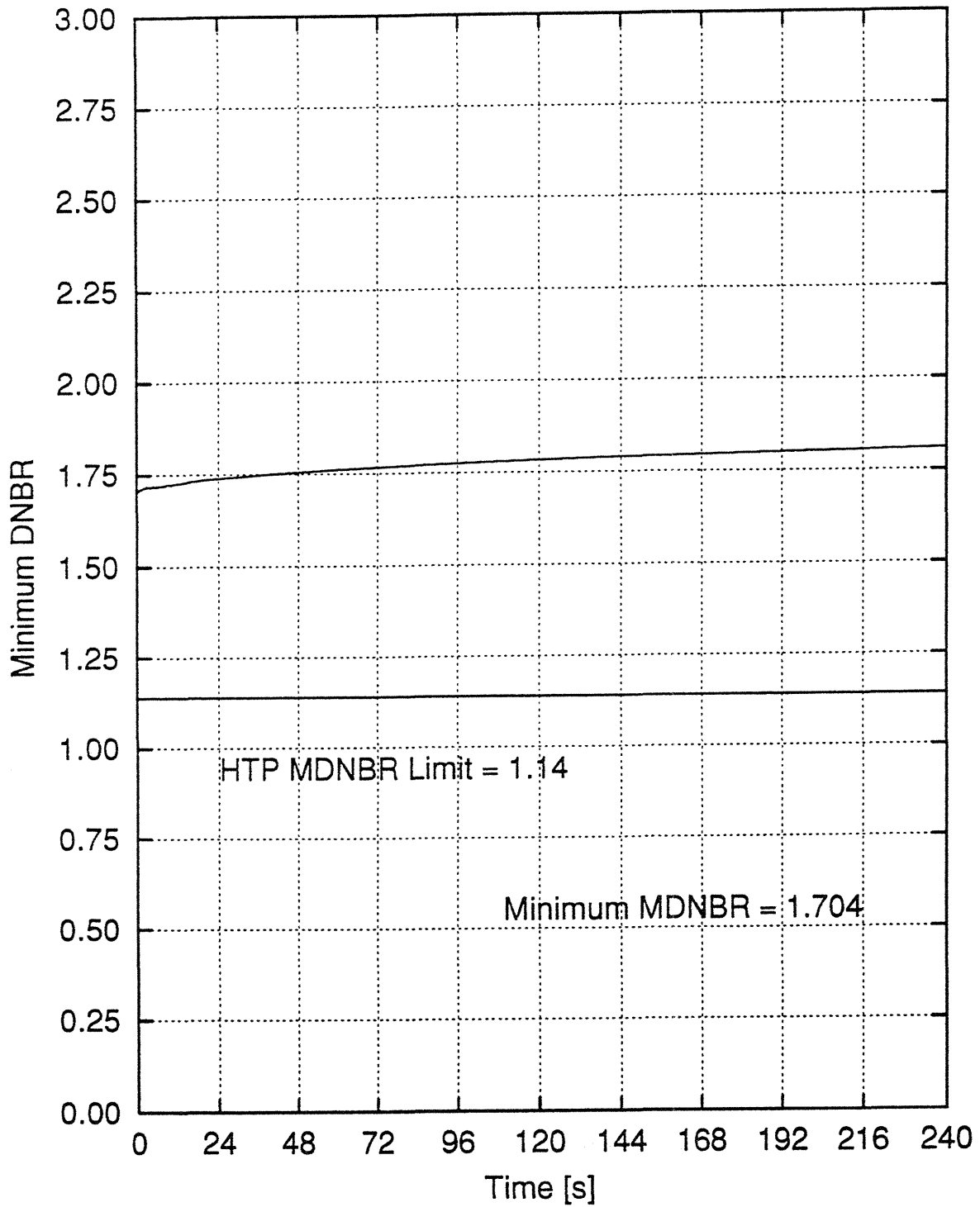


Figure 14.1.7-5
Excessive Load Increase - EOC Manual Control
Reactor Power vs. Time

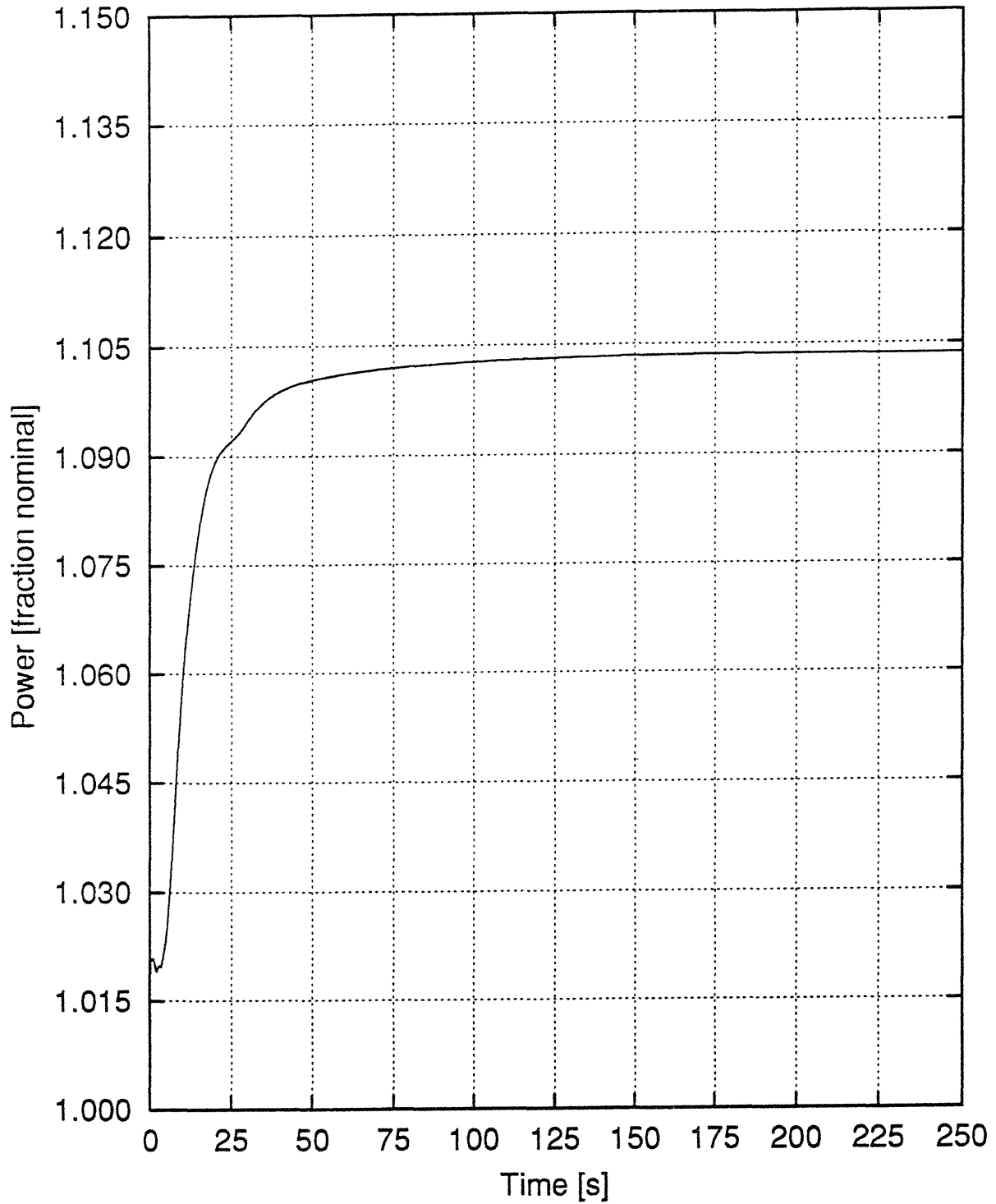


Figure 14.1.7-6
Excessive Load Increase - EOC Manual Control
Pressurizer Pressure vs. Time

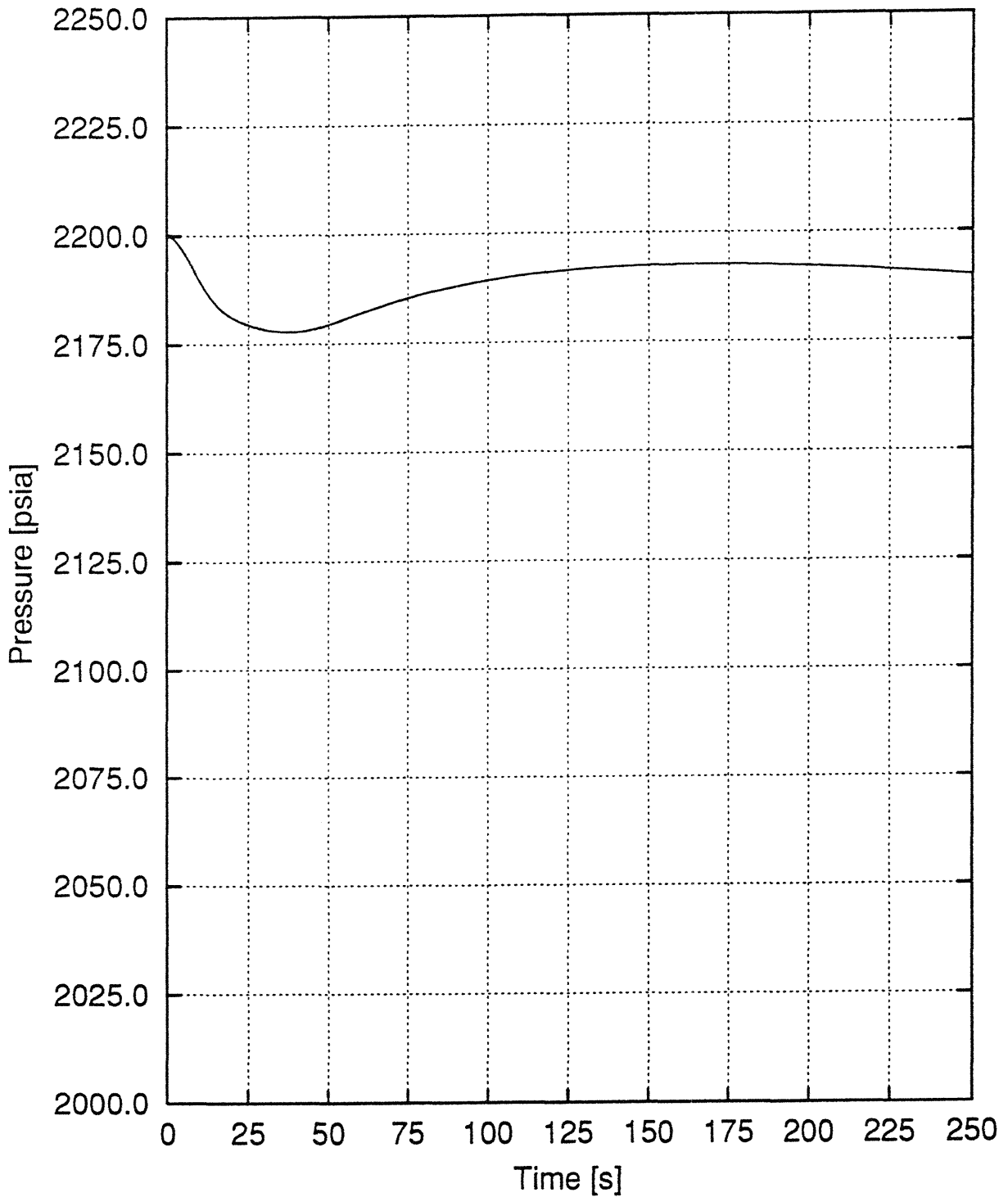


Figure 14.1.7-7
Excessive Load Increase - EOC Manual Control
 ΔT Loop vs. Time

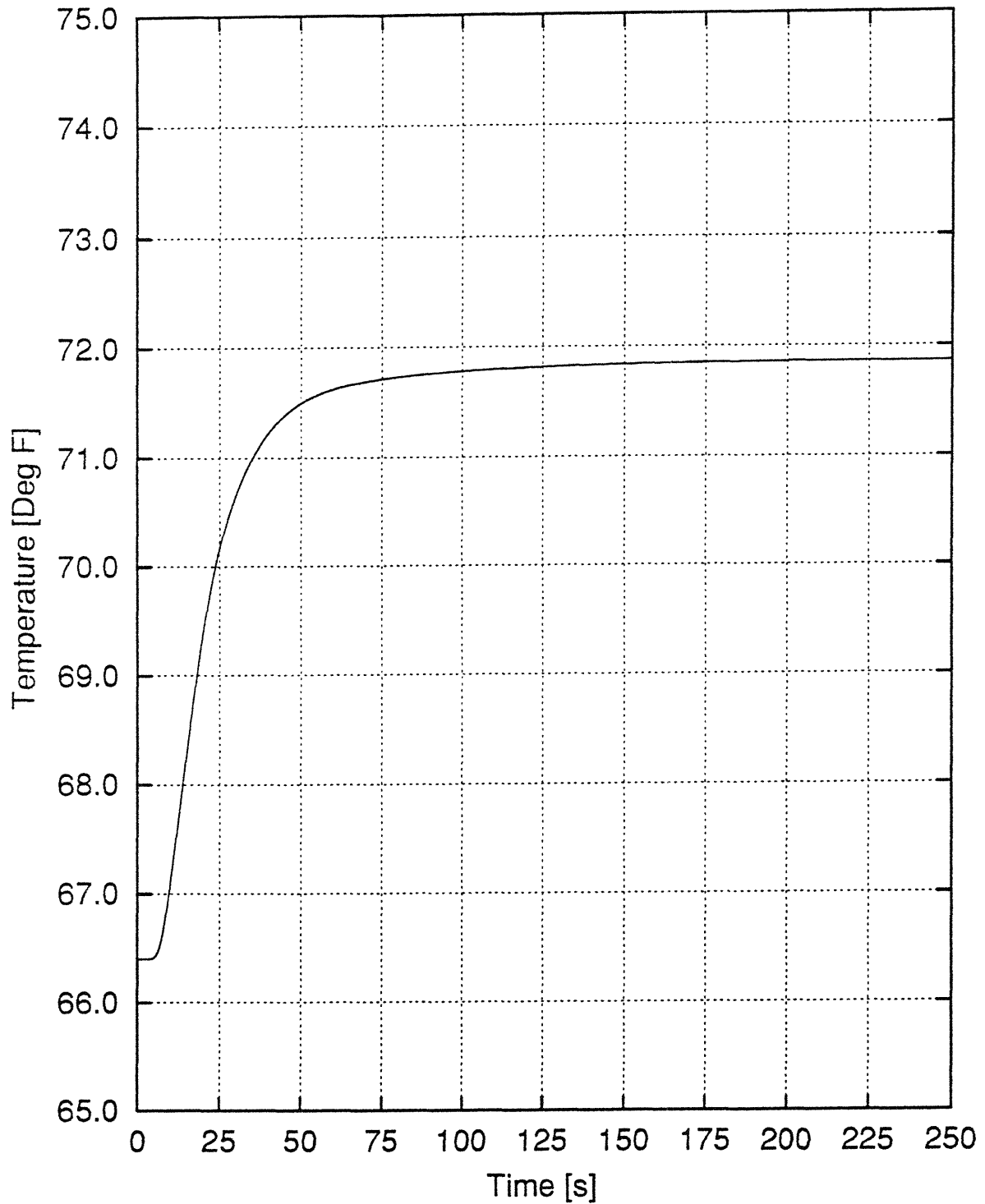


Figure 14.1.7-8
Excessive Load Increase - EOC Manual Control
Minimum DNBR vs. Time

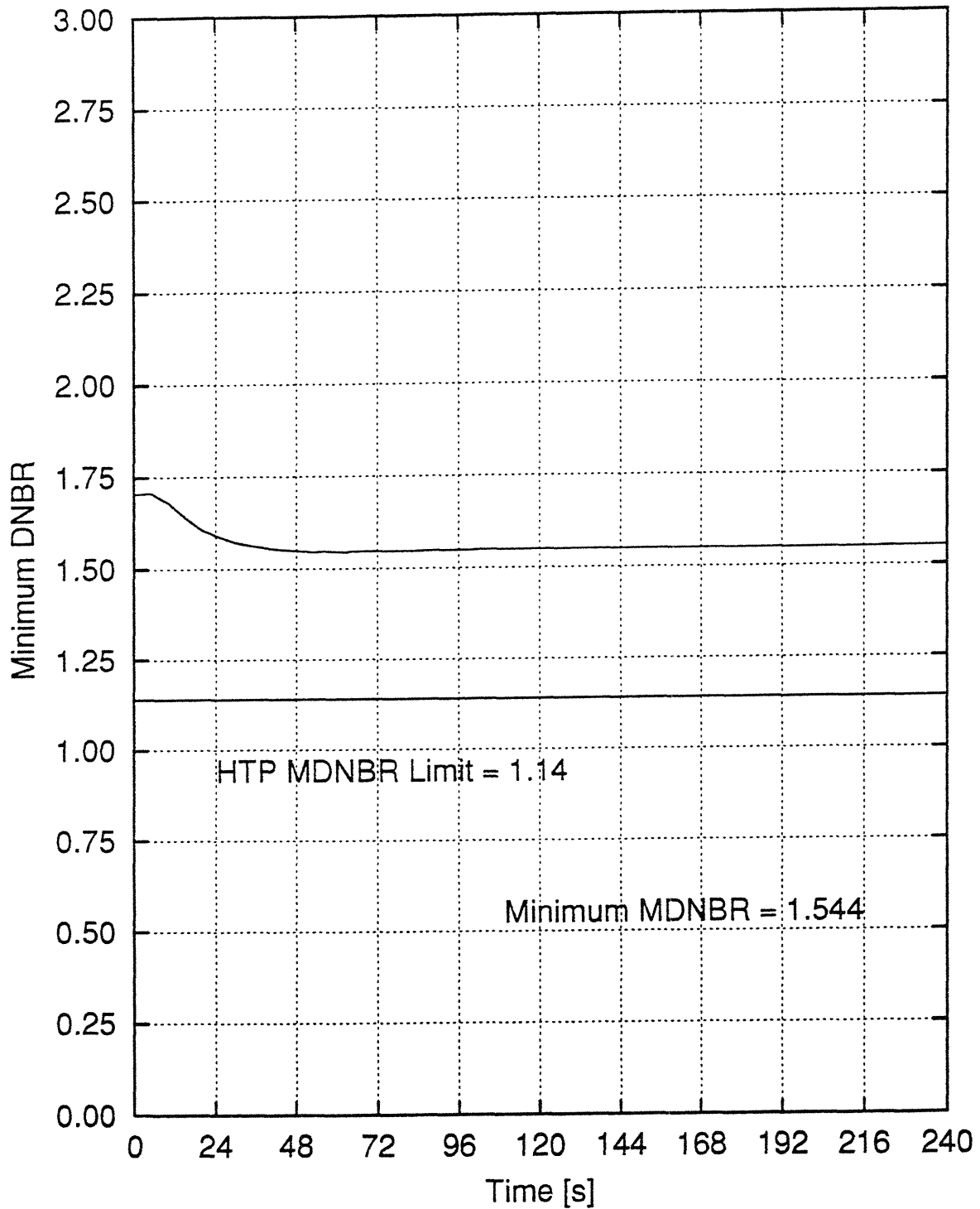


Figure 14.1.7-9
Excessive Load Increase - BOC Auto Control
Reactor Power vs. Time

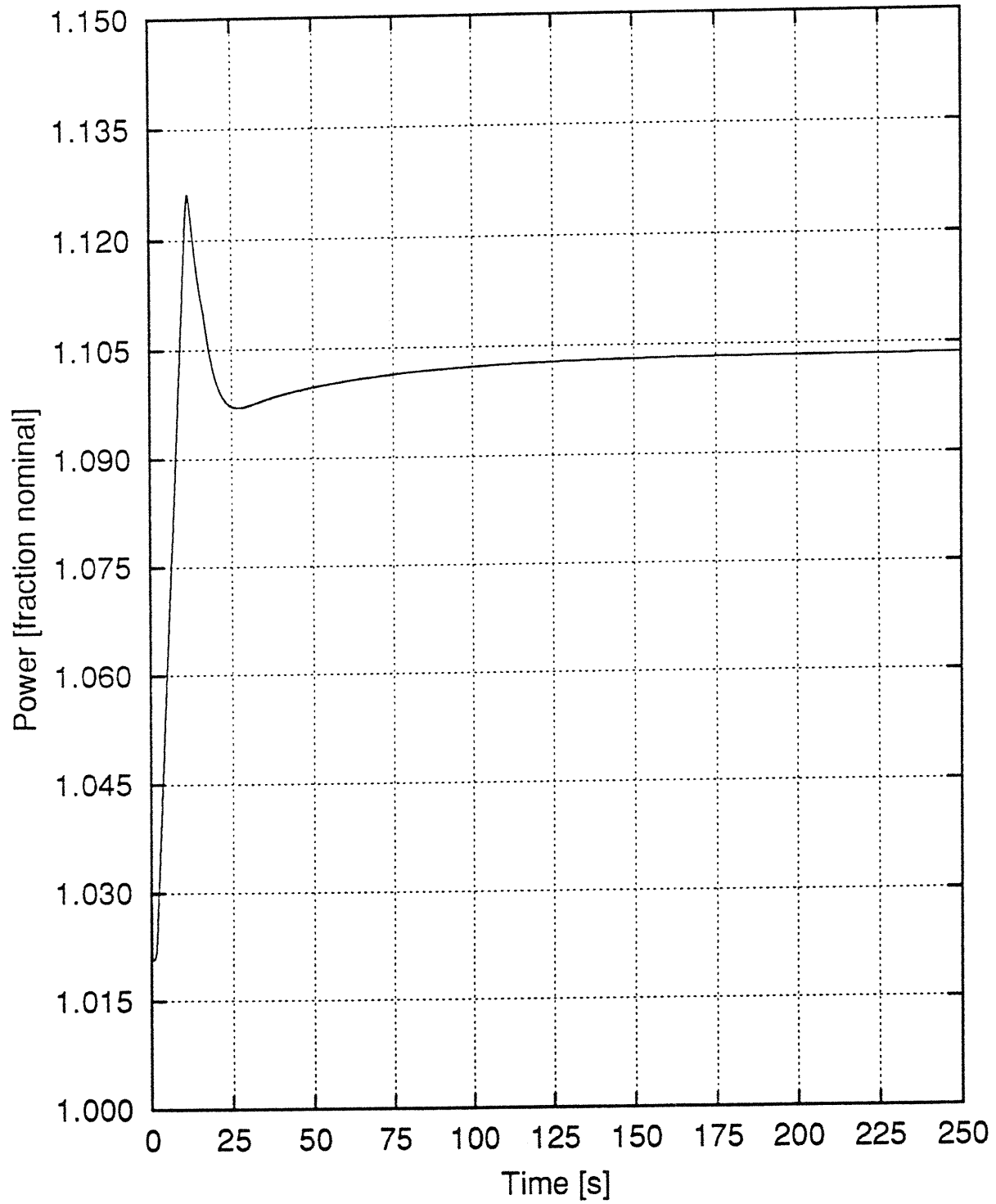


Figure 14.1.7-10
Excessive Load Increase - BOC Auto Control
Pressurizer Pressure vs. Time

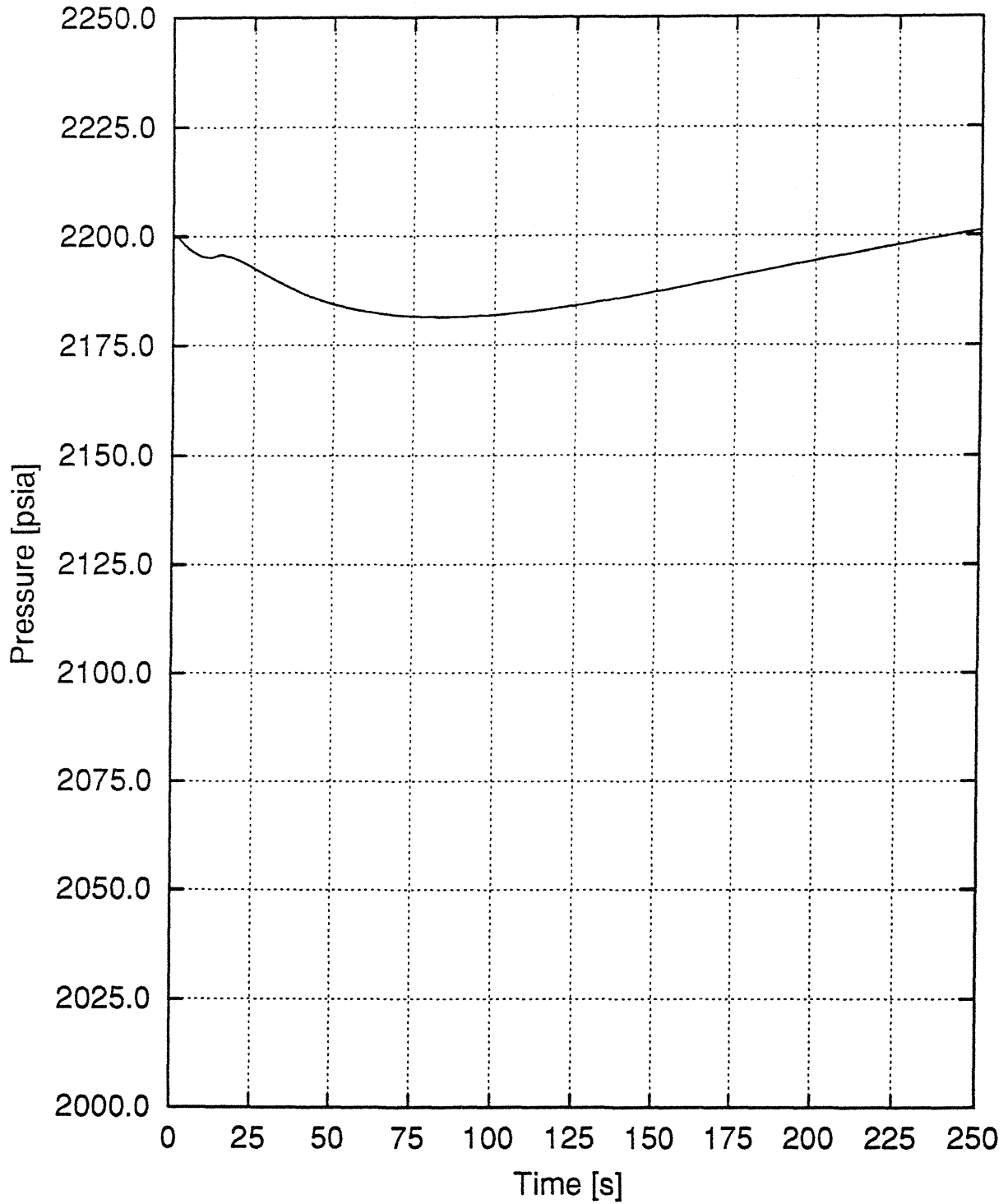


Figure 14.1.7-11
Excessive Load Increase - BOC Auto Control
 ΔT Loop vs. Time

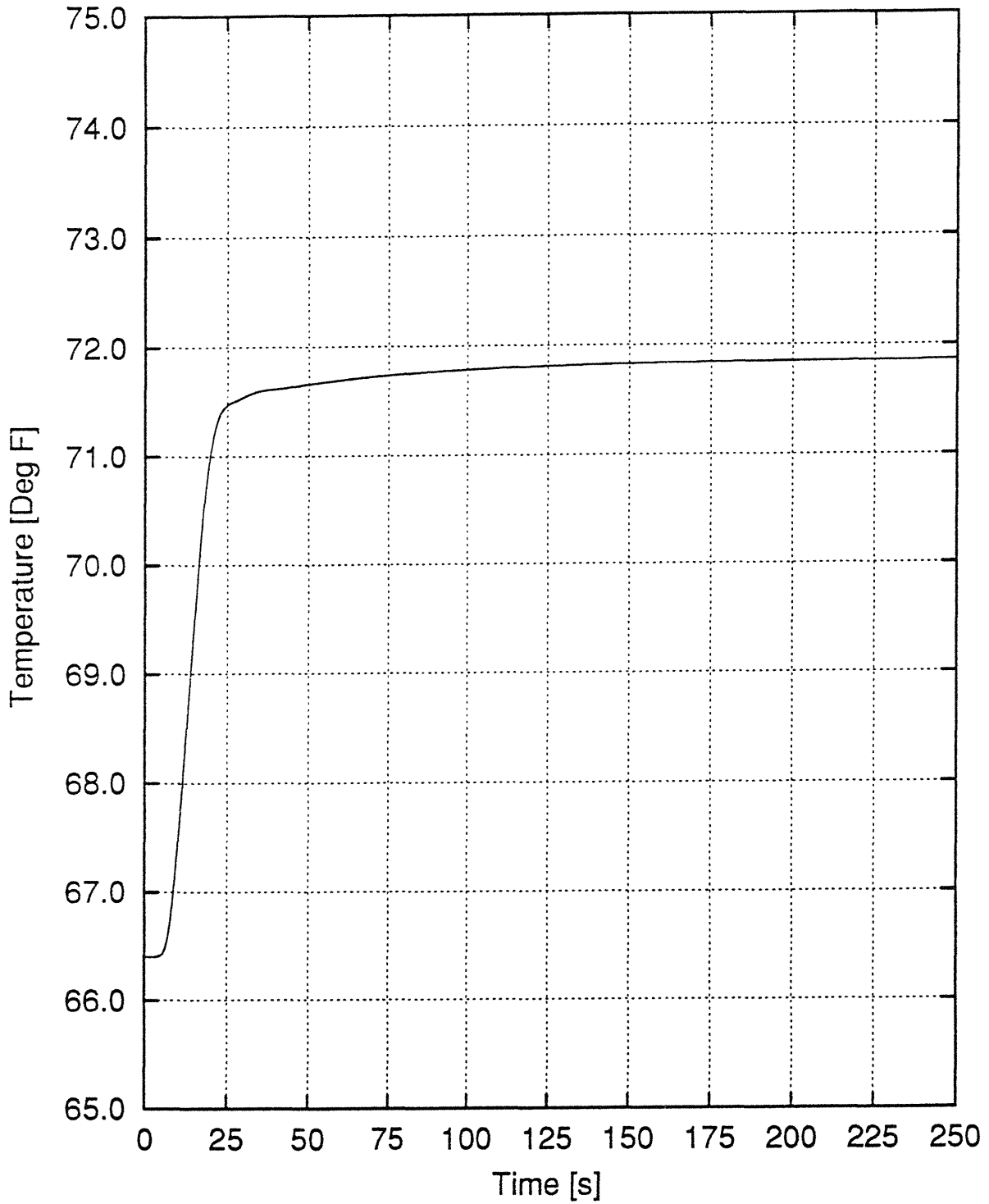


Figure 14.1.7-12
Excessive Load Increase - BOC Auto Control
 T_{ave} vs. Time

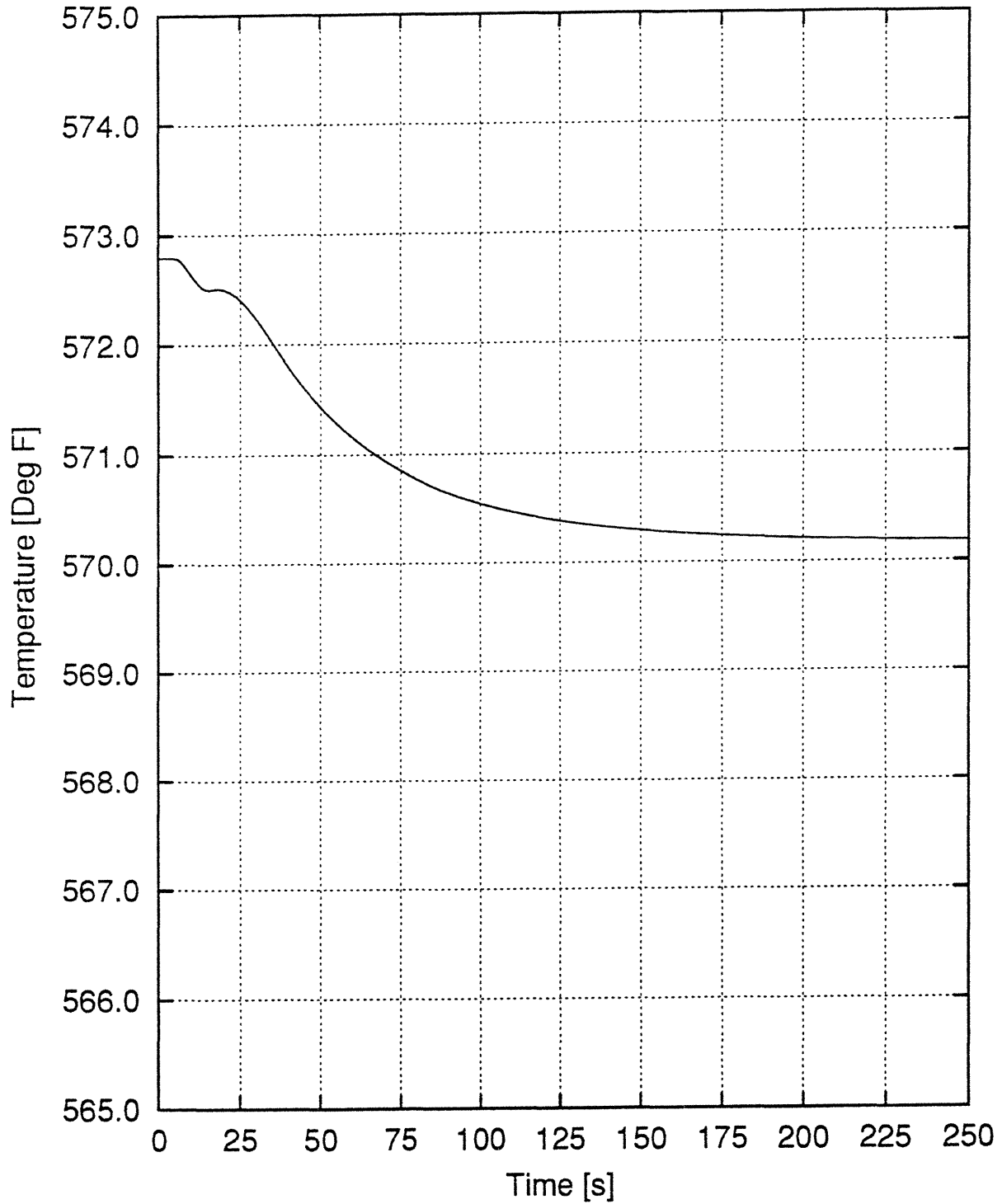


Figure 14.1.7-13
Excessive Load Increase - BOC Auto Control
Minimum DNBR vs. Time

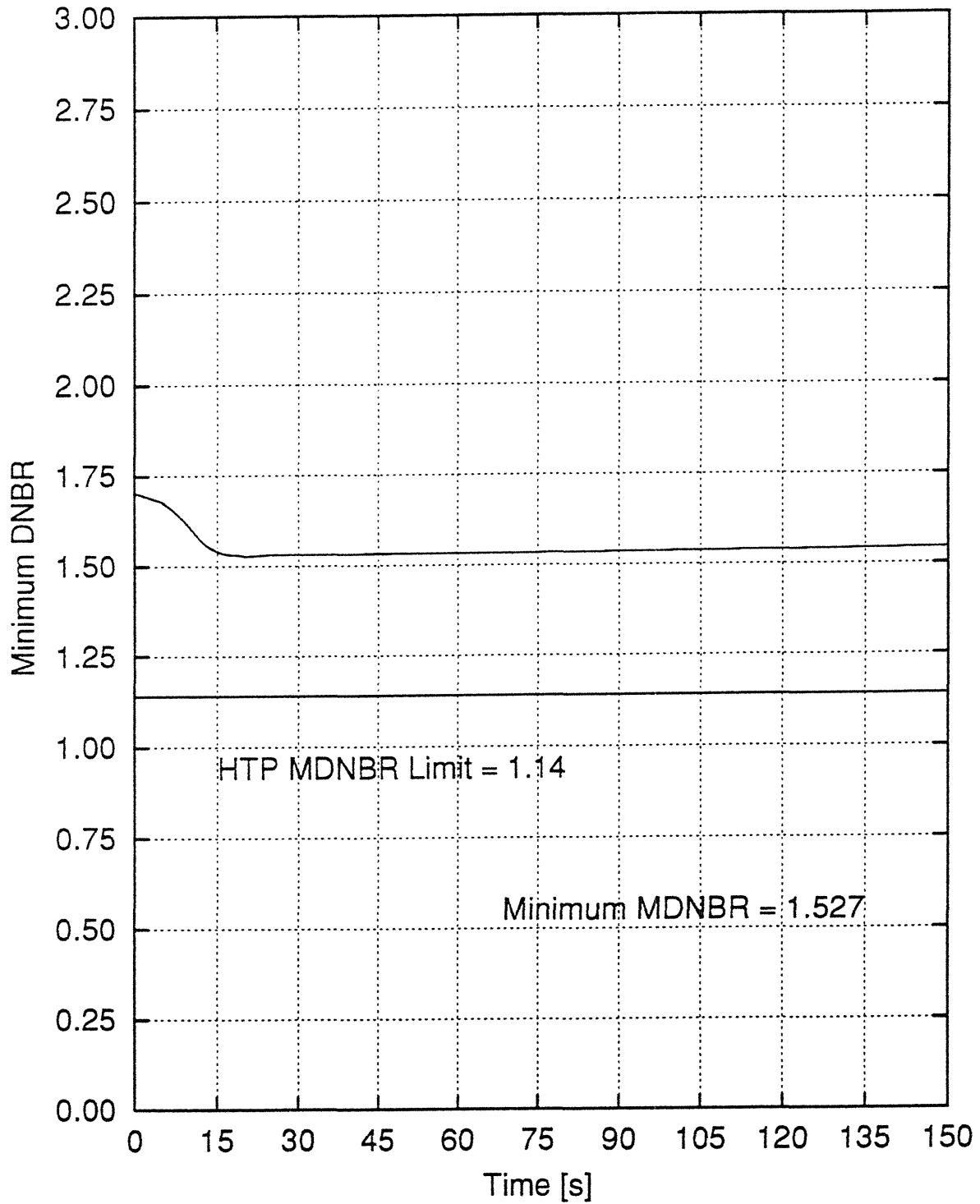


Figure 14.1.7-14
Excessive Load Increase - EOC Auto Control
Reactor Power vs. Time

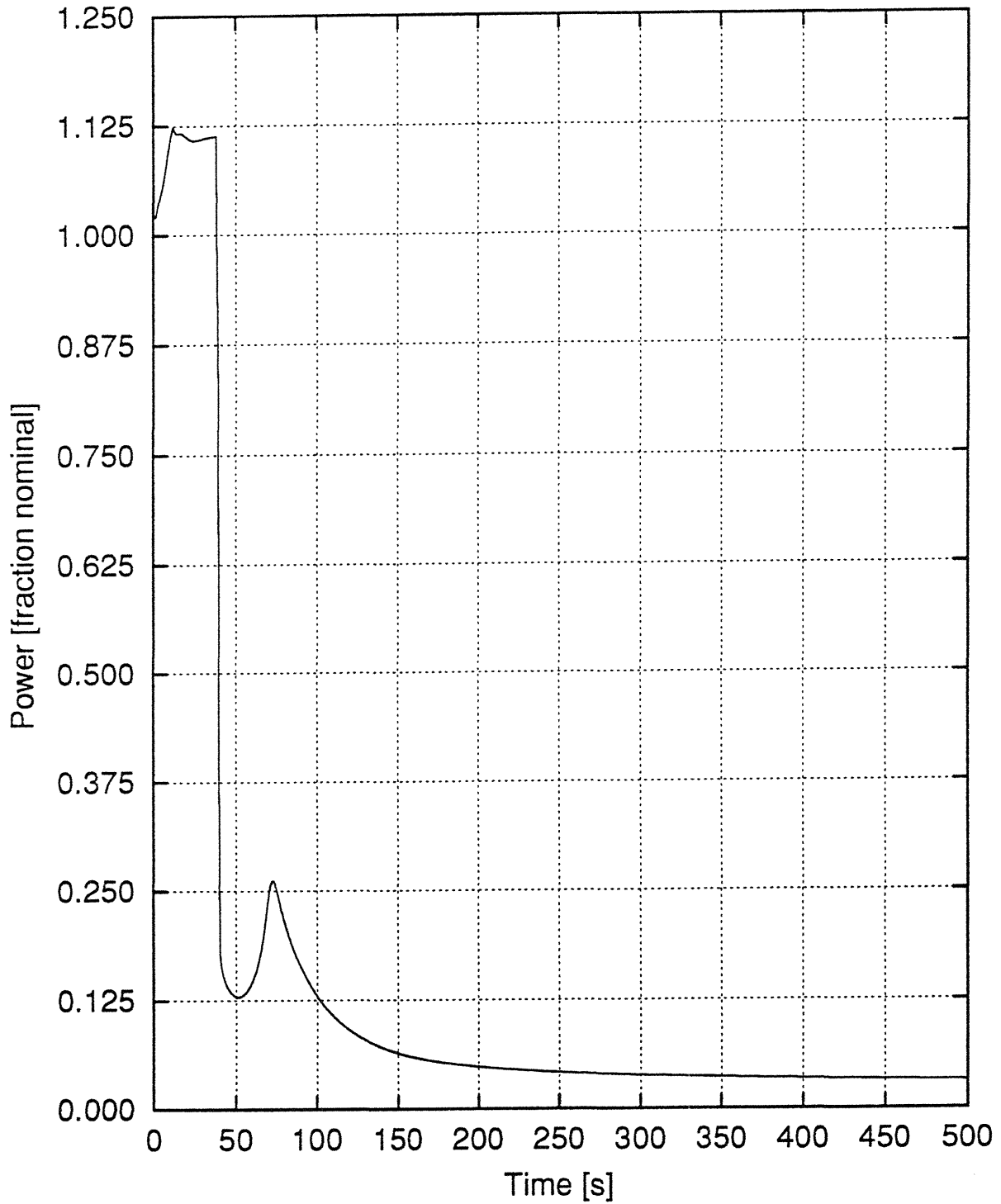


Figure 14.1.7-15
Excessive Load Increase - EOC Auto Control
Pressurizer Pressure vs. Time

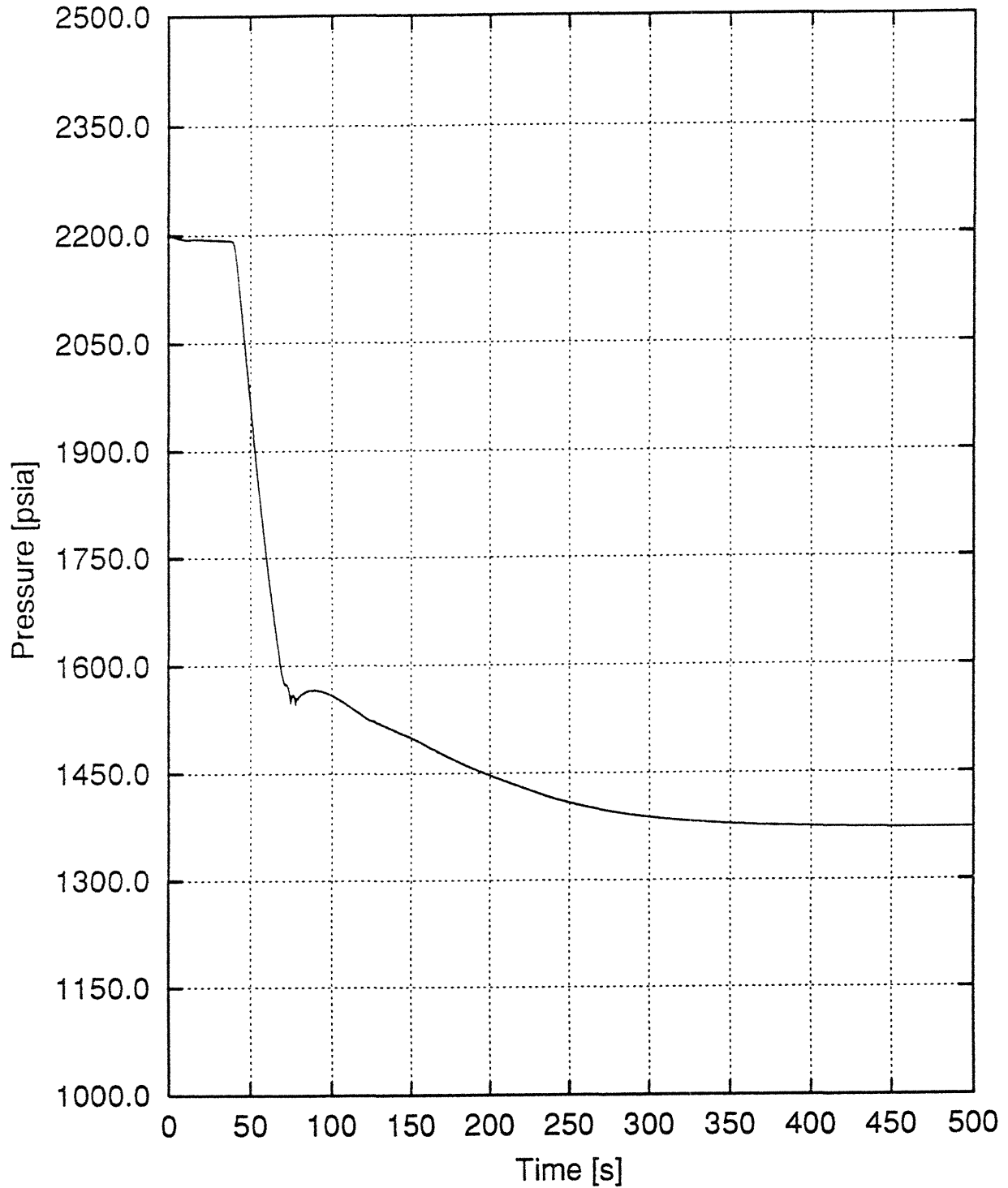


Figure 14.1.7-16
Excessive Load Increase - EOC Auto Control
 ΔT Loop vs. Time

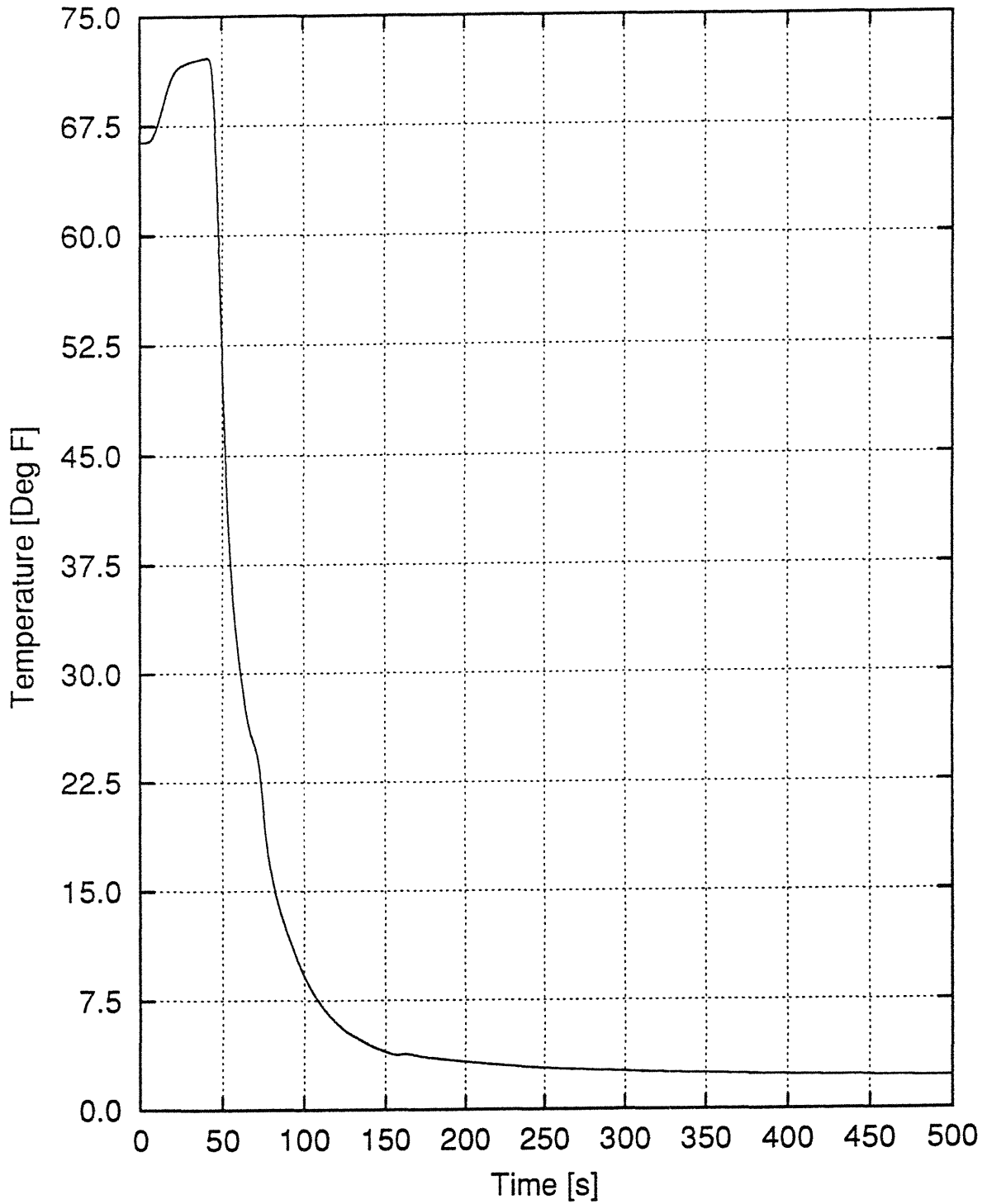


Figure 14.1.7-17
Excessive Load Increase - EOC Auto Control
 T_{ave} vs. Time

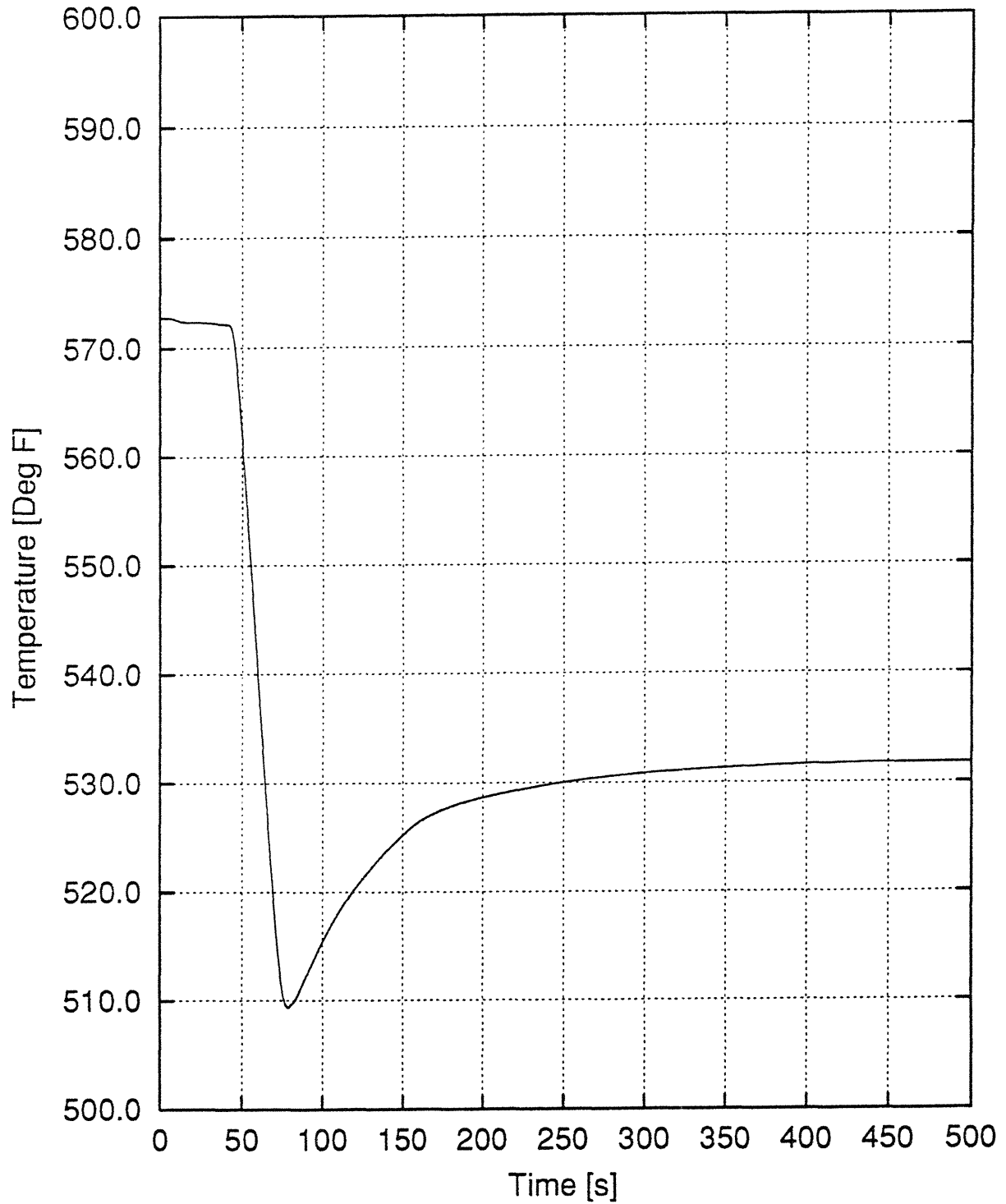


Figure 14.1.7-18
Excessive Load Increase -EOC Auto Control
Minimum DNBR vs. Time

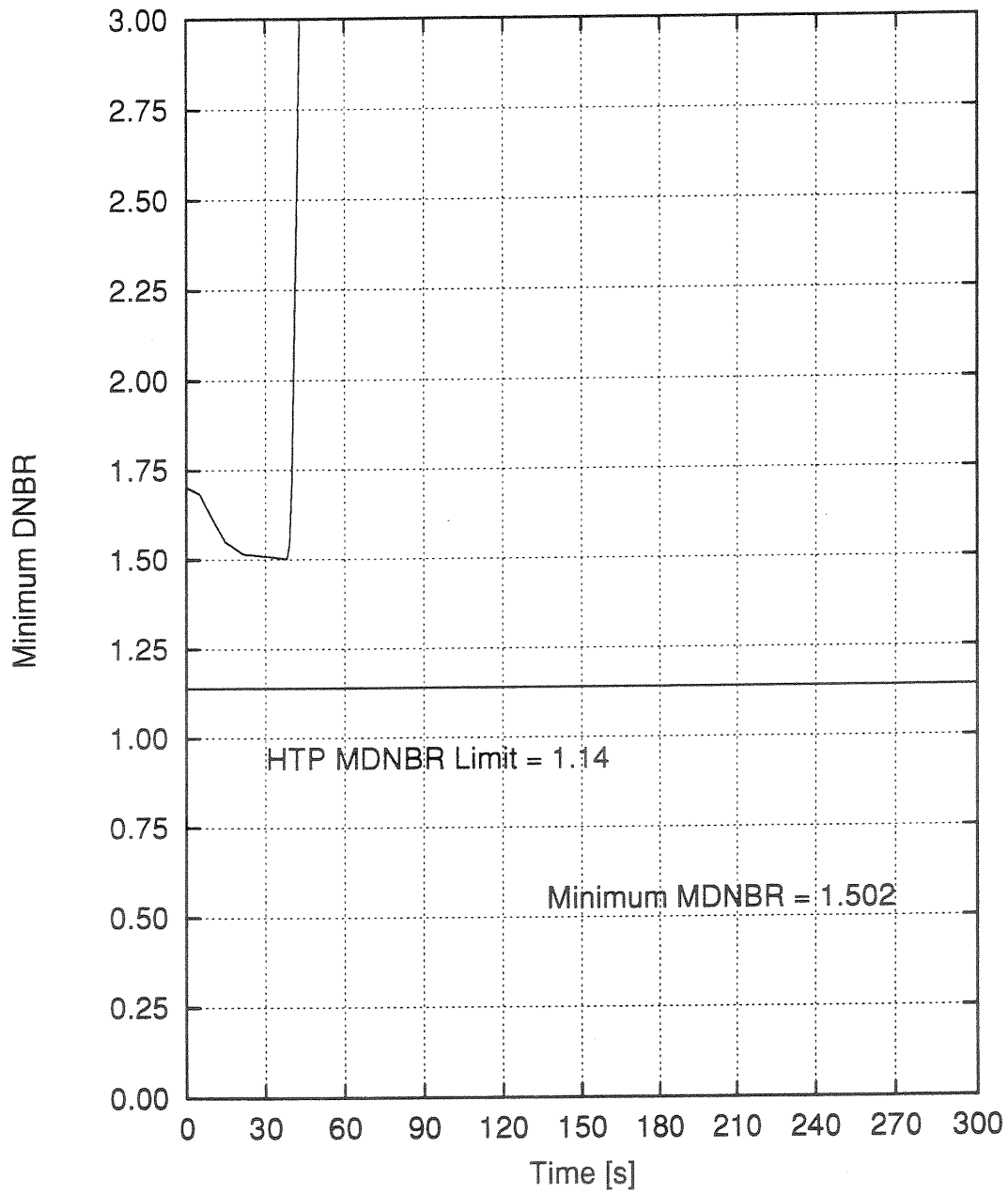


Figure 14.1.8-1
Partial Loss of Flow, One Pump Coasting Down (PLOF)
Total Core Inlet Flow vs. Time

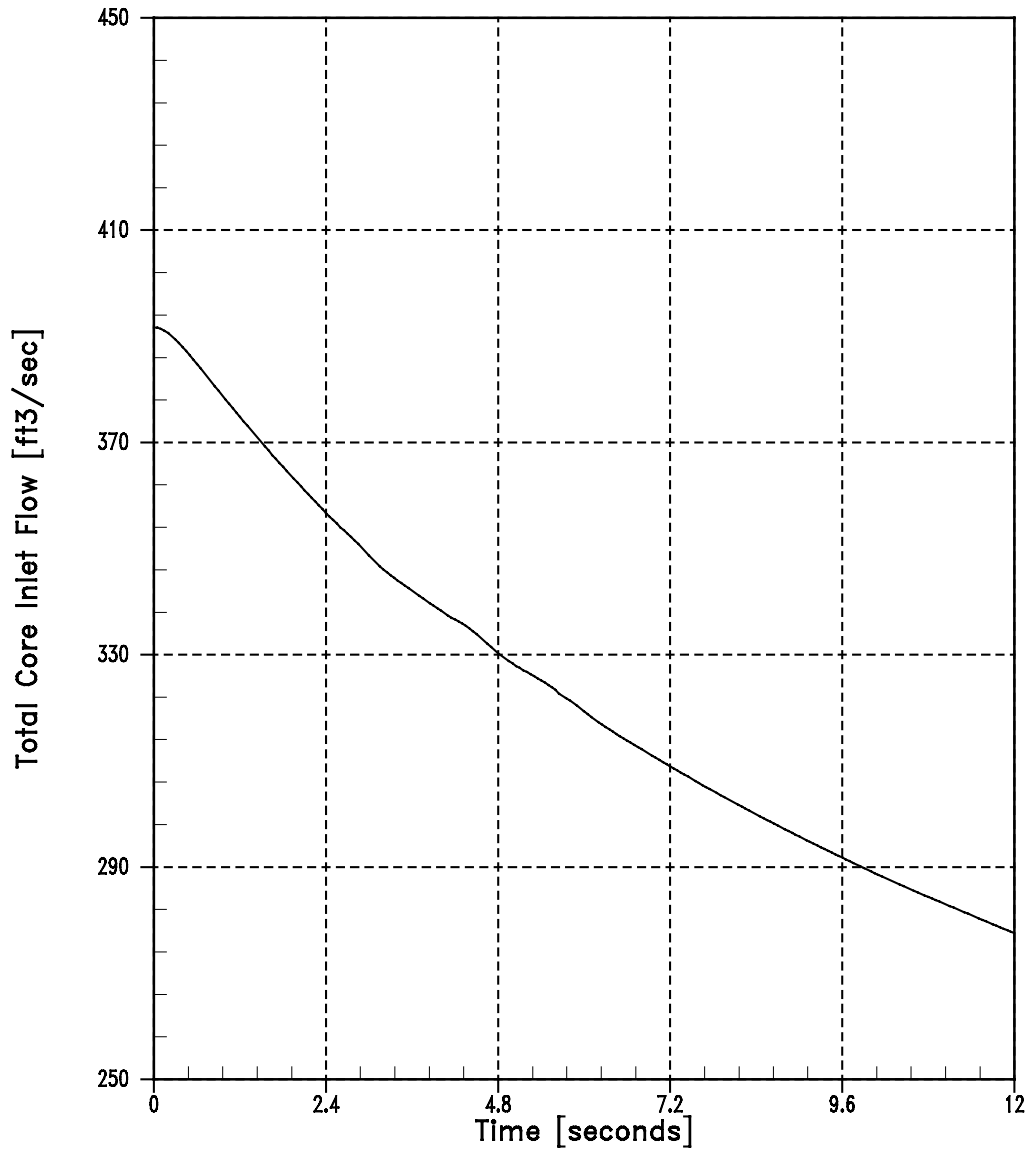


Figure 14.1.8-2
Partial Loss of Flow, One Pump Coasting Down (PLOF)
RCS Faulted Loop Flow vs. Time

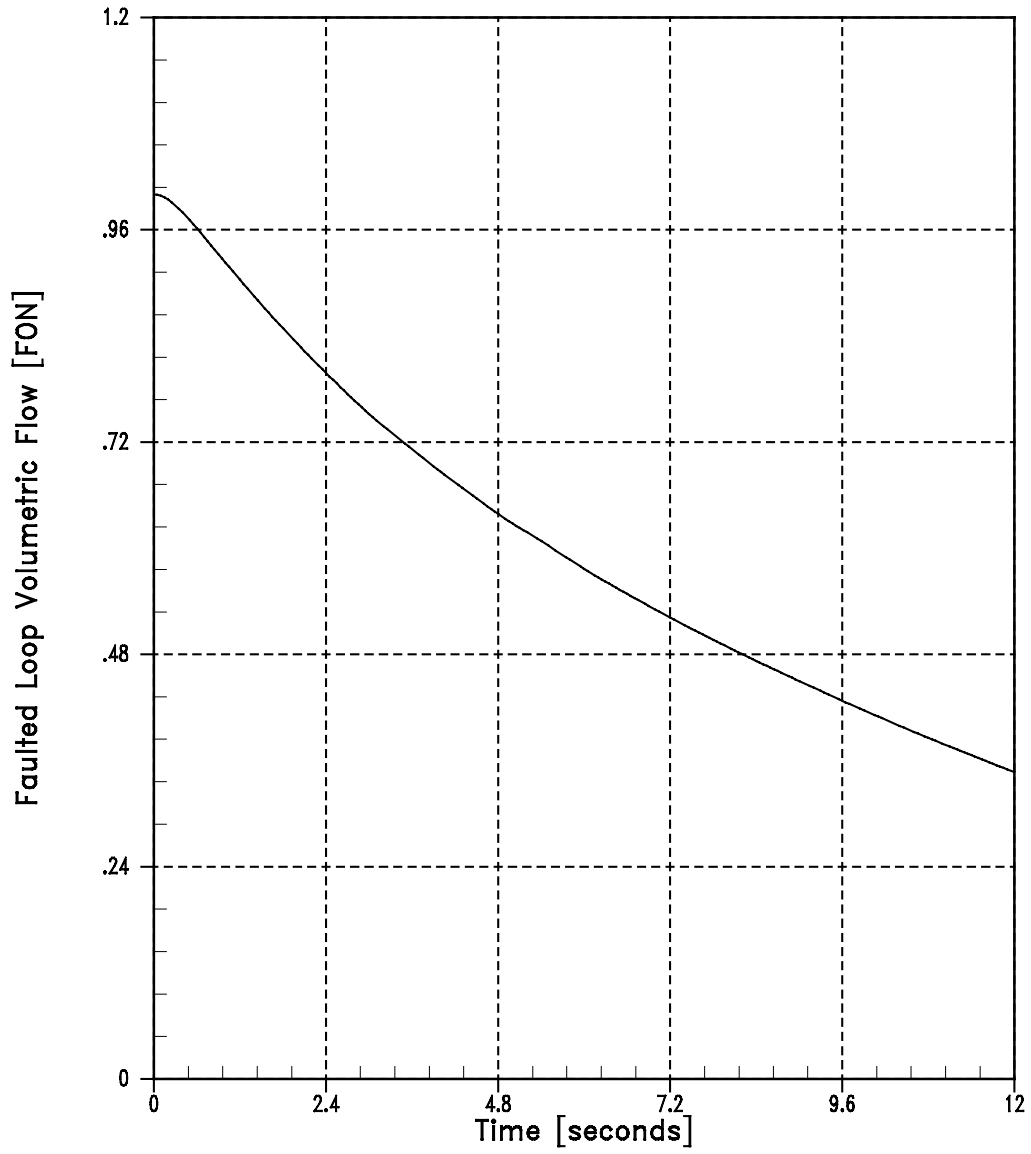


Figure 14.1.8-3
Partial Loss of Flow, One Pump Coasting Down (PLOF)
Nuclear Power vs. Time

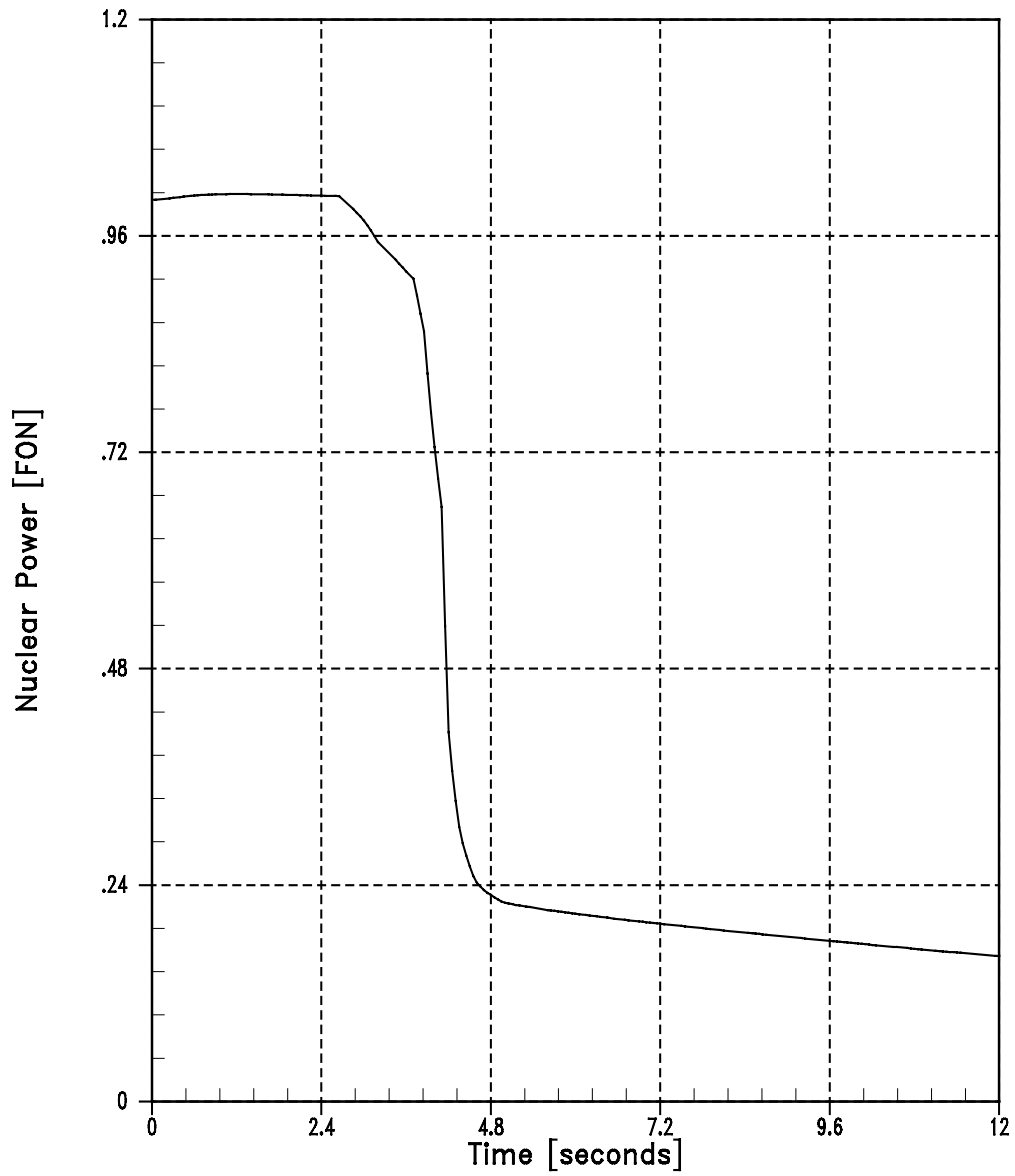


Figure 14.1.8-4
Partial Loss of Flow, One Pump Coasting Down (PLOF)
Core Average Heat Flux vs. Time

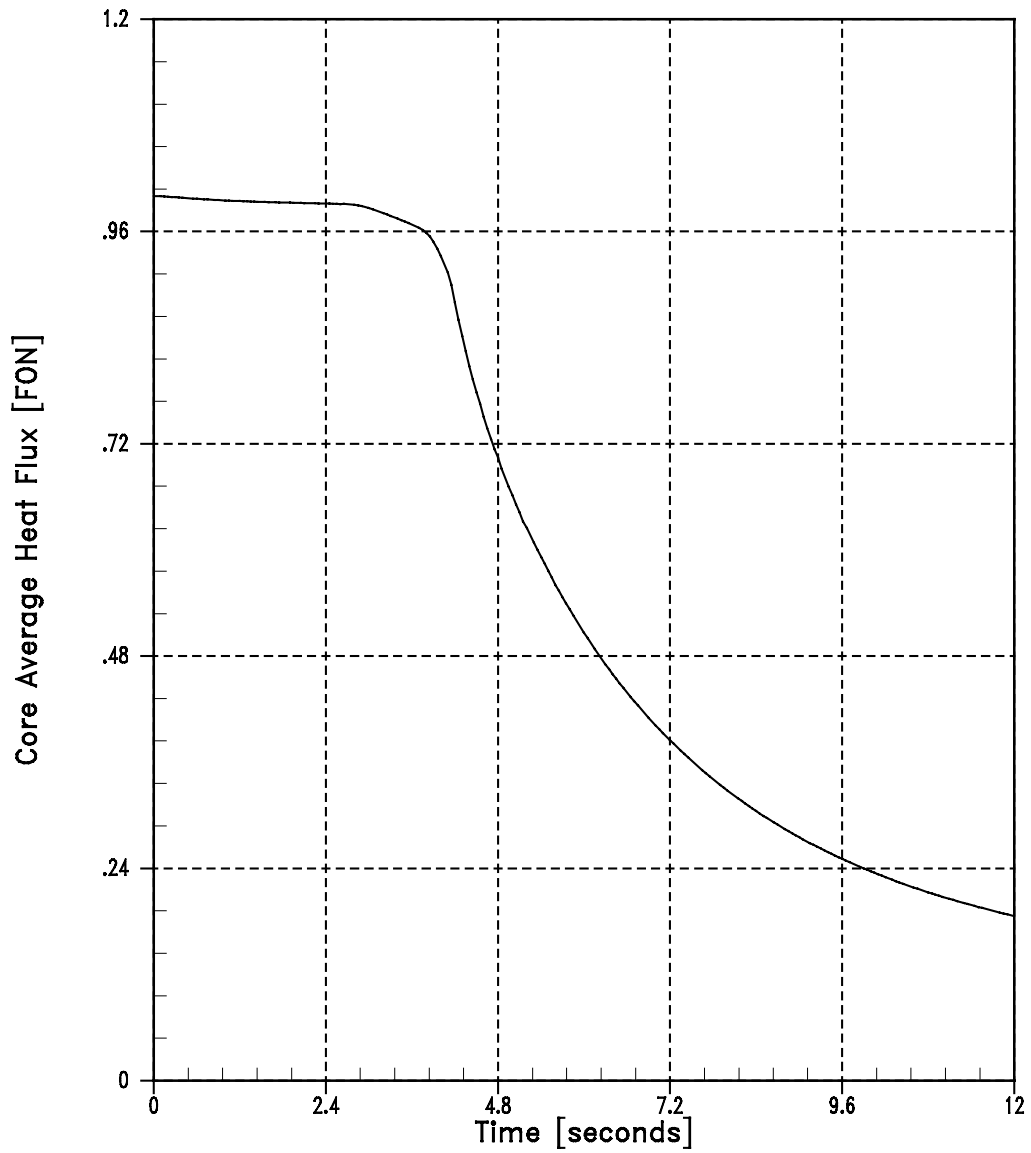


Figure 14.1.8-5
Partial Loss of Flow, One Pump Coasting Down (PLOF)
Pressurizer Pressure vs. Time

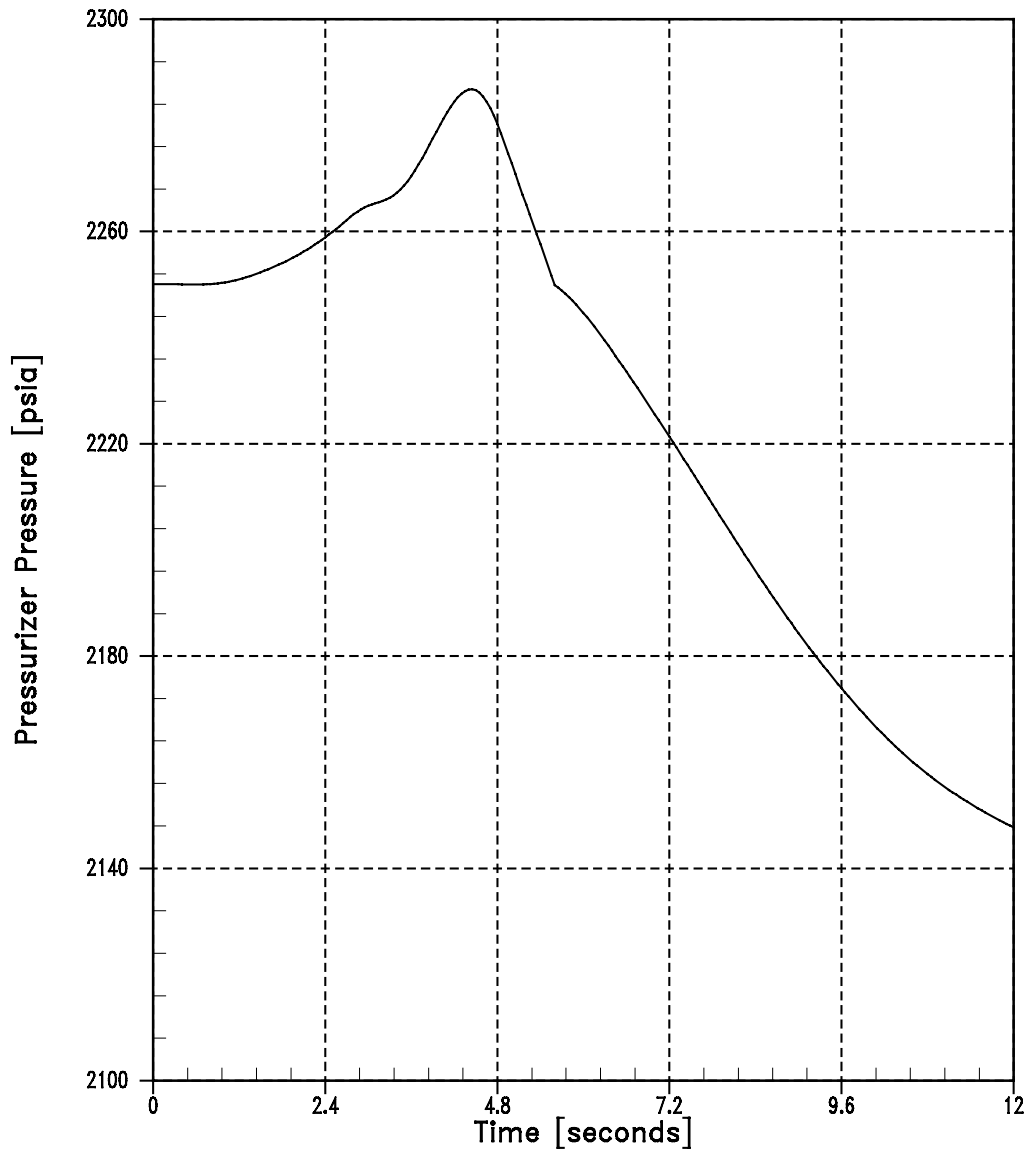


Figure 14.1.8-6
Partial Loss of Flow, One Pump Coasting Down (PLOF)
RCS Faulted Loop Temperature vs. Time

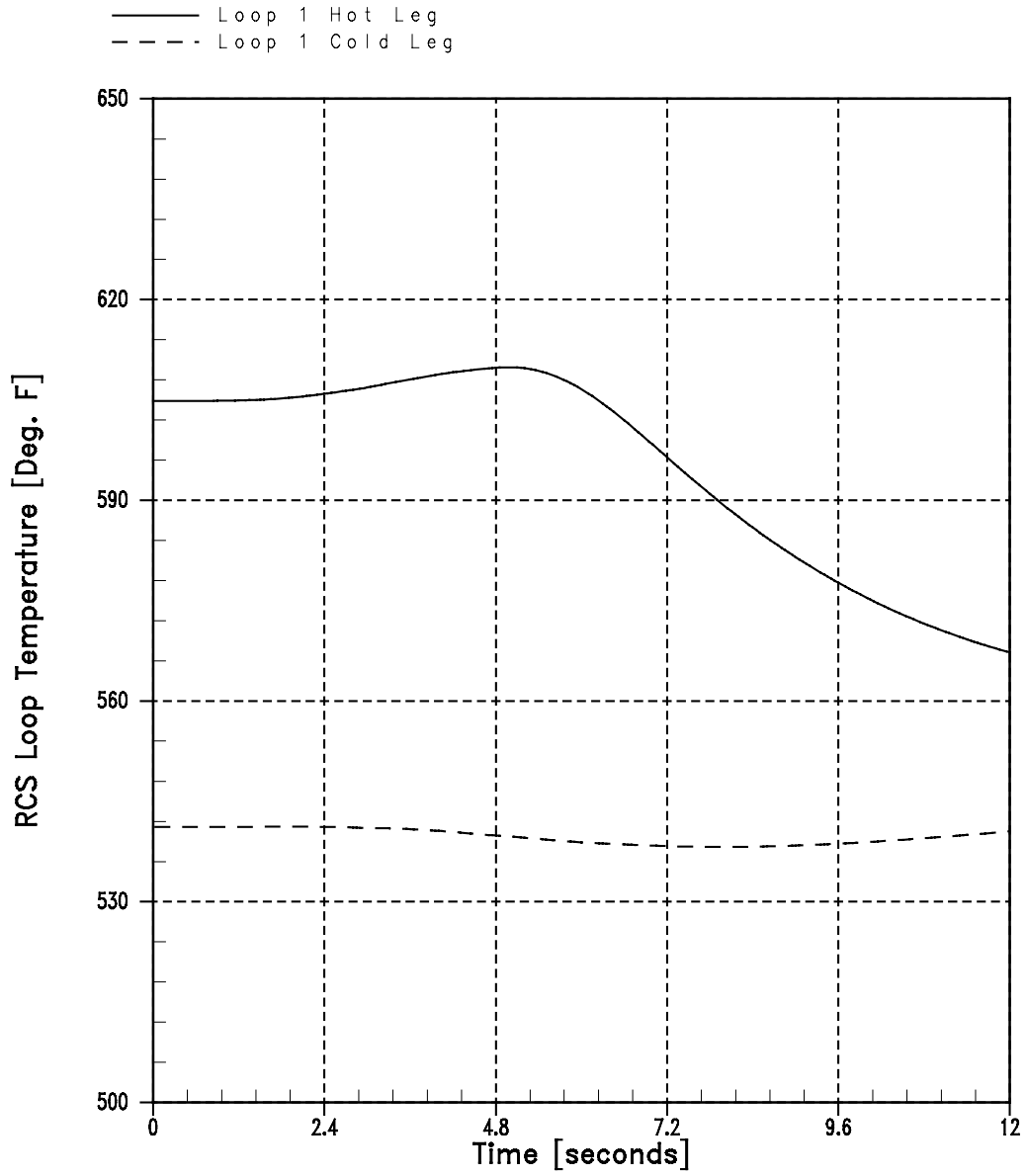


Figure 14.1.8-7
Partial Loss of Flow, One Pump Coasting Down (PLOF)
Hot Channel Heat Flux vs. Time

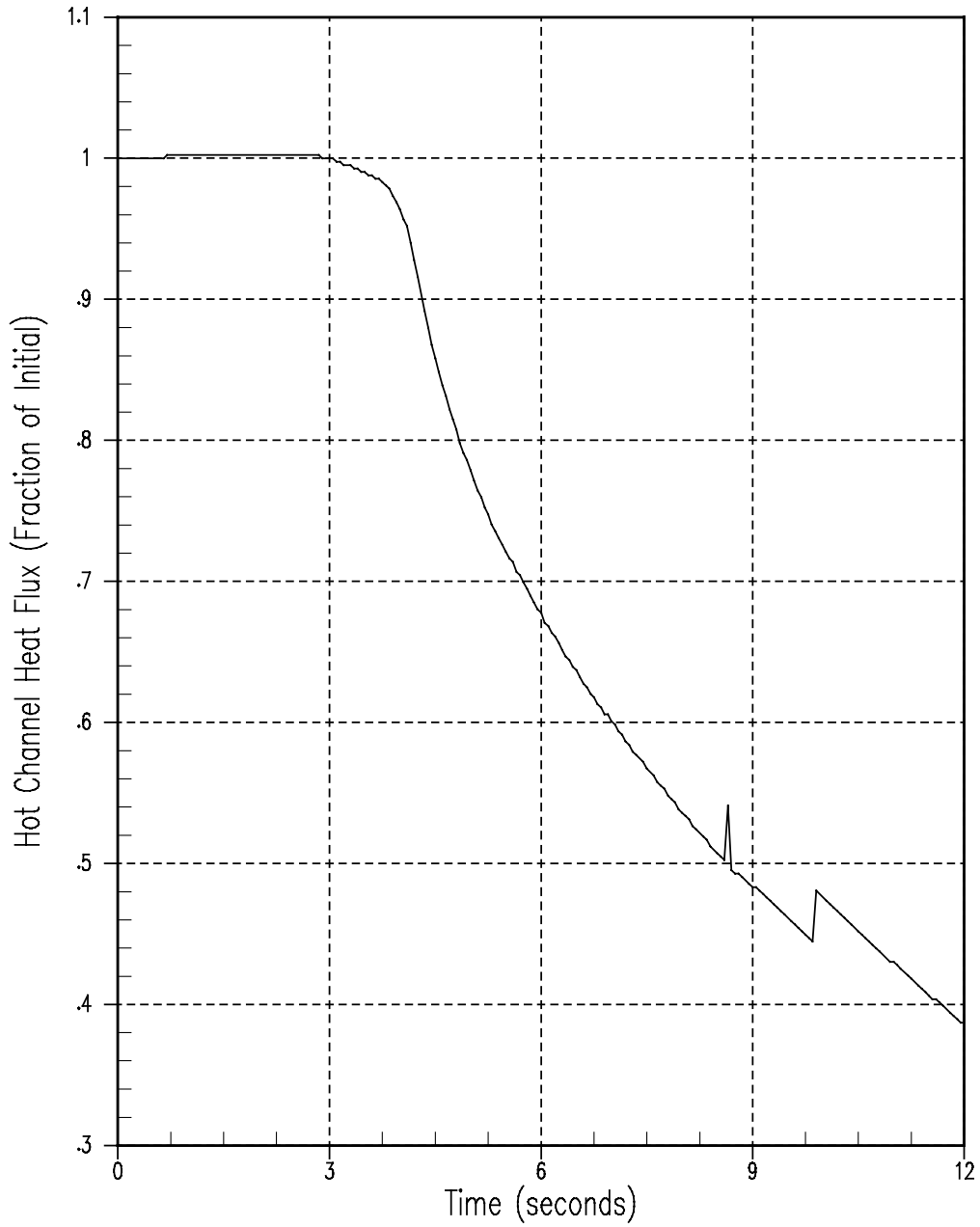


Figure 14.1.8-8
Partial Loss of Flow, One Pump Coasting Down (PLOF)
DNBR vs. Time

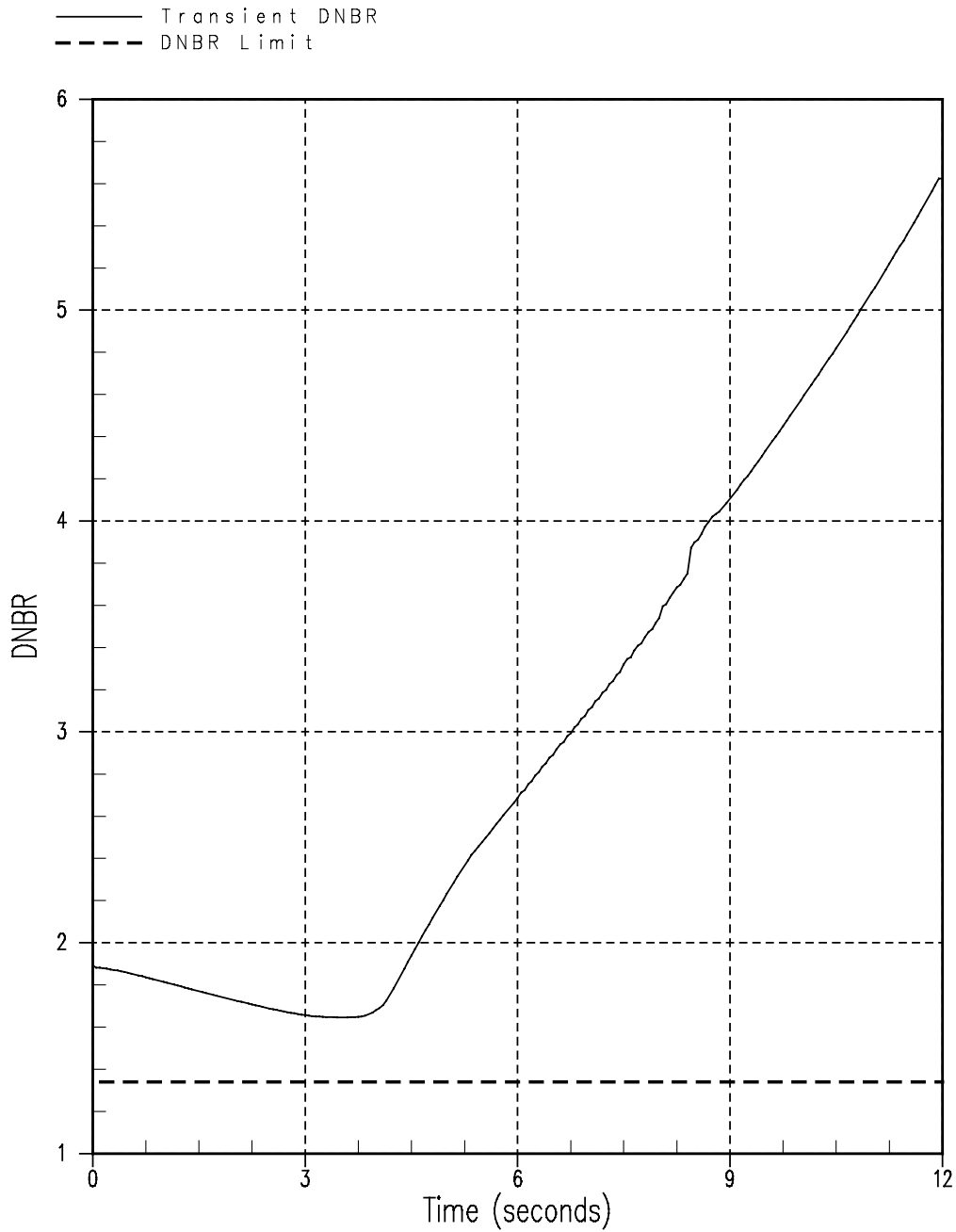


Figure 14.1.8-9
Complete Loss of Flow, Two Pump Coasting Down (CLOF)
Total Core Inlet Flow vs. Time

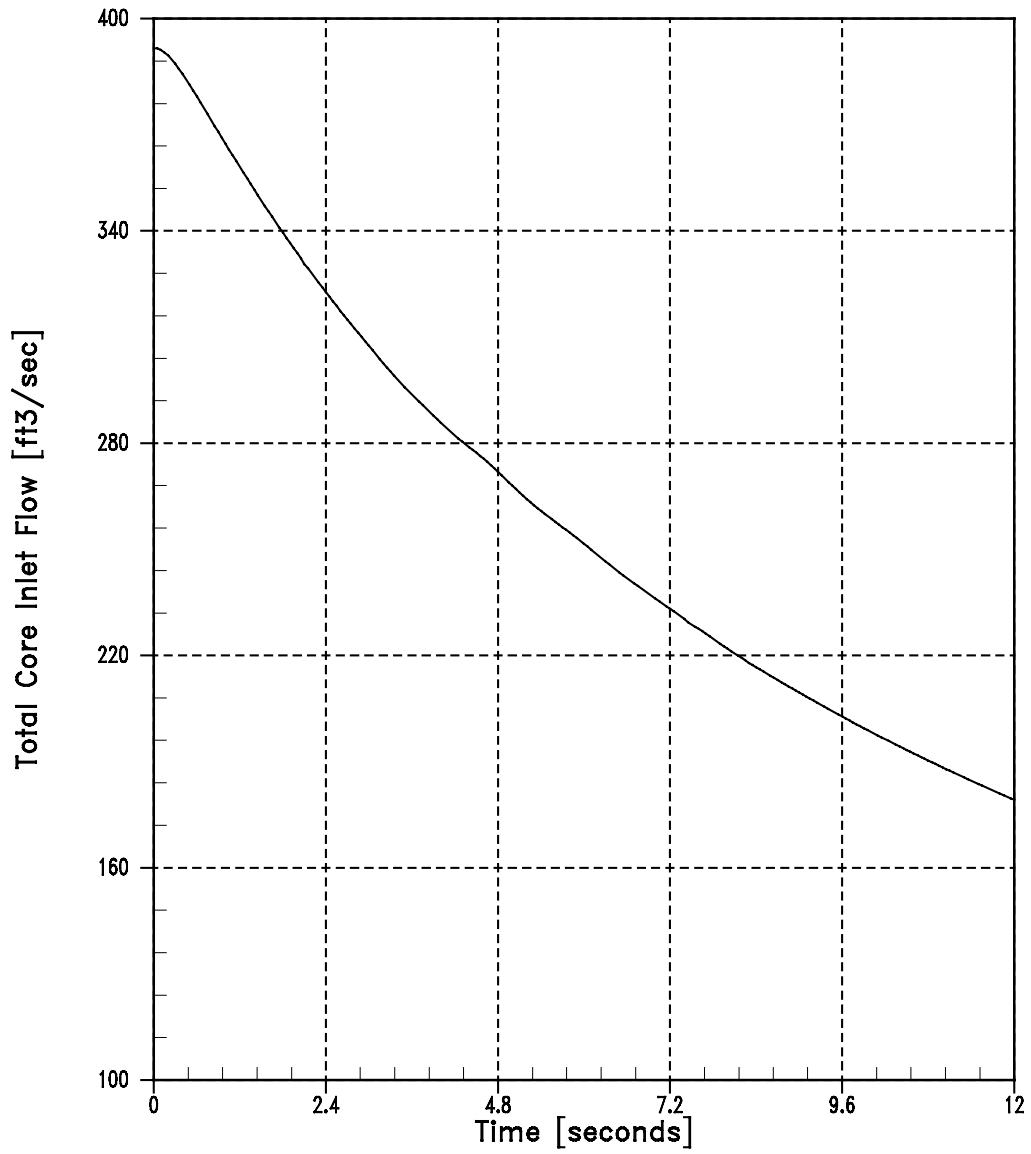


Figure 14.1.8-10
Complete Loss of Flow, Two Pumps Coasting Down (CLOF)
RCS Loop Flow vs. Time

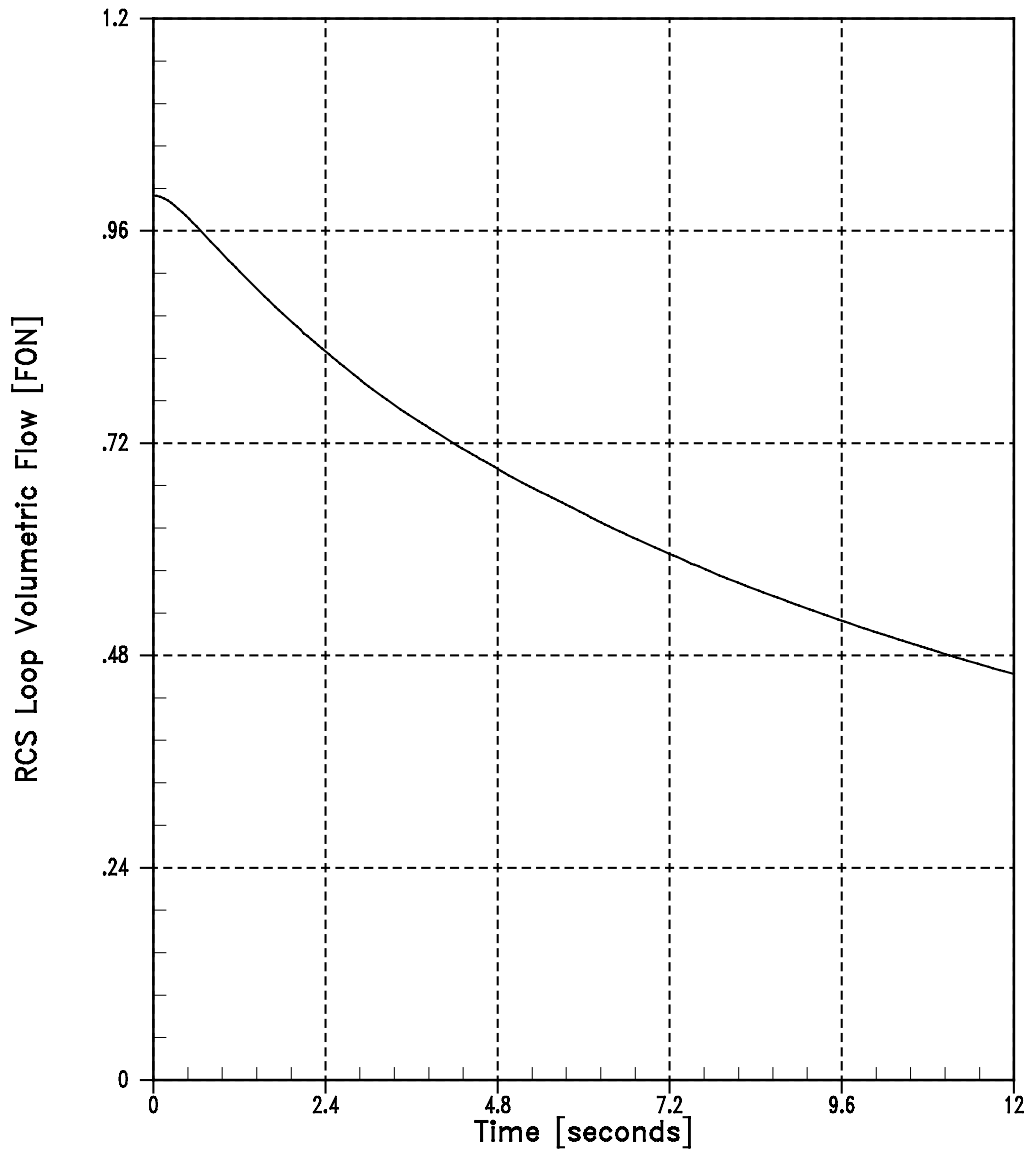


Figure 14.1.8-11
Complete Loss of Flow, Two Pumps Coasting Down (CLOF)
Nuclear Power vs. Time

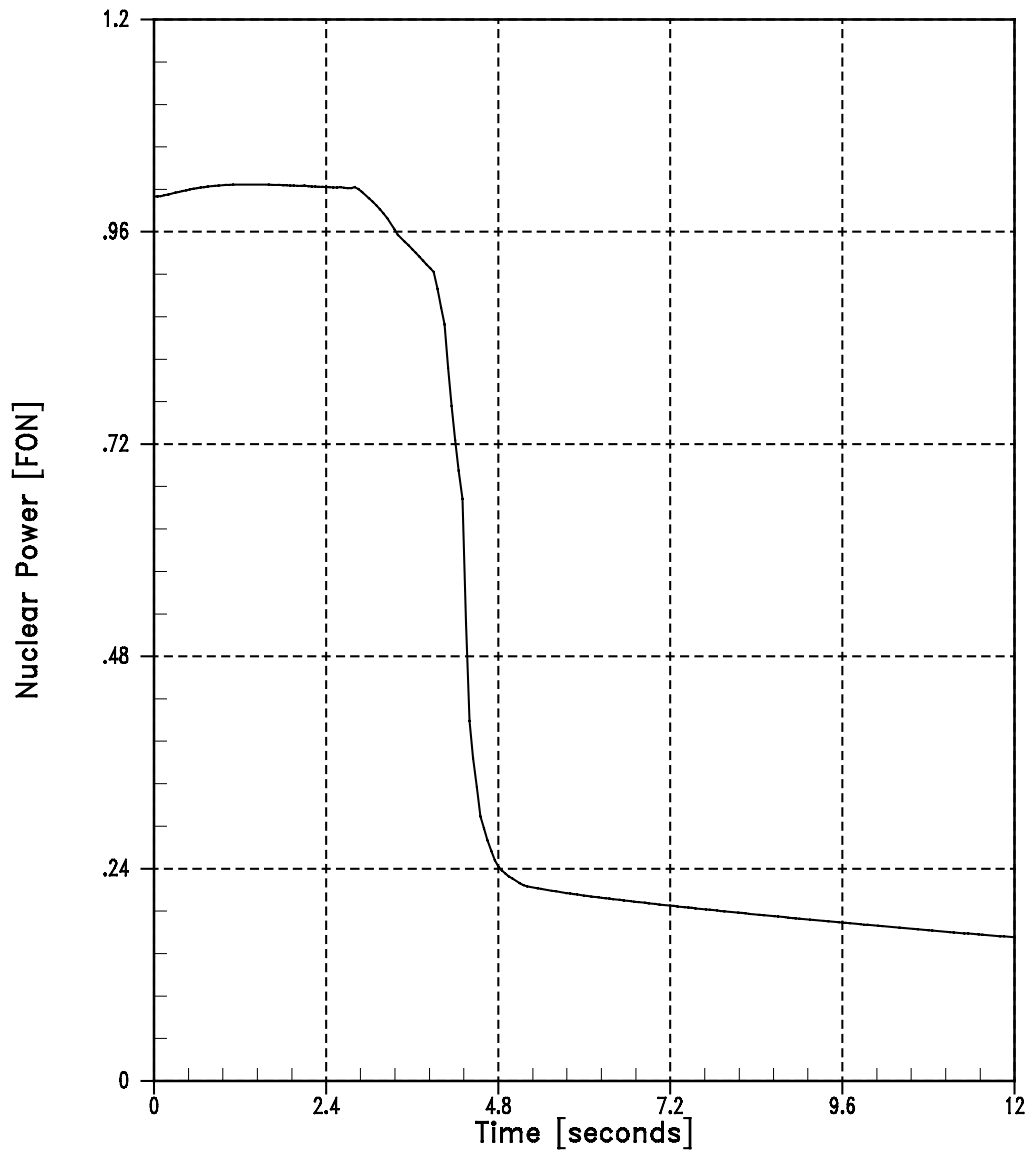


Figure 14.1.8-12
Complete Loss of Flow, Two Pumps Coasting Down (CLOF)
Core Average Heat Flux vs. Time

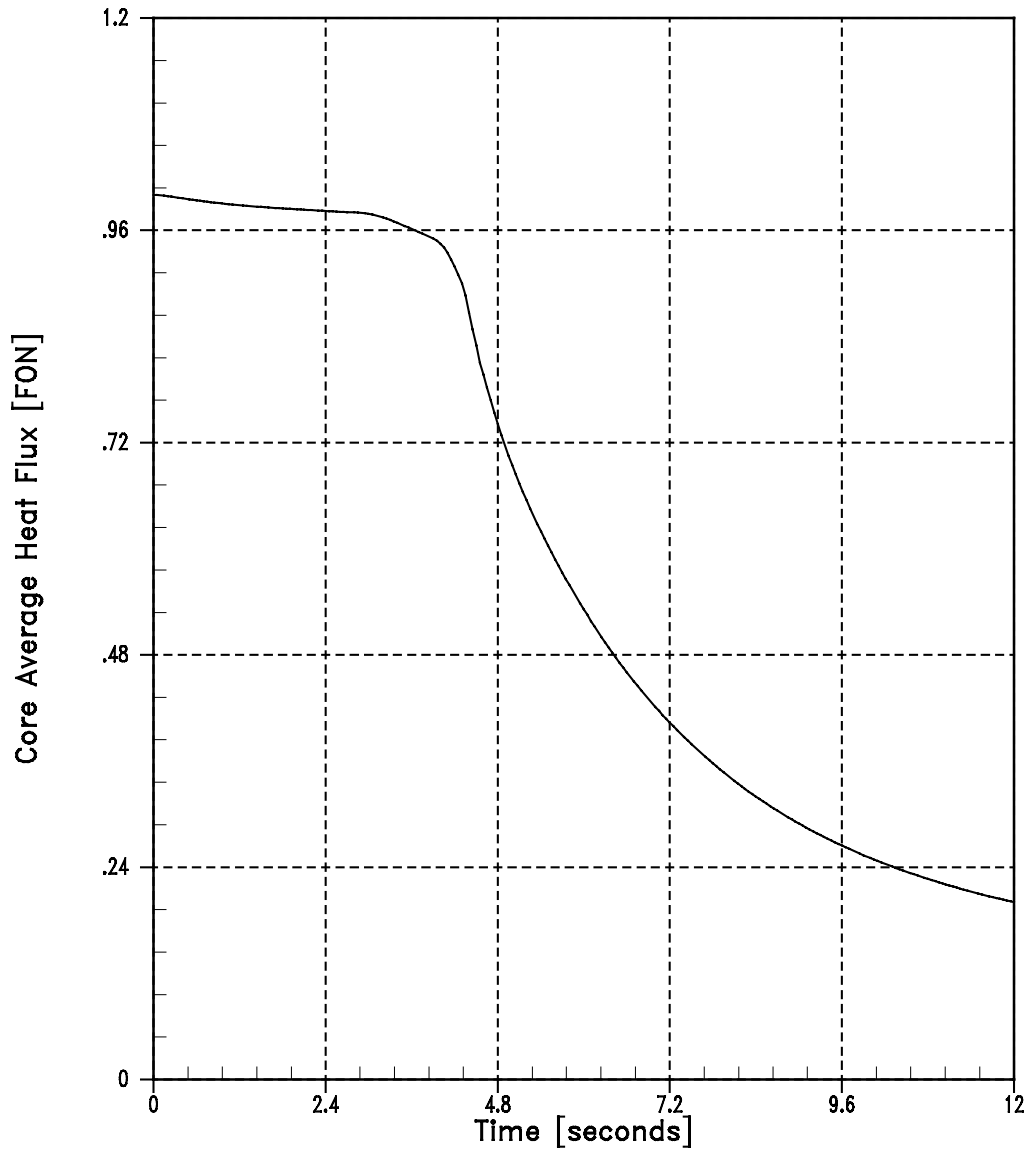


Figure 14.1.8-13
Complete Loss of Flow, Two Pumps Coasting Down (CLOF)
Pressurizer Pressure vs. Time

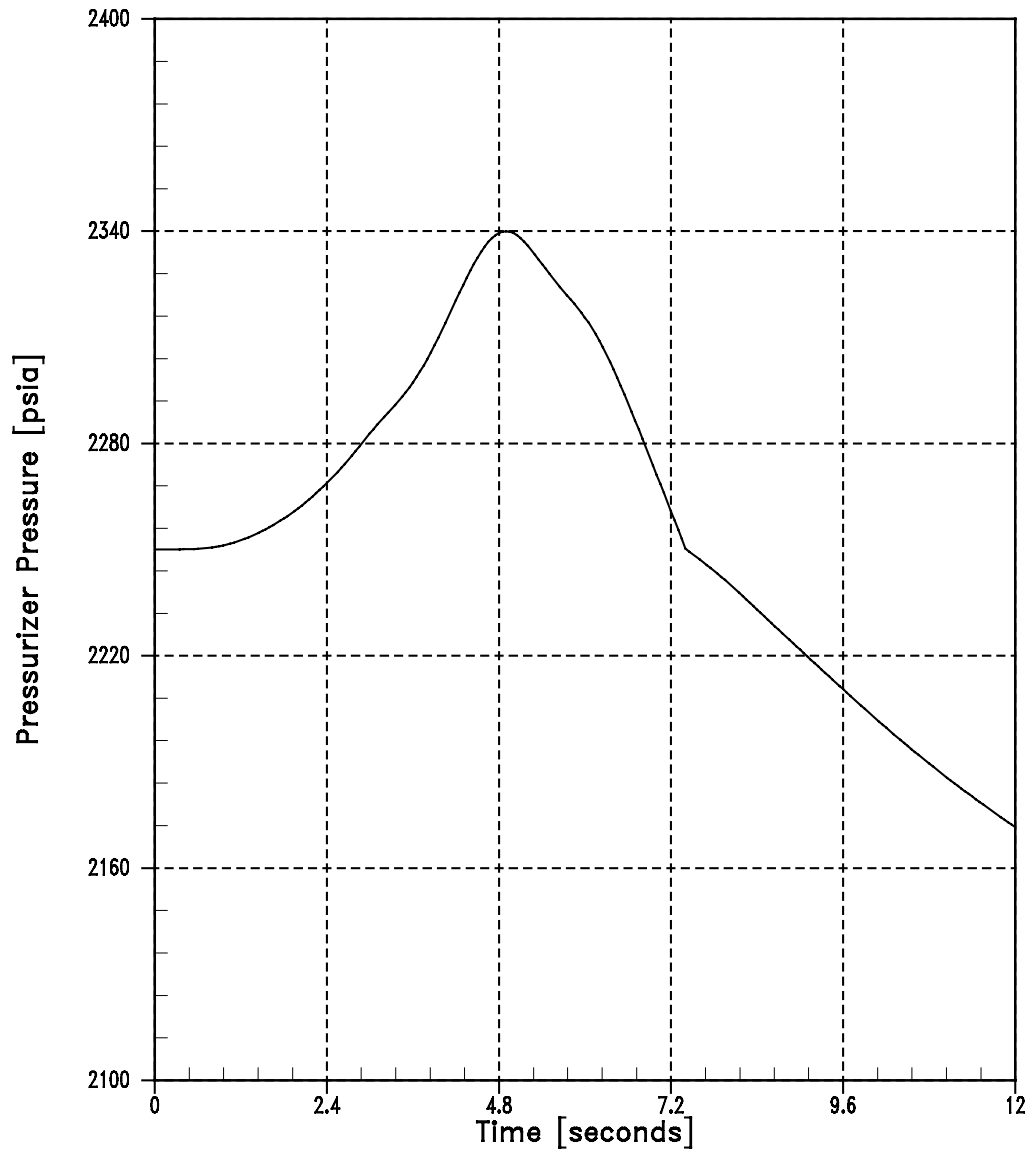


Figure 14.1.8-14
Complete Loss of Flow, Two Pumps Coasting Down (CLOF)
RCS Faulted Loop Temperature vs. Time

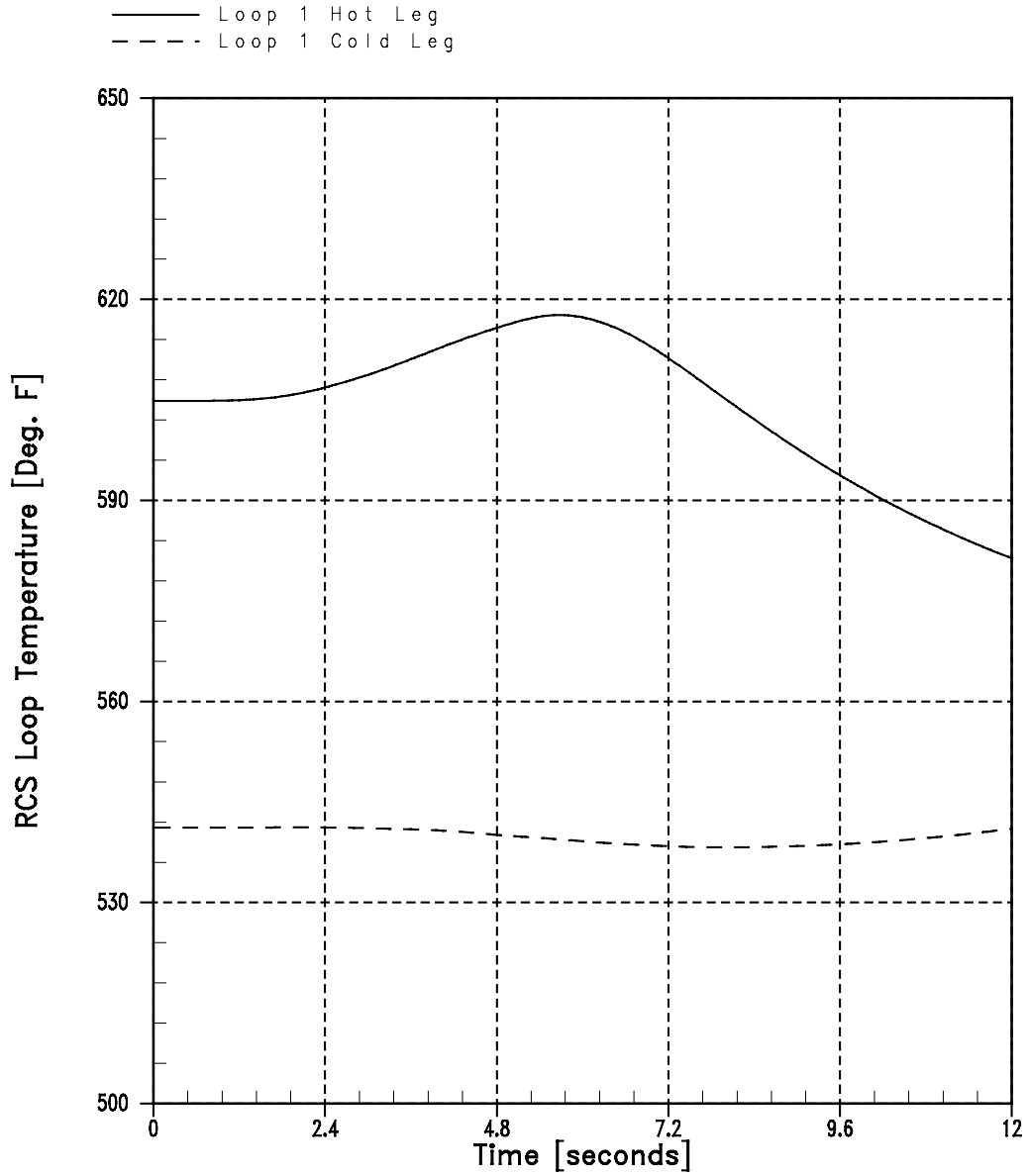


Figure 14.1.8-15
Complete Loss of Flow, Two Pumps Coasting Down (CLOF)
Hot Channel Heat Flux vs. Time

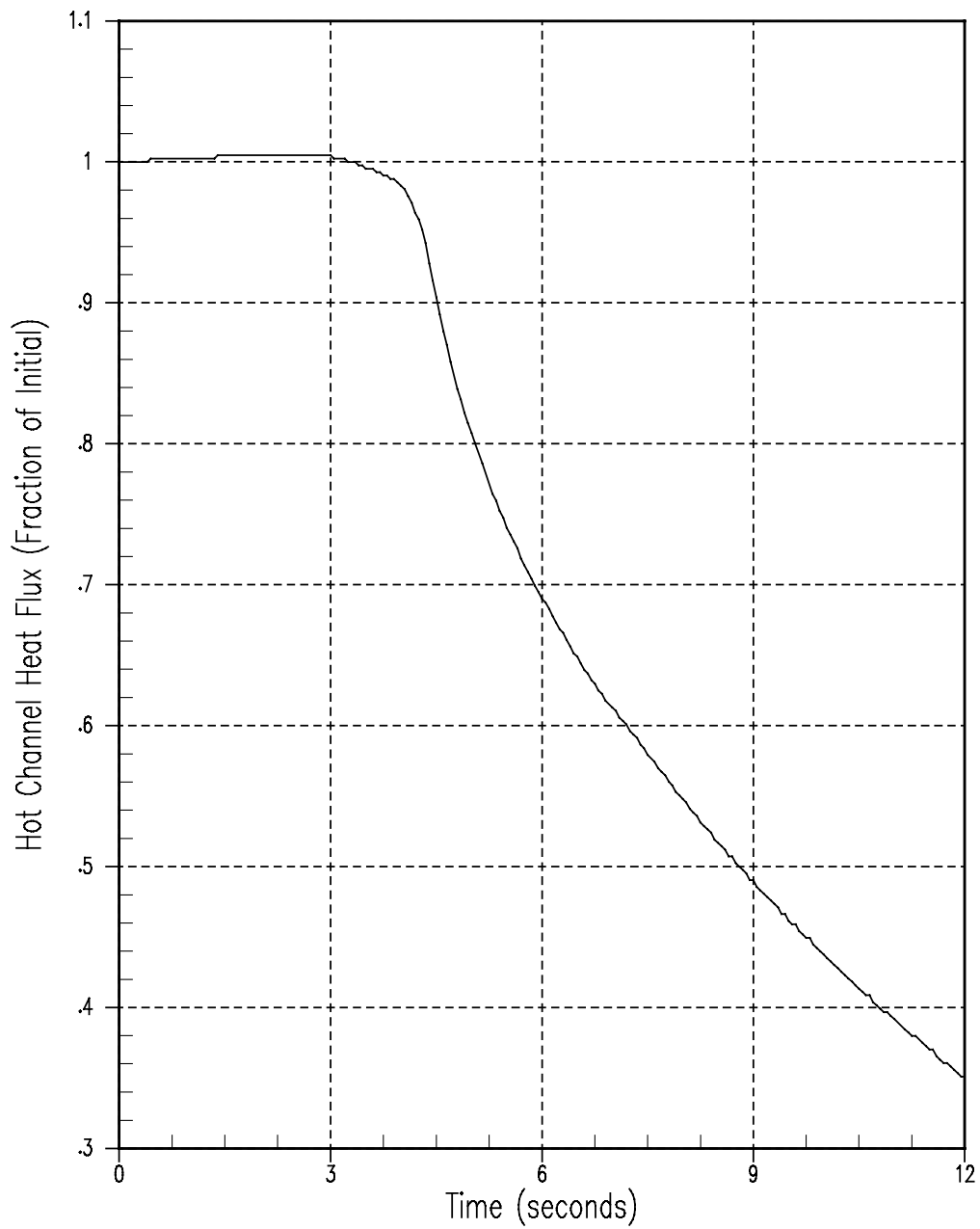


Figure 14.1.8-16
Complete Loss of Flow, Two Pumps Coasting Down (CLOF)
DNBR vs. Time

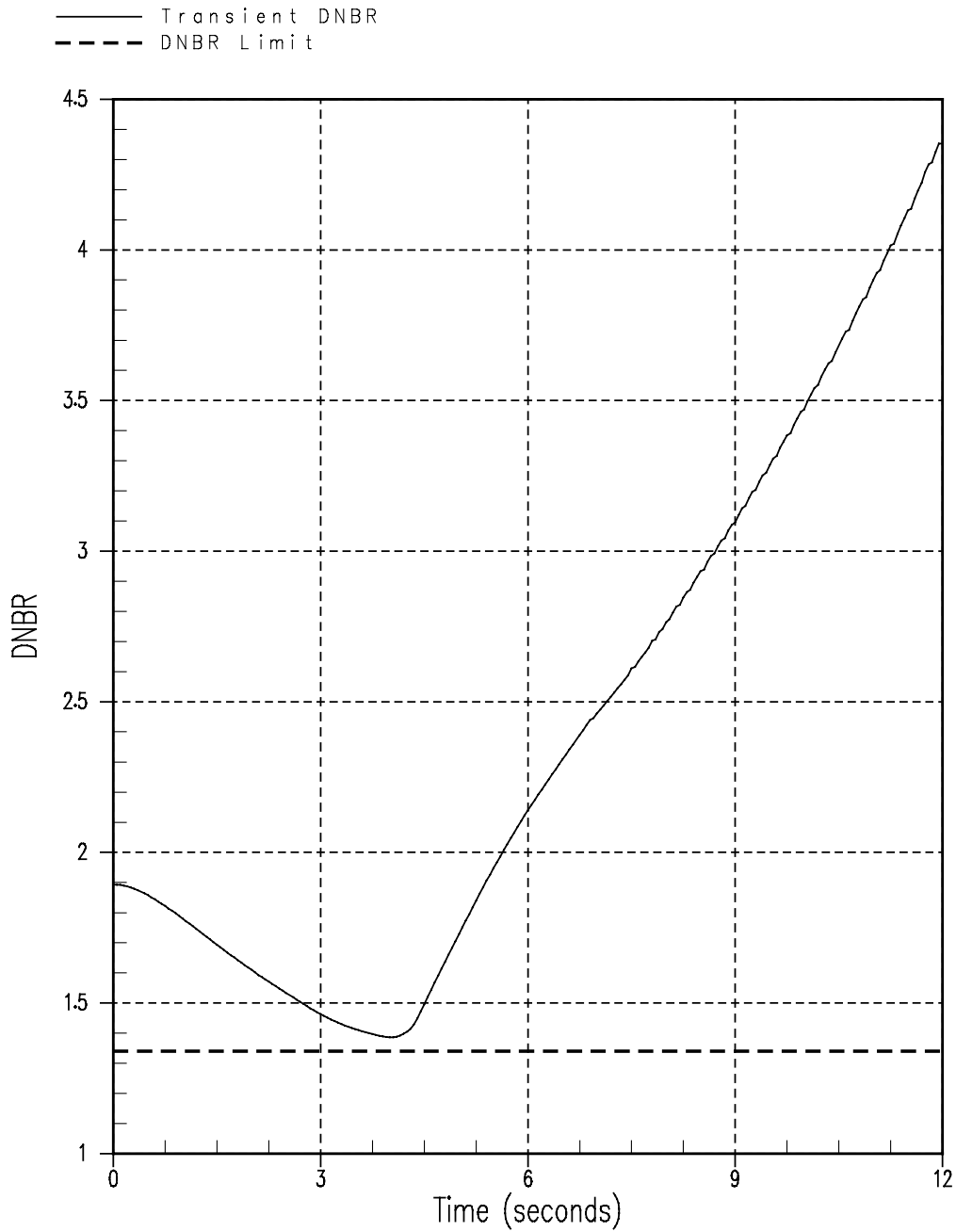


Figure 14.1.8-17
Complete Loss of Flow, Frequency Decay in Two Pumps (CLOF-UF)
Total Core Inlet Flow vs. Time

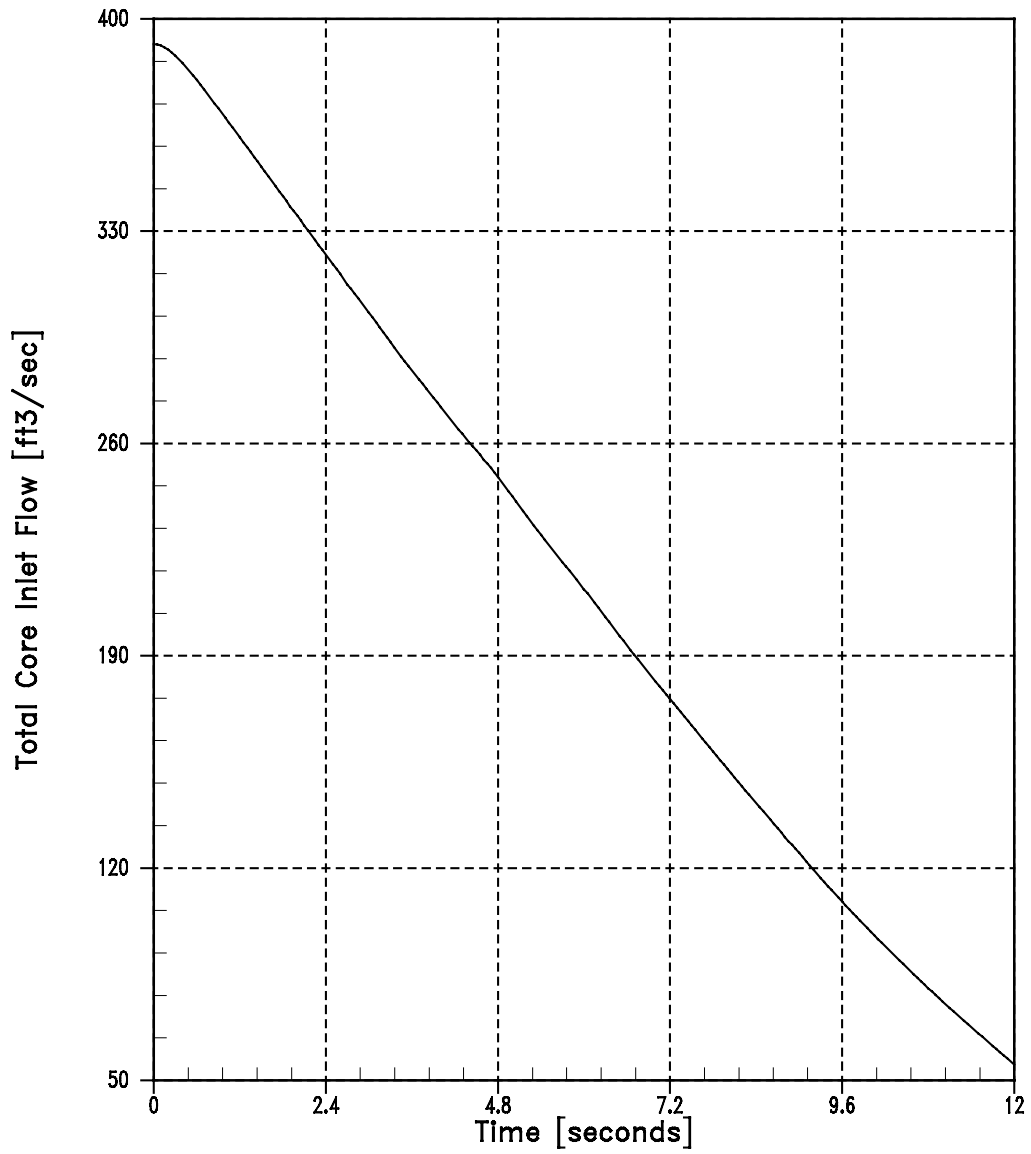


Figure 14.1.8-18
Complete Loss of Flow, Frequency Decay in Two Pumps (CLOF-UF)
RCS Loop Flow vs. Time

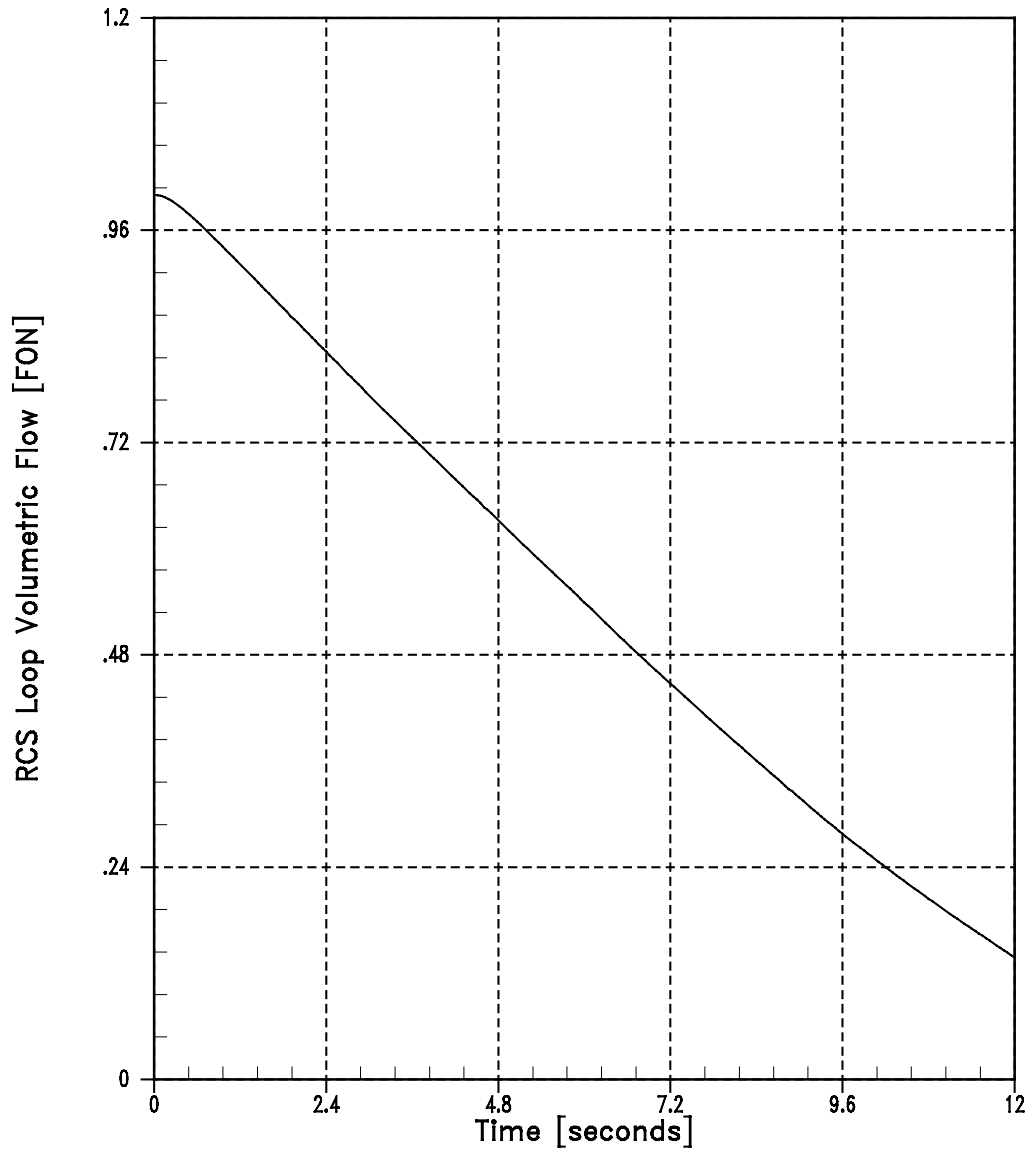


Figure 14.1.8-19
Complete Loss of Flow, Frequency Decay in Two Pumps (CLOF-UF)
Nuclear Power vs. Time

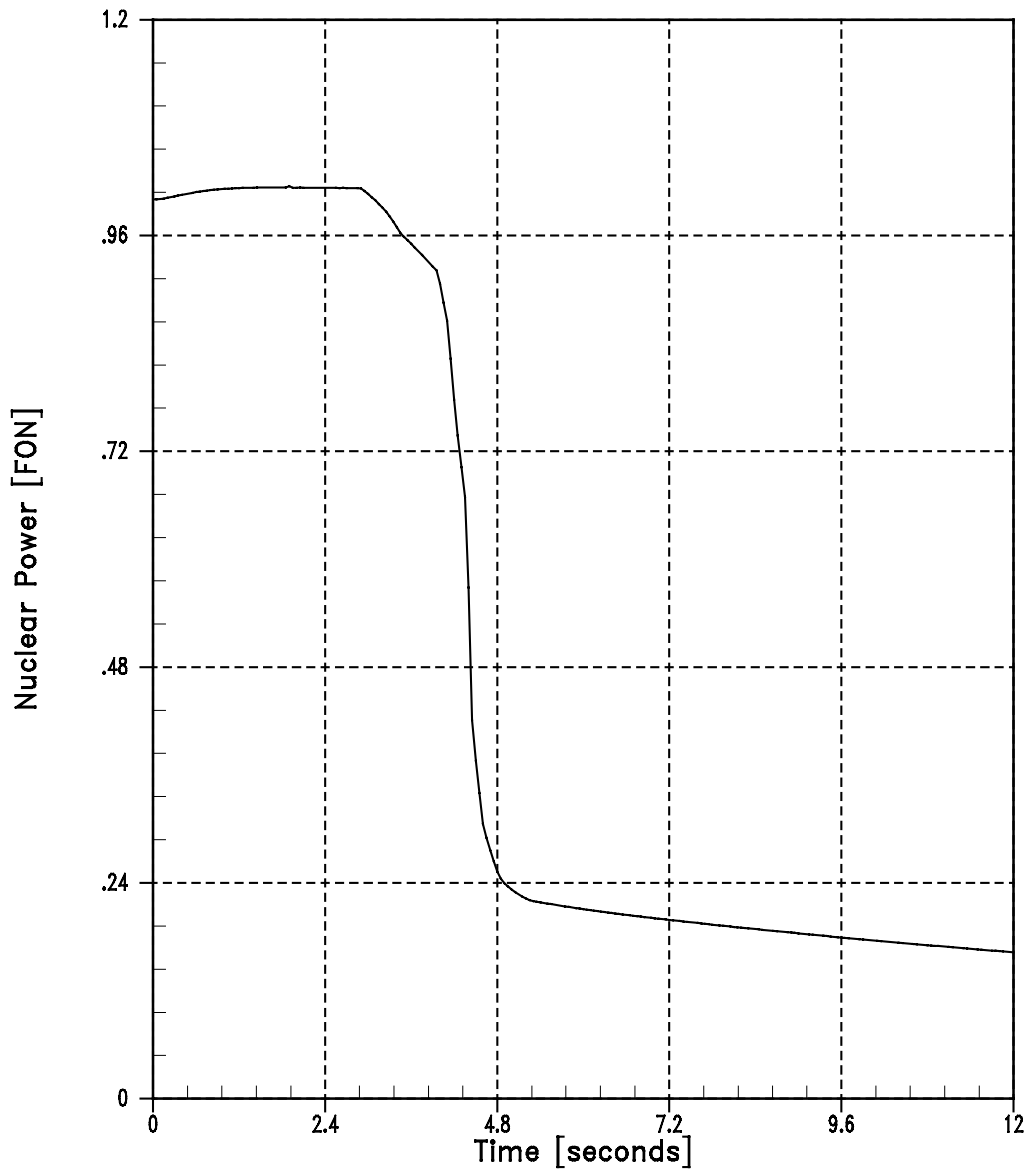


Figure 14.1.8-20
Complete Loss of Flow, Frequency Decay in Two Pumps (CLOF-UF)
Core Average Heat Flux vs. Time

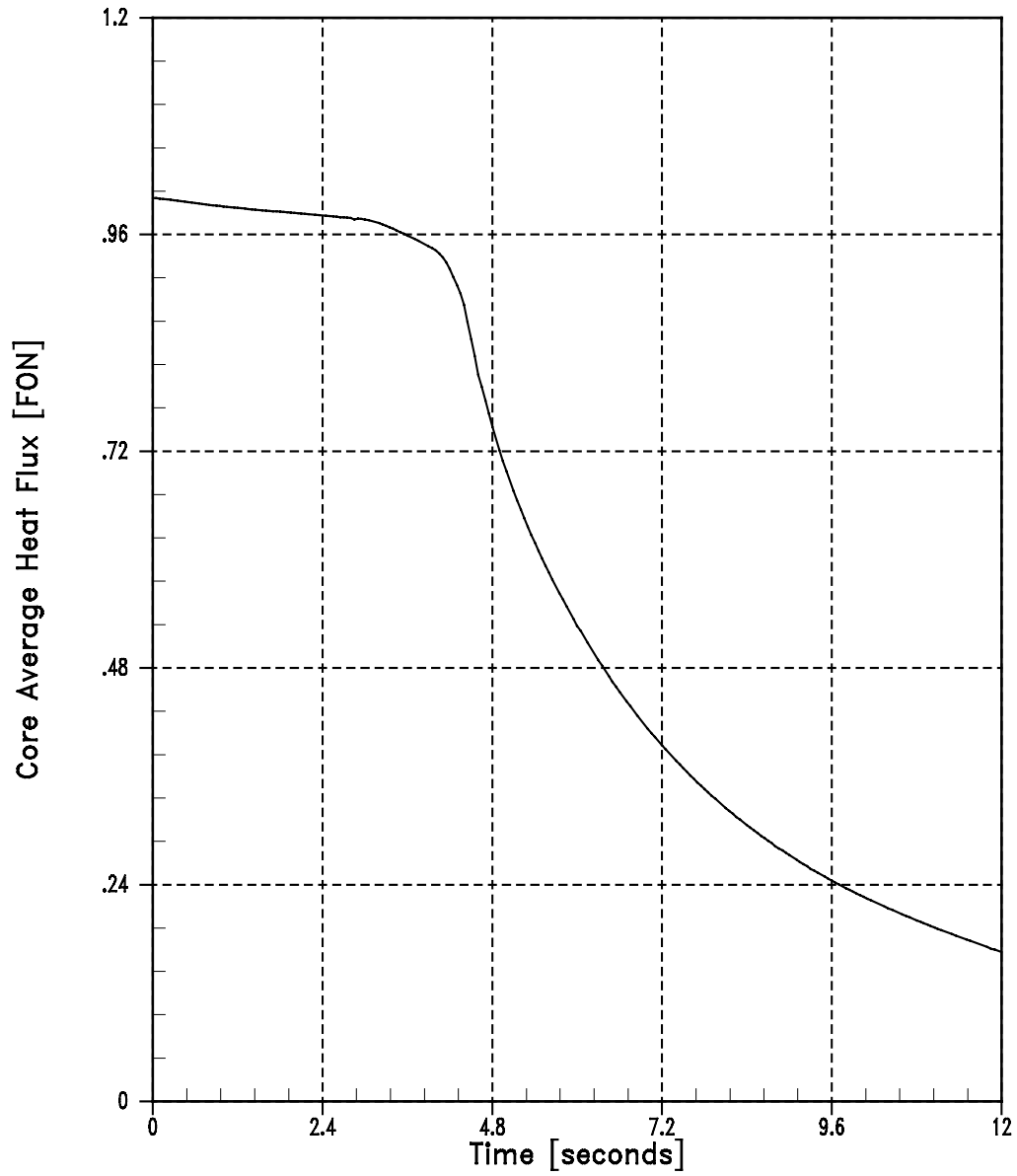


Figure 14.1.8-21
Complete Loss of Flow, Frequency Decay in Two Pumps (CLOF-UF)
Pressurizer Pressure vs. Time

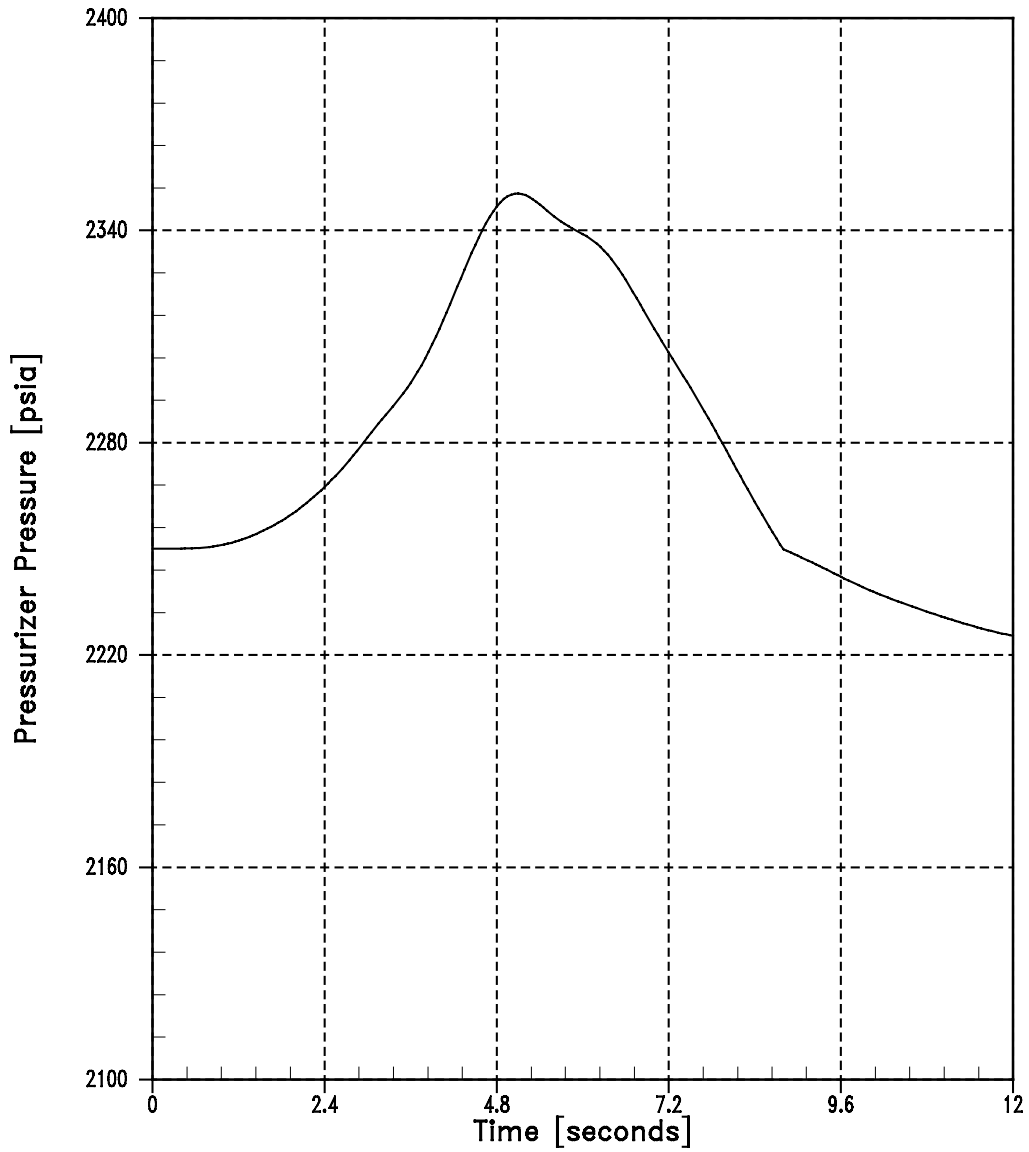


Figure 14.1.8-22
Complete Loss of Flow, Frequency Decay in Two Pumps (CLOF-UF)
RCS Loop Temperature vs. Time

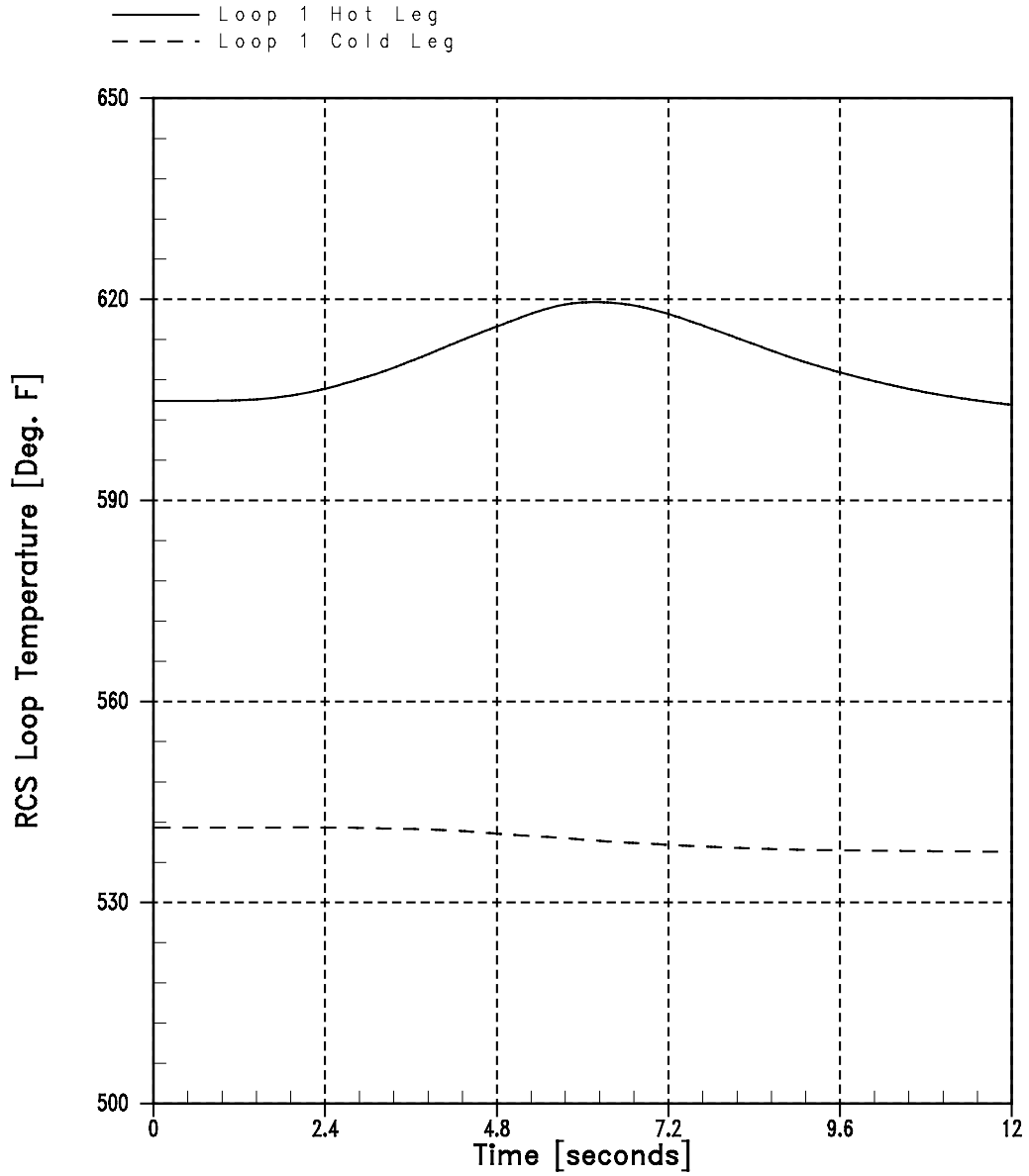


Figure 14.1.8-23
Complete Loss of Flow, Frequency Decay in Two Pumps (CLOF-UF)
Hot Channel Heat Flux vs. Time

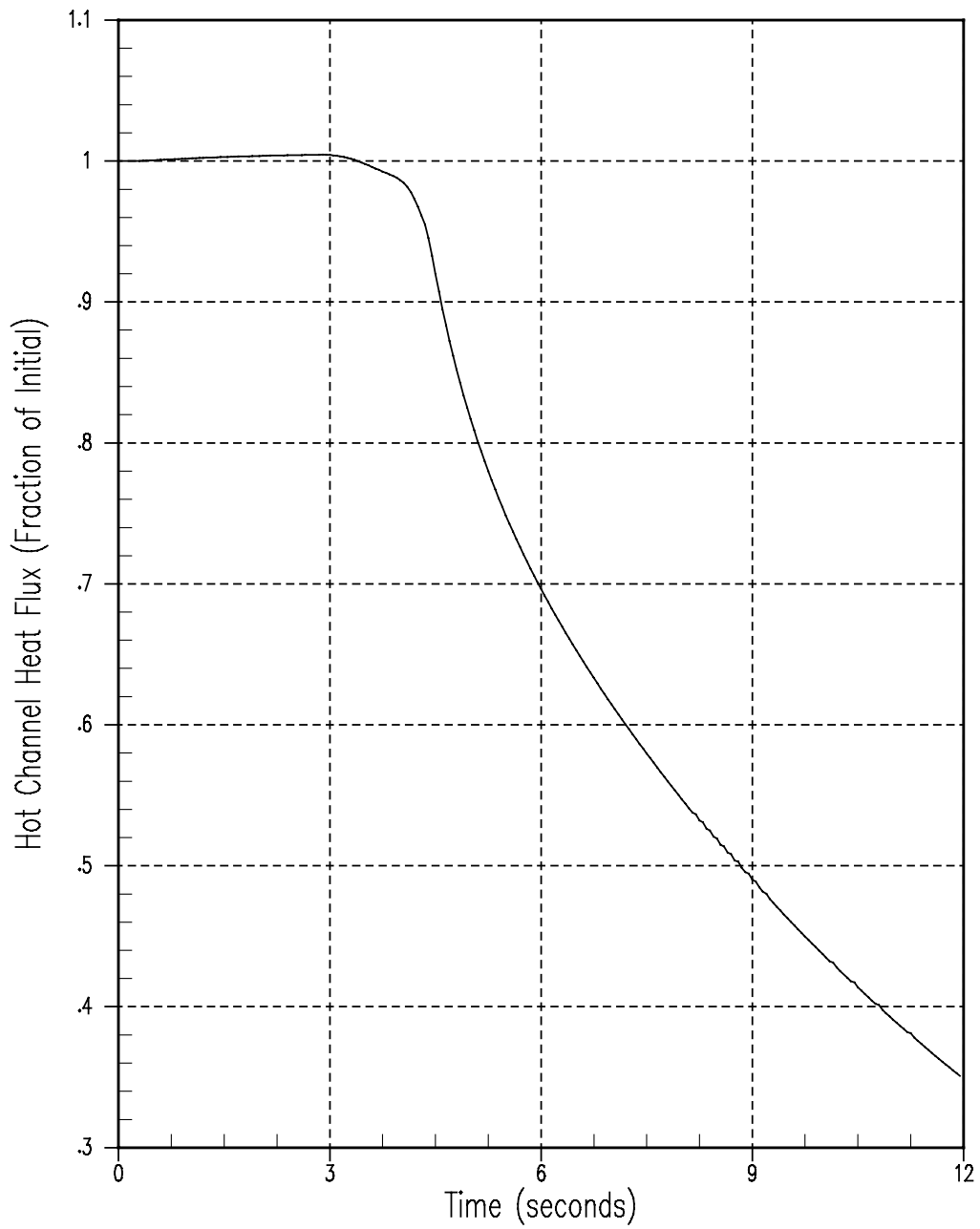


Figure 14.1.8-24
Complete Loss of Flow, Frequency Decay in Two Pumps (CLOF-UF)
DNBR vs. Time

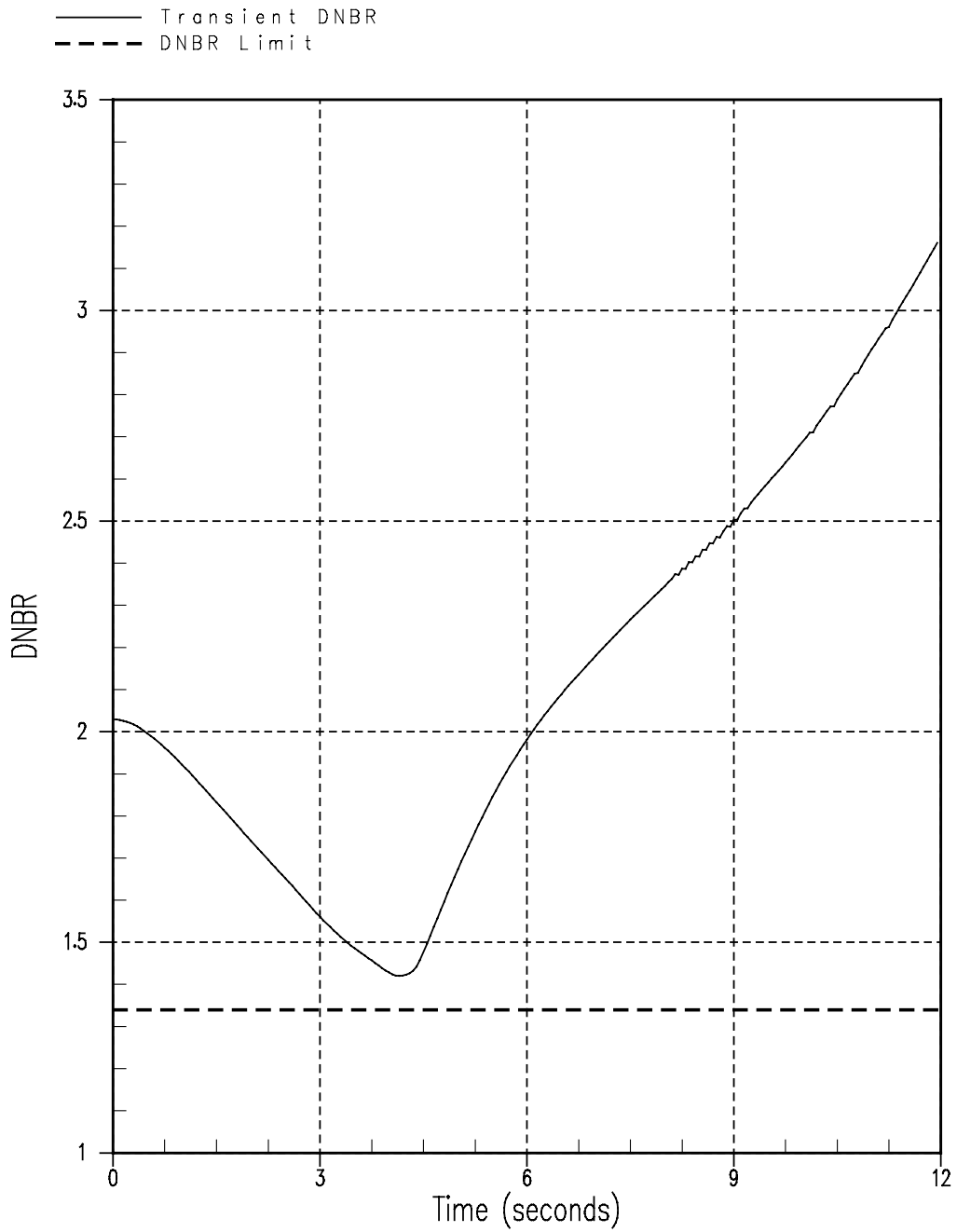


Figure 14.1.8-25
Locked Rotor/Shaft Break - RCS Pressure/Peak Cladding Temperature Case
Total Core Inlet Flow vs. Time

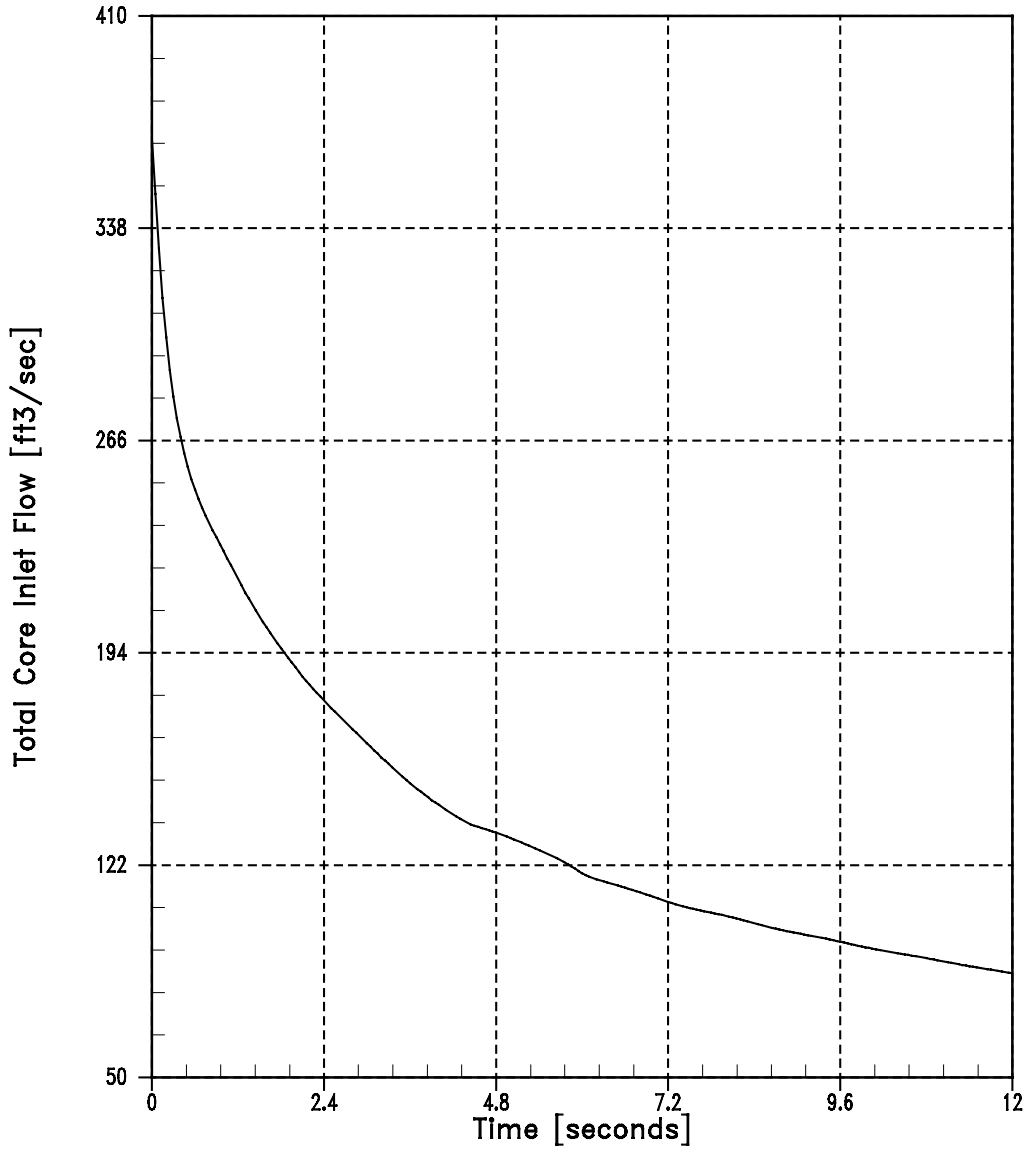


Figure 14.1.8-26
Locked Rotor/Shaft Break - RCS Pressure/Peak Cladding Temperature Case
RCS Loop Flow vs. Time

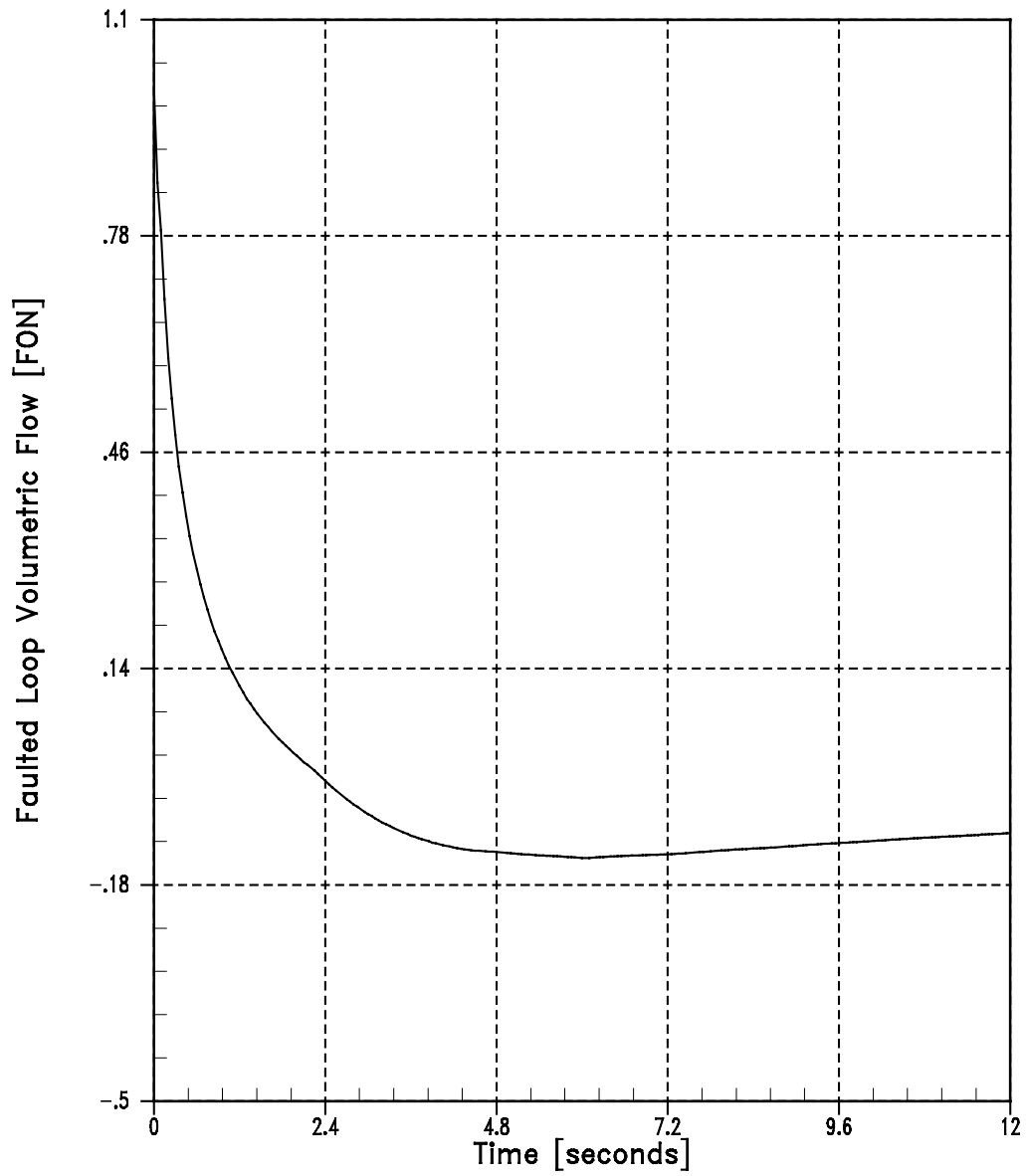


Figure 14.1.8-27
Locked Rotor/Shaft Break - RCS Pressure/Peak Cladding Temperature Case
Nuclear Power vs. Time

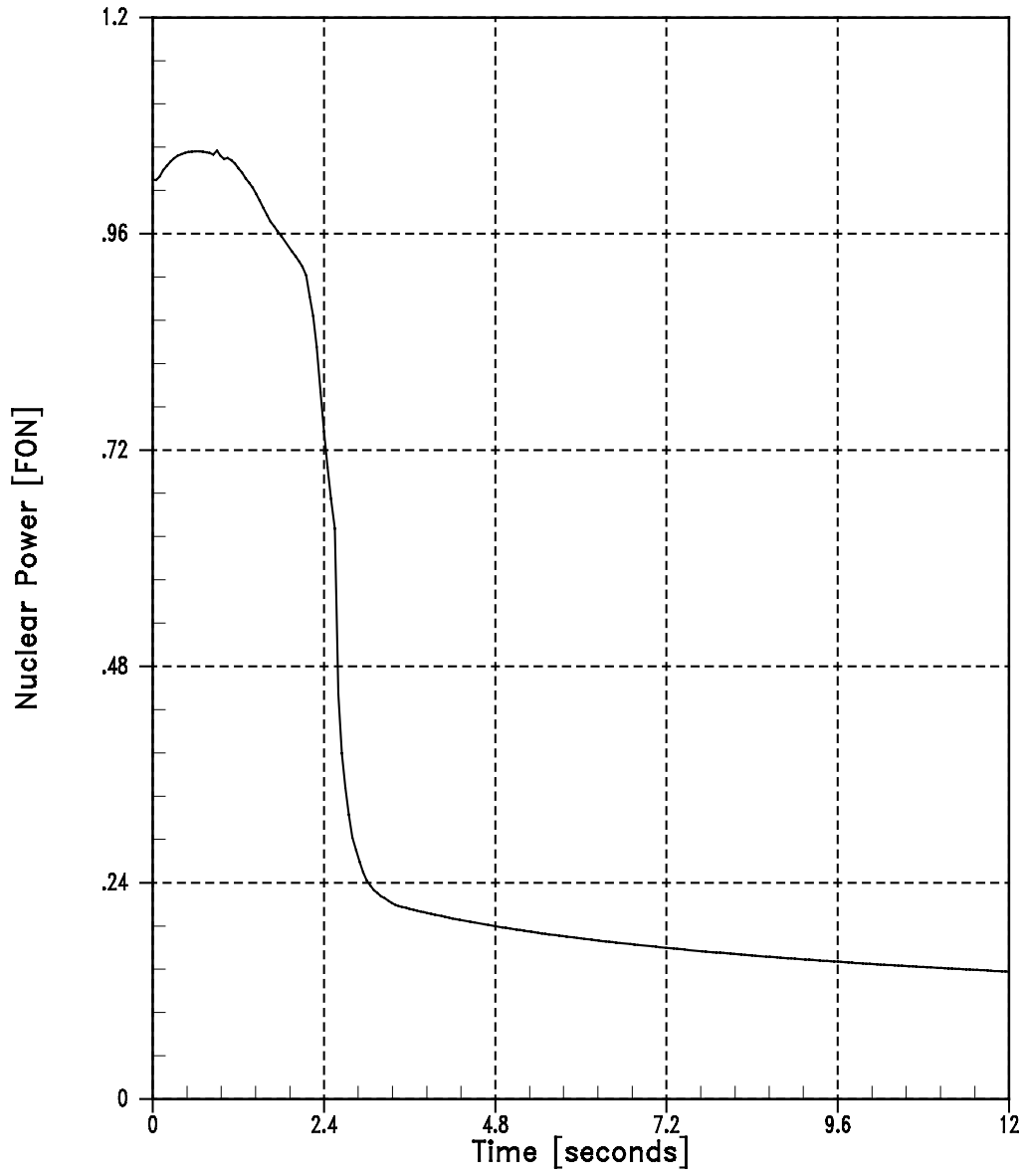


Figure 14.1.8-28
Locked Rotor/Shaft Break - RCS Pressure/Peak Cladding Temperature Case
Core Average Heat Flux vs. Time

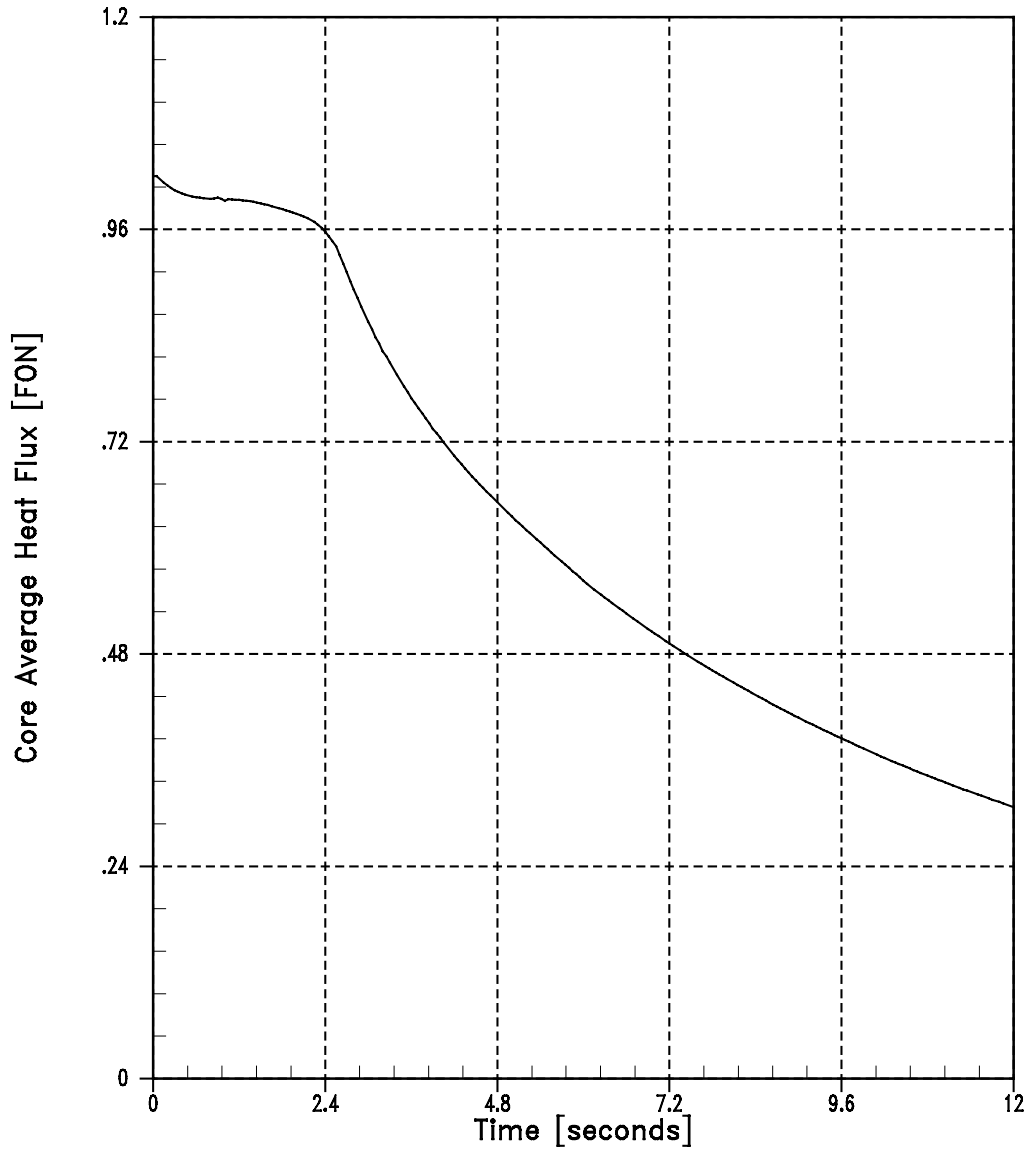


Figure 14.1.8-29
Locked Rotor/Shaft Break - RCS Pressure/Peak Cladding Temperature Case
Pressurizer Pressure vs. Time

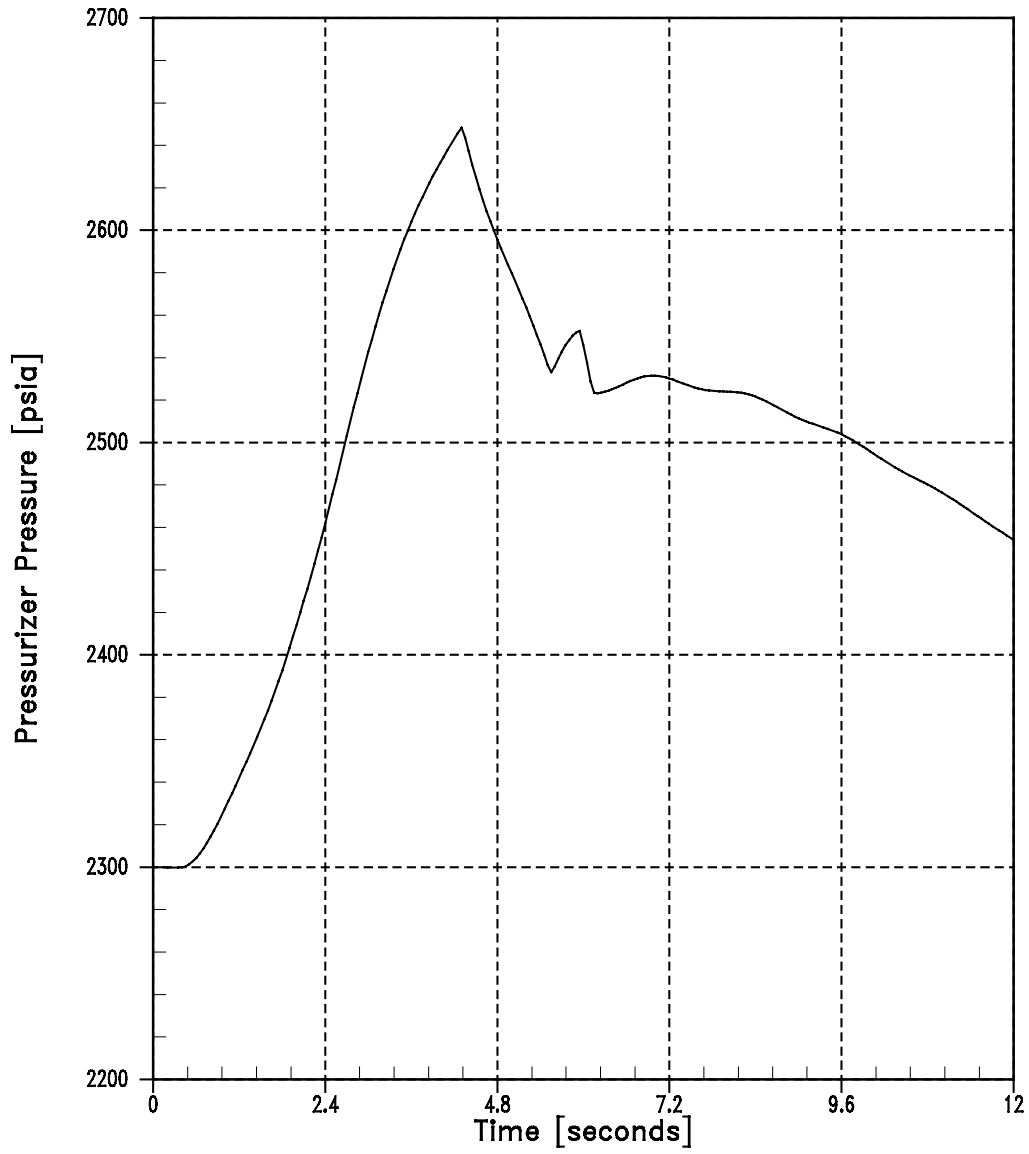


Figure 14.1.8-30
Locked Rotor/Shaft Break - RCS Pressure/Peak Cladding Temperature Case
Vessel Lower Plenum Pressure vs. Time

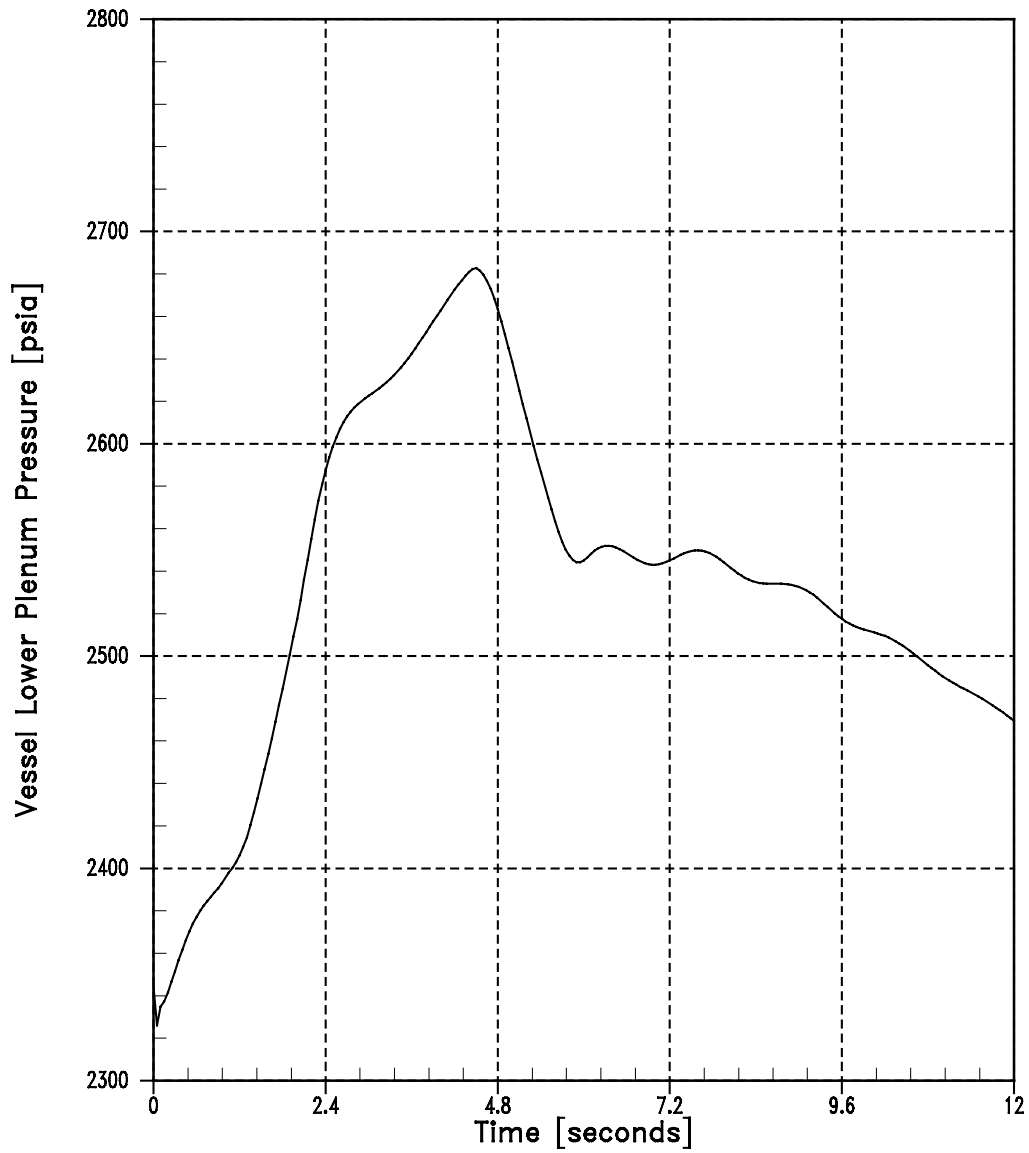


Figure 14.1.8-31
Locked Rotor/Shaft Break - RCS Pressure/Peak Cladding Temperature Case
RCS Loop Temperature vs. Time

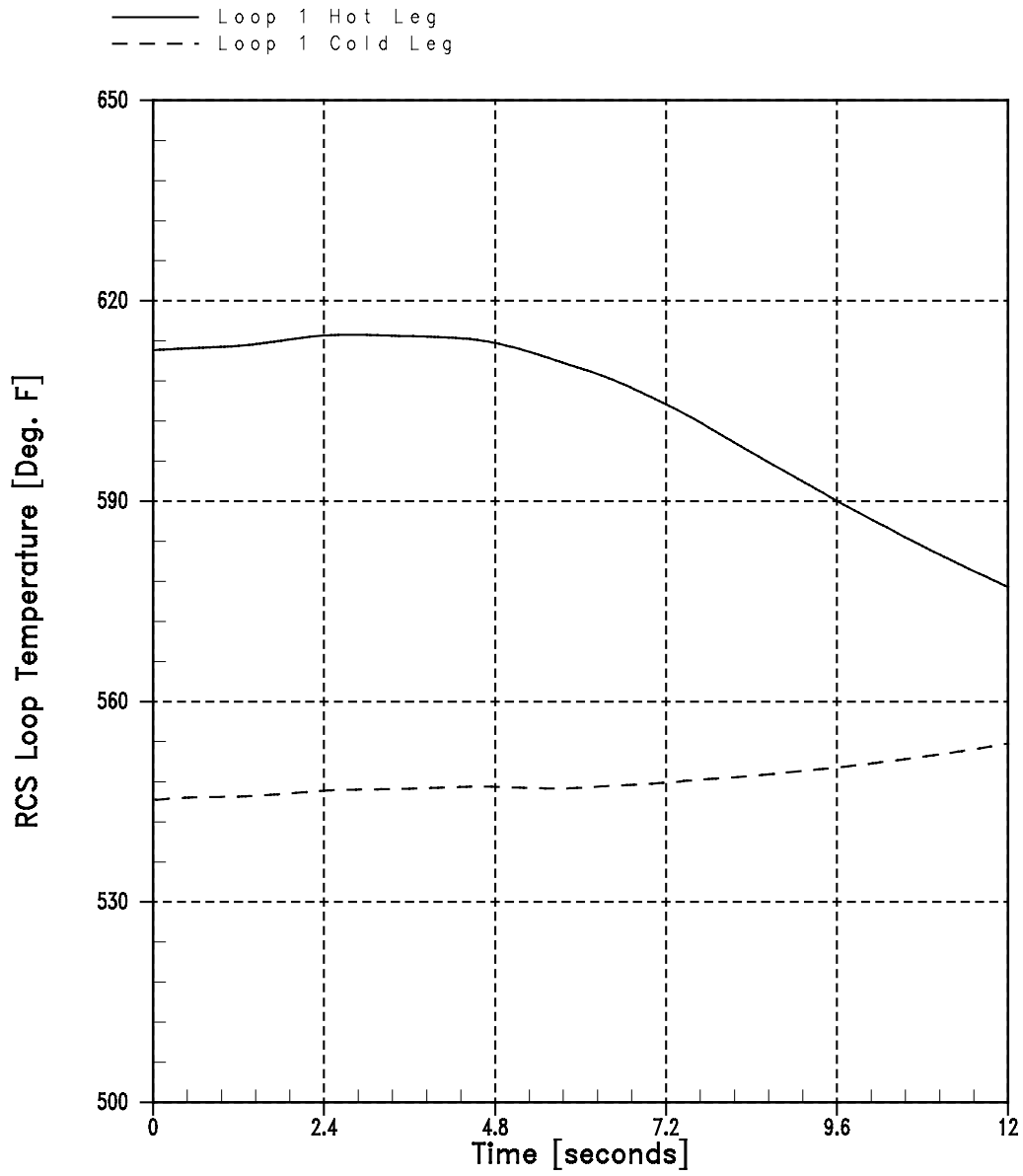


Figure 14.1.8-32
Locked Rotor/Shaft Break - RCS Pressure/Peak Cladding Temperature Case
Hot Channel Heat Flux vs. Time

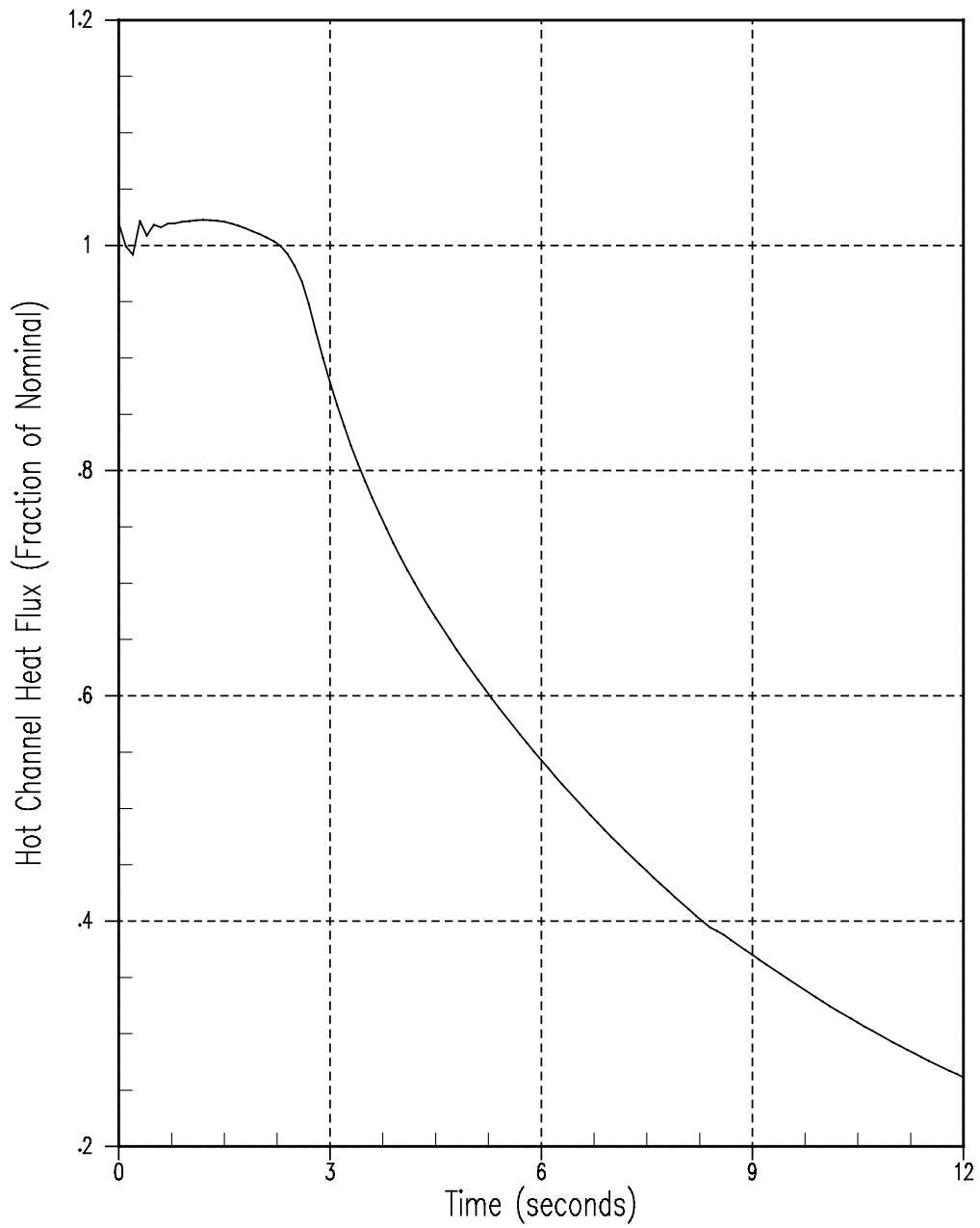


Figure 14.1.8-33
Locked Rotor/Shaft Break - RCS Pressure/Peak Cladding Temperature Case
Hot-Spot Cladding Inner Temperature vs. Time

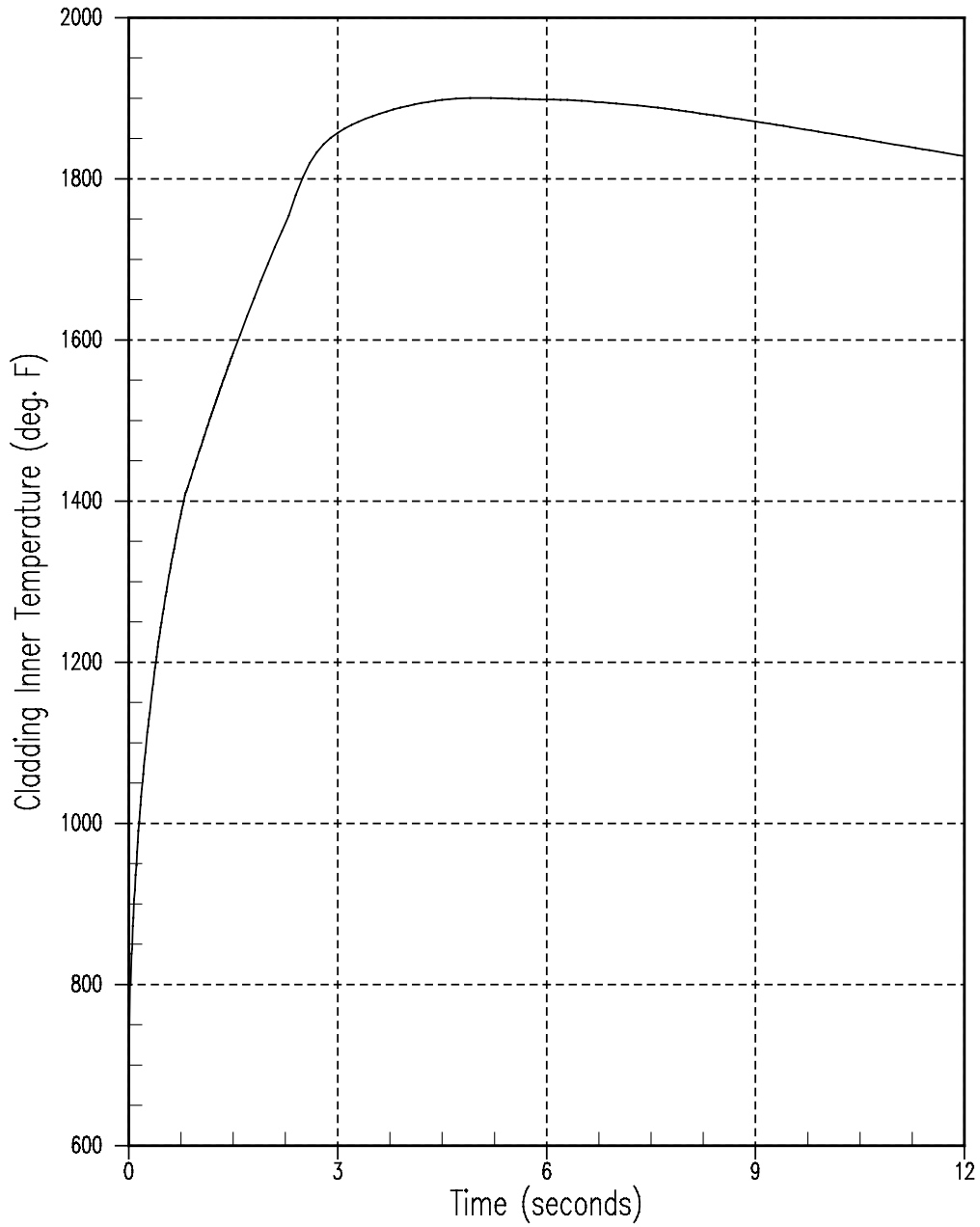


Figure 14.1.9-1
Loss of External Electrical Load With Automatic Pressure Control (DNB Case)
Nuclear Power vs. Time

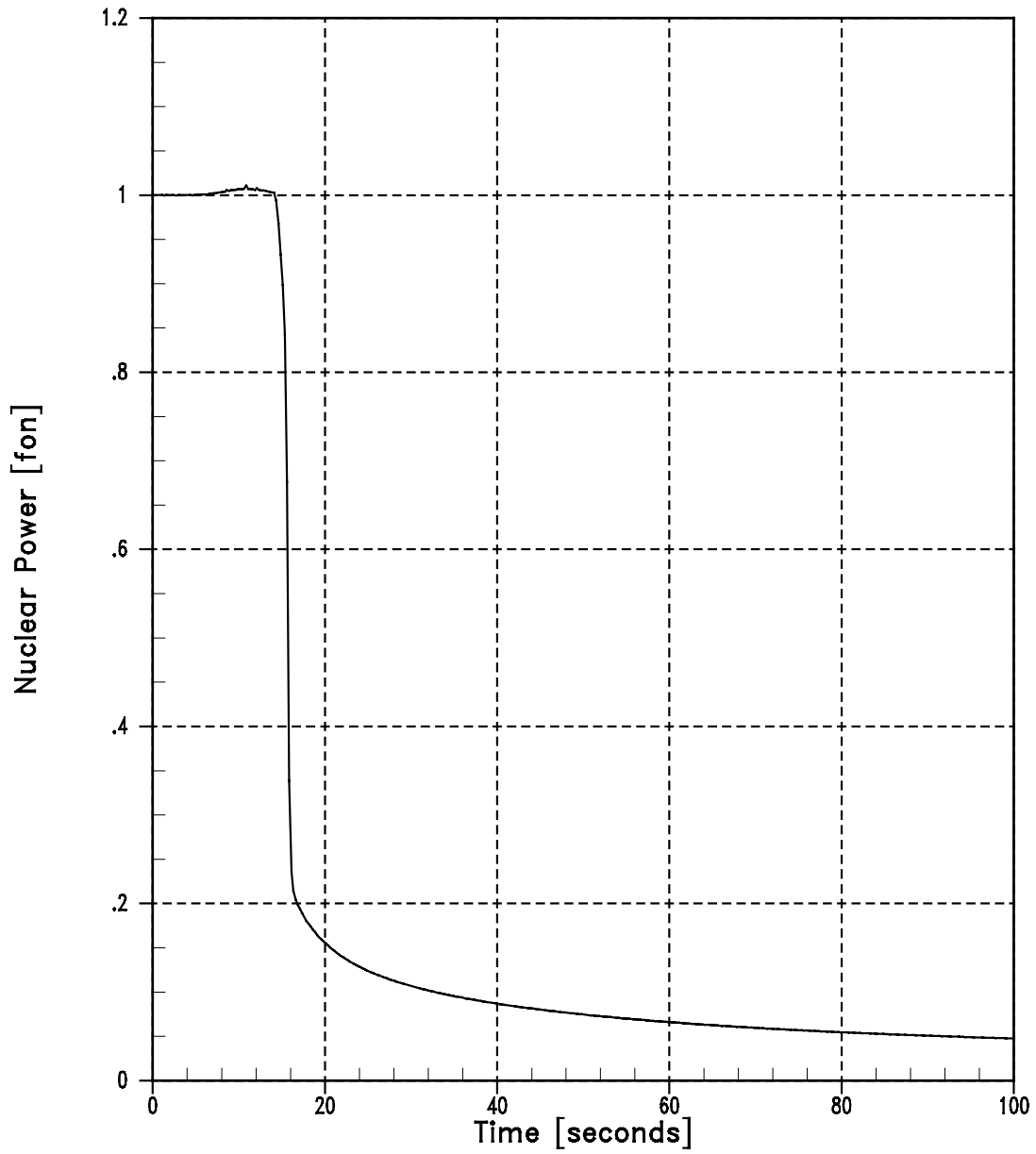


Figure 14.1.9-2
Loss of External Electrical Load With Automatic Pressure Control (DNB Case)
Vessel Average and Core Inlet Temperatures vs. Time

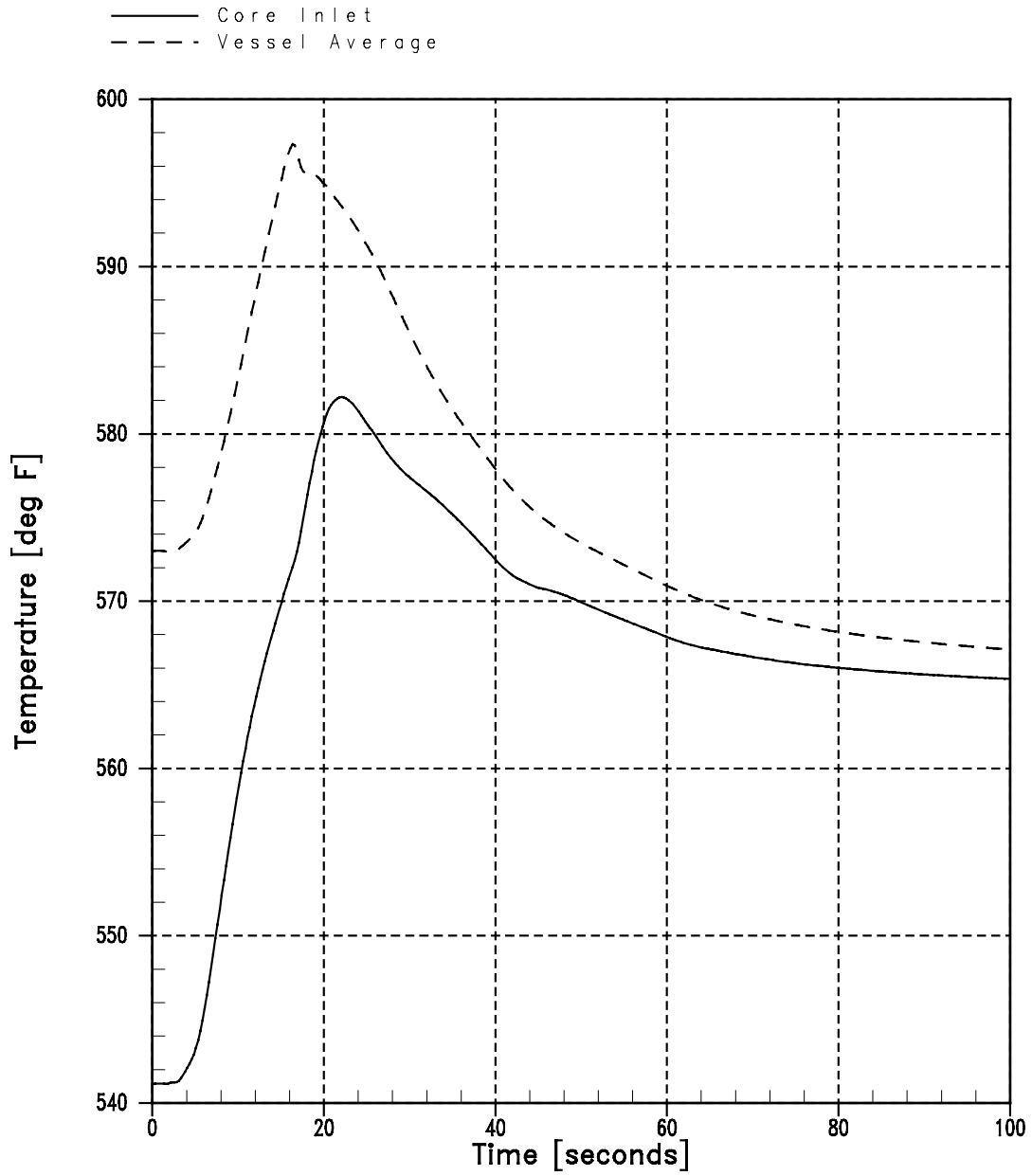


Figure 14.1.9-3
Loss of External Electrical Load With Automatic Pressure Control (DNB Case)
Pressurizer and RCP Exit Pressures vs. Time

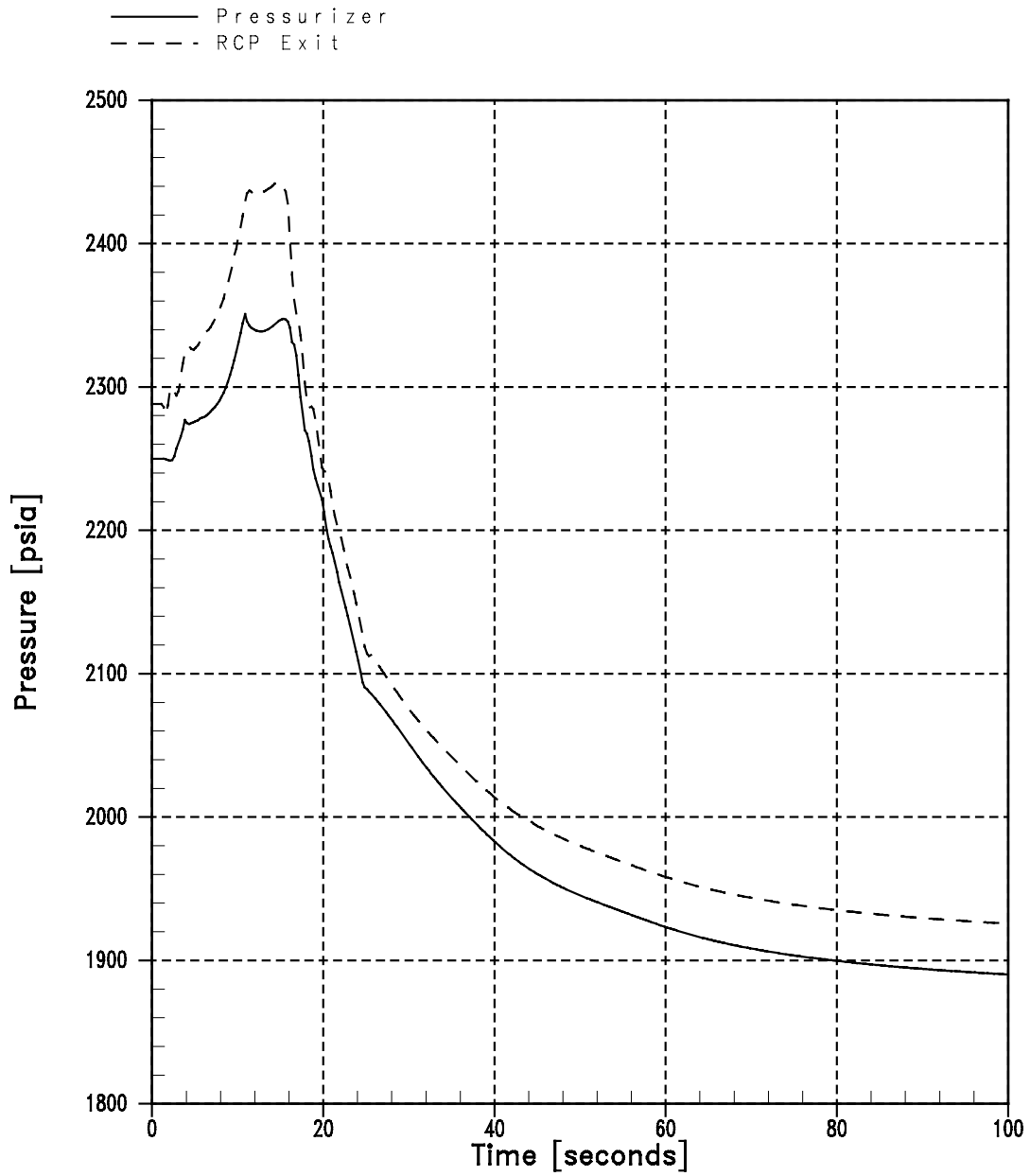


Figure 14.1.9-4
Loss of External Electrical Load With Automatic Pressure Control (DNB Case)
Pressurizer Water Volume vs. Time

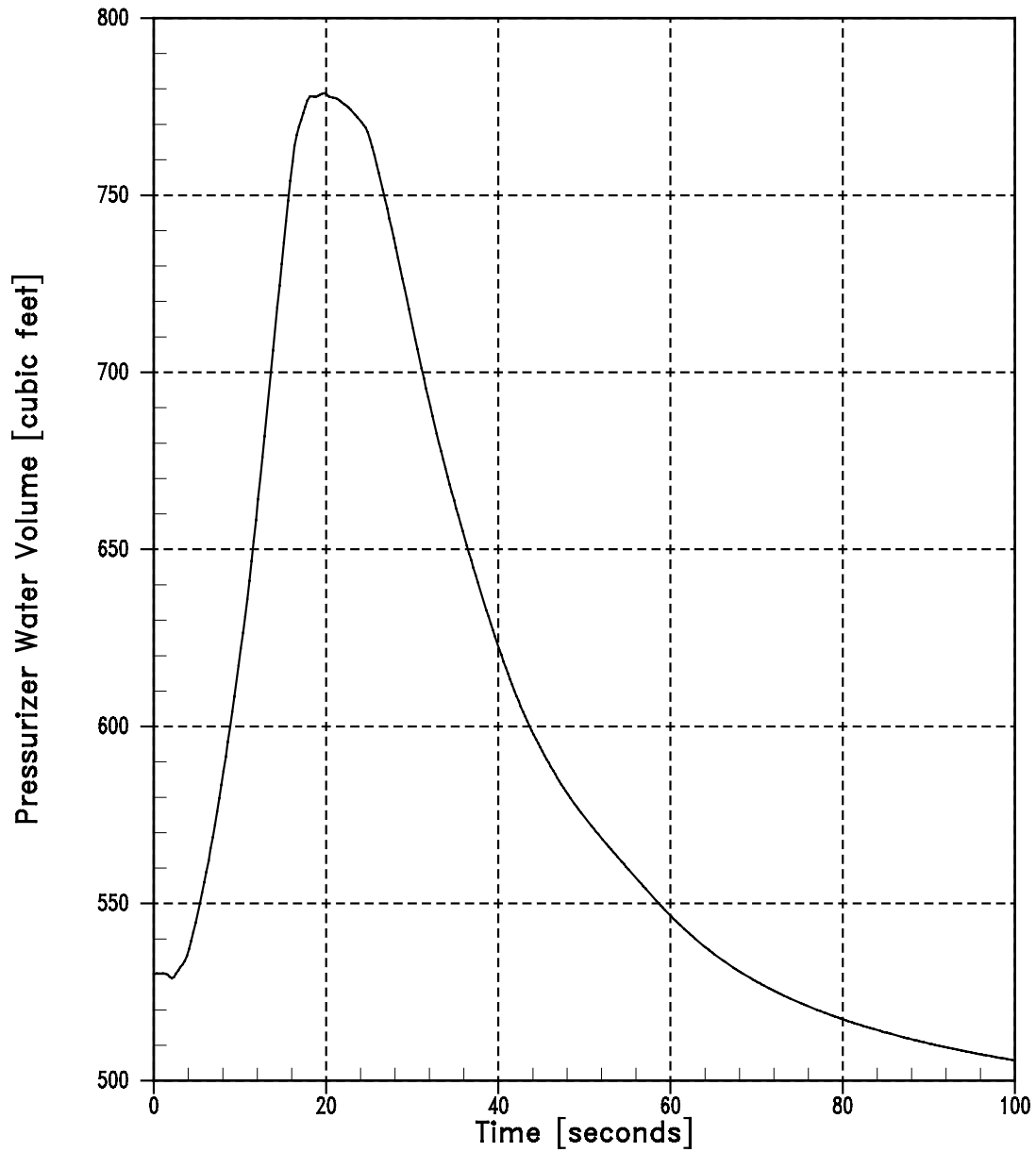


Figure 14.1.9-5
Loss of External Electrical Load With Automatic Pressure Control (DNB Case)
Steam Generator Pressure vs. Time

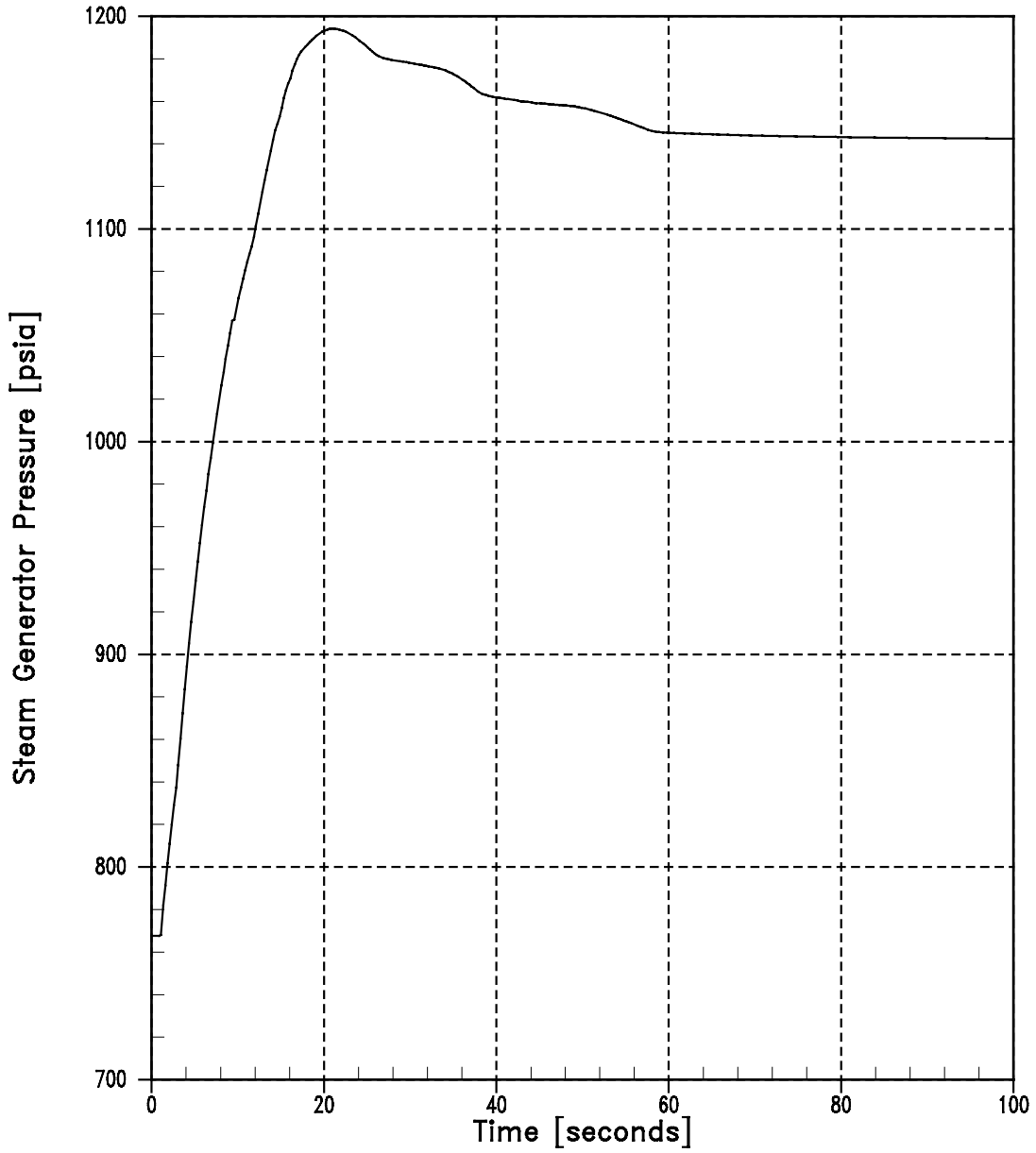


Figure 14.1.9-6
Loss of External Electrical Load With Automatic Pressure Control (DNB Case)
DNBR vs. Time

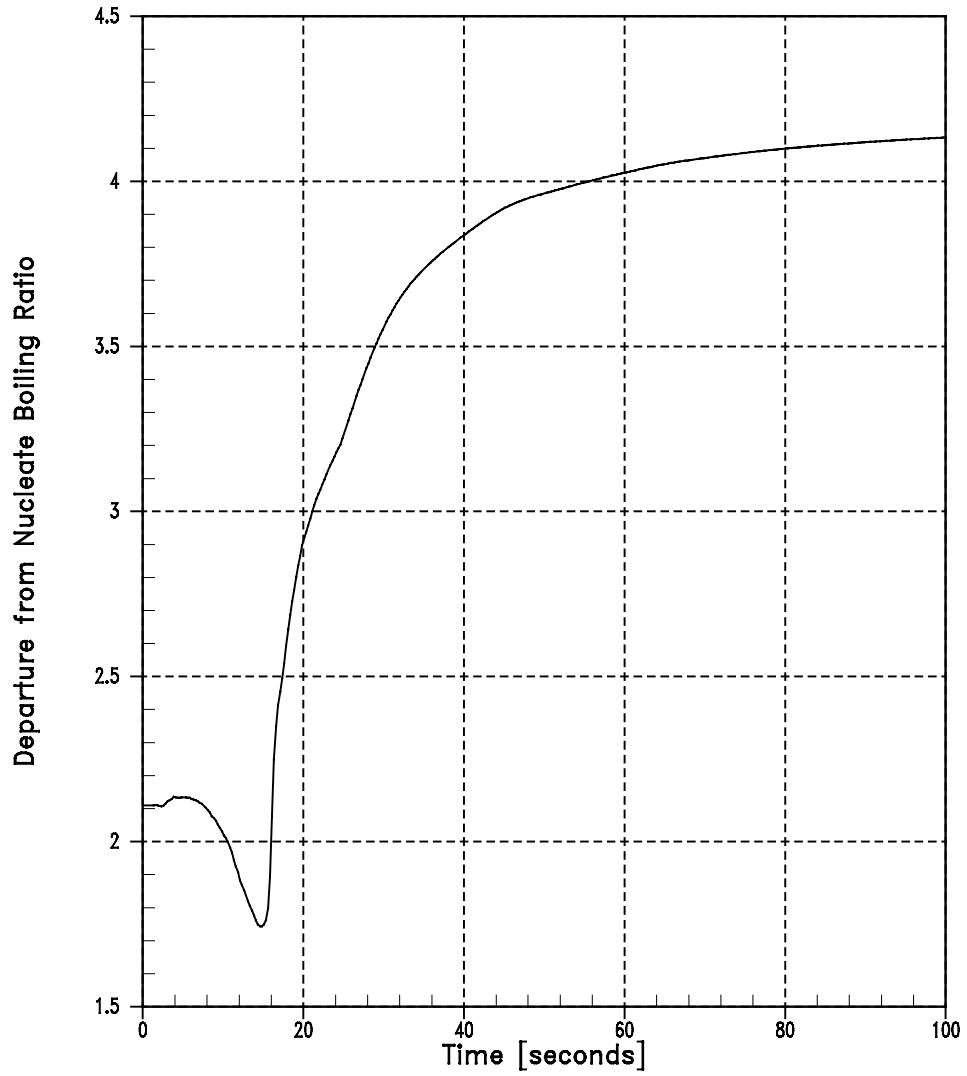


Figure 14.1.9-7
Loss of External Electrical Load Without Automatic Pressure Control (RCS Overpressure Case)
Nuclear Power vs. Time

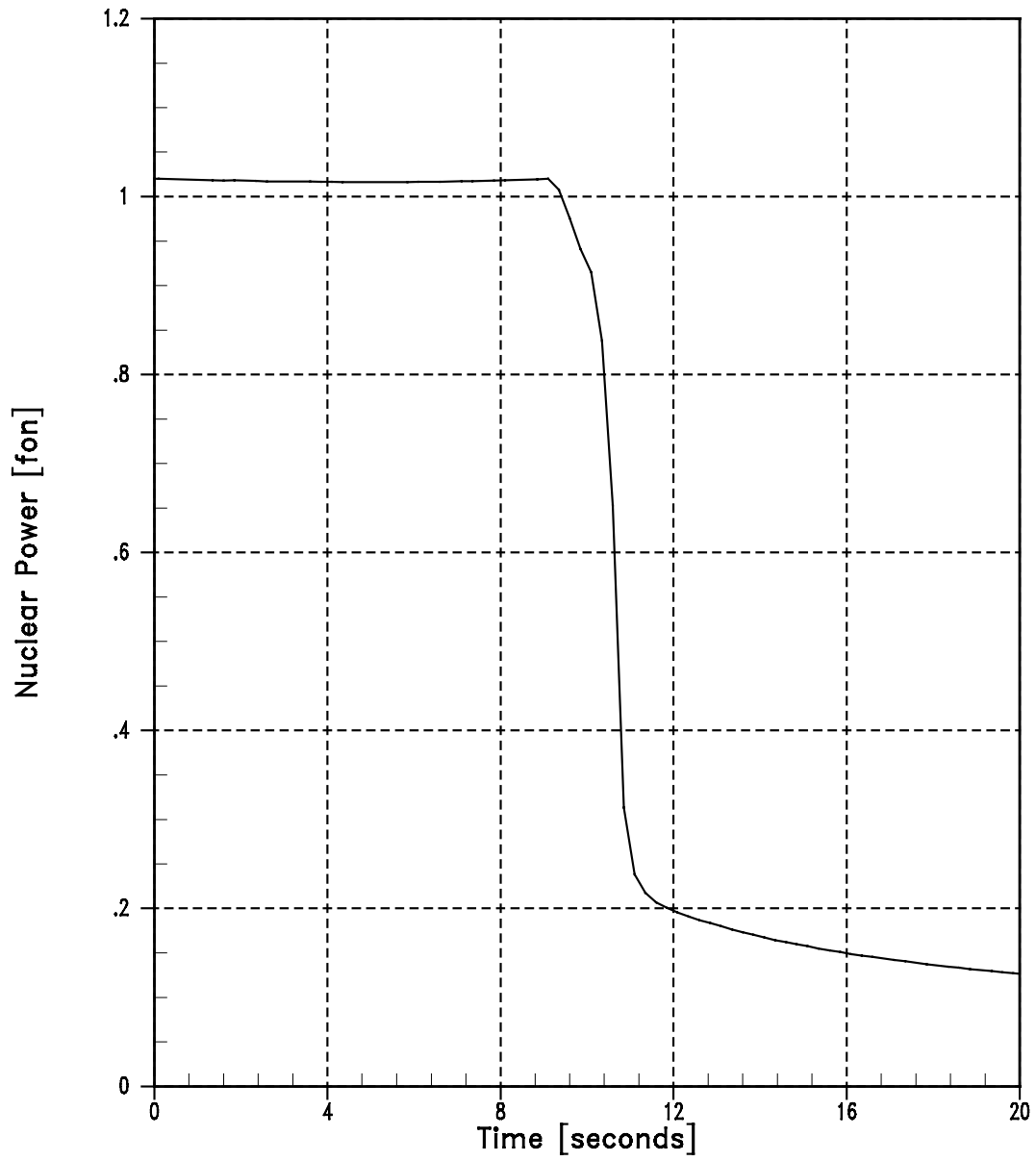


Figure 14.1.9-8
Loss of External Electrical Load Without Automatic Pressure Control (RCS Overpressure Case)
Vessel Average and Core Inlet Temperatures vs. Time

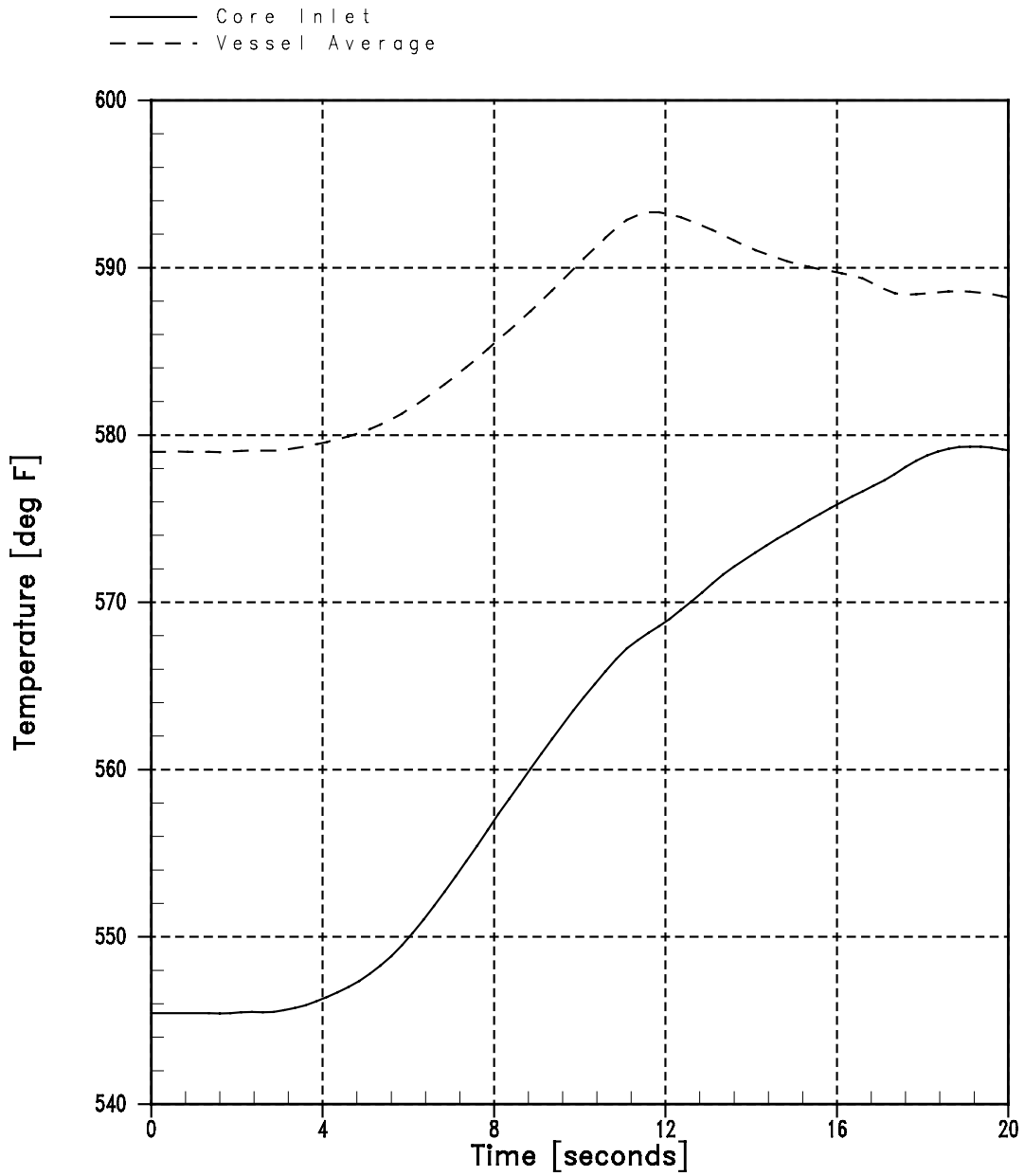


Figure 14.1.9-9
Loss of External Electrical Load Without Automatic Pressure Control (RCS Overpressure Case)
Pressurizer and RCP Exit Pressures vs. Time

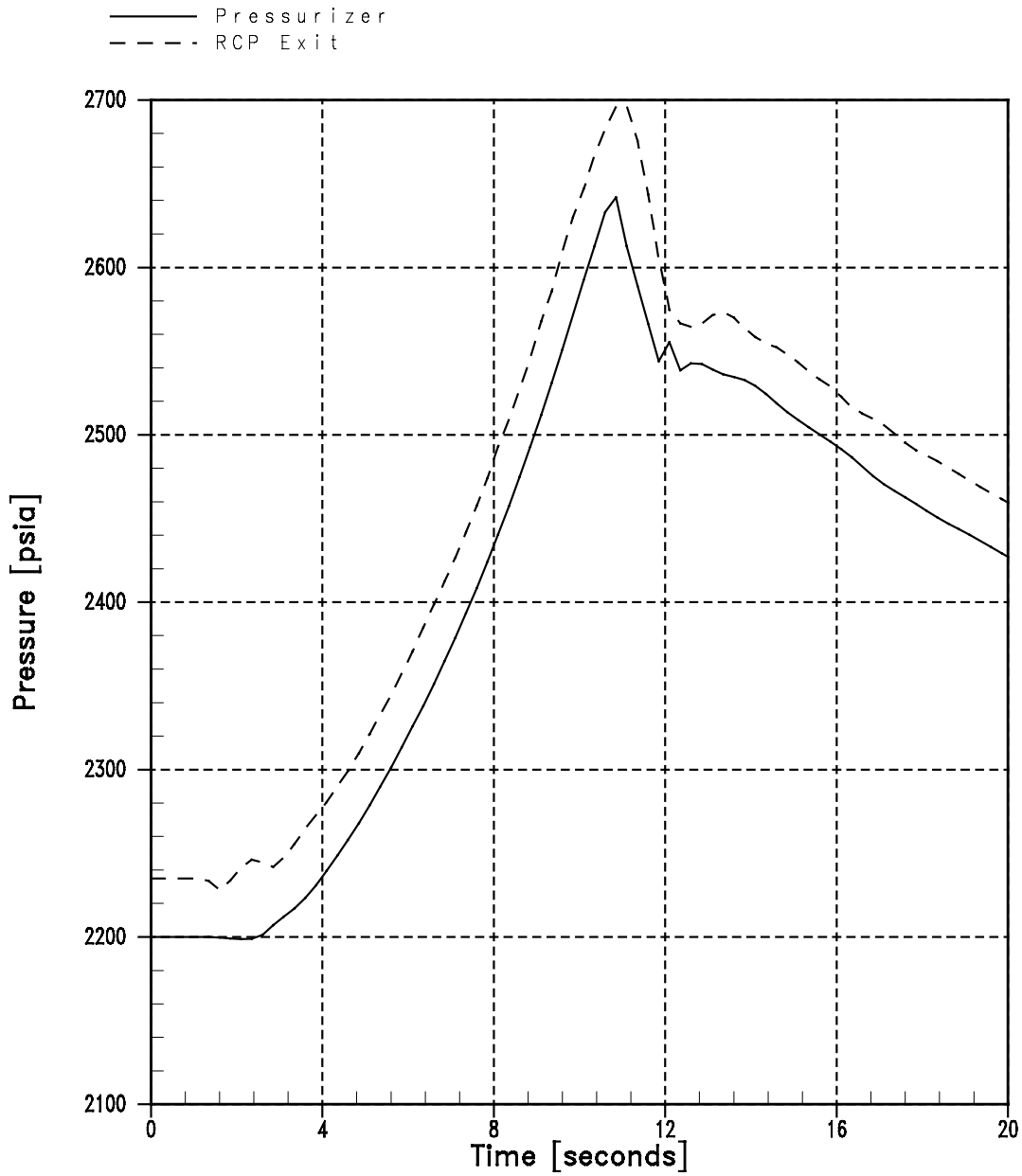


Figure 14.1.9-10
Loss of External Electrical Load Without Automatic Pressure Control (RCS Overpressure Case)
Pressurizer Water Volume vs. Time

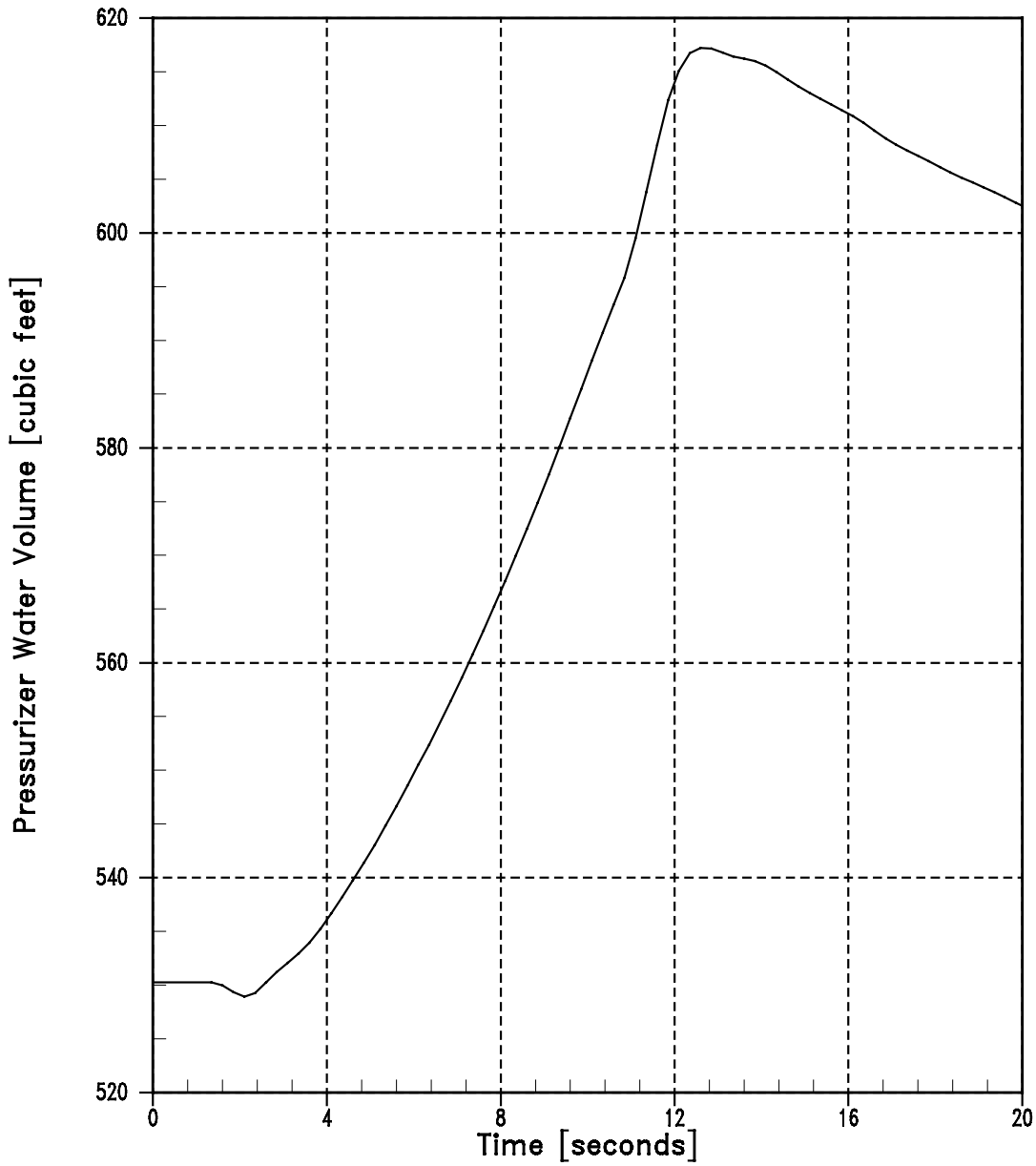


Figure 14.1.9-11
Loss of External Electrical Load Without Automatic Pressure Control (RCS Overpressure Case)
Steam Generator Pressure vs. Time

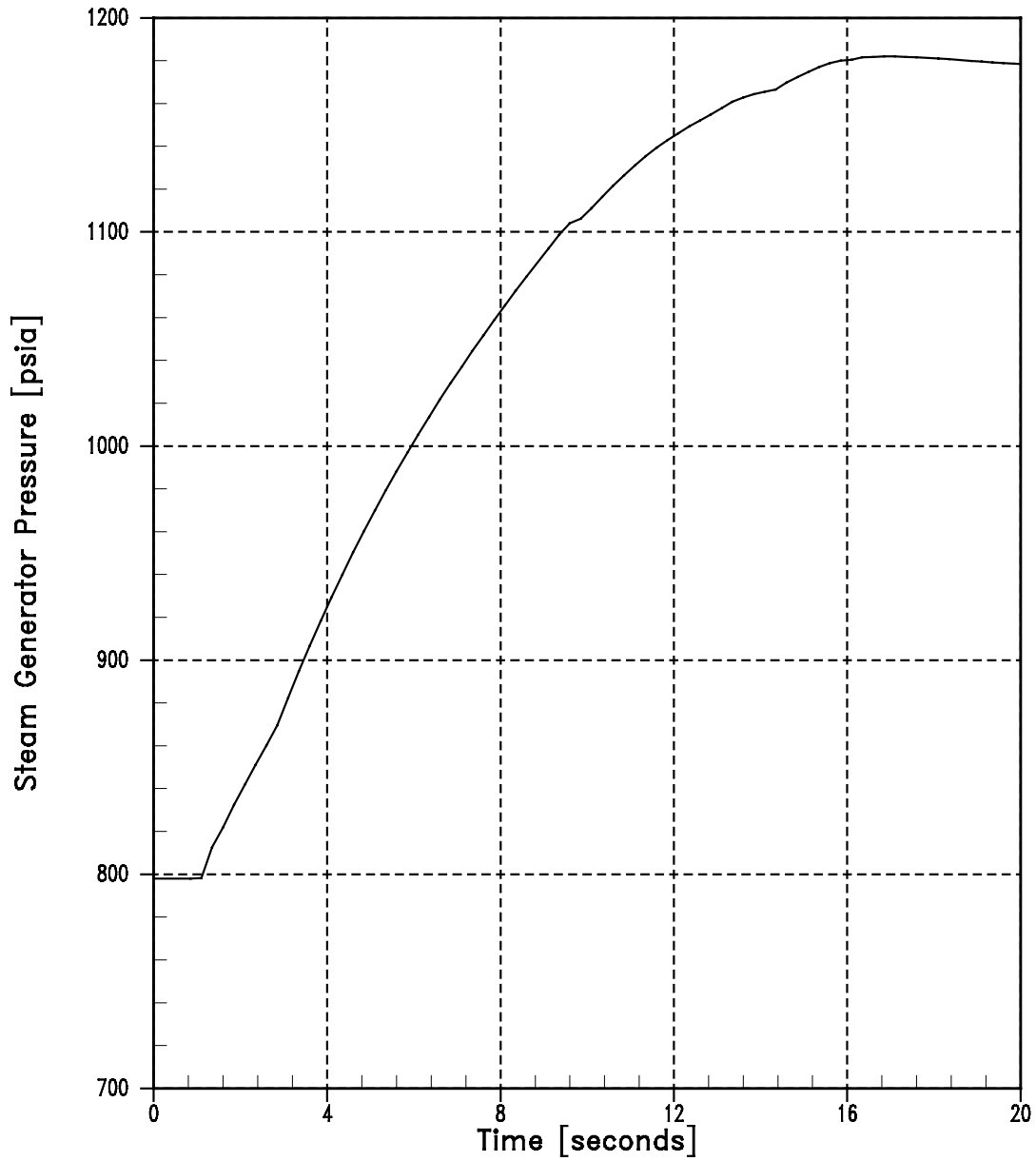


Figure 14.1.9-12
Loss of External Electrical Load With Automatic Pressure Control (MSS Overpressure Case)
Nuclear Power vs. Time

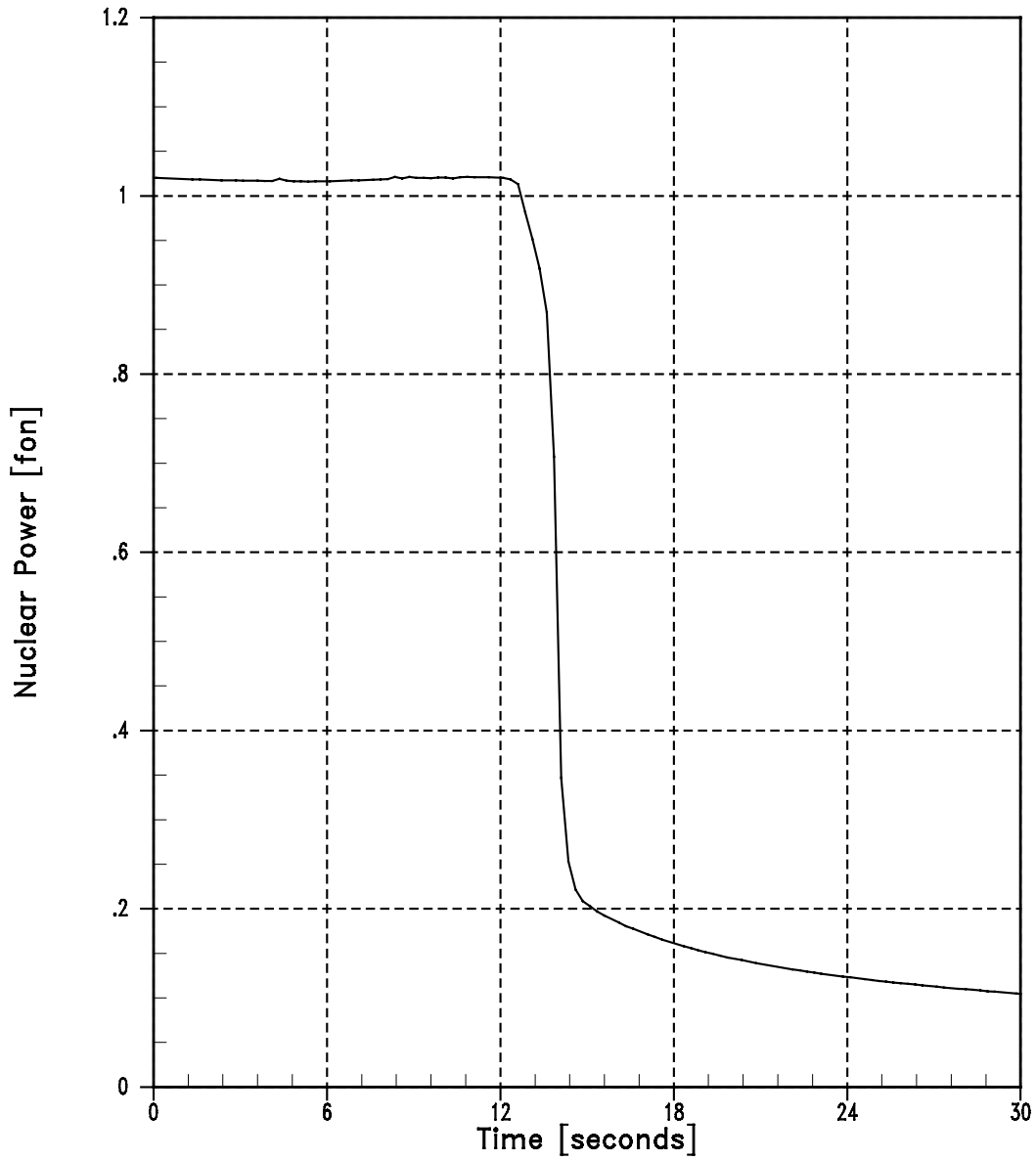


Figure 14.1.9-13
Loss of External Electrical Load With Automatic Pressure Control (MSS Overpressure Case)
Vessel Average and Core Inlet Temperatures vs. Time

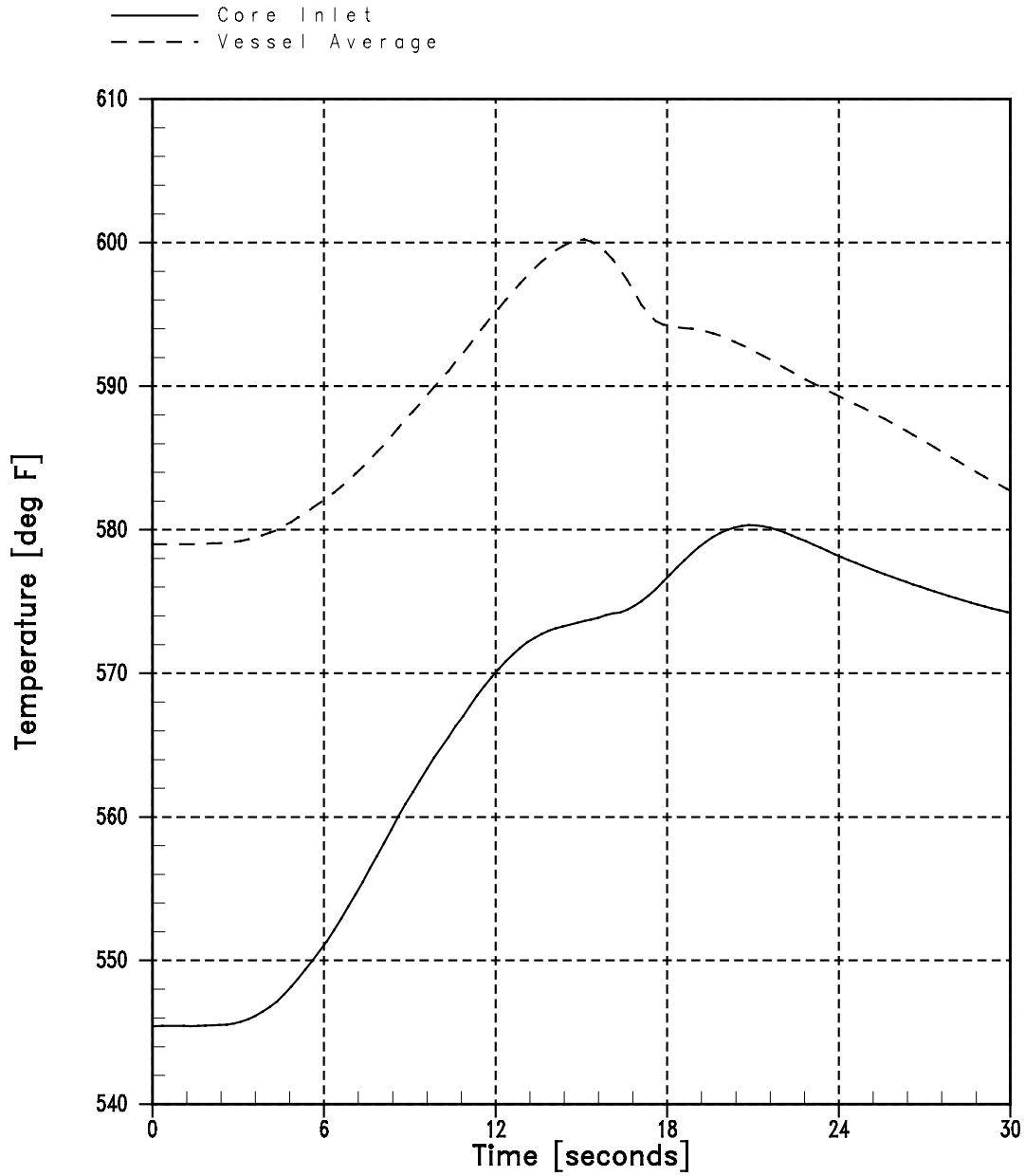


Figure 14.1.9-14
Loss of External Electrical Load With Automatic Pressure Control (MSS Overpressure Case)
Pressurizer and RCP Exit Pressures vs. Time

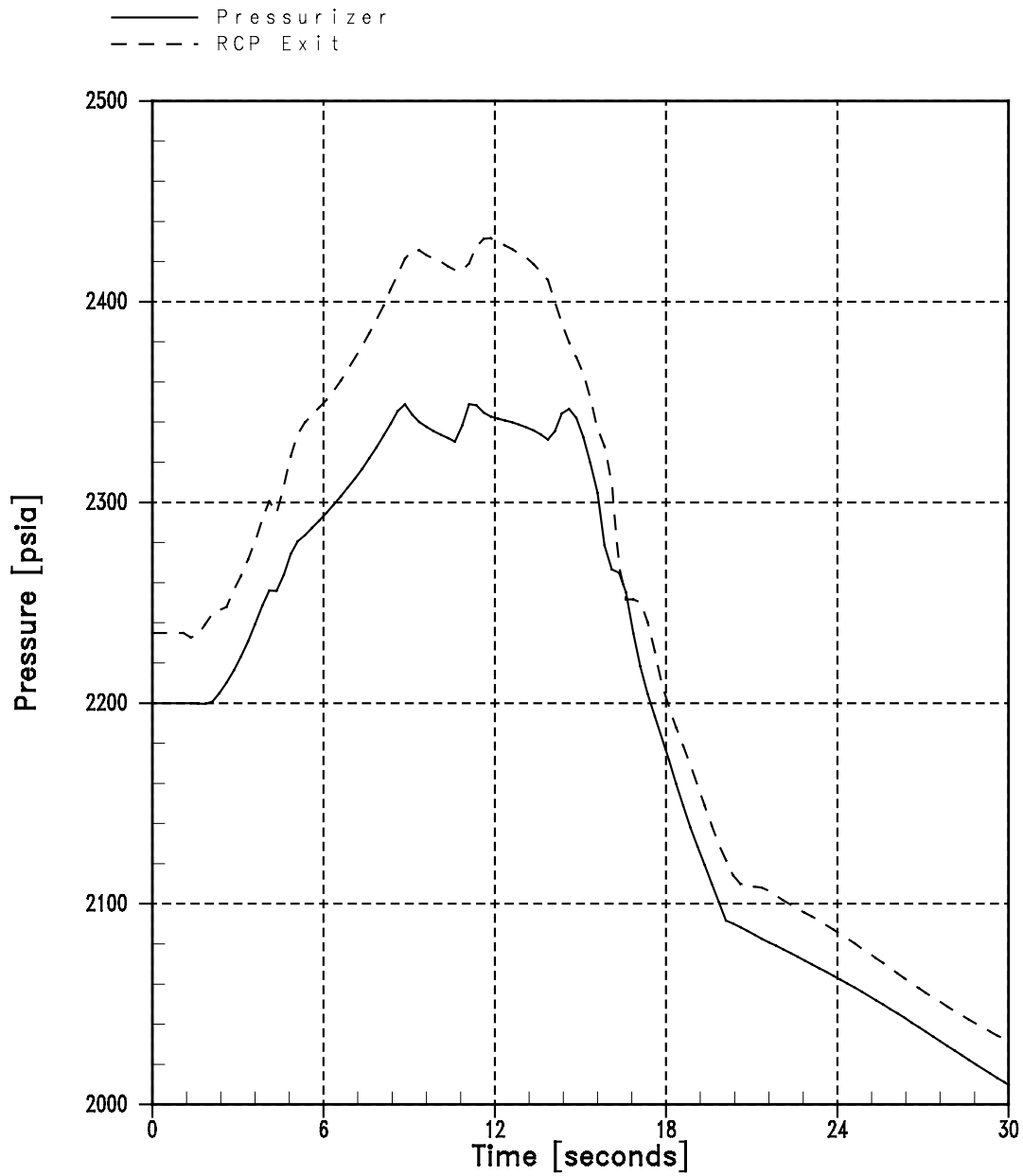


Figure 14.1.9-15
Loss of External Electrical Load With Automatic Pressure Control (MSS Overpressure Case)
Pressurizer Water Volume vs. Time

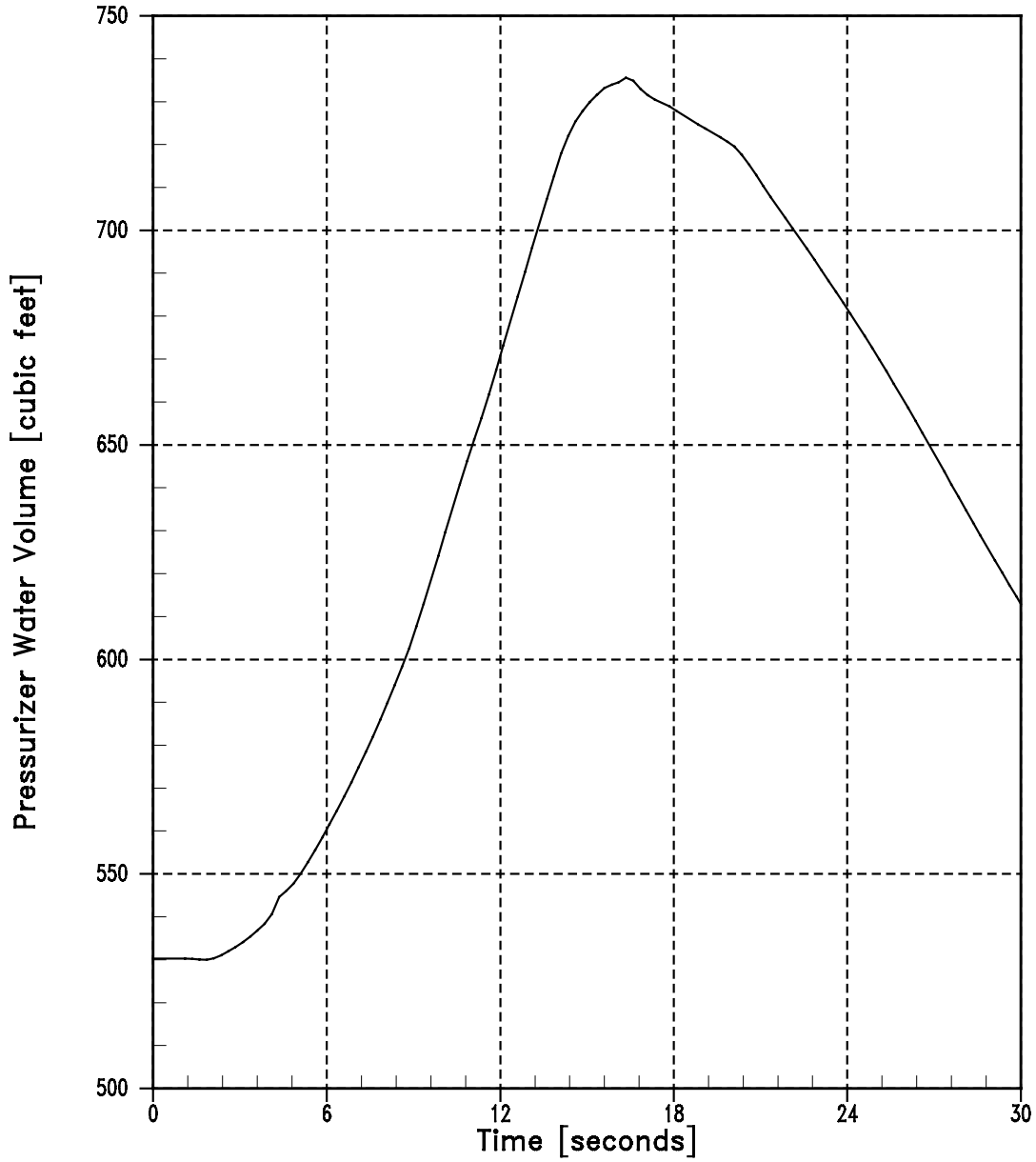


Figure 14.1.9-16
Loss of External Electrical Load With Automatic Pressure Control (MSS Overpressure Case)
Steam Generator Pressure vs. Time

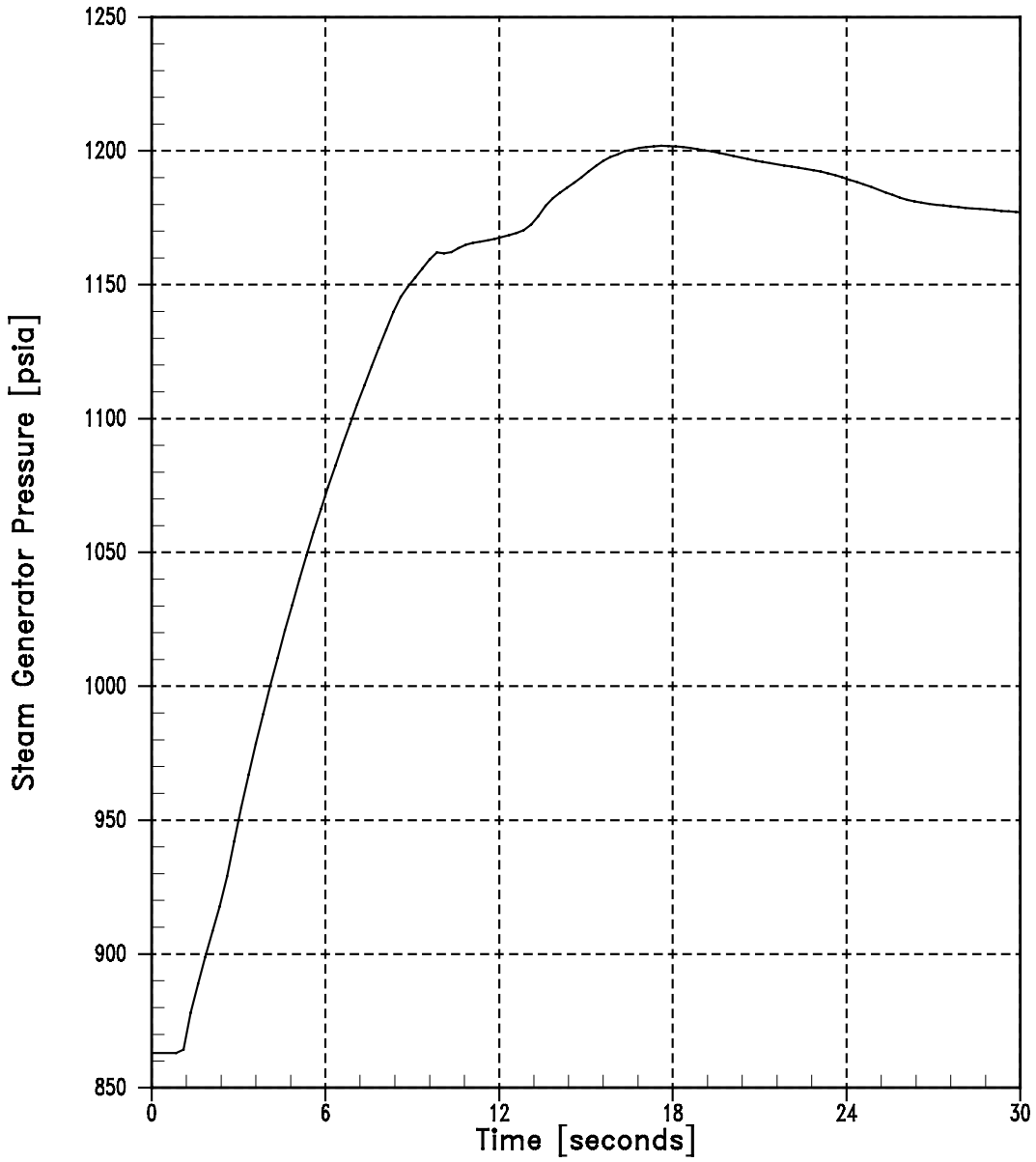


Figure 14.1.10-1
Loss of Normal Feedwater - High Pressure
T_{ave} Volume vs. Time

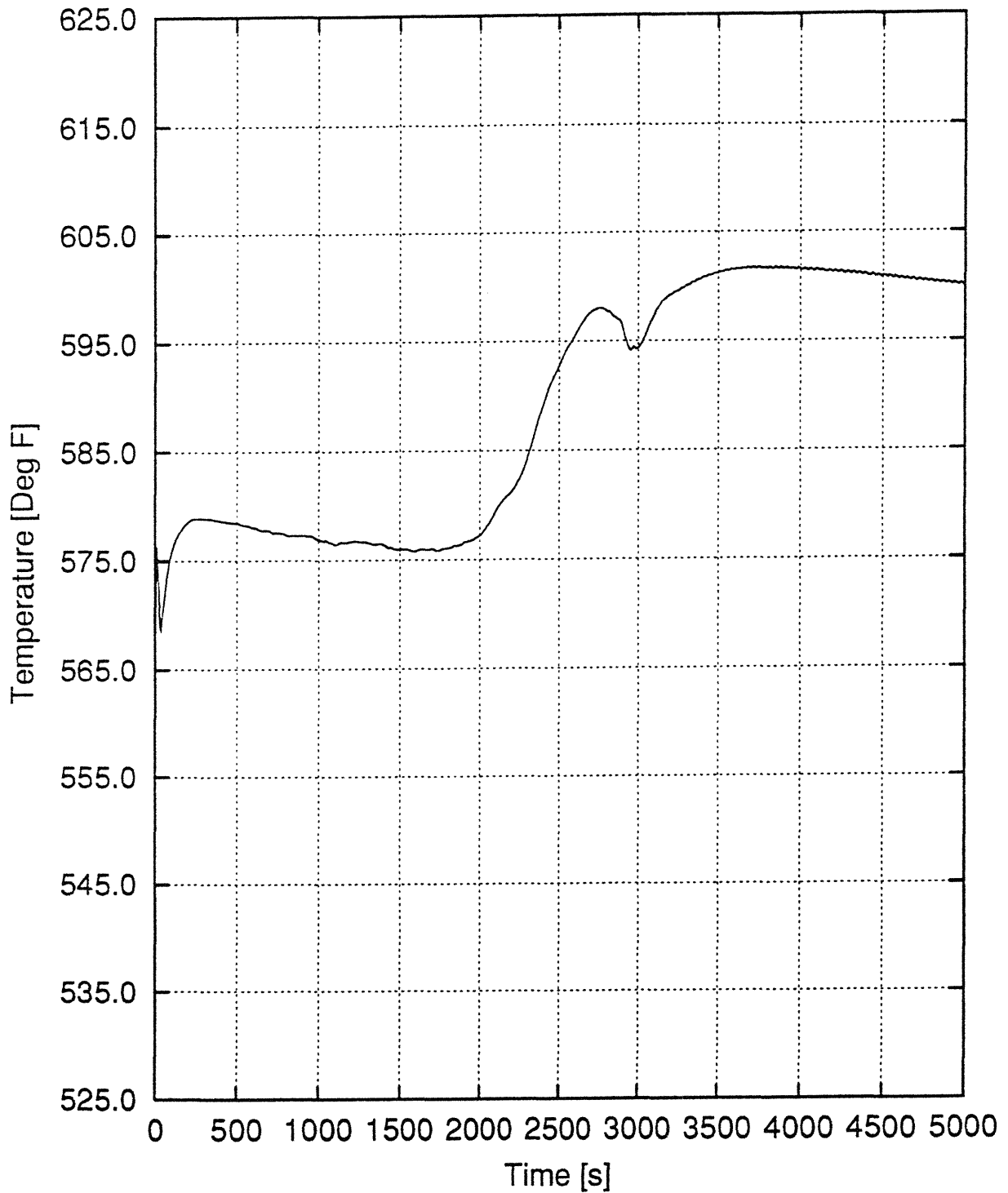


Figure 14.1.10-2
Loss of Normal Feedwater - High Pressure
Pressurizer Liquid Volume vs. Time

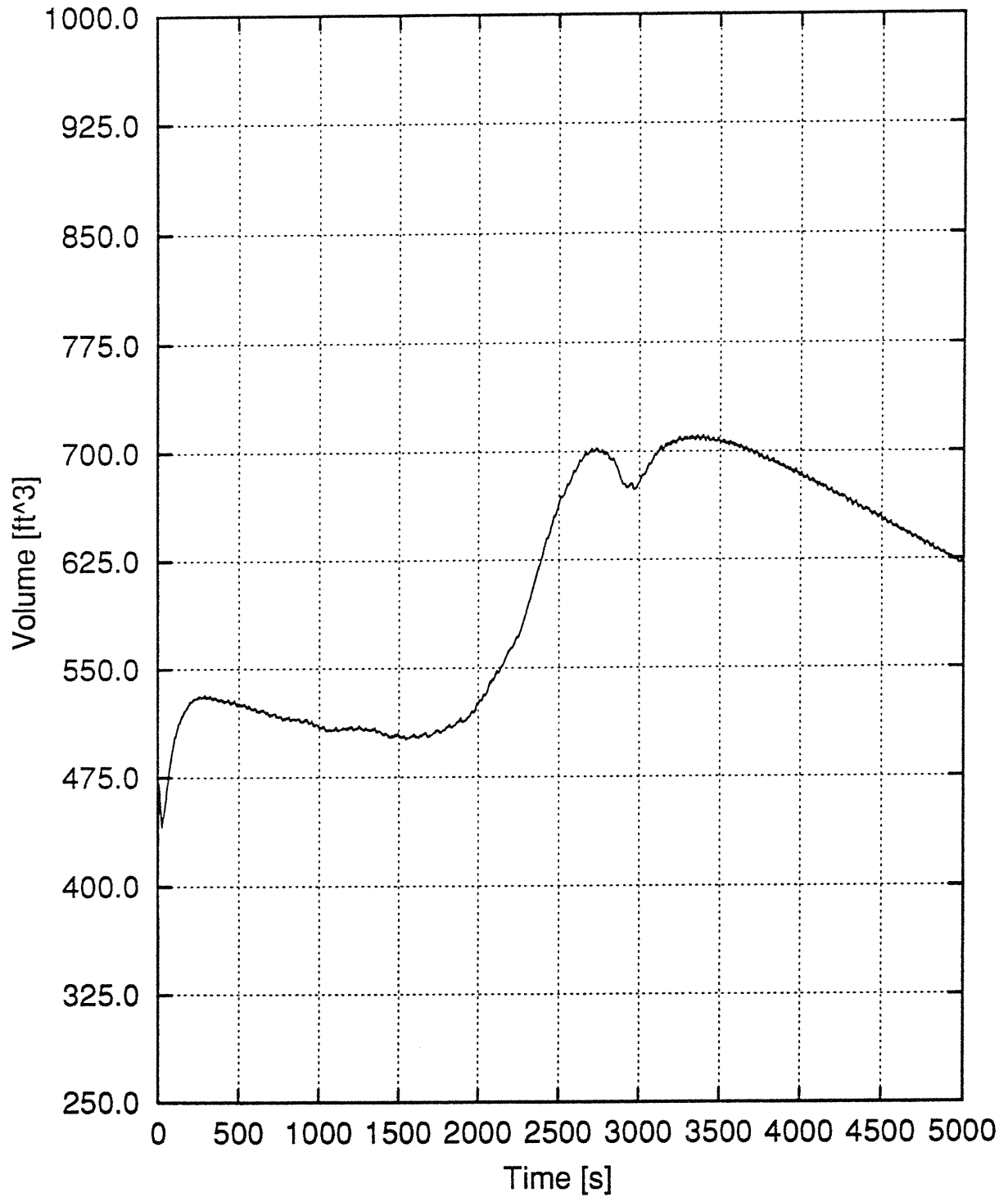


Figure 14.1.10-3
Loss of Normal Feedwater - High Pressure
SG A Wide Range Level vs. Time

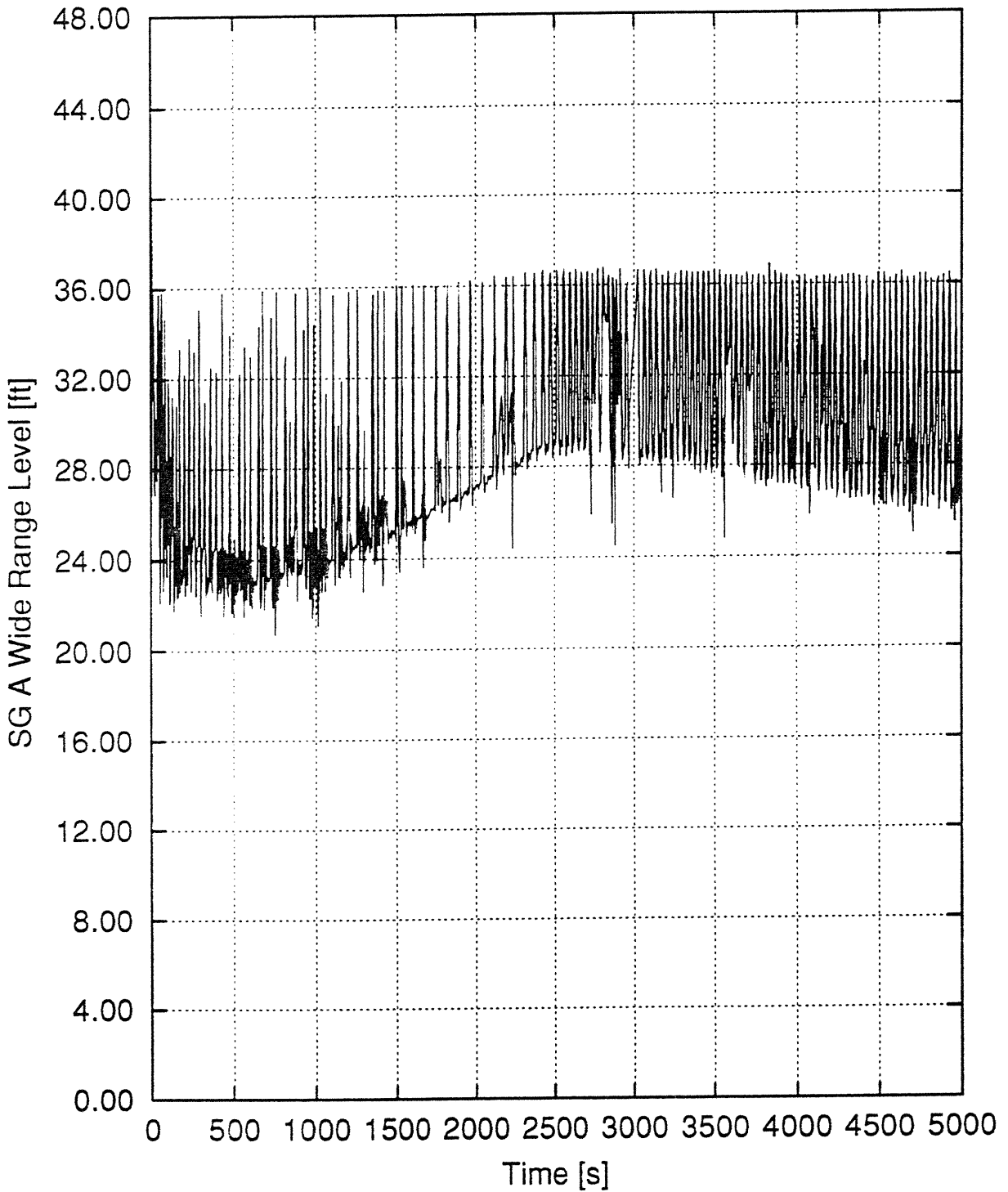


Figure 14.1.10-4
Loss of Normal Feedwater - High Pressure
SG B Wide Range Level vs. Time

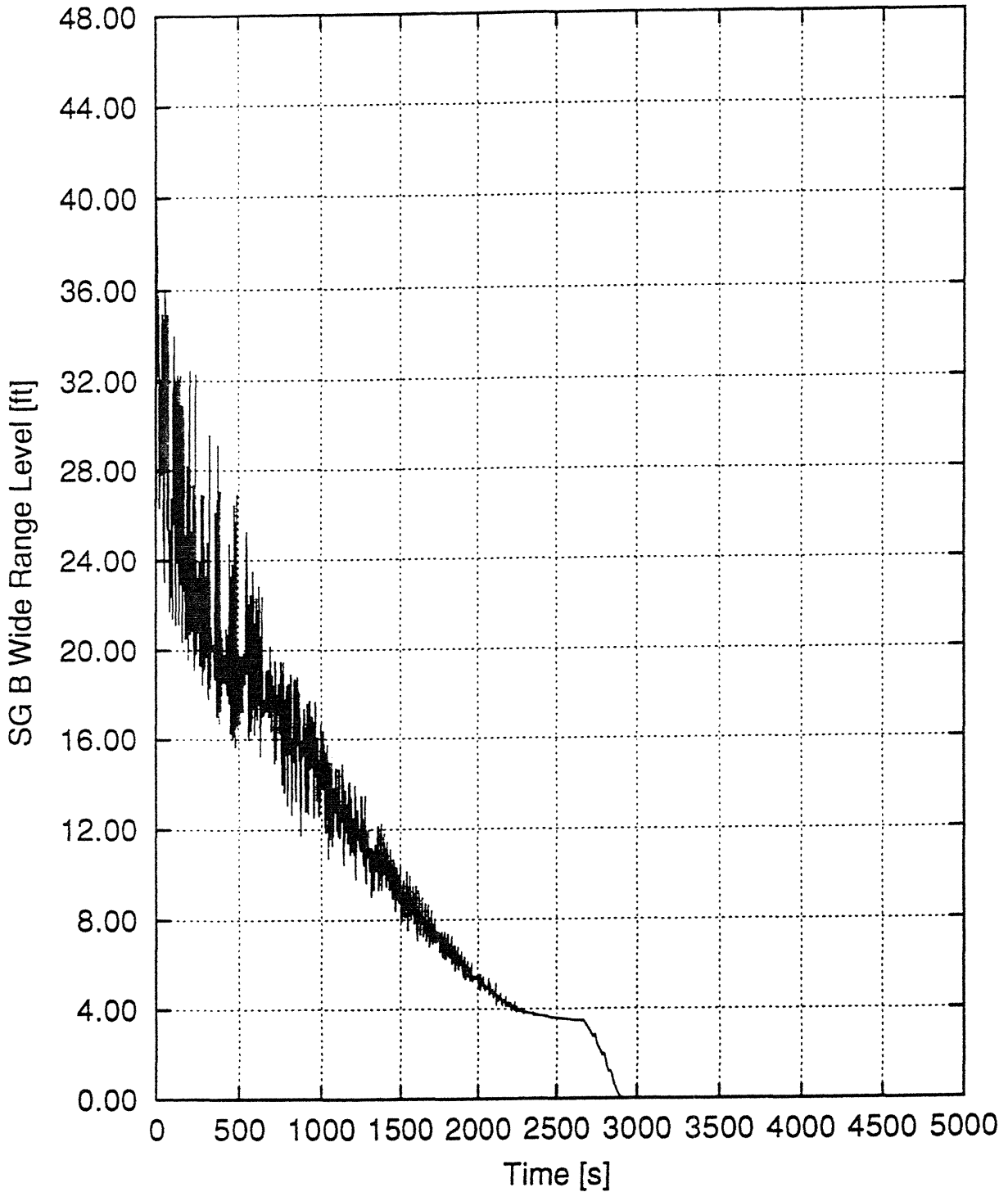


Figure 14.1.10-5
Loss of Normal Feedwater - High Pressure
Pressurizer Pressure vs. Time

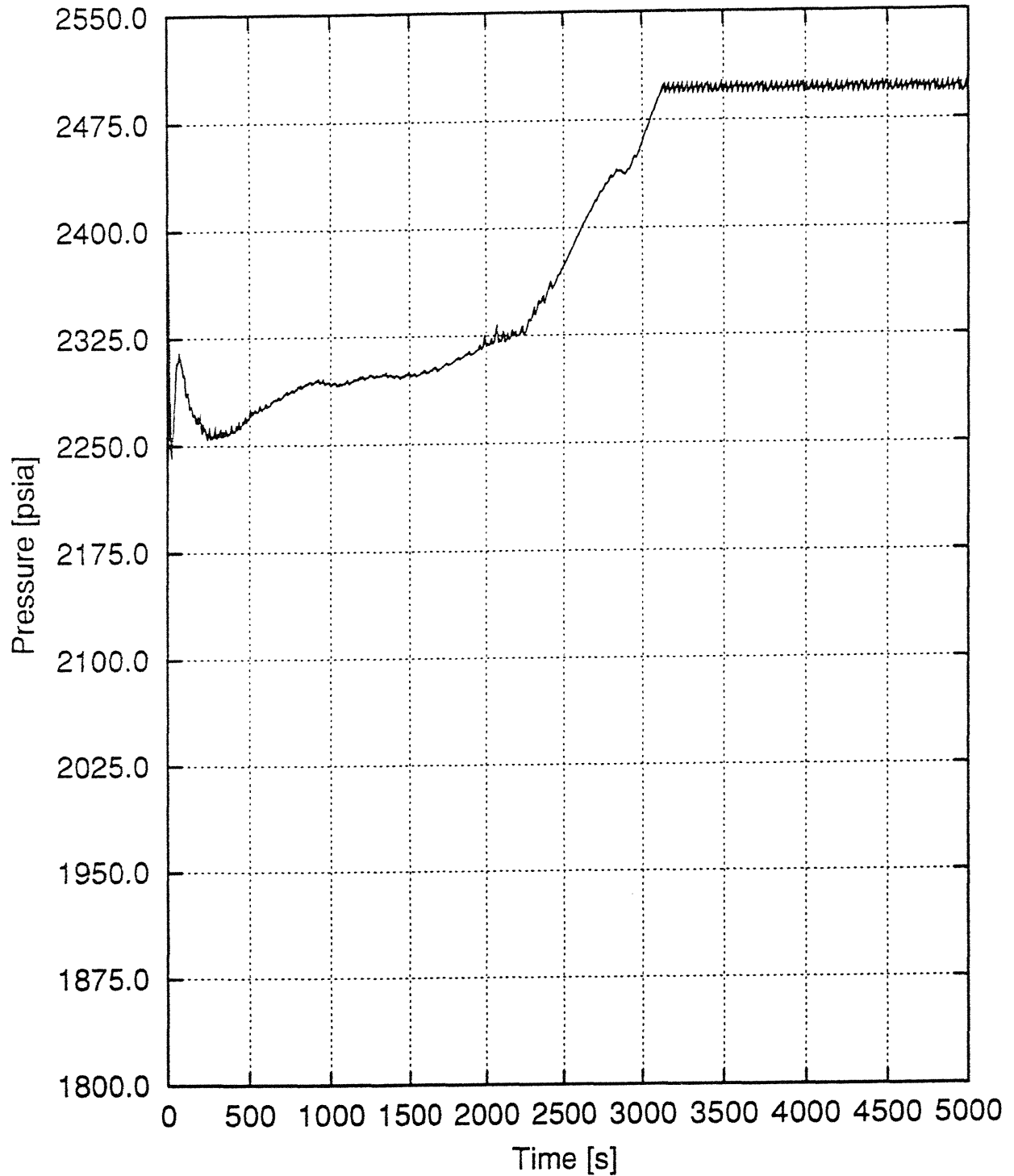


Figure 14.1.10-6
Loss of Normal Feedwater
Nuclear Power vs. Time

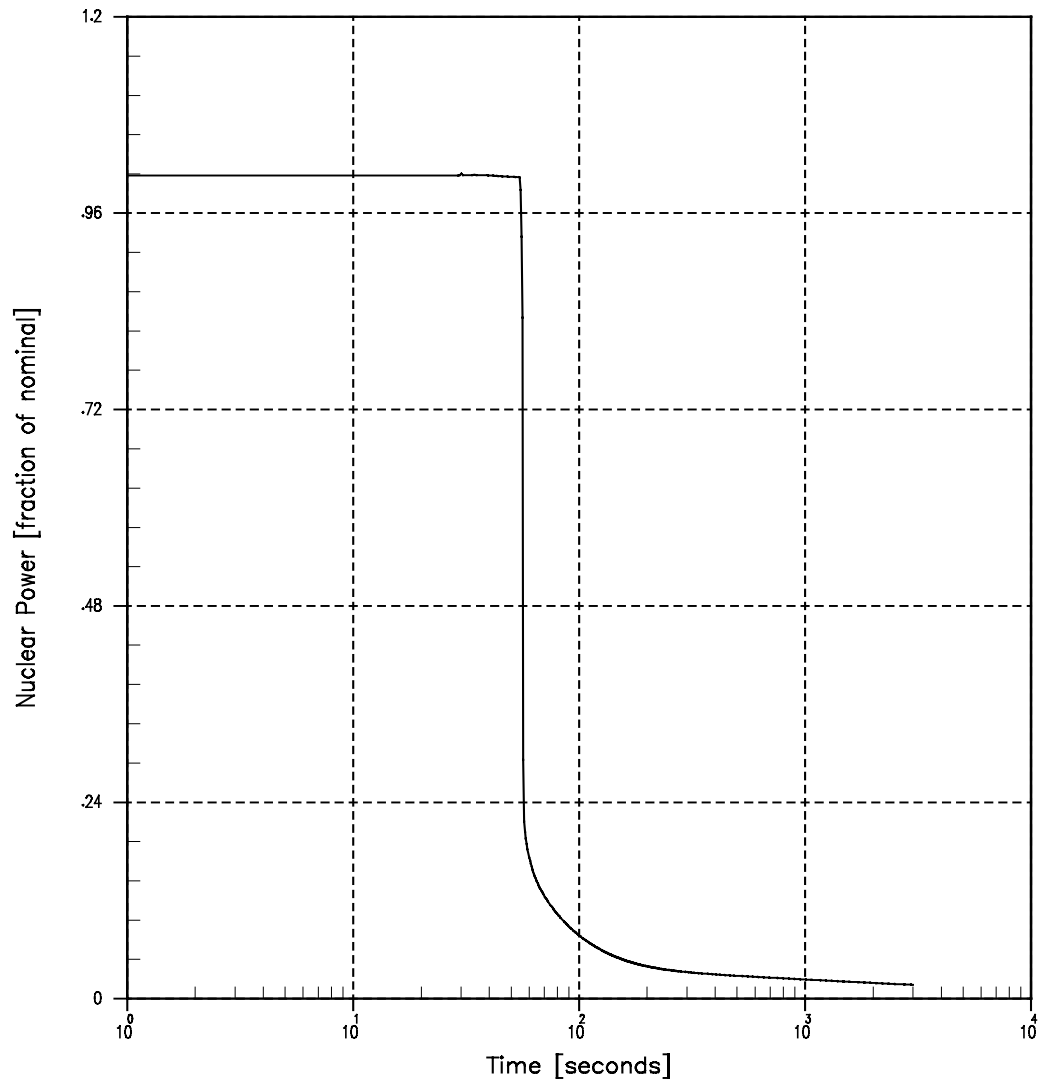


Figure 14.1.10-7
Loss of Normal Feedwater
Vessel Average Temperature vs. Time

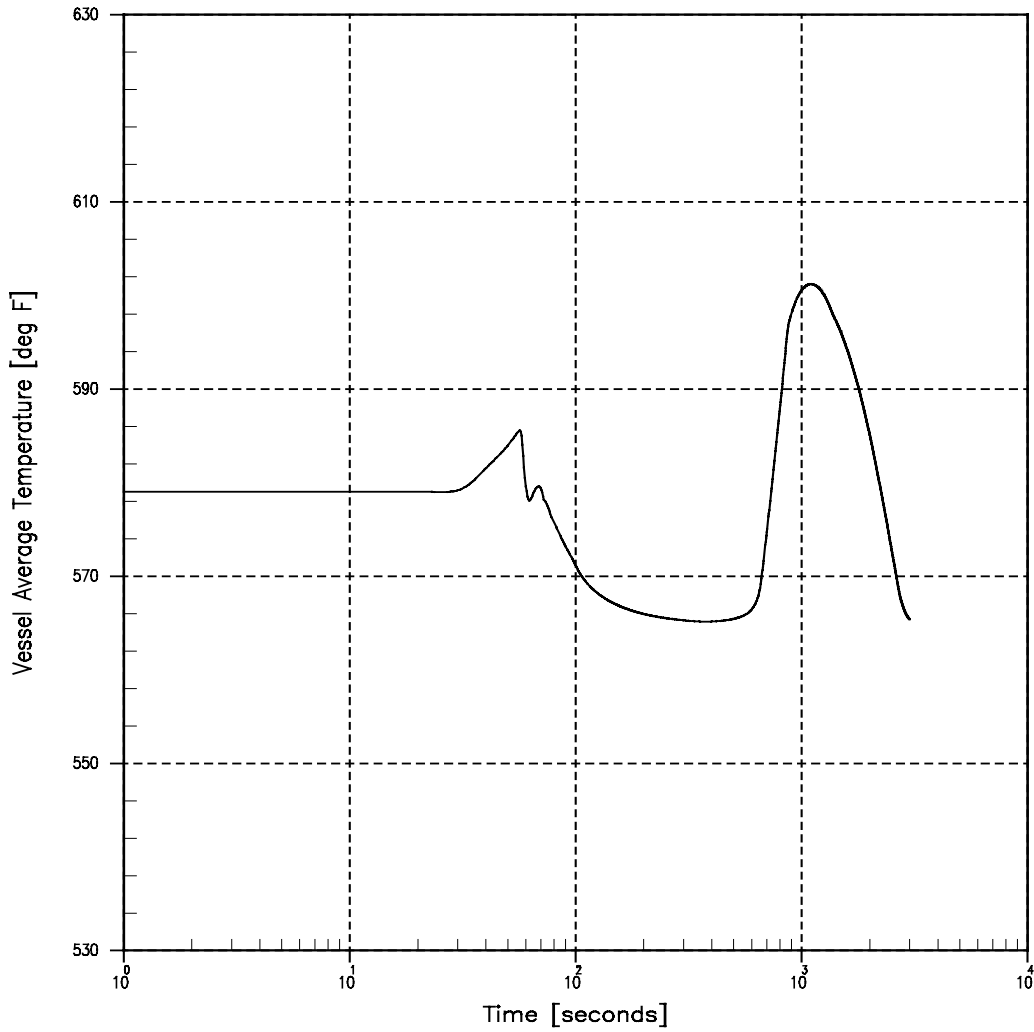


Figure 14.1.10-8
Loss of Normal Feedwater
Pressurizer Pressure vs. Time

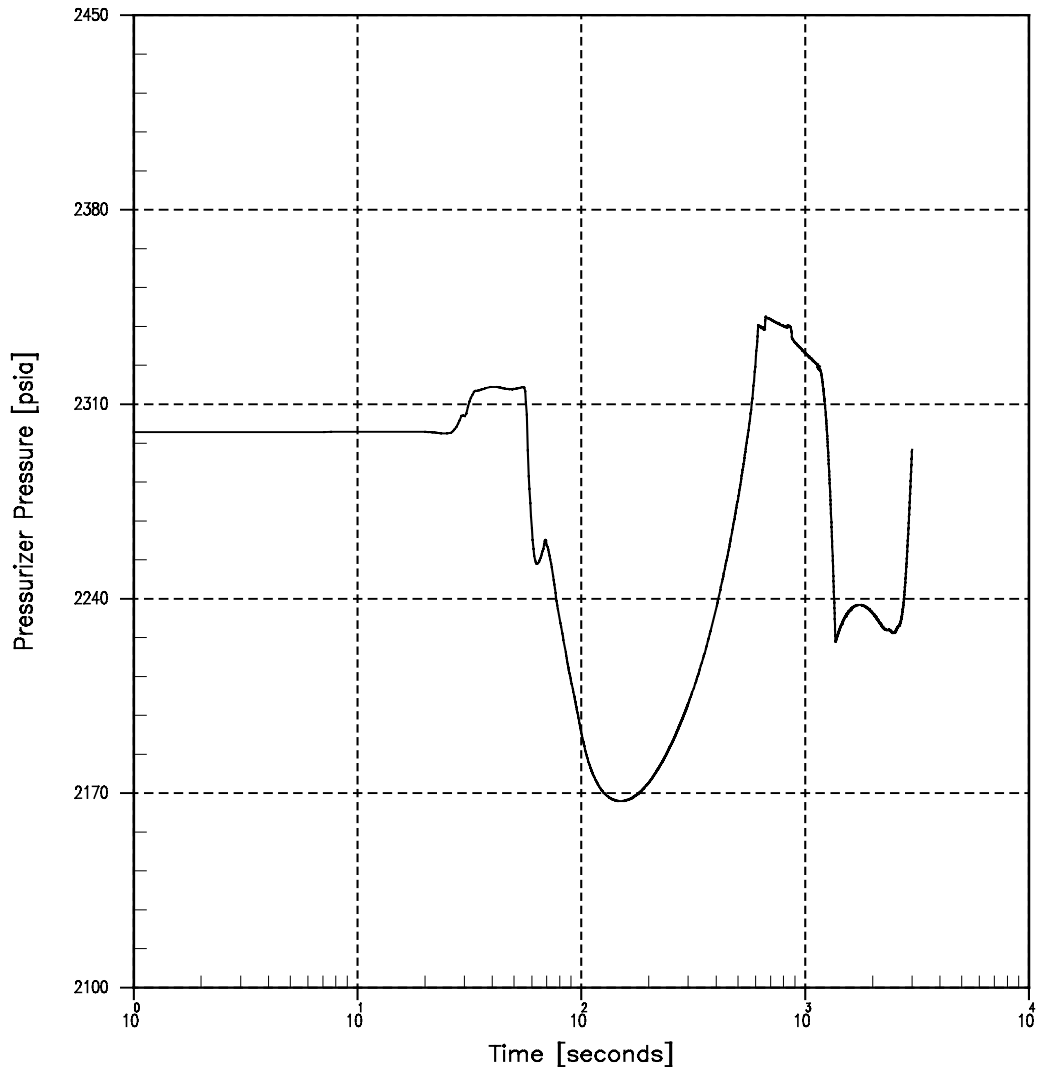


Figure 14.1.10-9
Loss of Normal Feedwater
Pressurizer Water Volume vs. Time

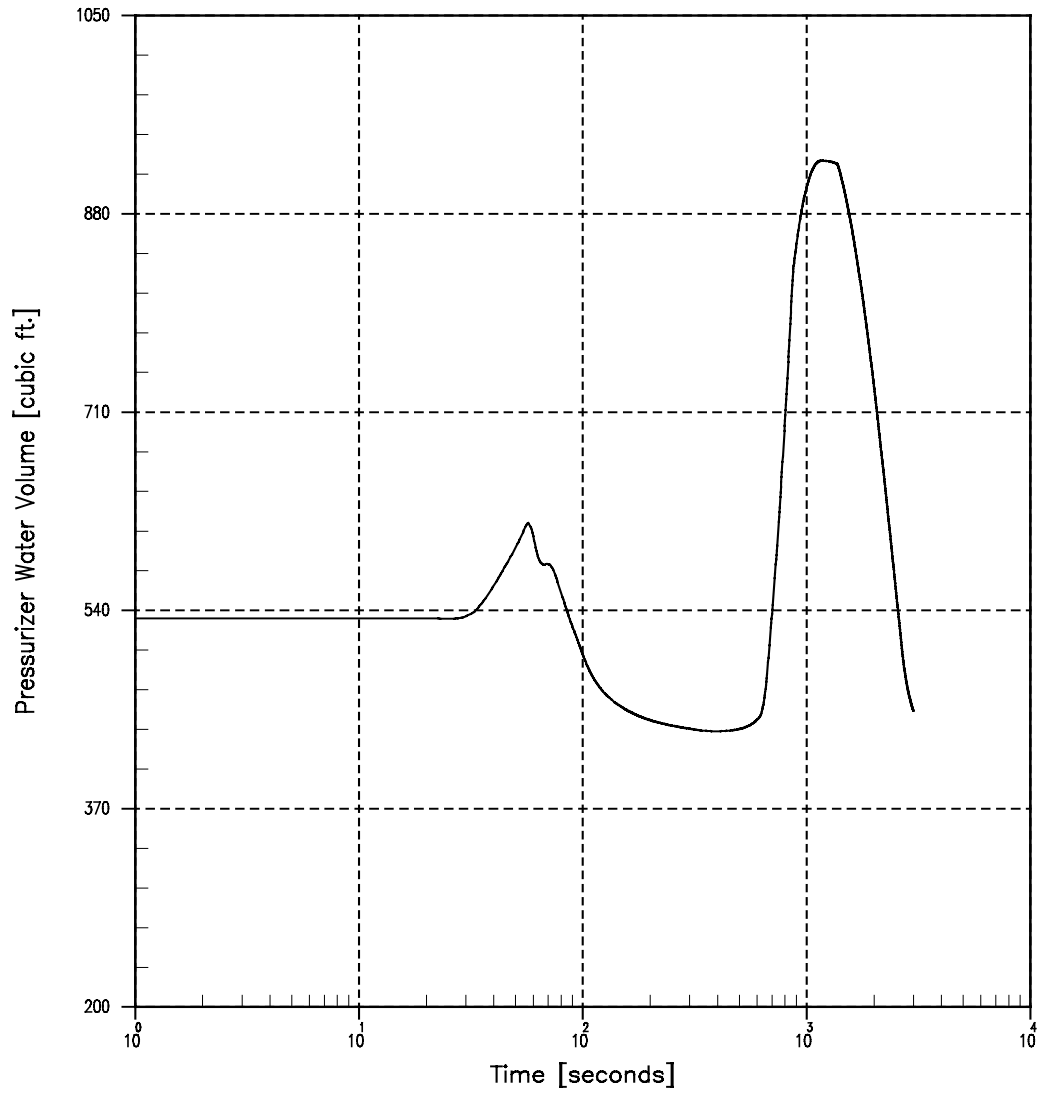


Figure 14.1.10-10
Loss of Normal Feedwater
Steam Generator Pressure vs. Time

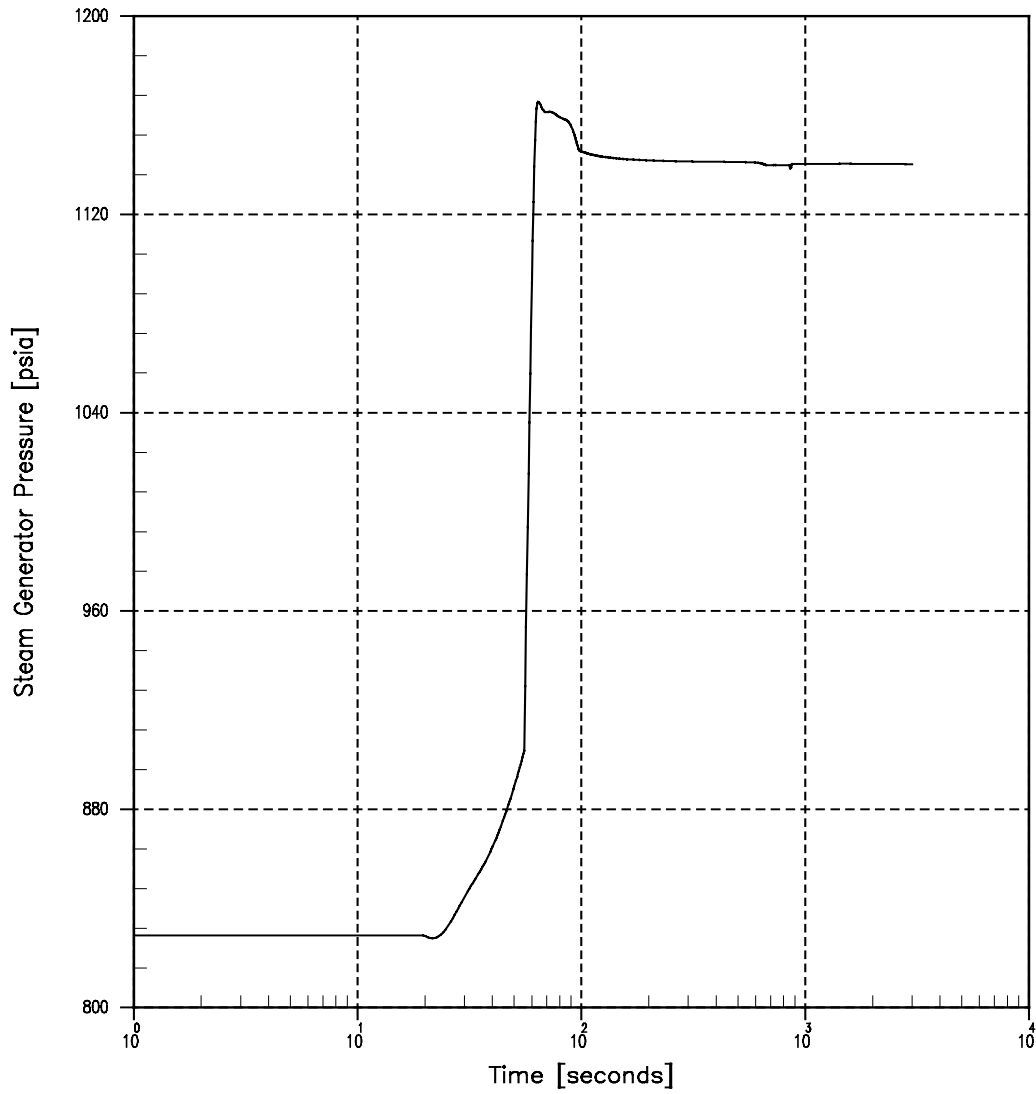


Figure 14.1.10-11
Loss of Normal Feedwater
Steam Generator Mass vs. Time

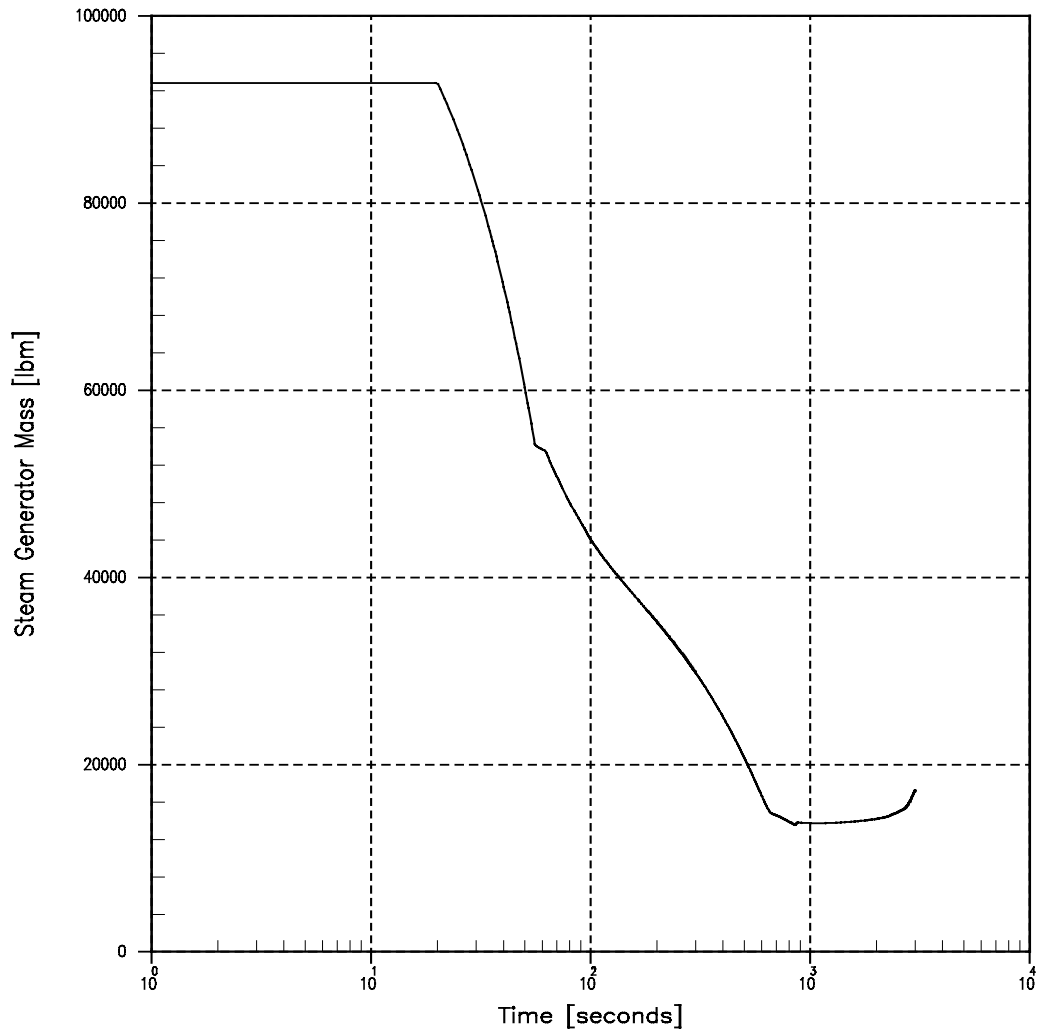
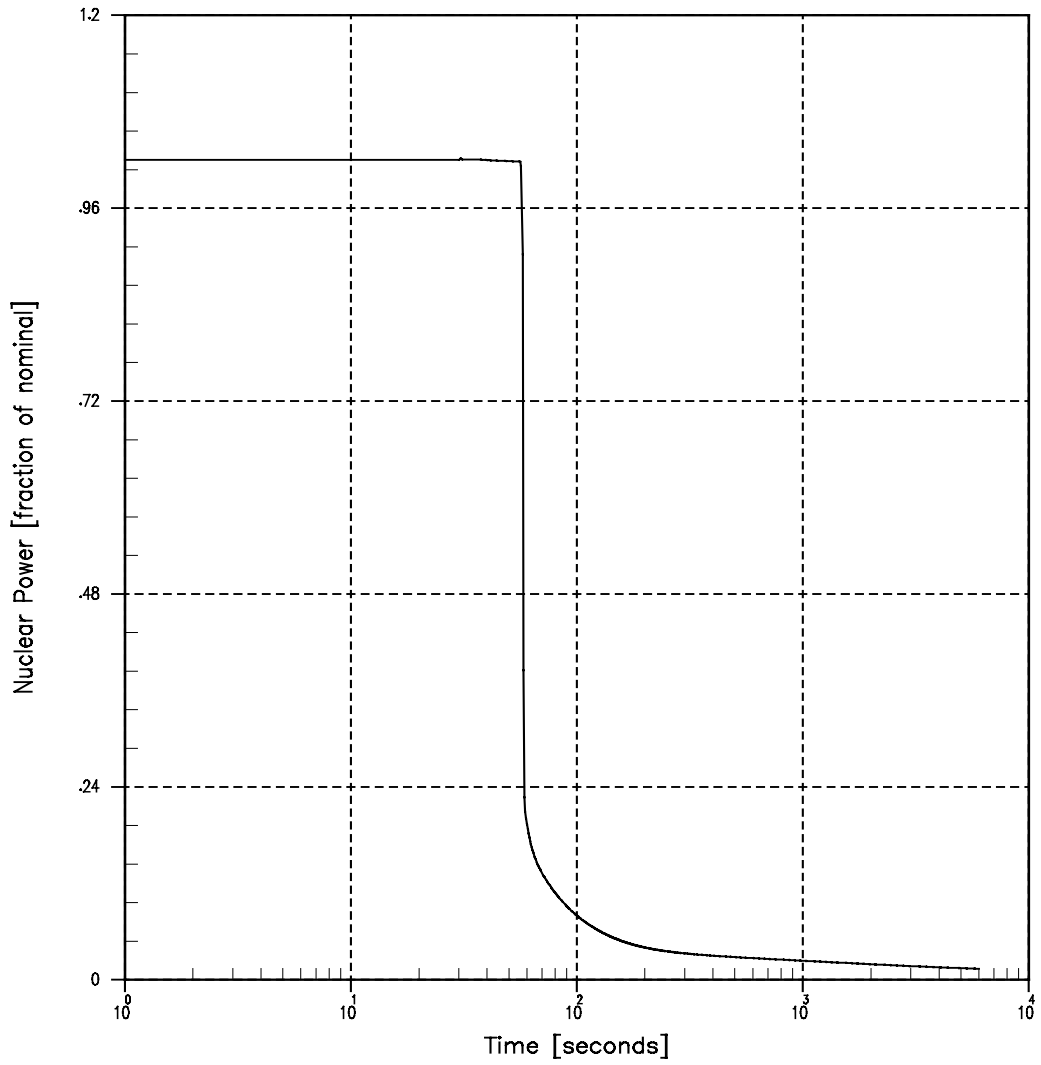
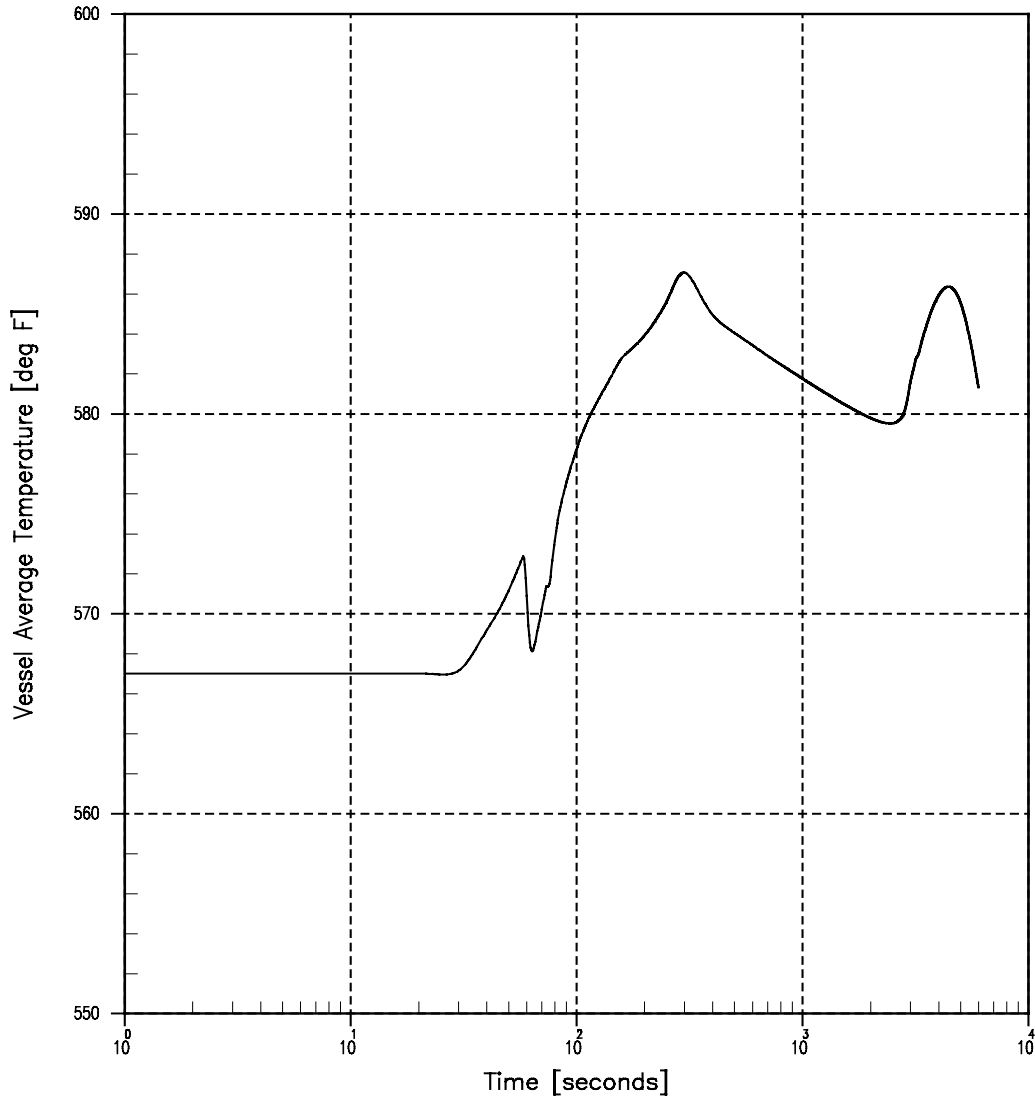


Figure 14.1.12-1
Loss of AC Power to the Plant Auxiliaries*
Nuclear Power vs. Time



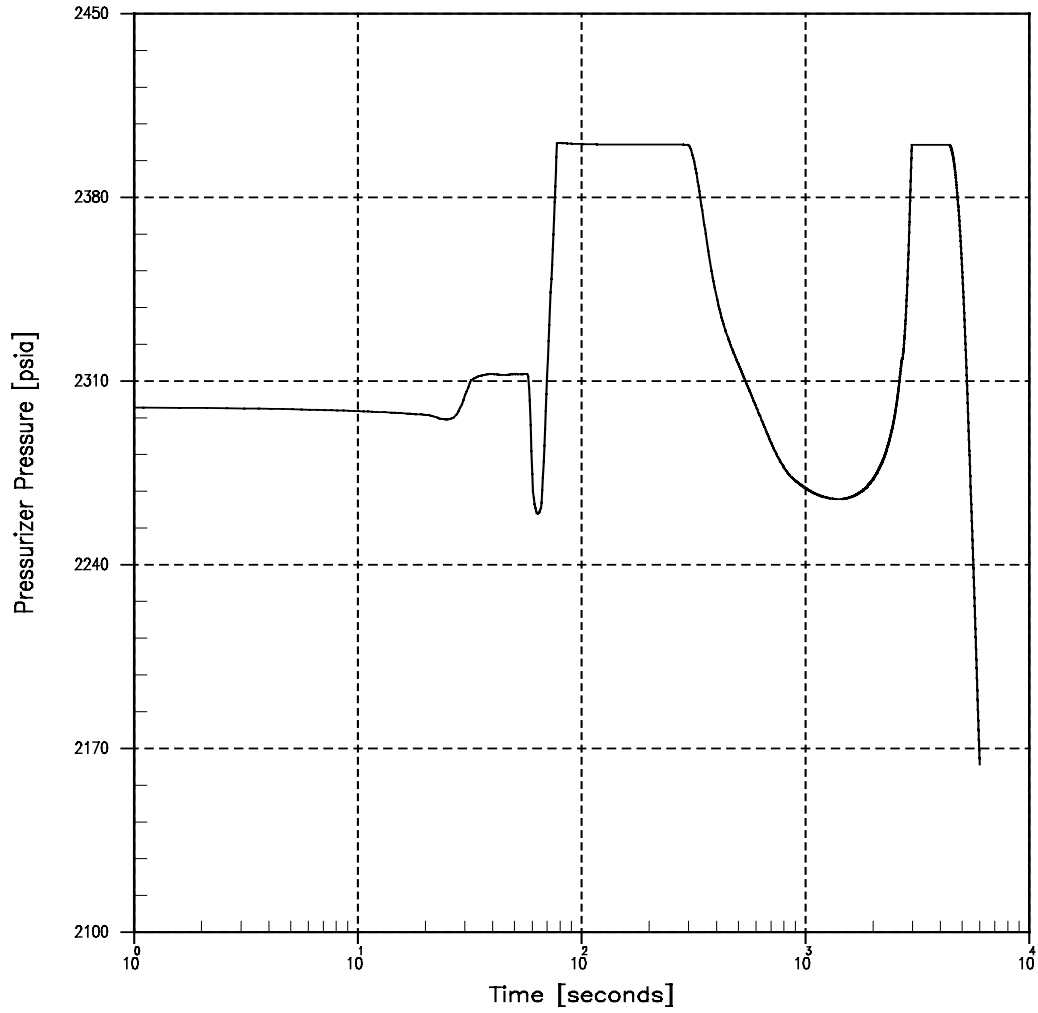
* Non-emergency AC power to station auxiliaries is lost following reactor trip.

Figure 14.1.12-2
Loss of AC Power to the Plant Auxiliaries*
Vessel Average Temperature vs. Time



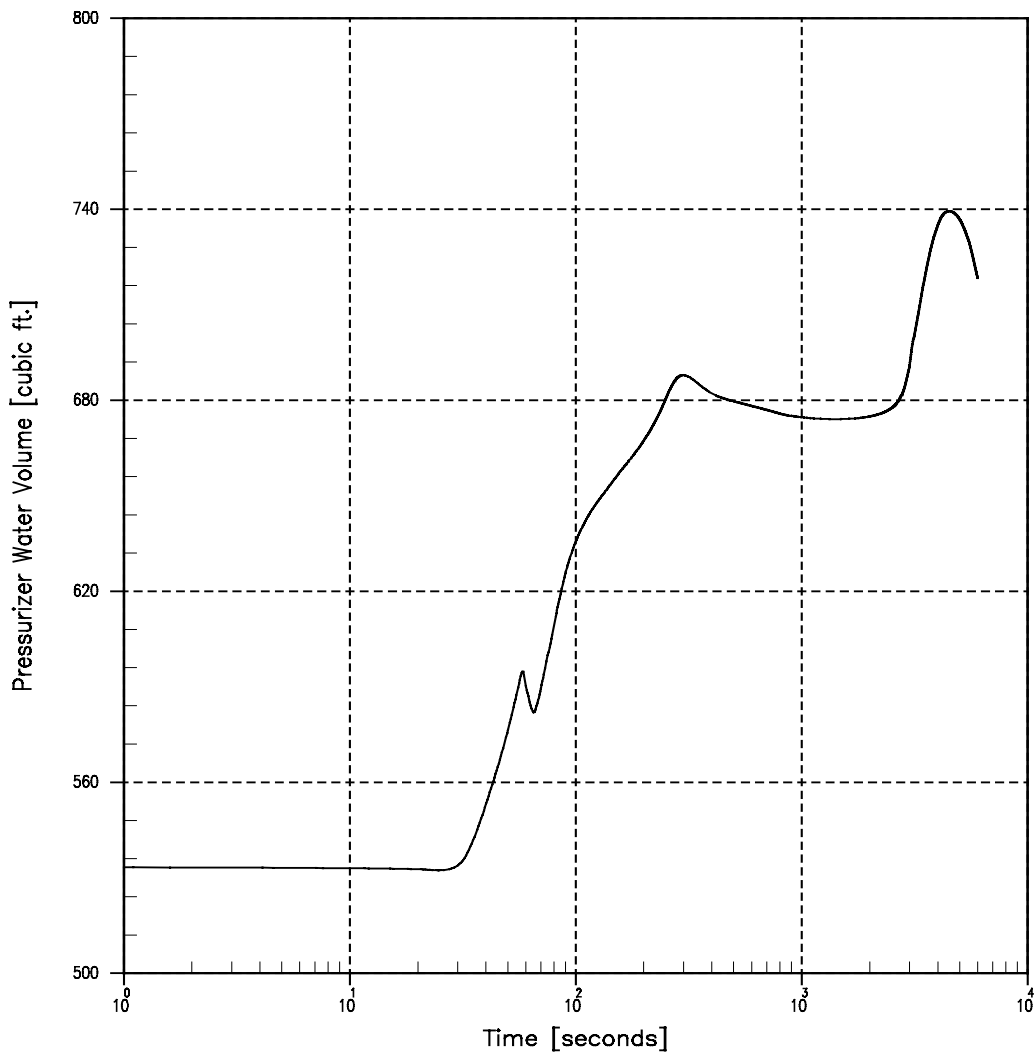
* Non-emergency AC power to station auxiliaries is lost following reactor trip.

Figure 14.1.12-3
Loss of AC Power to the Plant Auxiliaries
Pressurizer Pressure vs. Time



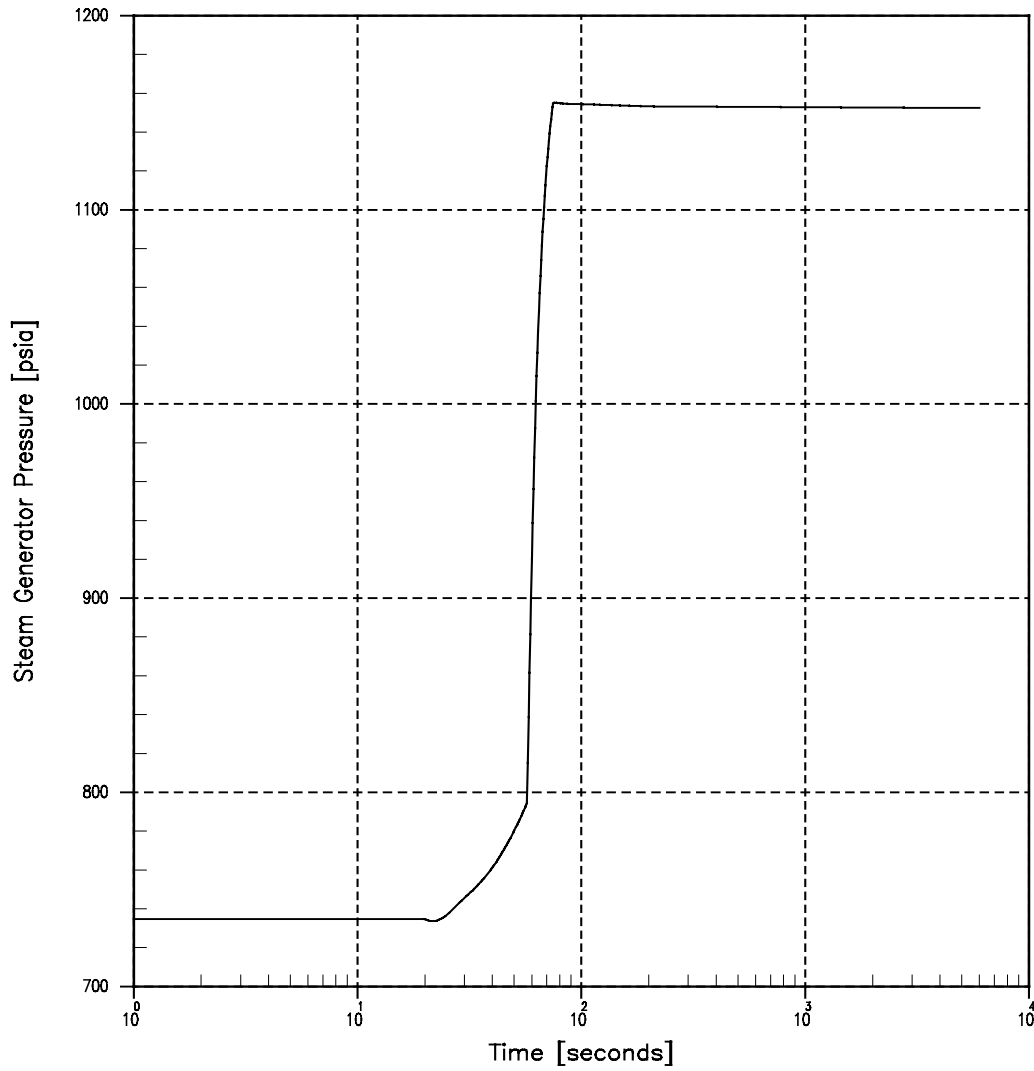
* Non-emergency AC power to station auxiliaries is lost following reactor trip.

Figure 14.1.12-4
Loss of AC Power to the Plant Auxiliaries*
Pressurizer Water Volume vs. Time



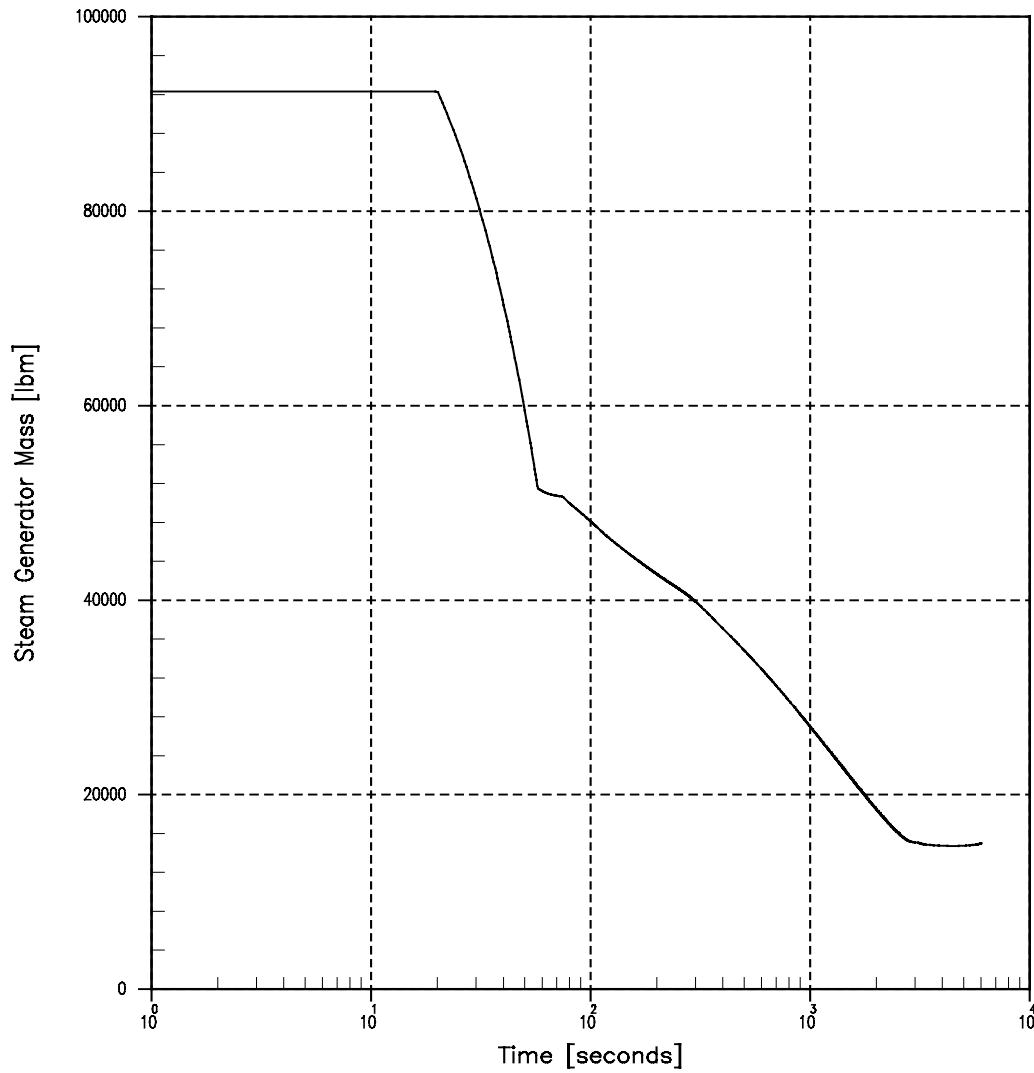
* Non-emergency AC power to station auxiliaries is lost following reactor trip.

Figure 14.1.12-5
Loss of AC Power to the Plant Auxiliaries*
Steam Generator Pressure vs. Time



* Non-emergency AC power to station auxiliaries is lost following reactor trip.

Figure 14.1.12-6
Loss of AC Power to the Plant Auxiliaries*
Steam Generator Mass vs. Time



* Non-emergency AC power to station auxiliaries is lost following reactor trip.

14.2 STANDBY SAFETY FEATURES ANALYSIS

Adequate provisions have been included in the design of the plant, and its standby engineered safeguards to limit potential exposure of the public to below the guidelines of 10 CFR 50.67 for situations which have a very low probability of occurrence, but which could conceivably involve uncontrolled releases of radioactive materials to the environment. The situations, which have been considered, are:

- Fuel Handling Accidents
- Accidental Release of Waste Liquid
- Accidental Release of Waste Gases
- Rupture of a Steam Generator Tube
- Steam Line Break
- Rupture of a Control Rod Drive Mechanism Housing - RCCA Ejection
- Turbine Missile Damage to Spent Fuel Pool

14.2.1 Fuel Handling Accidents

The following fuel-handling accidents are evaluated to ensure that no hazards are created:

- A fuel assembly becomes stuck inside the reactor vessel
- A fuel assembly or RCCA is dropped onto the floor of the reactor refueling cavity or spent fuel pool
- A fuel assembly becomes stuck in the penetration valve
- A fuel assembly becomes stuck in the transfer tube or the carriage becomes stuck.

14.2.1.1 Causes and Assumptions

The possibility of a fuel handling incident of the severity considered in the analysis is very remote because of the many administrative controls and physical limitations imposed on fuel handling operations. All refueling operations are conducted in accordance with prescribed procedures under direct surveillance of a supervisor technically trained in nuclear safety. Also, before any refueling operations begin, verification of complete RCCA insertion is obtained by weighing each control rod drive mechanism individually to verify that the control rods are disengaged from the control rod drive mechanisms. Boron concentration in the coolant is raised to the refueling concentration and verified by sampling. Refueling boron concentration is sufficient to maintain the clean, cold, fully loaded core sub-critical with all RCCAs withdrawn. The refueling cavity is filled with water meeting the same boric acid specifications.

As the vessel head is removed, a visual check is made to verify that RCCA drive shafts are free of the mechanism housings.

After the vessel head is removed, the RCCA drive shafts are disconnected from their respective assemblies using the manipulator crane and the shaft-unlatching tool. A spring scale is used to indicate that the drive shaft is free of the RCCA as the lifting force is applied.

The fuel handling manipulators and hoists are designed so that fuel cannot be raised above a position which provides adequate shield water depth for the safety of operating personnel. This safety feature applies to handling facilities in both the containment and in the spent fuel pool area. In the spent fuel pool, the design of storage racks and manipulation facilities is such that:

Fuel at rest is positioned by positive restraints in a safe, always sub-critical, geometrical array, with no credit for boric acid in the water.

Fuel can be manipulated only one assembly at a time.

Violation of procedures, by placing one fuel assembly in juxtaposition with any group of assemblies in racks does not result in criticality.

Crane facilities do not permit the handling of heavy objects, such as a spent fuel-shipping container, over the spent fuel storage area. A detailed description of crane movement limitations appears in Section 9.5.

Adequate cooling of fuel during underwater handling is provided by convective heat transfer to the surrounding water. The fuel assembly is immersed continuously while in the Refueling Cavity or Spent Fuel Pool.

Even if a spent fuel assembly becomes stuck in the transfer tube, the fuel assembly is completely immersed and natural convection maintains adequate cooling to remove the decay heat. The fuel handling equipment is described in detail in Section 9.5.

Two Nuclear Instrumentation System source-range channels are continuously in operation and provide warning of any approach to criticality during refueling operations. This instrumentation provides a continuous audible signal in the containment, and would annunciate a local horn and an annunciator in the plant control room if the count rate increases above a preset low level.

Refueling boron concentration is sufficient to maintain the clean, cold, fully loaded core sub-critical by at least 5 percent $\Delta k/k$ with all RCCAs inserted. At this boron concentration, the core would also be more than 2 percent sub-critical with all control rods withdrawn.

All these safety features make the probability of a fuel-handling incident very low. Nevertheless, it is possible that a fuel assembly could be dropped during the handling operations. Therefore, this incident is analyzed both from the standpoint of radiation exposure and accidental criticality.

Special precautions are taken in all fuel handling operations to minimize the possibility of damage to fuel assemblies during transport to and from the spent fuel pool and during installation

in the reactor. All handling operations of irradiated fuel are conducted under water. The handling tools used in the fuel handling operations are conservatively designed and the associated devices are of a fail-safe design.

In the fuel storage area, the fuel assemblies are spaced in a pattern that prevents any possibility of a criticality accident.

The motions of the cranes, which move the fuel assemblies, are limited to a low maximum speed. Caution is exercised during fuel handling to prevent the fuel assembly from striking another fuel assembly or structures in the containment or fuel storage building.

The fuel handling equipment suspends the fuel assembly in the vertical position during fuel movements, except when the fuel is moved through the transport tube.

The design of the fuel assembly is such that the fuel rods are restrained by grid clips which provide a total restraining force of approximately 40 pounds on each fuel rod at the end of life. The force transmitted to the fuel rods during normal handling is limited to the (grid frictional) restraining force and is not sufficient to breach the fuel rod cladding. If the fuel rods are not in contact with the fuel assembly bottom nozzles, the rods would have to slide against the 40-pound friction force. This would dissipate an appreciable amount of energy and thus limit the impact force on the individual fuel rods.

If one assembly is lowered on top of another, no damage to the fuel rods would occur that would breach the cladding. Considerable deformation would have to occur before the fuel rods would contact the top nozzle adapter plate and apply any appreciable load to the rods. Based on the above, it is unlikely that any damage would occur to the individual fuel rods during handling.

If during handling and subsequent translational motion the fuel assembly should strike against a flat surface, the fuel assembly lateral loads would be distributed axially along its length with reaction forces at the grid clips and essentially no damage would be expected in any fuel rods.

Analyses have been made assuming that fuel assembly is dropped vertically and strikes a rigid surface and where one fuel assembly is dropped vertically on another. The analysis of a dropped fuel assembly striking a rigid surface considers the stresses in the fuel cladding and any possible buckling of the fuel rods between the grid supports. The results show that the buckling load at the bottom section of the fuel rod, which would receive the highest loading, is below the critical buckling load and the stresses are below the yield stress. For the case in which a fuel assembly is assumed to be dropped on top of another assembly, the impact load is transmitted through the top nozzle and the RCCA guide tubes of the struck assembly before any of the loads reach the fuel rods. As a result, a significant amount of kinetic energy is absorbed by the top nozzle of the struck assembly and bottom nozzle of the falling assembly, thereby limiting the energy available for fuel rod deformation. The results of this analysis indicated that the buckling

load on the fuel rods is below the critical buckling load and stresses in the cladding are below yield.

Prototype fuel assemblies have been subjected to 3000 pounds of axial load without excessive lateral or axial deformation. The maximum column load expected to be experienced in service is approximately 1000 pounds. This information is used in the fuel handling equipment design to establish the limits for inadvertent axial loads.

For the purposes of evaluating the environmental consequences of a fuel-handling incident, a conservative upper limit of damage is assumed by considering the cladding rupture of all rods in one complete fuel assembly. The remaining fuel assemblies are so protected by the storage rack structure that no lateral bending loads would be imposed.

14.2.1.2 Activity Release Characteristics

For the assumed accident, there is a sudden release of the gaseous fission products held in the gap between the pellets and cladding of one fuel assembly. The low temperature of the fuel during handling operations precludes further significant release of gases from the pellets themselves after the cladding is breached. Molecular halogen release is also greatly minimized due to their low volatility at these temperatures. The strong tendency for iodine in vapor and particulate form to be scrubbed out of gas bubbles during their ascent to the water surface further reduces the quantity released from the water surface.

The fuel assembly gap activity was conservatively calculated with the plant assumed to be operated at 1683 MW_{th}. The iodine 131 gap activity is assumed to be 8 percent of total fuel iodine 131 activity. The Kr-85 gap activity is assumed to be 10 percent of the total fuel Kr-85 activity. All other iodine and noble gas gap activities are assumed to be 5 percent of the total fuel activity. The noble gas and iodine fission products calculated to be present in the average fuel rod at 100 hours following shutdown are given in Table D.3-2 of Appendix D. A factor of 1.7 is applied to the core average assembly activity to conservatively account for the peak radial peaking factor.

14.2.1.3 Method of Analysis

The volatile gaseous activities associated with the fuel handling accident could be released either inside the Containment Building or in the Auxiliary Building. Both of these areas have ventilation systems in operation under administrative control during fuel handling operations. Radioactivity monitors provide continuous indication of radiation levels and signal evacuation of these areas on high alarm. The Containment Building high-level alarm automatically closes the purge supply and exhaust ducts. Administrative evaluation of the containment activity would determine when purging could be resumed. A high-level alarm on the Auxiliary Building Vent Monitor would automatically activate the Zone Special Ventilation (SV) System with subsequent absolute and charcoal filtration. This system is described in Chapter 9.

In the analysis no credit is taken for the Spent Fuel Pool Ventilation System operation in the auxiliary building and no credit is taken for isolation of containment for the accident occurring in

containment. Since the assumptions and parameters for a fuel handling accident inside containment are identical to those for a fuel handling accident in the auxiliary building, the radiological consequences are the same regardless of the location of the accident.

In this analysis, all of the rods of one assembly (179 rodlets) are assumed to be damaged releasing the entire gap activity. Scrubbing of iodine by the borated water results in a decrease in the radioiodine activity available for release. A conservative value of 0.005 for scrubbing by the water is assumed. The activity released from the water surface is released to the outside environment over a 2 hour period.

Dispersion of this activity is computed using the Gaussian plume dispersion formula and taking credit for building wake dilution. A wind velocity of 1.5 meters per second is assumed to remain in one direction for the duration of the accident under Pasquill F conditions. The dispersion characteristics are discussed in Section 2.7 and curves, corrected for building wake effect by the volumetric source method, are presented on Figure 2.7-5. The site boundary, Exclusion Area Boundary χ/Q , dispersion factor is $2.232E-4 \text{ sec/m}^3$. The Low Population Zone χ/Q is $3.977E-5 \text{ sec/m}^3$.

The total effective dose equivalent (TEDE) doses at the site boundary and low population zone are 0.70 and 0.11 rem respectively.

Thus, it is concluded that a dropped fuel assembly would present no criticality hazard and would result in radiation levels at the site boundary and low population zone that are well below the 10 CFR 50.67 guidelines. This analysis was reviewed and approved by the NRC in Reference 2.

14.2.2 Accidental Release-Recycle of Waste Liquid

Accidents in the Auxiliary Building that result in the release of radioactive liquids are those that involve the rupture or leaking of system pipe lines or storage tanks. The largest vessels are the three liquid holdup tanks, sized such that two tanks can hold more than one reactor coolant liquid volume, used to store the normal recycle or water fluids produced. The contents of one tank are passed through the liquid processing train while the other tanks are being filled.

All liquid waste components except the reactor coolant drain tank are located in the Auxiliary Building and any leakage from the tank or piping will be collected in the building sump to be pumped back into the liquid waste system. The building sump and basement volume are sufficient to hold the full volume of a liquid holding tank without overflowing to areas outside the building. This also is true for the tanks in the Auxiliary Building.

The holdup tanks are also equipped with safety pressure relief and designed to accept the established seismic forces at the site. Liquids in the Chemical and Volume Control System flowing into and out of these tanks are controlled by manual valve operation and governed by prescribed administrative procedures.

The volume control tank design philosophy is similar in many respects to that applied for the holdup tanks. Level alarms, pressure relief valves and automatic tank isolation and valve control assure that a safe condition is maintained during system operation. Excess letdown flow is directed to either the holdup tanks via the reactor coolant drain tank or the volume control tank. The waste holdup tank is a horizontal tank, which is continuously maintained at atmospheric pressure. Its vent is routed to the atmosphere through the Auxiliary Building exhaust ducts.

The potential hazard from these process or waste liquid releases is derived only from the volatilized components. The releases are described and their effects summarized in Section 14.2.3.

The evaluation of the credibility of the accidental release of radioactive fluids above maximum normal concentration ($4E-5$ $\mu\text{Ci/cc}$) from the Waste Disposal System discharge is based upon the following review of waste discharge operating procedure, monitoring function description, monitor failure mode and the consequences of a monitor failure.

The process for discharging liquid wastes is as follows:

1. A batch of waste is collected in one Steam Generator Blowdown Treatment tank (capacity 10,000 gal); other lesser volume tank(s) can be used and follow the same process;
2. The tank, or tanks, is (are) isolated;
3. The tank(s) contents are recirculated to mix the liquid;
4. A sample is taken for radiochemical analysis;
5. If analysis indicates that release can be made within permissible limits, the quantity of activity to be released is recorded on the basis of the liquid volume in the tank(s) and its activity concentration. Each tank or batch is assessed for its radiological impact prior to and/or after each release. If release can not be made within permissible limits, the waste is returned for additional cleanup. Then the process begins again.
6. To release the liquid, the last stop valve in the discharge line (which is normally locked shut) must be unlocked and opened; a second valve, which trips shut automatically on high radiation signal from the effluent monitor, must be opened manually; a pump for the tank being released must be started manually and a flow rate established. The release flow rate is set at or below the maximum release flow rate as listed on the Radiological Liquid Waste Discharge Permit. Liquid is now being pumped to the discharge canal.

As the operating procedure indicates, the release of liquid waste is under administrative control. The effluent monitor is provided to maintain surveillance over the release.

The effluent monitor is provided with the following features:

1. A check source is provided to permit the operator to check the operation of the monitor before discharge from the control room.

2. If the monitor falls off scale at any time, an alarm condition is indicated in the control room and the waste disposal discharge valve is tripped closed automatically.
3. If the AC power supply to the monitor fails, a high radiation alarm is annunciated. The trip valve also closes.
4. The normally closed radiation trip valve fails closed.

It is concluded that the administrative controls imposed on the operator combined with the safety features built into the equipment provide a high degree of assurance against accidental release of waste liquids.

Should a complete failure of any tank located in the Auxiliary Building occur, its contents remains in this building. Any subsequent discharge of radioactive liquid to the lake is be conducted under the controls described above and does not result in activity concentrations in excess of the limits given in the Off-Site Dose Calculation Manual (ODCM).

Dilution of off-site liquid releases is discussed in Section 2.6.4.

14.2.3 Accidental Release-waste Gas

14.2.3.1 Gas Decay Tank Rupture

14.2.3.1.1 Causes and Assumptions

The gas decay tanks contain the gases vented from the RCS the volume control tank, and the liquid holdup tanks. Sufficient volume is provided in each of four tanks to store the gases evolved during a reactor shutdown. The system is adequately sized to permit storage of these gases for forty-five days prior to discharge.

This period is selected as the maximum foreseeable holdup time because in this period the shorter-lived radioactive gaseous isotopes received by the waste system will have decayed to a level, which is less significant than that of long-lived Kr⁸⁵.

The waste gas accident is defined as an unexpected and uncontrolled release to the atmosphere of the radioactive xenon and krypton fission gases that are stored in the waste gas storage system. Failure of a gas decay tank or associated piping could result in a release of this gaseous activity. This analysis shows that even with the worst expected conditions, the off-site doses following release of this gaseous activity would be very low.

The leakage of fission products through cladding defects can result in a buildup of radioactive gases in the reactor coolant. Based on experience with other operational closed cycle, pressurized water reactors, the number of defective fuel elements and the gaseous activity in the coolant is expected to be low. The principal source of radioactive gases in the Waste Disposal System is the bleeding of effluents from the RCS.

Nonvolatile fission product concentrations are greatly reduced as the cooled RCS liquid is passed through the purification demineralizers. (The removal factor for iodine, for example, is at

least 10.) The decontamination factor for iodine between the liquid and vapor phases, for example, is expected to be on the order of 10,000. Based on the above analysis and operating experience at Yankee-Rowe and Saxton, activity stored in a gas decay tank consists of the noble gases released from the processed coolant with only negligible quantities of the less volatile isotopes.

The components of the waste gas system are not subjected to any high pressures or stresses, are Class I design (see Appendix B), and are designed to the standards given in Table 11.1-2. A rupture or failure is highly unlikely. However, a rupture of a gas decay tank was analyzed to define the hazard caused by a malfunction in the radioactive waste disposal system.

14.2.3.1.2 Activity Release Characteristics

The activity in a gas decay tank is taken to be the maximum amount that could accumulate from operation with cladding defects in 1 percent of the fuel elements. This is at least ten times the expected number of defective fuel elements. The maximum activity is obtained by assuming the noble gases, xenon and krypton, are accumulated with no release over a full core cycle. The gas decay tank inventory is calculated assuming nuclide decay, degassing of the reactor coolant with letdown at the maximum rate, and periodic purging to the gas decay tank. The maximum inventory for each nuclide during the degas and purge cycle is given in Appendix D.

Samples taken from gas storage tanks in pressurized water reactor plants in operation show no appreciable amount of iodine.

To define the maximum doses, the release is assumed to result from gross failure of any process system storage tank, here represented by a gas decay tank giving a rapid release of its volatile and gaseous contents to the atmosphere.

14.2.3.2 Volume Control Tank Rupture

14.2.3.2.1 Causes and Assumptions

The volume control tank contains fission gases and low concentrations of halogens, which are normally a source of waste gas activity, vented to a gas decay tank. The iodine concentrations and volatility are quite low at the temperature, pH, and pressure of the fluid in the volume control tank. The same assumptions detailed in the preceding subsection apply to this tank. As the volume control tank and associated piping are not subjected to any high pressures or stresses, failure is very unlikely. However, a rupture of the volume control tank is analyzed to define the limit of the exposure that could result from such an occurrence.

14.2.3.2.2 Activity Release Characteristics

Rupture of the volume control tank is assumed to release all the contained noble gases and one percent of the halogen inventory of the tank plus that amount contained in the 88-gpm flow from the demineralizers, which would continue for up to five minutes before isolation would

occur. The one percent halogen release is a very conservative estimate of the decontamination factor expected for these conditions.

Based on one percent fuel defects, the activities available for release from the tank are given in Table D.6-1. The letdown flow release of noble gases is based on the RCS activities given in Table D.4-1. The iodine in the letdown flow is based on an assumed RCS iodine concentration of 60 $\mu\text{Ci/gm}$ DE I-131.

14.2.3.2.3 Method of Analysis

In calculating off-site plume centerline exposure, it is assumed that the activity is discharged to the atmosphere at ground level and is dispersed as a Gaussian plume downwind taking into account building wake dilution.

No credit is taken for the buoyant lift effect of the hydrogen present in the released gas. Dispersion coefficients based on the on-site meteorology program are used. A wind velocity of 1.5 meters per second is assumed to remain in one direction for the duration of the accident under Pasquill F conditions. The dispersion characteristics are discussed in Section 2.7.4 and curves corrected for building wake effects by the volumetric source method, are present on Figure 2.7-8.

The following parameters have been used in the dose assessment:

- A 0–2 hour χ/Q value of $2.232\text{E}-4 \text{ sec/m}^3$
- Breathing rate equal to $3.47\text{E}-4 \text{ m}^3/\text{sec}$
- The dose conversion factors for noble gases found in Table D.8-1
- The EPA Federal Guidance Report 11 committed effective dose equivalent (CEDE) dose conversion factors for iodine inhalation (Table D.8-1)
- The volume control tank specific activities are found in Table D.6-1
- The gas decay tank activities are found in Table D.7-1

14.2.3.2.4 Summary of Calculated Doses

The following tabulation summarizes the total effective dose equivalent doses at the site boundary (exclusion distance), consistent with a receptor on the plume centerline.

	TEDE Dose
Gas Decay Tank Rupture	0.1 rem
Volume Control Tank Rupture	0.1 rem
~25% of 10 CFR 50.67 Guidelines	6.3 rem

It is concluded that a rupture in the waste gas system or in the volume control tank would present no undue hazard to public health and safety.

14.2.4 Steam Generator Tube Rupture

14.2.4.1 Accident Description

The accident examined is the complete severance of a single steam generator tube with the reactor at power. This accident leads to an increase in contamination of the secondary system due to leakage of radioactive coolant from the RCS. In the event of a coincident loss of off-site power, or failure of the condenser dump system, discharge of activity to the atmosphere takes place via the steam generator safety and/or power operated relief valves.

The activity that is available for release from the system is limited by:

1. Activities in the steam generator secondary that are a consequence of operational leakage prior to the complete tube rupture.
2. The activity concentration in the reactor coolant.
3. Operator actions to isolate the mixed primary and secondary leakage to atmosphere.

The steam generator tube material is Alloy 690 and, as the material is highly ductile, it is considered that the assumption of a complete severance is conservative. The more probable mode of tube failure would be one or more minor leaks of undetermined origin. Activity in the Steam and Power Conversion System is subject to continuous surveillance and an accumulation of minor leaks that cause the activity to exceed the limits established in the Technical Specifications is not permitted during reactor operation.

The operator determines that a steam generator tube rupture has occurred, and identifies and isolates the ruptured steam generator on a restricted time scale in order to minimize contamination of the secondary system and ensure termination of radioactive release to the atmosphere from the ruptured steam generator. The recovery procedure is carried out on a time scale that ensures that break flow to the secondary system is terminated before water level in the ruptured steam generator rises into the main steam line. Sufficient indications and controls are provided to enable the operator to carry out these functions satisfactorily.

Assuming normal operation of the various plant control systems, the following sequence of events is initiated by a tube rupture:

1. Pressurizer low-pressure and low-level alarms are actuated and, prior to plant trip, charging pump flow increases in an attempt to maintain pressurizer level. On the secondary side there is a steam flow/feedwater flow mismatch before trip, as feedwater flow to the ruptured steam generator is reduced due to the additional break flow which is now being supplied to that generator.

2. Loss of reactor coolant inventory leads to falling pressure and level in the pressurizer until a reactor trip signal is generated by low pressurizer pressure. Resultant plant cooldown following reactor trip leads to a rapid change of pressurizer level, and the SI signal, initiated by low pressurizer pressure, follows soon after the reactor trip. The SI signal automatically terminates normal feedwater supply and initiates auxiliary feedwater addition; as discussed in Section 6.6; manual initiation of auxiliary feedwater may be required at low power levels.
3. The steam generator blowdown liquid monitor and the air-ejector radiation monitor will alarm, indicating a sharp increase in radioactivity in the secondary system.
4. The plant trip automatically shuts off steam supply to the turbine and if off-site power is available the condenser steam dump valves open permitting steam dump to the condenser. In the event of a coincident loss of off-site power, the condenser steam dump valves automatically close to protect the condenser. The steam generator pressure rapidly increases resulting in steam discharge to the atmosphere through the steam generator safety and/or power-operated relief valves.
5. Following plant trip, the continued action of auxiliary feedwater supply and borated SI flow (supplied from the refueling water storage tank) provide a heat sink, which absorbs some of the decay heat. Thus, steam bypass to the condenser, or in the case of loss of off-site power, steam relief to atmosphere, is attenuated during the thirty minutes in which the recovery procedure leading to isolation is being carried out.
6. SI flow results in increasing pressurizer water level. The time after trip at which the operator can clearly see returning level in the pressurizer is dependent upon the amount of operating auxiliary equipment.

14.2.4.2 Results

In determining the mass transfer from the RCS through the broken tube, several conservative assumptions are made as follows:

1. Plant trip occurs automatically as a result of low pressurizer pressure.
2. Following the initiation of the SI signal, both SI pumps are actuated and continue to deliver flow for thirty minutes.
3. After plant trip the break flow equilibrates at the point where incoming SI flow is balanced by outgoing break flow as shown in Figure 14.2.4-1. The resultant break flow persists from plant trip until thirty minutes after the accident.
4. The steam generators are controlled at the safety valve setting rather than the power-operated relief valve setting.
5. The operator identifies the accident type and terminates break flow to the ruptured steam generator within thirty minutes of accident initiation (see note below).

The above assumptions lead to a conservative estimate of 16,900 lb. of reactor coolant transferred to the ruptured steam generator as a result of a tube rupture accident from the start of the event until reactor trip and 138,000 lb. after reactor trip.

Note: Off-site and control room doses have been calculated for the KNPP SGTR accident with consideration of break flow continuing beyond the 30 minutes modeled in the licensing basis analysis. These supplemental SGTR analyses, performed for the Stretch Power Uprate (SUR), justify longer operator response times to a postulated steam generator tube rupture (SGTR). The supplemental SGTR analyses demonstrate that the licensing basis dose analysis which models 30 minutes of break flow in a simplistic manner is more limiting than a more realistic analysis with break flow continuing for 55 minutes. In addition the supplemental SGTR analyses demonstrate margin to SG overfill when the SGTR break flow is terminated 49 minutes from accident initiation.

Therefore, based on supplemental SGTR analyses, operator actions to terminate the SGTR break flow for periods up to 49 minutes from accident initiation have no adverse affect on the licensing basis radiological dose analysis. Terminating break flow in this 49 minute time period also provides sufficient margin to SG overfill.

14.2.4.3 Environmental Consequences of a Tube Rupture

The occurrence of a steam generator tube rupture, followed by immediate loss of off-site electrical power, has an extremely low probability. The effects have, however, been analyzed and the results show that the public health and safety are not endangered. The resulting off-site dose is calculated to be less than the 10 CFR 50.67 limits based on the following assumptions. The chronology of events subsequent to the tube failure is discussed above.

In assessing the consequences of the assumed accident, the inventory of halogens and noble gases available for release from the ruptured steam generator is based on the following:

1. The noble gas activity concentration in the reactor coolant is assumed to arise from continuous operation with one percent defective fuel clad (see Table D.4-1).
2. The maximum iodine activity in the reactor coolant is assumed to be 1.0 $\mu\text{Ci/gm}$ dose equivalent (DE) I-131. The analysis considers (separately) pre-accident and accident-initiated iodine spikes. The pre-accident iodine spike is assumed to have raised the RCS iodine concentration to 60 $\mu\text{Ci/gm}$ DE I-131 prior to the initiation of the tube rupture. The accident-initiated iodine spike is assumed to increase the rate iodine is released from the fuel to the coolant to a value 500 times the release rate corresponding to a maximum reactor coolant iodine concentration of 1.0 $\mu\text{Ci/gm}$ DE I-131.
3. The iodine concentration in the secondary coolant at the time of the tube rupture is assumed to be 0.1 $\mu\text{Ci/gm}$ DE I-131.
4. The amount of primary-to-secondary steam generator tube leakage to the intact steam generator is assumed to be 150 gpd.

5. An iodine partition factor in the steam generators of 0.01 (curies iodine/gm steam)/(curies iodine/gm water) is used. Prior to reactor trip and concurrent loss of off-site power, an iodine removal factor of 0.01 is taken for steam released to the condenser.
6. All noble gas activity carried of to the secondary side through steam generator tube leakage is assumed to be immediately released to the outside atmosphere.
7. Iodine contained in break flow that flashes upon entering the secondary side of the affected steam generator is assumed to be released immediately to the atmosphere with no partitioning. The amount of break flow that flashes to steam is conservatively calculated assuming that all break flow is from the hot leg side of the break and that the primary temperature remains constant. The pre-trip flashing fraction is 0.1993 and the post-trip flashing fraction is 0.1476.

In calculating off-site plume centerline exposure, it is assumed that the activity is discharged to the atmosphere at ground level and is dispersed as a Gaussian plume downwind taking into account building wake dilution.

Dispersion coefficients based on the on-site meteorology program are used. A wind velocity of 1.5 meters per second is assumed to remain in one direction for the duration of the accident under Pasquill F conditions. The dispersion characteristics are discussed in Section 2.7.4 and curves corrected for building wake effects by the volumetric source method, are presented in Figure 2.7-8.

The following parameters have been used in the dose assessment:

- A 0-2 hour λ/Q value of $2.232E-4 \text{ sec/m}^3$
- Breathing rate equal to $3.47E-4 \text{ m}^3/\text{sec}$
- Iodine dose conversion factors from EPA Federal Guidance Report 11 committed effective dose equivalent (CEDE) for inhalation (Table D.8-1)
- Noble gas dose conversion factors shown in Table D.8-1

14.2.4.4 Summary of Calculated Doses

The following tabulation summarizes the two-hour TEDE doses at the exclusion distance, consistent with a receptor on the plume centerline.

	TEDE Dose
Steam Generator Tube Rupture With Pre-Accident Iodine Spike	1.3 rem
10 CFR 50.67 Guidelines	25 rem
Steam Generator Tube Rupture With Accident-Initiated Iodine Spike	0.8 rem
10% of 10 CFR 50.67 Guidelines	2.5 rem

It is concluded that the complete failure of a steam generator tube preceded by a long-term leak history prior to its failure would present no undue hazard to public health and safety.

In 1992, Westinghouse completed a study (Reference 3) addressing the radiological consequences of steam generator tube bundle uncover coincident with a steam generator tube rupture, following a reactor trip. The results of the study indicated that there was little effect on radiological release due to tube uncover, and that the 10 CFR 50.67 limits continued to be met. It was concluded that steam generator tube uncover did not have significant impact on the accident analysis for steam generator tube rupture, and that no modifications to the analysis were necessary. A Westinghouse letter (Reference 4) transmitted the Westinghouse and NRC resolution stating that the issue was closed.

14.2.4.5 **Recovery Procedure**

The immediately apparent symptoms of a tube rupture accident such as falling pressurizer pressure and level, and increased charging pump flow are also symptoms of small steam-line breaks and LOCAs. It is therefore important for the operator to determine that the accident is a rupture of a steam generator tube to carry out the correct recovery procedure. The steam generator tube rupture is uniquely identified by high condenser air ejector radiation, high steam generator blowdown radiation, high steam line radiation, and decreased feedwater flow to the ruptured steam generator before the reactor trip. When the operators observe these indications, they enter the steam generator tube rupture recovery procedure.

The operators perform the following steps, which lead to isolation of the ruptured steam generator and termination of the leak.

1. Identify the ruptured steam generator by observing a higher level or higher radiation levels in one steam generator.
2. Isolate the ruptured steam generator by closing the main steam isolation valve (MSIV) and other smaller valves.
3. Stop auxiliary feedwater flow to the ruptured steam generator when the narrow range level returns to scale.
4. Control auxiliary feedwater flow in the intact steam generator so that the narrow range level remains on scale.
5. If off-site power is available, use condenser steam dumps to cool the RCS to enable RCS pressure to be reduced below the pressure of the ruptured steam generator. If off-site power is not available, atmospheric steam dumps or steam generator power-operated relief valves are used.

6. If off-site power is available, depressurize the RCS to below the pressure of the ruptured steam generator using pressurizer spray valves. If off-site power is not available, the reactor coolant pumps would not be running, making spray unavailable. In this case pressurizer power-operated relief valves or auxiliary spray are used for the depressurization.
7. Stop SI pumps.
8. Cool the RCS to cold shutdown. The ruptured steam generator is depressurized by either backfill into the RCS, blowdown into the Steam Generator Blowdown Treatment System, or steam dump into the condenser or atmosphere.

After the Residual Heat Removal System (RHR) is in operation, the condensate accumulated in the secondary system can be sampled and processed.

There is ample time to carry out the above recovery procedure such that isolation of the ruptured steam generator is established before water level rises into the main steam lines. The available time scale is improved by the termination of auxiliary feedwater flow to the ruptured steam generator. Normal operator vigilance therefore assures that excessive water level is not attained.

14.2.5 Steam Line Break

14.2.5.1 Accident Description

A steam line break transient would result in an uncontrolled increase in steam flow release from the steam generators, with the flow decreasing as the steam pressure drops. This steam flow release increases the heat removal from the RCS, which decreases the RCS temperature and pressure. With the existence of a negative MTC, the RCS cooldown results in a positive reactivity insertion, and consequently a reduction of the core shutdown margin. If the most reactive RCCA is assumed stuck in its fully withdrawn position after reactor trip, the possibility is increased that the core will become critical and return to power. A return to power following a steam line break is a concern with the high-power peaking factors that may exist when the most reactive RCCA is stuck in its fully withdrawn position. Following a steam line break, the core is ultimately shut down by the boric acid injected into the RCS by the emergency core cooling system (SI).

The steam line break core response analysis was performed to demonstrate that there is no consequential damage to the primary system and that the core remains in place and intact following a steam line break event. Assuming the most reactive RCCA is stuck in its fully withdrawn position, and applying the most limiting single failure of one SI train, steam line break core response cases were examined with and without off-site power available. Although DNB and fuel cladding damage are not necessarily unacceptable consequences of a steam line break transient, the analysis described below demonstrates that there is no consequential damage to the primary system, and that the core remains in place and intact, by showing that the DNB design basis is satisfied following a steam line break.

The steam line break containment integrity analysis was performed to demonstrate that the energy release to containment does not cause the failure of the containment structure following a steam line break event. Assuming a stuck RCCA and assuming a single failure in the engineered safety features or other system, structure or component important to safety, steam line break containment integrity cases were examined with and without off-site power available. The analysis described below demonstrates that the containment structure does not fail by showing that the containment pressure and temperature basis is satisfied following a steam line break.

The steam line break radiological consequences analysis was performed to demonstrate that the activity releases are within the 10 CFR 50.67 guidelines following a steam line break outside containment event. The analysis described below demonstrates acceptable radiological consequences by showing the radiological consequences basis is satisfied following a steam line break.

The systems and components that provide the necessary protection against a steam line break are listed as follows.

- SIS actuation by any of the following:
 - Two-out-of-three pressurizer pressure channels with low signals
 - Two-out-of-three steam line pressure channels on either loop with lo-lo signals
 - Two-out-of-three containment pressure channels with high signals
- The overpower reactor trips (neutron flux and ΔT) and the reactor trip occurring from the receipt of the SI signal.
- Redundant isolation of the main feedwater lines; sustained high feedwater flow would cause additional cooldown. In addition to normal control action that isolates main feedwater following a reactor trip, a SI signal will rapidly close all feedwater control valves, trip the main feedwater pumps, and close the feedwater pump discharge valves.
- Closure of the MSIVs. These valves are designed to close within five seconds after receipt of any of the following:
 - An SI signal coincident with one-out-of-two steam flow channels on Loop A with a hi-hi signal (isolates Loop A)
 - An SI signal coincident with one-out-of-two steam flow channels on Loop B with a hi-hi signal (isolates Loop B)
 - An SI signal coincident with one-out-of-two steam flow channels on Loop A with a high signal AND two-out-of-four T_{avg} channels with lo-lo signals (isolates Loop A)
 - An SI signal coincident with one-out-of-two steam flow channels on Loop B with a high signal AND two-out-of-four T_{avg} channels with lo-lo signals (isolates Loop B)
 - Two-out-of-three containment pressure channels with hi-hi signals

The MSS conducts steam in 30-inch piping from each of the two steam generators within the reactor containment, through a swing-disc type isolation valve (MSIV) and a swing-disc type non-return check valve to the turbine stop and control valves. The isolation and non-return check valves are located outside of the containment, and an equalizing line near the turbine interconnects the two steam lines. The non-return check valves prevent reverse flow of steam. Therefore, if a break occurs between a non-return check valve and a steam generator, only the affected steam generator would blow down. The steam generator blowdown from a steam line break located downstream of a non-return check valve would be terminated upon closure of both MSIVs.

Each main steam line contains a 16-inch diameter venturi-type flow restrictor located upstream of the MSIV and inside containment. These flow restrictors are used to measure the steam flow from each steam generator. Additional flow restrictors that are an integral part of the steam generator outlet nozzles serve to limit the steam release rate during a steam line break transient. The nozzle flow restrictors limit the effective maximum steam line break size to 1.4 ft² per steam generator.

14.2.5.2 Method of Analysis – Core Response

The analysis of the steam line break transient has been performed to demonstrate that the DNB design basis is satisfied. This is accomplished by showing that the calculated minimum DNBR is greater than the safety analysis limit DNBR of 1.472 (W-3 low pressure DNB correlation limit). The overall analysis process is described as follows.

Using the RETRAN code (Reference 11), transient values of key plant parameters identified as statepoints (core average heat flux, core pressure, core inlet temperature, RCS flow rate, and core boron concentration) were calculated first. Next, the advanced nodal code (ANC) core design code (Reference 12) was used to:

- Evaluate the nuclear response to the RCS cooldown so as to justify the RETRAN transient prediction of the average core power/reactivity
- Determine the peaking factors associated with the return to power in the region of the stuck RCCA

Finally, using the RETRAN-calculated statepoints and the ANC-calculated peaking factors, the detailed thermal and hydraulic computer code VIPRE (Reference 14) was used to calculate the minimum DNBR based on the W-3 DNB correlation.

The following assumptions were made in the analysis of the MSLB:

1. A hypothetical double-ended rupture (DER) of a main steam line was postulated at HZP/hot shutdown conditions. The maximum break size is effectively limited to the flow area of the steam generator outlet nozzle flow restrictors (1.4 ft² per steam generator). The assumed conditions correspond to a subcritical reactor, an initial vessel average temperature at the

no-load value of 547°F, and no core decay heat. These conditions are conservative for a steam line break transient because the resultant RCS cooldown does not have to remove any latent heat. Also, the steam generator water inventory is greatest at no-load conditions, which increases the capability for cooling the RCS.

2. Two DER cases were considered: one with offsite power and one with a loss-of-off-site-power. The difference being that both RCPs begin coasting down three seconds after the steam line break initiation for the case without off-site power. Note that steam line break transients associated with the inadvertent opening of a steam dump or relief valve were not analyzed because the resultant RCS cooldown, and thus the minimum DNBR, would be less limiting compared to the DER cases.
3. Perfect moisture separation within the steam generators was conservatively assumed.
4. An end-of-life shutdown margin of 1.3 percent $\Delta k/k$ corresponding to no-load, equilibrium xenon conditions, with the most reactive RCCA stuck in its fully withdrawn position was assumed. The stuck RCCA was assumed to be in the core location exposed to the greatest cooldown; that is, related to the faulted loop. The reactivity feedback model included a positive moderator density coefficient (MDC) corresponding to an end-of-life rodded core with the most reactive RCCA in its fully withdrawn position. The variation of the MDC due to changes in temperature and pressure was accounted for in the model. Figure 14.2.5-1 presents the k_{eff} versus temperature relationship at 1050 psia corresponding to the assumed negative MTC plus the Doppler temperature feedback effect.

The reactivity and power predicted by RETRAN were compared to those predicted by the ANC core design code. The ANC core analysis considered the following:

- Doppler reactivity feedback from the high fuel temperature near the stuck RCCA
- Moderator feedback from the high water enthalpy near the stuck RCCA
- Power redistribution effects
- Non-uniform core inlet temperature effects

The ANC core analysis confirmed that the RETRAN-predicted reactivity is acceptable.

5. Assuming no frictional losses, the Moody critical flow curve (Reference 5) was applied to conservatively maximize the break flow rate.
6. The non-return check valves were neglected to conservatively allow blowdown from both steam generators up to the time of MSIV closure. This assumption was made along with not crediting containment protection signals, to assure that any postulated break location or single failure assumption, is bounded by a single analysis.

7. The closure of the MSIV of the intact/unfaulted loop was conservatively modeled to be complete at 7.6 seconds after receipt of an SI signal due to the coincidence of a hi-hi steam flow rate (~200 percent of nominal full-power steam flow) signal and a lo-lo steam line pressure (495 psia) signal from the same loop.
8. The SI pumps were assumed to provide flow to the RCS at 25 seconds after receipt of a SI signal for the case with offsite power available, and at 30 seconds after a SI signal for the case without offsite power available. These delays account for signal processing and pump startup delays, and, as applicable, diesel generator startup time.
9. The minimum capability for the injection of highly concentrated boric acid solution, corresponding to the most restrictive single active failure in the SIS, was assumed. The assumed SI flow (see Figure 14.2.5-2) corresponds to the operation of one high-head SI pump. Boric acid solution from the refueling water storage tank (RWST), with a minimum concentration of 2400 ppm and a minimum temperature of 40°F, was the assumed source of the SI flow. The SI lines downstream of the RWST were assumed to initially contain unborated water to conservatively maximize the time it takes to deliver the highly concentrated RWST boric acid solution to the reactor coolant loops.
10. The SI accumulator tanks (one per loop) provide a passive injection of up to 2500 ft³ of borated water into the RCS. The accumulators were assumed to have a minimum boron concentration of 1850 ppm, a minimum temperature of 40°F, and an initial gas pressure of 714.7 psia.
11. Main feedwater flow equal to the nominal (100 percent power) value was assumed to initiate coincident with the postulated break, and was maintained until feedwater isolation occurs. The feedwater isolation was assumed to be complete at 85.7 seconds after the steam line pressure in the faulted loop reaches the lo-lo setpoint signal that generates the SI signal.
12. A minimum SGTP level of 0 percent was assumed to maximize the cooldown of the RCS.
13. Maximum (1200 gpm) auxiliary feedwater at a minimum temperature of 35°F was assumed to initiate coincident with the postulated break to maximize the cooldown of the RCS.

14.2.5.3 Results – Core Response

The results of the statepoint evaluation demonstrate that both cases analyzed meet the applicable DNBR acceptance criterion. The most limiting case is the case in which offsite power was assumed to be available. The time sequence of events for each case is presented in Table 14.2.5-1.

14.2.5.4 Double-Ended Rupture With Off-Site Power Available

Figure 14.2.5-3 through Figure 14.2.5-10 show the steam pressure, steam flow, pressurizer pressure, pressurizer water volume, reactor vessel inlet temperature, core heat flux, core boron concentration, and core reactivity following a double-ended rupture of a main steam line at initial no-load conditions with offsite power available (full reactor coolant flow). The effective break

size was limited to 1.4 ft² per steam generator by the flow area of the steam generator outlet nozzles, and both steam generators were assumed to discharge through the break until steam line isolation had occurred. It is important to note that at approximately 102 seconds the faulted loop (Loop 1) break (outlet nozzle) mass flow rate spikes (see Figure 14.2.5-4) as a result of the upper steam generator node becoming water-solid. This spike occurs after the peak heat flux is reached and does not invalidate the results.

14.2.5.5 Double-Ended Rupture Without Off-Site Power Available

Figure 14.2.5-11 through Figure 14.2.5-18 show the steam pressure, steam flow, pressurizer pressure, pressurizer water volume, reactor vessel inlet temperature, core heat flux, core boron concentration, and core reactivity following a double-ended rupture of a main steam line at initial no-load conditions with a loss-of-off-site-power (RCPs begin coasting down three seconds after break initiation). The effective break size was limited to 1.4 ft² per steam generator by the flow area of the steam generator outlet nozzles, and both steam generators were assumed to discharge through the break until steam line isolation had occurred.

14.2.5.6 Conclusions – Core Response

The MSLB transient was conservatively analyzed with respect to the reactor core response. Key analysis assumptions were made to conservatively maximize the cooldown of the RCS, so as to maximize the positive reactivity insertion, and thus maximize the peak return to power. Other key assumptions include: end-of-life shutdown margin with the most-reactive RCCA stuck in its fully withdrawn position, maximum delays in actuating engineered safeguard features such as SI, main steam isolation and feedwater isolation, and minimum SI flow with a minimum boron concentration.

A DNBR statepoint analysis was performed for two DER cases: one with offsite power and one with a loss-of-offsite power. The case with offsite power available—that is, the case with full reactor coolant flow—was found to be the limiting case. The minimum DNBR for each case was determined to be greater than the DNBR safety analysis limit, and thus the DNBR design basis is met.

14.2.5.7 Method of Analysis - Containment Integrity

There are four major factors that influence the release of mass and energy following a steam-line break. These are the initial steam generator fluid inventory, primary to secondary heat transfer, protective system operation, and the state of the secondary fluid blowdown. The following is a list of those plant variables that determine the influence of each of these factors.

- Plant Power Level
- Main Feedwater System Design
- Auxiliary Feedwater System Design
- Break Type, Area, Location

- Availability of Offsite Power
- Steam Generator Design
- Safety System Failures
- SG Reverse Heat Transfer and RCS Metal Heat Capacity

All of these variables are considered in the analyses and are conservatively selected based on Kewaunee plant design.

Steam-line break analysis cases are described based on a specific set of five parameters in the following manner:

1. Power Level: 0, 30, 70, and 102 percent for the rated power level.
2. Break Size: 0.1ft², 0.5ft², 0.8ft², 1.1ft², and 1.4ft²
3. Single Failures: There are three single failures which are:
 - a. One Feedwater (FW) Regulating Valve fails to isolate. This is denoted as R.
 - b. One MSIV fails to isolate. This is denoted as M.
 - c. One Containment Safeguards Train (one containment safeguard train is: one internal containment spray train and two containment fan cooler units) fails to activate. This is denoted as N.
4. Off-Site Power: Cases with and without the availability of off-site power are considered.
5. Entrainment: The quality of steam exiting the break is explicitly modeled and is dependent on break size and power level.

Based on the above parameters, steam-line break analysis cases are designated as follows:

- Break Size (Units of ft²)
- Single Failure
 - R - FW Reg Valve Failure
 - M - MSIV Failure
 - N - Containment Safeguards System Failure
- Off-Site Power
 - Y - Yes
 - N - No
- Entrainment
 - Y - Yes

- Power Level

0–0 percent

3–30 percent

7–70 percent

2–102 percent

For identification purposes, the cases are represented by a six number/letter identification tag. For example:

14NYY3 represents the steam line break case with:

14 = 1.4 ft² break

N = single active failure is one containment safeguards train

Y = off-site power is available

Y = entrainment is modeled

3 = initial power level is 30 percent

Further descriptions of the methods for steam-line break analysis follow:

1. The main feedwater flow is calculated using the following assumptions:
 - a. The feedwater pumps are running at full speed at the start of the transient and are tripped off on the SI signal. A conservative flow coastdown is modeled.
 - b. The condensate pumps are running at full speed throughout the transient.
 - c. The regulating valve for the unfaulted Loop remains at its initial position until the time at which it strokes to its fully-closed position at a rate of 5%/sec following an isolation signal. At that time, the valve is closed instantaneously.
 - d. The behavior of the regulating valve for the faulted loop is assumed to begin opening at $t = 0.0$ sec at an 8%/sec rate until the time the isolation signal occurs. It is held at that position until the time at which it strokes to its fully-closed position at a rate of 5%/sec following the isolation signal. At that time, the valve is closed instantaneously. For cases with a regulating valve failure, isolation is produced by closure of the FW isolation valve. The assumption used for the isolation valve is that it begins to close, at the time of the isolation signal, from full-open at a rate of 1.11%/sec. The initial opening of the regulating valve and the instantaneous FW isolation valve closure at the end of the stroke time are the same as for the case without a regulating valve closure failure.
2. The auxiliary feedwater (AFW) flow split between the two SGs is modeled. The AFW is initiated, prior to the time for the activation signal, at full capacity and using a conservatively high enthalpy. All three AFW pumps are assumed to be operating.

3. The core physics parameters are based on a bounding set corresponding to end-of-cycle conditions and minimum Core Operating Limit Report (COLR) shutdown requirements. The scram worth includes having the most reactive rod stuck out.
4. The dynamic reactor coolant pump model is used, which includes the gravity head and pump heat effects.
5. Conservative setpoints and time delays are used throughout.
6. No credit is taken for charging flow.
7. No credit is taken for SG tube plugging.
8. The following considerations are made in modeling the steam lines.
 - a. The pressure balancing line is modeled to allow communication between the steam lines in an unrestricted manner.
 - b. Main steam isolation for the unfaulted loop is assumed to occur instantaneously at the time required for the non-return check valve to close in the faulted loop, which is conservatively set to 5 seconds after the break occurs.
 - c. MSIV failure is modeled as a failure of the non-return check valve in the faulted loop. Steam flow from the unfaulted loop continues until the MSIV in the unfaulted main steam line closes. A closure assumption of 5 seconds is used for the MSIV. The time from the event initiation until MSIV closure signal receipt, plus signal instrumentation delays as applicable to the accident sequence analyzed, is added to the 5 second MSIV closure time assumption. At the time of the MSIV closure, the entire faulted and unfaulted loop steam lines from the MSIV to the turbine and the pressure balancing line are added to the total fluid mass and energy input to containment.
9. Entrainment analysis methods are used to obtain the time dependent quality of the faulted steam-line break flow which is power level and break size dependent. The quality of the unfaulted steam line break flow is conservatively assumed to be 1.0.
10. The turbine is tripped at $t = 0.0$ seconds for 0 percent power cases, and prior to or at the actual time of reactor trip for at power cases. These are conservative assumptions that maximize the available steam for blowdown.
11. A constant containment back pressure of 14.7 psia is conservatively assumed in all cases.
12. A conservatively high RCS flow rate is assumed.
13. Steam generator fluid inventory is maximized. Initial steam generator water level is 44 percent NRL plus uncertainties that depend on power level.

14.2.5.8 Results – Containment Integrity

Containment pressure and temperature responses for the limiting containment response steam line break analysis cases are presented in Figure 14.2.5-21 and Figure 14.2.5-22. The table below shows the peak calculated containment pressure and temperature for various MSLB cases. All cases analyzed result in a maximum containment pressure that is less than 46 psig and a containment vessel shell temperature that is less than 268°F. In addition, the limiting containment temperature and pressure profiles have been evaluated and shown to be less than the environmental qualification limits.

Peak Containment Pressures and Temperatures For MSLB Cases

Description	Peak Press (psig)	Peak Temp (°F)
0.1 ft ² break at 0% power	18.33	214.3
0.5 ft ² break at 0% power	35.71	251.1
0.8 ft ² break at 0% power	43.06	263.0
1.1 ft ² break at 0% power	45.16	265.8
1.4 ft ² break at 0% power	45.68	266.6
1.4 ft ² break at 30% power	41.87	260.9
1.4 ft ² break at 70% power	41.93	260.9
1.4 ft ² break at 102% power	43.33	263.4

14.2.5.9 Method of Analysis – Radiological Consequences

The steam line break outside containment results in the release to the atmosphere of the activity initially in the faulted steam generator. Activity contained in leakage from the RCS into the secondary side of the faulted steam generator is released as well, until the RCS is cooled sufficiently. Steam release from the unaffected steam generator to the atmosphere releases a portion of the activity initially in that steam generator as well as a portion of the activity transferred via primary to secondary leakage.

In assessing the consequences of the assumed accident, the amount of activity released to the atmosphere is based on the following:

1. The noble gas activity concentration in the reactor coolant is assumed to arise from continuous operation with one percent defective fuel clad (see Table D.4-1).

2. The maximum iodine activity in the reactor coolant is assumed to be 1.0 $\mu\text{Ci/gm}$ dose equivalent (DE) I-131. The analysis considers (separately) pre-accident and accident-initiated iodine spikes. The pre-accident iodine spike is assumed to have raised the RCS iodine concentration to 60 $\mu\text{Ci/gm}$ DE I-131 prior to the initiation of the tube rupture. The accident-initiated iodine spike is assumed to increase the rate iodine is released from the fuel to the coolant to a value of 500 times the release rate corresponding to a maximum reactor coolant iodine concentration of 1.0 $\mu\text{Ci/gm}$ DE I-131.
3. The iodine concentration in the secondary coolant at the time of the tube rupture is assumed to be 0.1 $\mu\text{Ci/gm}$ DE I-131.
4. All activity initially in the faulted steam generator is released in a short period after the start of the event. All activity transferred to the faulted steam generator via primary to secondary leakage is released immediately.
5. The amount of primary-to-secondary steam generator tube leakage is assumed to be 150 gpd per steam generator.
6. In the intact steam generator an iodine partition factor of 0.01 (curies iodine/gm steam)/(curies iodine/gm water) is used.
7. All noble gas activity carried over to the secondary side through steam generator tube leakage is assumed to be immediately released to the outside atmosphere.
8. A 0–2 hour λ/Q value of $2.232\text{E}-4 \text{ sec/m}^3$.
9. Breathing rate equal to $3.47\text{E}-4 \text{ m}^3/\text{sec}$.
10. Iodine dose conversion factors from EPA Federal Guidance Report 11 committed effective dose equivalent (CEDE) for inhalation (Table D.8-1).
11. Noble gas dose conversion factors shown in Table D.8-1.

14.2.5.10 Results – Radiological Consequences

The following tabulation summarizes the two-hour TEDE doses at the exclusion distance.

	TEDE Dose
Steam Line Break With Pre-Accident Iodine Spike	0.03 rem
10 CFR 50.67 Guidelines	25 rem
Steam Line Break With Accident –Initiated Iodine Spike	0.06 rem
10% of 10 CFR 50.67 Guidelines	2.5 rem

14.2.5.11 Conclusions

The analyses have shown that the MSLB acceptance criteria are satisfied.

Although DNB and possible clad perforation are not precluded in the acceptance criteria, the safety analysis has demonstrated that DNB does not occur, provided that core $F_{\Delta H}$ under steam line break conditions is ≤ 8.00 .

The peak pressure for the limiting containment response cases does not exceed 46 psig. The limiting temperature profile also does not create an environmental qualification concern for equipment in containment.

The consequences of these postulated accidents are well below the guidelines of 10 CFR 50.67 and it is concluded that the rupture of a steam line would present no undue hazard to public health and safety.

14.2.6 Rupture of a Control Rod Drive Mechanism Housing (RCCA Ejection)

14.2.6.1 Accident Description

This accident is the result of the extremely unlikely mechanical failure of a control rod drive mechanism pressure housing such that the RCS pressure would eject the RCCA and drive shaft. The consequences of this mechanical failure, in addition to being a minor LOCA, may also be a rapid reactivity insertion together with an adverse core power distribution, possibly leading to localized fuel rod damage.

Certain features in Westinghouse PWRs are intended to preclude the possibility of a rod ejection accident, or to limit the consequences if the accident were to occur. These include a sound, conservative mechanical design of the rod housings, along with a thorough quality control (testing) program during assembly, and a nuclear design that lessens the potential ejection worth of control rod assemblies and minimizes the number of assemblies inserted at high power levels.

The mechanical design is discussed in Chapter 3 of the USAR. A failure of the full-length control rod mechanism housing, sufficient to allow a control rod to be rapidly ejected from the core, is not considered credible for the following reasons:

- Each control rod drive mechanism housing is completely assembled and shop-tested at 3125 psi.
- The mechanism housings are individually hydrotested as they are installed on the reactor vessel head to the head adapters, and checked during the hydrotest of the completed RCS.
- Stress levels in the mechanism are not affected by system transients at power, or by the thermal movement of the coolant loops. Movements induced by the design earthquake can be accepted within the allowable primary working stress range specified by the American Society of Mechanical Engineers (ASME) Code, Section III, for Class A components.

- The latch mechanism housing and rod travel housing are each a single length of forged Type 316 stainless steel. This material exhibits excellent notch toughness at all temperatures that are encountered.

A significant margin of strength in the elastic range, together with the large energy absorption capability in the plastic range, gives additional assurance that gross failure of the housing will not occur. The reactor vessel head and CRDMs utilize butt welds to attach the rod travel housing to the control rod drive mechanism. Regulations require periodic inspections of those (and other) welds.

Even if a rupture of the control rod mechanism housing is postulated, the operation of a chemical shim plant is such that the severity of an ejected rod is inherently limited. In general, the reactor is operated with control rods inserted only far enough to permit load follow. Reactivity changes caused by core depletion and xenon transients are compensated by boron changes. Further, the location and groupings of control rod banks are selected during the core nuclear design to lessen the severity of an ejected control rod assembly. Therefore, should an RCCA be ejected from the reactor vessel during normal operation, there probably would be no reactivity excursion since most of the control rods are fully withdrawn from the core, or a minor reactivity excursion if an inserted RCCA is ejected from its normal position.

However, it may occasionally be desirable to operate with larger control rod insertions. For this reason, rod insertion limits are defined in the Technical Specifications as a function of power level. Operation with the RCCAs above this limit guarantees adequate shutdown capability and acceptable power distribution. The position of all RCCAs is continuously indicated in the control room. An alarm will occur if a bank of RCCAs approaches its insertion limit or if one RCCA deviates from its bank. There are low and lo-lo level insertion monitors with visual and audio signals. Operating instructions require boration when receiving either alarm.

If an RCCA ejection accident were to occur, a fuel rod thermal transient that could cause a DNB may occur together with limited fuel damage. The amount of fuel damage that can result from such an accident will be governed mainly by the worth of the ejected RCCA and the power distribution attained with the remaining control rod pattern. The transient is limited by the Doppler reactivity effects of the increase in fuel temperature and is terminated by reactor trip actuated by neutron flux signals. It is terminated before conditions are reached that can result in damage to the reactor coolant pressure boundary, or significant disturbances in the core, its support structures or other reactor pressure vessel internals that would impair the capability to cool the core.

The neutron flux response to a continuous reactivity insertion is characterized by a very fast flux increase terminated by the reactivity feedback effect of the negative DPC. This self limitation of the power burst is of primary importance since it limits the power to a tolerable level during the

delay time for protective action. Should an RCCA ejection accident occur, the following automatic features of the RPS are available to terminate the transient:

- The source-range high neutron flux reactor trip is actuated when either of two independent source-range channels indicates a neutron flux level above a pre-selected manually adjustable setpoint. This trip function may be manually bypassed when either intermediate-range flux channel indicates a flux level above a specified level. It is automatically reinstated when both intermediate-range channels indicate a flux level below a specified level.
- The intermediate-range high neutron flux reactor trip is actuated when either of two independent intermediate-range channels indicates a flux level above a pre-selected manually adjustable setpoint. This trip function may be manually bypassed when two-out-of-four power-range channels give readings above approximately 10 percent of full power and is automatically reinstated when three-out-of-four channels indicate a power below this value.
- The power-range high neutron flux reactor trip (low setting) is actuated when two-out-of-four power-range channels indicate a power level above approximately 25 percent of full power. This trip function may be manually bypassed when two-out-of-four power-range channels indicate a power level above approximately 10 percent of full power and is automatically reinstated when three-out-of-four channels indicate a power level below this value.
- The power-range high neutron flux reactor trip (high setting) is actuated when two-out-of-four power-range channels indicate a power level above a preset setpoint (typically, 109 percent power). This trip function is always active when the reactor is at power.
- The high nuclear flux rate reactor trip is actuated when the positive rate of change of neutron flux on two-out-of-four nuclear power-range channels indicates a rate above the preset setpoint. This trip function is always active.

Comprehensive studies of the threshold of fuel failure and of the threshold of significant conversion of the fuel thermal energy to mechanical energy have been carried out as part of the SPERT project by the Idaho Nuclear Corporation (Reference 7). Extensive tests of UO₂ - Zirconium-clad fuel rods representative of those in PWR-type cores have demonstrated failure thresholds in the range of 240 to 257 cal/g. However, other rods of a slightly different design have exhibited failures as low as 225 cal/g. These results differ significantly from the TREAT (Reference 8) results, which indicated a failure threshold of 280 cal/g. Limited results have indicated that this threshold decreases by about 10 percent with fuel burnup. The clad failure mechanism appears to be melting for zero burnup rods and brittle fracture for irradiated rods. Also important is the conversion ratio of thermal to mechanical energy. This ratio becomes marginally detectable above 300 cal/g for unirradiated rods and 200 cal/g for irradiated rods; catastrophic failure, (large fuel dispersal, large pressure rise) even for irradiated rods, does not occur below 300 cal/g.

The ultimate acceptance criteria for this event is that any consequential damage to either the core or the RCS must not prevent long-term core cooling, and that any off-site dose consequences

must be < 25 percent of 10 CFR 50.67. To demonstrate compliance with these requirements, it is sufficient to show that the RCS pressure boundary remains intact, and that no fuel dispersal in the coolant, gross lattice distortions, or severe shock waves will occur in the core. Therefore, the following acceptance criteria are applied to the RCCA ejection accident:

- Maximum average fuel pellet enthalpy at the hot spot must remain below 200 cal/g (360 Btu/lbm).
- Peak RCS pressure must remain below that which would cause the stresses in the RCS to exceed the faulted condition stress limits.
- Maximum fuel melting must be limited to the innermost 10 percent of the fuel pellet at the hot spot, independent of the above pellet enthalpy limit.

14.2.6.2 Method of Analysis

The calculation of the RCCA ejection transient is performed in two stages: a neutron kinetic analysis and a hot-spot fuel heat transfer analysis. The spatial neutron kinetics code TWINKLE (Reference 13) is used in a 1-D axial kinetics model to calculate the core nuclear power including the various total core feedback effects; that is, Doppler reactivity and moderator reactivity. The average core nuclear power is multiplied by the post-ejection hot-channel factor, and the fuel enthalpy and temperature transients at the hot spot are calculated with the detailed fuel and cladding transient heat transfer computer code, FACTRAN (Reference 10). The power distribution calculated without feedback is pessimistically assumed to persist throughout the transient. Additional details of the methodology are provided in WCAP-7588 (Reference 15).

The overpressurization of the RCS and number of rods in DNB, as a result of a postulated ejected rod, have both been analyzed on a generic basis for Westinghouse PWRs as detailed in Reference 15.

If the safety limits for fuel damage are not exceeded, there is little likelihood of fuel dispersal into the coolant or a sudden pressure increase from thermal-to-kinetic energy conversion. The pressure surge for this analysis can, therefore, be calculated on the basis of conventional heat transfer from the fuel and prompt heat generation in the coolant.

A detailed calculation of the pressure surge for an ejection worth of one dollar at beginning of life, HFP, indicates that the peak pressure does not exceed that which would cause stresses in the RCS to exceed their faulted condition stress limits. Since the severity of the KNPP analysis does not exceed this worst-case analysis, the RCCA ejection accident will not result in an excessive pressure rise or further damage to the RCS.

Reference 15 also documents a detailed three-dimensional THINC-III calculation, which demonstrates an upper limit to the number of rods-in-DNB for the RCCA ejection accident as 10 percent. Since the severity of the KNPP analysis does not exceed this worst-case analysis, the maximum number of rods in DNB following an RCCA ejection will be less than 10 percent, which is well within the 15 percent used in the radiological dose evaluation (see below). The most

limiting break size resulting from an RCCA ejection will not be sufficient to uncover the core or cause DNB at any later time. Since the maximum number of fuel rods experiencing DNB is limited to 15 percent, the fission product release will not exceed that associated with the guidelines of 10 CFR 50.67.

In calculating the nuclear power and hot-spot fuel rod transients following RCCA ejection, the following conservative assumptions are made:

1. The RTDP is not used for the RCCA ejection analysis. Instead, the STDP (maximum uncertainties in initial conditions) is employed. The analysis assumes uncertainties of 2.0 percent in nominal core power, 6.0°F in nominal vessel T_{avg} , and 50 psi in nominal pressurizer pressure. An additional 0.1-psi uncertainty has been determined to be negligible.
2. A minimum value for the delayed neutron fraction for BOC and EOC conditions is assumed, which increases the rate at which the nuclear power increases following RCCA ejection.
3. A minimum value of the Doppler power defect is assumed, which conservatively results in the maximum amount of energy deposited in the fuel following RCCA ejection. A minimum value of the moderator feedback is also assumed. A positive MTC is assumed for the BOC, zero-power case.
4. Maximum values of ejected RCCA worth and post-ejection total hot-channel factors are assumed for all cases considered. These parameters are calculated using standard nuclear design codes for the maximum allowed bank insertion at a given power level as determined by the rod insertion limits. No credit is taken for the flux flattening effects of reactivity feedback.
5. The start of rod motion occurs 0.65 seconds after the high neutron flux trip point is reached.

The analysis is performed to bound operation with Westinghouse 422V+ fuel and a maximum loop-to-loop SGTP imbalance of 10 percent.

14.2.6.3 Results

Figure 14.2.6-1 through Figure 14.2.6-8 present the nuclear power and hot-spot fuel rod thermal transients for the RCCA ejection cases analyzed. The transient results of the analysis are summarized in Table 14.2.6-1. A time sequence of events is provided in Table 14.2.6-2. For all cases, the maximum fuel pellet enthalpy remained below 200 cal/g. For the HFP cases, the peak hot-spot fuel centerline temperature reached the fuel melting temperature (4900°F at BOC and 4800°F at EOC). However, melting was restricted to less than 10 percent of the pellet. For the HZP cases, no fuel melting was predicted.

14.2.6.4 Conclusions

The analysis performed has demonstrated that, for the RCCA ejection event, the fuel thermal criteria are not exceeded. In addition, the peak pressure does not exceed that which would cause stresses to exceed the faulted condition stress limits. Also, the upper limit to the number of

rods-in-DNB is 15 percent, which ensures that off-site dose consequences are <25 percent of 10 CFR 50.67. Consequently, all applicable acceptance criteria are met.

14.2.6.5 Analysis – Radiological Consequences

As a result of the accident, fuel clad damage and a small amount of fuel melt are assumed to occur. Due to the pressure differential between the primary and secondary systems, radioactive reactor coolant is discharged from the primary into the secondary system. A portion of this radioactivity is released to the outside atmosphere through either the atmosphere relief valves or the main steam safety valves. Iodine activity is contained in the secondary coolant prior to the accident, and some of this activity is also released to the atmosphere as a result of steaming the steam generators following the accident. Finally, radioactive reactor coolant is discharged to the containment via the spill from the opening in the reactor vessel head. A portion of this radioactivity is released through containment leakage to the environment.

As a result of the rod ejection accident, less than 10 percent of the fuel rods in the core undergo DNB. In determining the off-site doses following rod ejection accident, it is conservatively assumed that 15 percent of the fuel rods in the core suffer sufficient damage in that all of their gap activity is released. In the rod ejection dose calculation, it is assumed that 10 percent of the core iodine and noble gas activity, and 12 percent of the core alkali metal activity, is contained in the gap. A small fraction of the fuel in the failed fuel rods is assumed to melt as a result of the rod ejection accident. This amounts to 0.375 percent of the core and the melting takes place in the centerline of the affected rods. Consistent with Regulatory Guide 1.183, one half of the iodine activity in the melted fuel is released when calculating release through the secondary system and one quarter of the iodine activity in the melted fuel is released when calculating release through containment. All of the noble gas and alkali metal activity in the melted fuel is assumed to be released.

A pre-existing iodine spike in the reactor coolant is assumed to have increased the primary coolant iodine concentration to 60 $\mu\text{Ci/gm}$ of dose equivalent I-131 prior to the rod ejection accident. The noble gas and alkali metal activity concentrations in the RCS at the time the accident occurs are based on operation with a fuel defect level of one percent. The iodine activity concentration of the secondary coolant at the time the rod ejection accident occurs is assumed to be 0.10 $\mu\text{Ci/gm}$ of dose equivalent I-131.

14.2.6.6 Results – Radiological Consequences

The following tabulation summarizes the two-hour TEDE doses at the exclusion distance taking into account both releases from the secondary system and the containment.

	TEDE Dose
Rod Ejection	0.4 rem
25% of 10 CFR 50.67 Guidelines	6.3 rem

14.2.6.7 Conclusions – Radiological Consequences

Even on the most pessimistic basis, the analyses indicated that the fuel and clad limits were not exceeded. It was concluded that there was no danger of sudden fuel dispersal into the coolant. The pressure surge was shown to be insufficient to exceed 2750 psia, and it was concluded that there was no danger of consequential damage to the primary coolant system. The off-site doses are well within the guidelines of 10 CFR 50.67.

14.2.7 Turbine Missile Damage to Spent Fuel Pool

14.2 References

1. Malinowski, D., M. J. Bell, E. R. Duhn, J. Locante, “Topical Report - Radiological Consequences of a Fuel Handling Accident,” WCAP 7518-L, June 1980 (Re-issued as WCAP-7828, December 1971)
2. Lamb, J. G., (NRC) to T. Coutu (NMC), transmitting the NRC SER for Amendment No. 166 to the Operating License, approving Implementation of Alternate Source Term, Letter No. K-03-040, March 17, 2003
3. WCAP-13132, “The Effect of Steam Generator Tube Bundle Uncovery on Radioiodine Release,” January 1992 (proprietary)
4. Letter WOG 93-066 from K. J. Voytell (WOG) to primary representatives (WPS), Transmittal of NRC Closure Letter on the Steam Generator Tube Rupture Uncovery Issue, March 31, 1993
5. Moody, F. J., “Maximum Flow Rate of a Single Component, Two-Phase Mixture,” transactions of the American Society of Mechanical Engineers, February 1965, p136
6. Burnett, T. W. T., “Reactor Protection System Diversity in Westinghouse Pressurized Water Reactor,” WCAP-7306, April 1969
7. Taxelius, T. G., ed. “Annual Report - Spert Project, October 1968, September 1969,” Idaho Nuclear Corporation TID-4500, June 1970
8. Liimatainen, R. C., and F. J. Testa, “Studies in TREAT of Zircaloy-2-Clad, UO₂ - Core Simulated Fuel Elements,” Argonne National Laboratory Chemical Engineering Division Semi-Annual Report, ANL-7225, January-June 1966
9. WCAP-7588, Revision 1-A, “An Evaluation of the Rod Ejection Accident in Westinghouse Pressurized Water Reactors Using Spatial Kinetics Methods,” January 1975
10. Hagrove, H. G., “FACTRAN – A FORTRAN IV Code for Thermal Transients in a UO₂ Fuel Rod,” WCAP-7908-A, December 1989
11. Huegel, D. S., et al., “RETRAN-02 Modeling and Qualification for Westinghouse Pressurized Water Reactor Non-LOCA Safety Analyses,” WCAP-14882-P-A, April 1999

12. Liu, Y. S., et al., “ANC: A Westinghouse Advanced Nodal Computer Code,” WCAP-10965-P-A, September 1986
13. Risher, D. H., Jr., and R. F. Barry, “TWINKLE – A Multi-Dimensional Neutron Kinetics Computer Code,” WCAP-7979-P-A (Proprietary) and WCAP-8028-A (Non-Proprietary), January 1975
14. Sung, Y. X., et al., “VIPRE-01 Modeling and Qualification for Pressurized Water Reactor Non-LOCA Thermal-Hydraulic Safety Analysis,” WCAP-14565-P-A (Proprietary), October 1999
15. Risher, D. H., “An Evaluation of the Rod Ejection Accident in Westinghouse Pressurized Water Reactors Using Spatial Kinetics Methods,” WCAP-7588, Revision 1-A, January 1975

Table 14.2.5-1
Steam Line Break Analysis Assumptions and Sequence Of Events

	Double-Ended Rupture With Offsite Power	Double-Ended Rupture Without Offsite Power
Steam Generator Model	54F	54F
Loss-of-Offsite Power	No	Yes
Time of Main Steam Line Rupture, seconds	0.01	0.01
Time Maximum AFW (600 gpm per loop) Initiated, seconds	0.01	0.01
Time Unfaulted Loop Steam Flow Reaches Hi-Hi Setpoint (~200% of Nominal), seconds	0.71	0.71
Time Steam Pressure Reaches Lo-Lo Setpoint (495 psia)		
• Faulted Loop, seconds	1.44	1.44
• Unfaulted Loop, seconds	2.01	2.01
Time of SI Signal Actuation Due to Coincidence of Hi-Hi Steam Flow and Lo-Lo Steam Pressure, seconds	2.72	2.72
Time of RCP Trip (Loss-of-Offsite-Power), seconds	N/A	3.00
Time of Steam Line Isolation (MSIV Closure) Due to SI Signal Actuation, seconds	10.22	10.22
Time Core Returns to Criticality, seconds	22.75	28.25
Time SI Pump Reaches Full Speed, seconds	27.72	32.72
Time Accumulator Tanks Begin Injecting into RCS, seconds	53.25	79.75
Time of Peak Heat Flux, seconds	56.50	132.75
Time of Minimum DNBR, seconds	56.25	~132.75
Time of Feedwater Isolation (Main Feedwater Isolation Valve Closure) Due to SI Signal Actuation, seconds	87.82	87.82
Peak Heat Flux, fraction of nominal	0.288	0.096
Minimum DNBR	2.29	Bounded by other case

Table 14.2.6-1
Assumptions and Results – RCCA Ejection

Beginning of Cycle	Full Power	Zero Power
Initial Power Level, %	102	0
Ejected RCCA Worth, % Δk	0.380	0.770
Delayed Neutron Fraction	0.0049	0.0049
Doppler Power Defect, % Δk	1.000	1.000
Feedback Reactivity Weighting	1.139	2.008
Trip Reactivity, % Δk	3.5	1.0
F_Q Before Ejection	2.5	N/A
F_Q After Ejection	4.2	11.0
Number of RCPs Operating	2	1
Maximum Fuel Pellet Enthalpy, cal/g	167.4	144.9
Maximum Fuel Melted, %	2.17	None
End of Cycle	Full Power	Zero Power
Initial Power Level, %	102	0
Ejected RCCA Worth, % Δk	0.370	0.930
Delayed Neutron Fraction	0.0043	0.0043
Doppler Power Defect, % Δk	0.900	0.900
Feedback Reactivity Weighting	1.316	2.144
Trip Reactivity, % Δk	3.5	1.0
F_Q Before Ejection	2.5	N/A
F_Q After Ejection	5.69	13.0
Number of RCPs Operating	2	1
Maximum Fuel Pellet Enthalpy, cal/g	170.3	161.6
Maximum Fuel Melted, %	5.89	None

Table 14.2.6-2
Sequence of Events – RCCA Ejection

Beginning of Cycle - Hot Zero Power	Time (seconds)
RCCA Ejection Occurs	0.000
High Neutron Flux Setpoint (Low Setting) is Reached	0.208
Peak Nuclear Power Occurs	0.252
Rods Begin to Fall Into the Core	0.858
Peak Cladding Average Temperature Occurs	2.134
Peak Heat Flux Occurs	2.150
Peak Fuel Average Temperature Occurs	2.273
Beginning of Cycle - Hot Full Power	Time (seconds)
RCCA Ejection Occurs	0.000
High Neutron Flux Setpoint (High Setting) is Reached	0.030
Peak Nuclear Power Occurs	0.135
Rods Begin to Fall Into the Core	0.680
Peak Fuel Average Temperature Occurs	1.904
Peak Cladding Average Temperature Occurs	2.024
Peak Heat Flux Occurs	2.040
End of Cycle - Hot Zero Power	Time (seconds)
RCCA Ejection Occurs	0.000
High Neutron Flux Setpoint (Low Setting) is Reached	0.147
Peak Nuclear Power Occurs	0.176
Rods Begin to Fall Into the Core	0.797
Peak Cladding Average Temperature Occurs	1.592
Peak Heat Flux Occurs	1.596
Peak Fuel Average Temperature Occurs	1.827

Table 14.2.6-2
Sequence of Events – RCCA Ejection

End of Cycle - Hot Full Power	Time (seconds)
RCCA Ejection Occurs	0.000
High Neutron Flux Setpoint (High Setting) is Reached	0.024
Peak Nuclear Power Occurs	0.129
Rods Begin to Fall Into the Core	0.674
Peak Fuel Average Temperature Occurs	1.902
Peak Cladding Average Temperature Occurs	2.035
Peak Heat Flux Occurs	2.050

Figure 14.2.4-1
Break Flow and SI Flow (Two Pumps) vs. Reactor Coolant Pressure

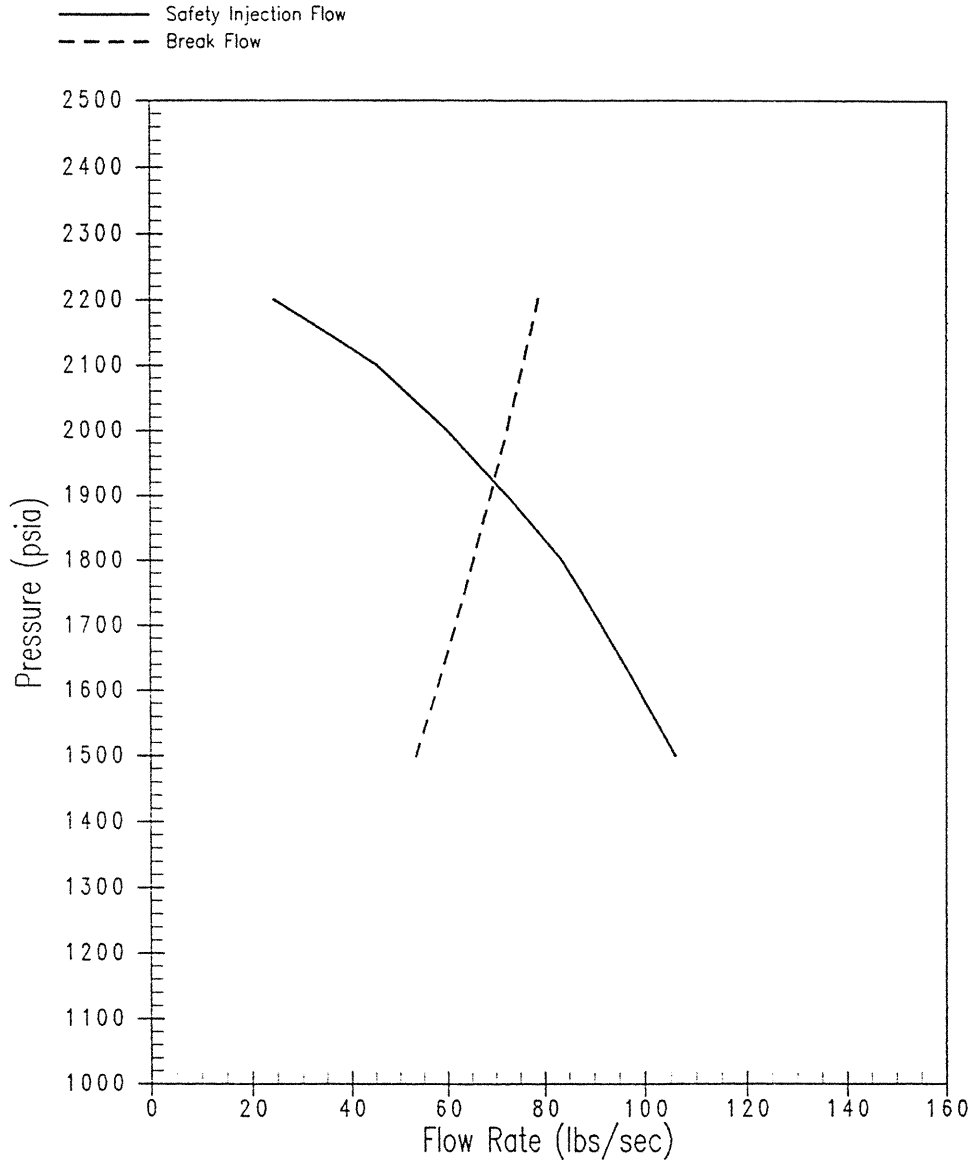


Figure 14.2.5-1
Variation of K_{eff} with Core Temperature

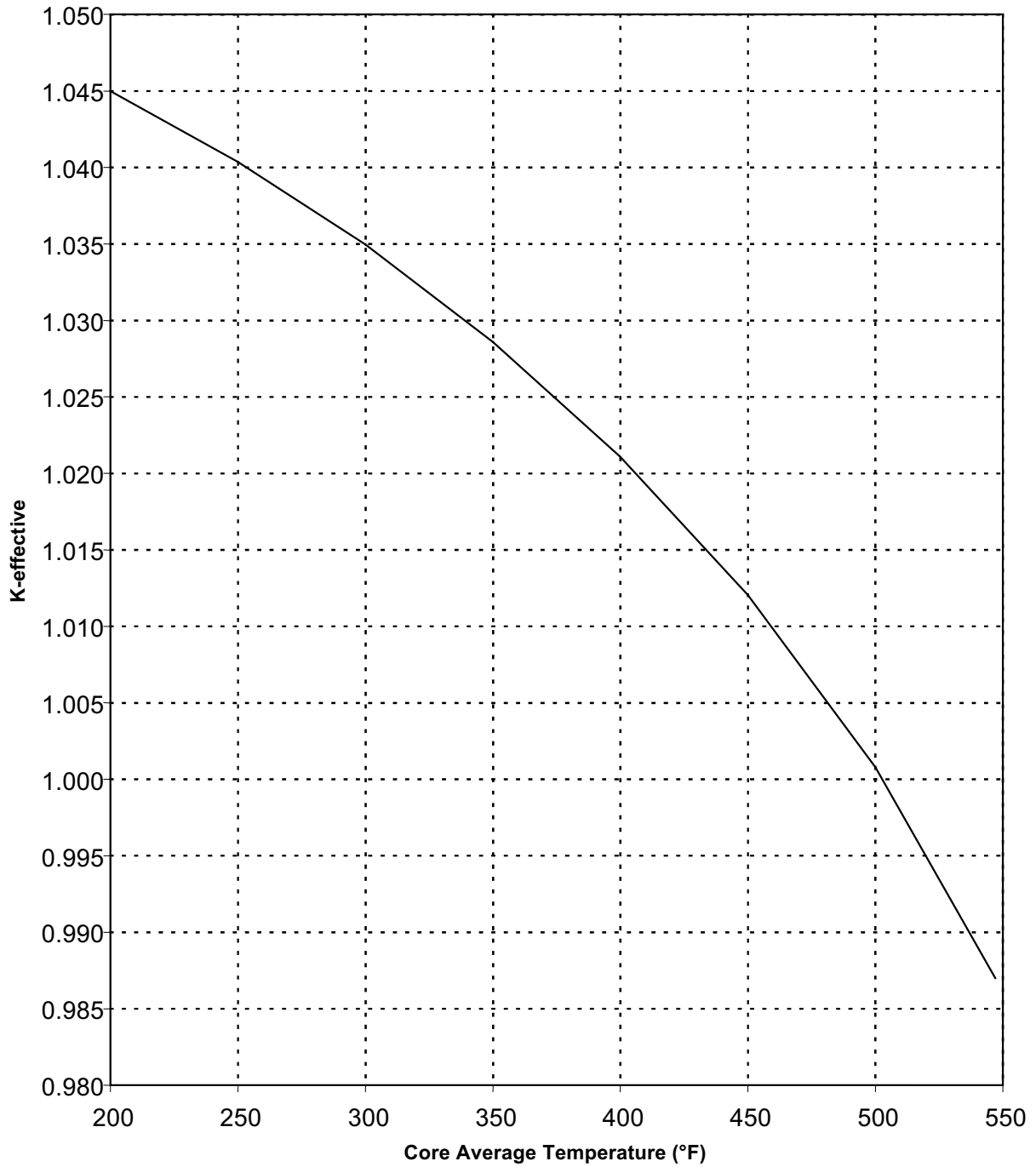


Figure 14.2.5-2
SI Curve

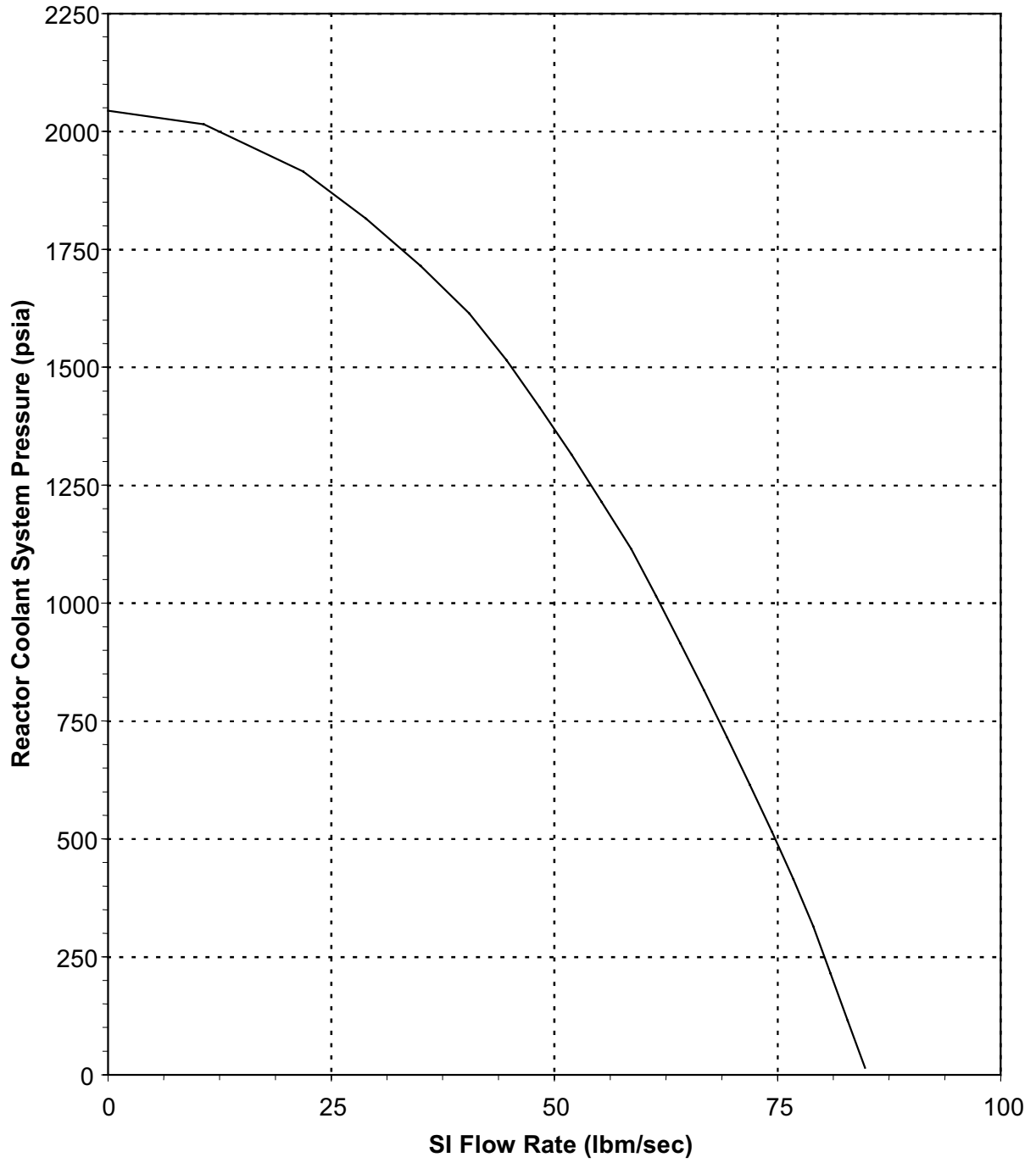


Figure 14.2.5-3
MSLB With Offsite Power
Steam Generator Steam Pressure vs. Time

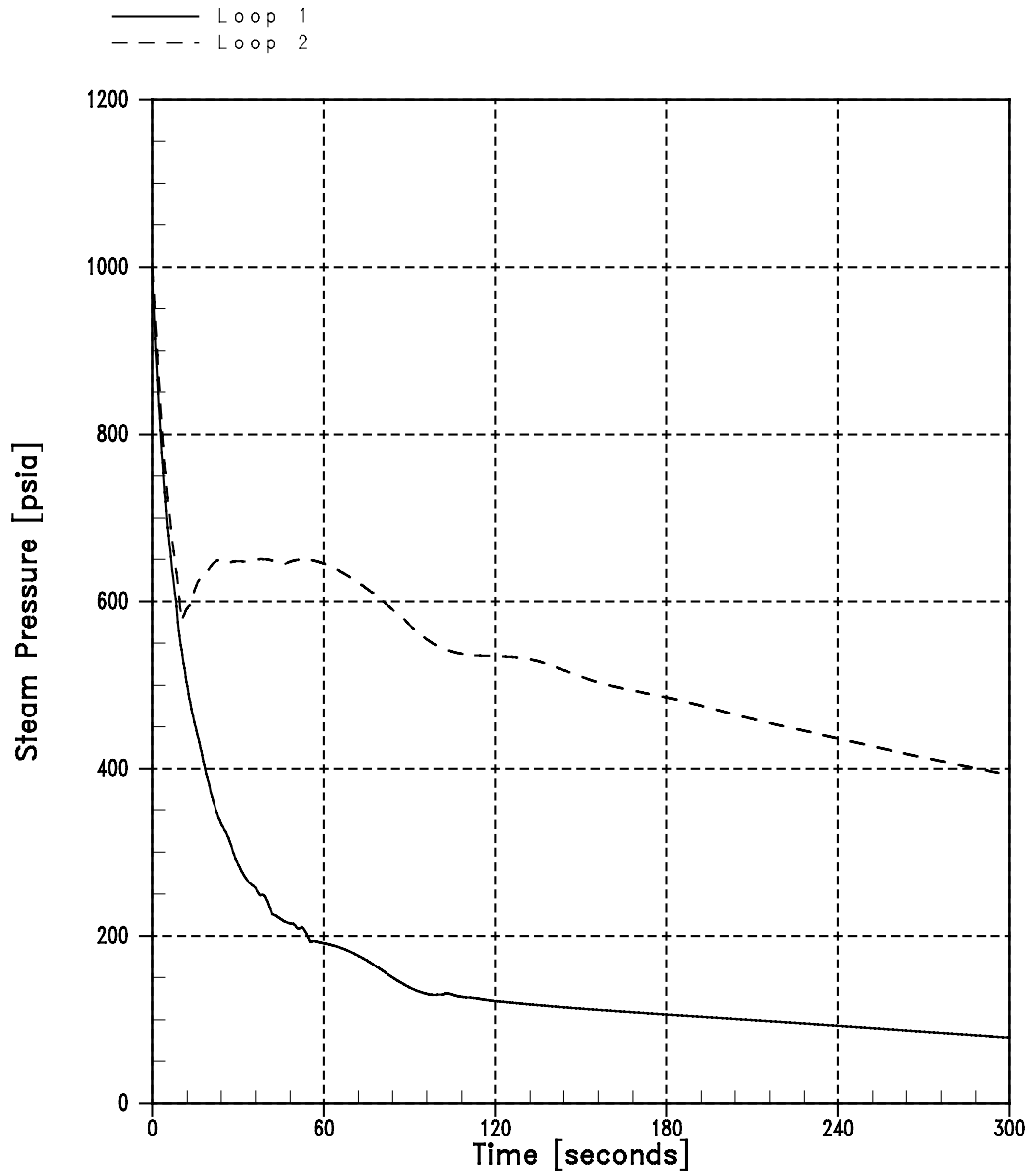


Figure 14.2.5-4
MSLB With Offsite Power
Steam Generator Outlet Nozzle Mass Flow Rate vs. Time

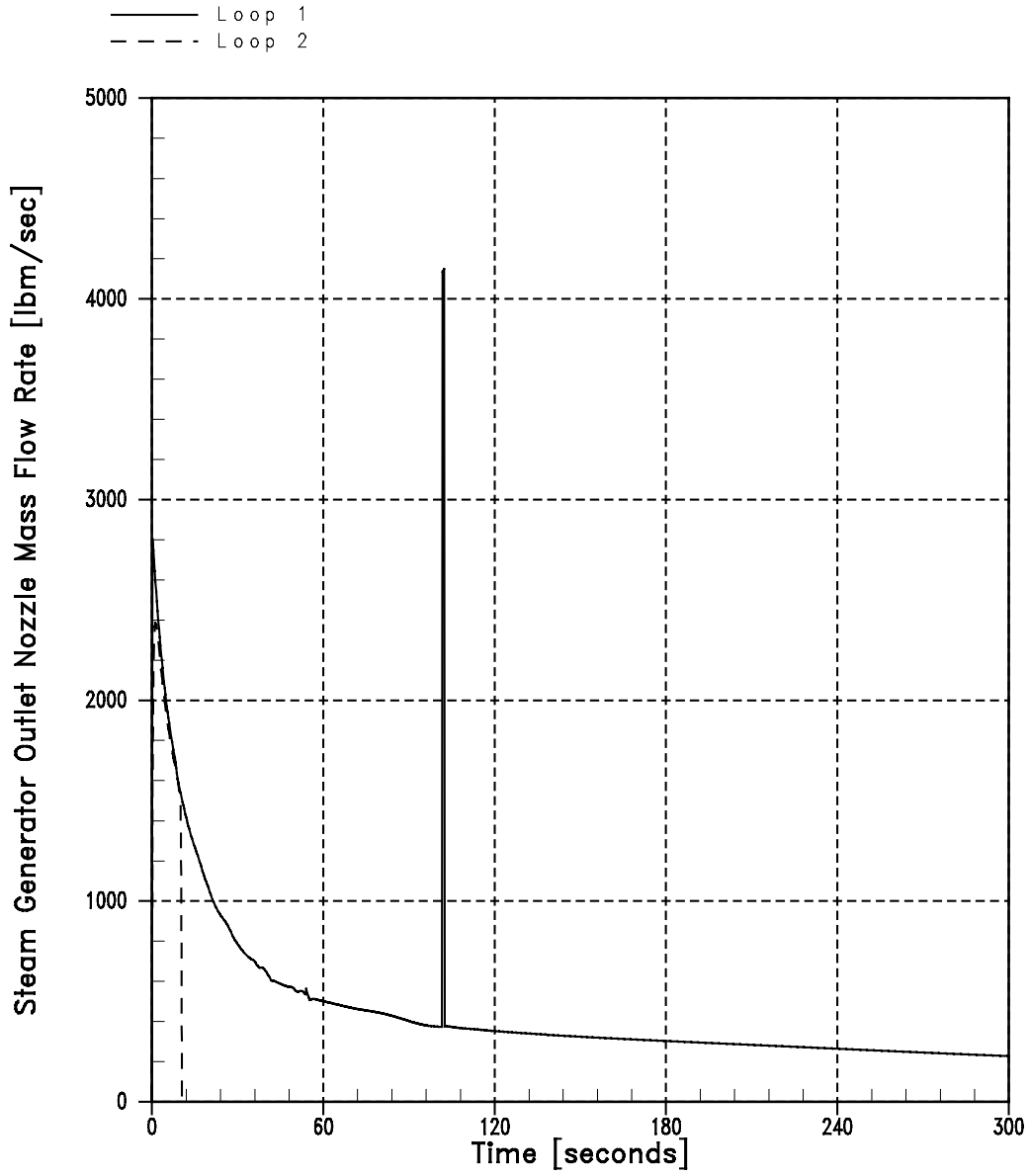


Figure 14.2.5-5
MSLB With Offsite Power
Pressurizer Pressure vs. Time

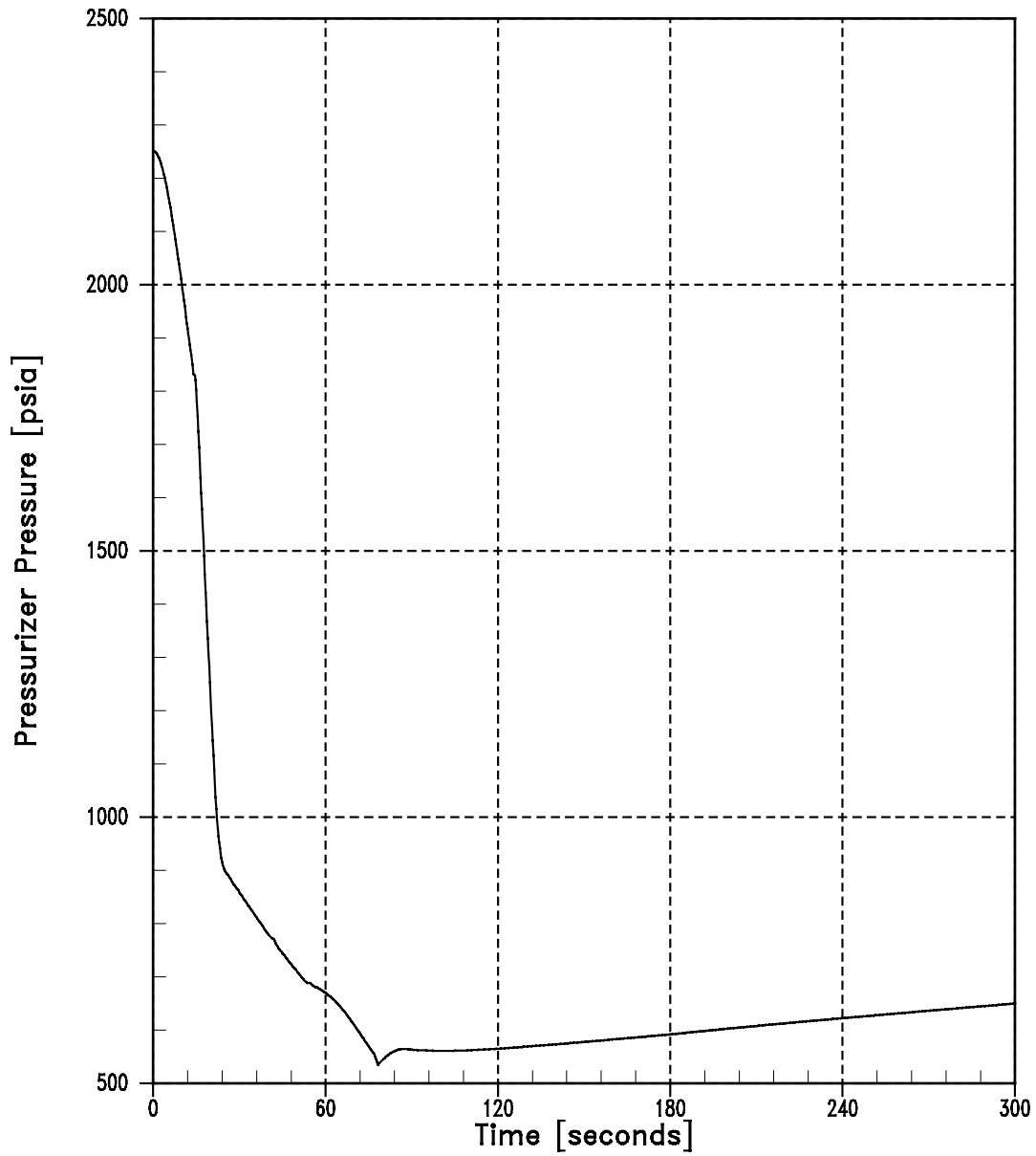


Figure 14.2.5-6
MSLB With Offsite Power
Pressurizer Water Volume vs. Time

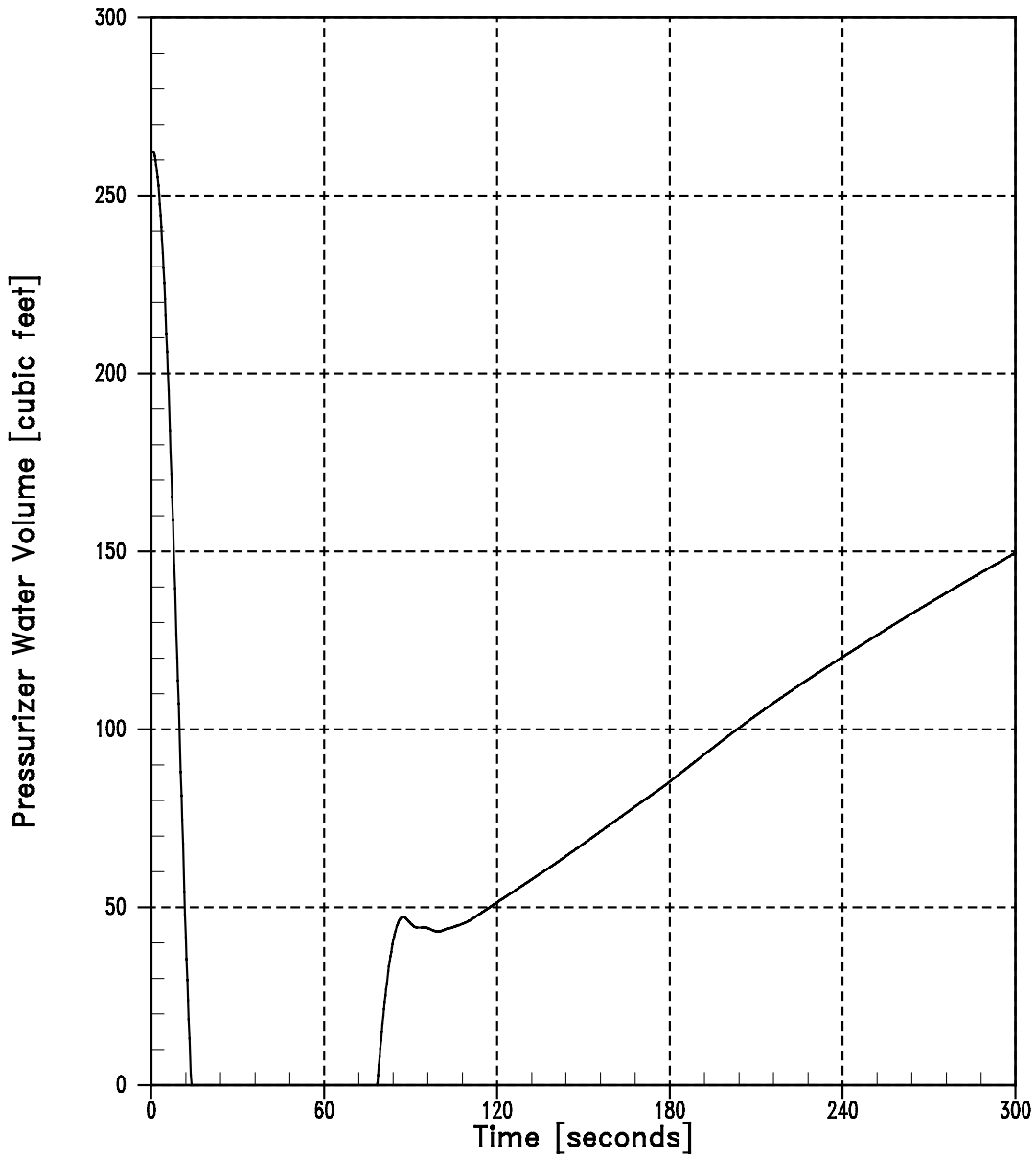


Figure 14.2.5-7
MSLB With Offsite Power
Reactor Vessel Inlet Temperature vs. Time

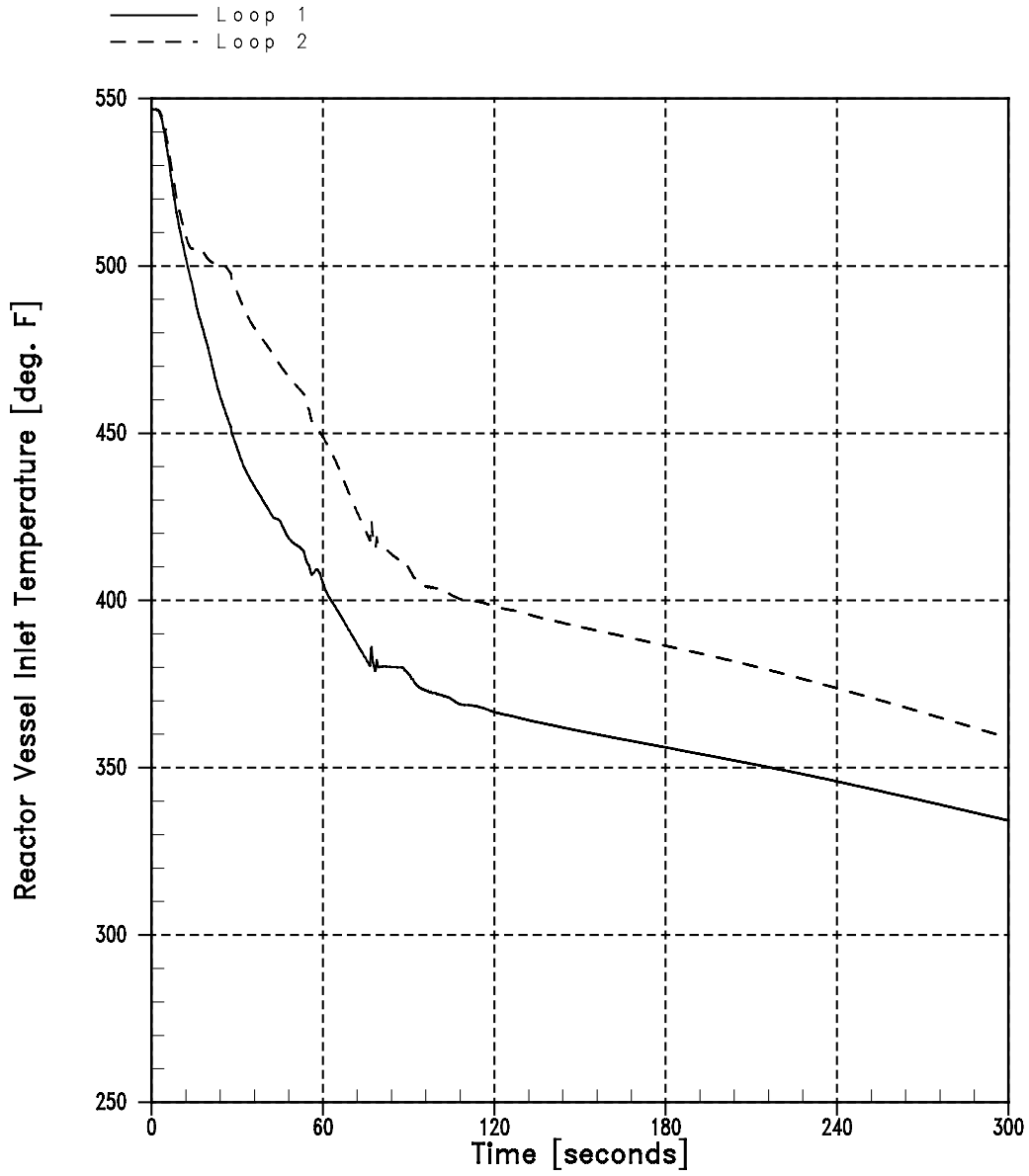


Figure 14.2.5-8
MSLB With Offsite Power
Core Heat Flux vs. Time

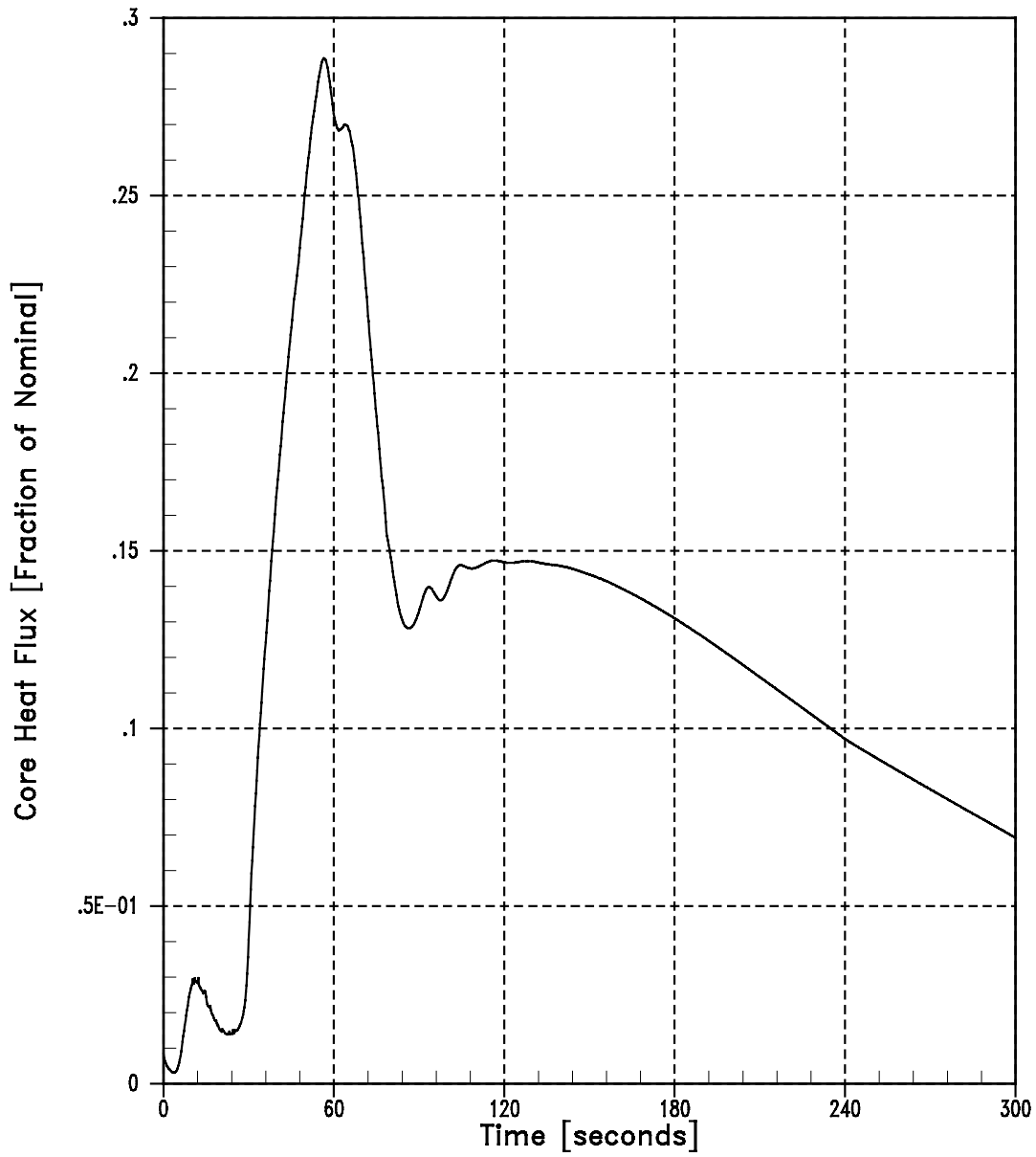


Figure 14.2.5-9
MSLB With Offsite Power
Core Averaged Boron Concentration vs. Time

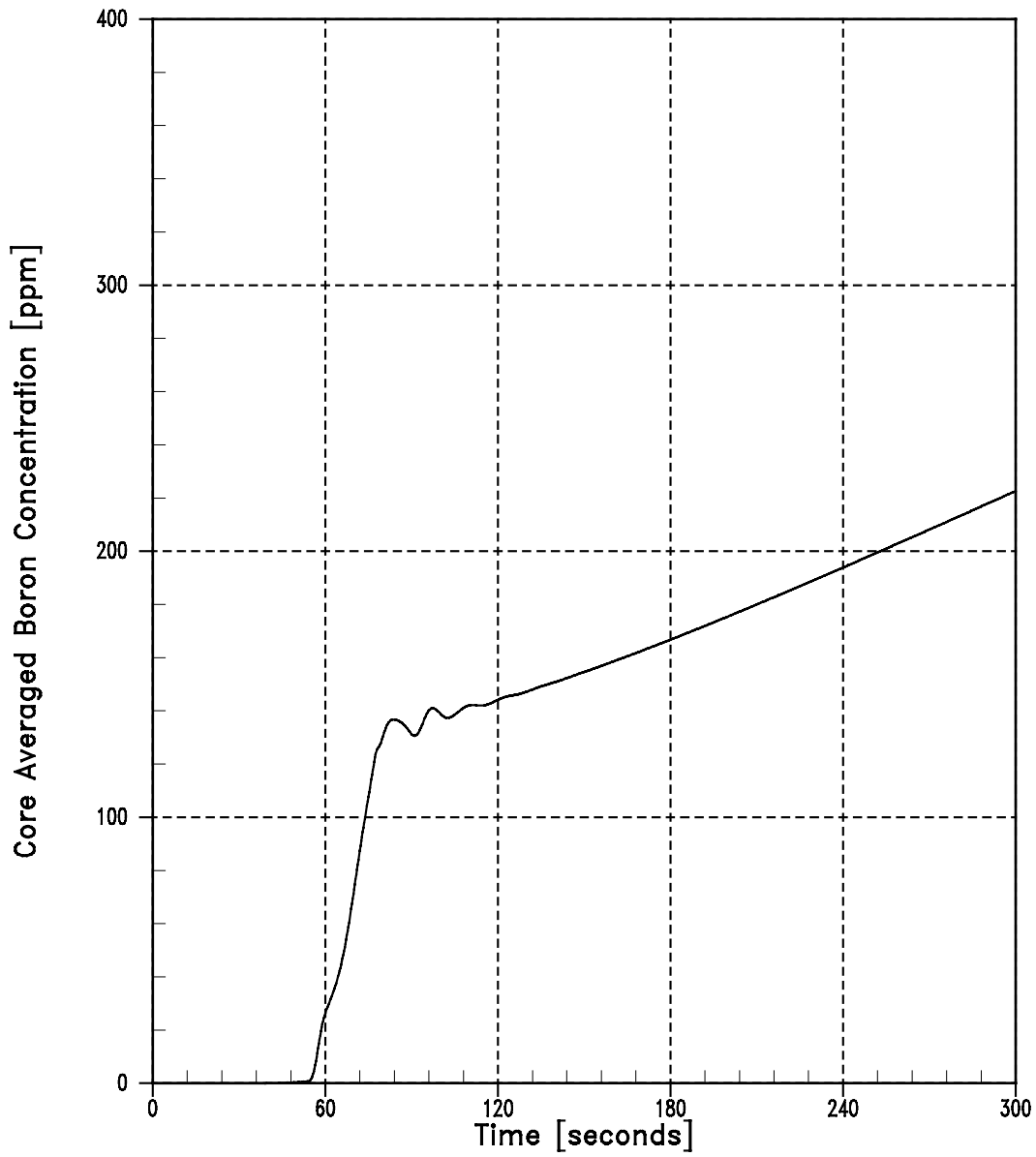


Figure 14.2.5-10
MSLB With Offsite Power
Reactivity vs. Time

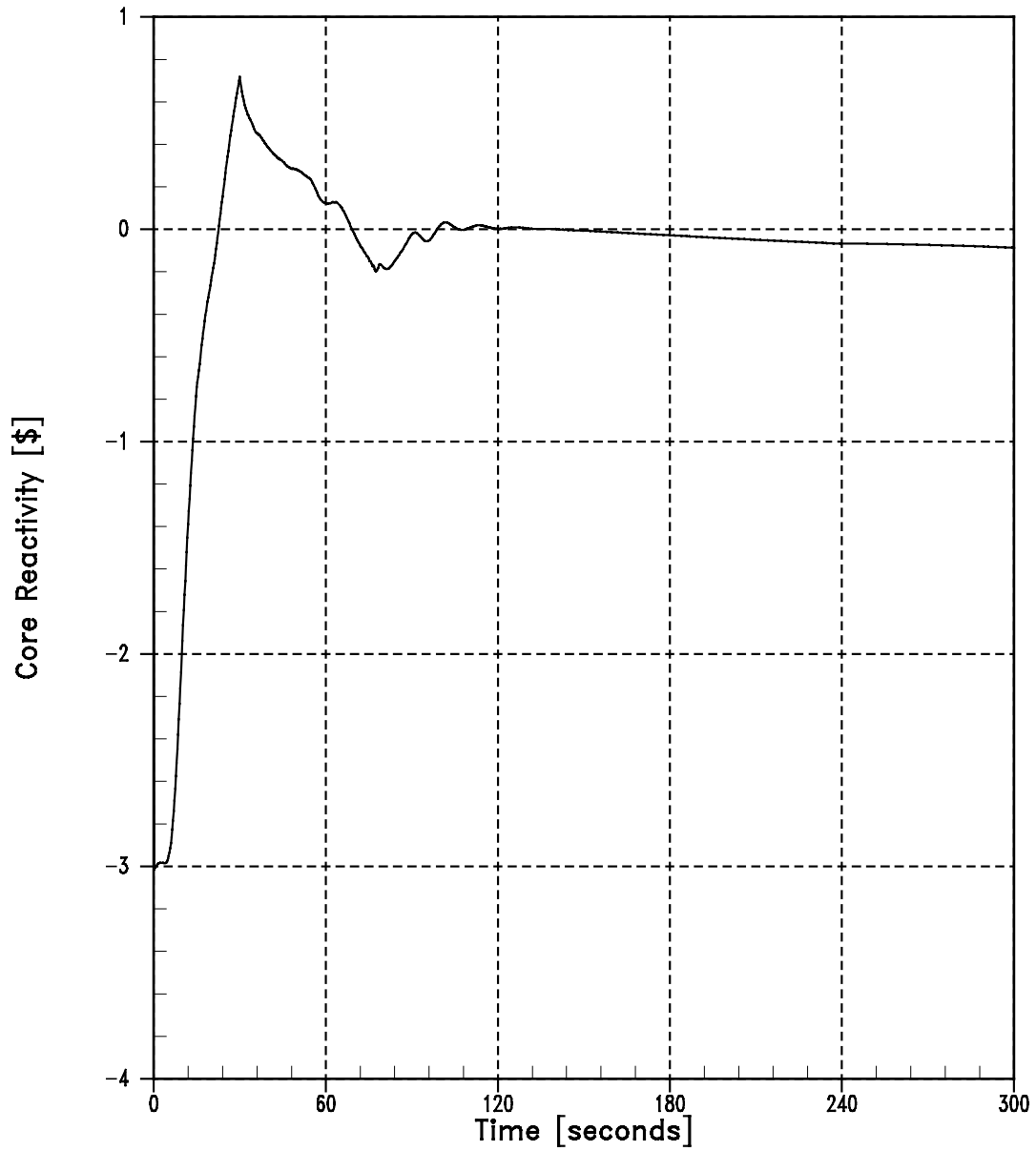


Figure 14.2.5-11
MSLB Without Offsite Power
Steam Pressure vs. Time

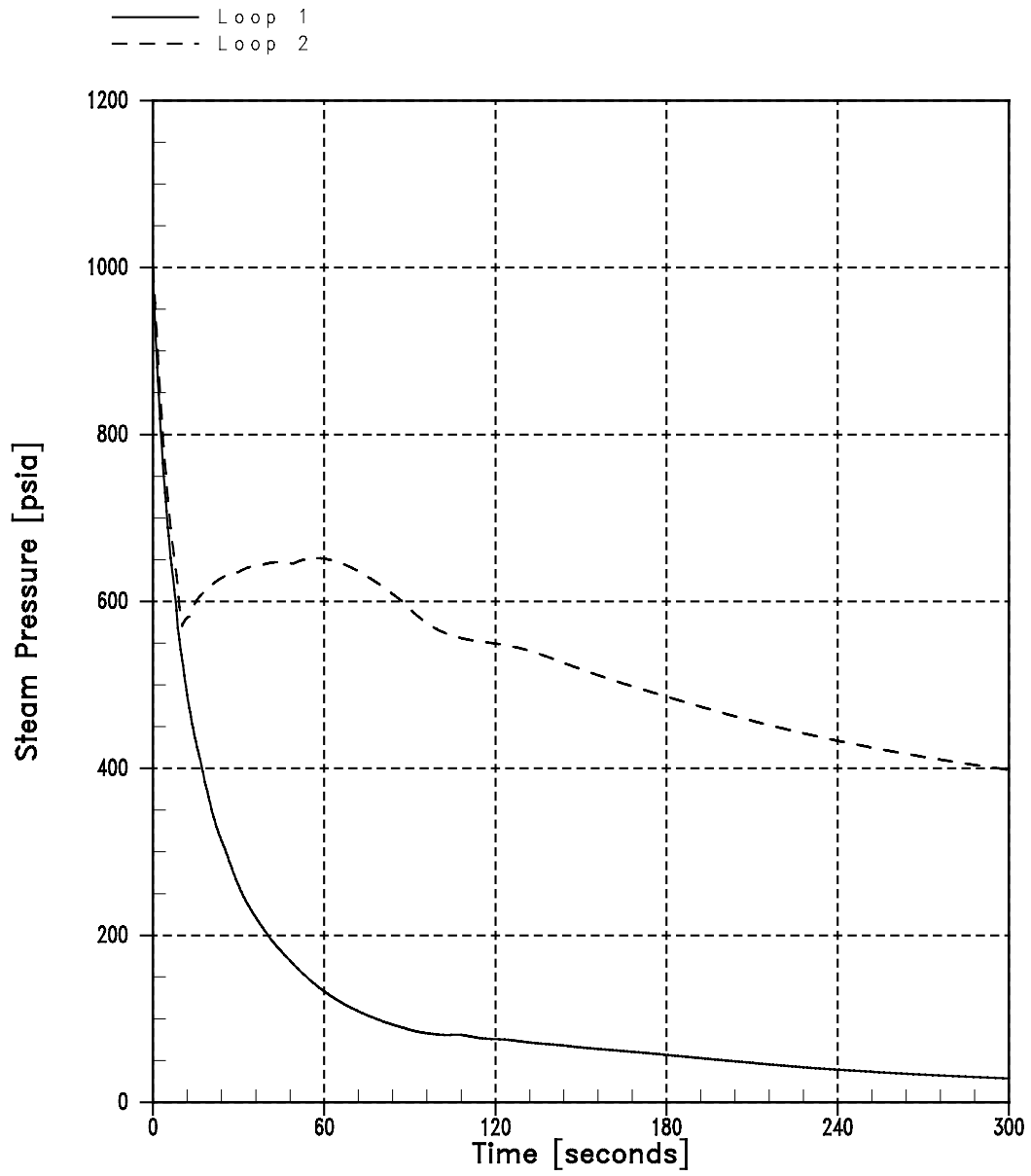


Figure 14.2.5-12
MSLB Without Offsite Power
Steam Generator Outlet Nozzle Mass Flow Rate vs. Time

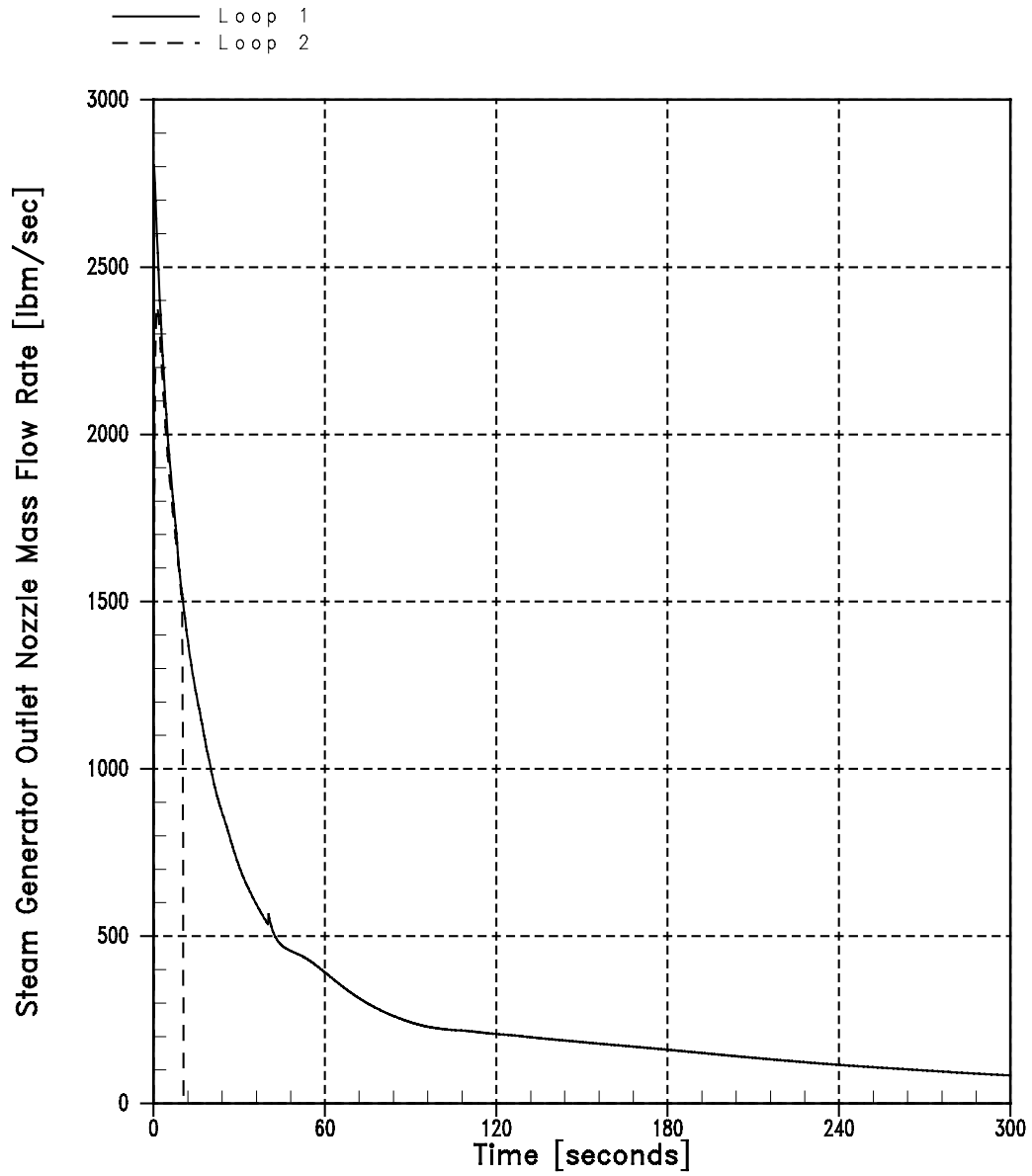


Figure 14.2.5-13
MSLB Without Offsite Power
Pressurizer Pressure vs. Time

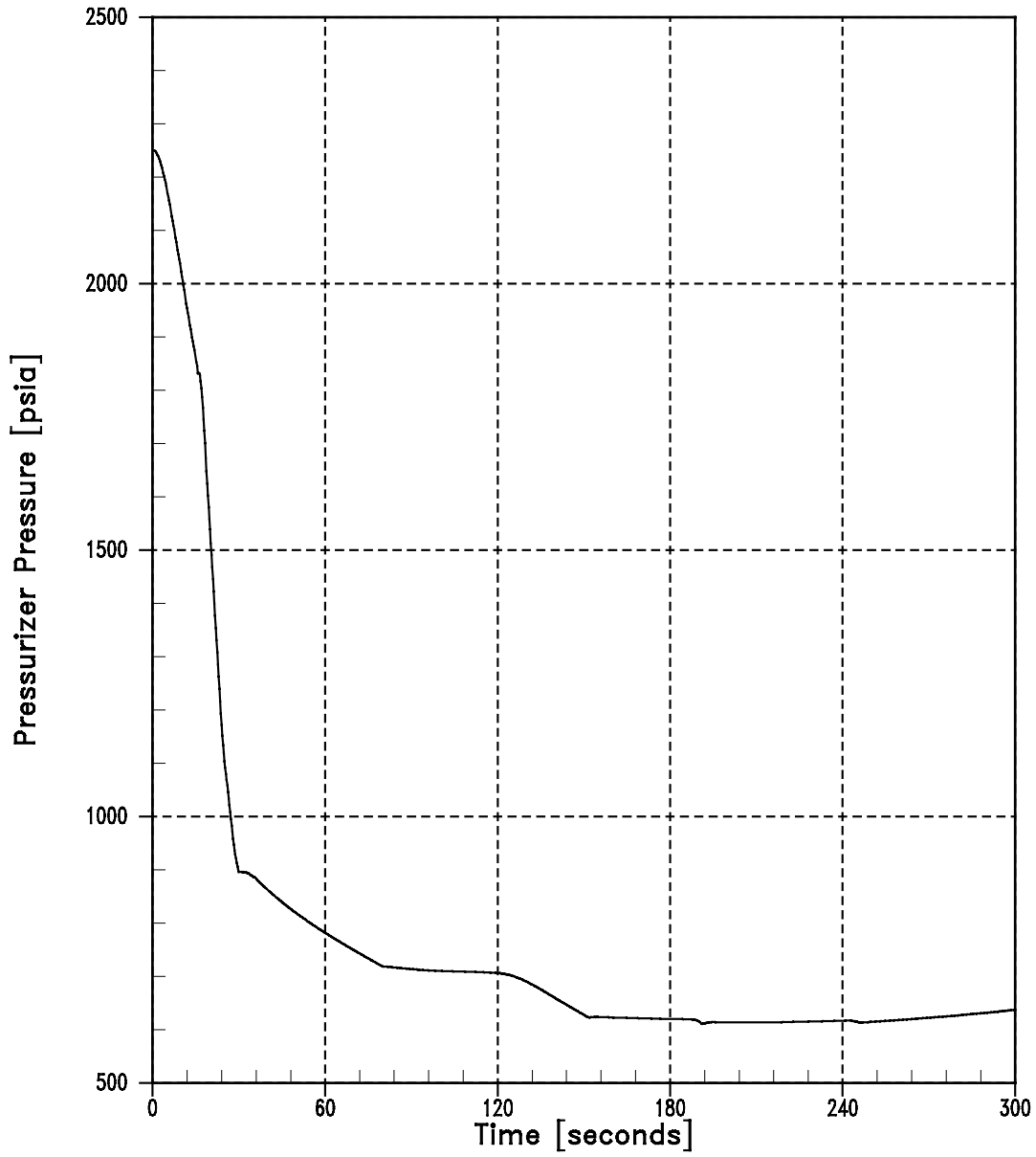


Figure 14.2.5-14
MSLB Without Offsite Power
Pressurizer Water Volume vs. Time

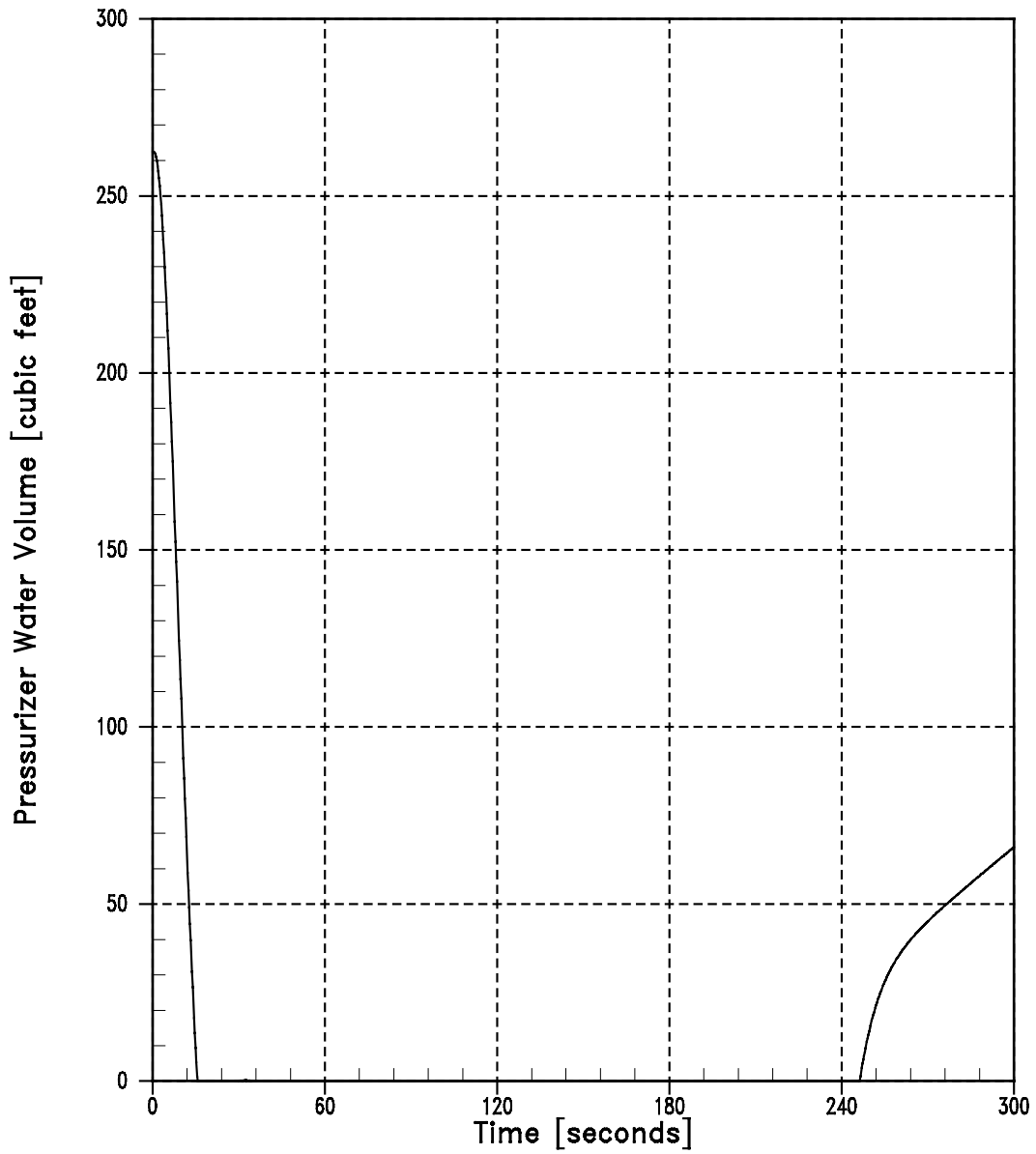


Figure 14.2.5-15
MSLB Without Offsite Power Reactor
Vessel Inlet Temperature vs. Time

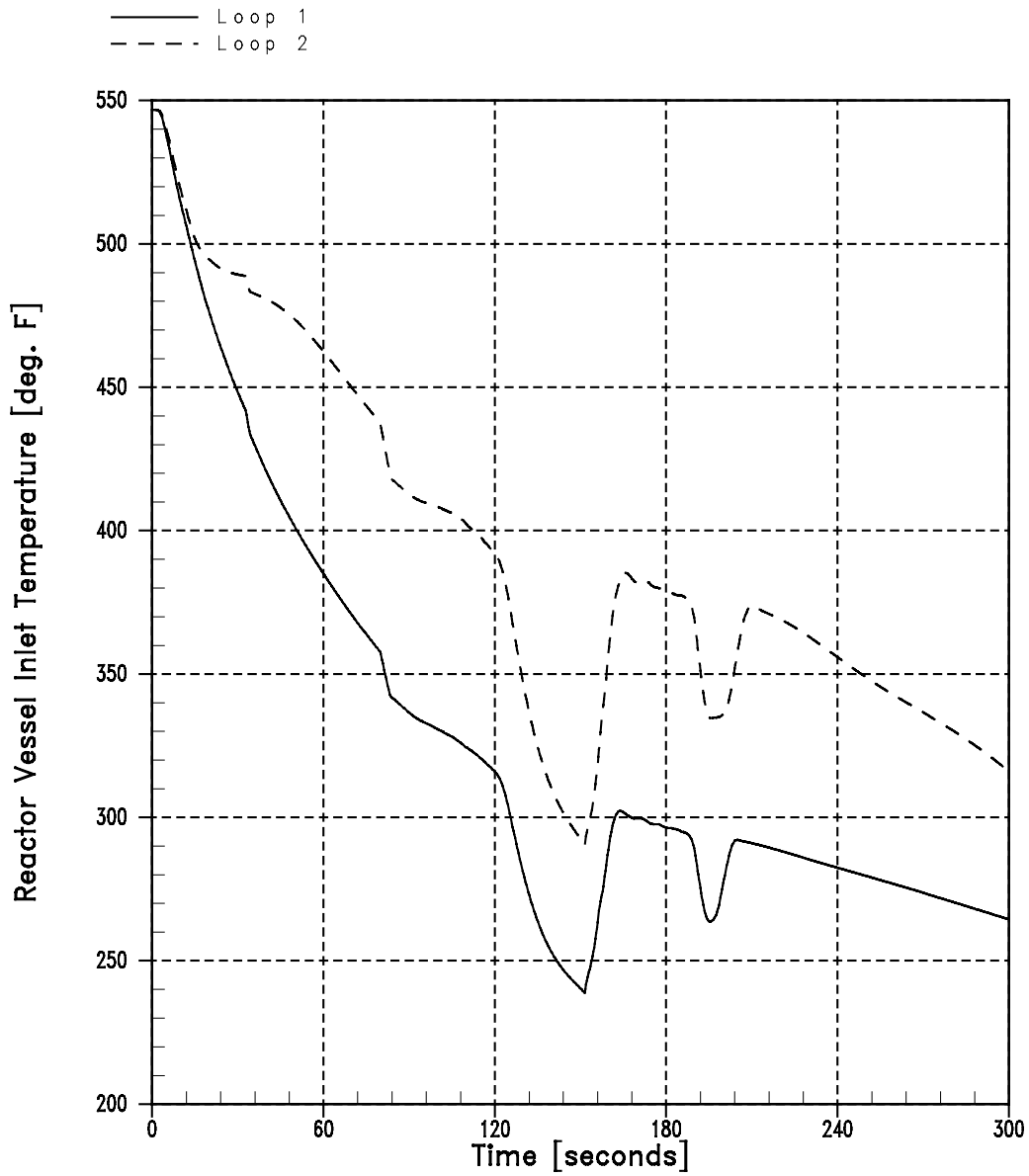


Figure 14.2.5-16
MSLB Without Offsite Power
Core Heat Flux vs. Time

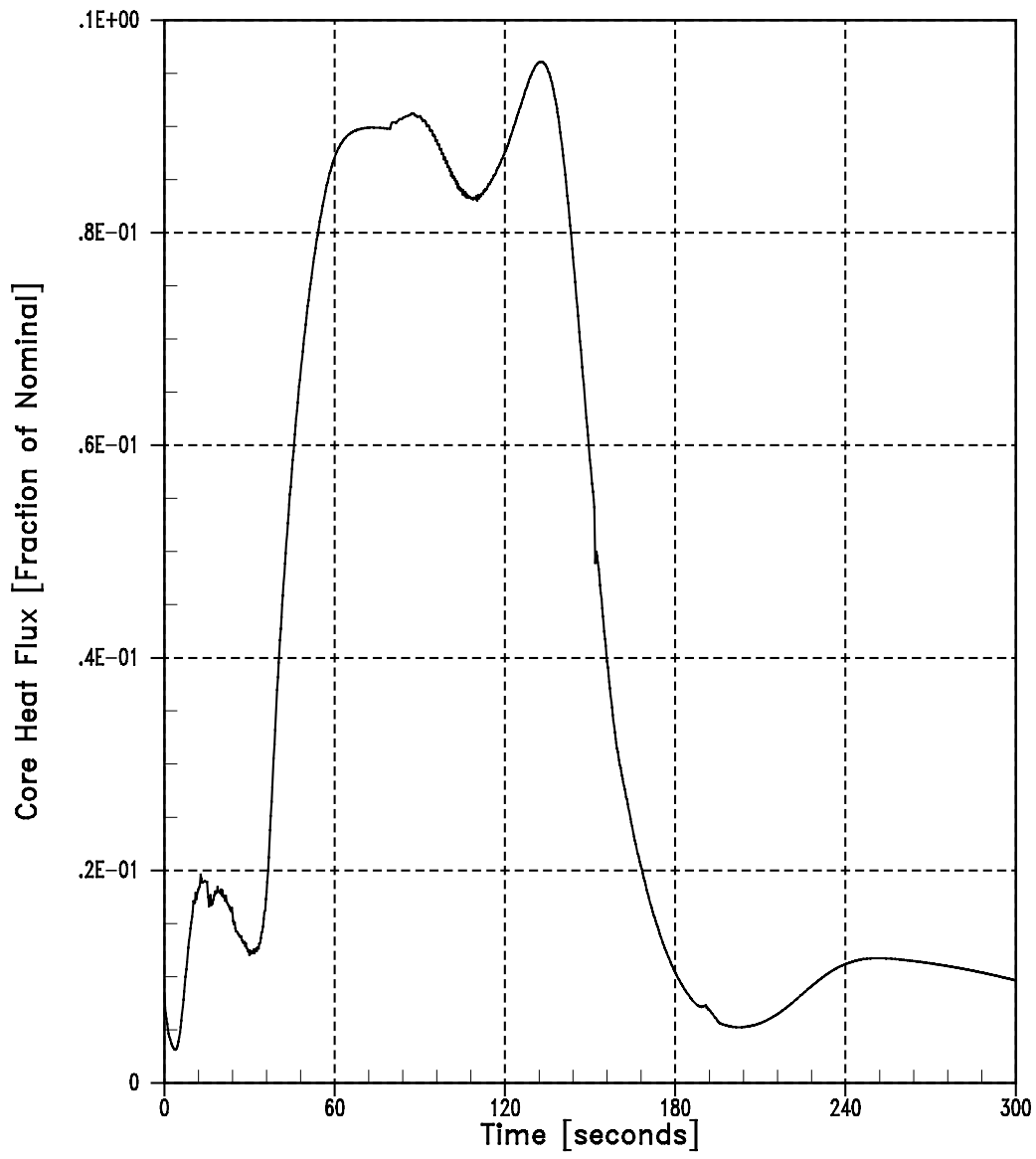


Figure 14.2.5-17
MSLB Without Offsite Power
Core Averaged Boron Concentration vs. Time

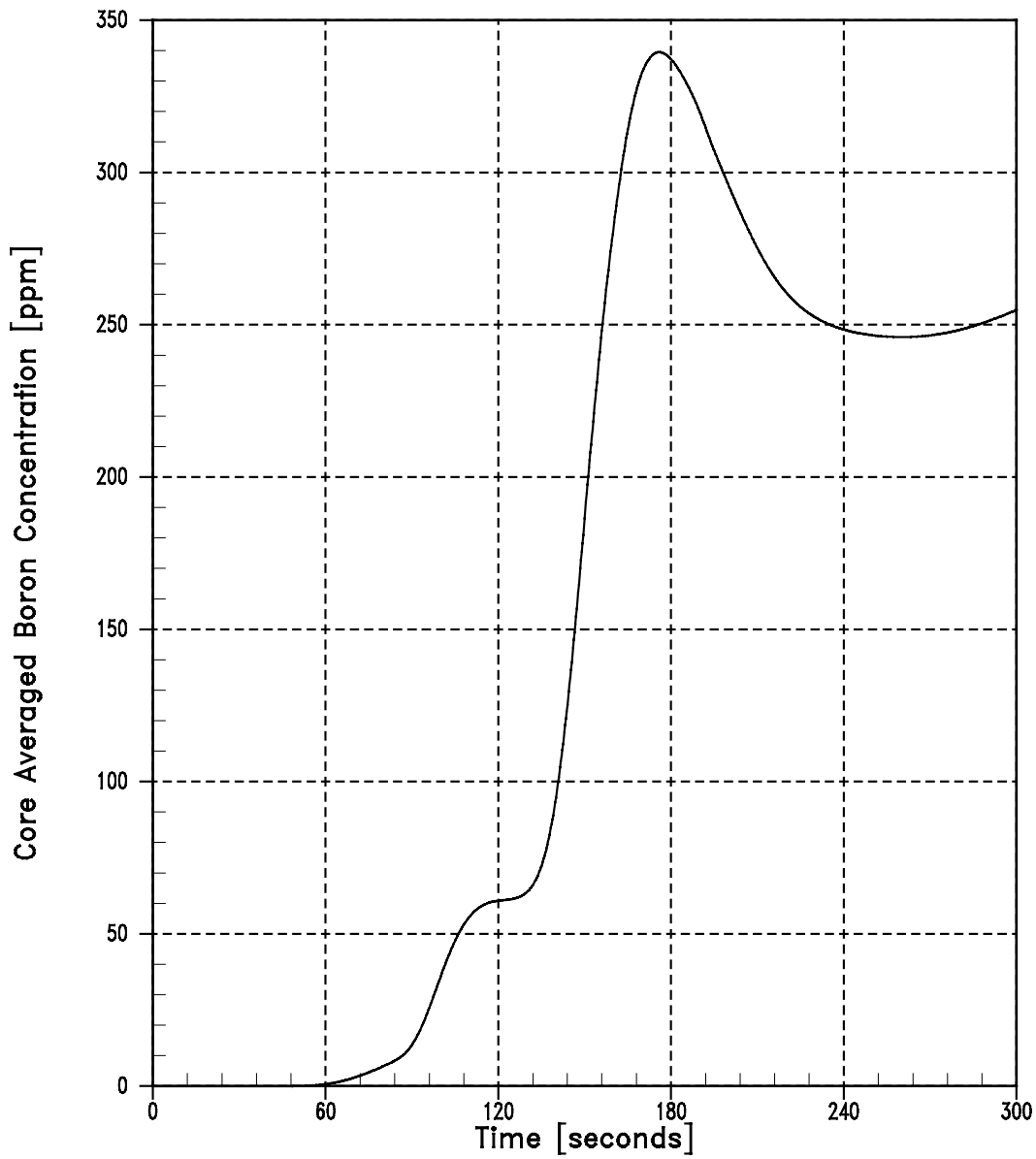


Figure 14.2.5-18
MSLB Without Offsite Power
Reactivity vs. Time

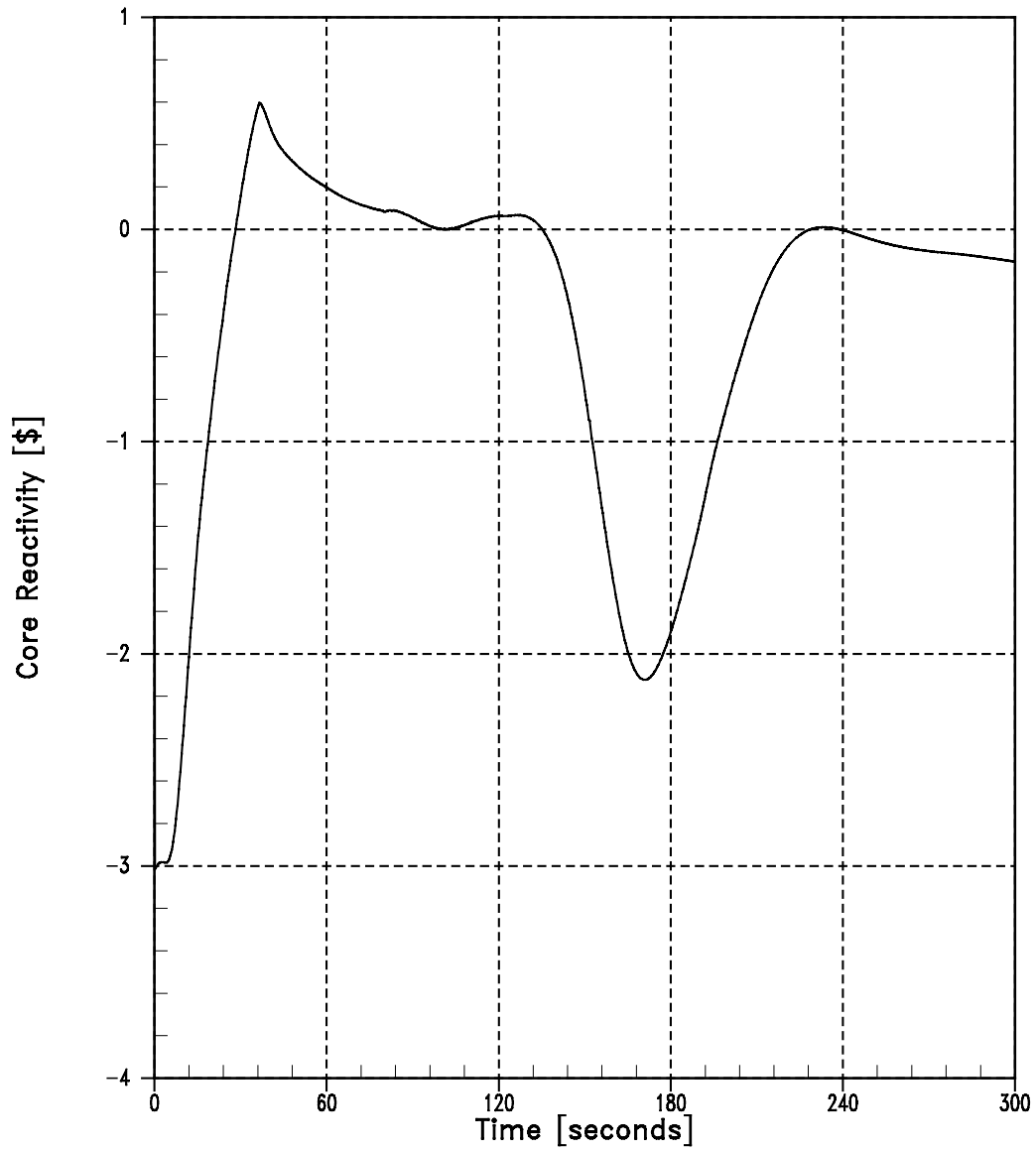


Figure 14.2.5-21
Limiting MSLB - Containment Pressure Response

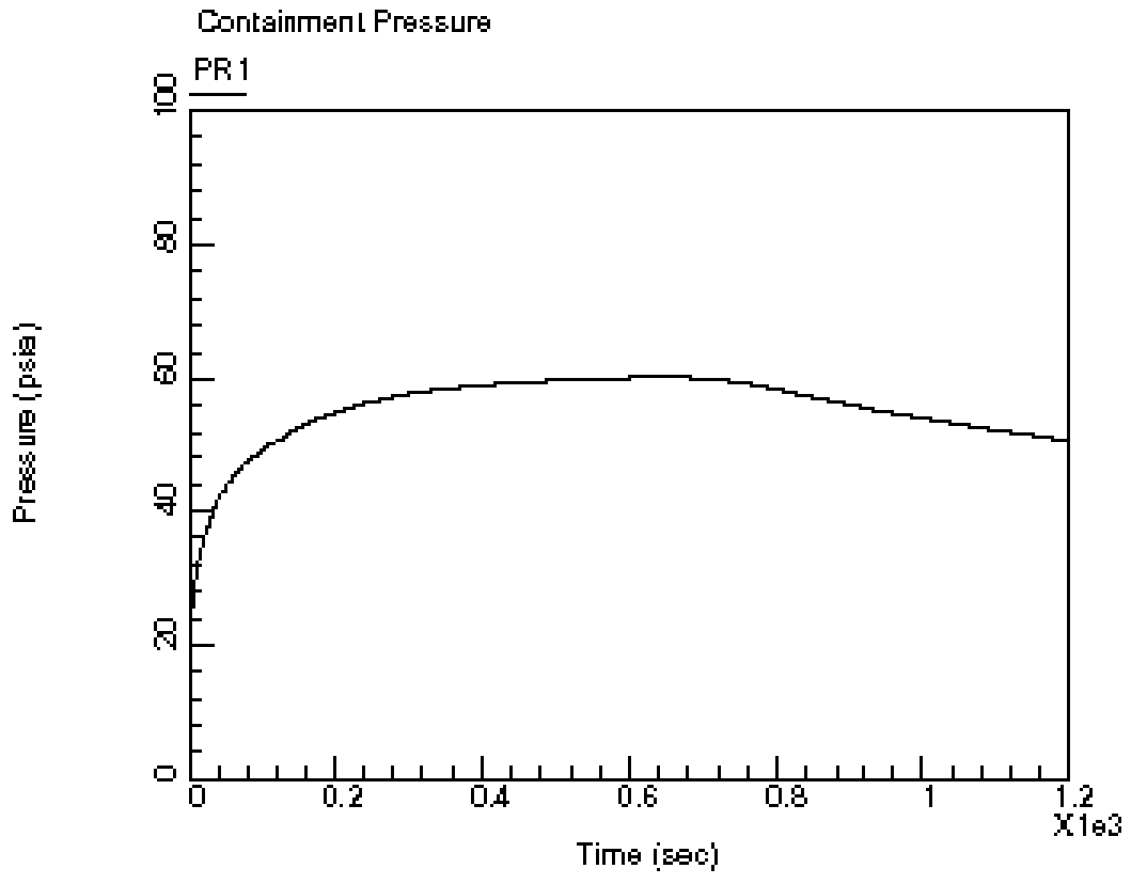


Figure 14.2.5-22
Limiting MSLB - Containment Temperature Response

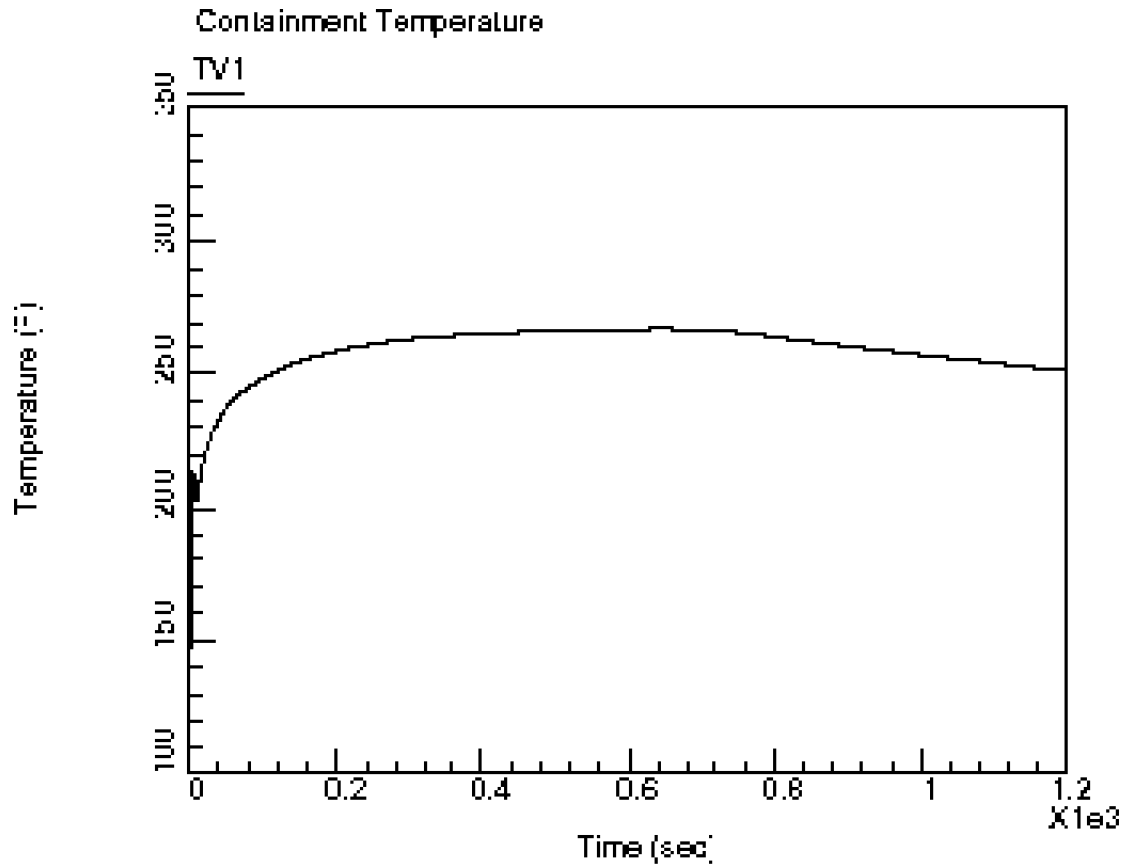


Figure 14.2.6-1
RCCA Ejection Accident from Full Power Beginning of Cycle
Reactor Power vs. Time

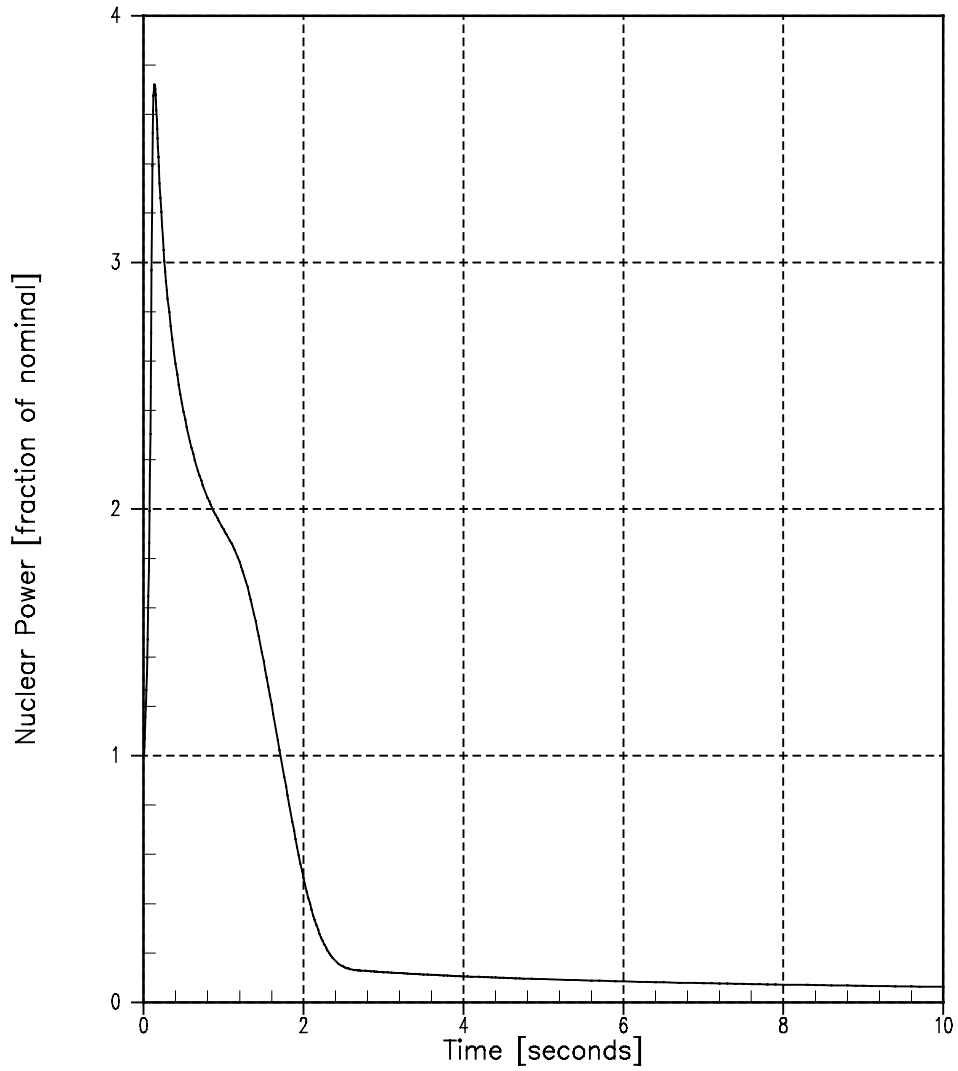


Figure 14.2.6-2
RCCA Ejection Accident from Full Power Beginning of Cycle
Fuel and Cladding Temperatures vs. Time

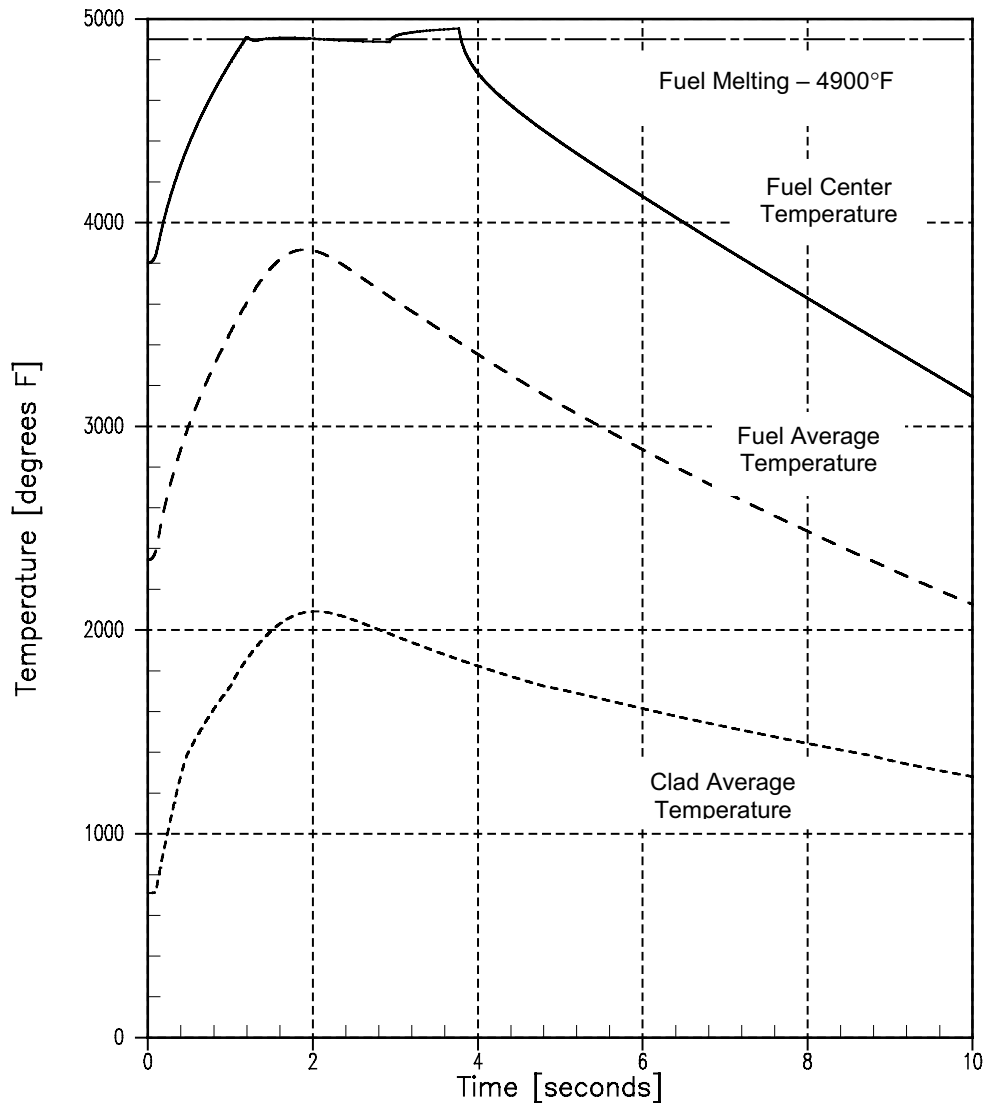


Figure 14.2.6-3
RCCA Ejection Accident from Zero Power Beginning of Cycle
Reactor Power vs. Time

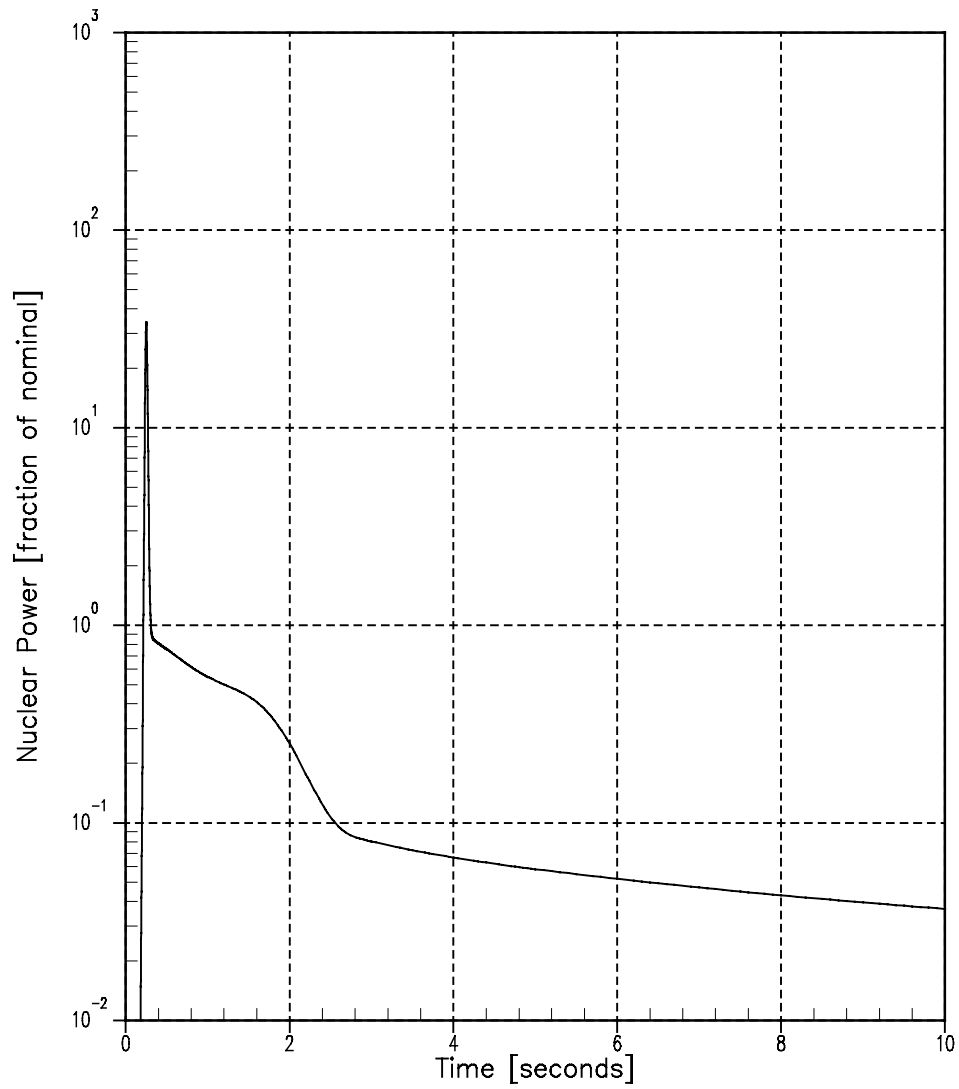


Figure 14.2.6-4
RCCA Ejection Accident from Zero Power Beginning of Cycle
Fuel and Cladding Temperatures vs. Time

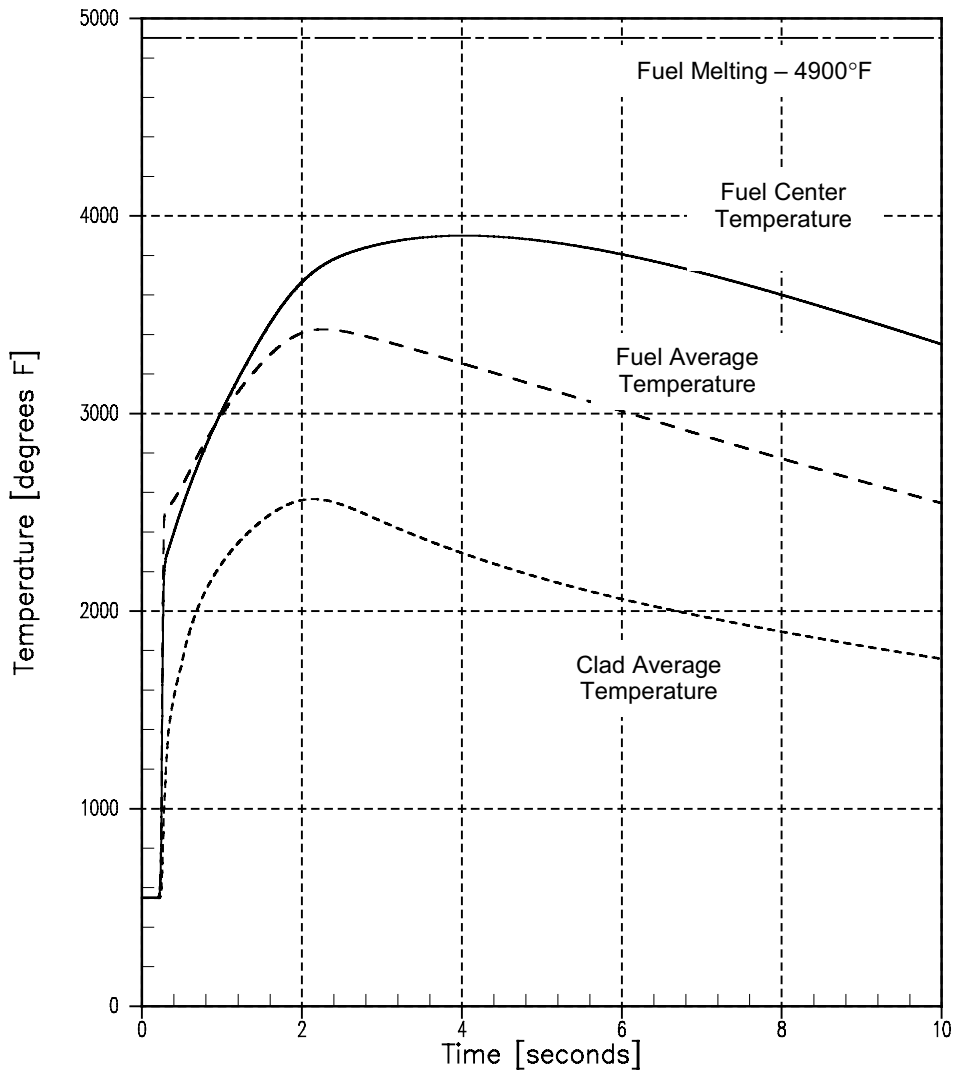


Figure 14.2.6-5
RCCA Ejection Accident from Full Power End of Cycle
Reactor Power vs. Time

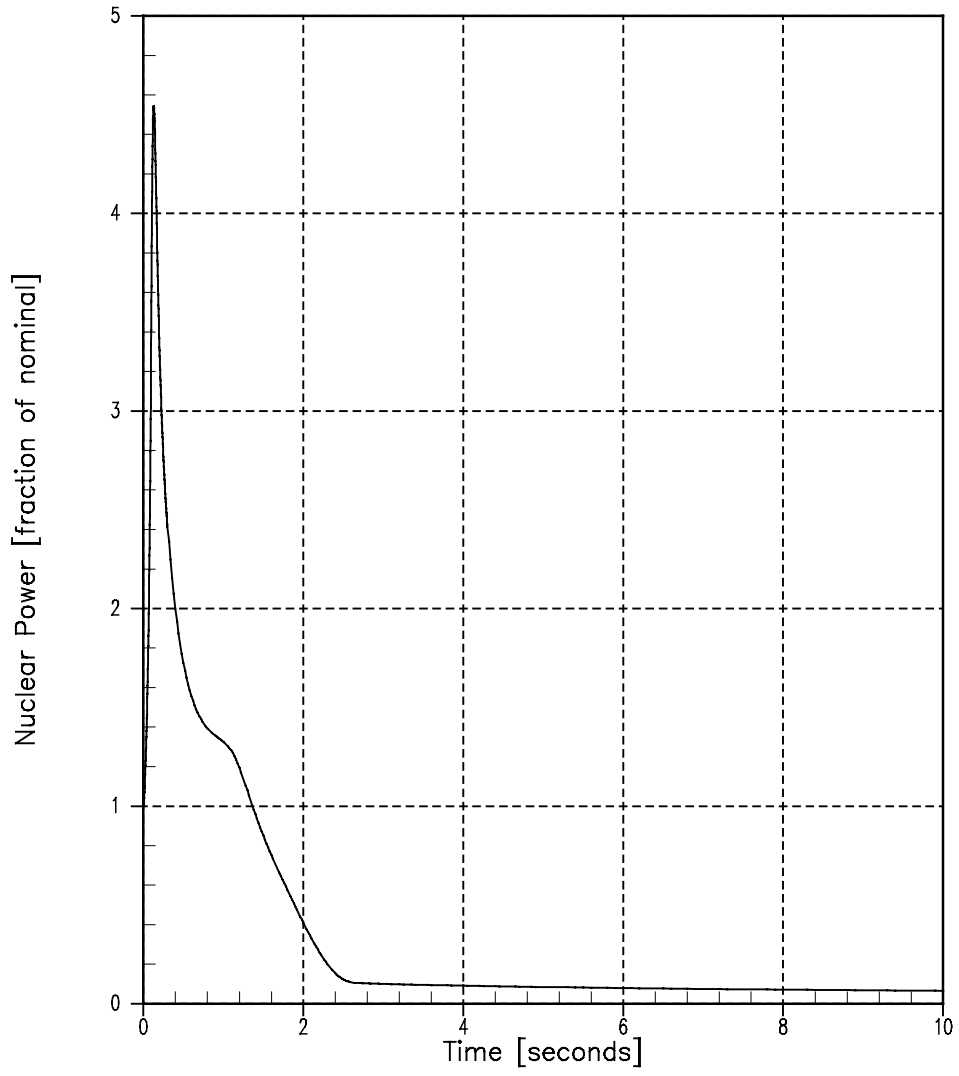


Figure 14.2.6-6
RCCA Ejection Accident from Full Power End of Cycle
Fuel and Cladding Temperatures vs. Time

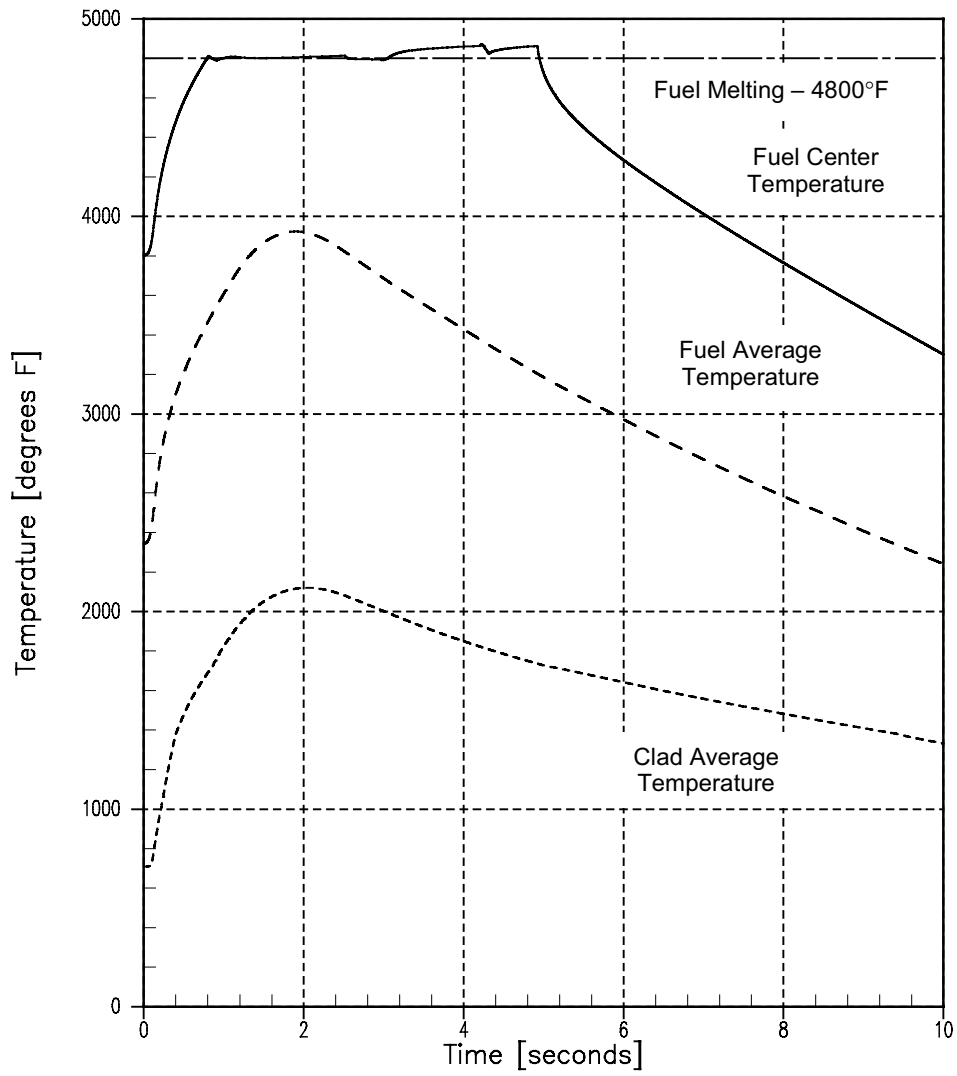


Figure 14.2.6-7
RCCA Ejection Accident from Zero Power End of Cycle
Reactor Power vs. Time

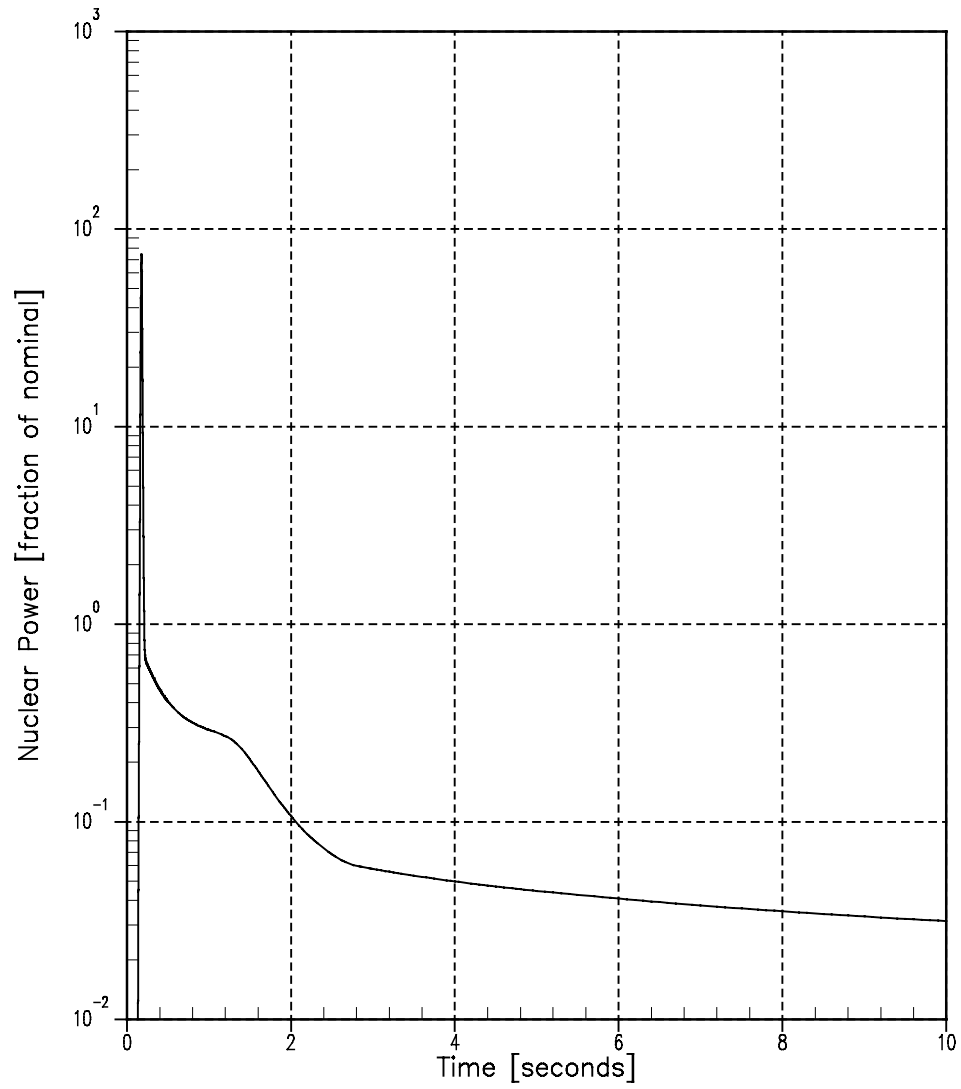
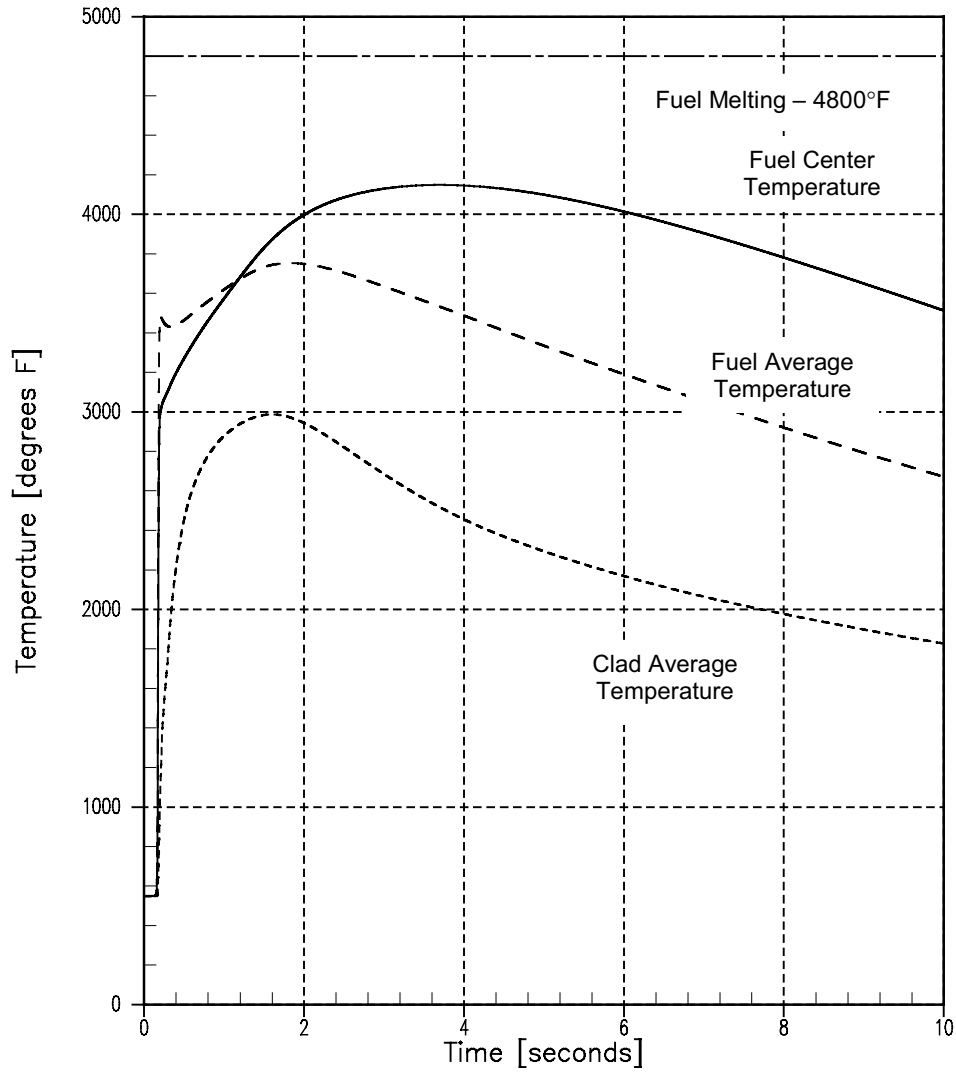


Figure 14.2.6-8
RCCA Ejection Accident from Zero Power End of Cycle
Fuel and Cladding Temperatures vs. Time



14.3 REACTOR COOLANT SYSTEM PIPE RUPTURES (LOCA)

14.3.1 General

14.3.1.1 Condition III - Infrequent Faults

By definition, Condition III occurrences are faults which may happen very infrequently during the life of the plant. They will be accommodated with the failure of only a small fraction of the fuel rods although sufficient fuel damage might occur to preclude resumption of the operation for a considerable outage time. The release of radioactivity will not be sufficient to interrupt or restrict public use of those areas beyond the exclusion radius. A Condition III fault will not, by itself, generate a Condition IV fault or result in a consequential loss of function of the RCS or of containment barriers.

The time sequence of events for the small breaks is shown in Table 14.3-1 and Table 14.3-2 presents the results of the analysis.

14.3.1.2 Condition IV - Limiting Faults

Condition IV occurrences are faults which are not expected to take place, but are postulated because their consequences would include the potential for the release of significant amounts of radioactive material. These are the most drastic occurrences which must be designed against, and they represent limiting design cases. Condition IV faults are not to cause a fission product release to the environment resulting in an undue risk to public health and safety in excess of guideline values of 10 CFR 50.67. A single Condition IV fault is not to cause a consequential loss of required functions of systems needed to cope with the fault including those of the Emergency Core Cooling System and the containment.

The analysis of total effective dose equivalent (TEDE) doses, resulting from events leading to fission product release, appears in Section 14.3.5. The fission product inventories, which form a basis for these calculations are presented in Appendix D. Section 14.3.4, Section 14.3.5 and Appendix H also include the discussions of systems interdependency contributing to limiting fission product leakage from the containment following a Condition IV occurrence.

The time sequence of events for a large break is shown in Table 14.3.3-8 and Figure 14.3.2-1, and Table 14.3.3-9 presents the results of these analyses.

14.3.1.3 Loss of Reactor Coolant From Small Ruptured Pipes or From Cracks In Large Pipes Which Actuates Emergency Core Cooling System

14.3.1.4 Identification of Causes and Accident Description

A LOCA is defined as a rupture of the RCS piping or of any line connected to the system. See Section 14.1.3 for a more detailed description of the loss of reactor coolant accident boundary limits. Ruptures of small cross sections will cause expulsion of the coolant at a rate which can be accommodated by the charging pumps which would maintain an operational water level in the

pressurizer permitting the operator to execute an orderly shutdown. The coolant, which would be released to the containment, contains the fission products existing in it.

Should a larger break occur, depressurization of the RCS causes fluid to flow to the RCS from the pressurizer resulting in a pressure and level decrease in the pressurizer. Reactor trip occurs when the pressurizer low-pressure trip setpoint is reached. The SIS is actuated when the appropriate setpoint is reached. The consequences of the accident are limited in two ways:

- Reactor trip and borated water injection complement void formation in causing rapid reduction of nuclear power to a residual level corresponding to the delayed fission and fission product decay
- Injection of borated water ensures sufficient flooding of the core to prevent excessive clad temperature

Before the break occurs the plant is in an equilibrium condition, i.e., the heat generated in the core is being removed via the secondary system. During blowdown, heat from decay, hot internals and the vessel continues to be transferred to the RCS. The heat transfer between the RCS and the secondary system may be in either direction depending on the relative temperatures. In the case of continued heat addition to the secondary side, system pressure increases and steam dump may occur. Makeup to the secondary side is provided by the auxiliary feedwater pumps. The SI signal stops normal feedwater flow by closing the main feedwater line isolation valves and initiates emergency feedwater flow by starting auxiliary feedwater pumps. As discussed in Section 6.6, manual initiation of auxiliary feedwater is acceptable at low power levels. The secondary flow aids in the reduction of RCS pressure. When the RCS depressurizes to 675 psig, the accumulators begin to inject water into the reactor coolant loops. Reactor coolant pump trip is assumed to be coincident with the reactor trip and effects of pump coast-down are included in the blowdown analyses.

14.3.1.5 Analysis of Effects and Consequences

14.3.1.5.1 Method of Analysis

The requirements of an acceptable ECCS Evaluation Model are presented in Appendix K of 10 CFR 50 (Reference 1). The requirements of Appendix K regarding specific model features were met by selecting models, which provide a significant overall conservatism in the analysis. The assumptions made pertain to the conditions of the reactor and associated safety system equipment at the time that the LOCA occurs and include such items as the core peaking factors, the containment pressure, and the performance of the ECCS system. Decay heat generated throughout the transient is also conservatively calculated as required by Appendix K of 10 CFR 50. The small-break LOCA analysis is documented in the Reload Transition Safety Report for the KNPP, July 2002.

14.3.1.6 **Small-Break LOCA Analysis Using NOTRUMP**

The Westinghouse NOTRUMP Small Break Evaluation Model consists of the NOTRUMP and SBLOCTA computer codes. NOTRUMP is used to model the system hydraulics and SBLOCTA calculates the fuel rod cladding heatup.

The postulated small-break LOCA is predominately a gravity dominated accident in which the slow draining of the RCS is accompanied by the formation of distinct mixture levels throughout the RCS. These mixture levels vary with time and are dependent upon the transient two-phase transport of mass and energy, which takes place within the RCS during the course of the accident. Consequently, the degree of accuracy with which a system model is capable of simulating the RCS response to a small-break LOCA is dependent upon the model's capability to accurately model the RCS transient mass and energy distribution.

For postulated LOCAs due to small breaks, the NOTRUMP computer code is used to calculate the transient depressurization of the RCS as well as to describe the mass and enthalpy of flow through the break. The NOTRUMP computer code is a state-of-the-art one-dimensional general network code incorporating a number of advanced features. Among these are calculation of thermal non-equilibrium in all fluid volumes, flow regime-dependent drift flux calculations with counter-current flooding limitations, mixture level tracking logic in multiple-stacked fluid nodes and regime dependent heat transfer correlation. The Westinghouse NOTRUMP Small Break Evaluation Model was developed to determine the RCS response to design basis small-break LOCAs, and to address NRC concerns expressed in NUREG-0611, "Generic Evaluation of Feedwater Transients and Small Break Loss-of-Coolant Accident in Westinghouse-Designed Operating Plants."

NOTRUMP (Reference 2, Reference 3 and Reference 6) is a general one-dimensional nodal network computer code which describes the spatial detail of the RCS with a network of fluid nodes (representing various system fluid volumes), flow links (representing various fluid flow paths), metal nodes (representing various metal masses), and heat transfer links (representing various heat transfer paths between metal structures and surrounding fluid). The use of NOTRUMP in the analysis involves, among other things, the representation of the reactor core as heated control volumes with an associated phase separation model to permit a transient mixture height calculation. The broken loop and intact loop are each modeled explicitly. Transient behavior of the system is determined from the governing conservation equations of mass, energy, and momentum. The multi-node capability of the program enables explicit, detailed spatial representation of various system components which, among other capabilities, enables a proper calculation of behavior of loop seal during a postulated small-break LOCA.

Peak clad temperature calculations are performed with the SBLOCTA code (Reference 4, Reference 5, and Reference 7), using the NOTRUMP calculated core pressure, fuel rod power history, uncovered core steam flow and mixture heights as boundary conditions. The code evaluates the fuel cladding and the coolant temperatures during the hypothetical small-break LOCA. Each of the fuel rods modeled by SBLOCTA is analyzed using finite-difference

conduction equations in both the axial and radial directions. It calculates the effect of cladding swell and burst and considers the exothermic reaction between zircaloy and water. A top skewed axial power shape is chosen for the hot rod because the power is concentrated in the upper regions of the core. Such a distribution is limiting for small-break LOCAs because it minimizes coolant swell, while maximizing vapor superheating and fuel rod heat generation at the uncovered elevations. The small-break LOCA analysis assumes the core continues to operate at full rated power until the control rods are completely inserted.

Small-break LOCA calculations are based on minimum safeguards assumptions designed to minimize pumped ECCS flow to the core. These calculations include loss of a train of ECCS and high head SI pump degradation of pump head by 15 percent. For a small-break LOCA with an equivalent break diameter less than the inner diameter of the high head SI line, pumped high head SI flow is delivered to both the intact and broken loop at the RCS backpressure (Figure 14.3-1). Justification for this assumption is provided in Reference 6. The effect of flow from the RHR pumps is not considered since their shutoff head is lower than RCS pressure during the portion of the transients considered here. For a small-break LOCA with an equivalent break diameter greater than or equal to the inner diameter of the high head SI line, pumped high head SI flow is delivered only to the intact loop with one line spilling to containment back pressure (Figure 14.3-2). This is assumed since the modeled break may include the severance of the high head SI line or an area of a severed high head SI line.

Delivery of the SI flow to the RCS was assumed to be delayed 30 seconds after the generation of a SI signal. This delay includes the time required for diesel startup and loading of the SI pumps onto the emergency buses and for the pump to come to full speed in order to deliver full flow. The assumed delay time is sufficient to account for degraded grid conditions. Finally, the new and approved SI condensation model (Reference 6) was used for all analysis cases.

14.3.1.7 Results

14.3.1.7.1 Reactor Coolant System Pipe Breaks

This section, presents results of the limiting break size in terms of highest peak clad temperature. The worst break size (small break) is a 3-inch diameter break. The depressurization transient for this break is shown in Figure 14.3-3. The extent to which the core is uncovered is shown in Figure 14.3-4.

During the earlier part of the small-break transient, the effect of the break flow is not strong enough to overcome the flow maintained by the reactor coolant pumps through the core as they are coasting down following reactor trip. Therefore, upward flow through the core is maintained. The resultant heat transfer cools the fuel rod and clad to very near the coolant temperatures as long as the core remains covered by a two-phase mixture.

The maximum hot spot clad temperature calculated during the transient is 1030°F. This analysis assumes the most limiting temperature conditions and includes the effects of fuel densification as described in Reference 5. The peak clad temperature transients are shown in

Figure 14.3-7 for the worst break size, i.e., the break with the highest peak clad temperature. The steam flow rate for the worst break is shown in Figure 14.3-5. When the mixture level drops below the top of the core, the steam flow computed by NOTRUMP provides cooling to the upper portion of the core. The core heat transfer coefficients for this phase of the transient are given in Figure 14.3-9. The hot spot fluid temperature for the worst break is shown in Figure 14.3-8. Finally, the safety injection flow to both the intact and broken loops is shown in Figure 14.3-6.

The reactor shutdown time (5.0 sec) is equal to the reactor trip signal time (2.0 sec) plus 3.0 sec for rod insertion. During this rod insertion period, the reactor is conservatively assumed to operate at rated power.

14.3.1.8 Conclusions

Analyses presented in this section show that the high head portion of the Emergency Core Cooling System, together with accumulators, provide sufficient core flooding to keep the calculated peak clad temperatures below required limits of 10 CFR 50.46. Hence, adequate protection is afforded by the Emergency Core Cooling System in the event of a small-break LOCA.

Following the TMI accident, Westinghouse performed generic studies of small-break LOCAs. Results of these studies indicated that peak clad temperatures greater than 2200°F may occur if the reactor coolant pumps are tripped after a significant loss of reactor coolant inventory. To prevent such a loss, the operators are instructed to trip the pumps early in the accident.

14.3.1.9 Additional Break Sizes

Additional break sizes and temperatures were analyzed, including the 2-inch and 4-inch breaks at high T_{avg} and the 3-inch break at low T_{avg} . Figure 14.3-10, Figure 14.3-11, and Figure 14.3-12 present the RCS pressure, core mixture level, and peak clad temperature plots for the 2-inch break. Figure 14.3-13, Figure 14.3-14, and Figure 14.3-15 present the RCS pressure, core mixture level, and peak clad temperature plots for the 4-inch break. Finally, for the 3-inch break at low T_{avg} conditions, Figure 14.3-16, Figure 14.3-17, and Figure 14.3-18 present the RCS pressure, core mixture level, and peak clad temperature plots.

The time sequence of events for small breaks analyzed is shown in Table 14.3-1, and Table 14.3-2 presents the results for these analyses.

14.3.2 Major Reactor Coolant System Pipe Ruptures (LOCA)

The analysis specified by 10 CFR 50.46 (Reference 1), “Acceptance Criteria for Emergency Core Cooling Systems for Light Water Power Reactors,” is presented in this section. The results of the best-estimate large-break LOCA analysis are summarized in Table 14.3.3-8, and show compliance with the acceptance criteria.

For the purpose of ECCS analyses, Westinghouse (W) defines a large-break LOCA as a rupture 1.0 ft² or larger of the RCS piping including the double ended rupture of the largest pipe in the RCS or of any line connected to that system. The boundary considered for LOCAs as related to connecting piping is defined in Section 4.1.3.

Should a major break occur, rapid depressurization of the RCS to a pressure nearly equal to the containment pressure occurs in approximately 35 seconds, with a nearly complete loss of system inventory. Rapid voiding in the core shuts down reactor power. A SIS signal is actuated when the low pressurizer pressure setpoint is reached. These countermeasures will limit the consequences of the accident in two ways:

1. Borated water injection complements void formation in causing rapid reduction of power to a residual level corresponding to fission product decay heat. An average RCS/sump mixed boron concentration is calculated to ensure that the post-LOCA core remains subcritical. However, no credit is taken for the insertion of control rods to shut down the reactor in the large break analysis.
2. Injection of borated water provides heat transfer from the core and prevents excessive cladding temperatures.

Before the break occurs, the reactor is assumed to be in a full power equilibrium condition, i.e., the heat generated in the core is being removed through the steam generator secondary system. At the beginning of the blowdown phase, the entire RCS contains sub-cooled liquid which transfers heat from the core by forced convection with some fully developed nucleate boiling. During blowdown, heat from fission product decay, hot internals and the vessel, continues to be transferred to the reactor coolant. After the break develops, the time to departure from nucleate boiling is calculated. Thereafter, the core heat transfer is unstable, with both nucleate boiling and film boiling occurring. As the core becomes voided, both transition boiling and forced convection are considered as the dominant core heat transfer mechanisms. Heat transfer due to radiation is also considered.

The heat transfer between the RCS and the secondary system may be in either direction, depending on the relative temperatures. In the case of the large-break LOCA, the primary pressure rapidly decreases below the secondary system pressure and the steam generators are an additional heat source. In the Kewaunee Nuclear Plant Large-Break LOCA analysis using the WCOBRA/TRAC UPI methodology, the steam generator secondary is conservatively assumed to be isolated (main feedwater and steam line) at the initiation of the event to maximize the secondary side heat load.

14.3.2.1 Performance Criteria for Emergency Core Cooling System

The reactor is designed to withstand thermal effects caused by a LOCA including the double-ended severance of the largest reactor cooling system cold leg pipe. The reactor core and internals together with the Emergency Core Cooling System (ECCS) are designed so that the reactor can be safely shut-down and the essential heat transfer geometry of the core preserved following the accident. Long-term coolability is maintained.

When the RCS depressurizes to approximately 750 psig, the accumulators begin to inject borated water into the reactor coolant loops. Borated water from the accumulator in the faulted loop is assumed to spill to containment and be unavailable for core cooling for breaks in the cold leg of the RCS. Flow from the accumulator in the intact loop may not reach the core during depressurization of the RCS due to the fluid dynamics present during the ECCS bypass period. ECCS bypass results from the momentum of the fluid flow up the downcomer due to a break in the cold leg, which entrains ECCS flow out toward the break. Bypass of the ECCS diminishes as mechanisms responsible for the bypassing are calculated to be no longer effective.

The blowdown phase of the transient ends when the liquid level in the lower plenum reaches its minimum. After the end of the blowdown, refill of the reactor vessel lower plenum begins. Refill is completed when emergency core cooling water has filled the lower plenum of the reactor vessel, which is bounded by the bottom of the active fuel region of the fuel rods (called bottom of core (BOC) recovery time).

The reflood phase of the transient is defined as the time period lasting from BOC recovery until the reactor vessel has been filled with water to the extent that the core temperature rise has been terminated. From the latter stage of blowdown and on into the beginning of reflood, the intact loop accumulator tank rapidly discharges borated cooling water into the RCS. Although a portion injected prior to end of bypass is lost out the cold leg break, the accumulator eventually contributes to the filling of the reactor vessel downcomer. The downcomer water elevation head provides the driving force required for the reflooding of the reactor core. The high head safety injection (HHSI) pump aids in the filling of the downcomer and core and subsequently supply water to help maintain a full downcomer and complete the reflooding process. The low head safety injection (LHSI), which injects into the upper plenum (hence, upper plenum injection - UPI) also aids the reflooding process by providing water to the core through the vessel upper plenum.

Continued operation of the ECCS pumps supplies water during long-term cooling. Core temperatures have been reduced to long-term steady state levels associated with dissipation of residual heat generation. After the water level of the refueling water storage tank (RWST) reaches a minimum allowable value, coolant for long-term cooling of the core is obtained by switching from the injection mode to the sump recirculation mode of ECCS operation. Spilled borated water is drawn from the engineered safety features (ESF) containment sumps by the LHSI pumps (also called the Residual Heat Removal pumps, or RHR pumps) and returned to the upper plenum and

RCS cold legs. Figure 14.3.2-1 contains a schematic of the bounding sequence of events for the Kewaunee large-break LOCA transient.

For the Best-Estimate large-break LOCA analysis, one ECCS train, including one HHSI pump and one RHR (low-head) pump, starts and delivers flow through the injection lines. One branch of the HHSI injection line spills to the containment backpressure; the other branch connects to the intact loop cold leg accumulator line. The RHR injection line connects directly into the upper plenum. Both emergency diesel generators (EDGs) are assumed to start in the modeling of the containment fan coolers and spray pumps. Modeling full containment heat removal systems operation is required by Branch Technical Position CSB 6-1 (Reference 14) and is conservative for the large-break LOCA.

To minimize delivery to the reactor, the HHSI branch line chosen to spill is selected as the one with the minimum resistance. In addition, the pump performance curves are degraded, with the high head degraded by 15 percent of design head and the low head degraded by 10 percent of design head.

14.3.2.2 Large-Break LOCA Analytical Model

In 1988, as a result of the improved understanding of LOCA thermal-hydraulic phenomena gained by extensive research programs, the NRC staff amended the requirements of 10 CFR 50.46 and Appendix K, “ECCS Evaluation Models,” so that a realistic evaluation model may be used to analyze the performance of the ECCS during a hypothetical LOCA (Reference 7). Under the amended rules, best-estimate thermal-hydraulic models may be used in place of models with Appendix K features. The rule change also requires, as part of the analysis, an assessment of the uncertainty of the best-estimate calculations. It further requires that this analysis uncertainty be included when comparing the results of the calculations to the prescribed acceptance limits. Further guidance for the use of best-estimate codes was provided in Regulatory Guide 1.157 (Reference 8).

To demonstrate use of the revised ECCS rule, the NRC and its consultants developed a method called the Code Scaling, Applicability, and Uncertainty (CSAU) evaluation methodology (Reference 9). This method outlined an approach for defining and qualifying a best-estimate thermal-hydraulic code and quantifying the uncertainties in a LOCA analysis.

A LOCA evaluation methodology for three- and four-loop PWR plants based on the revised 10 CFR 50.46 rules was developed by Westinghouse with the support of EPRI and Consolidated Edison and was approved by the NRC (Reference 10). The methodology is documented in WCAP-12945, “Code Qualification Document (CQD) for Best Estimate LOCA Analysis” (Reference 11). Extension of this methodology to plants equipped with residual heat removal (RHR) injection into the upper plenum was approved in May 1999 (Reference 15) and is documented in Reference 12.

The thermal-hydraulic computer code which was reviewed and approved for the calculation of fluid and thermal conditions in the PWR during a large-break LOCA is WCOBRA/TRAC Version MOD7A, Rev. 1 (Reference 11).

WCOBRA/TRAC combines two-fluid, three-field, multi-dimensional fluid equations used in the vessel with one-dimensional drift-flux equations used in the loops to allow a complete and detailed simulation of a PWR. This best-estimate computer code contains the following features:

- Ability to model transient three-dimensional flows in different geometries inside the vessel
- Ability to model thermal and mechanical non-equilibrium between phases
- Ability to mechanistically represent interfacial heat, mass, and momentum transfer in different flow regimes
- Ability to represent important reactor components such as fuel rods, steam generators, reactor coolant pumps, etc.

The reactor vessel is modeled with the three-dimensional, three-field fluid model, while the loop, major loop components, and SI points are modeled with the one-dimensional fluid model.

The basic building block for the vessel is the channel, a vertical stack of single mesh cells. Several channels can be connected together by gaps to model a region of the reactor vessel. Regions that occupy the same level form a section of the vessel. Vessel sections are connected axially to complete the vessel mesh by specifying channel connections between sections. Heat transfer surfaces and solid structures that interact significantly with the fluid can be modeled with rods and unheated conductors. The fuel parameters are generated using the Westinghouse fuel performance code (PAD 4.0, Reference 6).

One-dimensional components are connected to the vessel. Special purpose components exist to model specific components such as the steam generator and pump.

A typical calculation using WCOBRA/TRAC begins with the establishment of a steady-state initial condition with all loops intact. The input parameters and initial conditions for this steady-state calculation are discussed in the next section.

Following the establishment of an acceptable steady-state condition, the transient calculation is initiated by introducing a break into one of the loops. The evolution of the transient through blowdown, refill, and reflood follows continuously, using the same computer code (WCOBRA/TRAC) and the same modeling assumptions. Containment pressure is modeled with the BREAK component using a time dependent pressure table. Containment pressure is calculated using the COCO code (Reference 5) and mass and energy releases from the WCOBRA/TRAC calculation. The parameters used in the containment analysis to determine this pressure curve are presented in Table 14.3.3-1 through Table 14.3.3-3.

The methods used in the application of WCOBRA/TRAC to the large-break LOCA are described in Reference 10 through Reference 12. A detailed assessment of the computer code WCOBRA/TRAC was made through comparisons to experimental data. These assessments were used to develop quantitative estimates of the code's ability to predict key physical phenomena in a PWR large-break LOCA. Modeling of a PWR introduces additional uncertainties which are identified and quantified in the plant-specific analysis (Reference 13). The final step of the best-estimate methodology is to combine all the uncertainties related to the code and plant parameters and estimate the PCT at the 95th percentile (PCT^{95%}). The steps taken to derive the PCT uncertainty estimate are summarized below:

1. Plant Model Development

In this step, a WCOBRA/TRAC model of the KNPP is developed. A high level of nodding detail is used, in order to provide an accurate simulation of the transient. However, specific guidelines are followed to assure that the model is consistent with models used in the code validation. This results in a high level of consistency among plant models, except for specific areas dictated by hardware differences such as in the upper plenum of the reactor vessel or the ECCS injection configuration.

2. Determination of Plant Operating Conditions

In this step, the expected or desired range of the plant operating conditions to which the analysis applies is established. The parameters considered are based on a "key LOCA parameters" list that was developed as part of the methodology. A set of these parameters, at mostly nominal values, is chosen for input as initial conditions to the plant model. A split break in the cold leg (a longitudinal break along the side of the pipe) is modeled initially, as was determined to be limiting for a typical two-loop plant (Reference 12). A transient is run utilizing these parameters and is known as the "initial transient." Next, several confirmatory runs are made, which vary a subset of the key LOCA parameters over their expected operating range in one-at-a-time sensitivities. The results of these calculations for KNPP are discussed in Section 4 of Reference 13. The most limiting input conditions, based on these confirmatory runs, are then combined into a single transient, which is then called the "reference transient."

3. PWR Sensitivity Calculations

A series of PWR transients are performed in which the initial fluid conditions and boundary conditions are ranged around the nominal conditions used in the reference transient. The results of these calculations for KNPP form the basis for the determination of the initial condition bias and uncertainty discussed in Section 5 of Reference 13.

Next, a series of transients are performed which vary the power distribution, taking into account all possible power distributions during normal plant operation. The results of these calculations for KNPP form the basis for the determination of the power distribution bias and uncertainty (response surface) discussed in Section 6 of Reference 13.

Finally, a series of transients are performed which vary parameters that affect the overall system response (“global” parameters) and local fuel rod response (“local” parameters). The results of these calculations for KNPP form the basis for the determination of the model bias and uncertainty (response surface) discussed in Section 7 of Reference 13.

4. Response Surface Calculations

The results from the power distribution and global model WCOBRA/TRAC runs performed in Step 3 are fit by regression analyses into equations known as response surfaces. The results of the initial conditions run matrix are used to generate a PCT uncertainty distribution.

5. Uncertainty Evaluation

The total PCT uncertainty from the initial conditions, power distribution, and model calculations is derived using the approved methodology (Reference 12). The uncertainty calculations assume certain plant operating ranges which may be varied depending on the results obtained. These uncertainties are then combined to determine the initial estimate of the total PCT uncertainty distribution for the split and limiting guillotine breaks. The results of these initial estimates of the total PCT uncertainty are compared to determine the limiting break type. If the guillotine break is limiting, an additional set of guillotine transients are performed which vary overall system response (“global” parameters) and local fuel rod response (“local” parameters). The results of these calculations form the basis for the determination of the model bias and uncertainty for guillotine breaks discussed in Section 8 of Reference 13. Finally, an additional series of runs is made to quantify the bias and uncertainty due to assuming that the above three uncertainty categories are independent. The final PCT uncertainty distribution is then calculated for the limiting break type, and the 95th percentile PCT (PCT^{95%}) is determined, as described later under Uncertainty Evaluation.

6. Plant Operating Range

The plant operating range over which the uncertainty evaluation applies is defined. Depending on the results obtained in the above uncertainty evaluation, this range may be the desired range established in Step 2, or may be narrower for some parameters to gain additional margin.

There are three major uncertainty categories or elements:

- Initial condition bias and uncertainty
- Power distribution bias and uncertainty
- Model bias and uncertainty

Conceptually, these elements may be assumed to affect the reference transient PCT as shown below:

$$PCT_i = PCT_{REF,i} + \Delta PCT_{IC,i} + \Delta PCT_{PD,i} + \Delta PCT_{MOD,i} \quad (14.3.2-1)$$

where

$PCT_{REF,i}$ = Reference transient PCT: The reference transient PCT is calculated using WCOBRA/TRAC at the nominal conditions identified in Table 14.3.3-4, for the blowdown and reflood periods.

$\Delta PCT_{IC,i}$ = Initial condition bias and uncertainty: This bias is the difference between the reference transient PCT, which assumes several nominal or average initial conditions, and the average PCT taking into account all possible values of the initial conditions. This bias takes into account plant variations which have a relatively small effect on PCT. The elements which make up this bias and its uncertainty are plant-specific.

$\Delta PCT_{PD,i}$ = Power distribution bias and uncertainty: This bias is the difference between the reference transient PCT, which assumes a nominal power distribution, and the average PCT taking into account all possible power distributions during normal plant operation. Elements which contribute to the uncertainty of this bias are calculational uncertainties, and variations due to transient operation of the reactor.

$\Delta PCT_{MOD,i}$ = Model bias and uncertainty: This component accounts for uncertainties in the ability of the WCOBRA/TRAC code to accurately predict important phenomena which affect the overall system response (“global” parameters) and the local fuel rod response (“local” parameters). The code and model bias is the difference between the reference transient PCT, which assumes nominal values for the global and local parameters, and the average PCT taking into account all possible values of global and local parameters.

The separability of the bias and uncertainty components in the manner described above is an approximation, since the parameters in each element may be affected by parameters in other elements. The bias and uncertainty associated with this assumption is quantified as part of the overall uncertainty methodology and included in the final estimates of $PCT^{95\%}$.

14.3.2.3 Large-Break LOCA Analysis Results

A series of WCOBRA/TRAC calculations were performed using the KNPP input model, to determine the effect of variations in several key LOCA parameters on peak cladding temperature (PCT). From these studies, an assessment was made of the parameters that had a significant effect as will be described in the following sections.

14.3.2.3.1 LOCA Transient Description

The plant-specific analysis performed for the KNPP indicated that the split break is more limiting than the double-ended cold leg guillotine (DECLG) break. The plant conditions used in the split break reference transient are listed in Table 14.3.3-4. The results of the initial transient and the confirmatory calculations performed to determine the final reference transient are listed in Table 14.3.3-5. Note that the initial transient and confirmatory calculations were performed at a slightly lower power (1.4 percent lower) and a slightly larger T_{avg} operating window than the final reference transient. This was done to incorporate a mid-analysis request to reduce the calorimetric uncertainty from 2.0 percent to 0.6 percent. Neither change is considered to be a significant perturbation to the plant initial operating conditions and will not affect the relative outcome of the confirmatory and break spectrum calculations. Table 14.3.3-4 reflects the final reference transient conditions at the higher power. Since many of these parameters are at their bounded values, the calculated results are a conservative representation of the response to a large-break LOCA. The following is a description of the final reference transient.

The LOCA transient can be conveniently divided into a number of time periods in which specific phenomena are occurring. For a typical large break, the blowdown period can be divided into the critical heat flux (CHF) phase, the upward core flow phase, and the downward core flow phase. These are followed by the refill, reflood, and long term core cooling phases. The important phenomena occurring during each of these phases in the reference transient are discussed below.

The containment back pressure curve used in all of the calculations is calculated using the COCO code (Reference 5) and mass and energy releases from the WCOBRA/TRAC transient at the lower power. The parameters used in the containment analysis to determine this pressure are listed in Table 14.3.3-1 through Table 14.3.3-3. The mass and energy releases from the lower powered transient are shown in Table 14.3.3-6. These mass and energy releases were used to calculate the final containment pressure curve (Figure 14.3.2-1) used in the reference transient shown on Table 14.3.3-5 and all of the subsequent WCOBRA/TRAC calculations. This containment pressure was assessed to be a lower bound to pressure calculated using the mass and energy releases from the final reference transient at the final uprated power.

A subsequent evaluation was performed to assess the impact of additional metal introduced to the containment building due to the sump strainer modifications. It was concluded that the impact of the additional containment metal is bounded by the available margin in the analysis. Table 14.3.3-3 has been updated accordingly.

14.3.2.3.2 Critical Heat Flux (CHF) Phase (0–5 seconds)

The reactor coolant pumps are assumed to trip coincident with the break opening. Shortly after the break is assumed to open, the vessel depressurizes rapidly and the core flow decreases as subcooled liquid flows out of the vessel into the broken cold leg. The fuel rods go through departure from nucleate boiling (DNB) and the cladding rapidly heats up (Figure 14.3.2-3) while the core power shuts down due to voiding in the core. Control rod insertion is not modeled. The hot water in the core and upper plenum flashes to steam. The water in the upper head flashes and is forced down through the guide tubes. The break flow becomes saturated and is substantially reduced (Figure 14.3.2-4).

At approximately 4 seconds, the pressure in the pressurizer has fallen to the point where the SI signals are initiated.

14.3.2.3.3 Upward Core Flow Phase (4–8 seconds)

The colder water in the downcomer and lower plenum flashes, and the mixture swells. Since the intact loop pump is assumed to trip at the initiation of the break, it begins to coast down and does not serve to enhance upflow cooling by pushing fluid into the core. The upflow phase is short-lived for this reason. However, there is sufficient upflow cooling to begin significantly reducing the heat up in the fuel rods. As the lower plenum fluid depletes, upflow through the core ends (Figure 14.3.2-5).

14.3.2.3.4 Downward Core Flow Phase (8–30 seconds)

The break flow begins to dominate and pulls flow down through the core. Figure 14.3.2-5 shows the total core flow at the core midplane. The blowdown PCT of 1654°F occurs as the downflow increases in intensity and continues to decrease while downflow is sustained. At approximately 11 seconds, the pressure in the cold leg falls to the point where accumulators begin injecting cold water into the cold legs (Figure 14.3.2-6). Because the break flow is still high, much of the accumulator emergency core cooling system (ECCS) water entering the downcomer is bypassed out of the break. As the system pressure continues to decrease, the break flow, and consequently the core flow, is reduced. The break flow further reduces and the accumulator water begins to fill the downcomer and lower plenum. The core flow is nearly stagnant during this period and the hot assembly experiences a near adiabatic heat up.

14.3.2.3.5 Refill Phase (30–40 seconds)

The HHSI pump begins to inject (Figure 14.3.2-7) into the cold leg at approximately 34 seconds assuming a delay time of 30 seconds after the SI signal is initiated when a loss of offsite power is assumed. Since the break flow has significantly reduced by this time, much of the ECCS entering the downcomer via the cold leg is retained in the downcomer and refills the lower plenum. The LHSI pump is assumed to begin injecting (Figure 14.3.2-8) cold ECCS water into the upper plenum at approximately 39 seconds, assuming a delay of 35 seconds for the loss of offsite power case, after the SI signal has been actuated. The water enters the vessel at the hot leg

nozzle centerline elevation and falls down to the upper core plate through the outer global channels. The liquid drains down through the low power region via the open hole channel of the counter-current flow limiting (CCFL) region. The hot assembly experiences a nearly adiabatic heatup as the lower plenum fills with ECCS water (Figure 14.3.2-3 and Figure 14.3.2-10).

14.3.2.3.6 Reflood (40–250 seconds)

At approximately 40 seconds, the intact loop accumulator is empty of water, and begins injecting nitrogen into the cold leg (Figure 14.3.2-6). The insurge in the downcomer forces the downcomer liquid into the lower plenum and core regions (Figure 14.3.2-9 through Figure 14.3.2-11). During this time, core cooling is increased, and the hot assembly clad temperature decreases slightly.

The clad temperature in the hot assembly returns to nearly adiabatic heatup for about 30 seconds, until the core again begins to refill. The LHSI liquid flows down through the low power region and crossflows into the average assemblies near the bottom of the core. This water quenches the bottom of the core, which produces vapor that flows up through the average and hot assemblies, providing bottom-up cooling. The reflood PCT of 1763°F occurs at approximately 70 seconds.

14.3.2.3.7 Long Term Core Cooling

At the end of the WCOBRA/TRAC calculation, the core and downcomer levels are increasing as the pumped SI flow exceeds the break flow. The core and downcomer levels would be expected to continue to rise, until the downcomer mixture level approaches the loop elevation. At that point, the break flow would increase, until it roughly matches the injection flowrate. The core would continue to be cooled until the entire core is eventually quenched.

14.3.2.3.8 Confirmatory Sensitivity Studies

A number of sensitivity calculations were carried out to investigate the effect of the key LOCA parameters, and to develop the required data for the uncertainty evaluation. In the sensitivity studies performed, LOCA parameters were varied one at a time. For each sensitivity study, a comparison between the base case and the sensitivity case transient results was made.

The results of the sensitivity studies are summarized in Table 14.3.3-5 and Table 14.3.3-7. A full report on the results for all sensitivity study results is included in Section 4 of Reference 13. The results of these analyses lead to the following conclusions:

1. The limiting break type is a cold leg split break, and the limiting split break area is 0.7 times the area of a cold leg pipe ($C_D = 0.7$), which is 2.88 ft². This split break size is then modeled in the reference transient, as well as in the subsequent calculations used in the determination of uncertainties.
2. Modeling the pressurizer on the broken loop results in a higher PCT than modeling the pressurizer on the intact loop.

3. Modeling loss-of-offsite power (LOOP) results in a higher PCT than when the reactor coolant pumps are assumed to continue to run (no-LOOP).
4. Maximum steam generator tube plugging (10 percent) results in the highest PCT.
5. Modeling the minimum value of vessel average temperature ($T_{\text{avg}} = 556.3^{\circ}\text{F}$) results in the highest PCT.
6. Modeling the maximum power fraction ($P_{\text{LOW}} = 0.6$) in the low power/periphery channel of the core results in the highest PCT.

14.3.2.3.9 Initial Conditions Sensitivity Studies

Several calculations were performed to evaluate the effect of change in the initial conditions on the calculated LOCA transient. These calculations analyzed key initial plant conditions over their expected range of operation. These studies included effects of ranging RCS conditions (pressure and temperature), SI temperature, and accumulator conditions (pressure, temperature, volume, and line resistance). The results of these studies are presented in Section 5 of Reference 13.

The calculated results were used to develop initial condition uncertainty distributions for the blowdown and reflood peaks. These distributions are then used in the uncertainty evaluation to predict the PCT uncertainty component resulting from initial conditions uncertainty ($\Delta\text{PCT}_{\text{IC},i}$).

14.3.2.3.10 Power Distribution Sensitivity Studies

Several calculations were performed to evaluate the effect of power distribution on the calculated LOCA transient. The power distribution attributes which were analyzed are the peak linear heat rate relative to the core average, the maximum relative rod power, the relative power in the bottom third of the core (P_{BOT}), and the relative power in the middle third of the core (P_{MID}). The choice of these variables and their ranges are based on the expected range of plant operation. The ranges for each of these variables can be superimposed upon a scatter plot of all possible power shapes for a typical KNPP fuel cycle (including 18-month fuel cycles). The box surrounding the power shapes encompasses the range on P_{BOT} and P_{MID} that was analyzed with this power distribution run matrix, as shown in Section 6 of Reference 13.

The power distribution parameters used for the reference transient are biased to yield a relatively high PCT. The reference transient uses the maximum $F_{\Delta\text{H}}$, a skewed to the top power distribution, and a F_{Q} at the midpoint of the sample range.

A run matrix was developed in order to vary the power distribution attributes singly and in combination. The calculated results are presented in Section 6 of Reference 13. The sensitivity results indicated that power distributions with peak powers shifted towards the middle of the core produced higher PCTs as a result of some steam cooling in the top of the core for UPI plants.

The calculated results were used to develop response surfaces, as described in Step 4 of Section 14.3.2.2, which could be used to predict the change in PCT for various changes in the

power distributions for the blowdown and reflood peaks. These were then used in the uncertainty evaluation, to predict the PCT uncertainty component resulting from uncertainties in power distribution parameters, ($\Delta PCT_{PD,i}$).

14.3.2.4 Global Model Sensitivity Studies

Several calculations were performed to evaluate the effect of break flow path resistance and upper plenum drain distribution on the PCT for the split break with the limiting break area ($C_D = 0.7$). As in the power distribution study, these parameters were varied singly and in combination in order to obtain a data base which could be used for response surface generation. The run matrix and ranges of the break flow parameters are described in Reference 12. The limiting guillotine break was also identified using the methodology described in Reference 12. The plant specific calculated results are presented in Section 7 of Reference 13. The results of these studies indicated that the split break calculation resulted in much higher PCTs than the guillotine break calculations. Therefore, no further guillotine calculations needed to be performed.

The calculated results were used to develop response surfaces as described in Section 14.3.2.2, which could be used to predict the change in PCT for various changes in the flow conditions. These were then used in the uncertainty evaluation to predict the PCT uncertainty component resulting from uncertainties in global model parameters ($\Delta PCT_{MOD,i}$).

14.3.2.4.1 Uncertainty Evaluation and Results

The PCT equation was presented in Section 14.3.2.2. Each element of uncertainty is initially considered to be independent of the other. Each bias component is considered a random variable, whose uncertainty and distribution is obtained directly, or is obtained from the uncertainty of the parameters of which the bias is a function. For example, $\Delta PCT_{PD,i}$ is a function of F_Q , $F_{\Delta H}$, P_{BOT} , and P_{MID} . Its distribution is obtained by sampling the plant F_Q , $F_{\Delta H}$, P_{BOT} , and P_{MID} distributions and using a response surface to calculate $\Delta PCT_{PD,i}$. Since ΔPCT_1 is the sum of these biases, it also becomes a random variable. Separate initial PCT frequency distributions are constructed as follows for the split break and the limiting guillotine break size:

1. Generate a random value of each ΔPCT element.
2. Calculate the resulting PCT using Equation 14.3.2-1.
3. Repeat the process many times to generate a histogram of PCTs.

A final verification step is performed in which additional calculations (known as “superposition” calculations) are made with WCOBRA/TRAC, simultaneously varying several parameters which were previously assumed independent (for example, power distributions and models). Predictions using Equation 14.3.2-1 are compared to this data, and additional biases and uncertainties are applied.

The estimate of the PCT at 95 percent probability is determined by finding that PCT below which 95 percent of the calculated PCTs reside. This estimate is the licensing basis PCT, under the revised ECCS rule.

The results for the KNPP are given in Table 14.3.3-8, which shows the reflood 95th percentile PCT ($PCT^{95\%}$) of 2084°F. As expected, the difference between the 95 percent value and the average value increases with increasing time, as more parameter uncertainties come into play.

14.3.2.5 Evaluations

The transition from Siemens Standard/Heavy Fuel Assemblies to Westinghouse 14x14 Vantage+ fuel with Performance+ features (422V+) fuel has been evaluated for the effects of hydraulic mismatch and differences in fuel designs. The Reference Transient for the KNPP was used to determine the transition core effects.

Two additional calculations were performed for this assessment. For one calculation, the hot assembly was modeled with the fresh 422V+ fuel, surrounded by Siemens Heavy fuel, once burned. For the second calculation, the hot assembly was modeled with Siemens Heavy fuel (once burned), surrounded by fresh 422V+ assemblies. In both calculations, the low power/peripheral region was modeled with Siemens Heavy fuel (once burned). The results of the assessment indicate that the Best-Estimate analysis with a full core of 422V+ fuel for the KNPP bounds the transition core cycles.

14.3.2.6 Large-Break LOCA Conclusions

It must be demonstrated that there is a high level of probability that the limits set forth in 10 CFR 50.46 are met. The demonstration that these limits are met for the KNPP is as follows:

1. There is a high level of probability that the peak cladding temperature (PCT) shall not exceed 2200°F. The results presented in Table 14.3.3-8 indicate that this regulatory limit has been met with a reflood $PCT^{95\%}$ of 2084°F.
2. The maximum calculated local oxidation of the cladding shall nowhere exceed 0.17 times the total cladding thickness before oxidation. The approved Best-Estimate LOCA methodology assesses this requirement using a plant-specific transient which has a PCT in excess of the estimated 95 percentile PCT ($PCT^{95\%}$). Based on this conservative calculation, a maximum local oxidation of 8.44 percent is calculated, which meets the regulatory limit.
3. The calculated total amount of hydrogen generated from the chemical reaction of the cladding with water or steam shall not exceed 0.01 times the hypothetical amount that would be generated if all of the metal in the cladding cylinders surrounding the fuel were to react. The total amount of hydrogen generated, based on this conservative assessment is 0.0074 times the maximum theoretical amount, which meets the regulatory limit.

4. Calculated changes in core geometry shall be such that the core remains amenable to cooling. This requirement is met by demonstrating that the PCT does not exceed 2200°F, the maximum local oxidation does not exceed 17 percent, and the seismic and LOCA forces are not sufficient to distort the fuel assemblies to the extent that the core cannot be cooled. The BE UPI methodology (Reference 11 and Reference 12) specifies that the effects of LOCA and seismic loads on core geometry do not need to be considered unless grid crush extends to in-board assemblies. Fuel assembly structural analyses performed for Kewaunee indicate that this condition does not occur. Therefore, this regulatory limit is met.
5. After any calculated successful initial operation of the ECCS, the calculated core temperature shall be maintained at an acceptably low value and decay heat shall be removed for the extended period of time required by the long lived radioactivity remaining in the core. The conditions at the end of the WCOBRA/TRAC calculations indicates that the transition to long term cooling is underway even before the entire core is quenched.

14.3.2.6.1 SER Requirements

The SER requirements for three- and four-loop plants (Reference 11) have been met for this KNPP analysis. The BE UPI Evaluation Model has additional requirements to verify that the plant conditions fall within the range of conditions represented by the test simulations used for assessment of phenomena unique to upper plenum injection plants (Reference 15). Table 14.3.3-9 compares the plant conditions for KNPP to the test conditions utilized in the BE UPI methodology (Reference 12). From this table, it is clear that KNPP conditions fall within the range of test conditions. Thus, the BE UPI SER requirements have been met for Kewaunee.

14.3.2.6.2 Plant Operating Range

The expected PCT and its uncertainty developed above is valid for a range of plant operating conditions. In contrast to current Appendix K calculations, many parameters in the base case calculation are at nominal values. The range of variation of the operating parameters has been accounted for in the estimated PCT uncertainty. Table 14.3.3-10 and Figure 14.3.2-12 through Figure 14.3.2-14 summarize the operating ranges for the KNPP. If operation is maintained within these ranges, the LOCA analysis developed in Reference 13 is considered to be valid.

14.3.3 Core and Internals Integrity Analysis

The response of the reactor core and vessel internals under excitation produced by a simultaneous complete severance of a reactor coolant pipe and seismic excitation of typical two loop plant internals has been determined. A detailed description of the analysis applicable to the KNPP design appears in WCAP 7822, (Reference 1) Indian Point Unit 2 Reactor Internals Mechanical Analysis for Blowdown Excitation (Westinghouse Proprietary).

See Steam Generator Replacement and T_{avg} Operating Window Program Licensing Report (Reference 6), Section 5.2 for Updates to Internals Qualifications.

14.3.3.1 **Reactor Internals Response Under Blowdown and Seismic Excitation**

A LOCA may result from a rupture of reactor coolant piping. During the blowdown of the coolant, critical components of the core are subjected to vertical and horizontal excitation as a result of rarefaction waves propagating inside the reactor vessel.

For these large breaks, the reduction in water density greatly reduces the reactivity of the core, thereby shutting down the core whether the rods are tripped or not. (The subsequent refilling of the core by the Emergency Core Cooling System uses borated water to maintain the core in a sub-critical state.) Therefore, the main requirement is to assure effectiveness of the Emergency Core Cooling System. Insertion of the control rods, although not needed, gives further assurance of ability to shut the plant down and keep it in a safe shutdown condition.

The pressure waves generated within the reactor are highly dependent on the location and nature of the postulated pipe failure. In general, the more rapid the severance of the pipe, the more severe the imposed loadings on the components. A one-millisecond severance time is taken as the limiting case.

In the case of the hot leg break, the vertical hydraulic forces produce an initial upward lift of the core. A rarefaction wave propagates through the reactor hot leg nozzle into the interior of the upper core barrel. Since the wave has not reached the flow annulus on the outside of the barrel, the upper barrel is subjected to an impulsive compressive wave. Thus, dynamic instability (buckling) or large deflection of the upper core barrel or both is the possible response of the barrel during hot leg blowdown. In addition to the above effects, the hot leg break results in transverse loading on the upper core components as the fluid exits the hot leg nozzle.

In the case of the cold leg break, a rarefaction wave propagates along a reactor inlet pipe arriving first at the core barrel at the inlet nozzle of the broken loop. The upper barrel is then subjected to a nonaxisymmetric expansion radial impulse, which changes as the rarefaction wave propagates both around the barrel and down the outer flow annulus between vessel and barrel. After the cold leg break, the initial steady-state hydraulic lift forces (upward) decrease rapidly (within a few milliseconds) and then increase in the downward direction. These cause the reactor core and lower support structure to move initially downward.

If a simultaneous seismic event with the intensity of the design basis earthquake (DBE) is postulated with the LOCA, the imposed loading on the internals component may be additive in certain cases, and therefore, the combined loading must be considered. In general, however, the loading imposed by the earthquake is small compared to the blowdown loading.

14.3.3.2 **Acceptance Criteria for Results of Analyses**

The criteria for acceptability in regard to mechanical integrity analysis is that adequate core cooling and core shutdown must be assured. This implies that the deformation of the reactor internals must be sufficiently small so that the geometry remains substantially intact. Consequently, the limitations established on the internals are concerned principally with the

maximum allowable deflections and/or stability of the parts, in addition to a stress criterion, to assure integrity of the components.

14.3.3.3 Allowable Deflection and Stability Criteria

Upper Barrel - The upper barrel deformation has the following limits:

1. To insure a shutdown and cooldown of the core during blowdown, the basic requirement is a limitation on the outward deflection of the barrel at the locations of the inlet nozzles connected to the unbroken lines. A large outward deflection of the barrel in front of the inlet nozzles, accompanied with permanent strains, could close the inlet area and stop the cooling water coming from the accumulators. (The remaining distance between the barrel and the vessel inlet nozzle after the accident must be such that the inlet flow area be approximately the same as that of the accumulator pipes.) Consequently, a permanent barrel deflection in front of the unbroken inlet nozzles larger than a certain limit called the “no-loss of function” limit, could impair the efficiency of the Emergency Core Cooling System.
2. To assure rod insertion and to avoid disturbing the Control Rod Cluster guide structure, the barrel should not interfere with the guide tubes. This condition also requires a stability check to assure that the barrel will not buckle under the accident loads.

Control Rod Cluster Guide Tubes - The guide tubes in the upper core support package house the control rods. The deflection limits were established from tests.

Fuel Assembly - The limitations for this case are related to the stability of the thimbles in the upper end. The upper end of the thimbles shall not experience stresses above the allowable dynamic compressive stresses. Any buckling of the upper end of the thimbles due to axial compression could distort the guideline and thereby affect the free fall of the control rod.

Upper Package – The maximum allowable local deformation of the upper core plate where a guide tube is located is 0.100 inch. This deformation will cause the plate to contact the guide tube since the clearance between plate and guide tube is 0.100 inches. This limit will prevent the guide tubes from undergoing compression. For a plate local deformation of 0.150 inches, the guide tube will be compressed and deformed transversely to the upper limit previously established; consequently, the value of 0.150 inches is adopted as the no loss-of-function local deformation, with an allowable limit of 0.100 inches.

14.3.3.4 Allowable Stress Criteria

For this faulted condition, the allowable stress criteria is given by Figure 14.3-20. This figure defines various criteria based upon their corresponding method of analysis.

To account for multi-axial stresses, the Von Mises Theory is also considered.

14.3.3.5 Method of Analysis

14.3.3.5.1 Blowdown Model

BLODWN-2 is a digital computer program developed for the purpose of calculating local fluid pressure, flow, and density transients that occur in PWR coolant systems during a LOCA (Reference 2). This program applies to the sub-cooled, transition, and saturated two-phase blowdown regimes. BLODWN-2 is based on the method of characteristics wherein the resulting set of ordinary differential equations, obtained from the laws of conservation of mass, momentum, and energy, are solved numerically using a fixed mesh in both space and time.

Although spatially one-dimensional conservation laws are employed, the code can be applied to describe three-dimensional system geometries by use of the equivalent piping networks. Such piping networks may contain any number of pipes or channels of various diameters, dead ends, branches (with up to six pipes connected to each branch), contractions, expansions, orifices, pumps, and free surfaces (such as in the pressurizer). System losses such as friction, contraction, expansion, etc., are considered.

BLODWN-2 predictions have been compared with numerous test data as reported in WCAP-7401 (Reference 3). It is shown that the BLODWN-2 digital computer program correlates well with both the sub-cooled and the saturated blowdown regimes.

14.3.3.5.2 FORCE Model for Blowdown

BLODWN-2 evaluates the pressure and velocity transients for a maximum of 2400 locations throughout the system. These pressure and velocity transients are stored as a permanent tape file and are made available to the program FORCE which utilizes a detailed geometric description in evaluating the loadings on the reactor internals.

Each reactor component for which FORCE calculations are required is designated as an element and assigned an element number. Forces acting upon each of the elements are calculated summing the effects of:

- The pressure differential across the element
- Flow stagnation on, and unrecovered orifice losses across the element
- Friction losses along the element

Input to the code, in addition to the BLODWN-2 pressure and velocity transients includes the effective area of each element on which the force acts, due to the pressure differential across the element, a coefficient to account for flow stagnation, unrecovered orifice losses, and the total area of the element along which the shear forces act.

The mechanical analysis has been performed using conservative assumptions in order to obtain results with extra margin. Some of the most significant are:

- The mechanical and hydraulic analysis has been performed separately without including the effect of the water-solid interaction. Peak pressures obtained from the hydraulic analysis will be attenuated by the deformation of the structures.
- When applying the hydraulic forces, no credit is taken for the stiffening effect of the fluid environment, which will reduce the deflections and stresses in the structure.
- The multi-mass model described below is considered to have a sufficient number of degrees of freedom to represent the most important modes of vibration in the vertical direction. This model is conservative in the sense that further mass-spring resolution of the system would lead to further attenuation of the shock effects obtained with the present model.

14.3.3.5.3 Method of Blowdown Re-Analysis

Re-analysis performed in support of increased full power primary coolant temperature range and new fuel products (such as Siemens-Designed 14 x 14 fuel) have made use of the MULTIFLEX (Reference 4 and Reference 5) computer code, rather than BLOWDN-2 described above. These analyses use the FORCE2 computer code (described in Reference 5) to post process MULTIFLEX hydraulic transient results into vertical forces as described above for the FORCE code. Lateral forces are computed using the LATFORC code (described in Reference 5). Additional details of these re-analysis are found in Section 6.5 of the Steam Generator Replacement and T_{avg} Operating Window Program Licensing Report (Reference 6). As described in Section 5.2 of Reference 6, the core and internals integrity calculations found the re-analysis loads to remain bounded by the calculations described above.

14.3.3.5.4 Vertical Excitation Model for Blowdown

For the vertical excitation, the reactor internals are represented by a multi-mass system connected with springs and dashpots simulating the elastic response and the viscous damping of the components. Also incorporated in the multi-mass system is a representation of the motion of the fuel elements relative to the fuel assembly grids. The fuel elements in the fuel assemblies are kept in position by friction forces originating from the preloaded fuel assembly grid fingers. Coulomb-type friction is assumed in the event that sliding between the rods and the grid fingers occurs. Figure 14.3-19 shows the spring-mass system used to represent the internals. In order to obtain an accurate simulation of the reactor internals response, the effects of internal damping, clearances between various internals, snubbing action caused by solid impact, Coulomb friction induced by fuel rods motion relative to the grids, and pre-loads in hold-down springs have been incorporated in the analytical model. The reactor vessel is regarded as a fixed base while the internals undergo relative displacement with respect to their initial position. The modeling is conducted in such a way that uniform masses are lumped into easily identifiable discrete masses

while elastic elements are represented by springs. Table 14.3-3 lists the various masses, springs, etc.

The appropriate dynamic differential equations for the multi-mass model describing the aforementioned phenomena are formulated and the results obtained using a digital computer program which computes the response of the multi-mass model when excited by a set of time dependent forcing functions. The appropriate forcing functions are applied simultaneously and independently to each of the masses in the system. The results from the program give the forces, displacements and deflections as functions of time for all the reactor internals components (lumped masses). Reactor internals response to both hot and cold leg pipe ruptures are analyzed. The forcing functions used in the study are obtained from hydraulic analyses of the pressure and flow distribution around the entire RCS as caused by double-ended severance of a RCS pipe.

14.3.3.5.5 Vertical Excitation Model for Earthquake

As shown in WCAP-7822 (Reference 1) the reactor internals are modeled as a single degree-of-freedom system for vertical earthquake analysis. The maximum acceleration at the vessel support is increased by amplification due to the building-soil interaction.

14.3.3.5.6 Transverse Excitation Model for Blowdown

Various reactor internal components are subjected to transverse excitation during blowdown. Specifically, the barrel, guide tubes, and upper support columns are analyzed to determine their response to this excitation.

14.3.3.5.7 Core Barrel

For the hydraulic analysis of the pressure transients during hot leg blowdown, the maximum pressure drop across the barrel is a uniform radial compressive impulse. The barrel is then analyzed for dynamic buckling using these conditions and the following conservative assumptions:

- The effect of the fluid environment is neglected (water stiffening is not considered).
- The shell is treated as simply supported.

During cold leg blowdown, the upper barrel is subjected to a nonaxisymmetric expansion radial impulse, which changes as the rarefaction wave propagates both around the barrel and down the outer flow annulus between vessel and barrel.

The analysis of transverse barrel response to cold leg blowdown is performed as follows:

1. The upper core barrel is treated as a simply supported cylindrical shell of constant thickness between the upper flange weldment and the lower core barrel weldment without taking credit for the supports at the barrel mid-span offered by the outlet nozzles. This assumption leads to conservative deflection estimates of the upper core barrel.

2. The upper core barrel is analyzed as a shell with four variable sections to model the support flange, upper barrel, reduced weld section, and a portion of the lower core barrel.
3. The barrel with the core and thermal shield is analyzed as a beam fixed at the top and elastically supported at the lower radial support and the dynamic response is obtained.

Guide Tubes - The dynamic loads on RCC guide tubes are more severe for a LOCA caused by hot leg rupture than for an accident by cold leg rupture since the cold leg break leads to much smaller changes in the transverse coolant flow over the RCC guide tubes. Thus, the analysis is performed only for a hot leg blowdown.

The guide tubes in closest proximity to the ruptured outlet nozzle are the most severely loaded. The transverse guide tube forces during the hot leg blowdown decrease with increasing distance from the ruptured nozzle location.

A detailed structural analysis of the RCC guide tubes was performed to establish the equivalent cross-section properties and elastic and support conditions. An analytical model was verified both dynamically and statically by subjecting the control rod cluster guide tube to a concentrated force applied at the transition plate. In addition, the guide tube was loaded experimentally using a triangular distribution to conservatively approximate the hydraulic loading. The experimental results consisted of a load deflection curve for the RCC guide tube plus verification of the deflection criteria to assure RCC insertion.

The response of the guide tubes to the transient loading due to blowdown may be found by utilizing the equivalent single freedom system for the guide tube using experimental results for equivalent stiffness and natural frequency.

The time dependence of the hydraulic transient loading has the form of a step function with constant slope front with a rise time to peak force of the same order of the guide tube fundamental period in water. The dynamic application factor in determining the response is a function of the ramp impulse rise time divided by the period of the structure.

Upper Support Columns - Upper support columns located close to the broken nozzle during hot leg break will be subjected to transverse loads due to cross flow.

The loads applied to the columns were computed with a similar method to the one for the guide tubes, i.e., taking into consideration the increase in flow across the column during the accident. The columns were studied as beams with variable section and the resulting stresses were obtained using the reduced section modulus at the slotted portions.

14.3.3.5.8 Transverse Excitation Model for Earthquake

The reactor building with the reactor vessel support, the reactor vessel, and the reactor internals are included in this analysis. The mathematical model of the building, attached to ground, is identical to that used to evaluate the building structure. The reactor internals are mathematically modeled by beams, concentrated masses and linear springs.

All masses, water and metal are included in the mathematical model. All beam elements have the component weight or mass distribution uniformly, e.g., the fuel assembly-mass and barrel mass. Additionally, wherever components are attached uniformly their mass is included as an additional uniform mass, e.g., baffles and formers acting on the core barrel. The water near and about the beam elements is also included as a distributed mass. Horizontal components are considered as a concentrated mass acting on the barrel. This concentrated mass also includes components attached to the horizontal members, since these are the media through which the reaction is transmitted. The water near and about these separated components is considered as being additive at these concentrated mass points.

The concentrated masses attached to the barrel represent the following:

- the upper core support structure, including the upper vessel head and one-half the upper internals,
- the upper core plate, including one-half the thermal shield and the other one-half of the upper internals,
- the lower core plate, including one-half of the lower core support columns,
- the lower one-half of the thermal shield, and
- the lower core support, including the lower instrumentation and the remaining half of the lower core support columns.

The modulus of elasticity is chosen at its hot value for the three major materials found in the vessel, internals, and fuel assemblies. In considering shear deformation, the appropriate cross-sectional area is selected along with a value for Poisson's ratio. The fuel assembly moment of inertia is derived from experimental results by static and dynamic tests performed on fuel assembly modes. These tests provide stiffness values for use in this analysis.

The fuel assemblies are assumed to act together and are represented by a single beam. The following assumptions are made in regard to connection restraints. The vessel is pinned to the vessel support and part of the containment building. The barrel is clamped to the vessel at the barrel flange and spring-connected to the vessel at the lower core barrel radial support. This spring corresponds to the radial support stiffness for two opposite supports acting together. The beam representing the fuel assemblies is pinned to the barrel at the locations of the upper and lower core plates.

The response spectrum method has been used in the calculation. After computing the transverse natural frequency and obtaining the normal modes of the complete structure, the maximum response is obtained from the superposition of the usual mode response with the conservative assumptions that all the modes are in phase and that all the peaks occur simultaneously.

14.3.3.5.9 Conclusions - Mechanical Analysis

The results of the analysis applicable to the Kewaunee design are presented in Table 14.3-4 and Table 14.3-5. These tables summarize the maximum deflections and stresses for blowdown, seismic, and blowdown plus seismic loadings.

The stresses due to the DBE (vertical and horizontal components) were combined in the most unfavorable manner with the blowdown stresses in order to obtain the largest principal stress and deflection.

These results indicate that the maximum deflections and stress in the critical structures are below the established allowable limits. For the transverse excitation, it is shown that the upper barrel does not buckle during a hot leg break and that it has an allowable stress distribution during a cold leg break. Section 5.9, under Primary Piping, discusses the restraints which were added to restrain the reactions of jet forces in the primary loop piping caused by pipe rupture, to limit the LOCA loads.

Even though control rod insertion is not required for plant shutdown, this analysis shows that most of the guide tubes will deform within the limits established experimentally to assure control rod insertion with the exceptions shown in Table 14.3-4. It can be seen in the table that 31 of the 33 guide tubes are below the NLF limit. For those guide tubes deflected above the NLF limit, it must be assumed that the rods will not drop. However, the conclusion reached is that the core will shutdown in an orderly fashion due to the formation of voids, and this orderly shutdown will be aided by the great majority of rods that do drop.

14.3.4 Containment Integrity Evaluation

14.3.4.1 Long Term LOCA Mass and Energy Releases

The uncontrolled release of pressurized high-temperature reactor coolant, termed a LOCA, will result in release of steam and water into the containment. This, in turn, will result in increases in the local subcompartment pressures, and an increase in the global containment pressure and temperature. Therefore, there are both long- and short-term issues reviewed relative to a postulated LOCA that must be considered for the KNPP.

The long-term LOCA mass and energy releases are analyzed to approximately 10^6 seconds and are utilized as input to the containment integrity analysis. This demonstrates the acceptability of the containment safeguards systems to mitigate the consequences of a hypothetical large-break LOCA. The containment safeguards systems must be capable of limiting the peak containment pressure to less than 46 psig. For this program, Westinghouse generated the mass and energy releases using the March 1979 model, described in Reference 1. The NRC review and approval letter is included with Reference 1. The following sections discuss the long-term LOCA mass and energy releases. The results of this analysis were provided for use in the containment integrity analysis.

14.3.4.1.1 Input Parameters and Assumptions

The mass and energy release analysis is sensitive to the assumed characteristics of various plant systems, in addition to other key modeling assumptions. Where appropriate, bounding inputs are utilized and instrumentation uncertainties are included. For example, the RCS operating temperatures are chosen to bound the highest average coolant temperature range of all operating cases and a temperature uncertainty allowance of (+6.0°F) is then added. Nominal parameters are used in certain instances. For example, the RCS pressure in this analysis is based on a nominal value of 2250 psia plus an uncertainty allowance (+50.1 psi). All input parameters are chosen consistent with accepted analysis methodology.

Some of the most critical items are the RCS initial conditions, core decay heat, SI flow, and primary and secondary metal mass and steam generator heat release modeling. Specific assumptions concerning each of these items are discussed in the following paragraphs. Table 14.3.4-1 through Table 14.3.4-3 present key data assumed in the analysis.

The core rated power of 1782.6 MWt adjusted for calorimetric error (i.e., 100.6 percent of 1772 MWt) was used in the analysis. As previously noted, the use of RCS operating temperatures to bound the highest average coolant temperature range were used as bounding analysis conditions. The use of higher temperatures is conservative because the initial fluid energy is based on coolant temperatures that are at the maximum levels attained in steady-state operation. Additionally, an allowance to account for instrument error and deadband is reflected in the initial RCS temperatures. The selection of 2250 psia as the limiting pressure is considered to affect the blowdown phase results only, since this represents the initial pressure of the RCS. The RCS rapidly depressurizes from this value until the point at which it equilibrates with containment pressure.

The rate at which the RCS blows down is initially more severe at the higher RCS pressure. Additionally the RCS has a higher fluid density at the higher pressure (assuming a constant temperature) and subsequently has a higher RCS mass available for releases. Thus, 2250 psia plus uncertainty was selected for the initial pressure as the limiting case for the long-term mass and energy release calculations.

The selection of the fuel design features for the long-term mass and energy release calculation is based on the need to conservatively maximize the energy stored in the fuel at the beginning of the postulated accident (i.e., to maximize the core stored energy). The core stored energy that was selected was 4.68 full power seconds (FPS). The margins in the core stored energy include +15 percent in order to address the thermal fuel model and associated manufacturing uncertainties and the time in the fuel cycle for maximum fuel densification. Thus, the analysis very conservatively accounts for the stored energy in the core.

Margin in RCS volume of 3 percent (which is composed of 1.6 percent allowance for thermal expansion and 1.4 percent allowance for uncertainty) was modeled.

A uniform steam generator tube plugging level of 0 percent was modeled. This assumption maximizes the reactor coolant volume and fluid release by virtue of consideration of the RCS fluid in all steam generator tubes. During the post-blowdown period, the steam generators are active heat sources since significant energy remains in the secondary metal and secondary mass that has the potential to be transferred to the primary side. The 0 percent tube plugging assumption maximizes the heat transfer area and, therefore, the transfer of secondary heat across the steam generator tubes. Additionally, this assumption reduces the reactor coolant loop resistance, which reduces the ΔP upstream of the break for the pump suction breaks and increases break flow. Thus, the analysis conservatively accounts for the level of steam generator tube plugging.

The secondary-to-primary heat transfer is maximized by assuming conservative heat transfer coefficients. This conservative energy transfer is ensured by maximizing the initial internal energy of the inventory in the steam generator secondary side. This internal energy is based on full-power operation plus uncertainties.

Regarding SI flow, the mass and energy release calculation considered configurations/failures to conservatively bound respective alignments. The cases include: a) a minimum safeguards case (one HHSI and one LHSI pump) (see Table 14.3.4-2); and b) a maximum safeguards case, (two HHSI and two LHSI pumps) (see Table 14.3.4-3). In addition, the containment backpressure is assumed to be equal to the containment design pressure. This assumption was shown in Reference 1 to be conservative for the generation of mass and energy releases.

In summary, the following assumptions were employed to ensure that the mass and energy releases are conservatively calculated, thereby maximizing energy release to containment:

1. Maximum expected operating temperature of the RCS (100 percent full-power conditions)
2. Allowance for RCS temperature uncertainty (+6.0°F)
3. Margin in RCS volume of 3 percent (which is composed of 1.6 percent allowance for thermal expansion, and 1.4 percent allowance for uncertainty)
4. Core rated power of 1772 MWt
5. Allowance for calorimetric error (+0.6 percent of power)
6. Conservative heat transfer coefficients (i.e., steam generator primary/secondary heat transfer, and RCS metal heat transfer)
7. Allowance in core stored energy for effect of fuel densification
8. A margin in core stored energy (+15 percent to account for manufacturing tolerances)
9. An allowance for RCS initial pressure uncertainty (+50.1 psi)
10. A maximum containment backpressure equal to 46 psig

11. Steam generator tube plugging leveling (0 percent uniform)

- Maximizes reactor coolant volume and fluid release
- Maximizes heat transfer area across the steam generator tubes
- Reduces coolant loop resistance, which reduces the ΔP upstream of the break for the pump suction breaks and increases break flow

Thus, based on the previously discussed conditions and assumptions, an analysis of Kewaunee was made for the release of mass and energy from the RCS in the event of a LOCA at 1782.6 MWt.

14.3.4.1.2 Description of Analyses

The evaluation model used for the long-term LOCA mass and energy release calculations is the March 1979 model described in Reference 1.

This report section presents the long-term LOCA mass and energy releases generated in support of the Kewaunee SGR Program. These mass and energy releases are then subsequently used in the containment integrity analysis.

The mass and energy release rates described form the basis of further computations to evaluate the containment following the postulated accident. Discussed in this section are the long-term LOCA mass and energy releases for the hypothetical double-ended pump suction (DEPS) rupture with minimum safeguards and maximum safeguards and double-ended hot leg (DEHL) rupture break cases. The mass and energy releases for these three cases are presented in Section 6.4.1.1 of Reference 8. Section 6.4.1.1 of Reference 8 is considered to be incorporated by reference into the KPS USAR. These three LOCA cases are used for the long-term containment integrity analyses in Section 14.3.4.2.

14.3.4.1.3 LOCA Mass and Energy Release Phases

The containment system receives mass and energy releases following a postulated rupture in the RCS. These releases continue over a time period, which, for the LOCA mass and energy analysis, is typically divided into four phases.

1. Blowdown – the period of time from accident initiation (when the reactor is at steady-state operation) to the time that the RCS and containment reach an equilibrium state.
2. Refill – the period of time when the lower plenum is being filled by accumulator and emergency core cooling system (ECCS) water. At the end of blowdown, a large amount of water remains in the cold legs, downcomer, and lower plenum. To conservatively consider the refill period for the purpose of containment mass and energy releases, it is assumed that

this water is instantaneously transferred to the lower plenum along with sufficient accumulator water to completely fill the lower plenum. This allows an uninterrupted release of mass and energy to containment. Thus, the refill period is conservatively neglected in the mass and energy release calculation.

3. Reflood – begins when the water from the lower plenum enters the core and ends when the core is completely quenched.
4. Post-reflood (Froth) – describes the period following the reflood phase. For the pump suction break, a two-phase mixture exits the core, passes through the hot legs, and is superheated in the steam generators prior to exiting the break as steam. After the broken loop steam generator cools, the break flow becomes two phase.

14.3.4.1.4 Computer Codes

The Reference 1 mass and energy release evaluation model is comprised of mass and energy release versions of the following codes: SATAN VI, WREFLOOD, FROTH, and EPITOME. These codes were used to calculate the long-term LOCA mass and energy releases for Kewaunee.

SATAN VI calculates blowdown, the first portion of the thermal-hydraulic transient following break initiation, including pressure, enthalpy, density, mass and energy flow rates, and energy transfer between primary and secondary systems as a function of time.

The WREFLOOD code addresses the portion of the LOCA transient where the core reflooding phase occurs after the primary coolant system has depressurized (blowdown) due to the loss of water through the break and when water supplied by the ECCS refills the reactor vessel and provides cooling to the core. The most important feature of WREFLOOD is the steam/water mixing model.

FROTH models the post-reflood portion of the transient. The FROTH code is used for the steam generator heat addition calculation from the broken and intact loop steam generators.

EPITOME continues the FROTH post-reflood portion of the transient from the time at which the secondary equilibrates to containment design pressure to the end of the transient. It also compiles a summary of data on the entire transient, including formal instantaneous mass and energy release tables and mass and energy balance tables with data at critical times.

14.3.4.1.5 Break Size and Location

Generic studies have been performed with respect to the effect of postulated break size on the LOCA mass and energy releases. The double-ended guillotine break has been found to be limiting due to larger mass flow rates during the blowdown phase of the transient. During the reflood and froth phases, the break size has little effect on the releases.

Three distinct locations in the RCS loop can be postulated for a pipe rupture for mass and energy release purposes:

- Hot leg (between vessel and steam generator)
- Cold leg (between pump and vessel)
- Pump suction (between steam generator and pump)

The break locations analyzed for this program are the DEPS rupture (10.46 ft²) and the DEHL rupture (9.154 ft²). Break mass and energy releases have been calculated for the blowdown, reflood, and post-reflood phases of the LOCA for the DEPS cases. For the DEHL case, the releases were calculated only for the blowdown. The following information provides a discussion on each break location.

The DEHL rupture has been shown in previous studies to result in the highest blowdown mass and energy release rates. Although the core flooding rate would be the highest for this break location, the amount of energy released from the steam generator secondary is minimal because the majority of the fluid that exits the core vents directly to containment bypassing the steam generators. As a result, the reflood mass and energy releases are reduced significantly as compared to either the pump suction or cold leg break locations where the core exit mixture must pass through the steam generators before venting through the break. For the hot leg break, generic studies have confirmed that there is no reflood peak (i.e., from the end of the blowdown period the containment pressure would continually decrease). Therefore, only the mass and energy releases for the hot leg break blowdown phase are calculated and presented in this section of the report.

The cold leg break location has also been found in previous studies to be much less limiting in terms of the overall containment energy releases. The cold leg blowdown is faster than that of the pump suction break, and more mass is released into the containment. However, the core heat transfer is greatly reduced, and this results in a considerably lower energy release into containment. Studies have determined that the blowdown transient for the cold leg is, in general, less limiting than that for the pump suction break. During reflood, the flooding rate is greatly reduced and the energy release rate into the containment is reduced. Therefore, the cold leg break is bounded by other breaks and no further evaluation is necessary.

The pump suction break combines the effects of the relatively high core flooding rate, as in the hot leg break, and the addition of the stored energy in the steam generators. As a result, the pump suction break yields the highest energy flow rates during the post-blowdown period by including all of the available energy of the RCS in calculating the releases to containment. Thus, only the DEHL and DEPS cases are used to analyze long-term LOCA containment integrity.

14.3.4.1.6 Application of Single-Failure Criterion

An analysis of the effects of the single-failure criterion has been performed on the mass and energy release rates for each break analyzed. An inherent assumption in the generation of the mass and energy release is that offsite power is lost. This results in the actuation of the emergency diesel generators, required to power the SIS. This is not an issue for the blowdown period, which is limited by the DEHL break.

Two cases have been analyzed to assess the effects of a single failure. The first case assumes minimum safeguards SI flow based on the postulated single failure of an emergency diesel generator. This results in the loss of one train of safeguards equipment. The other case assumes maximum safeguards SI flow based on no postulated failures that would impact the amount of ECCS flow. The analysis of the cases described provides confidence that the effect of credible single failures is bounded.

14.3.4.1.7 Acceptance Criteria for Analyses

A large-break LOCA is classified as an American Nuclear Society (ANS) Condition IV event, an infrequent fault. To satisfy the NRC acceptance criteria presented in the Standard Review Plan, Section 6.2.1.3, the relevant requirements are the following:

- 10 CFR 50, Appendix A
- 10 CFR 50, Appendix K, Paragraph I.A

To meet these requirements, the following must be addressed:

- Sources of energy
- Break size and location
- Calculation of each phase of the accident

14.3.4.1.8 Blowdown Mass and Energy Release Data

The SATAN-VI code is used for computing the blowdown transient. The code utilizes the control volume (element) approach with the capability for modeling a large variety of thermal fluid system configurations. The fluid properties are considered uniform and thermodynamic equilibrium is assumed in each element. A point kinetics model is used with weighted feedback effects. The major feedback effects include moderator density, moderator temperature, and Doppler broadening. A critical flow calculation for subcooled (modified Zaloudek), two-phase (Moody), or superheated break flow is incorporated into the analysis. The methodology for the use of this model is described in Reference 1.

Section 6.4.1.1 of Reference 8 presents the calculated mass and energy release for the blowdown phase of the DEHL break for Kewaunee. For the hot leg break mass and energy release tables, Break Path 1 refers to the mass and energy exiting from the reactor vessel side of the

break; Break Path 2 refers to the mass and energy exiting from the steam generator side of the break.

Section 6.4.1.1 of Reference 8 presents the calculated mass and energy releases for the blowdown phase of the DEPS break. For the pump suction breaks, Break Path 1 in the mass and energy release tables refers to the mass and energy exiting from the steam generator side of the break. Break Path 2 refers to the mass and energy exiting from the pump side of the break.

14.3.4.1.9 Reflood Mass and Energy Release Data

The WREFLOOD code is used for computing the reflood transient. The WREFLOOD code consists of two basic hydraulic models — one for the contents of the reactor vessel and one for the coolant loops. The two models are coupled through the interchange of the boundary conditions applied at the vessel outlet nozzles and at the top of the downcomer. Additional transient phenomena such as pumped SI and accumulators, reactor coolant pump performance, and steam generator release are included as auxiliary equations that interact with the basic models as required. The WREFLOOD code permits the capability to calculate variations during the core reflooding transient of basic parameters such as core flooding rate, core and downcomer water levels, fluid thermodynamic conditions (pressure, enthalpy, density) throughout the primary system, and mass flow rates through the primary system. The code permits hydraulic modeling of the two flow paths available for discharging steam and entrained water from the core to the break, i.e., the path through the broken loop and the path through the unbroken loops.

A complete thermal equilibrium mixing condition for the steam and ECCS injection water during the reflood phase has been assumed for each loop receiving ECCS water. This is consistent with the usage and application of the Reference 1 mass and energy release evaluation model in recent analyses, e.g., D. C. Cook Docket (Reference 3). Even though the Reference 1 model credits steam/water mixing only in the intact loop and not in the broken loop, the justification, applicability, and NRC approval for using the mixing model in the broken loop has been documented (Reference 3). Moreover, this assumption is supported by test data and is further discussed below.

The model assumes a complete mixing condition (i.e., thermal equilibrium) for the steam/water interaction. The complete mixing process, however, is made up of two distinct physical processes. The first is a two-phase interaction with condensation of steam by cold ECCS water. The second is a single-phase mixing of condensate and ECCS water. Since the steam release is the most important influence to the containment pressure transient, the steam condensation part of the mixing process is the only part that need be considered. (Any spillage directly heats only the sump.)

The most applicable steam/water mixing test data have been reviewed for validation of the containment integrity reflood steam/water mixing model. This data was generated in 1/3-scale tests (Reference 4), which are the largest scale data available and thus most clearly simulates the flow regimes and gravitational effects that would occur in a pressurized water reactor (PWR).

These tests were designed specifically to study the steam/water interaction for PWR reflood conditions.

A group of 1/3-scale tests corresponds directly to containment integrity reflood conditions. The injection flow rates for this group cover all phases and mixing conditions calculated during the reflood transient. The data from these tests were reviewed and discussed in detail in Reference 1. For all of these tests, the data clearly indicate the occurrence of very effective mixing with rapid steam condensation. The mixing model used in the containment integrity reflood calculation is, therefore, wholly supported by the 1/3-scale steam/water mixing data.

Additionally, the following justification is also noted. The post-blowdown limiting break for the containment integrity peak pressure analysis is the pump suction double-ended rupture break. For this break, there are two flow paths available in the RCS by which mass and energy may be released to containment. One is through the outlet of the steam generator, the other via reverse flow through the reactor coolant pump. Steam that is not condensed by ECCS injection in the intact RCS loops passes around the downcomer and through the broken loop cold leg and pump in venting to containment. This steam also encounters ECCS injection water as it passes through the broken loop cold leg, complete mixing occurs and a portion of it is condensed. It is this portion of steam that is condensed that is taken credit for in this analysis. This assumption is justified based upon the postulated break location, and the actual physical presence of the ECCS injection nozzle. A description of the test and test results are contained in Reference 1 and Reference 3.

Section 6.4.1.1 of Reference 8 presents the calculated mass and energy releases for the reflood phase of the pump suction double-ended rupture, minimum safeguards, and maximum safeguards cases, respectively.

The transient response of the principal parameters during reflood are given in Section 6.4.1.1 of Reference 8 for the DEPS cases.

14.3.4.1.10 Post-Reflood Mass and Energy Release Data

The FROTH code (Reference 2) is used for computing the post-reflood transient. The FROTH code calculates the heat release rates resulting from a two-phase mixture present in the steam generator tubes. The mass and energy releases that occur during this phase are typically superheated due to the depressurization and equilibration of the broken loop and intact loop steam generators. During this phase of the transient, the RCS has equilibrated with the containment pressure. However, the steam generators contain a secondary inventory at an enthalpy that is much higher than the primary side. Therefore, there is a significant amount of reverse heat transfer that occurs. Steam is produced in the core due to core decay heat. For a pump suction break, a two-phase fluid exits the core, flows through the hot legs, and becomes superheated as it passes through the steam generator. Once the broken loop cools, the break flow becomes two phase. During the FROTH calculation, ECCS injection is addressed for both the injection phase and the recirculation phase. The FROTH code calculation stops when the secondary side equilibrates to

the saturation temperature (T_{sat}) at the containment design pressure, after this point the EPITOME code completes the steam generator depressurization.

The methodology for the use of this model is described in Reference 1. The mass and energy release rates are calculated by FROTH and EPITOME until the time of containment depressurization. After containment depressurization (14.7 psia), the mass and energy release available to containment is generated directly from core boil-off/decay heat.

Section 6.4.1.1 of Reference 8 presents the two-phase post-reflood mass and energy release data for the pump suction double-ended break cases.

14.3.4.1.11 Decay Heat Model

On November 2, 1978, the Nuclear Power Plant Standards Committee (NUPPSCO) of the ANS approved ANS Standard 5.1 (Reference 5) for the determination of decay heat. This standard was used in the mass and energy release model for Kewaunee. Section 6.4.1.1 of Reference 8 presents the decay heat curve used in the Kewaunee mass and energy release analysis.

Significant assumptions in the generation of the decay heat curve for use in the LOCA mass and energy releases analysis include the following:

1. The decay heat sources considered are fission product decay and heavy element decay of U-239 and Np-239.
2. The decay heat power from fissioning isotopes other than U-235 is assumed to be identical to that of U-235.
3. The fission rate is constant over the operating history of maximum power level.
4. The factor accounting for neutron capture in fission products has been taken from Reference 5.
5. The fuel has been assumed to be at full power for 10^8 seconds.
6. The total recoverable energy associated with one fission has been assumed to be 200 MeV/fission.
7. Two sigma uncertainty (two times the standard deviation) has been applied to the fission product decay.

Based upon NRC staff review, (Safety Evaluation Report [SER] of the March 1979 evaluation model [Reference 1]), use of the ANS Standard-5.1, November 1979 decay heat model was approved for the calculation of mass and energy releases to the containment following a LOCA.

14.3.4.1.12 Steam Generator Equilibration and Depressurization

Steam generator equilibration and depressurization is the process by which secondary-side energy is removed from the steam generators in stages. The FROTH computer code calculates the heat removal from the secondary mass until the secondary temperature is the saturation temperature (T_{sat}) at the containment design pressure. After the FROTH calculations, the EPITOME code continues the FROTH calculation for steam generator cooldown removing steam generator secondary energy at different rates (i.e., first- and second-stage rates). The first-stage rate is applied until the steam generator reaches T_{sat} at the user specified intermediate equilibration pressure, when the secondary pressure is assumed to reach the actual containment pressure. Then the second-stage rate is used until the final depressurization, when the secondary reaches the reference temperature of T_{sat} at 14.7 psia, or 212°F. The heat removal of the broken loop and intact loop steam generators are calculated separately.

During the FROTH calculations, steam generator heat removal rates are calculated using the secondary-side temperature, primary-side temperature and a secondary-side heat transfer coefficient determined using a modified McAdam's correlation. Steam generator energy is removed during the FROTH transient until the secondary-side temperature reaches saturation temperature at the containment design pressure. The constant heat removal rate used during the first heat removal stage is based on the final heat removal rate calculated by FROTH. The steam generator energy available to be released during the first stage interval is determined by calculating the difference in secondary energy available at the containment design pressure and that at the (lower) user-specified intermediate equilibration pressure, assuming saturated conditions. This energy is then divided by the first-stage energy removal rate, resulting in an intermediate equilibration time. At this time, the rate of energy release drops substantially to the second-stage rate. The second-stage rate is determined as the fraction of the difference in secondary energy available between the intermediate equilibration and final depressurization at 212°F, and the time difference from the time of the intermediate equilibration to the user-specified time of the final depressurization at 212°F. With current methodology, all of the secondary energy remaining after the intermediate equilibration is conservatively assumed to be released by imposing a mandatory cooldown and subsequent depressurization down to atmospheric pressure at 3600 seconds, i.e., 14.7 psia and 212°F (the mass and energy balance tables have this point labeled as "Available Energy").

14.3.4.1.13 Sources of Mass and Energy

The sources of mass considered in the LOCA mass and energy release analysis are the RCS, accumulators, and pumped SI.

The energy sources considered in the LOCA mass and energy release analysis are the following:

- RCS water
- Accumulator water (both inject)
- Pumped SI water
- Decay heat
- Core-stored energy
- RCS metal (includes steam generator tubes)
- Steam generator metal (includes transition cone, shell, wrapper, and other internals)
- Steam generator secondary energy (includes fluid mass and steam mass)
- Secondary transfer of energy (feedwater into and steam out of the steam generator secondary)

The analysis used the following energy reference points:

- Available energy: 212°F; 14.7 psia [energy available that could be released]
- Total energy content: 32°F; 14.7 psia [total internal energy of the RCS]

The mass and energy inventories are presented at the following times, as appropriate:

- Time zero (initial conditions)
- End of blowdown time
- End of refill time
- End of reflood time
- Time of broken loop steam generator equilibration to pressure setpoint
- Time of intact loop steam generator equilibration to pressure setpoint
- Time of full depressurization (3600 seconds)

In the mass and energy release data presented, no Zirc-water reaction heat was considered because the cladding temperature does not rise high enough for the rate of the Zirc-water reaction heat to proceed.

14.3.4.2 Long-Term LOCA Containment Response Analysis

The KPS containment system is designed so that for all LOCA break sizes, up to and including the double-ended severance of a reactor coolant pipe, the containment peak pressure remains below the design pressure. This section details the containment response subsequent to a hypothetical LOCA. The containment response analysis uses the long-term LOCA mass and energy release data from Section 14.3.4.1.

The containment response analysis demonstrates the acceptability of the containment safeguards system to mitigate the consequences of a LOCA inside containment. The impact of LOCA mass and energy releases on the containment pressure is addressed to ensure that the containment pressure remains below 46 psig at the licensed core power conditions. In support of equipment design and licensing criteria (for example, qualified operating life), with respect to post-accident environmental conditions, long-term containment pressure and temperature transients are generated to conservatively bound the potential post-LOCA containment conditions.

14.3.4.2.1 Accident Description

A break in the primary RCS piping causes a loss-of-coolant, which results in a rapid release of mass and energy to the containment atmosphere. Typically the blowdown phase for the large LOCA events (DEHL, cold leg, or pump suction pipe breaks) is over in less than 30 seconds. This large and rapid release of high-energy, two-phase fluid causes a rapid increase in the containment pressure, which results in the actuation of the emergency fan cooler and containment spray systems.

The RCS accumulators begin to refill the lower plenum and downcomer of the reactor vessel with water after the end of blowdown. The reflood phase begins after the vessel fluid level reaches the bottom of the fuel. During this phase, the core is quenched with water from both the accumulators and pumped SI. The quenching process creates a large amount of steam and entrained water that is released to containment through the break. This two-phase mixture would have to pass through the steam generators and also absorb energy from the secondary side coolant if the break were located in the cold leg or pump suction piping.

The LOCA mass and energy release decreases with time as the system cools and depressurizes. Core decay heat is removed by nucleate boiling after the reflood phase is complete. After the reflood is complete, the core fluid level is maintained by pumping water back into the vessel from either the SI or sump recirculation system. The containment heat removal systems continue to condense steam and slowly reduce the containment pressure and temperature over time.

14.3.4.2.2 Input Parameters and Assumptions

A series of analyses, using different break sizes and locations, was performed for the LOCA containment response. Section 14.3.1 documents the mass and energy releases for the DEPS and DEHL breaks. The DEPS break cases were run with both minimum and maximum safeguards. The three minimum safeguards cases assume a diesel train failure. This assumption leaves one of two containment spray pumps and two of four containment fan coil units (CFCUs) available for containment heat removal. Three variations on the RHR/CCW configuration were considered for the minimum safeguards case. The first case assumes the operation of one RHR heat exchanger with CCW flow of 1550 gpm, 1 CCW heat exchanger with SW flow and one CCW heat exchanger without SW flow. The second case assumes 1 RHR heat exchanger with CCW flow, 1 RHR heat exchanger without CCW flow, 1 CCW heat exchanger with SW flow and 1 CCW heat exchanger without SW flow. The third case is the same as the first except that the CCW flow to the RHR heat exchanger is reduced to 1100 gpm. Two single-failure cases were modeled for the maximum safeguards DEPS case. In the first case, one of the two containment spray pumps was assumed to fail, and in the second case one of the four CFCUs was assumed to fail. Only one RHR heat exchanger was credited for recirculation cooling in the maximum safeguards DEPS cases.

The containment initial conditions (pressure, temperature, and humidity) assumed for the containment response analyses are shown in Table 14.3.4-4.

Table 14.3.4-4 also includes the temperature of the service water system (SWS), the initial temperature of the refueling water storage tank (RWST), and the containment cooling system assumptions used in the analysis.

The heat sink data for the Kewaunee containment model is summarized in Table 14.3.4-5. The thermo-physical properties of the containment heat sink materials are shown in Table 14.3.4-6. The CFCU performance data (heat removal as a function of containment temperature) is shown in Table 14.3.4-7.

The major assumptions made in the containment response analysis are listed below:

- The LOCA mass and energy release input to the containment model is described in Section 14.3.4.1.
- Homogeneous mixing is assumed. The steam-air mixture and the water phases each have uniform properties. More specifically, thermal equilibrium between the air and the steam is assumed. However, this does not imply thermal equilibrium between the steam-air mixture and the water phase.
- Air is taken as an ideal gas, while compressed water and steam tables are employed for water and steam thermo-dynamic properties.

- For the blowdown portion of the LOCA analysis, the discharge flow separates into steam and water phases at the breakpoint. The saturated water phase is at the total containment pressure, while the steam phase is at the partial pressure of the steam in the containment. Steam and water releases are input separately for the post-blowdown portion of the LOCA analysis.
- The saturation temperature at the steam partial pressure is used for heat transfer to the heat sinks and the fan coolers.

14.3.4.2.3 Description of the Kewaunee GOTHIC Containment Model

Calculation of the containment pressure and temperature is accomplished by use of the digital computer code GOTHIC. The GOTHIC version 7.1 Patch 1 was used for this analysis. The analysis and the methodology were approved by the NRC as part of the power uprate license amendment (Reference 9).

An improved recirculation heat removal system model was added to the Kewaunee containment model to more accurately determine the RHR and CCWS temperatures during sump recirculation for the LOCA analysis. The containment peak pressure and temperature occur prior to the transfer to recirculation; the improved recirculation model only affects the long-term LOCA containment pressure and temperature response.

The recirculation system model uses GOTHIC component models for the RHR and CCW heat exchangers and the CCW pump. The GOTHIC heat exchanger input data was taken from the heat exchanger specification sheets. The heat exchanger models were benchmarked against design conditions and output data from the COCO code.

The RHR System model uses a flow boundary condition to draw suction from the sump through the RHR heat exchanger. The RHR heat exchanger transfers energy from the sump to the CCWS. The CCWS model calculates the secondary side inlet conditions for the RHR heat exchanger. The CCW pump provides flow through the CCW heat exchanger to transfer heat to the Service Water System (SWS). The service water flow rate and temperature are boundary conditions to the CCW heat exchanger model. The CCW heat exchanger outlet flow is split between the RHR heat exchanger and the other CCW heat loads. The other heat loads are modeled using a constant heat source.

14.3.4.2.4 Acceptance Criteria

The containment response for design-basis containment integrity is an American Nuclear Society (ANS) Condition IV event, an infrequent fault. The containment analysis methodology satisfies the current NRC acceptance criteria from 10 CFR 50, Appendix A and SRP 6.2.1.1.A. The relevant general design criteria (GDC) requirements that are met are as follows:

- GDC 16 and GDC 50: To satisfy the requirements of GDC 16 and GDC 50, the peak calculated containment pressure should be less than the containment maximum internal pressure design limit of 46 psig considering the most severe single failure.

- GDC 38 and GDC 50: To satisfy the requirements of GDC 38 and GDC 50, the calculated pressure at 24 hours should be less than 50 percent of the peak calculated value. (This is related to the criteria for doses at 24 hours.)

The Kewaunee plant was originally licensed with the FSAR containing text from the interim criteria that was derived from the draft Atomic Industrial Forum (AIF) GDCs. The Kewaunee SER indicated that the operating license was granted because "...the plant design generally conforms to the intent..." of the requirements of 10 CFR 50 Appendix A. The specific interim criteria were:

- Interim GDC 10 - Containment
- Interim GDC 49 - Containment Design Basis
- Interim GDC 52 - Containment Heat Removal Systems

14.3.4.2.5 Analysis Results

The containment response calculations for the DEPS case with minimum SI was performed for 3 million seconds (approximately 35 days). The containment response calculations for the DEPS case with maximum SI was performed for 10 million seconds (approximately 11.6 days). Since the steam generator secondary side energy is effectively isolated for hot leg breaks, the containment response calculation for the DEHL case was performed for the blowdown phase only (approximately 20 seconds). The containment pressure, steam temperature, and water (sump) temperature profiles from each of the LOCA cases are shown in Figure 14.3.4-1 through Figure 14.3.4-12. Table 14.3.4-8 summarizes the LOCA containment response results for the three cases studied.

14.3.4.3 Conclusions

The LOCA containment response analyses have been performed as part of the Power Uprate Program for Kewaunee. The analyses included long-term pressure and temperature profiles for each case. The calculated peak containment pressure was less than 46 psig for all cases. In addition, the containment pressure was less than 50 percent of the peak value within 24 hours. Based on the results, all applicable containment integrity acceptance criteria have been met.

14.3.5 Off-Site Dose Consequences

14.3.5.1 Introduction

The NRC has established guidelines in 10 CFR 50.67 for radiation doses resulting from accidental releases of radioactivity from a reactor plant. This section shows the capability of the Kewaunee Power Station to stay within the dose criteria set forth in 10 CFR 50.67 following the design basis accident with conservative assumptions including assumed conditions of release consistent with those of NRC Regulatory Guide 1.183.

The Kewaunee Power Station Containment System is described in detail in Chapter 5. One feature of particular importance to the environmental consequences of a LOCA is the presence of two barriers, in series, to fission product leakage: the Reactor Containment Vessel and the Shield Building.

Reactor Containment Vessel leakage is collected within an annular volume between these barriers before release; the annulus is, therefore, effective as a means of holding leakage for decay and providing additional dilution prior to release. Release from the Shield Building to the environment is through absolute and charcoal filters provided in the Shield Building Ventilation (SBV) system. For reference in the evaluation of environmental consequences, a schematic diagram of this system is shown in Figure 14.3-23.

Shield Building Ventilation System fans establishes a negative pressure with respect to the atmosphere in the annulus within six minutes after the accident. The amount of filtered annulus air released to the environment is just sufficient to maintain the negative annulus pressure and compensate for in-leakage. The balance of the filtered annulus air is recirculated to the Shield Building to provide for further decay and filtration.

A limited amount of containment leakage could potentially bypass the Shield Building annulus through certain lines that terminate in the Auxiliary Building. This leakage will be collected and processed by the Auxiliary Building Special Ventilation System. An even smaller amount of containment leakage may bypass both the Shield Building and the Auxiliary Building and go directly to the environment. Both of these pathways have been evaluated.

14.3.5.1.1 Cause of Activity Release

The postulated cause of radioactivity release to the environment analyzed in this section is an extremely improbable double-ended rupture of a 29-inch inside diameter pipe in the reactor coolant loop. Following the assumptions of NRC Regulatory Guide 1.183, it is assumed that the Design Basis Accident will release to the Reactor Containment Vessel the following portions of the core activity:

- 100 percent of the noble gases (Xe, Kr) (5 percent in the gap and 95 percent in the fuel)
- 40 percent of the iodines (5 percent in the gap and 35 percent in the fuel)
- 30 percent of the alkali metals (Cs, Rb) (5 percent in the gap and 25 percent in the fuel)
- 5 percent of the tellurium metals (Te, Sb)
- 2 percent of the barium and strontium
- 0.25 percent of the noble metals (Ru, Rh, Mo, Tc)
- 0.05 percent of the cerium group (Ce, Pu, Np)

- 0.02 percent of the lanthanides (La, Zr, Nd, Nb, Pr, Y, Cm, Am)

The release of activity to containment occurs over a 1.8-hour interval. The gap activity is released in the first 30 minutes, and the fraction of the core activity that is released does so over the next 1.3 hours. A gap fraction of 5 percent is assumed for iodines, noble gases, and alkali metals. Gap activity of the other nuclides is not considered. With the exception of the iodines and noble gases, all activity released to containment is modeled as particulates. The iodine in containment is modeled as 4.85 percent elemental, 0.15 percent organic, and 95 percent particulate. A homogeneous mixture of this activity within the containment atmosphere is assumed to occur instantaneously. Because of the multiple redundancy in engineered safety features, such a release is considered incredible.

14.3.5.1.2 Sequence of Events Following a LOCA

As discussed previously, the Shield Building Ventilation System is designed to provide three functions during the course of the LOCA:

- Provide a negative pressure region to control and limit environmental leakage
- Enhance mixing and dilution of any Containment Vessel leakage to the annulus
- Provide holdup and long-term filtration of annulus air

Immediately following the accident, the Shield Building pressure increases due to heat transferred from the containment shell. Operation of one of the Shield Building Ventilation System's two redundant fans establishes a negative pressure within ten minutes. During this period no credit is taken for the filtered exhaust of air by the Shield Building Ventilation System. Instead it is assumed that the Shield Building does not exist. From 0 to 10 minutes, 90 percent of the containment leakage is assumed to be released directly to the atmosphere without holdup or filtering. The remaining 10 percent goes to the Auxiliary Building Special Ventilation Zone where it is filtered before release to the atmosphere.

At 10 minutes into the accident, the Shield Building Ventilation System is assumed to be fully effective in controlling leakage into the Shield Building. It is assumed that from 10 minutes on, 89 percent of the containment leakage is processed by the Shield Building Ventilation System. Of the remaining 11 percent, 10 percent is assumed to go to the Auxiliary Building Special Ventilation Zone where it is subject to processing by the Auxiliary Building Special Ventilation System and one percent is assumed to be released directly to the atmosphere. These leakage assumptions are regarded as conservative upper limits as stated in the Technical Specifications for Kewaunee. A filter efficiency of 90 percent is applied to the removal of elemental and organic iodine and a filter efficiency of 99 percent is applied to the removal of particulates.

Figure 14.3-24 shows results of a shield building ventilation performance test. Also shown is a curve enveloping all data points with a considerable margin. This envelope is the basis for the conservative exhaust rates used in calculating offsite doses following a LOCA.

As described in Chapter 5, the shield building ventilation fans take a filtered suction from the annulus and their discharge is apportioned between atmospheric discharge and annulus recirculation flow. The atmospheric discharge (or SBV exhaust flow as shown in Figure 14.3-24) is dependent on the amount of annulus in leakage at the vacuum setpoint chosen for the Shield Building Ventilation System Control. The SBV exhaust flow will reach 2700 cfm at 20 minutes post-LOCA. Using the envelope in Figure 14.3-24, this exhaust flow will maintain a negative 1-inch wc (water column) in the annulus. It is recognized that exhaust flow rates must be higher early in the accident due to annulus heating. This is shown in Figure 14.3-26. To simplify the analysis a constant exhaust rate of 6000 ± 10 percent cfm has been used from 10 to 30 minutes and 3100 cfm from 30 minutes to 30 days. This simplification can be made due to the size of the envelope in Figure 14.3-24 and Figure 14.3-26.

The Containment Vessel Internal Spray System is described in Section 6.4. The primary purpose of the spray system is to spray cool water into the containment atmosphere in the event of a LOCA and thereby ensuring that containment pressure does not exceed its design value. However, the spray system also has the property of removing iodine and particulates from the containment vessel atmosphere. The iodine removal coefficients due to containment spray are given in Table 14.3-7. During spray operation, no credit is taken for sedimentation removal of particulates, although it would take place. Recirculation sprays are not credited. Credit is taken for sedimentation removal of particulates after spray termination. The analysis credits a sedimentation coefficient of 0.1h^{-1} . Table 14.3-7 also provides a summary of the other parameters used in the analysis, which was documented in Reference 1.

14.3.5.1.3 Method of Analysis

The evaluation of the environmental consequences of a loss-of-coolant accident consists of determining the radiation dose resulting from inhalation of radioiodine discharged from the Shield Building and of determining the dose due to direct gamma radiation from the radioactive cloud created by the discharge of Containment Vessel leakage from the Shield Building.

The evaluation of the environmental consequences of a loss-of-coolant is based on the assumptions of NRC Regulatory Guides 1.183. The analysis model describing the activity release is shown in Figure 14.3-23. This figure illustrates the basic assumptions of the analysis. A portion of the Containment Vessel activity inventory is assumed to leak into the Shield Building and form the Shield Building activity inventory. Activity leaves the Shield Building by passing through the charcoal filters. Of the activity passing through the filters, a portion is released via the shield building vent and the rest is recirculated back into the Shield Building. The Shield Building activity is also a function of the assumed annular participation fraction. This fraction is a measure of the mixing efficiency in the annulus.

When ECCS recirculation is established following the LOCA, leakage is assumed to occur from ECCS equipment outside containment. There are two pathways considered for the ECCS recirculation leakage. One is the leakage directly into the auxiliary building and the other is

back-leakage into the RWST. Although recirculation is not initiated until the RWST has drained to the pre-determined setpoint level the analysis conservatively considers leakage from the start of the event. For the ECCS leakage analysis, all iodine activity released from the fuel is assumed to be in the sump solution until removed by radioactive decay or leakage from the ECCS. The iodine activity that becomes airborne after being released by the leakage is modeled as 97 percent elemental and 3 percent organic.

The analysis models leakage to the auxiliary building of 12 gallon/hr (twice the System Integrity Program limit of 6 gallons/hr per Regulatory Guide 1.183). The analysis models a conservative airborne fraction of 10 percent when the sump temperature is above 212°F. Once the sump solution temperature drops below 212°F, the airborne fraction is reduced to one percent. The reduction in airborne fraction is conservatively delayed until 3 hours from the start of the event.

RHR back-leakage to the RWST is assumed at a rate of 3 gpm for the first 24 hours, and 1.5 gpm for the remainder of the event. It is assumed that one percent of the iodine contained in the leak flow becomes airborne. The one percent value is applied even when the sump is above 212°F since any incoming water would be cooled by the water remaining in the RWST. The RWST vents to the auxiliary building.

It is assumed that half the iodine activity that becomes airborne in the auxiliary building from the two leak sources is removed by plateout on surfaces. Releases from the auxiliary building are subject to filtration by the auxiliary building special ventilation system.

The analysis is documented in Reference 1. Dose results are listed in Table 14.3-9. Reference 1 also demonstrates that the 30 day dose to control room operators is within the limit specified in 10 CFR 50.67.

14.3.5.2 Conservatism Between Analysis and Physical Situation

Many conservative assumptions have been made in the application of the NRC Regulatory Guide 1.183 to the Kewaunee Plant. Elimination of this conservatism would be expected to reduce the calculated dose by orders of magnitude. In order to place the above analysis in perspective, major assumptions applied in the analysis which affect the calculated dose are reviewed below:

1. In accordance with NRC Regulatory Guide 1.183, a release of activity from melted fuel to the containment atmosphere was assumed. As shown in Section 14.3.2, the SIS will prevent fuel rod clad melting and will limit the zirconium-water reaction to an insignificant amount. However, as a result of the cladding temperature increase and the rapid system depressurization following the accident, cladding failures may occur in the hotter regions of the core. These failures would release only the inventory of volatile fission products in the gap between the fuel pellet and the cladding.
2. No reduction of activity has been assumed by plateout in the Shield Building.

3. Recirculation filtration has been assumed to take place with only one of two redundant systems operable. Since the combined flow capability of the two recirculating fans will be double that used in the analysis, a significant reduction of iodine and particulate activity in the Shield Building would result.

14.3.6 Charcoal Filter Ignition Hazard Due to Iodine Absorption

The radioactive iodine, which collects on the charcoal filters generates a significant amount of decay heat. A detailed analysis was made of the potential for spontaneous ignition of the charcoal during post-LOCA operation of the Shield Building Ventilation (SBV) system. To maximize the charcoal filter temperature, it was assumed that forced air-cooling is lost at the time of maximum heat load.

Using the assumptions of NRC Safety Guide 4, i.e., 50 percent halogen release from the fuel and 50 percent plateout in the Reactor Containment Vessel, the iodine released and the heat generated from that iodine are estimated to be:

Isotope	Curies (10^7)	Decay Heat (kW)
I-131	1.21	41.55
I-132	1.718	262.7
I-133	2.26	143.7
I-134	2.575	450.3
I-135	2.0	292.7

The maximum amount of heat that can be generated on the filters is limited by the rate at which the iodine leaks out of the Reactor Containment Vessel onto the filters, and by the decay of the isotopes that are collected on the filter.

In the analysis performed, the following conservative assumptions are made:

1. It is assumed that no holdup takes place in the Shield Building, i.e., all of the activity released via Containment Vessel leakage goes directly on the filters.
2. No credit is taken for plateout in the Shield Building.
3. All of the activity is assumed to collect on one train of the SBV filters with 100 percent efficiency.

With those assumptions, the maximum rate of heat generated on the charcoal filters was predicted to occur at one day following the accident. At this time of maximum heat load, the forced air cooling through the filter assembly is assumed to be lost. Assuming the charcoal filter is at 190°F (based on calculated post-accident shield building temperature) when forced cooling is lost, results in a charcoal filter centerline temperature of 258°F, which is significantly lower than

the 626°F ignition temperature of the charcoal used. This temperature is also below the 356°F at which iodine desorption is expected to begin.

This analysis is conservative by at least an order of magnitude for the following reasons:

1. The analysis was based upon a NRC Safety Guide 4 release.
2. The maximum allowable containment vessel leak rate is assumed to occur for the first day following accident initiation. Peak containment pressure occurs only a few minutes following accident initiation and decays quickly. This would result in a leak rate much less than maximum allowable.
3. All plateout of iodine in the Shield Building was neglected.
4. All activity was assumed to collect on one of two filters.
5. All activity leakage from the Containment Vessel was assumed to collect, at 100 percent filter efficiency, on the filter without holdup or decay in the Shield Building.
6. No heat dissipation from the filter housing to the surrounding room environment is assumed.

A spray system is provided which is activated automatically upon occurrence of high temperature adjacent to the charcoal. The analysis has shown that actuation of this system is not expected to occur.

14.3.7 Generation and Disposition of Hydrogen

14.3.7.1 General

The design basis LOCA and its off-site consequences are discussed earlier in this section. It is recognized that a LOCA could be followed by the possible generation of hydrogen from radiolysis of water, from chemical corrosion of materials by spray liquids, and from possible metal-water reactions accompanying the accident.

The equilibrium concentrations that could theoretically result have been calculated to exceed the lower flammability limit of 4.1 volume percent hydrogen; therefore, it is necessary to provide means of limiting the accumulation of hydrogen to an acceptable lower concentration.

The simplest means of control is to purge, venting the mixture of air and hydrogen to the environment, at a rate sufficient to maintain a hydrogen concentration that is below the lower flammability limit.

The capability of venting is an essential part of any system of hydrogen control because the eventual containment cleanup must be by controlled dispersal of containment gases to the environment; hydrogen control and eventual containment purge by venting are inseparable considerations of the same LOCA because any primary means of control cannot be terminated until conditions permit venting to proceed at a rate sufficient to supplant it and prevent further rise in hydrogen concentration. Complete analysis must be based on a reference condition of

acceptable venting at which venting can later proceed at a rate greater than that necessary to control hydrogen. This condition is conveniently defined as the occurrence of 1 MPC at the site boundary (i.e., when the summation of the fractions of the maximum permissible concentrations given in 10 CFR 20 equals unity).

14.3.7.2 **Summary of Reanalysis Based on Safety Guide 7**

Initial studies were based on conservative estimates of hydrogen sources provided by the reactor supplier, and they included the assumptions of Safety Guide 4. These studies indicated that 3.5 v/o concentrations would be reached in 56 days, that venting could be deferred until 86 days after the accident without the lower flammability limit being reached, and that initiation of venting through a charcoal filter at a rate sufficient to arrest hydrogen accumulation would then result in instantaneous site boundary concentrations no greater than 1 MPC. Thus, direct venting through charcoal was indicated to be sufficient means of hydrogen control.

The present reanalysis uses a Containment Vessel leak rate of one percent per day. A conservative filter efficiency of 90 percent for the Shield Building Ventilation System is used in the reanalysis, but doses are also given for a filter efficiency of 95 percent.

Also, additional considerations are now incorporated in the analysis, based on information published subsequent to initial submittal of this USAR:

- Safety Guide 7 now prescribes even more conservative assumptions regarding hydrogen sources.
- Test data indicate that, at least for higher initial post-accident containment temperatures, substantial amounts of hydrogen could be released from painted surfaces during the first day following the accident.

Both the time at which hydrogen control must be initiated and the doses associated with venting are extremely sensitive to the assumptions regarding hydrogen sources. The above two effects, for example, would alone advance the calculated time of occurrence of 3.5 percent hydrogen concentration—from 56 days to 18 days and from 56 days to 41 days, respectively. Together they result in occurrence of 3.5 percent concentration on the eleventh day.

The collective assumptions prescribed in Safety Guide 4 and Safety Guide 7 are regarded as being unnecessarily conservative. Also, for conservatism it is found necessary to overestimate the potential contribution from protective coatings, which is the remaining source, because the test data are for simulated post-accident conditions of temperature much more severe than those predicted. The hydrogen generation and venting problem will consequently be far less severe than determined from these assumptions.

A method of venting is proposed which is indicated to attain reasonable off-site doses, even under these conditions of early venting requirements. In addition, means are provided to defer

venting, if necessary, by compressing the containment atmosphere, thus diluting the hydrogen within the containment, and thereby reducing the potential dose from venting.

14.3.7.3 **Methods of Control**

Two modes of operation are being provided, any of which employed alone would provide adequate means of hydrogen control.

1. Controlled vent flow and processing of this flow with recirculation filtering by the SBVS before its release to the environment.
2. Deferment of venting, if necessary, by adding air to the containment to compress the atmosphere, and thus, dilute its hydrogen concentration.

In addition to these two methods of hydrogen control, the capability to utilize an external hydrogen recombiner, has been provided.

14.3.7.4 **Venting to the Shield Building Annulus**

The Shield Building Ventilation System affords the benefit of recycle through charcoal filters. When venting must first be initiated, at least one-of-two redundant trains of equipment will already be in continuous operation, maintaining vacuum and collecting and processing containment vessel leakage before its discharge to the environment. Any vent flow necessary to maintain acceptable hydrogen concentrations within the containment will be directed into the Shield Building annulus at a controlled rate, to be processed along with the containment leakage which would represent part of the required vent flow.

The effect of recycle through the filters of the Shield Building Ventilation System is to reduce the iodine effluent concentration by an additional factor that is essentially equal to the ratio of recirculation flow to discharge flow to the environment. This is the same factor that has been applied to the standby ventilation system for a boiling water reactor plant (Reference 1).

Analysis demonstrates that venting at greater than 1 MPC would be unnecessary on the basis of reasonably conservative assumptions, which include the conservative allowance for protective coatings. The need to vent at higher activity concentrations might be required only for the extremely conservative basis of Safety Guide 7. If post-accident hydrogen generation were in accordance with this most conservative estimate, the resulting doses from the processed vent flow are indicated to be a small fraction of those of the accident analysis. The time delay before initiation of venting and the conservative allowances made in the initial phases of the accident analysis for direct filtered and unfiltered release of containment leakage are not applicable during the equilibrium recycle operation which will be established before venting is necessary.

14.3.7.5 **Dilution by Containment Pressure Raise**

Dilution of hydrogen concentration by modest increases in containment pressure is one of several simpler methods of hydrogen control that were first proposed and investigated in 1970 for Wisconsin Public Service Corporation and other participants of the same study program.

Partial pressurizing of the containment can defer the occurrence of limiting hydrogen concentrations, and consequently defer the need to vent until appreciable decay of containment activity has occurred. The objective is to defer venting until venting at an acceptable dose level alone can arrest the further accumulation of hydrogen and permit termination of the method used to defer venting. Such deferral of venting is the identical objective of other methods, such as the use of recombiners.

Controlled venting with the accompanying replenishment of vented containment air requires that a pressure differential exist at least intermittently across the containment shell. The venting system can readily be designed for an operating differential in either direction, but design for positive internal pressure during venting provides the option of deferred venting.

Analysis indicates that a rather small increase in pressure can significantly reduce the venting doses associated with the most conservative estimates of hydrogen sources, and that the method provides a practical means of utilizing the benefits of recirculation filtration provided by the Shield Building Ventilation System.

14.3.7.6 Hydrogen Recombination

In addition to the two methods of hydrogen control described above, the capability to use an external hydrogen recombiner for recombination of hydrogen and oxygen into water vapor has been provided. Permanent piping, valving, and power source connections are provided at two separate locations for the connection and operation of an external hydrogen recombiner within the Auxiliary Building. The two locations allow recombiner placement at approximately opposite sides of Containment; in the unlikely situation that one of the two areas will be unavailable or be required for continual personnel occupancy, the remaining location will remain available for recombiner placement and operation.

14.3.7.7 Analysis of Materials of Construction and Protective Coatings

Analysis has been made of the materials of construction and the protective coatings used within the containment, particularly as they affect the potential of hydrogen generation by reaction with spray solution.

14.3.7.8 Description of Materials

The original specified coatings for structural steel items were 3 mils of Carbo-zinc 11 primer plus a 4-mil finish coat of Phenoline 305. The same protective coatings were specified for the inner surface of the steel containment vessel, plus an additional 4-mil finish coat between elevations 606 feet and 660 feet. These coatings will be maintained by application of an appropriate Service Level I protective coating or coating system, depending on the extent of repair. Appropriate Service Level I coatings for use in containment are determined by KPS engineering specifications and procedures. Periodic inspections are performed to assess the condition of protective coatings on the vessel and structural steel.

All concrete walls, floors, ceilings, and other surfaces within the containment were originally protectively coated with sealer, surfacer, and/or finish coats of Carboline or Phenoline. Neither of these coatings included Carbo-zinc. The coatings on concrete walls, floors, ceilings, and other surfaces are also maintained by application of appropriate Service Level I protective coatings. Periodic inspections are performed to assess the condition of protective coatings on concrete surfaces.

The use of unqualified coatings in containment is minimized. Unqualified coatings were used in containment on structural and architectural steel, piping, various equipment and components, and other miscellaneous items. Analysis has shown that the current amount of unqualified paint will not affect the operability of the emergency core cooling system and the internal containment spray system following a LOCA. Components with factory coatings, which are unqualified will not be stripped of the coating and re-coated. This is in the interest of equipment reliability and nuclear safety.

Galvanized steel is used for ventilation ducts, gratings, stair treads, etc., and some aluminum is used in components and protective coatings associated with the reactor equipment and the reactor building crane. The use of these materials has been minimized in design to the extent practical.

The surface areas and amount of the materials are summarized in Table 14.3-10.

Other materials in contact with the spray solution, such as stainless steel and copper alloys, are not significant with regard to corrosive generation of hydrogen.

The effects of corrosion on component integrity are of possible concern only with regard to potential chloride stress corrosion of stainless steel by the boric acid spray solution. Sufficient caustic will be added with containment spray so that both the initial spray and the recirculated sump solution will be at pH of 7 or higher. Means are provided to monitor the chloride content of the recirculated sump water. Corrosion effects are not otherwise of concern with regard to component integrity. For example, if the zinc-bearing coating of galvanized ductwork were to be completely consumed by reaction with the spray, there would be negligible further corrosion of the exposed steel.

14.3.7.9 Zinc-Bearing Surfaces

A zinc-bearing primer is used as an undercoat on original structural steel and on the inner surface of the containment vessel.

The results of ORNL experiments indicate that substantial amounts of hydrogen can evolve from such undercoats during the initial conditions of a LOCA. This effect appears to be independent of the type of spray solution and of the amount and type of coating over the primer. The outer coating is reported to typically appear unaffected after exposure conditions even though measurable releases of hydrogen from the under-coatings were produced.

The most relevant experiments (Reference 2) involved exposure of vendors' test coupons to spray solution under temperature conditions intended to simulate those of a LOCA in a PWR: 5 minutes at 300°F, 105 minutes at 284°F, and the remainder of a day at 225°F. For a boric acid spray solution of 3000 ppm boron without additives, the most applicable paint sample (3 mils of Carbo-zinc plus a 2 mil overcoat) yielded 2.3 cc of hydrogen per cm² of surface or 0.075 scf/ft². With 0.15N NaOH added to the solution, the yield was 2.0 cc/cm² or 0.066 scf/ft². The hydrogen release from these tests was typically about 60 percent of that released in previous tests in which the exposure temperature was maintained constant at 266°F for 24 hours.

The test conditions for both sets of tests were much more severe than those predicted for the design basis accident, and substantially less hydrogen generation would therefore be expected. It is conservatively assumed in the analysis that the first-day contribution from the painted surface is given by half the product of the total area given in Table 14.3-10 and the release per unit area given by the higher temperature experiments intended to simulate accident conditions.

The factor of two is perhaps justified alone on the basis of the fraction of total zinc-bearing surface that will be directly exposed to the spray solution, but even greater reduction factors should result from the reduced temperatures relative to the experiment. The post-accident air and steam temperatures are predicted to be only 265°F maximum during the first 5 minutes; a decrease from 238°F initial temperature to 140°F during the next 105 minutes; and 140°F or less thereafter.

An approximate indication of the effect of temperature is given by the relation of Arrhenius for the case of constant activation energy: $R(T_1)/R(T_0) = \exp [\alpha(T_1 - T_0)/T_1 T_0]$. Many reactions double or triple in rate for a 10°C rise in temperature in accordance with this relation (Reference 3). Its direct application to the typical relative yields of the ORNL tests (those for the simulated accident conditions versus those for constant temperature exposure at 266°F for 24 hours) implies a doubling in rate for every 4°C rise.

To obtain indication of the reduced reaction that might be expected at the lower temperatures predicted for the design basis accident, the same relation is applied identically to the time-temperature sequence of the accident-simulation experiment and to the predicted first-day post-accident temperature curve. With reaction rates near 300°F assumed to double for temperature increments ranging from 4°C to 30°C, the resulting reduction factors in the first-day reaction are indicated to vary from 109 to 4.2, respectively, relative to the accident simulation tests.

These indications suggest that a reduction factor of 10 to 100 would be appropriate. However, in the absence of lower temperature data or direct indication of temperature sensitivity of the reaction rates, an overall reduction factor of only two is conservatively assumed.

14.3.7.10 Aluminum Surfaces

Corrosion of aluminum surfaces would be negligible with an acidic borated spray being a factor of a hundred or more less than with a basic spray solution (Reference 4).

For the case of buffered spray solution, reaction rates of aluminum are available as a function of temperature (Reference 5). Application of this information to the temperature transient predicted for the design basis accident indicates 1 mil reaction on the first day, plus a continuing rate thereafter that is less than the 200 mils/year prescribed by Safety Guide 7.

14.3.7.11 Net Effect of Spray Additive

The total hydrogen production from protective coatings (see Table 14.3-11) has been calculated with and without spray additive, and with first-day production from galvanized coating treated identically as the paint, because of the absence of relevant information for the case of no additive and because the zinc content of most of the galvanized surface is similar to that of the paint. Addition of spray additive justifies use of a lower conservative estimate for painted surfaces and neglect of the first-day contribution from the galvanized surface.

An added allowance is made for aluminum reaction with additive, based on full consumption of the 110 pounds of aluminum paint on the first day and 200 mils/year consumption of the remaining aluminum, assuming $\frac{1}{4}$ -inch effective thickness and 20 scf hydrogen generation per pound consumed.

From Table 14.3-11, it can be noted that the calculated total coating contribution at 10 days would not increase with the use of additive. Also, the coating contribution is only a minor part of total continuing production; therefore, the adjustment for additive is not significant. Effectively, the extremely conservative allowance for zinc-bearing surfaces that is necessitated by the absence of lower temperature data, and the appropriate adjustments in this conservative estimate, obscure the net increase in hydrogen that should result from the directly calculable effect of spray additive on aluminum.

14.3.7.12 Analysis of Methods of Hydrogen Control

14.3.7.12.1 Sources and Assumptions

Studies have been based primarily on the results of conservative hydrogen generation calculations provided by the reactor supplier. The major assumptions for this “reasonably conservative case” are summarized in Table 14.3-12, and compared with those for a “most conservative case” which includes the assumptions of Safety Guide 7. Both cases described in this table include the conservative allowance for first-day reaction of the zinc-bearing surfaces described in the previous section.

The significant differences introduced by Safety Guide 7 are the increase in assumed zirconium reaction, the higher value of G, and the greater core gamma absorption in the coolant. These assumptions add a half percent more hydrogen concentration for zirconium and increase

the radiolytic sources by factors of 1.67 in the core and 1.6 in the coolant. The overall effect is to alter entirely the urgency and magnitude of the hydrogen problem, as shown by comparison of the first several lines of Table 14.3-13.

The source contributions and venting requirements for the most conservative case that based on Safety Guide 7 are shown in Figure 14.3-28.

14.3.7.13 Analysis of Venting Through Shield Building Annulus

The first case analyzed is that of controlled venting through the Shield Building Ventilation System without pressurizing, and neglecting any effects of the positive pressure differential that would be used to accomplish such venting.

It is assumed that venting is initiated upon measured occurrence of 3.5 v/o concentration (as shown in Figure 14.3-28), and continued at a diminishing rate which maintains that concentration until the effects of decay and purge depletion result in instantaneous venting concentrations of 1 MPC at the site boundary. The purge and vent rate is then increased with further decay and purge depletion while maintaining 1 MPC off-site, causing containment activity and hydrogen content to decrease monotonically until purging is complete.

Calculations with regard to venting are based on the initial activity inventories described in Appendix D, Table D.1-1 (consistent with Safety Guide 4) and on the dispersion factors and breathing rate appropriate to the two-day to thirty-day period of the meteorological studies:

$$\begin{aligned} \chi/Q &= 3.882\text{E-}6 \text{ sec/m}^3 \text{ at the site boundary} \\ &= 4.473\text{E-}7 \text{ sec/m}^3 \text{ at 4800 meters} \\ \beta &= 2.32\text{E-}4 \text{ m}^3/\text{sec} \end{aligned}$$

Venting is assumed to be through the Shield Building annulus with equilibrium recirculation flow of 4000 cfm through filters which remove 90 percent of the iodine and all solid fission products, and with constant discharge flow of 200 cfm. These conservatively chosen flow conditions are consistent with the equilibrium phase of the calculations of shield building activity discharge during the design basis accident.

The resulting venting doses are presented in Table 14.3-13.

The reasonably conservative case described in the Table 14.3-13 results in very low off-site venting doses because it represents a rather trivial case of venting. For consistency in comparison of the two cases, it has been assumed that venting is initiated upon occurrence of 3.5 percent hydrogen. However, the initial activity levels from venting at this time would be about 7 MPC at the site boundary and, by simply deferring venting and allowing the concentration to rise further (to 4.07 percent), venting could later be initiated at a rate sufficient to arrest the concentration at this higher value without exceeding 1 MPC at the site boundary.

Greater venting doses are indicated in Table 14.3-13 for the most conservative case, but these represent a minor portion of the leakage doses associated with the maximum design accident. They might be regarded as an added penalty from venting, except that occurrence of the postulated accident leakage would have deferred and greatly reduced the consequence of venting (or would have obviated the need to vent, for example, in the case of normal initial leak rate of one percent per day).

Thus, the need to vent at off-site concentrations greater than tolerance in order to maintain safe hydrogen concentrations can be predicted only on the basis of the most conservative assumptions—those of Safety Guide 7.

For purposes of evaluation of the venting doses, it may be noted that the recycle advantage factor which is incorporated in all the thyroid doses in Table 14.3-13, and which affects the occurrence of 1 MPC vent capability, reduces effectively to $nP/L_2 = 0.90 \times 4000 \text{ cfm} / 200 \text{ cfm} = 18$, where P is the recycle flow, L_2 is the discharge flow, and n is the removal efficiency of the charcoal. This advantage factor is independent of the partition factor or effective volume fraction assumed for mixing in the annulus. The reduction factor would instead be 45 at the expected conditions of 5000 cfm recirculation and 100 cfm discharge, and the iodine doses would then be 40 percent of those indicated in Table 14.3-13. The thyroid doses would be similarly affected by the removal of iodine by containment spray liquid, which effect, with additive, should further reduce the indicated thyroid doses by a large factor.

14.3.7.14 Analysis of Effects of Pressure Increase

The lower limit of flammability for hydrogen in air is reported to be 4.1 volume percent at atmospheric pressure, and this limit is reported to increase slightly with pressure, rather than to decrease (Reference 6).

Thus, compression of a hydrogen-air mixture by addition of more air to a fixed volume decreases the volume fraction of hydrogen and permits more hydrogen to be accumulated for a given limiting volume fraction. The calculation assumes that once a limiting concentration C_o is reached (3.5 percent), as hydrogen production continues, the containment pressure P is raised by injecting air at a rate sufficient to maintain C_o , where a concentration C(t) would otherwise result if dilution by pressure increase did not occur:

$$P(t) = 14.7 \frac{C(t)}{C_o}$$

Doubling of the absolute pressure, for example, would permit hydrogen to be maintained at 3.5 percent until 7 percent would otherwise have accumulated.

A second effect is that, when purging and venting are initiated, the fractional vent-flow necessary to maintain a given concentration at any time is less at pressure. The mass flow required is independent of pressure, but the flow expressed in fraction of containment volume is less by the ratio of absolute pressures, as is the fractional release rate of contained activity.

As well as deferring the need to vent, overpressure causes leakage to occur from the containment to the annulus. The assumed leakage is based on one percent per day at the design pressure of 42 psi:

$$L(t) = .01/day \sqrt{\frac{P(t) - 14.7}{42}}$$

Out-leakage and vented gases are necessarily processed identically by the Shield Building Ventilation System. They are consequently equivalent from the standpoint of radiation dose, as well as with regard to their effectiveness in hydrogen control when they are replenished by purge flow. Out-leakage, thus, simply represents a portion of the venting rate that is not deferred when venting is otherwise deferred by pressure increase.

The effects of pressure increase on venting requirements and containment leakage are described by Figure 14.3-29 and Figure 14.3-30, and the resulting doses are presented in Table 14.3-14.

The upper curves of Figure 14.3-29 are for a limited pressure rise of 6.1 psig, sufficient to maintain 3.5 percent hydrogen up to 30 days. Venting is then initiated at the same rate that compressed air is being added, with pressure consequently remaining constant. This constant pressure purge continues at a rate no more than necessary to maintain constant concentration, until decay and diminishing vent rate cause the concentrations at the site boundary to reduce to 1 MPC. Purging then proceeds at the rate which theoretically maintains 1 MPC and which rapidly increases as a consequence of further decay and purge depletion.

Pressure relief could be initiated between 30 and 62 days in this case, by allowing the vent rate to exceed the purging or replenishment rate necessary to maintain constant hydrogen, but this would unnecessarily increase the venting dose. Similarly, beyond 62 days, pressure relief cannot fully proceed by unreplenished vent relief at the vent rate permitted by off-site concentration limits. Continued existence of hydrogen sources requires instead that some part of the permissible vent flow be replenished as a purging flow to prevent the limiting concentration being exceeded during this period of final cleanup. The solid-line blowdown curves in Figure 14.3-29 are the lines of earliest pressure relief, which maintain both the limiting hydrogen concentration and the limiting off-site radiation concentration during a controlled blowdown plus purge. The time for complete cleanup is independent of pressure or purging considerations; it is determined only by the venting rate and venting depletion of the contained activity, which effect is also idealized in the figures for the case of earliest cleanup.

The resulting doses are shown in Table 14.3-14 and compared with the previous case of no deferment of venting. Deferment to 30 days is seen to gain a reduction of 10 in venting dose, but the containment leakage dose resulting from the overpressure reduces this factor to 5 or 6.

The out-leakage rates are shown in Figure 14.3-30 and compared with the vent rates. The dose from leakage is additive only up to the time when venting is initiated because the purge rates are the total replenished out-flow required to maintain concentration, either by leakage or venting.

Out-leakage should be less than that estimated on the basis of the design leakage, and it will be assured to be less by surveillance testing of the containment. The effects of out leakage are conservatively considered in the calculations but the compensating depletion, which it would cause is neglected because the actual leakage that would occur is uncertain.

The effect of pressure on purge rate may be noted from Figure 14.3-30, where the top solid curve is the fractional purge rate necessary to maintain concentration C_o at atmospheric pressure:

$$L(t) = \frac{Q(t)N}{C_o}$$

with $Q(t)$ the uncompressed volumetric production rate of hydrogen at time t in the containment air volume V that is used to define concentration.

The dashed line describes the initial purge rate at time t that supplants a pressure increase that was maintaining C_o :

$$L(t) = \frac{14.7/P(t)}{C_o} \times Q(t)N = \frac{Q(t)N}{C(t)}$$

where $C(t)$ is the concentration that would occur at time t without dilution by pressure increase.

The solid curve for constant pressure purge initiated at thirty day is:

$$L(t) = \frac{Q(t)N}{C(30)} = \frac{14.7}{P(30)} \times \frac{QtN}{C_o}$$

Thus, required purge rate is reduced with pressure increase directly in the ratio of absolute pressures. Both solid curves in the figure correspond to the same mass flow of air and hydrogen, but they differ with regard to fractional release rate of the contained volume, and hence, with regard to fractional release rate of the contained activity.

The lower curves in Figure 14.3-29 correspond to sustained pressure rise until a 1 MPC venting capability is attained, sufficient to control hydrogen. As shown in Table 14.3-14, the dose is all from out-leakage and little is gained relative to initiating venting at thirty days. However, the containment is tested initially at 46 psig, and thus, its design does not preclude continuing the pressure rise as far as required.

An additional case has been considered wherein recycle credit for iodine is neglected, as would be the case if all leakage and vent flow were somehow to be discharged directly to a 90 percent filter without recirculation.

The diagonal line in Figure 14.3-30 corresponding to a 1 MPC vent of leak rate would effectively be displaced downward in this case by loss of the recirculation advantage factor of 18.1 for iodine, and the 1 MPC venting intersection would be accordingly deferred in time. It can also be seen from the figure that further pressure rise would cause the containment leakage to exceed the vent rate necessary to control concentration, the intersection occurring at 67 days and 12.8 psi for a one percent leak rate. At this point leakage alone would control hydrogen, the air supply could be reduced to match the leakage and prevent further rise.

A 1 MPC venting capability is deferred in this case to about 90 days, and the total leakage dose is 18.1 rad to the thyroid and 0.107 R whole body radiation. The doses would be less and the maximum useful pressure would be slightly greater for lower containment leak rates.

Thus, even without the recycle advantage at the Shield Building Ventilation System, acceptable doses are indicated for the method of pressure control alone.

14.3.7.15 Provisions for Mixing, Sampling, and Venting of Containment Gases

The provisions for mixing, sampling, and venting of containment gases are shown schematically in Figure 14.3-31.

14.3.7.15.1 Mixing

Two containment dome vent fans are provided to circulate and mix gases within the containment during the period following the postulated LOCA when combustible gases could conceivably accumulate. Each fan draws a combined 8000-cfm through two-of-four inlet ducts located in the dome area of the Containment Vessel. The discharge from each fan is conveyed downward through separate ductwork and returned to the containment volume near the operating floor.

These systems are completely independent and redundant to each other, and they satisfy the requirements of Engineered Safety Features. The fans are started manually from the control room, and surveillance testing of the capability of these systems to start and operate as intended is performed during refueling outages.

14.3.7.16 Venting to Shield Building Annulus

Two vent valve systems are provided to accomplish venting of pressurized containment gases to the Shield Building annulus. The two systems will each vent containment gases from the ductwork associated with one of the containment dome vent fans and transfer them by means of positive pressure differential through separate penetrations of the Containment Vessel. Each penetration has remote-manually operated isolation valves that are normally closed and that can be separately opened to permit venting, or sampling, through either penetration. Each penetration

exhausts gases through a remotely controlled throttle valve directly into the Shield Building annulus where they will be processed and discharged by the Shield Building Ventilation System.

Each penetration has a remote-indicating flow meter located in the annulus and upstream of the throttle valve so as to indicate fractional containment volume vent rate, independent of containment pressure.

The vent relief systems are located entirely within the annulus to preclude concern for leakage. The systems and their power supplies meet the requirements for engineered safeguards.

The vent system flow requirements are:

- that each throttle valve can accomplish the maximum vent rate necessary to control hydrogen (~25 scfm) at a nominal driving pressure (~2 psi, or greater if necessary); and
- that the combined capacity should not present a significant limitation with regard to time requirements for the completion of containment purge when transfer is eventually made to direct filtered discharge.

Analysis indicates that, for a design leak rate of one percent per day, the resulting out-leakage limits the useful pressure increase to about 13 psi, and this, or an even lower pressure, can be set as an operational limit. The vent system was tested in conjunction with the Shield Building Ventilation System to establish acceptable limits, and limits were set by operating procedures and, if necessary, can be set by means of fixed orifices downstream of the throttle valves.

Compression and replenishment of containment gases is through either of two penetrations that span the annulus to admit fresh air through the instrument air system. These penetrations will each initially be equipped with normally closed, remote manually opened isolation valves, throttle valve, and connections for use of oil-free portable air compressors. Design supply will be 100 scfm for each penetration at the maximum anticipated pressure.

Initial tests of the vent systems included startup, calibration of flow versus control position at varying pressure following integrated leak rate tests, and establishment of limits with regard to the Shield Building Ventilation System.

14.3.7.17 Provisions for Sampling

Monitoring of the containment hydrogen concentration is accomplished by two Comsip Model K-111 hydrogen analyzers. As stated in Reference 7, the analyzers fulfill the requirements of Item II.F.1.6 of NUREG-0737. The hydrogen monitors have indication in the control room and a range of 0 percent to 10 percent by volume under positive or negative containment pressure. The monitors are normally kept in standby mode, but indication is available on demand. The system is operated from its remote control panel located outside the high radiation sampling room. A hydrogen sample is drawn from the post-LOCA hydrogen control system sample ports in

containment. These ports are located near the discharge of the containment dome fans, which permits rapid detection of hydrogen escaping from the reactor. The fans draw suction from the upper areas of containment, which prevents the formation of a stratified atmosphere. The fans are powered from safeguard buses and are designed to operate in a post-LOCA environment (see NRC SER in Reference 7).

14.3.8 Steam Generator Tube Plugging

Steam generator tube plugs may be periodically installed to remove tubes from service based on reported degradation. When installed, the plugs become the primary pressure boundary for the subject tube. Plugs are installed at both ends of the tube, effectively isolating tube wall defects (corrosion, etc.). Tube plugging levels up to and including 10 percent of the total tubes have been analyzed.

A number of plug types and designs have been qualified for use in the KNPP steam generators. Plug types include expanded mechanical plugs, rolled plugs and welded plugs. Plug integrity is ensured by the qualification of the design and installation process through laboratory testing and observed field performance. Analytical verification of plug integrity used design and operating transient parameters selected to bound those loads imposed during normal and postulated accident conditions. Fatigue and stress analysis of steam generator tube plugs were performed in accordance with the ASME B&PV Code Section III.

14.3.9 Steam Generator Tube Fatigue Analysis

The NRC issued Bulletin 88-02 which required several actions to be implemented in order to minimize the potential for a steam generator tube rupture event caused by a rapidly propagating fatigue crack. This Bulletin is not applicable to the KNPP replacement steam generators due to material/manufacturing process upgrades.

14.3.10 Steam Generator Tube Removal

Portions of steam generator tubes may be removed periodically for laboratory analysis to determine degradation morphology, extent, and cause. Upon removal, the affected tube portions remaining inside the steam generator are plugged on both ends to maintain the integrity of the pressure boundary. Analyses have been performed which justify tube plugging up to a level of 10 percent of the total tubes in the generator. The plugs installed to restore pressure boundary integrity are qualified to the requirements of ASME B&PV Code Section III.

14.3.1 References

1. “Acceptance Criteria for Emergency Core Cooling System for Light Water Cooled Nuclear Power Reactors,” 10 CFR 50.46 and Appendix K of 10 CFR 50. Federal Register, Volume 39, Number 3, January 4, 1974
2. Meyer, P. E. and J. Kornfilt, “NOTRUMP. A Nodal Transient Small Break and General Network Code,” WCAP-10079-P-A (Proprietary) and WCAP 10080-A, (Non-Proprietary), August 1985
3. Lee, N., W. D. Tauche, W. R. Schwarz, “Westinghouse Small Break ECCS Evaluation Model Using the NOTRUMP Code,” WCAP-10054-P-A (Proprietary) and WCAP-10081-A (Non-Proprietary), August 1985
4. Bordelon, F. M., et al., “LOCTA-IV Program: Loss of Coolant Transient Analysis,” WCAP-8301, (Proprietary) and WCAP-8305 (Non-Proprietary), June 1974
5. Hellman, J. M., “Fuel Densification Experimental Results and Model For Reactor Application,” WCAP-8219, October 1973
6. Thompson, C. M., et al., “Addendum To The Westinghouse Small Break ECCS Evaluation Model Using The NOTRUMP Code: Safety Injection Into The Broken Loop and COSI Condensation Model.” WCAP-10054-P-A, Addendum 2, Revision 1 (Proprietary) and WCAP-10081-NP (Non-Proprietary), July 1997
7. Shimeck, D. J., “1-D Heat Conduction Model for Annular Fuel Pellets,” WCAP-147/8-P-A, May 1998

14.3.2 References

1. “Acceptance Criteria for Emergency Core Cooling Systems for Light Water Cooled Nuclear Power Reactors: 10 CFR 50.46 and Appendix K of 10 CFR 50.46,” Federal Register, Volume 39, Number 3, January 4, 1974
2. Hochreiter, L. E., W. R. Schwarz, K. Takeuchi, C. K. Tsai, and M. Y. Young, “Westinghouse Large-Break LOCA Best-Estimate Methodology, Volume 1: Model Description and Validation,” WCAP-10924-P-A, Volume 1, Revision 1, (Proprietary Version), December 1988
3. Dederer, S. I., L. E. Hochreiter, W. R. Schwarz, D. L. Stucker, C. K. Tsai, and M. Y. Young, “Westinghouse Large-Break LOCA Best-Estimate Methodology, Volume 2: Application to Two-Loop PWRs Equipped with Upper Plenum Injection,” WCAP-10924-P-A, Volume 2, Revision 2, December 1988
4. NRC Staff Report, “Emergency Core Cooling System Analysis Methods,” USNRC-SECY-83-472, November 1983

5. Bordelon, F. M., and E. T. Murphy, "Containment Pressure Analysis Code (COCO)," WCAP-8327 (Proprietary Version), WCAP-8326 (Non-Proprietary Version), June 1974
6. Foster, J. P., et al., "Westinghouse Improved Performance Analysis and Design Model (PAD 4.0)," WCAP-15063-P-A, Revision 1, with Errata, 2000
7. Federal Register, "Emergency Core Cooling Systems: Revisions to Acceptance Criteria," V53, N180, pp. 35996-36005, September 16, 1988
8. USNRC Regulatory Guide 1.157, "Best-Estimate Calculations of Emergency Core Cooling System Performances," May 1989
9. Boyack, B., et al., 1989, "Qualifying Reactor Safety Margins: Application of Code Scaling Applicability and Uncertainty (CSAU) Evaluation Methodology to a Large Break Loss-of-Coolant-Accident," NUREG/CR-5249
10. Letter, R. C. Jones (USNRC) to N. J. Liparulo (W), "Acceptance for Referencing of the Topical Report WCAP-12945 (P), Westinghouse Code Qualification Document for Best Estimate Loss-of-Coolant Analysis," June 28, 1996
11. Bajorek, S. M., et al., 1998, "Westinghouse Code Qualification Document for Best Estimate Loss of Coolant Accident Analysis," WCAP 12945-P-A (Proprietary), Volume I, Revision 2, and Volumes II-V, Revision 1, and WCAP-14747 (Non-Proprietary)
12. Dederer, S. I., et al., "Application of Best Estimate Large Break LOCA Methodology to Westinghouse PWRs with Upper Plenum Injection," W CAP-14449-P-A (Proprietary), Revision 1, and WCAP-14450 (Non-Proprietary), October 1999
13. Kellerman, B. E., et al., "Best Estimate Analysis of the Large Break Loss of Coolant Accident for Kewaunee Nuclear Power Plant to Support Up-rating and Transition to Westinghouse Fuel," WCAP-15708, July 2002
14. Branch Technical Position CSB 6-1, "Minimum Containment Pressure Model for PWR ECCS Performance Evaluation," July, 1981
15. Letter, C. A. Carpenter (USNRC) to N. J. Liparulo (W), "Acceptance for Referencing of the Topical Report WCAP-14449(P), Application of Best Estimate Large Break LOCA Methodology to Westinghouse PWRs With Upper Plenum Injection," (TAC No. M94035), May 21, 1999

14.3.3 References

1. Bohm, G. J., "Indian Point Unit No. 2 Reactor Internals Mechanical Analysis for Blowdown Excitation," WCAP-7822, December 20, 1971, W Class III
2. Fabric, S., "BLODWN-2: Digital Computer Program for Calculation of Hydraulic Transients During a Loss-of-Coolant Accident," Transactions Am. Nucl. Soc. p. 358, 1969 Annual Meeting, Seattle, June 15-19

3. Fabric, S., “Loss-of-Coolant Analysis: Comparison Between BLODWN-2 Code Results and Test Data,” WCAP-7401, November 1969
4. Takeuchi, K., et al., “MULTIFLEX 3.0, A FORTRAN-IV Computer Program For Analyzing Thermal-Hydraulic-Structure System Dynamics Advanced Beam Model,” WCAP-9735, Revision 2 (Proprietary), WCAP-9736, Revision 1 (Non-Proprietary), February 1998
5. Takeuchi, K., et al., “MULTIFLEX 3.0, A FORTRAN-IV Computer Program For Analyzing Thermal-Hydraulic-Structure System Dynamics,” WCAP-8708-P-A (Proprietary), WCAP-8709-A (Non-Proprietary), February 1998
6. Kewaunee Nuclear Power Plant, Steam Generator Replacement and Tavq Operating Window Program Licensing Report, November 2000

14.3.4 References

1. “Westinghouse LOCA Mass and Energy Release Model for Containment Design - March 1979 Version,” WCAP-10325-P-A (Proprietary), WCAP-10326-A (Nonproprietary), May 1983
2. “Westinghouse Mass and Energy Release Data For Containment Design,” WCAP-8264-P-A, Rev. 1 (Proprietary), WCAP-8312-A (Nonproprietary), August 1975
3. “Amendment No. 126, Facility Operating License No. DPR-58 (TAC No. 71062), for D. C. Cook Nuclear Plant Unit 1,” Docket No. 50-315, June 9, 1989
4. EPRI 294-2, “Mixing of Emergency Core Cooling Water with Steam; 1/3-Scale Test and Summary,” WCAP-8423, Final Report, June 1975
5. ANSI/ANS-5.1 1979, “American National Standard for Decay Heat Power in Light Water Reactors,” August 1979
6. Ranz, E. W., and W. R. Marshall, Jr., “Evaporation for Drops,” Chemical Engineering Progress, 48, pp. 141-146, March 1952
7. Parsly, L. F., “Design Consideration of Reactor Containment Spray System, Part VI, The Heating of Spray Drops in Air-Steam Atmospheres,” ORNL-TM-2412 Part VI, January 1970
8. WCAP 16040-P, “KNPP Power Uprate Project NSSS and BOP Licensing Report,” February 2003
9. Lamb, J. G., (NRC) to T. Coutu (NMC), transmitting “Kewaunee Nuclear Power Plant – Issuance of Amendment (TAC No. MB 9031),” February 27, 2004, with attached Safety Evaluation Docket No. 50-305

14.3.5 References

1. Lamb, John, (NRC) to Tom Coutu (NMC), transmitting the NRC SER for Amendment No. 172 to the Operating License, approving the Stretch Power Uprate, Letter No. K-04-035, February 27, 2004

14.3.9 References

1. Docket 50-322, DRL Staff Evaluation of Shoreham Application, February 20, 1970
2. ORNL-TM-3342, "ORNL Safety Research and Development Program Bimonthly Report for January-February, 1971"
3. Getman and Daniels, "Outlines of Theoretical Chemistry," sixth edition, John Wiley and Sons, p. 332
4. Row, T. H., "Reactor Containment - Building Spray Systems for Fission Product Removal," Nuclear Safety, September-October, 1971, p. 516
5. Docket 50-255, Palisades FSAR, Figure 14.22-5
6. Cottrell, Wm. B. and A. W. Savolainen, "U.S. Reactor Containment Technology," ORNL-NSIC-5, p. 5.82
7. NRC Safety Evaluation Report, S. A. Varga (NRC) to C. W. Giesler (WPS), Letter No. K-83-101, May 2, 1983

Table 14.3-1
Small-Break LOCA Time Sequence of Events

Event Time (sec)	High T_{avg}			Low T_{avg}
	2-in.	3-in.	4-in.	3-in.
Break Initiation	0	0	0	0
Reactor Trip Signal	44.4	18.7	10.4	11.7
S-Signal	52.5	25.2	14.6	12.6
AFW Initiation	112.5	85.2	74.6	72.6
Loop Seal Clearing	560	262	153	287
Core Uncovery	1318	558	307	659
Accumulator Injection	1987	725	372	729
PCT Time	1919	812	165	817
Core Recovery	2141	1428	482	1400

Table 14.3-2
Small-Break LOCA Fuel Cladding Results

Results	High T_{avg}			Low T_{avg}
	2-in.	3-in.	4-in.	3-in.
Peak Clad Temperature (°F)	916	1030	938	861
Peak Clad Temperature Elevation (ft)	11.00	11.00	9.75	11.00
Maximum Local Zinc/Water Reaction, (%)	<17.0	<17.0	<17.0	<17.0
Maximum Local Zinc/Water Reaction Elevation (ft)	11.25	11.00	10.25	11.25
Total Zinc/Water Reaction (%)	<1.0	<1.0	<1.0	<1.0
Hot Rod Burst Time (sec)	no burst	no burst	no burst	no burst
Hot Rod Burst Elevation (ft)	N/A	N/A	N/A	N/A
Reactor Core Rated Thermal Power ^a	772 MWt			
Peak Linear Power	16.73 kW/ft			
Total Peaking Factor (F_Q)	2.5			

a. 0.6% is added to the core thermal power to account for calorimetric uncertainties.

Table 14.3.3-1

Large Break Local Containment Data Used for Calculation of Containment Pressure

Net Free Volume	1,370,000 ft ³
Initial Conditions	
Pressure	14.7 psid
Temperature	90.0°F
RWST Temperature	40.0°F
Service Water Temperature	32.0°F
Temperature Outside Containment	-20.0°F
Initial Spray Temperature	40.0°F
Spray System	
Number of spray pumps operating	2
Post-accident spray system initiation delay without LOOP	15 sec
Maximum spray system flow	3200 gal/min
Containment Fan Coolers	
Post-accident initiation fan coolers	0 sec
Number of fan coolers operating	4
Fan cooler heat removal data	See Table 14.3.3-2
Structural Heat Sinks	See Table 14.3.3-3

Table 14.3.3-2
Fan Cooler Heat Removal Data Used for Calculation of Containment Pressure

Temperature (°F)	Heat Removal Rate Per Fan Cooler (Btu/s)
120	1800
136	5670
205	12,550
244	16,970
270	20,080

Table 14.3.3-3
 Large Break Structural Heat Sink Data
 Used for Calculation of Containment Pressure

Structural Heat Sinks

Description	Material (ft ²)	Area (ft ²)	Thickness (inches)
Containment Cylinder (Paint Coating #3)	Carbon Steel	26,381.35	1.5
Containment Dome (Paint Coating #4)	Carbon Steel	17,318.0	0.75
Reactor Vessel Liner & Refueling Canal	Stainless Steel –	7860.0	0.25
	Concrete Backup	7860.0	12.00
Containment Cylinder (Paint Coating #4)	Carbon Steel	17,823.35	1.5
Crane (Paint Coating #5)	Carbon Steel	9877.0	0.75
Pipes	Carbon Steel	6800.0	0.375
Miscellaneous Supports	Carbon Steel	44,000.0	0.50
Crane (unpainted)	Carbon Steel	4823.0	0.75
Miscellaneous Supports	Carbon Steel	32,000.0	0.25
Ventilation Ductwork	Carbon Steel	35,125.0	0.1875
Gratings	Carbon Steel	12,400.00	0.090
Hand Rails	Carbon Steel	1695.0	0.144
Exposed Conduit and Cable Trays	Carbon Steel	6000.0	0.100
Accumulators	Carbon Steel	2200.0	1.440
Heavy Walls (unpainted)	Concrete	3400.0	12.0
Heavy Walls (Paint Coating #1)	Concrete	37,400.0	12.0
Medium Floors (unpainted)	Concrete	19,770.0	6.0
Medium Floors (Paint Coating #2)	Concrete	5300.0	6.0
Light Floors (unpainted)	Concrete	2370.0	3.0
Light Floor (Paint Coating #2)	Concrete	5200.0	3.0
Sump B Recirculation Strainer Pipe	Stainless Steel	145.0	0.25
Sump B Recirculation Strainer Perforated Plate	Stainless Steel	575.0	0.048

Table 14.3.3-3
 Large Break Structural Heat Sink Data
 Used for Calculation of Containment Pressure

Structural Heat Sinks

Description	Material (ft ²)	Area (ft ²)	Thickness (inches)
Paint Coating Systems:			
Coating #1: Phenoline 305 Primer – 4 mils; Phenoline 305 Finish – 4 mils			
Coating #2: Phenoline 300 Finish – 8 mils			
Coating #3: Carbozinc 11 Primer – 3 mils; Phenoline 305 Finish – 4 mils			
Coating #4: Carbozinc 11 Primer – 3 mils; Phenoline 305 Finish – 8 mils			
Coating #5: Carbozinc 11 Primer – 3 mils			

Table 14.3.3-4
Key LOCA Parameters and Reference Transient Assumptions

Parameter	Reference Transient	Uncertainty or Bias
1.0 Plant Physical Description		
a. Dimensions	Nominal	ΔPCT_{MOD}^1
b. Flow resistance	Nominal (KN=1.58)	ΔPCT_{MOD}
c. Pressurizer location	Opposite broken loop	Bounded
d. Hot assembly location	Under limiting location	Bounded
e. Hot assembly type	<u>W</u> Vantage+ (422V+)	Bounded
f. SG tube plugging level	High (10%)	Bounded ⁴
2.0 Plant Initial Operating Conditions		
2.1 Reactor Power		
a. Core average linear heat rate (AFLUX)	Nominal - 100% of uprated power (6.853 kw/ft)	ΔPCT_{PD}^2
b. Peak linear heat rate (PLHR)	15.43 kw/ft ($F_Q=2.252$), derived from Tech Spec (TS) F_Q limit of 2.50 and maximum baseload steady-state depletion F_Q of 2.10	ΔPCT_{PD}
c. Hot rod average linear heat rate (HRFLUX)	12.52 kw/ft ($F_{\Delta H} = 1.83$), derived from $F_{\Delta H}$ limit of 1.80 Note 5	ΔPCT_{PD}
d. Hot assembly average linear heat rate (HAFLUX)	12.04 kw/ft (HRFLUX/1.04)	ΔPCT_{PD}
e. Hot assembly peak linear heat rate (HAPHR)	14.82 kw/ft (PLHR/1.04)	ΔPCT_{PD}
d. Axial power distribution (P_{BOT} , P_{MID})	Figure 14.3.2-12	ΔPCT_{PD}
g. Low power region relative power (P_{LOW})	$0.2 \leq P_{LOW} \leq 0.6$	Bounded ⁸
h. Hot assembly burnup	BOL	Bounded

Table 14.3.3-4
Key LOCA Parameters and Reference Transient Assumptions

Parameter	Reference Transient	Uncertainty or Bias
i. Prior operating history	Equilibrium decay heat	Bounded
j. Moderator Temperature Coefficient (MTC)	Tech Spec Maximum (0)	Bounded
k. HFP boron	800 ppm	Generic
2.2 Fluid Conditions		
a. T_{avg}	Minimum nominal $T_{avg} = 556.3^{\circ}\text{F}$	Nominal is bounded, ⁴ unc'y is in $\Delta\text{PCT}_{\text{IC}}$
b. Pressurizer pressure	Nominal (2250.0 psia)	$\Delta\text{PCT}_{\text{IC}}$
c. Loop flow	89,000 gpm ⁹	$\Delta\text{PCT}_{\text{MOD}}^6$
d. TUH	Best Estimate	0
e. Pressurizer level	Nominal (362.5 ft ³) ⁷	0
f. Accumulator temperature	Nominal (90.0°F)	$\Delta\text{PCT}_{\text{IC}}^3$
g. Accumulator pressure	Nominal (764.7 psia)	$\Delta\text{PCT}_{\text{IC}}$
h. Accumulator liquid volume	Nominal (1250 ft ³)	$\Delta\text{PCT}_{\text{IC}}$
i. Accumulator line resistance	Nominal	$\Delta\text{PCT}_{\text{IC}}$
j. Accumulator boron	Minimum (1850 ppm)	Bounded
3.0 Accident Boundary Conditions		
a. Break location	Cold leg	Bounded
b. Break type	Split	$\Delta\text{PCT}_{\text{MOD}}$
c. Break size	Limiting ¹⁰	$\Delta\text{PCT}_{\text{MOD}}$
d. Offsite power	Loss-of-Offsite-Power (LOOP)	Bounded ⁴
e. SI flow	Minimum	Bounded
f. SI temperature	Nominal (85°F)	$\Delta\text{PCT}_{\text{IC}}$
g. SI delay	Maximum delay ¹¹	Bounded

Table 14.3.3-4
Key LOCA Parameters and Reference Transient Assumptions

Parameter	Reference Transient	Uncertainty or Bias
h. Containment pressure	Minimum based on <u>WC/T</u> M&E from the Limiting Split Break	Bounded
i. Single failure	ECCS: Loss of one Train of SI	Bounded
j. Control rod drop time	No control rods	Bounded
4.0 Model Parameters		
a. Critical Flow	Nominal (as coded)	ΔPCT_{MOD}
b. Resistance uncertainties in broken loop	Nominal (as coded)	ΔPCT_{MOD}
c. Initial stored energy/fuel rod behavior	Nominal (as coded)	ΔPCT_{MOD}
d. Core heat transfer	Nominal (as coded)	ΔPCT_{MOD}
e. Delivery and bypassing of ECC	Nominal (as coded)	Conservative
f. Steam binding/entrainment	Nominal (as coded)	Conservative
g. Noncondensable gases/ accumulator nitrogen	Nominal (as coded)	Conservative
h. Condensation	Nominal (as coded)	ΔPCT_{MOD}

Notes:

1. ΔPCT_{MOD} indicates this uncertainty is part of code and global model uncertainty.
2. ΔPCT_{PD} indicates this uncertainty is part of power distribution uncertainty.
3. ΔPCT_{IC} indicates this uncertainty is part of initial condition uncertainty.
4. Confirmed in Section 4 of Reference 13.
5. $F_{\Delta H}$ value bounds the Technical Specification limit.
6. Assumed to be result of loop resistance uncertainty.
7. Pressurizer level at the minimum nominal T_{avg} of 556.3°F.
8. A P_{LOW} of 0.6 is bounding, as determined in Section 4 of Reference 13.
9. Based on 10 percent SGTP.

Table 14.3.3-4
Key LOCA Parameters and Reference Transient Assumptions

Parameter	Reference Transient	Uncertainty or Bias
10. The limiting split break was determined to be 70 percent of the area of the cold leg in Section 4 of Reference 13.		
11. The maximum SI delay times for loss-of-offsite-power (LOOP) are 30.0 sec for HHSI and 35.0 sec.		

Table 14.3.3-5
 KNPP Confirmatory Calculation PCT Results Summary

Case ^a	Blowdown PCT (°F)	Reflood PCT (°F)
Initial Transient	1613	1739
Pressurizer on Intact Loop	1633	1723
LOOP	1639	1770
Reduced SGTP (0%)	1606	1735
Increased T_{avg} (575.3°F)	1593	1626
Reduced P_{LOW} (0.2)	1620	1736
Final Reference Transient ^b	1654	1763

a. All confirmatory cases were performed at the 6.0% uprated nominal core power of 1749 MWt.

b. The final reference transient was performed at the 7.4% uprated nominal core power of 1772 MWt and at the low nominal T_{avg} operating point of 556.3°F.

Table 14.3.3-6
Large-Break LOCA Mass and Energy Releases Used for COCO Calculation

Time (sec)	Mass Flow (lbm/s)	Energy Flow (Btu/s)
0.0	0	0
0.5	35,141	17,812,478
1.0	34,677	17,577,966
2.0	31,183	15,845,205
3.0	27,078	13,878,829
4.0	22,624	11,742,809
5.0	17,199	9,025,576
6.0	14,714	7,799,808
8.0	12,516	6,900,154
10.0	10,377	6,070,358
12.0	8685	5,206,006
14.0	6690	4,151,783
16.0	5729	3,323,195
18.0	5276	2,635,818
20.0	4141	1,580,523
22.0	1762	419,772
24.0	3339	799,974
26.0	2236	602,920
28.0	2594	640,592
30.0	1449	266,043
32.0	1166	231,838
34.0	307	103,518
35.5	-90	0
36.5	-22	0
40.0	398	225,543
45.0	310	292,109
50.0	247	250,334

Table 14.3.3-6
Large-Break LOCA Mass and Energy Releases Used for COCO Calculation

Time (sec)	Mass Flow (lbm/s)	Energy Flow (Btu/s)
55.0	211	212,803
60.5	191	198,064
70.0	94	111,254
80.0	97	115,882
90.5	86	101,908
100.0	64	75,931
110.0	50	59,802
120.0	59	68,805
130.0	161	114,731
160.0	639	205,201
190.0	201	163,290
220.0	300	117,634
249.5	40	46,593

Table 14.3.3-7
 KNPP Break Size and Type Sensitivity PCT Results Summary

Break Type ^a	Discharge Coefficient (C_D)	Flow Resistance (K_N)	Reflood PCT (°F)
Split	0.5	1.58	1075
Split	0.6	1.58	1593
Split	0.7	1.58	1740
Split	0.8	1.58	1705
Split	0.9	1.58	1633
Split	1.0	1.58	1550
Limiting Split ^b	0.7	1.58	1739
DECLG	0.8	0.77	1408
DECLG	0.8	1.58	1481
DECLG	0.8	2.40	1562
DECLG	1.0	1.58	1287

- a. All split cases were performed at the 6.0% uprated nominal core power of 1749 MWt. The DECLG cases were performed at the same conditions as the Final Reference Transient (7.4% uprated nominal core power of 1772 MWt and at the low nominal T_{avg} operating point of 556.3°F).
- b. The limiting split ($C_D=0.7$) was rerun with minor input corrections.

Table 14.3.3-8
 KNPP Best-Estimate Large-Break LOCA Results

Component	Blowdown	First Reflood	Second Reflood	Criteria
50th Percentile PCT (°F)	< 1672	< 1600	< 1760	N/A
95th Percentile PCT (°F)	< 1924	< 1892	< 2084	< 2200
Maximum Local Oxidation (%)		< 8.44		< 17.0
Maximum Total Hydrogen Generation (%)		< 0.74		< 1.0

Table 14.3.3-9

KNPP Conditions Analyzed with WCOBRA/TRAC Compared to be UPI Test Conditions

Condition	BE UPI Test	KNPP
Core Power, MWt	1980	1772
Low Power Region Average Linear Heat Rate (kW/ft)	6.9	1.35 – 4.11
Hot Assembly Peak Linear Heat Rate (kW/ft)	17.0	16.955 ^a

a. This is a higher peak linear heat rate than would be allowed by the Tech Specs.

Table 14.3.3-10
Plant Operating Range Allowed by the Best-Estimate
Large-Break LOCA Analysis (KNPP)

Parameter	Operating Range
1.0 Plant Physical Description	
a. Dimensions	No in-board assembly grid deformation during LOCA +SSE
b. Flow resistance	N/A
c. Pressurizer location	N/A
d. Hot assembly location	Anywhere in core
e. Hot assembly type	Fresh 14 x14 Vantage+ (422V+) fuel assembly
f. SG tube plugging level	$\leq 10\%$
2.0 Plant Initial Operating Conditions	
2.1 Reactor Power	
a. Core average linear heat rate	Core power $\leq 100.6\%$ of 1772 MWt (6.853 kw/ft)
b. Peak linear heat rate	$F_Q \leq 2.50$
c. Hot rod average linear heat rate	$F_{\Delta H} \leq 1.80$
d. Hot assembly average linear heat rate	$\bar{P}_{HA} \leq 1.731$
e. Hot assembly peak linear heat rate	$F_{Q,HA} \leq 2.40$
f. Axial power dist. (P_{BOT} , P_{MID})	Figure 14.3.2-12
g. Low power region relative power (P_{LOW})	$0.2 \leq P_{LOW} \leq 0.6$
h. Hot assembly burnup	≤ 75000 MWD/MTU, lead rod
i. Prior operating history	All normal operating histories
j. MTC	≤ 0 at HFP
k. HFP boron	Normal letdown
2.2 Fluid Conditions	
a. T_{avg}	$556.3 \pm 10^\circ F \leq T_{avg} \leq 575.3 \pm 10^\circ F$
b. Pressurizer pressure	$2150 \leq P_{RCS} \leq 2350$ psia

Table 14.3.3-10
Plant Operating Range Allowed by the Best-Estimate
Large-Break LOCA Analysis (KNPP)

Parameter	Operating Range
c. Loop flow	$\geq 89,000$ gpm/loop
d. T_{UH}	Current upper internals, T_{hot} UH
e. Pressurizer level	Normal level, automatic control
f. Accumulator temperature	$40 \leq$ accumulator temp $\leq 130^{\circ}\text{F}$
g. Accumulator pressure	$675 \leq P_{ACC} \leq 825$ psig
h. Accumulator volume	$1225 \leq V_{ACC} \leq 1275$ ft ³
i. Accumulator fL/D	Current line configuration
j. Minimum accumulator boron	≥ 1850 ppm
3.0 Accident Boundary Conditions	
a. Break location	N/A
b. Break type	N/A
c. Break size	N/A
d. Offsite power	Available or LOOP
e. SI flow	Figure 14.3.2-13 and Figure 14.3.2-14
f. SI temperature	$40 \leq$ SI Temp $\leq 130^{\circ}\text{F}$ (40°F spray temp assumed)
g. SI delay	LHSI ≤ 25.0 seconds (with offsite power) ≤ 35.0 seconds (with LOOP) HHSI ≤ 20.0 seconds (with offsite power) ≤ 30.0 seconds (with LOOP)
h. Containment pressure	Bounded - Based on minimum containment pressure of 14.7 psia. Bounding pressure curve (Figure 14.3.2-2) is based on COCO containment pressure calculation using conditions supplied in Table 14.3.3-1 through Table 14.3.3-3.
i. Single failure	Loss of one train of SI
j. Control rod drop time	N/A

Table 14.3-3
Components Nomenclature

Component	Element
Vessel Supports	Numbers 1 and 49
Barrel Flange and Hold-Down Spring	Numbers 2 through 6
Barrel	Numbers 7 through 10
Lower Core Supports	Numbers 11 through 15
Major Fuel Assembly	Even Numbers 16 through 38
Minor Fuel Assemblies	Odd Numbers 17 through 39
Upper Internals	Numbers 40 through 48

Table 14.3-4
Maximum Deflections Under Blowdown (Inches)(1-millisecond Double-Ended Break)

Component	Cold Leg	Hot Leg	Seismic Horizontal	Maximum Total	Allowable Limit	No Loss of Function Limit
Upper Barrel - radial inward	0.0	0.064	0.002	0.066	2.0	4.0
- radial outward	0.093	0.021	0.002	0.095	0.5	1.0
Upper Core Plate	0.004	0.014	0	0.014	0.100 ^a	0.150
RCC Guide Tubes (deflection as a beam)		31 < Allowable	0.006 (ALL)	31 < Allowable	0.72 (ALL)	1.15(ALL)
Total (33)		2 < N.L.F.	0.006 (ALL)	2 < N.L.F.	0.72 (ALL)	1.15(ALL)
Fuel Assembly Thimbles (cross section distortion)	~ 0	~ 0	~ 0	~ 0	0.036	0.072

a. Only to verify that the plate will not touch a guide tube.

Table 14.3-5
Summary of Maximum Stress Intensities (PSI)(1-millisecond Pipe Break and Seismics)

Component	Hot Leg Break		Cold Leg Break		Maximum Total Seismic		Maximum Total Blowdown Plus Seismic
	Maximum Membrane	Maximum Total	Maximum Membrane	Maximum Total	Vertical	Horizontal	
Barrel (Girth Weld)	10,430	20,199	32,000	45,300	718	2170	48,188
Barrel Flange (Weld)	7778	29,568	25,000	44,500	313	1007	45,820
Fuel Assembly Top Nozzle Plate	--	10,380	0	850	0	0	10,380
Fuel Assembly Bottom Nozzle Plate	0	44,060	0	25,080	0	0	44,060
Upper Support Columns	10,228	10,228	14,043	14,043	--	--	14,043

Allowable Stress, S_m :

S_m at 588°F = 16,600 psi^a

maximum membrane stress = $P_m = 2.4 S_m = 39,800$ psi

maximum total stress = $P_m + P_b = 49,800$ psi

a. Per Winter 1969 Addenda ASME Section III Code.

Table 14.3-6
Internal Energy Balance^a

	Double Ended	4.5 ft ²	3.0 ft ²	0.5 ft ²
U _i	4.15	4.15	4.15	4.15
a/Blowdown	180.11	179.61	179.09	171.98
	0.00	0.00	0.00	0.00
Σ (mh)in b/Sprays				
Σ Qin	~ 0	~ 0	~ 0	~ 0
a/Structure	7.03	7.81	8.45	12.09
	0	0	0	0.61
Σ Qout b/Fans				
Total U _f	177.23	175.95	174.79	163.83
From COCO the final conditions are:				
Steam	131.67	130.50	130.29	123.41
Air	4.11	4.10	4.10	4.05
Sump	40.27	40.66	40.03	37.18
	176.05	175.26	174.42	164.64

a. All energy values in 10⁶ Btu.

Table 14.3-7
Major Assumptions for Design Basis LOCA Analysis

Source Term	
Core Activity	See Table D.1-1
Nuclide Parameters	See Table D.1-1
Activity Release Timing	
Gap Release	First 30 minutes
Fuel Release	1.3 hours (ending at 1.8 hours)
Activity Release From The Fuel	
Noble Gases	5% gap, 95% fuel (100% total)
Iodines	5% gap, 35% fuel (40% total)
Alkali Metals	5% gap, 25% fuel (30% total)
Tellurium Metals	0% gap, 5% fuel (5% total)
Barium, Strontium	0% gap, 2% fuel (2% total)
Noble Metals	0% gap, 0.25% fuel (0.25% total)
Cerium Group	0% gap, 0.05% fuel (0.05% total)
Lanthanides	0% gap, 0.02% fuel (0.02% total)
Iodine Chemical Form in Containment	4.85% elemental, 0.15% organic & 95% particulates
Iodine Chemical Form Released to Atmosphere from ECCS Leakage	97% elemental, 3% organic
Containment Release Path	
Containment, Shield Building and Auxiliary Building Modeling	See Table 14.3-8
Spray Operation	
Time to Initiate Sprays	0.0 hours
Termination of Spray Injection	0.91 hours
Recirculation Spray	Not credited
Injection Spray Flow Rate	1148 gpm
Spray Fall Height	150 feet

Table 14.3-7
Major Assumptions for Design Basis LOCA Analysis

Source Term	
Removal Co-efficients	
Elemental Iodine Injection Spray Removal	20.0 hr ⁻¹
Particulate Injection Spray Removal	4.5 hr ⁻¹
Sedimentation Particulate Removal (after spray termination)	0.1 hr ⁻¹
ECCS Leakage Release Path	
Credited Sump Volume	315,000 gal
ECCS Leak Rate to Auxiliary Building	12 gal/hr ^a
Airborne Fraction for ECCS Leakage to Auxiliary Building	
0–3 hours	10%
>3 hours	1%
ECCS Leak Rate to RWST	
0–24 hours	3 gpm
>24 hours	1.5 gpm
Airborne Fraction for ECCS Leakage to RWST	1%
ECCS Leakage Plateout in Auxiliary Building	50%
Shield Building & Auxiliary Building Filter Efficiencies	
Elemental	90%
Organic	90%
Particulates	99%
Off-Site Atmospheric Dispersion Factors	
See Table D.8-4	
Off-Site Breathing Rates	
See Table D.8-3	

a. Twice the System Integrity Program limit per Regulatory Guide 1.183.

Table 14.3-8
Containment, Shield Building
and Auxiliary Building Modeling Used for LBLOCA

Containment Net-Free Volume	1.32E7 (ft ³)
Shield Building Volume	3.74E5 (ft ³)
Shield Building Participation Fraction	0.5
Auxiliary Building Volume	Not modeled, no holdup credited
Containment Leak Rates	
0–24 hours	0.5 (weight %/day)
> 24 hours	0.25 (weight %/day)
Containment Leak Path Fractions	
0–10 minutes	
Through Shield Building	0.0
Through Auxiliary Building SV	0.1
Direct to Environment	0.9
>10 minutes	
Through Shield Building	0.89
Through Auxiliary Building SV	0.1
Direct to Environment	0.01
Shield Building Air Flows	
0–10 minutes	
Shield Building to Environment	Not applicable
Shield Building Recirculation	Not applicable
10 minutes–30 minutes	
Shield Building to Environment	6000 + 10% scfm
Shield Building Recirculation	0.0 scfm
>30 minutes	
Shield Building to Environment	3100 scfm
Shield Building Recirculation	2300 scfm

Table 14.3-8
Containment, Shield Building
and Auxiliary Building Modeling Used for LBLOCA

Shield Building and Auxiliary Building
Filter Efficiencies

Elemental	90%
Organic	90%
Particulate	99%

Table 14.3-9
Doses for Design Basis Loss-of-Coolant Accident

	Total Effective Dose Equivalent (TEDE) Dose
Limiting Site Boundary 2-Hour Exposure (1.8 – 3.8 hours)	1.31 rem
30-Day Low Population Zone Exposure	0.22 rem
10 CFR 50.67 Limit	25.0 rem

Table 14.3-10
Exposed Zinc and Aluminum Bearing Surfaces Within Kewaunee Containment Vessel

	Square Feet	Thickness or Weight/Area	Pounds of Metal
<u>Galvanized Steel Surfaces</u>			
Platform and gratings, all surfaces	12,400	2.0 oz Zn/ft ²	1550
All ductwork, both sides	35,253	0.60 oz Zn/ft ²	1322
Conduit, trays and supports exposed to spray	13,250	0.60 oz Zn/ft ²	497
Stair treads	2305	0.60 oz Zn/ft ²	86
Cable restraints	338	--	68
Total Galvanized	63,596		3523
<u>Zinc-Bearing Undercoats</u>			
Primer on structural steel, Carbozine 11	95,400	3 mils specified	5540
Primer on containment vessel interior, Carbozine 11	51,500	3 mils specified	2243
Total Undercoat	146,900		8530
<u>Aluminum Surfaces</u>			
Reactor equipment, including contingency	144.5	--	424
Crane lights and fixtures	Undetermined	--	160
Connectors on rod drive cables	58.7	--	110
Total Aluminum	Undetermined		694
Aluminum Paint on Reactor Equipment	Undetermined	--	110

Table 14.3-11
Hydrogen Gas Production in Acidic and Basic Solutions

	First Day Reaction Rate	Area or Weight	First Day scf	Continuing scf/day
<u>No additive (pH < 7)</u>				
Zinc-bearing paint	2.3 cc/cm ²	146,900/2 ft ²	5542	
Galvanized surface	2.3 cc/cm ²	63,596/2 ft ²	2400	36.4
Total				36.4
<u>With additive (pH > 7)</u>				
Zinc-bearing paint	2.0 cc/cm ²	146,900/2 ft ²	4819	
Galvanized surface	low	63,596/2 ft ²	--	36.4
Aluminum paint	all	110 lb	2200	
Aluminum structure	1 mil	694 lb	66	36.4
Total			7085	72.8

Table 14.3-12
Sources and Assumptions for Hydrogen Calculations

	Reasonably Conservative Estimate	Most Conservative Estimate Using Safety Guide 7
<u>Coolant Absorption of Radiation from Fuel</u>		
Halogens in fuel	50%	50%
Noble gases in fuel	100%	0
Other fission products in fuel	99%	99%
Gamma energy fraction absorbed in water	0.071	0.10
Beta energy fraction absorbed in water	0	0
G(H ₂), molecules/100 ev	0.44	0.50
<u>Sources in Coolant</u>		
Halogens in coolant	50%	50%
Noble gases in coolant	0	0
Other fission products in coolant	1%	1%
Gamma energy fraction absorbed	1.0	1.0
Beta energy fraction absorbed	1.0	1.0
G(H ₂) molecules/100 ev	0.30	0.50
Initial Zirconium-Water Reaction	2% (4862 scf)	5% (12,155 scf)
<u>Initial Zinc Reaction</u>		
1.15 cc/cm ² × 200,146 ft ²	7550 scf	7550 scf
Continuing Zinc Reaction	30.5 scf/day	30.5 scf/day
<u>Plant Characteristics</u>		
Thermal power	1721.4 Mw	
Containment free volume	1,320,000 ft ³	
Initial containment temperature	120°F	
Zirconium cladding	30,858 lb	

Table 14.3-13
Venting Requirements and Venting Doses without Pressure Increase

	Reasonably Conservative Estimate	Most Conservative Estimate Using Safety Guide 7
Time of occurrence of 3.5 ^v / _o hydrogen	41 days	10.1 days
Time of occurrence of 4.1 ^v / _o hydrogen	65 days	17 days
Initial vent rate necessary to maintain 3.5 ^v / _o hydrogen	7.3 scfm or 0.90% day at 41 days	24.2 scfm or 3.05% day at 10.1 days
Occurrence of 1 MPC at site boundary ^a	63 days ^a	60 days
Initial 1 MPC vent flow at time indicated above	5.8 scfm	9.3 scfm
Earliest completion of purge with 1 MPC maintained at site boundary	122 days	98 days
Venting dose at site boundary up to 30 post-accident days	—	6.37 rem thyroid ^b ; 0.75 rem whole body
Venting dose at site boundary up to occurrence of 1 MPC	0.166 rem thyroid 0.017 rem whole body	6.88 rem thyroid ^c 0.79 rem whole body
Venting dose at 4800 meters up to 30 post-accident days	—	0.734 rem thyroid; 0.087 rem whole body
Venting dose at 4800 meters up to Occurrence of 1 MPC at site boundary	19.1 mrem thyroid; 2.0 mrem whole body	0.792 rem thyroid; 0.091 rem whole body

a. In the reasonable conservative case, a 1 MPC vent capability would occur at 63 days and 4.07% hydrogen concentration if venting were deferred and not initiated at 3.5% concentration.

b. Dose is 3.02 rem for an SBVS filter efficiency of 95%.

c. Dose is 3.25 rams for an SBVS filter efficiency of 95%.

Table 14.3-14
Effects of Pressure Increase on Venting Doses

	No Deferment of Venting	Venting Deferred Until 30 Days	Venting Deferred Until 1 MPC
Occurrence of 3.5 % Hydrogen Concentration	10.1 days	10.1 days	10.1 days
Action at 10.1 days	Vent at 24.2 scfm initial	Compress hydrogen with 24.2 scfm air initial	Compress hydrogen with 24.2 scfm air initial
Stop Pressure Rise and Begin Venting	--	30 days	30 days
Peak Containment Pressure	0 psig	6.1 psig	12.2 psig
Occurrence of 1 MPC at site Boundary	60 days	62 days	63 days
Earliest Completion of 1 MPC Final Purge	98 days	119 days	131 days
Site Boundary Doses up to Occurrence of 1 MPC: From Venting:			
Thyroid Dose			
Whole Body Dose	6.88 rem ^a	0.64 rem	0 rem
From Pressure-Induced Leakage Before Venting: ^b			
Thyroid Dose	0.72 rem		
Whole Body Dose	0 rem	0.99 rem	0.097 rem
TOTAL DOSE			
Thyroid Dose			
Whole Body Dose	6.88 rem ^a	1.36 rem	0.99 rem

a. Dose is 3.25 rem for an SBVS filter efficiency of 95%.

b. Based on 0.01/day leakage at design test pressure.

Table 14.3.4-1
System Parameters Initial Conditions

Parameters	Value
Core thermal power (MWt)	1782.6
RCS total flow rate (lbm/sec)	18852
Vessel outlet temperature (°F)	612.8
Core inlet temperature (°F)	545.2
Vessel average temperature (°F)	579.0
Initial steam generator steam pressure (psia)	809
Steam generator design	Model 54F
Steam generator tube plugging (%)	0
Initial steam generator secondary-side mass (lbm)	115250.3
Assumed maximum containment backpressure (psia)	60.7
Accumulator	
Water volume (ft) per accumulator	1275
N ₂ cover gas pressure (psia)	714.7
Temperature (°F)	120
SI delay, total (sec) (from beginning of event)	33.8

Note: Core thermal power, RCS total flow rate, RCS coolant temperatures and steam generator secondary side mass include appropriate uncertainty and/or allowance.

Table 14.3.4-2
 SI Flow Minimum Safeguards
 Injection Mode (Re-flood Phase)

RCS Pressure (psig)	Total flow (lbm/sec)
0	305.0
20	288.9
40	269.4
60	247.3
80	221.9
100	189.7
120	142.8
140	82.1
160	81.7
180	81.4

Recirculation Sequence

Time (sec)	Vessel Injection (lbm/sec)	
	From RWST	From Sump
3953.0	84.8	0
4143.0	84.8	33.3
6352.0	0.0	33.3
6382.0	0.0	186.2
10,000.0	0.0	186.2
500,000.0	0.0	186.2

Table 14.3.4-3
 SI Flow Maximum Safeguards
 Injection Mode (Re-flood Phase)

RCS Pressure (psig)	Total flow (lbm/sec)
0	711.5
20	671.9
40	628.4
60	581.5
80	528.8
100	465.2
120	388.1
140	270.9
160	173.8
180	173.1

Recirculation Sequence

Time (sec)	Vessel Injection (lbm/sec)	
	From RWST	From Sump
1253.0	304.9	0.0
1443.0	304.9	66.6
1473.0	304.9	186.2
2707.0	0.0	186.2
2919.0	0.0	186.2
500,000.0	0.0	186.2

Table 14.3.4-4
Containment Response Analysis Parameters

Service Water Temperature (°F)	80 (0-24 hrs) 73 (24-168 hrs) 70 (>168 hrs)
RWST Water Temperature (°F)	120
Initial Containment Temperature (°F)	120
Initial Containment Pressure (psia)	16.85
Initial Relative Humidity (%)	17.7
Net Free Volume (ft ³)	1.32×10^6
CFCU	
<hr/>	
Total	4
Analysis Maximum	4
Analysis Minimum	2
Containment High Pressure Setpoint (psig)	5.00
Delay Time (sec)	
With Offsite Power	75.0
Without Offsite Power	85.0
Containment Spray Pumps	
<hr/>	
Total	2
Analysis Maximum	2
Analysis Minimum	1
Flow Rate (gpm)	
Injection Phase (per pump)	1170
Recirculation Phase	Not modeled
Containment High-High Pressure Setpoint (psig)	23.0
Delay time (sec)	
With Offsite Power (delay after high-high pressure setpoint)	106.0
Without Offsite Power (delay after high-high pressure setpoint)	135.0
CS Termination Time, (sec)	
Minimum Safeguards	3953
Maximum Safeguards (stop one pump/stop second pump)	1253/2707

Table 14.3.4-4
Containment Response Analysis Parameters

RHR System

Recirculation Switchover, Full Flow Established, (sec)	
Minimum Safeguards	6382
Maximum Safeguards	1473
Number of Heat Exchangers Modeled in the Analysis	1
RHR Flows through RHR Heat Exchangers	
Minimum Safeguards	
Time (sec)	Flow (lbm/s)
0.0	0.0
4143	0.0
4143.1	33.3
6382	33.3
6382.1	186.2
3.1E+6	186.2
Maximum Safeguards	
Time (sec)	Flow (lbm/s)
0.0	0.0
1472	0.0
1473	186.2
3.1E+6	186.2
CCW Flow per RHR Heat Exchangers (gpm)	1000

CCW Heat Exchangers

Number of Heat Exchangers Modeled in the Analysis	1
CCW Flow per CCW Heat Exchanger (gpm)	1600
Service Water Flow (gpm)	2000
Additional Heat Loads, Btu/hr	9.6×10^6

Table 14.3.4-5
Kewaunee Structural Heat Sinks for Containment Integrity Analysis^{1,2,3}

Sink	Surfaces Description	Material	Total Exposed Area (ft ²)	Thickness (in)
1	Containment Cylinder – Coating #4	Carbon Steel	41,300	1.5
2	Containment Dome - Coating #4	Carbon Steel	17,300	0.75
3	Reactor Vessel Liner – Coating #4	Carbon Steel - Concrete Backup	1260 1260	0.25 12.00
4	Refueling Canal	Stainless Steel - Concrete Backup	1100 1100	0.1875 12.0
5	Refueling Canal	Stainless Steel - Concrete Backup	5500 5500	0.25 12.0
6	Misc. Supports – Coating #4	Carbon Steel	4055	0.168
7	Misc. Supports – Coating #4	Carbon Steel	16,925	0.25
8	Misc. Supports – Coating #4	Carbon Steel	28,500	0.375
9	Crane – Coating #5	Carbon Steel	2000	0.75
10	Crane – Coating #5	Carbon Steel	500	1.0
11	Hand Rails – Coating #4	Carbon Steel	1695	0.0725
12	Grating – Coating #4	Carbon Steel	12,400	0.045
13	Exposed Conduit and Cable Trays – Coating #4	Carbon Steel	10,733	0.10
14	Ductwork – Coating #4	Carbon Steel	18,000	0.035
15	Walls 1' to 1.9' – Exposed 2 sides – Coating #2	Concrete	2806	6.0
16	Floors 12.0 in and Greater – Coating #2	Concrete	12,896	12.0
17	Walls 4' to 7'-4" – Exposed 2 Sides – Coating #2	Concrete	18,588	24.0
18	Floor (in contact with sump) – Coating #2	Concrete	1088	12.0
19	Walls 2' to 3'-2" – Exposed 2 Sides – Coating #2	Concrete	28,898	12.0

Table 14.3.4-5
Kewaunee Structural Heat Sinks for Containment Integrity Analysis^{1,2,3}

Sink	Surfaces Description	Material	Total Exposed Area (ft ²)	Thickness (in)
20	Floors 4 in to 10 in – Coating #2	Concrete	6810	4.0
21	Accumulator Upper Dome Coating #4	Carbon Steel Stainless Steel Liner	307	1.375
22	Accumulator Upper Cylinder Coating #4	Carbon Steel Stainless Steel Liner	494	2.75
23	Accumulator Lower Cylinder Coating #4	Carbon Steel Stainless Steel Liner	869	2.75
24	Accumulator Lower Dome Coating #4	Carbon Steel Stainless Steel Liner	307	1.375

Notes:

1. The accumulator conductors are included for the MSLB models only. A separate volume is modeled for the water and nitrogen in the accumulators. The inside of the accumulator upper dome and cylinder are in contact with the nitrogen in the accumulators with a natural convection heat transfer coefficient. The inside of the accumulator lower dome and cylinder are in contact with the water in the accumulators with a natural convection heat transfer coefficient. The assumed water volume in each accumulator is 1225 gallons (minimum volume).
2. Using 11 mil paint thickness.
3. There is an air annulus (shield building) between the concrete containment cylinder and dome and steel shell. For the MSLB models, a separate volume was included for the shield building with natural convection to the outside surface of the containment dome and cylinder.

Paint Coating Systems

Coating #1: Plastite 9028 surfacer – flush; Phenoline 305 Primer – 4 mils;
Phenoline 305 Finish - 4 mils

Coating #2: Phenoline 9028 Amine-Epoxy filler – flush; Plastite 9009 Primer – 6 mils;
Phenoline 300 Finish – 8 mils

Coating #3: Carbozinc 11 Primer – 3 mils; Phenoline 305 Finish – 4 mils

Coating #4: Carbozinc 11 Primer – 3 mils; Phenoline 305 Finish – 8 mils

Coating #5: Carbozinc 11 Primer – 3 mils

1 mil = 1/1000 inch

Table 14.3.4-6
Thermo-Physical Properties of Containment Heat Sinks^a

Material	Conductivity (Btu/hr-ft-°F)	Volumetric Heat Capacity (Btu/ft ³ -°F)
Carbon Steel	26.0	56.4
Stainless Steel	8.0	56.6
Concrete	0.80	28.8
Phenoline 300 Finish	0.25	32.4
Phenoline 305 Finish	0.25	32.4
Phenoline 305 Primer	0.25	32.4
Carbozinc 11 Primer	0.9	28.8

Notes:

- a. For the LOCA cases more conservative values of 0.083 and 28.8 for the conductivity and heat capacity, respectively.

Table 14.3.4-7
Containment Fan Coil Unit Performance (CFCU)

Containment Temperature (°F)	Heat Removal Rate (Btu/sec) per CFCU
100	0
136	1858.3
205	8338.9
244	12691.7
270	15230.6
300	15230.6

Table 14.3.4-8
LOCA Containment Response Results (Loss-of-Offsite Power Assumed)

Case	Peak Press (psig)	Peak Temp. (°F)	Pressure (psig) @ 24 hours	Temperature (°F) @ 24 hours
DEPSMINSI	43.1 @ 58.2 sec	261.6 @ 38.2 sec	10.1 @ 86,400 sec	167.1 @ 86,400 sec
DEPSMAXSI1 Fan Cooler Fails	42.6 @ 58.1 sec	261.7 @ 38.0 sec	8.2 @ 86,400 sec	153.4 @ 86,400 sec
DEPSMAXSI1 Spray Pump Fails	42.6@ 58.1 sec	261.7 @ 38.0 sec	7.1 @ 86,400 sec	145.4 @ 86,400 sec
DEHL	44.6 @ 19.9 sec	265.0 @ 19.8 sec	Not applicable	Not applicable

Figure 14.3-1
SI Flow, Spill to RCS

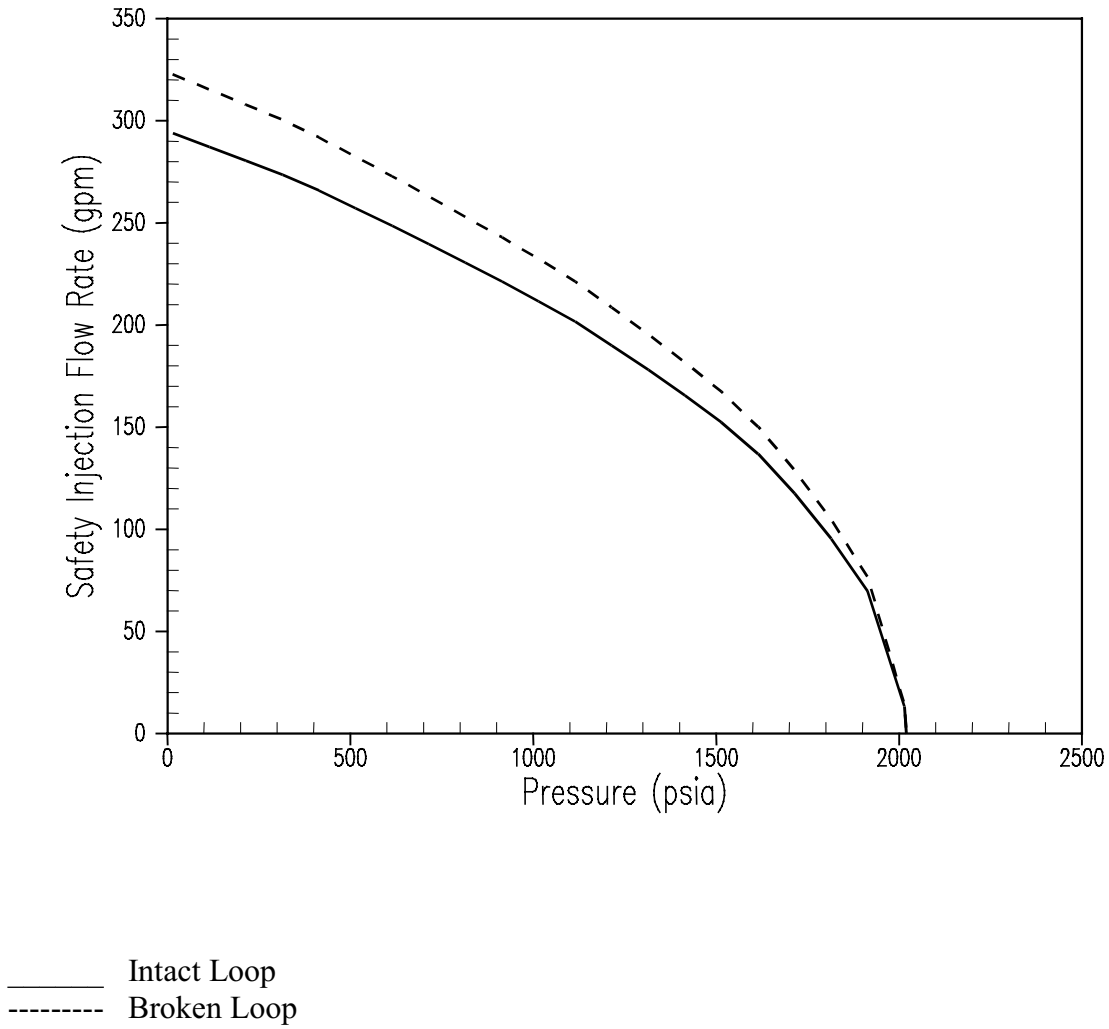
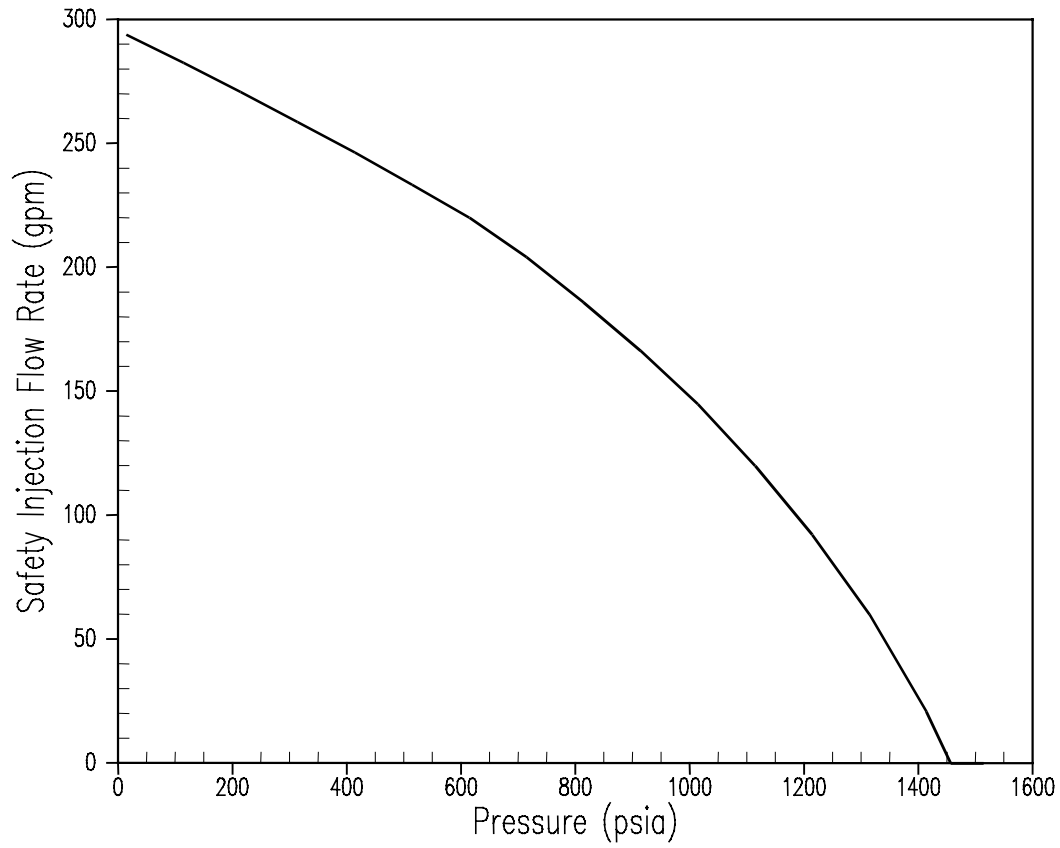


Figure 14.3-2
SI Flow, Spill to Containment



_____ Intact Loop

Figure 14.3-3
Pressurizer Pressure 3-Inch Break High T_{avg}

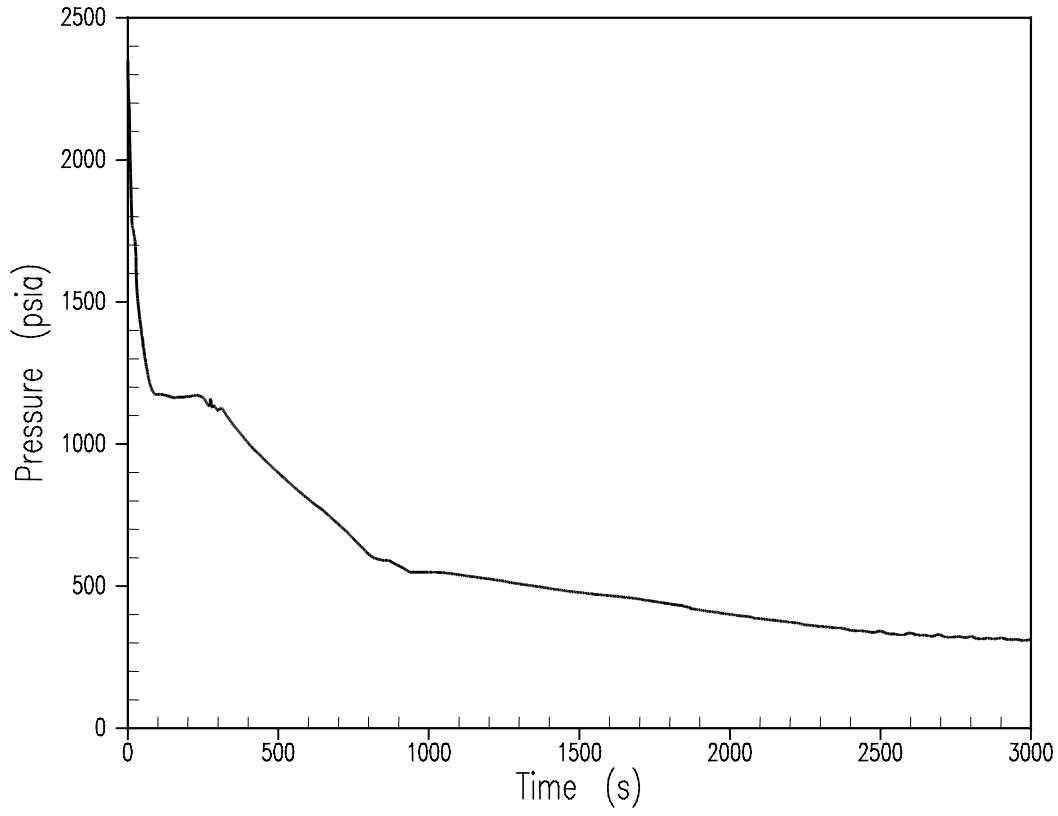


Figure 14.3-4
Core Mixture Level 3-Inch Break High T_{avg}

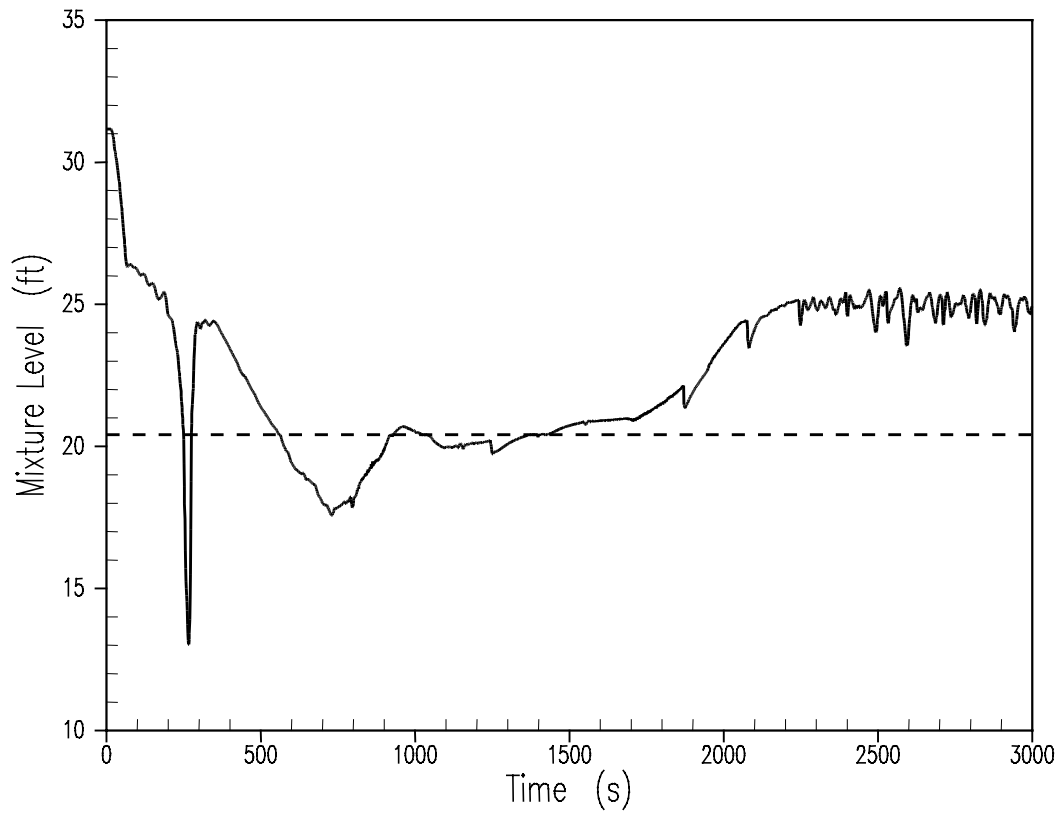


Figure 14.3-5
Core Exit Steam Flow 3-Inch Break High T_{avg}

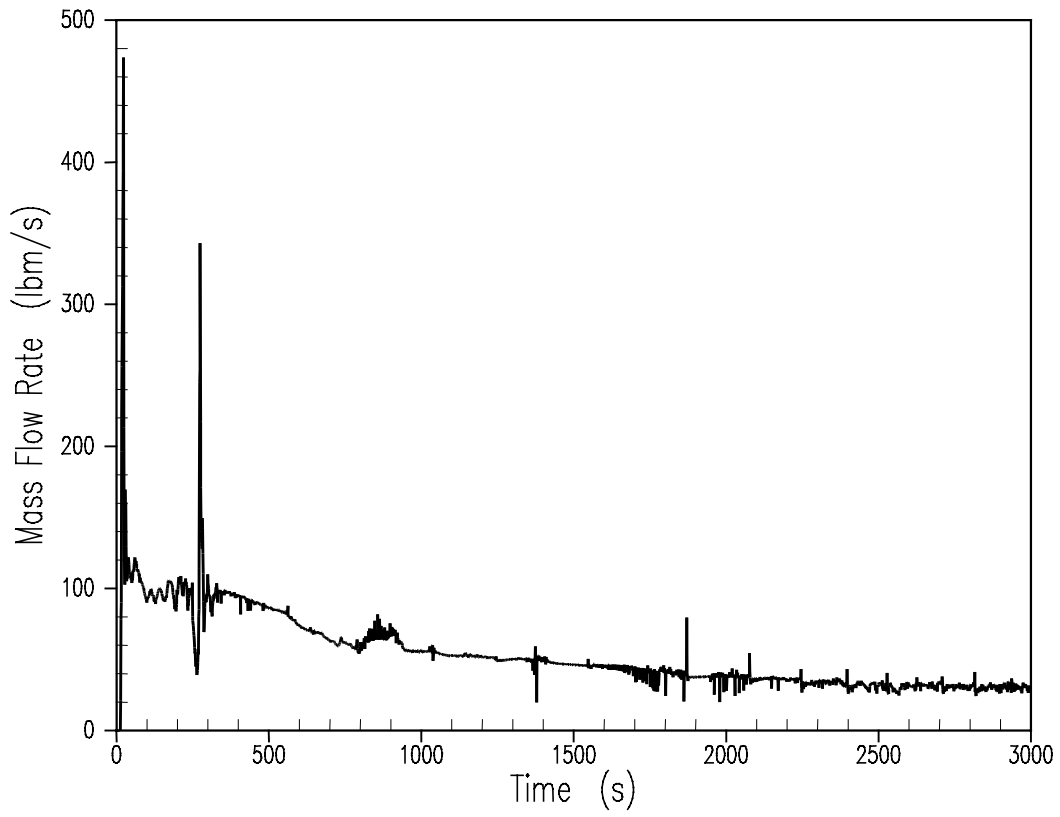
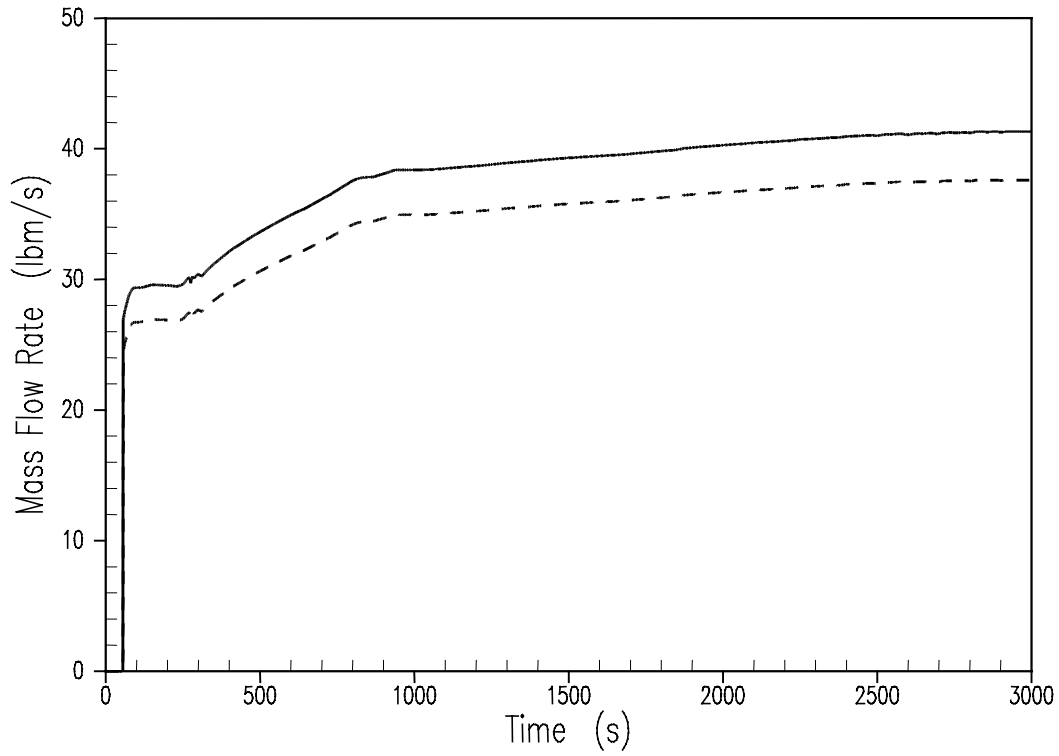


Figure 14.3-6
BL & IL Pumped SI Flow Rate 3-Inch Break High T_{avg}



—— Broken Loop
----- Intact Loop

Figure 14.3-7
Peak Clad Temp at PCT Elevation 3-Inch Break High T_{avg}

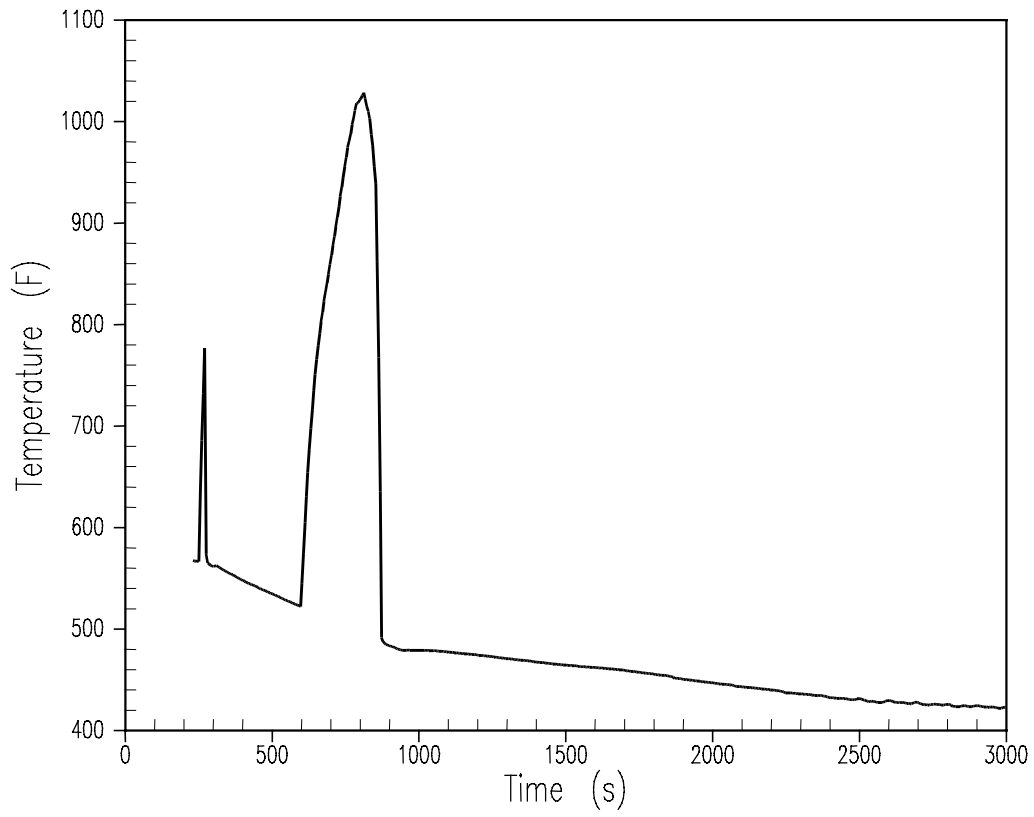


Figure 14.3-8
Hot Spot Fluid Temp at PCT Elevation 3-Inch Break High T_{avg}

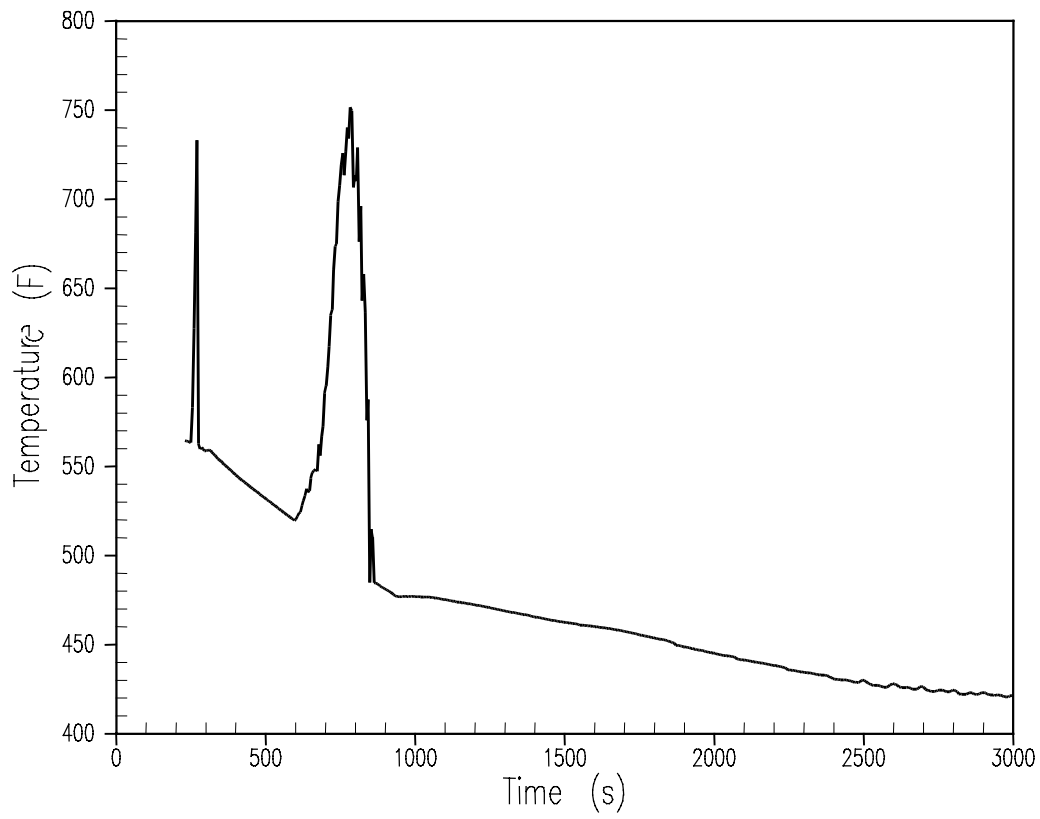


Figure 14.3-9
Hot Rod HCT at PCT Elevation 3-Inch Break High T_{avg}

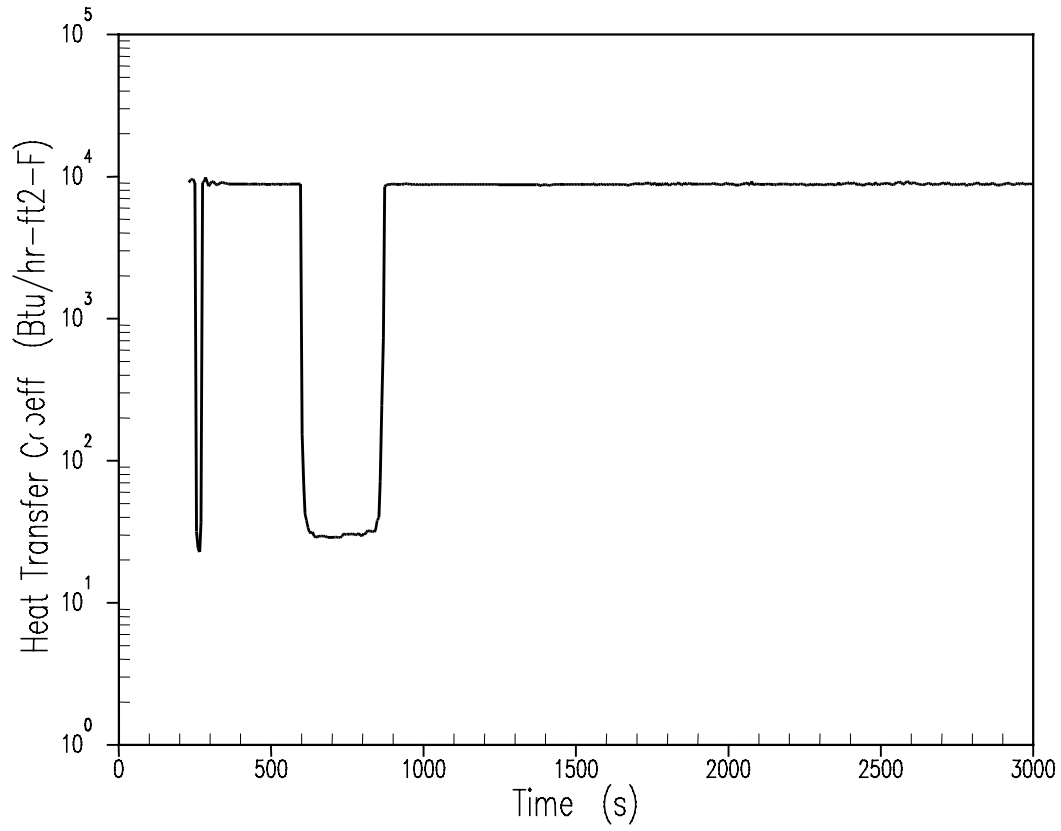


Figure 14.3-10
Pressurizer Pressure 2-Inch Break High T_{avg}

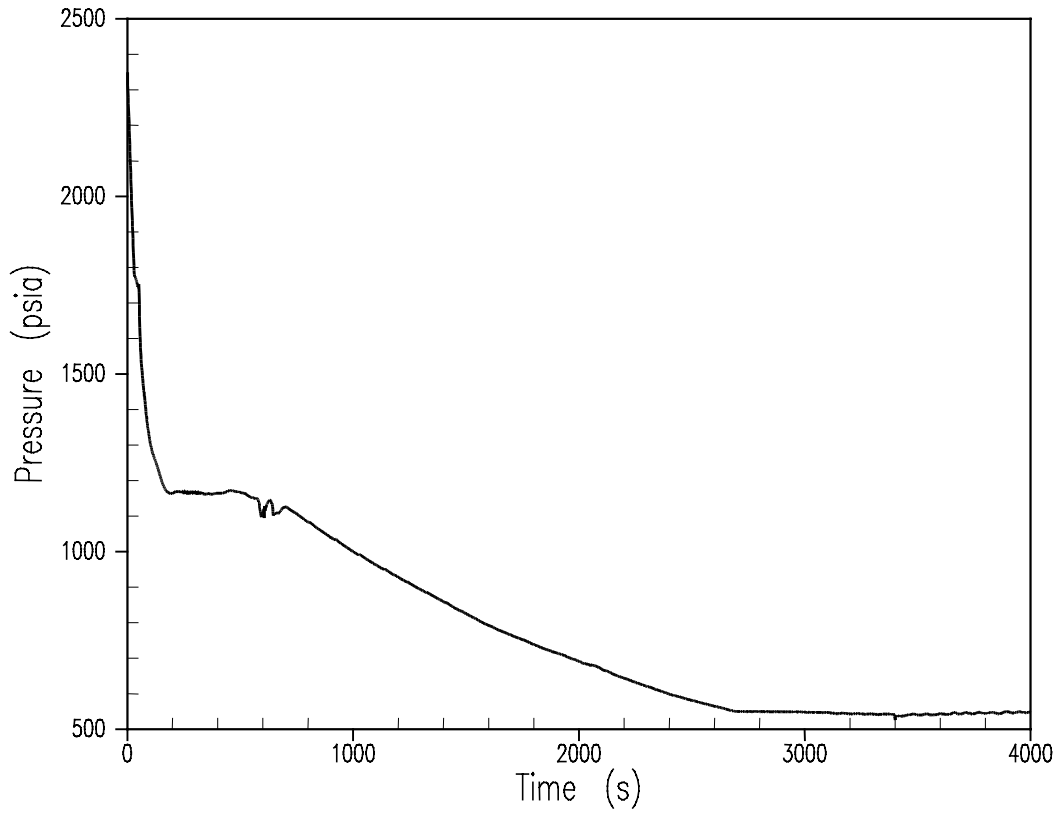


Figure 14.3-11
Core Mixture Level 2-Inch Break High T_{avg}

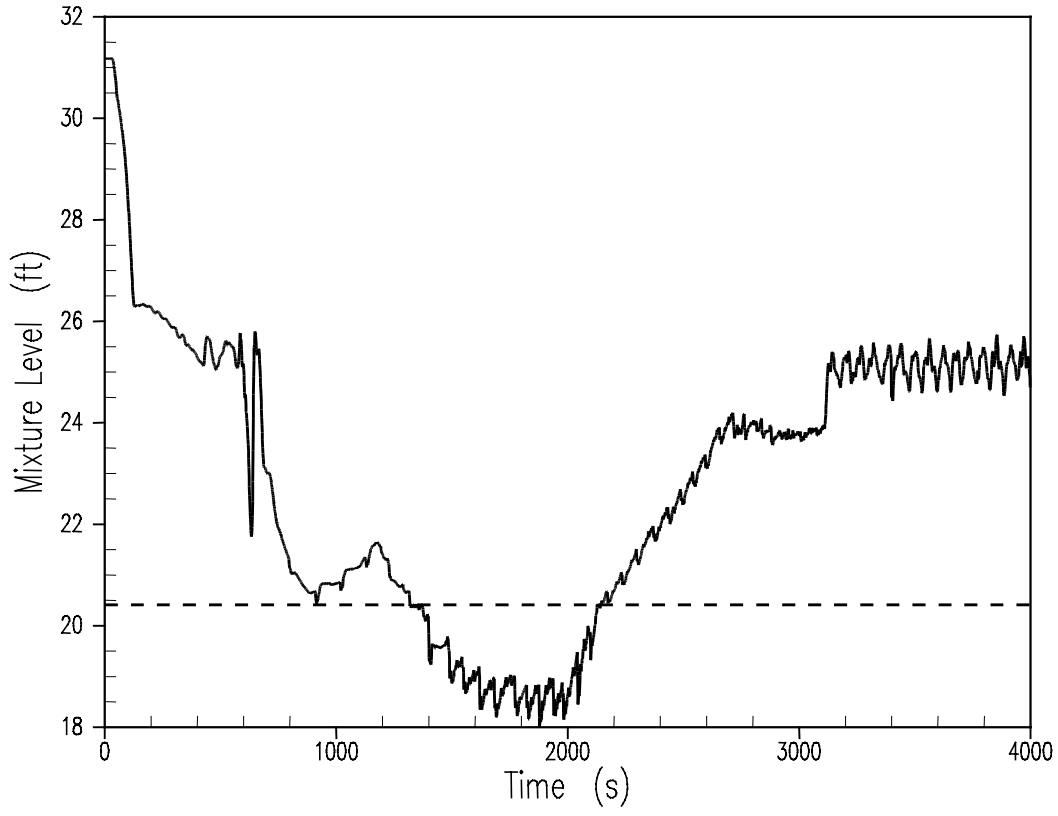


Figure 14.3-12
Peak Clad Temp at PCT Elevation 2-Inch Break High T_{avg}

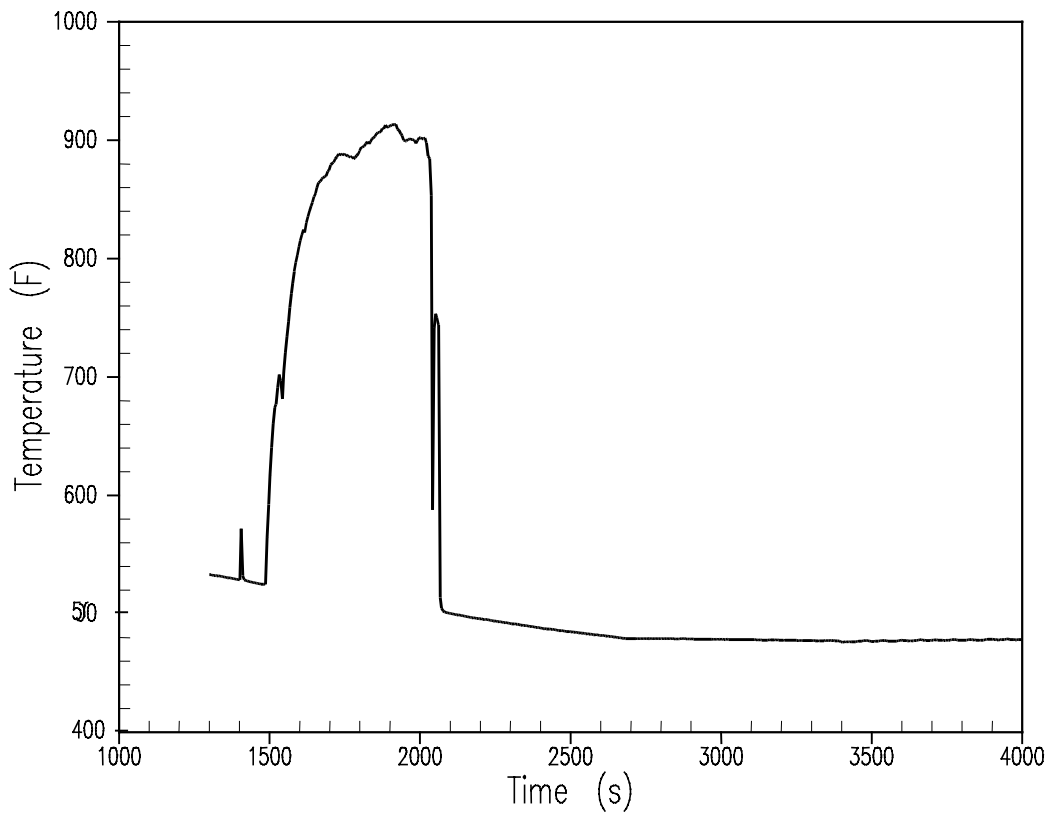


Figure 14.3-13
Pressurizer Pressure 4-Inch Break High T_{avg}

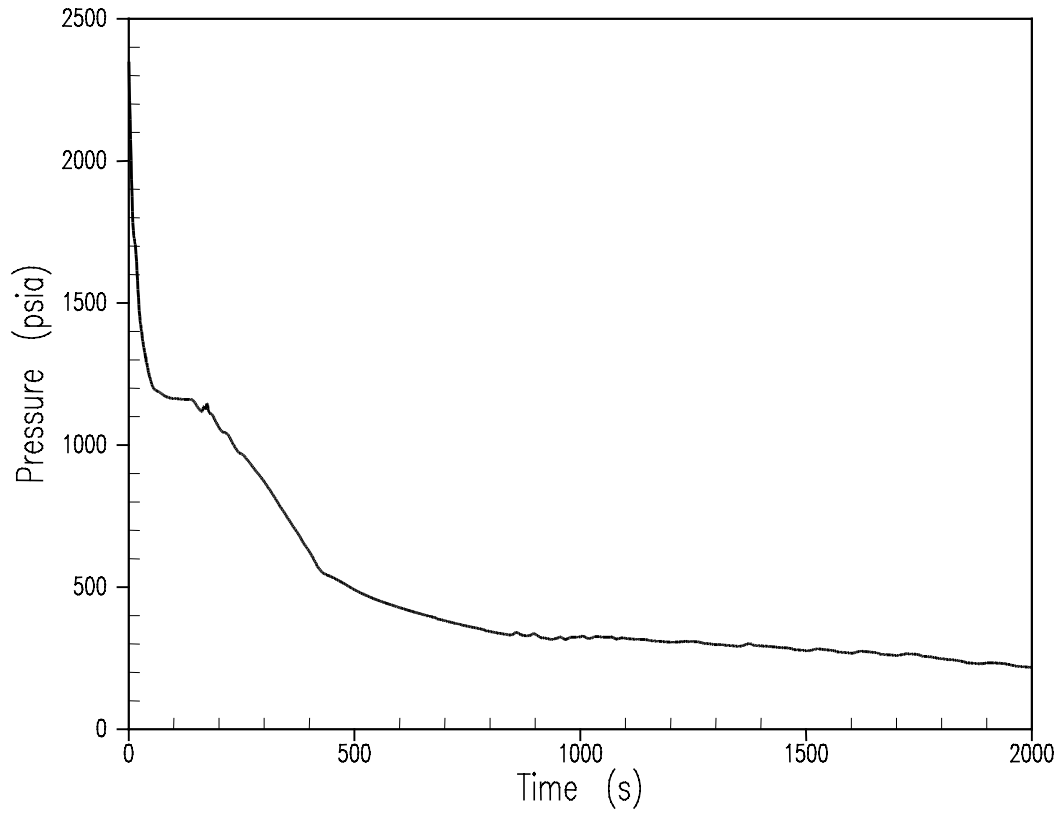


Figure 14.3-14
Core Mixture Level 4-Inch Break High T_{avg}

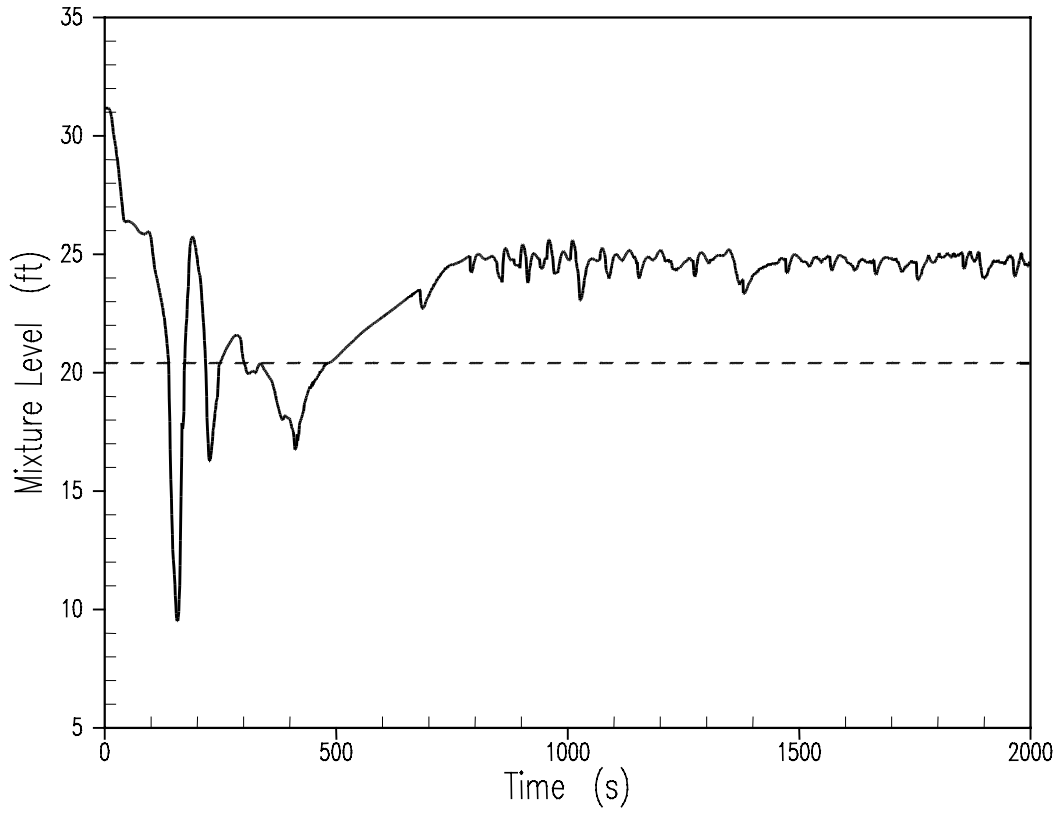


Figure 14.3-15
Peak Clad Temp at PCT Elevation 4-Inch Break High T_{avg}

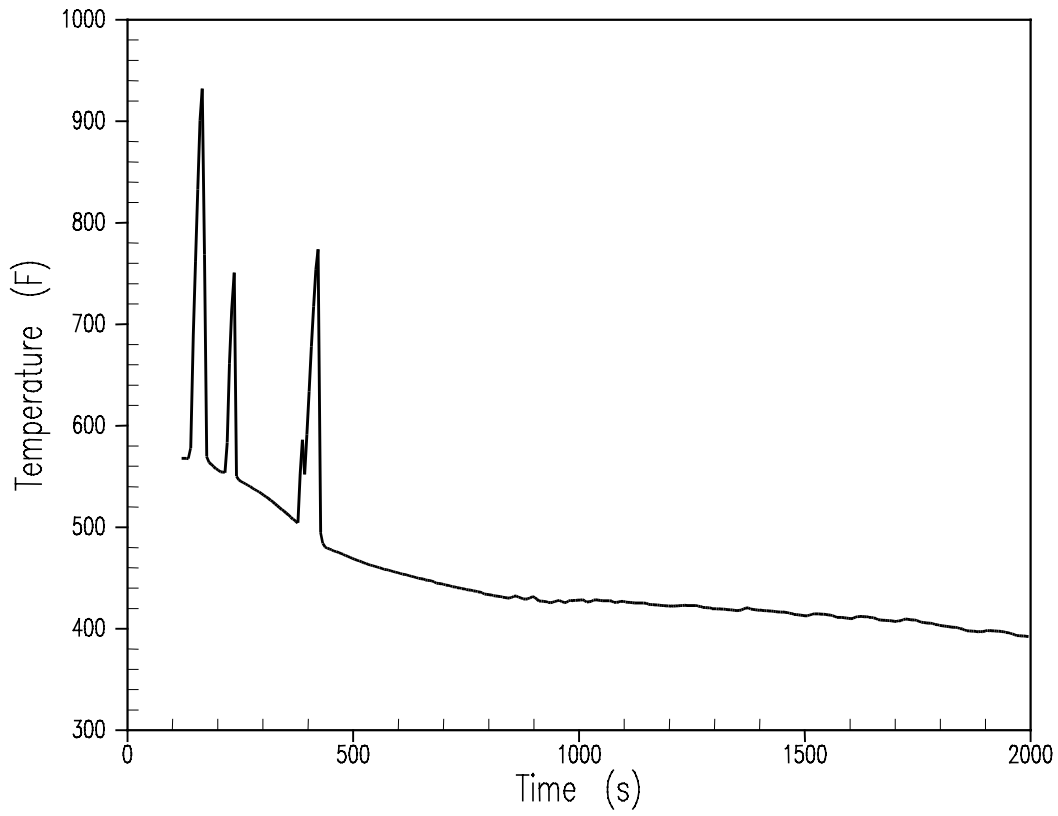


Figure 14.3-16
Pressurizer Pressure 3-Inch Break Low T_{avg}

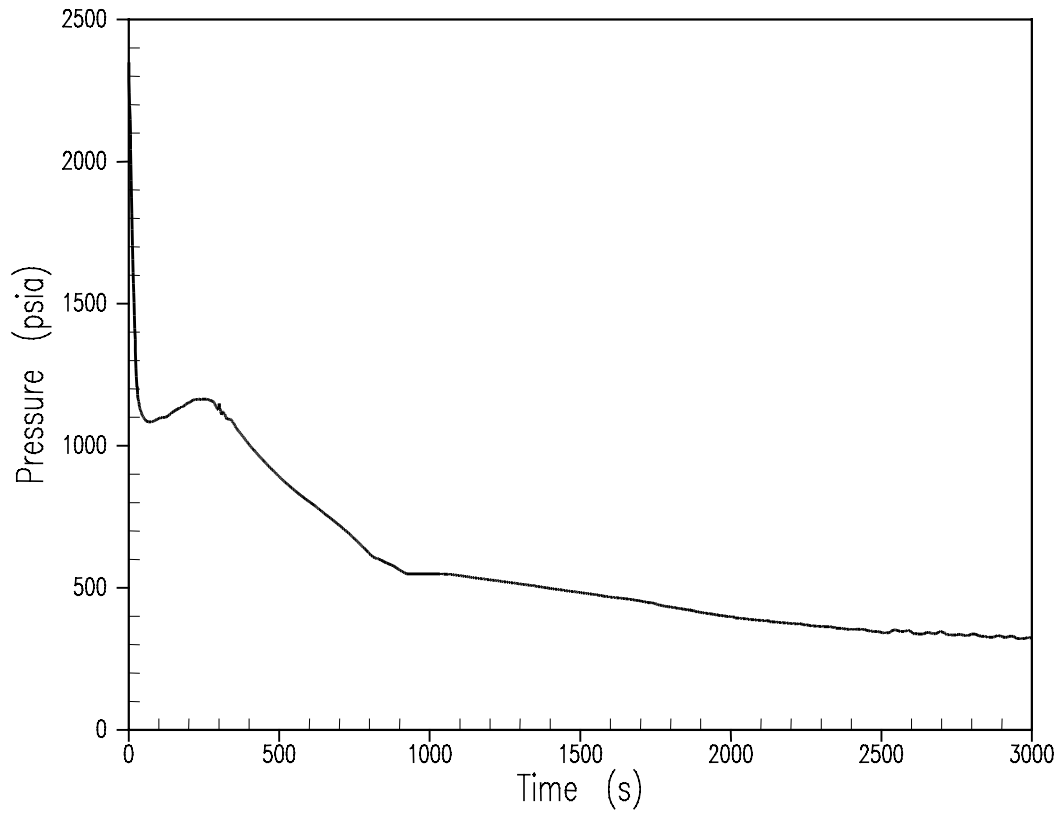


Figure 14.3-17
Core Mixture Level 3-Inch Break Low T_{avg}

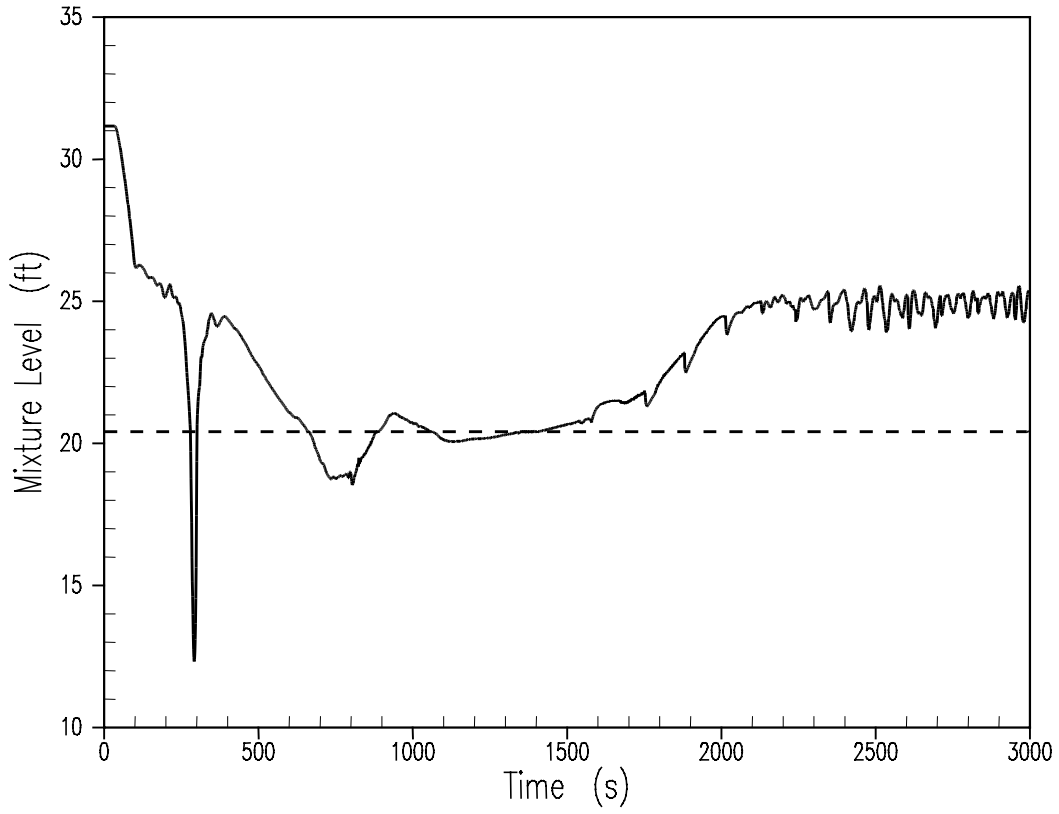


Figure 14.3-18
Peak Clad Temp at PCT Elevation 3-Inch Break Low T_{avg}

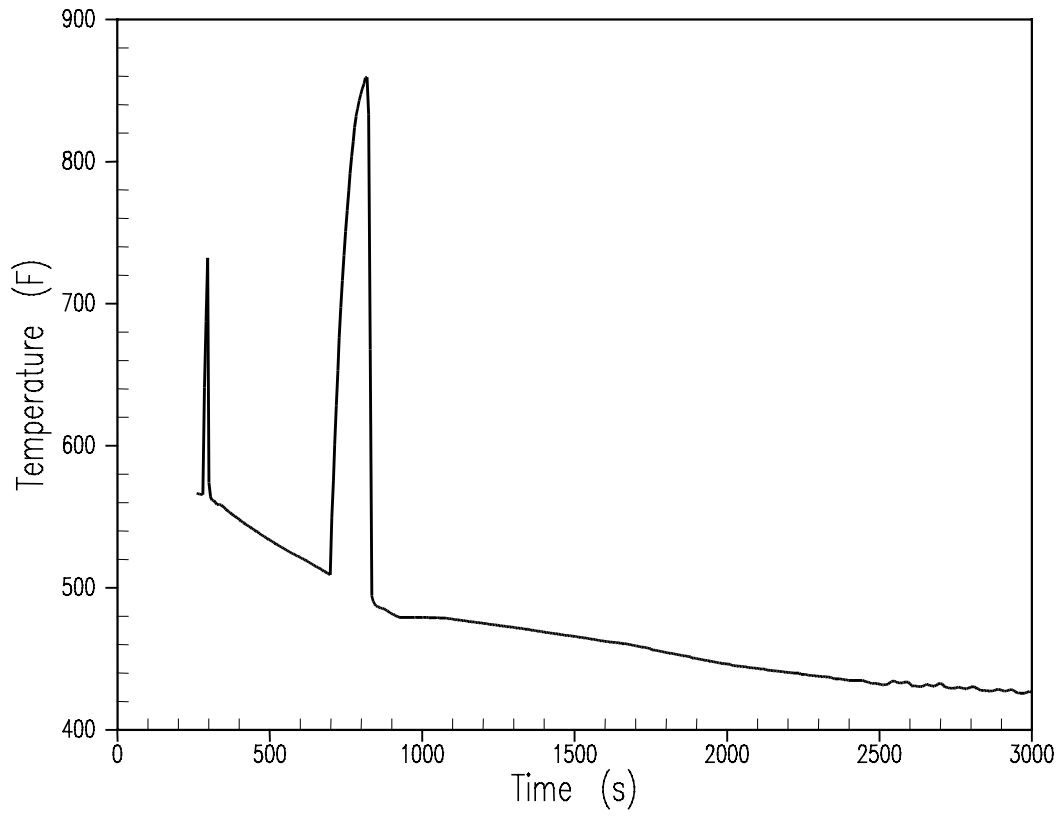


Figure 14.3-19
 Loop Reactor Mathematical Model for Vertical Response

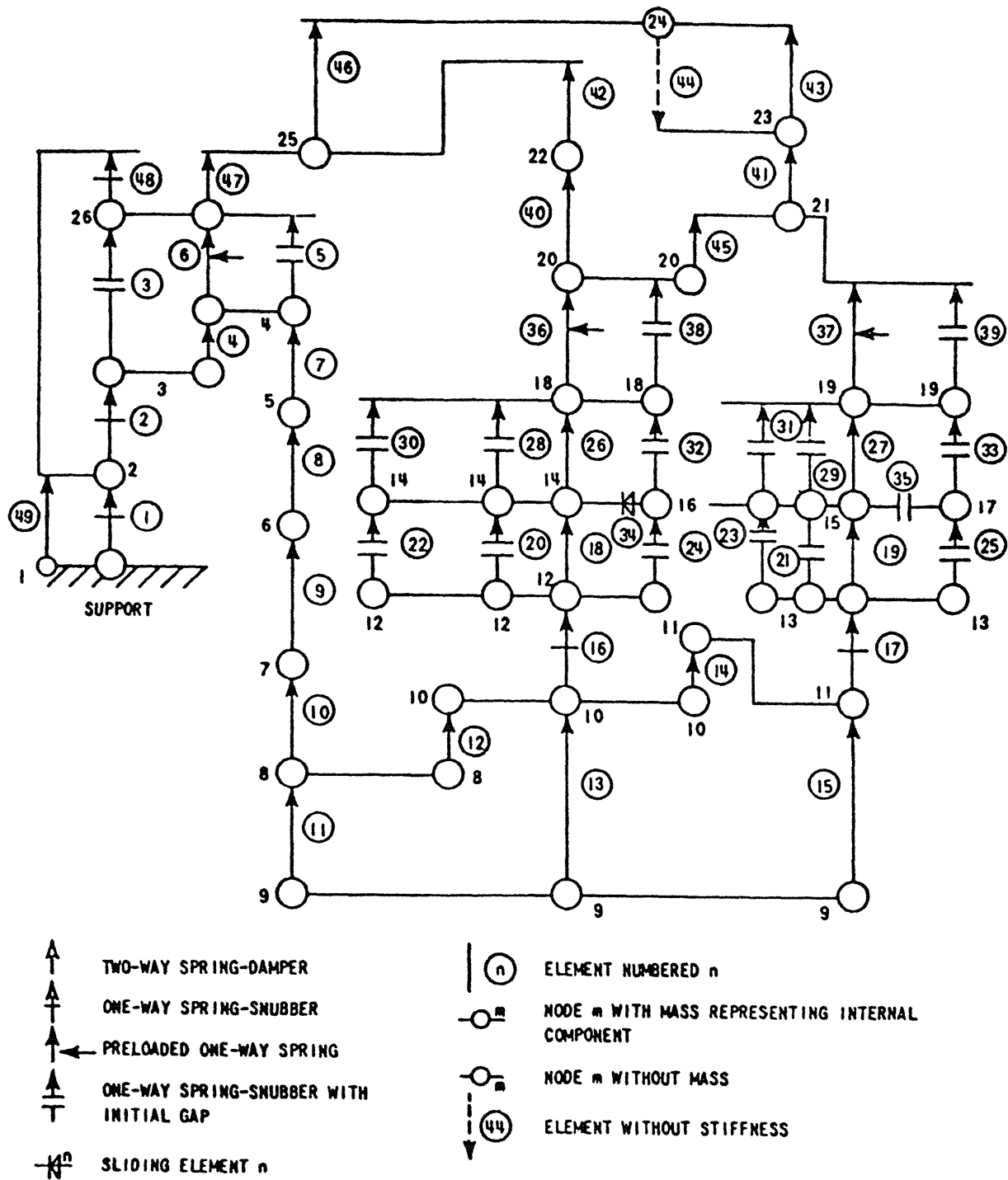


Figure 14.3-20
 Reactor Internals Allowable Stress Criteria

S_m = DESIGN STRESS INTENSITY VALUE AT TEMPERATURE, GIVEN BY THE ASME SECTION III CODE
 PRIMARY STRESSES (NOTES 1, 2, 9 AND 10)

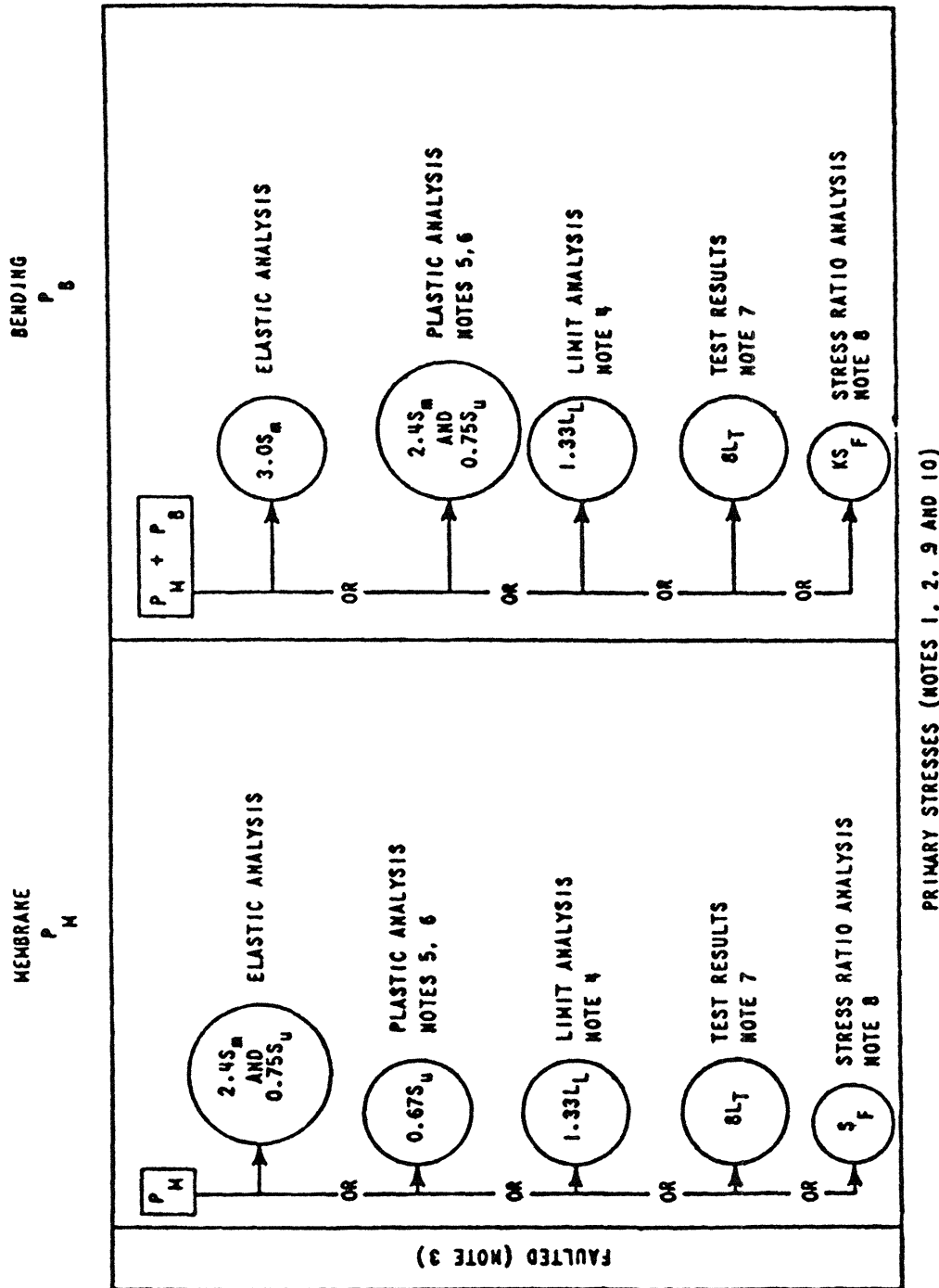


Figure 14.3-21
Notes for Figure 14.3-20

- Note 1. The symbols P_M , P_B do not represent single quantities but rather sets of six quantities representing the six quantities representing the six stress components σ_t , σ_l , σ_r , τ_{lr} , τ_{rt} , and τ_{ll} .
- Note 2. When loads are dynamically applied, consideration should be given to the use of dynamic load amplification and possible changes in modulus or elasticity.
- Note 3. For configurations where compressive stresses occur, the stress limits shall be revised to take into account critical buckling stresses. The permissible equivalent static external pressure shall be taken as 2.5 times that given by the rules of Section III Pressure Vessel ASME Code. Where dynamic pressures are involved, the permissible external pressure shall be limited to 75 percent of the dynamic instability pressures.
- Note 4. L_L = Lower bound limit load with an assumed yield point equal to $1.5 S_m$. The “lower bound limit load” is here defined as that produced from the analysis of an ideally plastic (non-strain hardening) material where deformations increase with no further increase in applied load. The lower bound load is one in which the material everywhere satisfies equilibrium and nowhere exceeds the defined material yield strength using either a shear theory or a strain energy of distortion theory to relate multiaxial yielding to the uniaxial case.
- Note 5. S_u - Ultimate strength at temperature. Multi-axiality effects on uniform strength shall be considered.
- Note 6. Elastic plastic evaluated nominal primary stress. Strain hardening of the material may be used for the actual stress strain curve at the temperature of loading or any approximation to the actual stress-strain curve which everywhere has a lower stress for the same strain as the actual curve may be used. Either the shear or strain energy of distortion flow rule shall be used to account for multi-axial effects.
- Note 7. The stress limits given in this criterion need not be satisfied if it can be shown from the test of a prototype or model that the specified loads do not exceed 80 percent or L_T , for Faulted conditions. L_T is the ultimate load or load combination used in the test. In using this method, account shall be taken of the dimensional tolerances which may exist between the actual part and the tested part or parts as well as differences which may exist in the ultimate strength or other governing material properties of the actual part and the tested parts to assure that the loads obtained from the test are a conservative representation of the load carrying capability of the actual component under postulated loading for Faulted Conditions.

Figure 14.3-21

Notes for Figure 14.3-20

- Note 8. Stress rasion is a method of plastic analysis which uses the stress ratio combinations (combination of stresses that consider the rasion of the actual stress to the allowable plastic or elastic stress) to compute the maximum load a strain hardening material can carry. For Faulted condition use $S_F < 2.4S_m$ and $0.75 S_u$, whichever is smaller.
- Note 9. Where deformation is of concern in a component, the deformation shall be limited to 80 percent of the value given in the Design Specification (no loss of function) for Faulted Conditions.
- Note 10. No limit requirements are established for fatigue and secondary stresses, however evaluation of these conditions are recommended when safety requirements are involved.

Figure 14.3-22
Containment Fan Cooler Heat Removal Rate vs. Containment Pressure

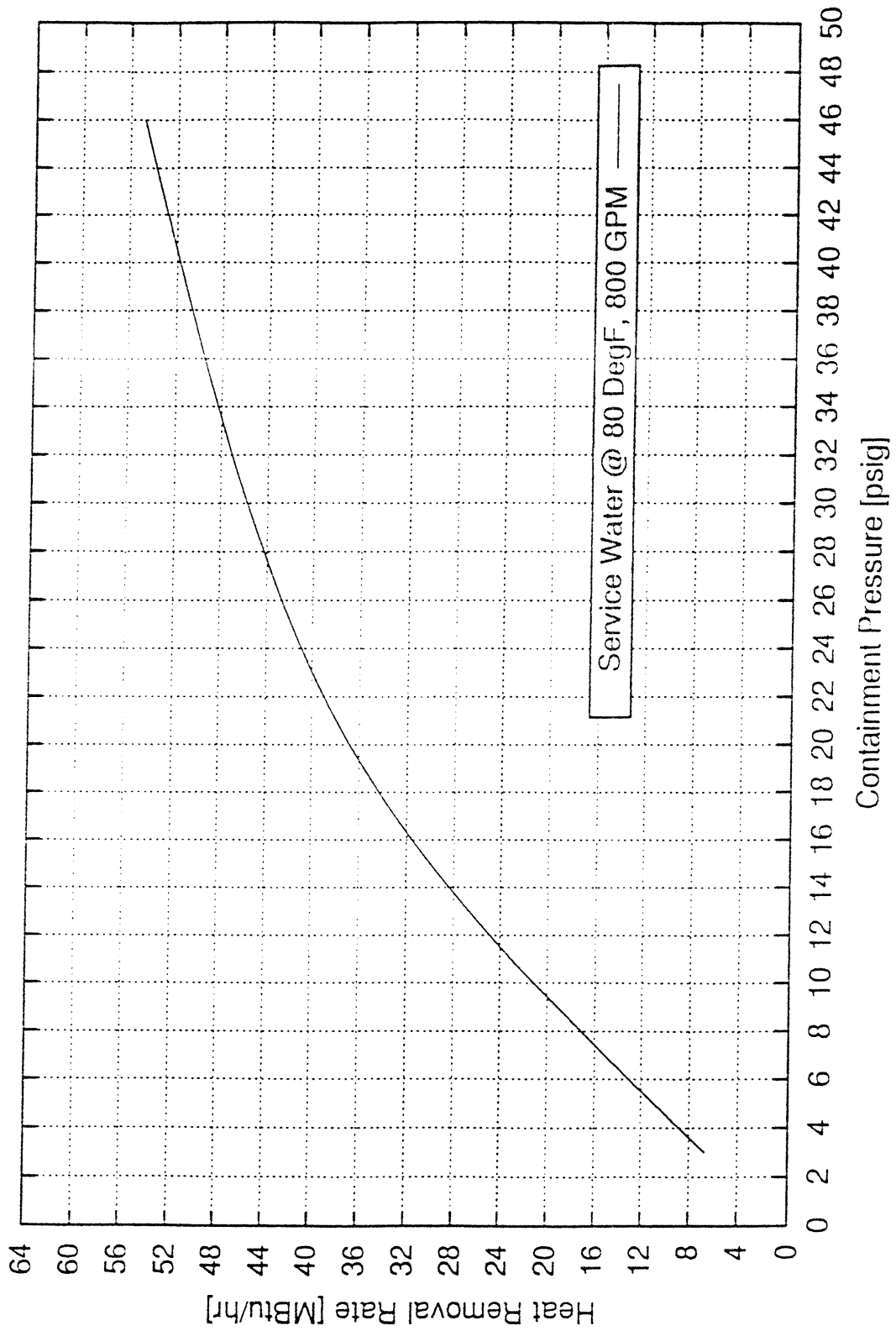
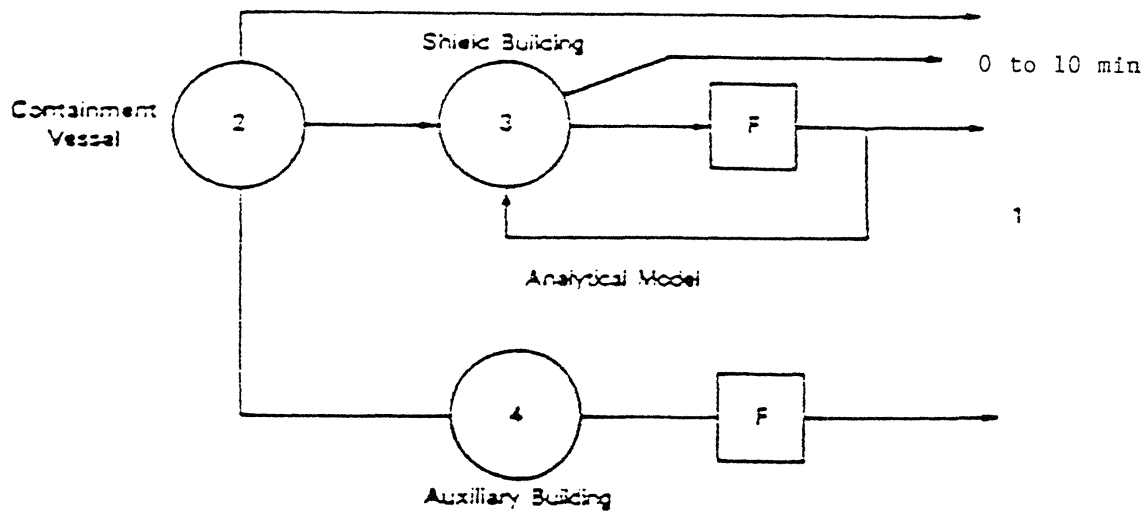
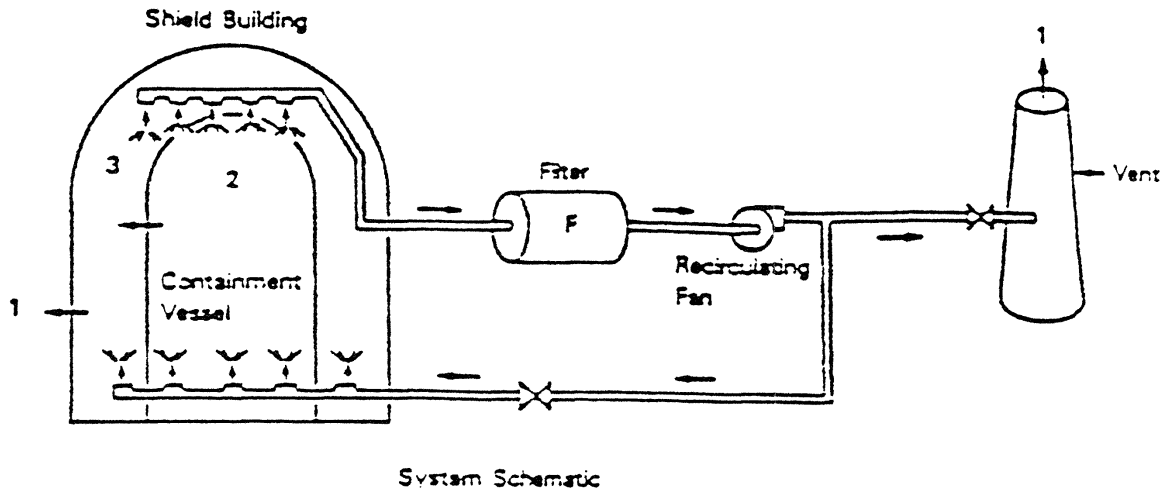


Figure 14.3-23
Shield Building Ventilation System



Regions

1. Environment
2. Containment Vessel
3. Shield Building
4. Auxiliary Building Special Ventilation Zone

Figure 14.3-24
Shield Building Ventilation Performance Test Curve and Shield Building Performance Curve

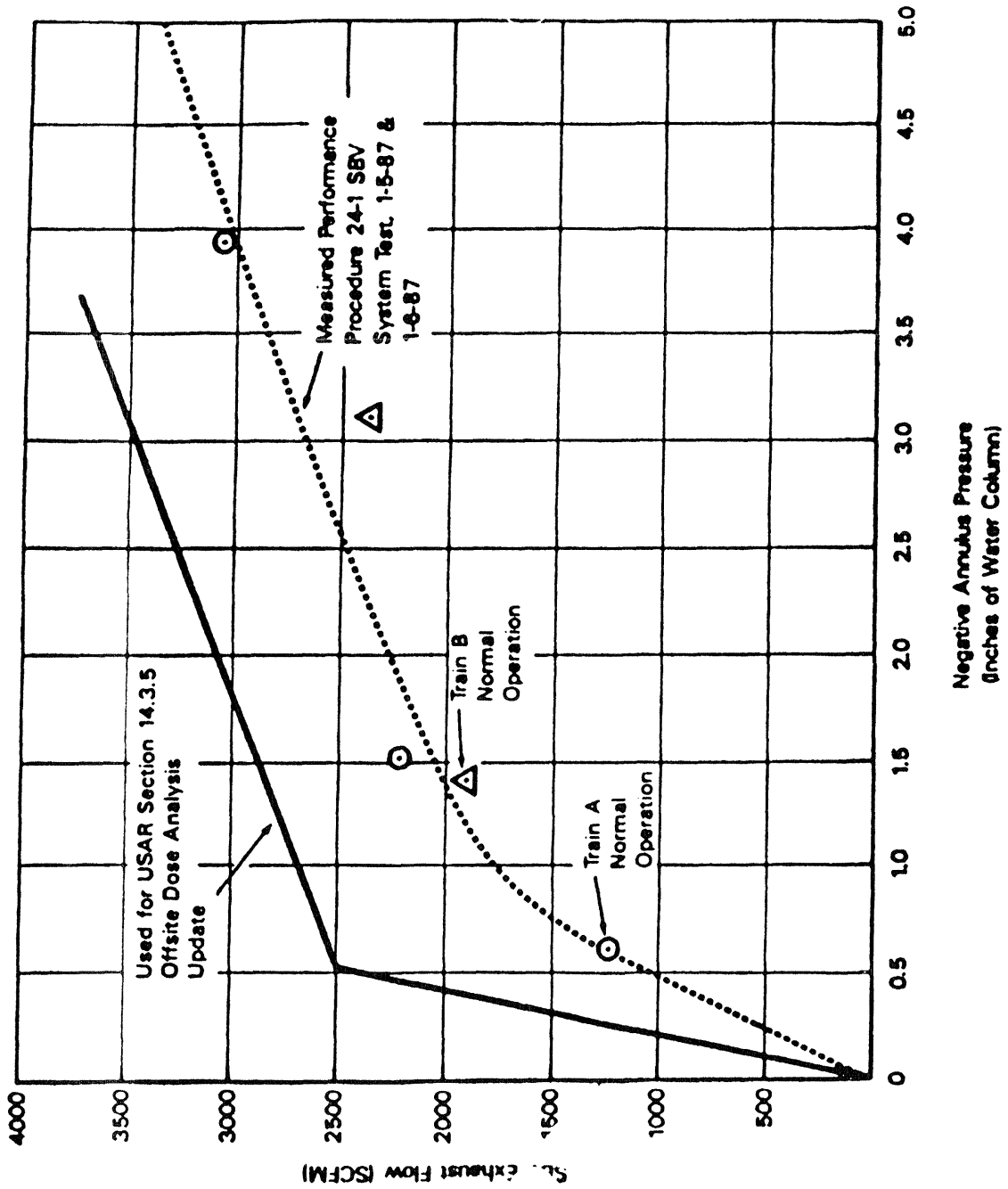


Figure 14.3-25
Annulus Pressure with Steel Shell Expansion Design Basis Transient

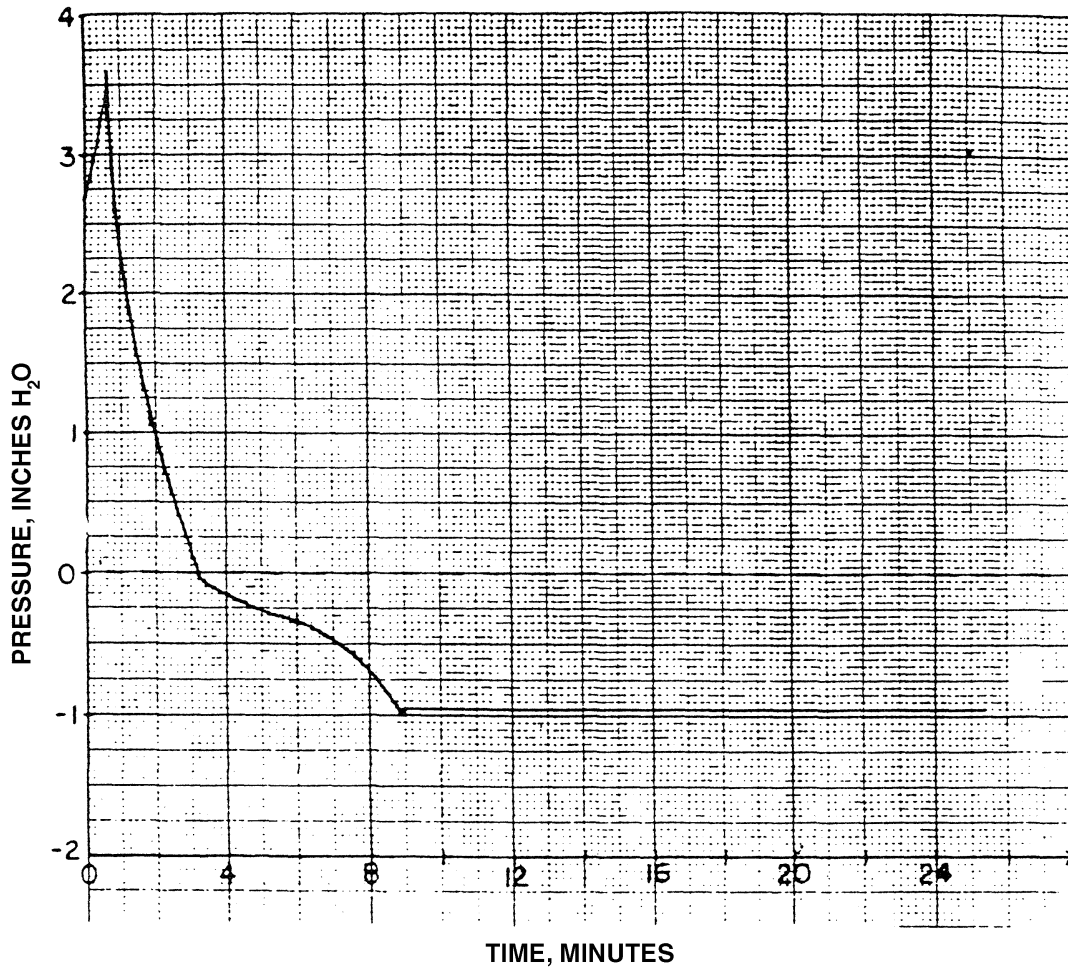


Figure 14.3-26
Flow Out of the SBVS with Steel Shell Expansion Design Basis Transient

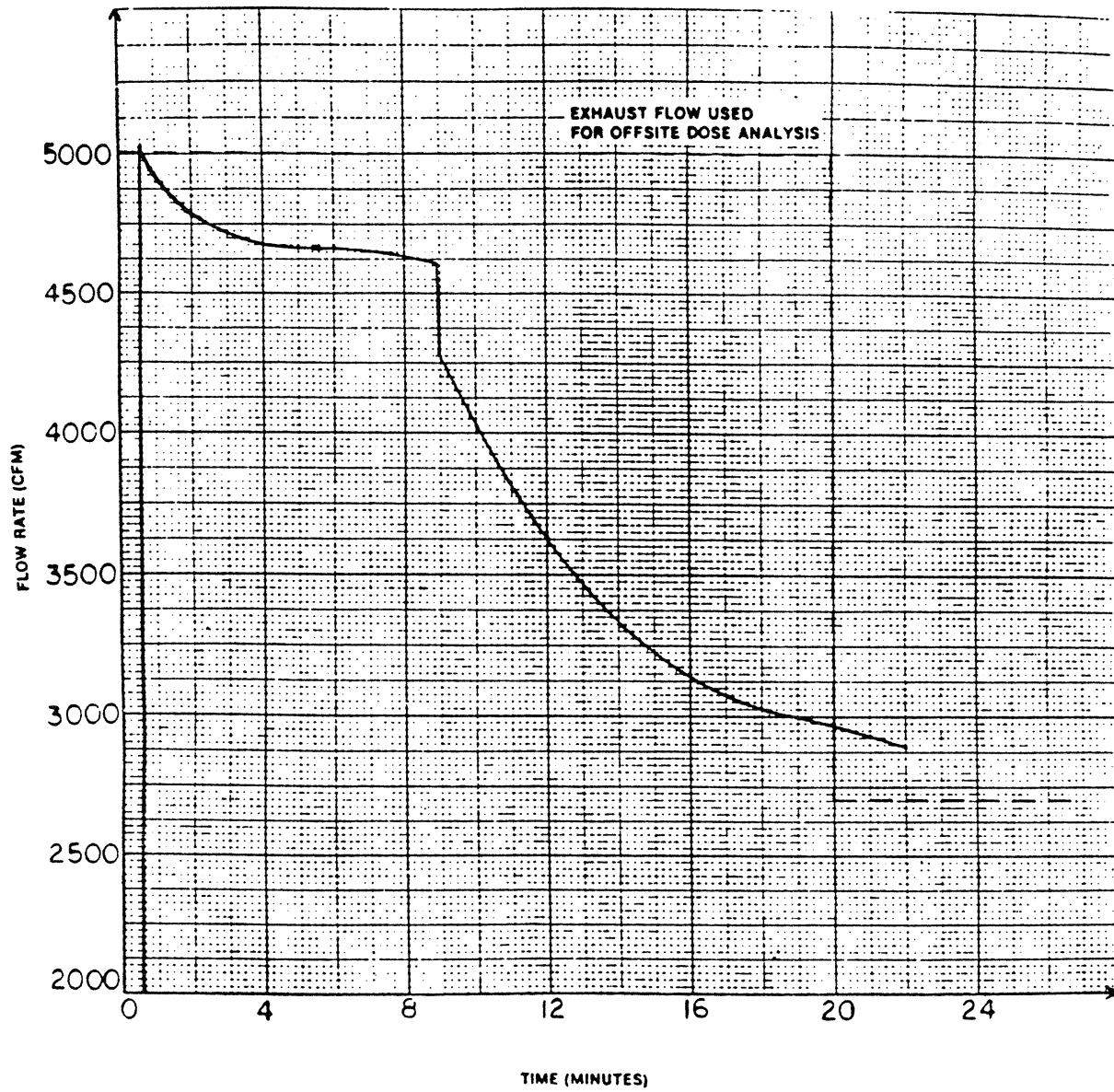


Figure 14.3-27
[Deleted]



Figure 14.3-28
Hydrogen Control By Purging and Venting Through Shield Building Vent System Without Pressure Increase

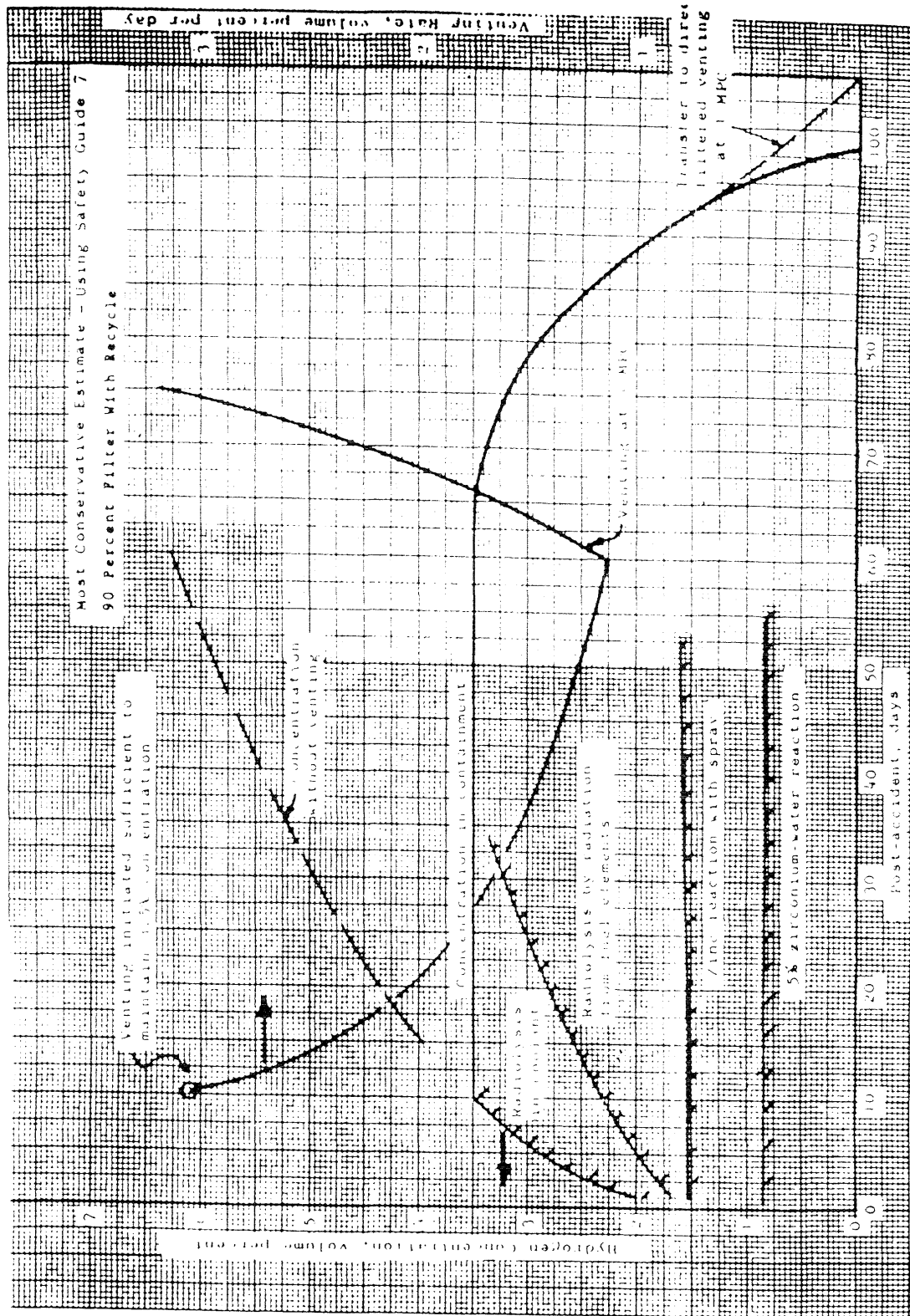


Figure 14.3-30
Containment Leakage and Venting Requirements as Affected by Pressure Increase

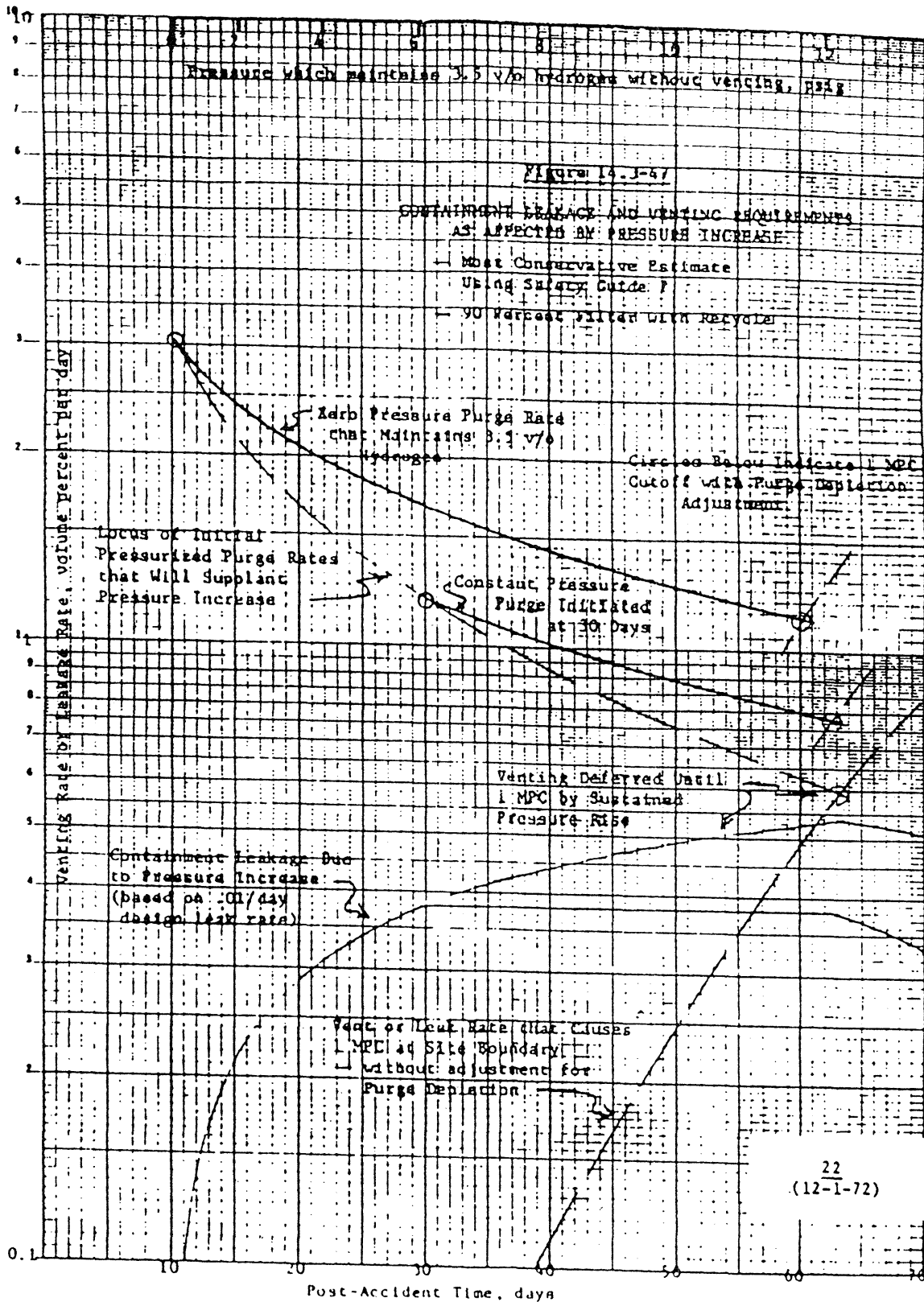
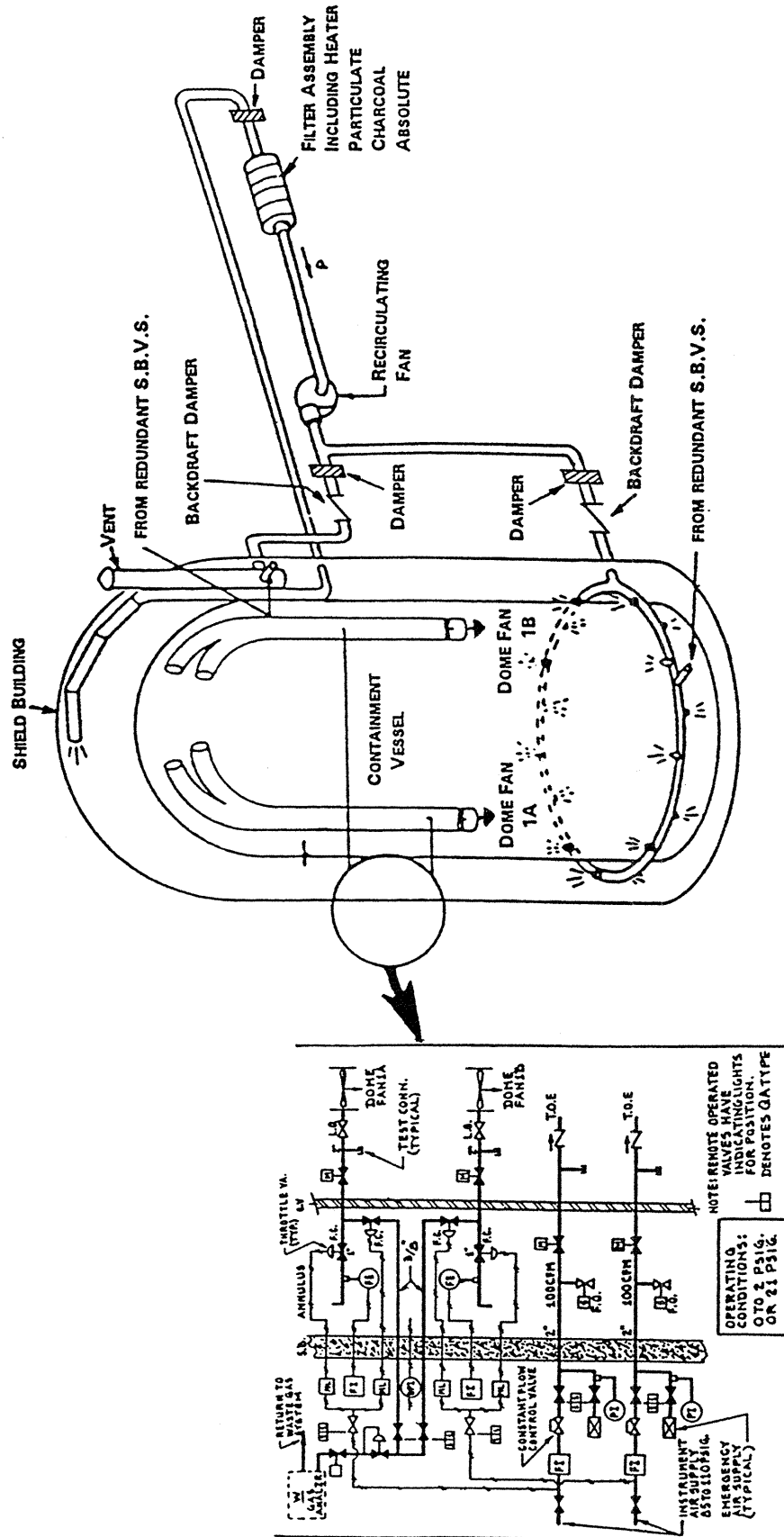
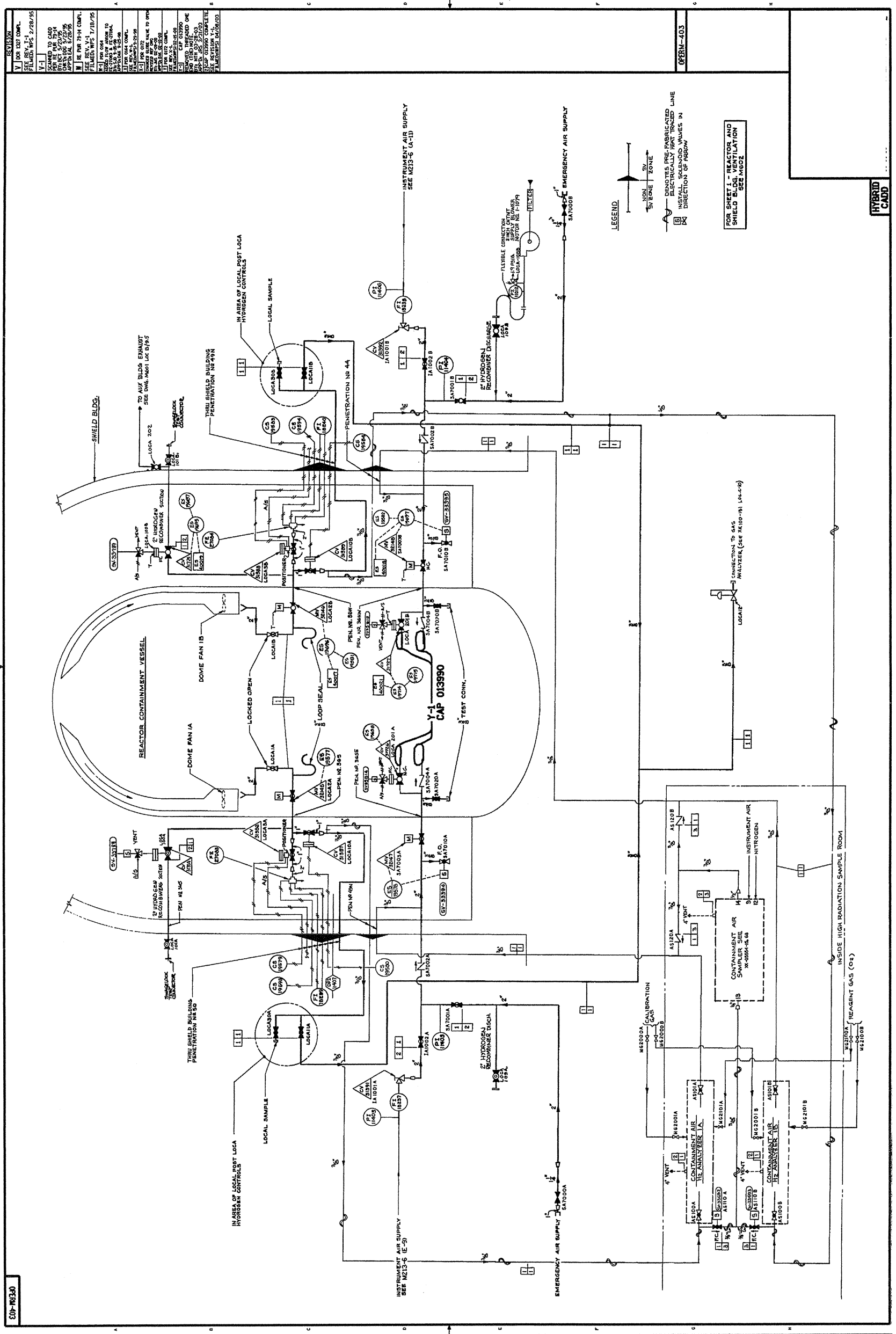


Figure 14.3-31
Provisions for Mixing, Sampling and Venting of Containment Gases



Intentionally Blank

Figure 14.3-32 Reactor Building Ventilation System Post LOCA-H₂ Control Flow Diagram



Intentionally Blank

Figure 14.3.2-1
 Typical Time Sequence of Events for the KNPP BELOCA Analysis

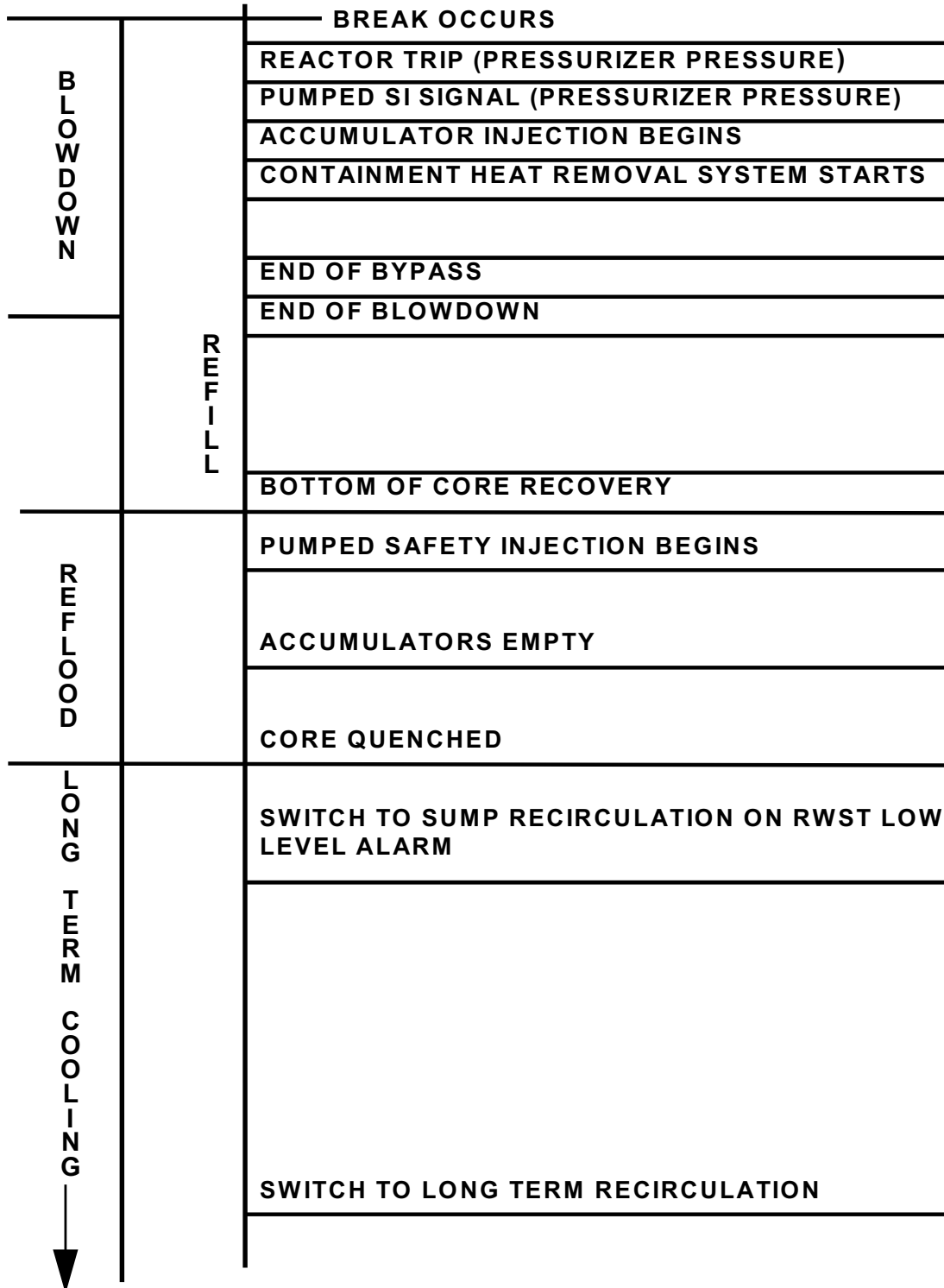


Figure 14.3.2-2
Containment Pressure Curve Used in the KNPP BELOCA Analysis

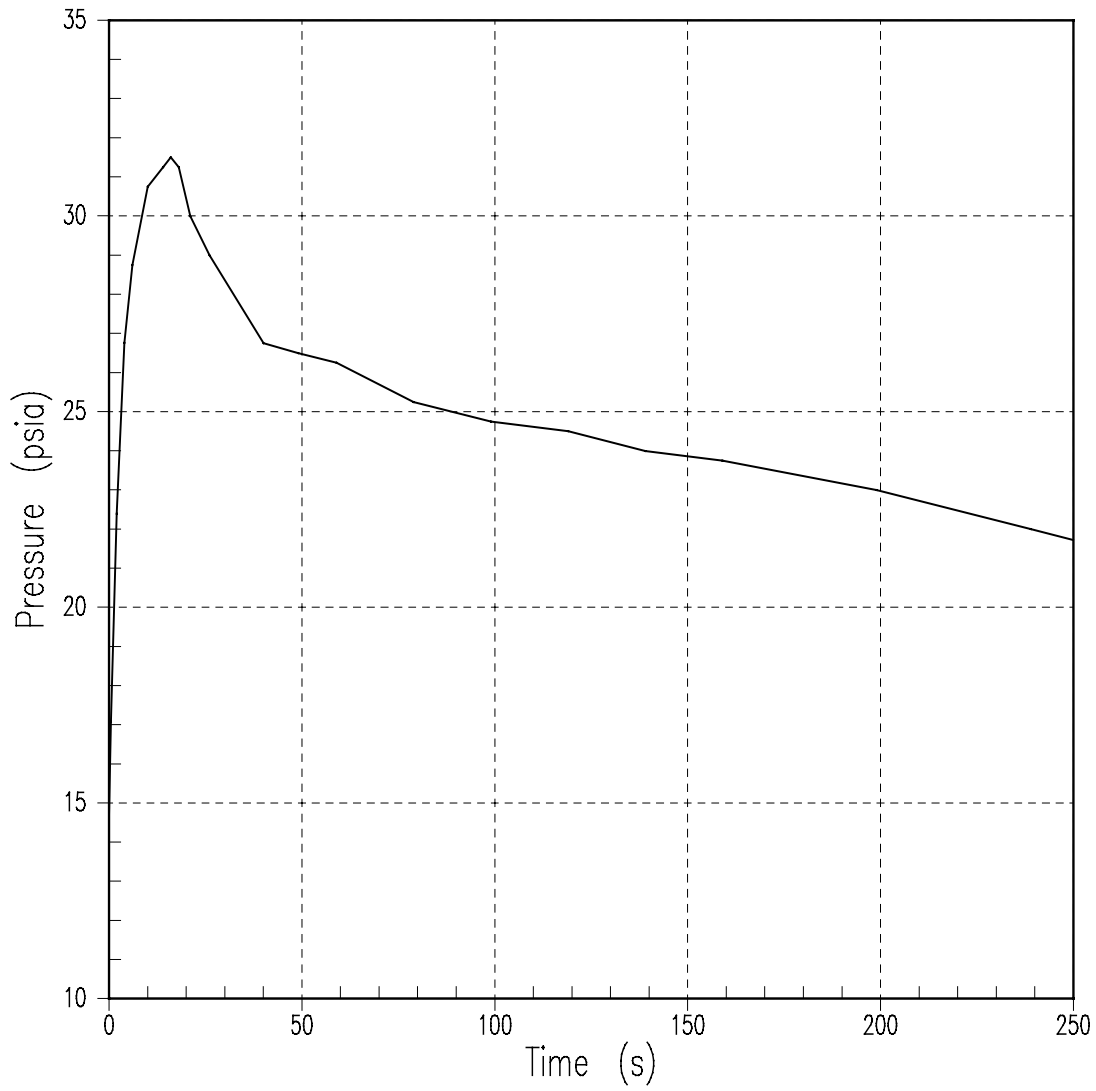


Figure 14.3.2-3
KNPP Reference Transient-Peak Clad Temperature

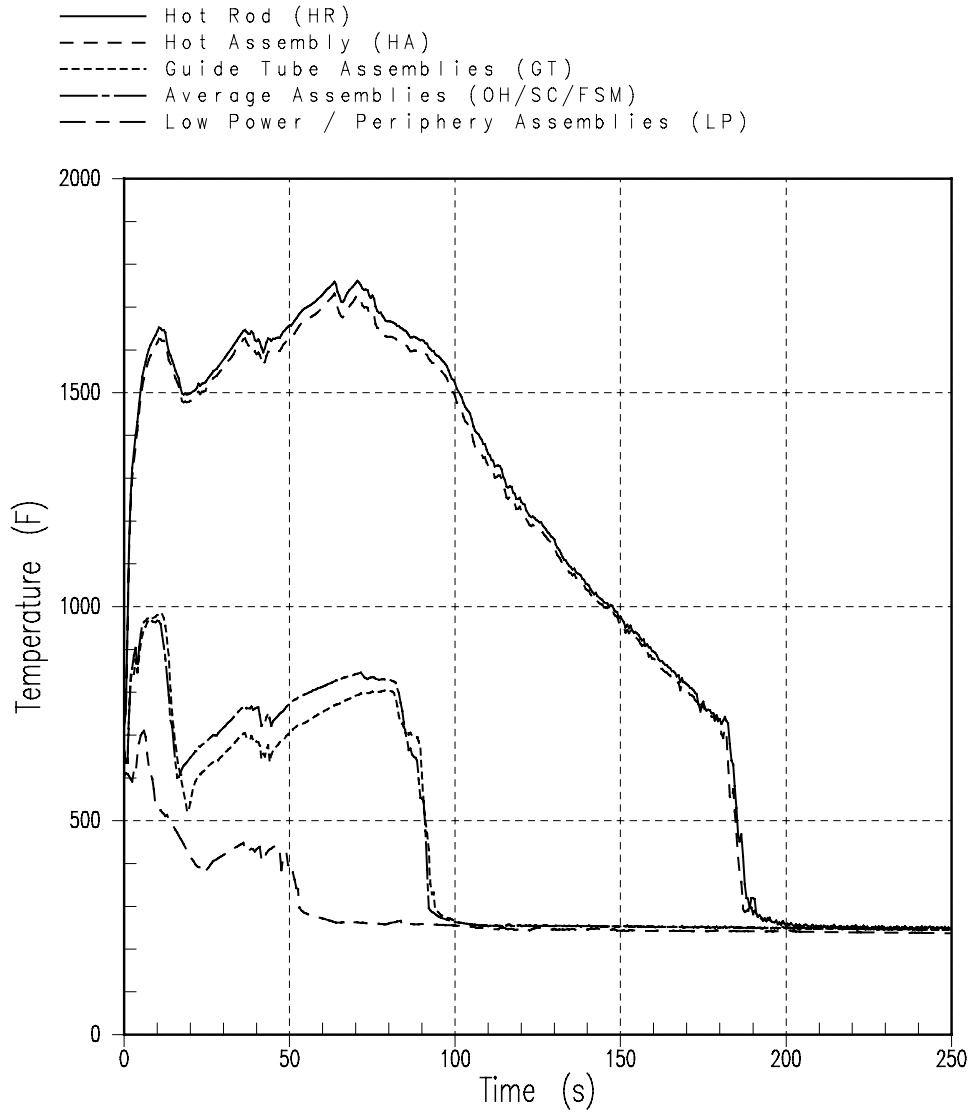


Figure 14.3.2-4
KNPP Reference Transient-Split Break Flow

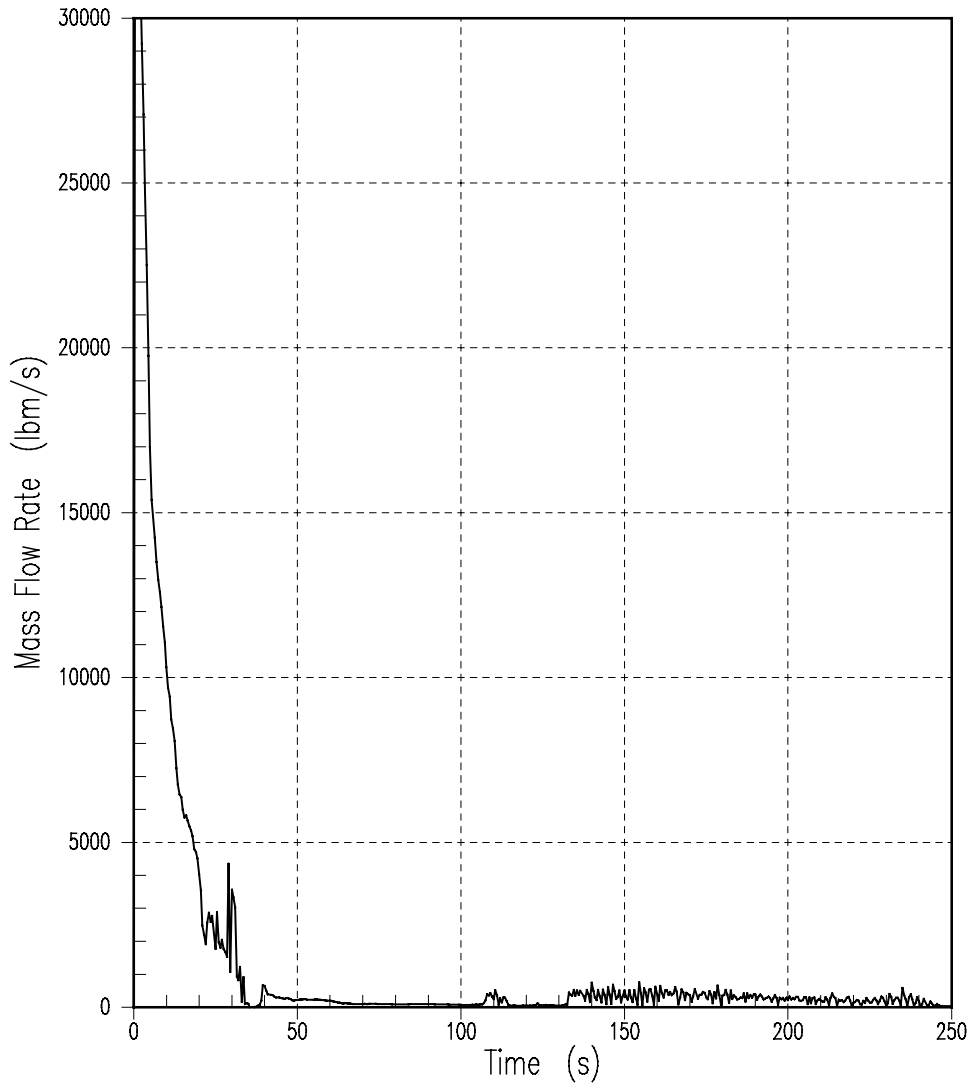


Figure 14.3.2-5
KNPP Reference Transient-Total Core at Midplane

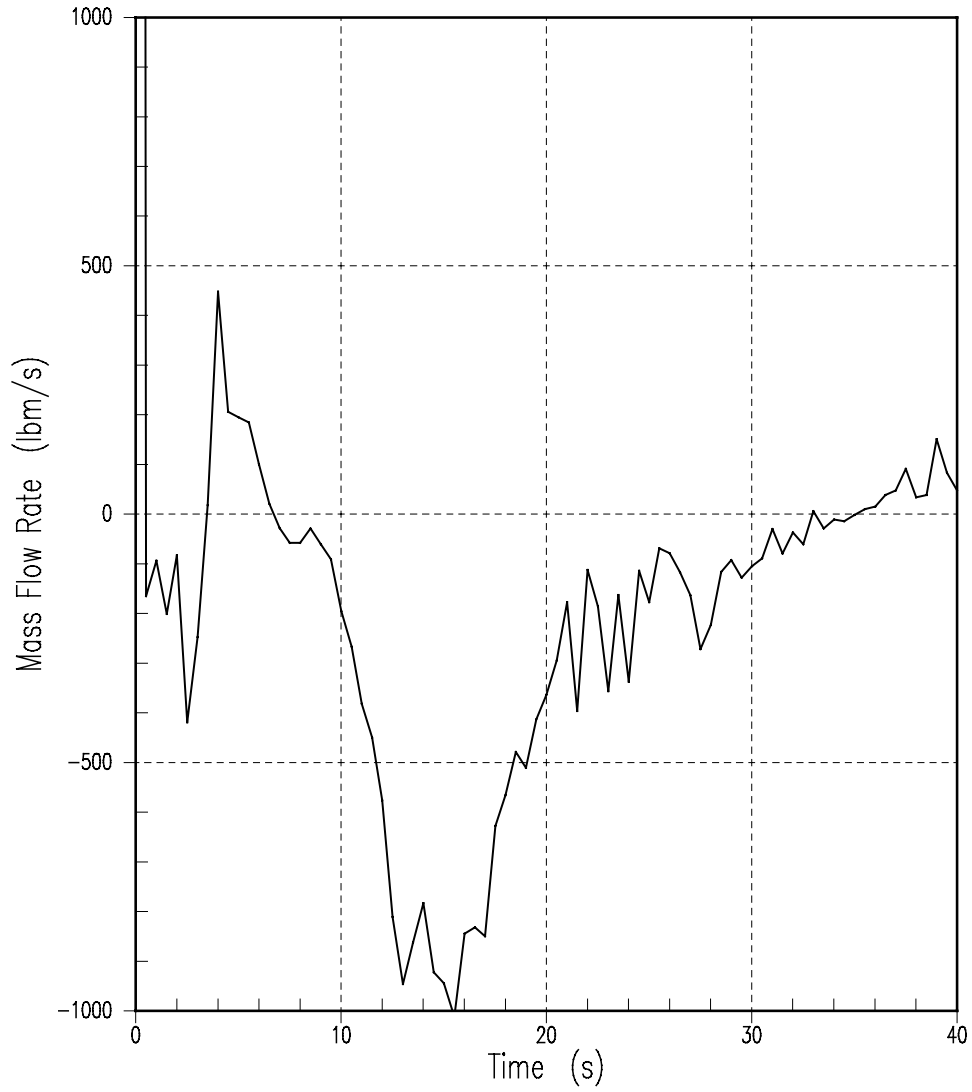


Figure 14.3.2-6
KNPP Reference Transient-Accumulator Flow

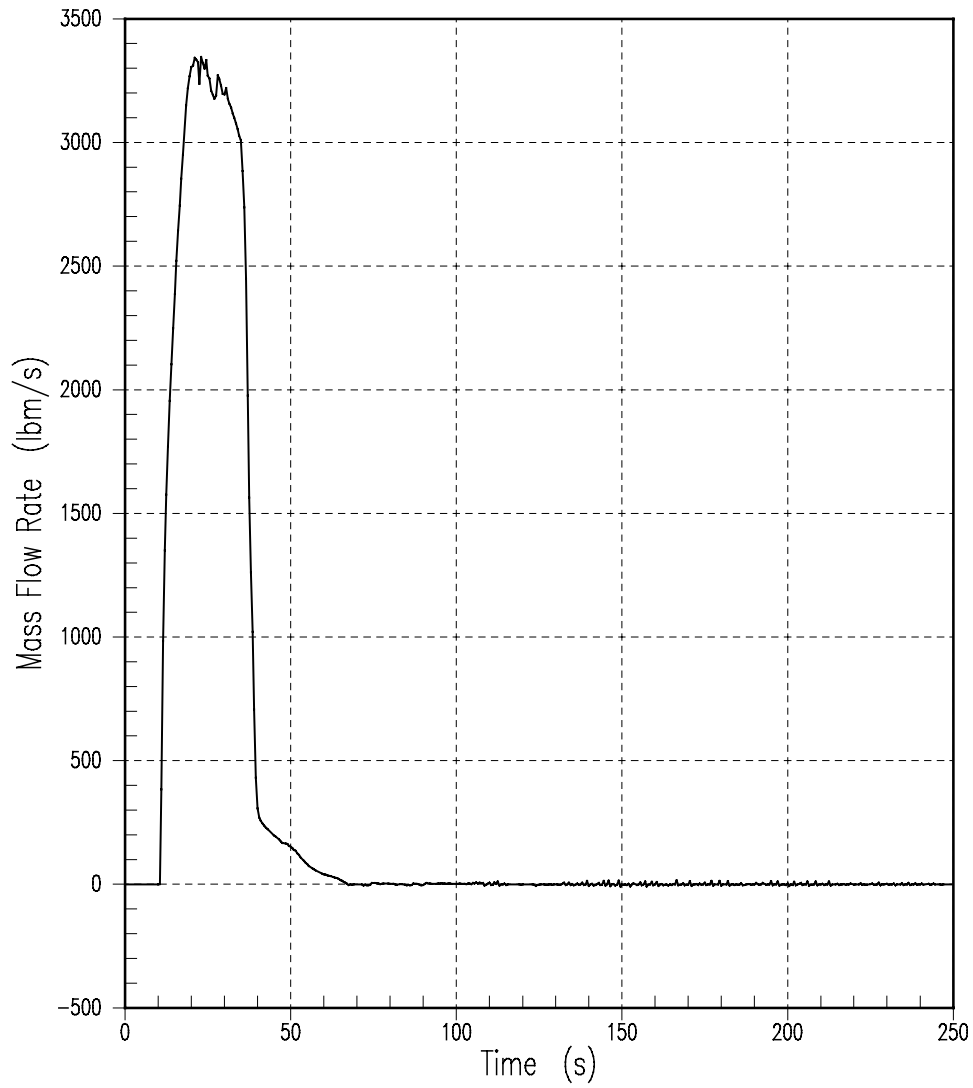


Figure 14.3.2-7
KNPP Reference Transient-HHSI Flow

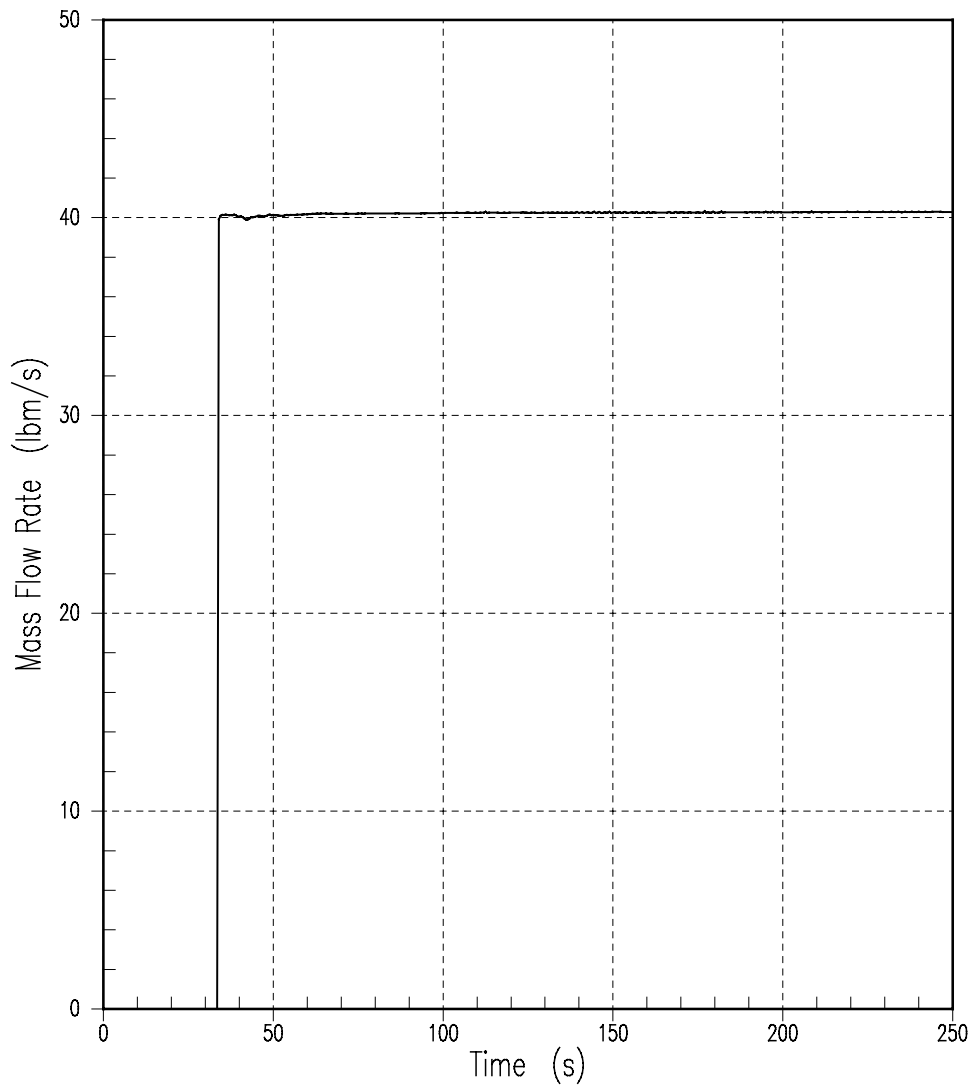


Figure 14.3.2-8
KNPP Reference Transient-LHSI Flow

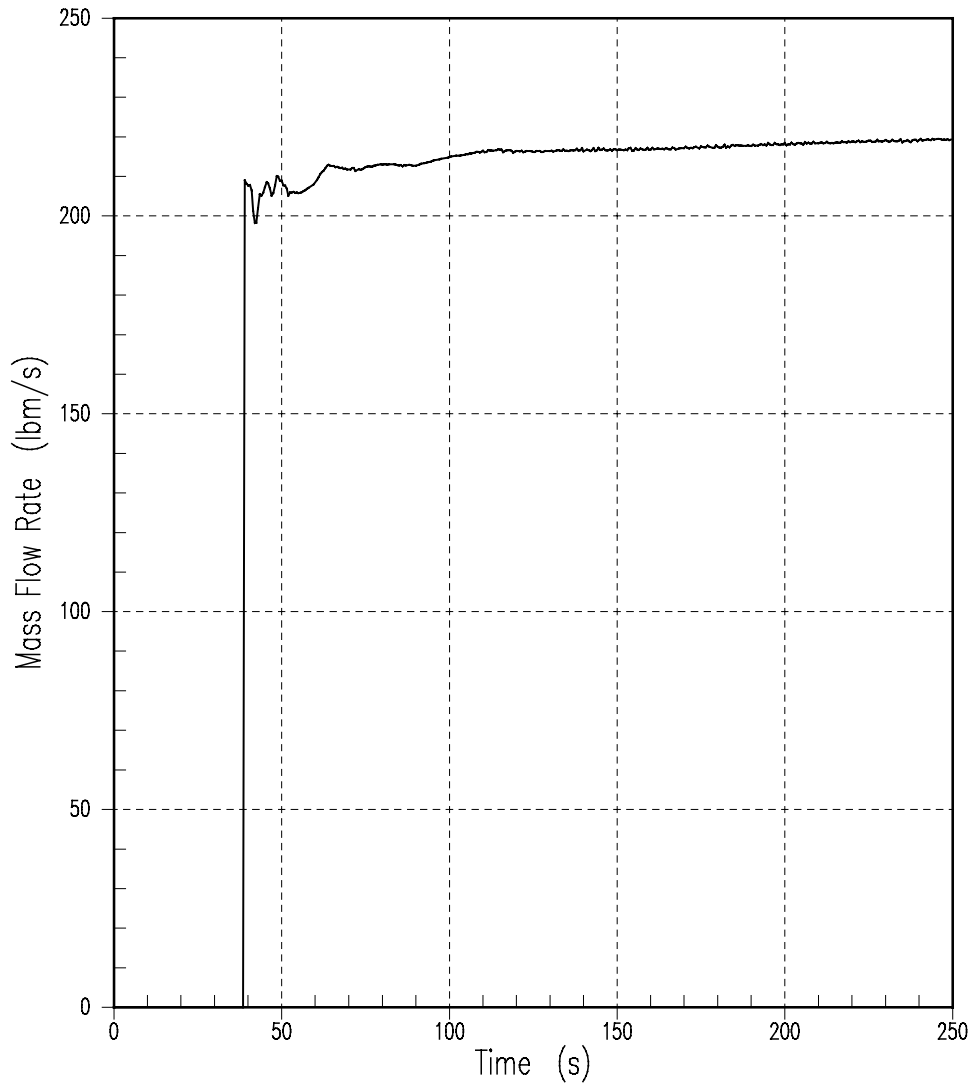


Figure 14.3.2-9
KNPP Reference Transient-Average Liquid Levels in the Downcomer Channels

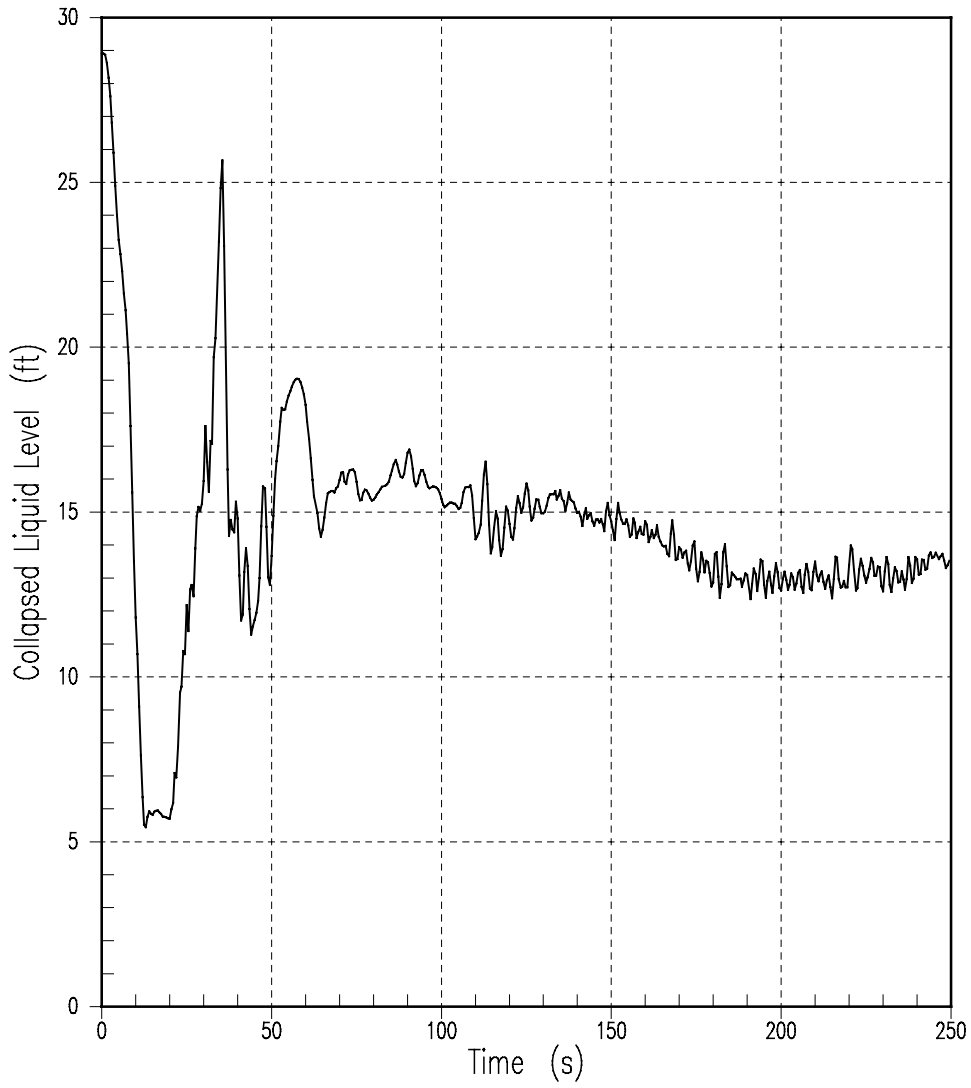


Figure 14.3.2-10
KNPP Reference Transient-Lower Plenum Liquid Level

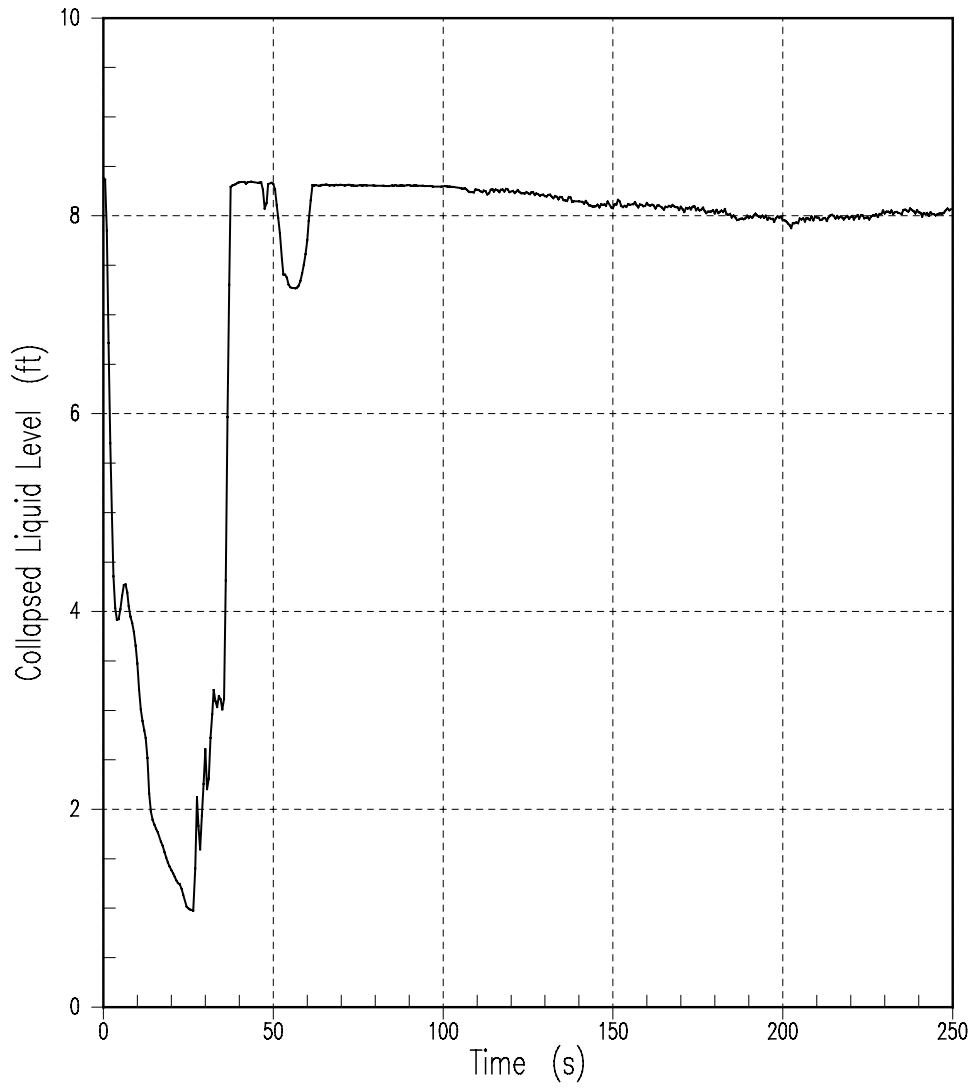


Figure 14.3.2-11
KNPP Reference Transient-Core Channel Liquid Level

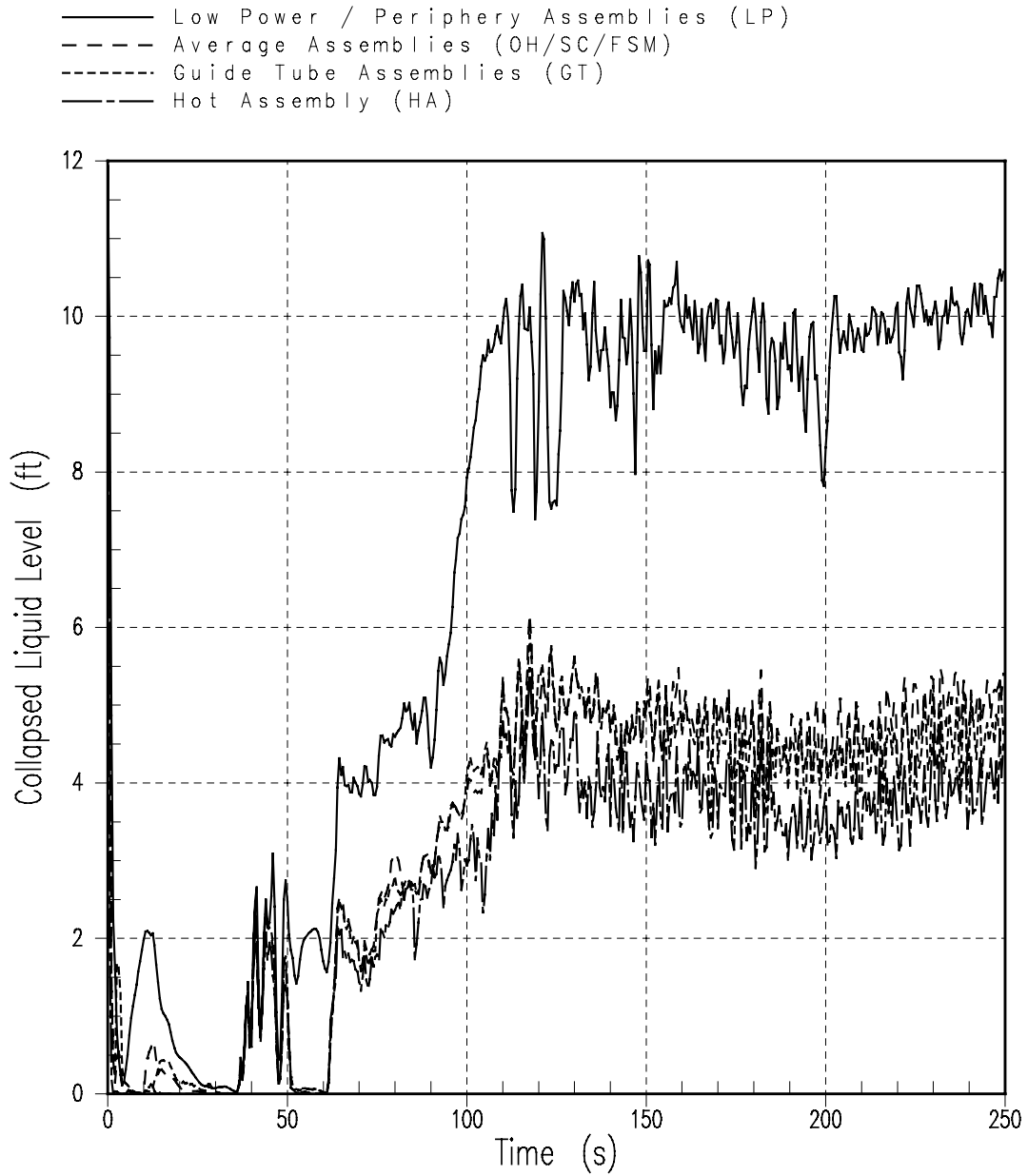


Figure 14.3.2-12
KNPP P_{BOT}/P_{MID} Limits Superimposed on a Plot of All Possible Power Shapes

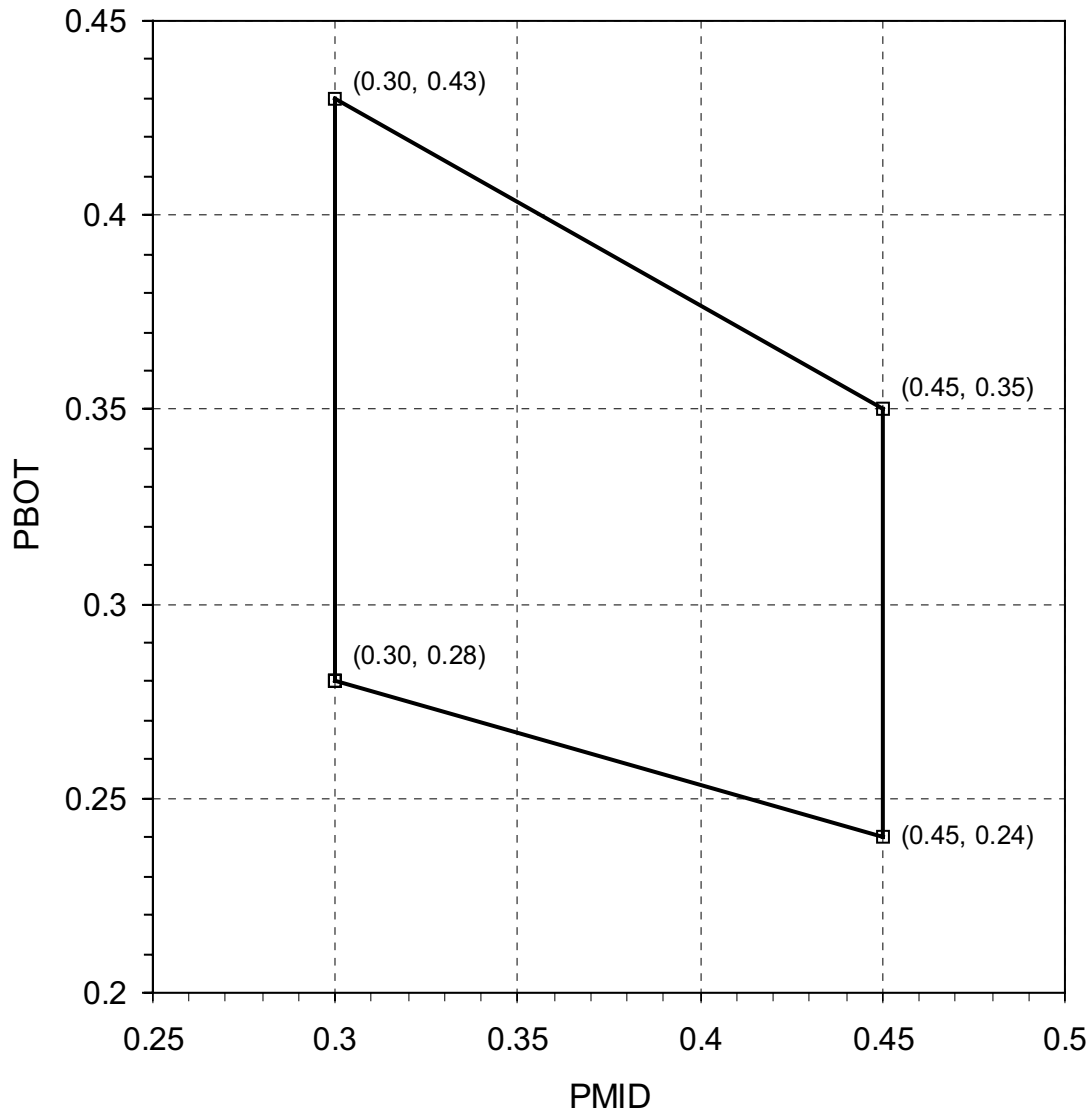


Figure 14.3.2-13
KNPP LHSI Flow (One 10% Degraded LHSI Pump)

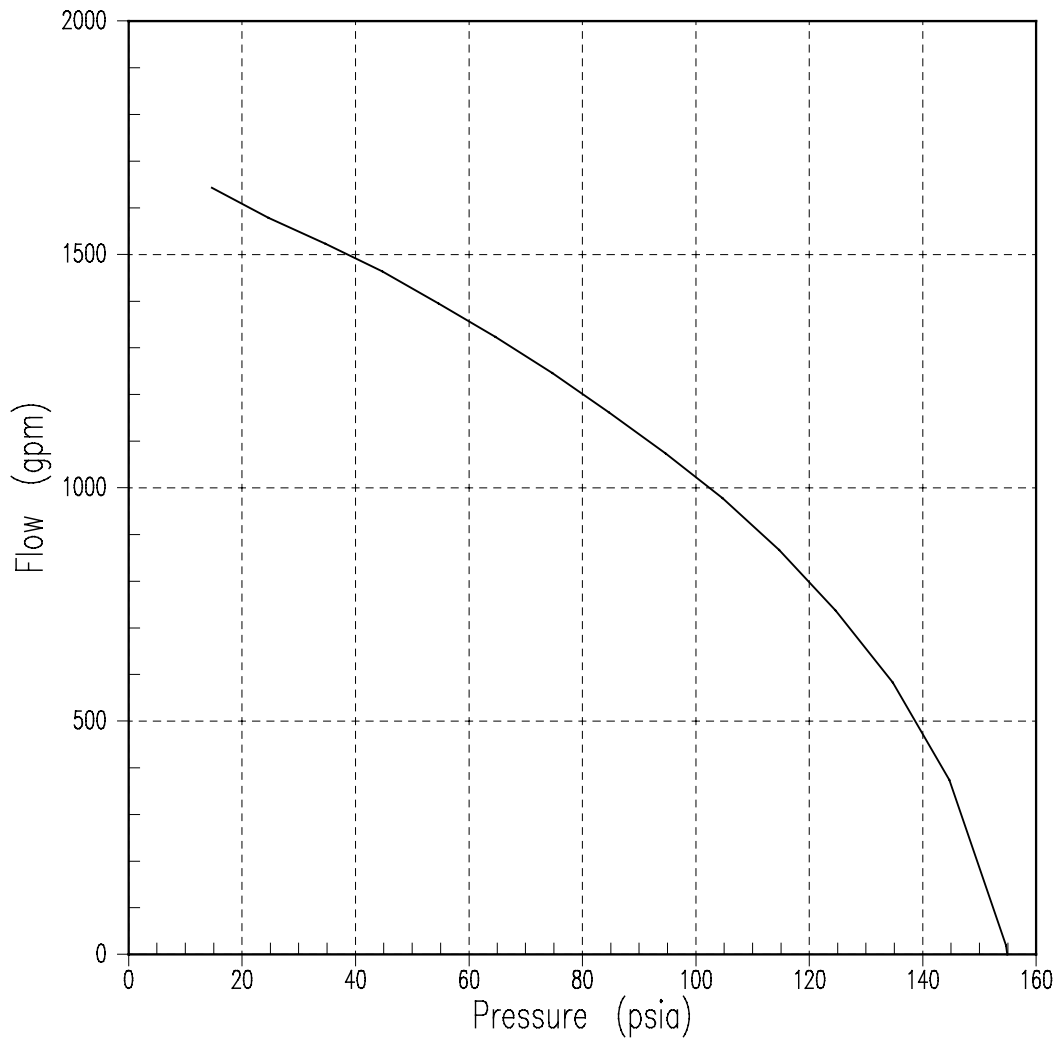


Figure 14.3.2-14
KNPP HHSI Flow (One 15% Degraded HHSI Pump)

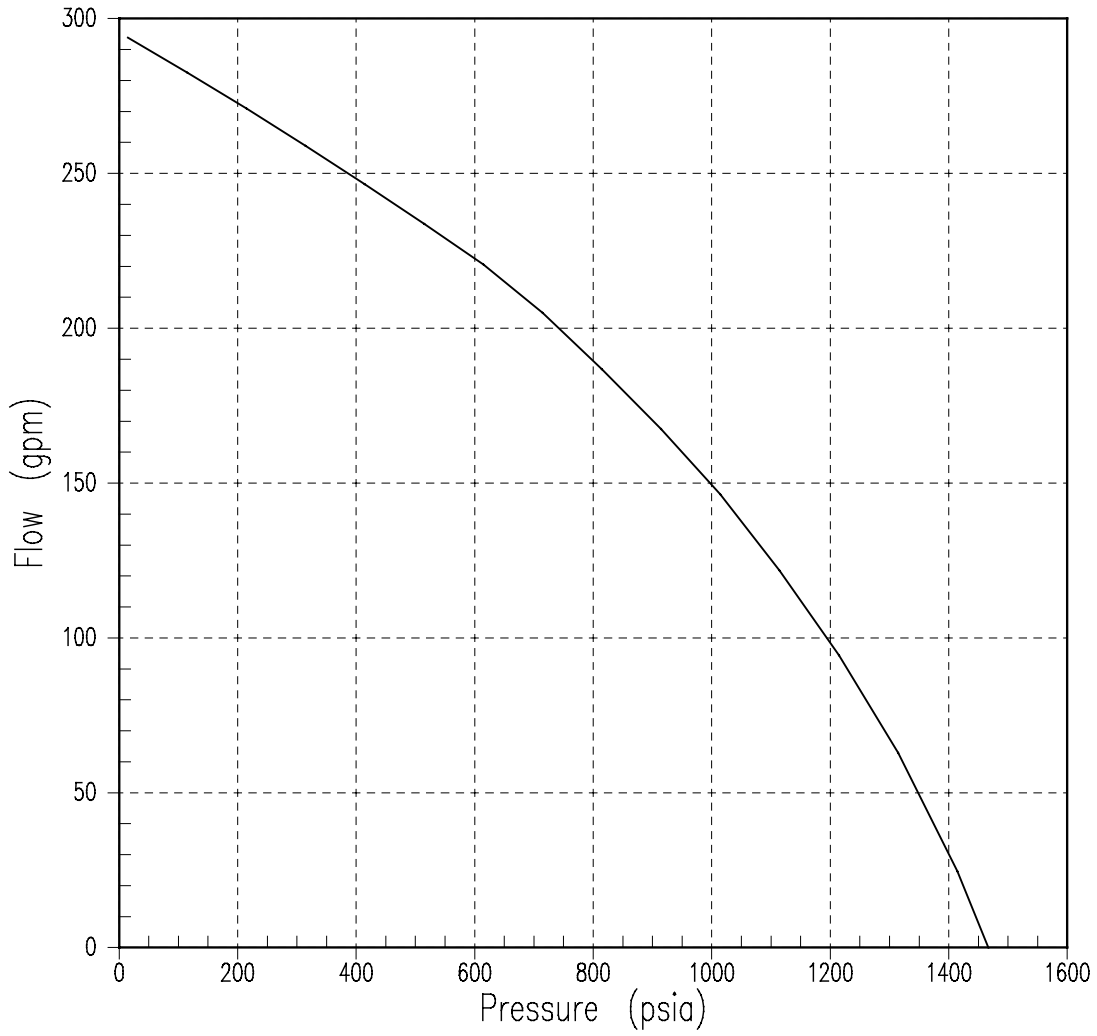


Figure 14.3.4-1
Double-Ended Hot Leg Break - Containment Pressure

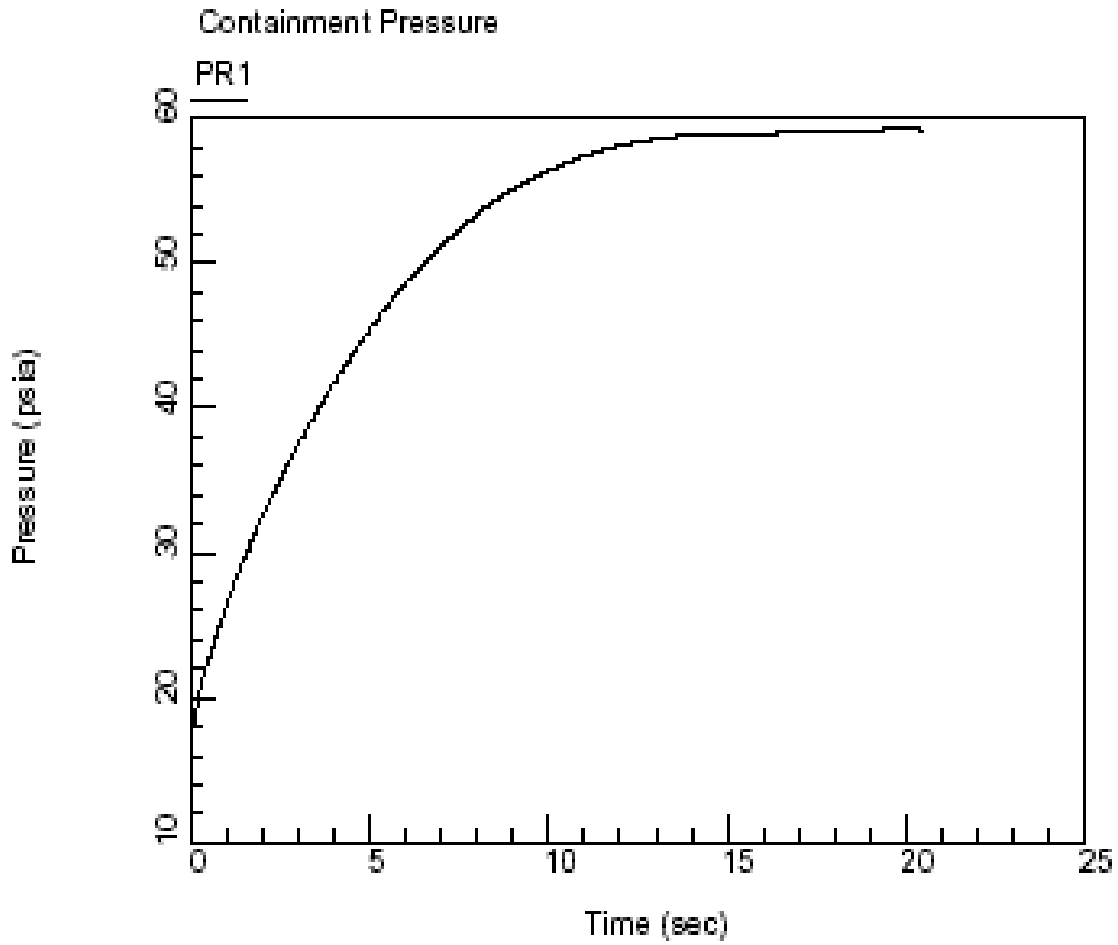


Figure 14.3.4-2
Double-Ended Hot Leg Break - Containment Atmosphere Temperature

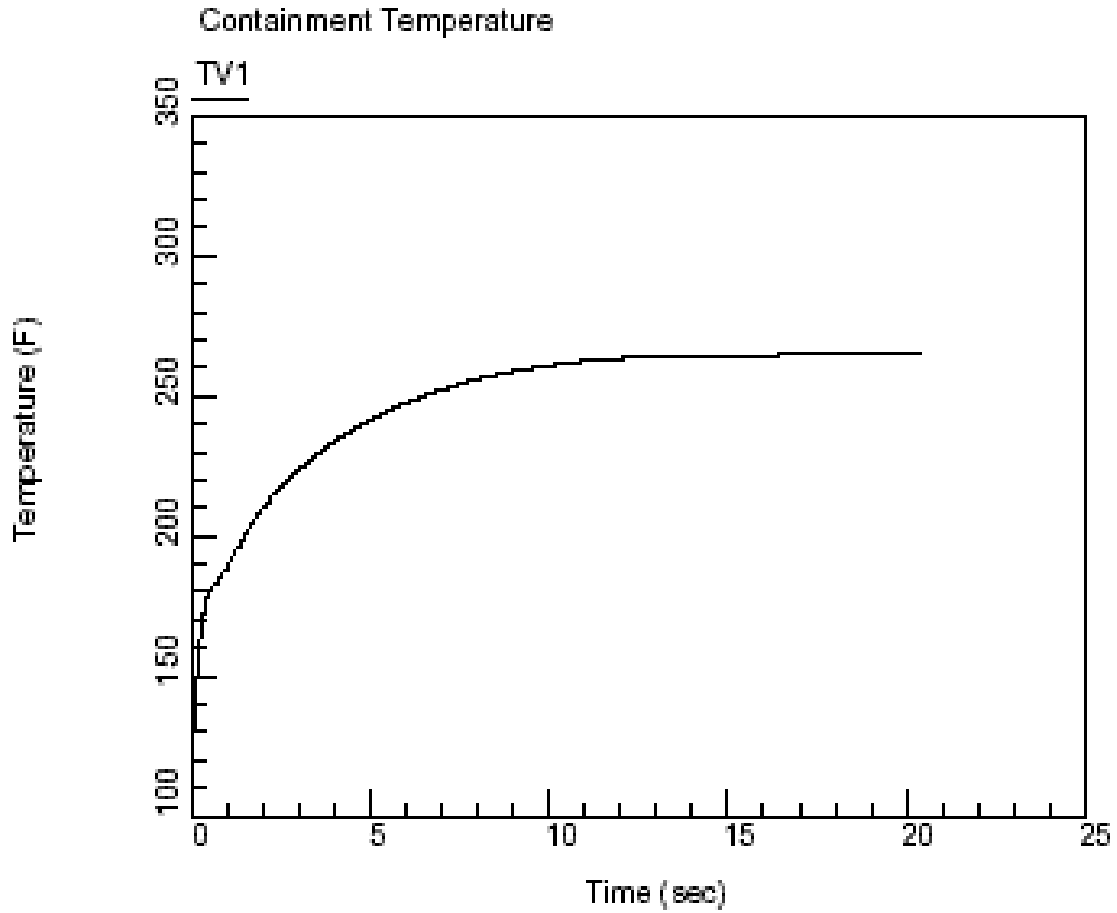


Figure 14.3.4-3
Double-Ended Hot Leg Break - Containment Sump Temperature

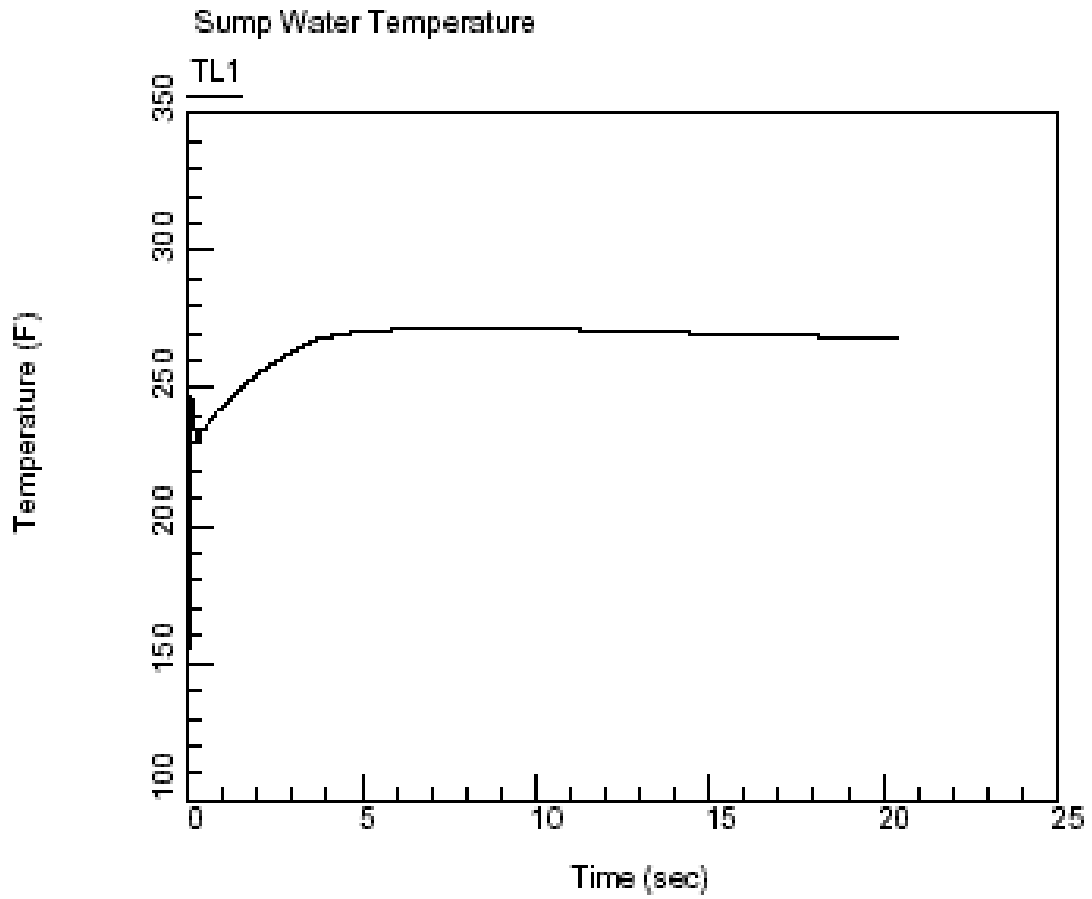


Figure 14.3.4-4
Double-Ended Pump Suction Break with Minimum Safeguards - Containment Pressure

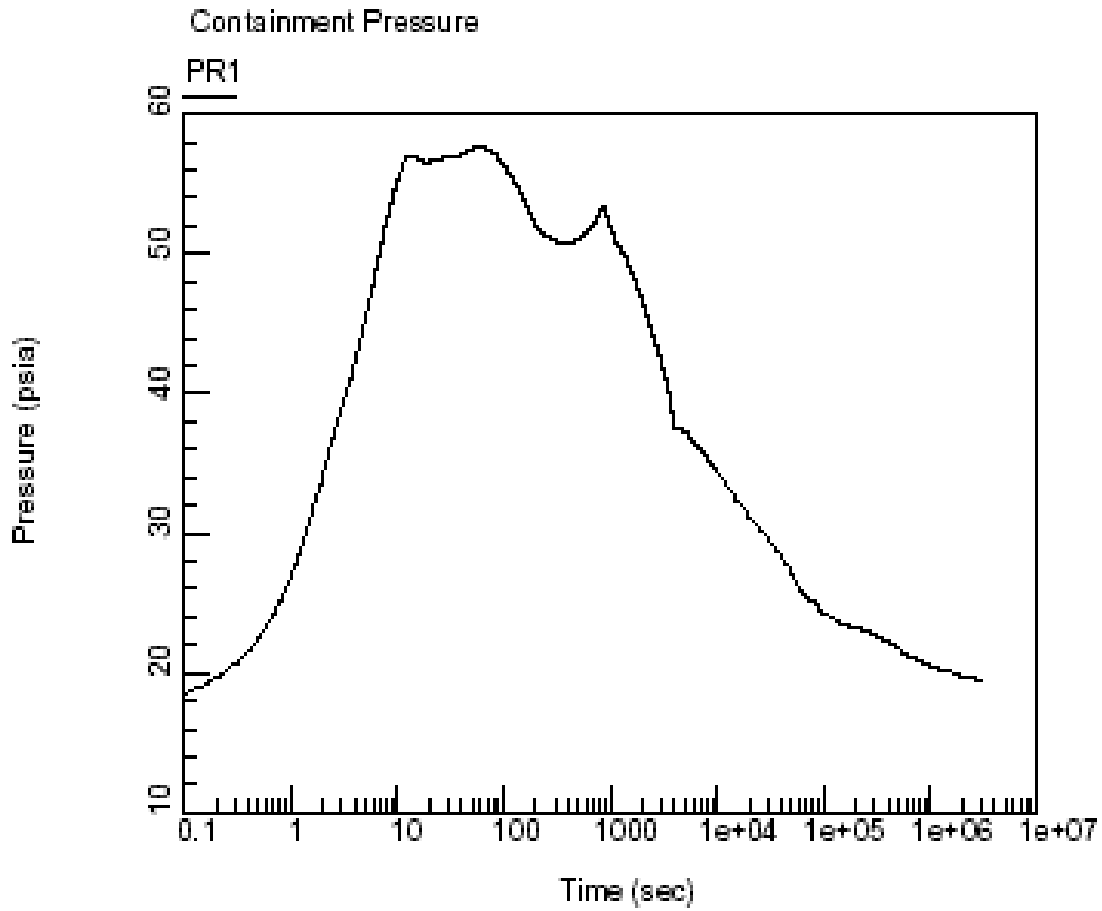


Figure 14.3.4-5
Double-Ended Pump Suction Break with Minimum Safeguards - Containment Atmosphere
Temperature

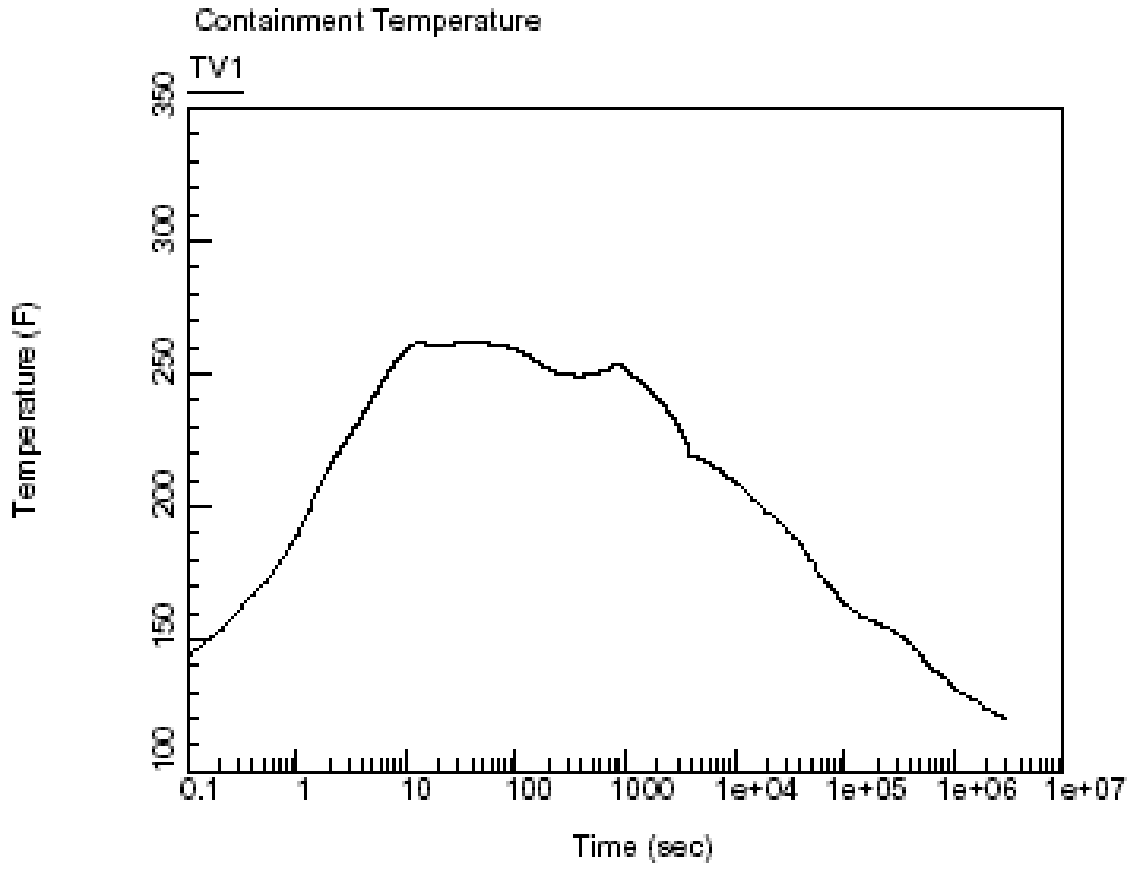


Figure 14.3.4-6
Double-Ended Pump Suction Break with Minimum Safeguards - Containment Sump Temperature

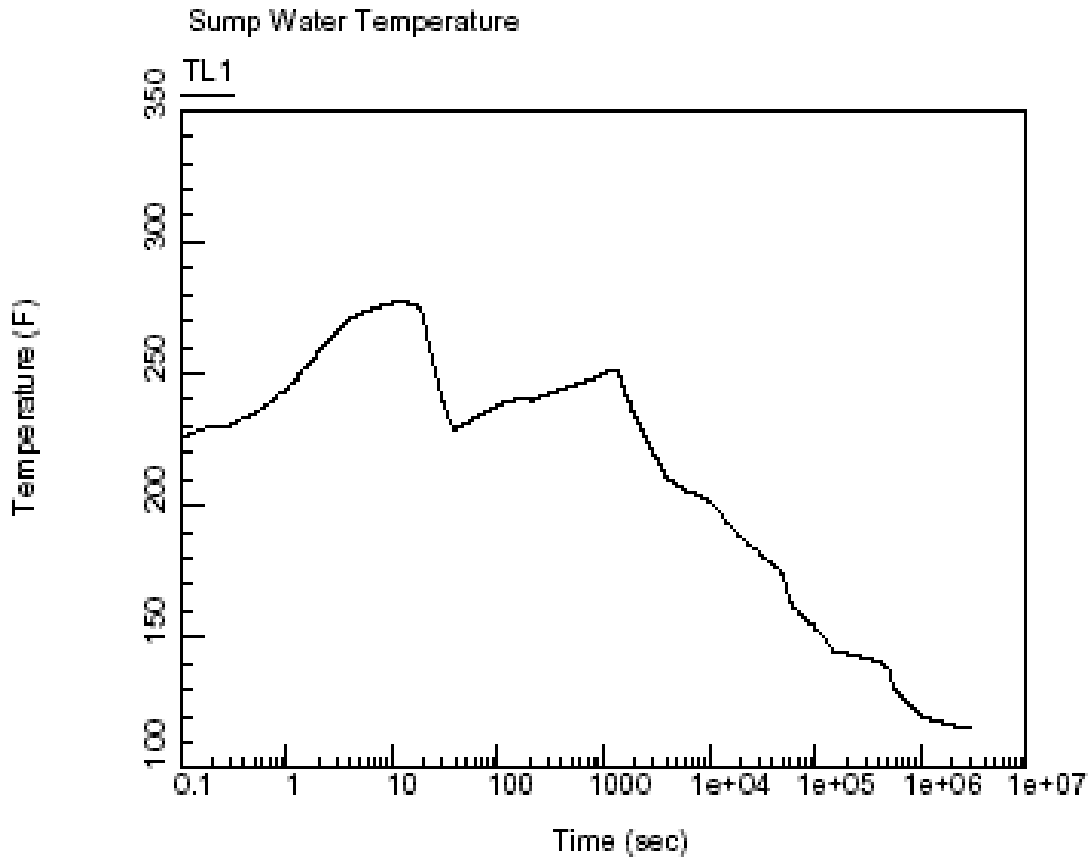


Figure 14.3.4-7
Double-Ended Pump Suction Break with Maximum Containment Safeguards - 1 Spray Pump
Failure Containment Pressure

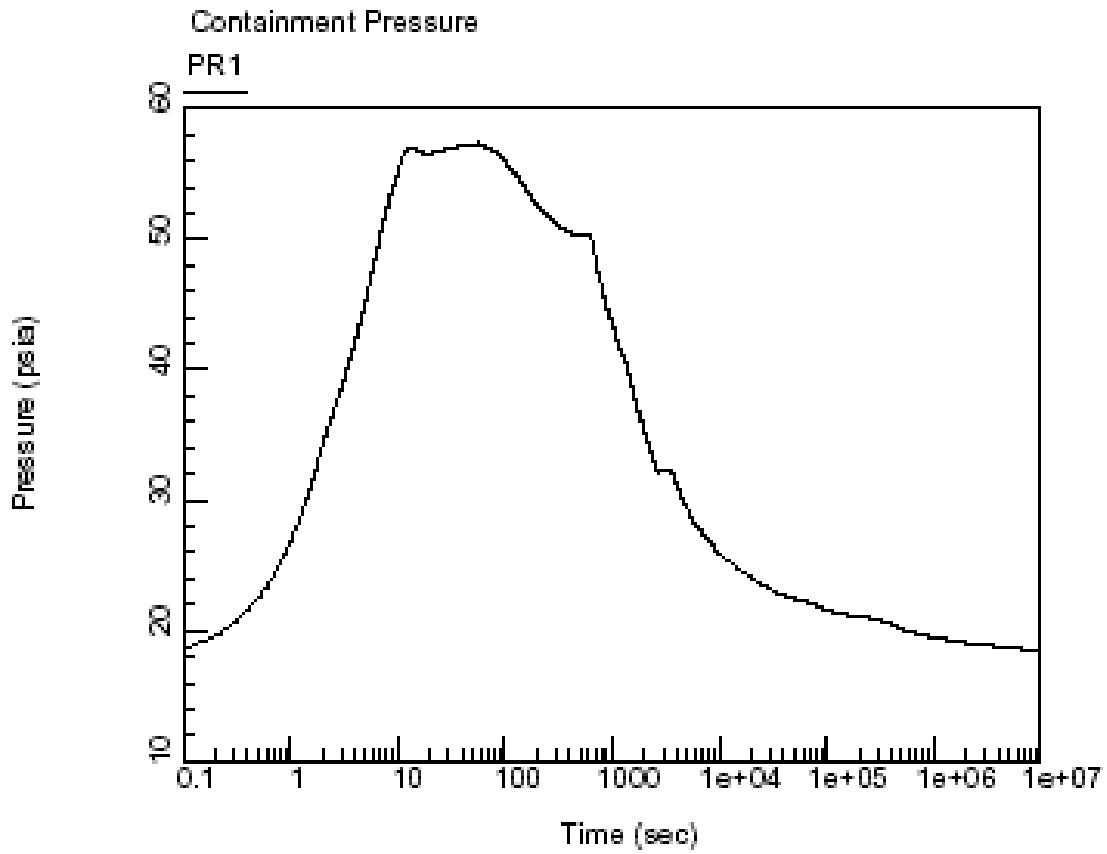


Figure 14.3.4-8
Double-Ended Pump Suction Break with Maximum Containment Safeguards - 1 Spray Pump
Failure Containment Atmosphere Temperature

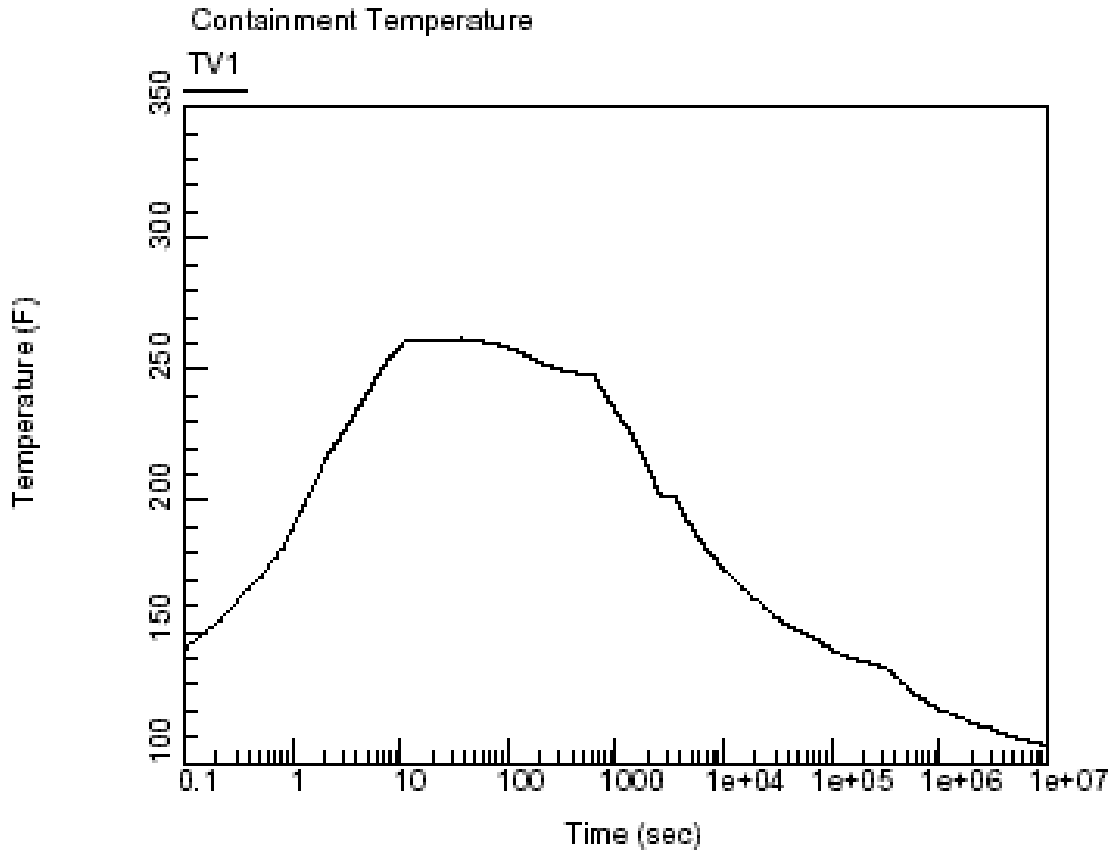


Figure 14.3.4-9
Double-Ended Pump Suction Break with Maximum Containment Safeguards - 1 Spray Pump
Failure Containment Sump Temperature

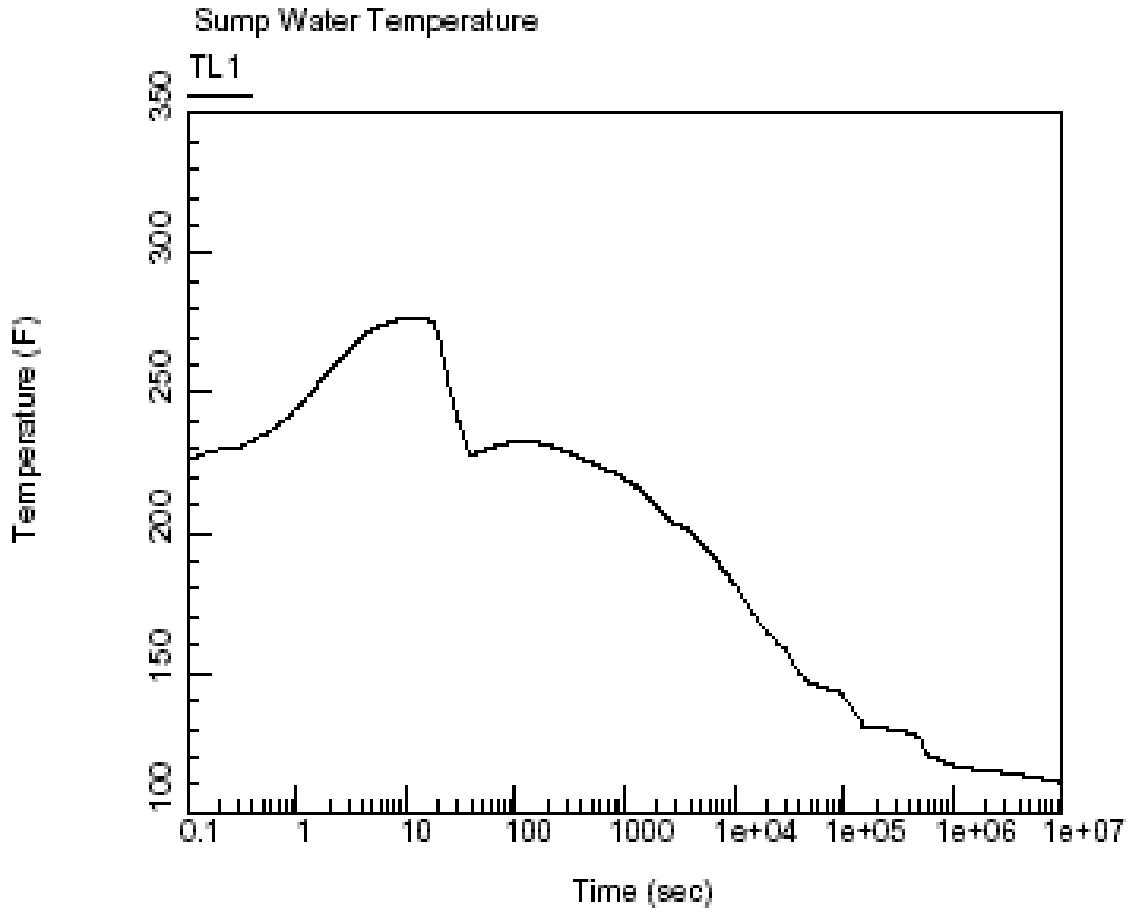


Figure 14.3.4-10
Double-Ended Pump Suction Break with Maximum Containment Safeguards - 1 Fan Cooler
Failure Containment Pressure

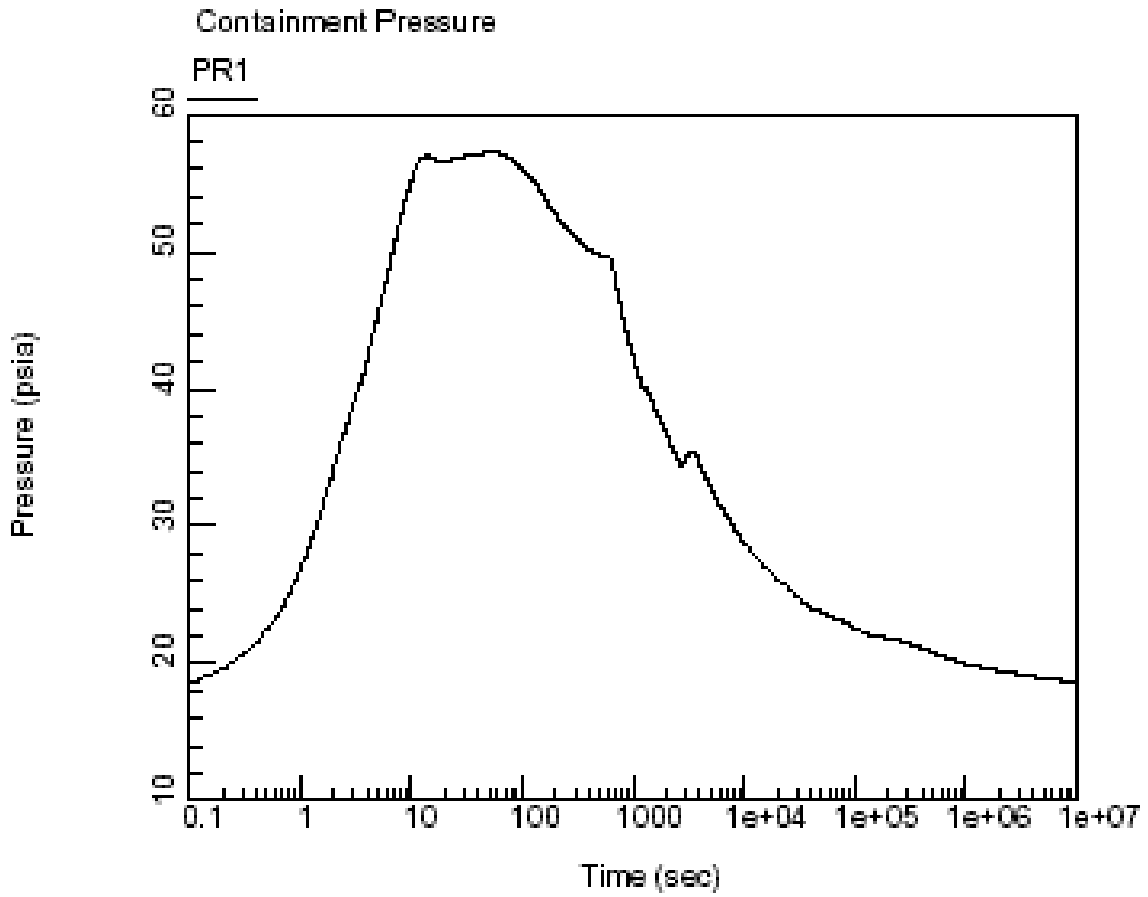


Figure 14.3.4-11
Double-Ended Pump Suction Break with Maximum Containment Safeguards - 1 Fan Cooler
Failure Containment Atmosphere Temperature

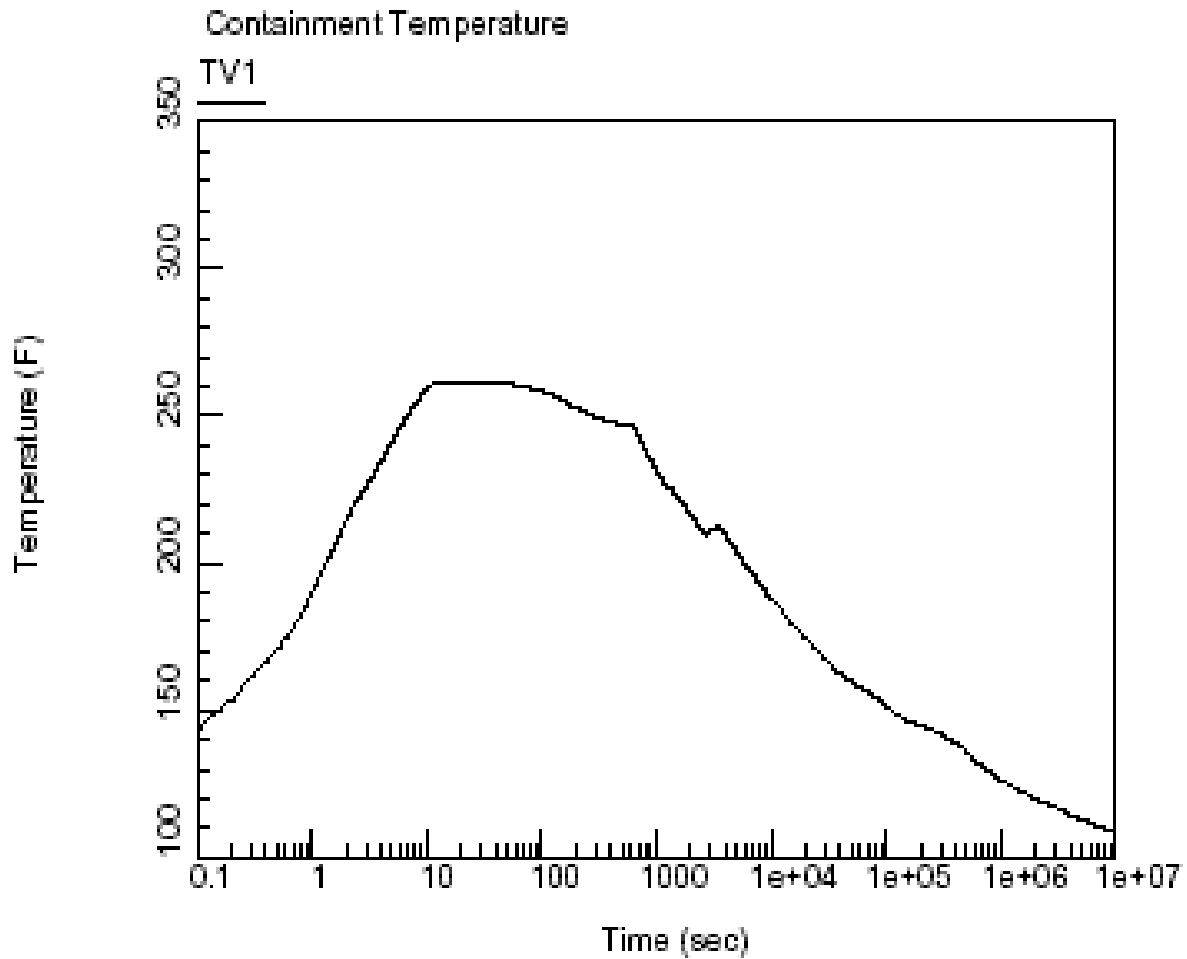
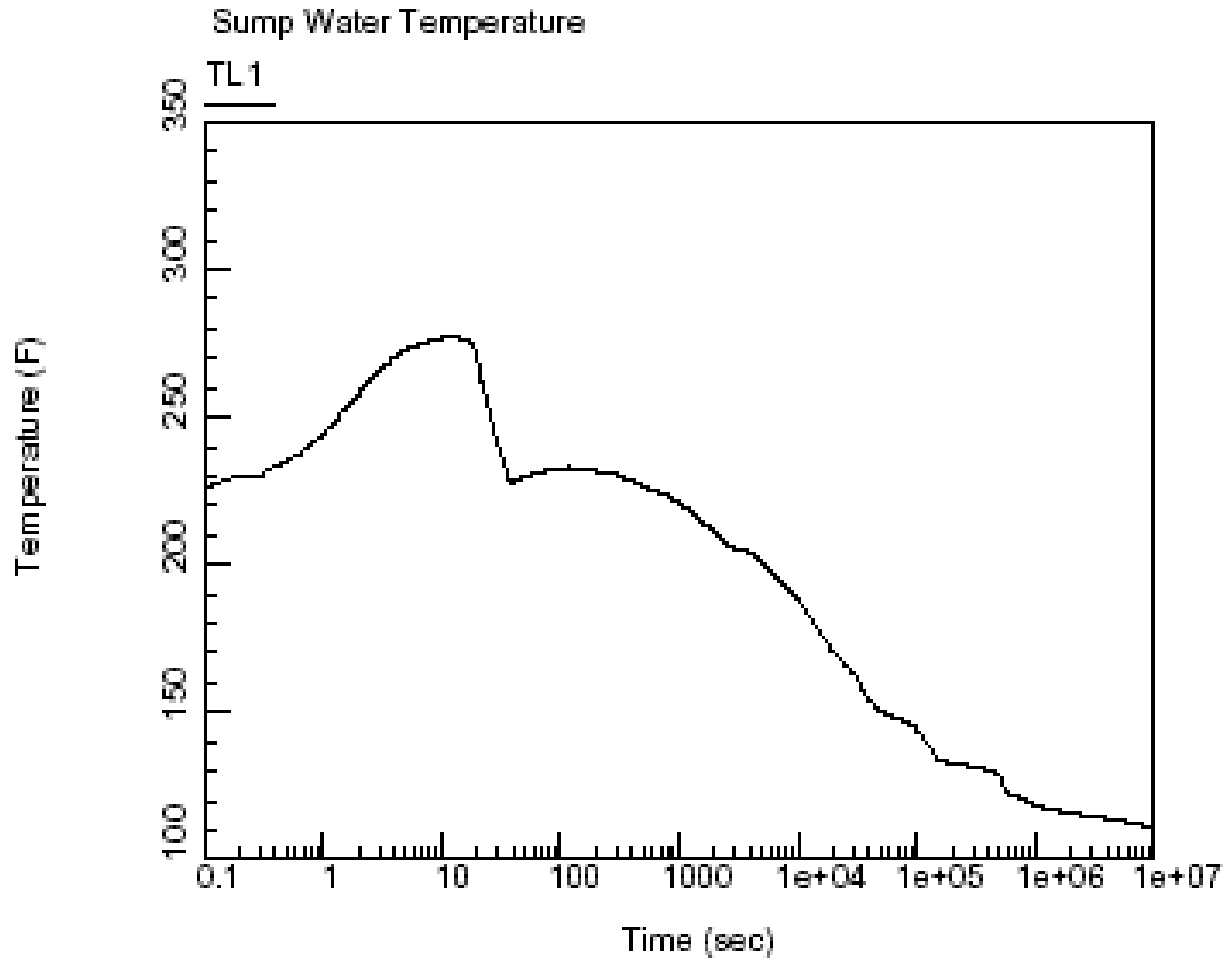


Figure 14.3.4-12
Double-Ended Pump Suction Break with Maximum Containment Safeguards - 1 Fan Cooler
Failure Containment Sump Temperature



APPENDIX 14A
HEAT TRANSFER COEFFICIENTS - LOCTA-R

Intentionally Blank

APPENDIX 14A
HEAT TRANSFER COEFFICIENTS
USED IN LOCTA-R2

Heat Transfer Regime	Heat Transfer Correlation
1. Sub-cooled nucleate boiling	Jens and Lottes ⁽¹⁾
$T_w - T_{sat} = 1.9e^{-P/900}(q'')^{1/4}$	(1)
2. Stable film boiling	
X > 0.0	Dougall and Rohsenow ⁽²⁾
$H = 0.023 \frac{k_v}{D_e} \left(\frac{\rho_v D_e}{\mu_v} \cdot \frac{Q_1 + Q_v}{A_c} \right)^{0.8} \left(\frac{C_p \mu}{k} \right)_v^{0.4}$	(2)
X < 0.0	Sandberg et al. ⁽³⁾
$\left(\frac{hD_e}{k} \right)_f = 0.0193 \left(\frac{D_e G}{\mu} \right)_f^{0.80} \left(\frac{C_p \mu}{k} \right)_f^{1.23}$	(3)
$\left(\frac{\rho_g}{\rho_b} \right)^{0.68} \left(\frac{\rho_g}{\rho_l} \right)^{0.068}$	
3. Turbulent forced convection to steam	McEligot et al. ^(4,5)
$\frac{hD_e}{k} = 0.020 [Re b]^{0.8} [Pr b]^{0.4} \left[\frac{T_w}{b} \right]^{-0.5}$	(4)
4. Laminar forced convection to steam	Hausen ⁽⁶⁾ and Kays ⁽⁷⁾
$\left(\frac{hD_e}{k} \right)_{iso} = 3.66v$	(5)
$h/h_{iso} = \left(\frac{T_b}{T_w} \right)^{0.25}$	

Heat Transfer Regime	Heat Transfer Correlation
5. Radiation to steam	Hottel ⁽⁸⁾ (6)
$q'' = \varepsilon \times 0.1713 \left[\frac{\left(\frac{T_w}{100}\right)^4 - \left(\frac{T_b}{100}\right)^4}{T_w - T_b} \right]$	
6. Pool film boiling	Bromley ⁽⁹⁾ , Hsu and Westwater ⁽¹⁰⁾ (7)
$h = 0.7 \left(\frac{k_v 3 \rho_v (\rho L - \rho v) g h_{fg}}{L (T_w - T_b) \mu_v} \right)^{0.25}$	
7. Mist heat transfer in a dispersed flow	Dougall and Rohsenow ⁽²⁾ (8)
$h = 0.023 \frac{h_v}{D_e} \left[\frac{p_e D}{\mu_e} \frac{Q_1 + Q_v}{A_c} \right]^{0.08} \left(\frac{C_p \mu}{k} \right)_v^{0.4}$	

NOMENCLATURE SYMBOLS

A_c = Area of flow channel

C_p = Specific heat

D_e = Equivalent diameter

G = Mass velocity

L = Length of heat source

P = System pressure

Pr = Prandtl number

Q_1 = Volumetric flow rate of liquid

Q_v = Volumetric flow rate of vapor

Re = Reynolds number

T = Temperature

g = Gravity constant

h = Heat transfer coefficient

h_{fg} = Latent heat of vaporization

k = Thermal conductivity

q'' = Heat flux

X = Quality

e = Effective emissivity

m = Dynamic viscosity

ρ = Density

SUBSCRIPTS

b = Quantities evaluated at bulk fluid temperature

f = Quantities evaluated at film temperature

g = Saturated vapor

iso = Evaluation of the parameter when the temperature difference ($T_w - T_b$) is small

l = Saturated liquid

sat = Refers to saturated condition

v = Saturated vapor

L = Refers to liquid

w = Wall

14A References

1. Jens, W. H., and P. A. Lottes, "Analyses of Heat Transfer, Burnout, Pressure Drop, and Density Data for High Pressure Water," USAEC Report ANL-4627, 1951
2. Dougall, R. S., and W. M. Rohsenow, "Film Boiling on the Inside of Vertical Tubes with Upward Flow of Fluid at Low Quantities," MIT Report 9079-26
3. Sandberg, R. O., A. A. Bishop, L. S. Tong, "Forced Convection Heat Transfer at High Pressure After the Critical Heat Flux," ASME Paper No. 65-HT-31, 1965
4. McEligot, D. M., P. M. Magee, and G. Leppert, "Effect of Large Temperature Gradients on Convective Heat Transfer: The Downstream Region," J. of Heat Transfer, Vol. 87, 1965, pp 67-76

5. McEligot, D. M., L. W. Ormand, and H. C. Perkins, "Internal Low Reynolds-Number Turbulent and Transitional Gas Flow with Heat Transfer," J. of Heat Transfer, Vol. 88, 1966, pp. 239-245
6. Hausen, H., "Darstellung des Wärmeüberganges in Rohren durch verallgemeinerte Potenzbeziehungen," VDI Zeit., No. 4, p. 91, 1943
7. Kays, W. M., "Numerical Solutions for Laminar-Flow Heat Transfer in Circular Tubes," Trans. ASME, Vol. 77, 1955, pp. 1265-2374
8. Hottel, H. C., "Radiation Heat Transmission," Ch. 4 of Heat Transmission by W. H. McAdams, McGraw-Hill, 1954
9. Bromley, L. A., "Heat Transfer in Stable Film Boiling," Chemical Engineering Progress, Vol. 46, No. 5, 1950, pp. 221-227
10. Hsu, Y. Y., S. W. Westwater, "Approximation Theory for Film Boiling on Vertical Surfaces," Chemical Engineering Process Symposium, Storrs, Conn., 1959

APPENDIX 14B
WESTINGHOUSE HEAT TRANSFER
RESEARCH AND DEVELOPMENT PROGRAMS

Intentionally Blank

APPENDIX 14B

WESTINGHOUSE HEAT TRANSFER RESEARCH AND DEVELOPMENT PROGRAMS

Several Westinghouse Research and Development Programs have resulted in confirmation of the usage of the above heat transfer correlations for loss-of-coolant analyses and also in the development of a transition boiling heat transfer correlation.

From the results of the Flashing Heat Transfer Program, the following conclusions were made:

- Heat transfer in the transition to film boiling regime during the blowdown of a LOCA can be conservatively predicted by a correlation developed from steady-state film boiling and transition boiling data.
- The McEligot, et al. correlation (Reference 1, Reference 2) realistically predicts the convective heat transfer coefficients in turbulent flow.
- In turbulent flow, the radiant heat transfer contributions to the total heat transfer coefficient is adequately predicted by Hottel's (Reference 3) technique.
- In laminar flow the total heat transfer coefficient is conservatively predicted by using the correlation of Hausen (Reference 4) and Kays (Reference 5) for the convective contribution and the method of Hottel (Reference 3) for the radiant contribution.

In progress at the time of this application was the Full-length Emergency Cooling Heat Transfer (FLECHT) Program. The objective was to investigate the behavior of a simulated pressurized water reactor during the core recovery (re-flooding) period, which follows a LOCA. The Group I and Group II test series of this program, which included 7 x 7 and 10 x 10 rod bundle arrays, have been completed.

APPENDIX 14C
CONTAINMENT PRESSURE RESPONSE TO LOCA

Intentionally Blank

APPENDIX 14C

CONTAINMENT PRESSURE RESPONSE TO LOCA

14C.1 Steam Generators as an Active Heat Source

The containment pressure response has been analyzed considering the steam generators as an active heat source during re-flood. The analysis presented is for the 3.0 ft² pump suction break, which has been found to be most conservative. In addition, sensitivity studies are presented to show the containment pressure transient as a function of break size and location.

The calculational model may be divided into three parts: Blowdown, when the system pressure drops from 2250 psia to containment pressure; Refill, when the vessel inventory is increased to the bottom of the core; and Re-flood, where the water level moves into the core.

BLOWDOWN - The model for blowdown is essentially the same as that used in the FSAR containment analysis. The SATAN code is used to simulate breaks in the various locations. All accumulators inject for breaks other than the cold leg.

The steam generator is modeled using several well-known heat transfer correlations. When the heat flow in the steam generators is from primary to secondary, the heat transfer coefficient on the tube side is calculated using the Dittus Boelter (Reference 1) correlation for sub-cooled forced convection, while the shell side uses the well known Jens-Lottes (Reference 2) correlation for nucleate boiling. For secondary to primary heat flow, the tube side heat transfer coefficient is calculated using the Jens-Lottes correlation for nucleate boiling. This calculation will be bypassed if the tubes experience Departure from Nucleate Boiling (DNB). The DNB ratio is calculated using Macbeth's (Reference 3) correlation of the critical heat flux. When the value of this ratio drops below an input value, the Dougall-Rohsenow (Reference 4) film boiling correlation is used. Should the fluid in the steam generator tubes become superheated, the superheat forced convection correlation developed by McEligot (Reference 5) is used. The shell side heat transfer coefficient when the heat flow is from secondary to primary, is the only difference in the steam generator model used in the FSAR and the present model.

Previously, this value was maintained at the high initial value, thus allowing an exceedingly high heat flow from the secondary to the primary side of the steam generators. In the present model the heat transfer coefficient on the shell side when heat flow is from secondary to primary is calculated using McAdam's (Reference 6) recommended correlation for turbulent boundary layers on vertical surfaces.

Table 14C-1 lists all of the heat transfer correlations referenced formerly. The heat flow rates vs. time curves for the broken loop steam generator and the intact loop steam generator are presented in Figure 14C-1 and Figure 14C-2 for the worst case (3-ft² pump suction break).

The fluid volume contained in the primary system has been adjusted slightly. This volume reflects the correct system volume, calculated from component dimensions, plus 1.6 percent to account for thermal expansion and 1.4 percent to account for uncertainties. The initial fluid energy presented in the FSAR was based on a fluid volume in excess of that calculated using the standard procedure described above.

The initial fluid energy is also based on coolant temperatures, which are the maximum levels attained in steady-state operation including allowance for instrument error and deadband.

The previous SATAN initial stored energy in the core has been identified as being exceedingly conservative. The stored energy has been evaluated using a detailed temperature model of the pellet, clad and gap. The temperature distribution within the fuel pellet is predominantly a function of the local power density and the UO₂ thermal conductivity. However, the computation of radial fuel temperature distributions combines crud, oxide, clad, gap and pellet conductances. The factors which influence these conductances, such as gap size (or contact pressure), internal gas pressure, gas composition, pellet density, and radial power distribution within the pellet, etc., have been combined into a semi-empirical thermal model. This thermal model has been incorporated into a computer code to enable the determination of these factors and their net effects on temperature profiles. The temperature predictions of the code have been compared to in-pile fuel temperature measurements and melt radius data with good results. Table 14C-2 presents the results of sensitivity study on core stored energy, in full power seconds above average coolant temperature, varying the following parameters:

- Average Power Level
- Number of nodes assumed in the pellet
- Effect of fuel densification

A conservative value of 7.9 (6.6 x 1.2) full power seconds, which includes fuel densification and additional margin, was used in this analysis. Moreover, core stored energy was based on a conservative value of 102 percent of the engineered safeguards design rating power level.

Table 14C-3 summarizes the core stored energy plus core power generation (during blowdown) used in this analysis. The margins cited above clearly indicate that the values employed in this analysis represent a conservative upper bound of the core-stored energy.

The amount of heat released from the core over blowdown has been studied and an upper bound has been determined by a suitably conservative analysis. The SATAN code heat release predictions were compared to those of an average channel analysis using the LOCTA code.

The LOCTA code, for calculation of heat release, was modified to obtain a conservatively high value. Coefficients in the transition boiling correlation were modified to obtain a realistic fit

of the approximately 500 data points. An informal submittal (proprietary) was made to the NRC in November 1971.

The DNB time was increased to 2.5 seconds. The modified transition boiling correlation and the larger DNB time are in the direction of a conservative heat release for containment pressure. Separate analyses provide for simulation of more detailed effects in the pellet temperature calculation, and thus, in the core energy release calculation. Moreover, the incremental energy associated with the different schemes is small compared to total blowdown release.

The difference between the LOCTA heat release and the SATAN heat release is added directly to the blowdown energy rate transient by the following method:

$$(mh)_{to\ containment} = (mh)_{SATAN\ Blowdown} + m_{SATAN\ Blowdown} \times \bar{h}$$

$$\text{where: } \bar{h} = \frac{Q_{LOCTA} - Q_{SATAN}}{M_{Blowdown}}$$

where: mh = Enthalpy flow rate

m = Mass flow rate predicted by SATAN

\bar{h} = Incremental blowdown enthalpy

Q_{LOCTA} = LOCTA core heat release

Q_{SATAN} = SATAN core heat release

$M_{Blowdown}$ = Mass released over blowdown

In summary, the following items insure that the energy release is conservatively analyzed for maximum containment pressure.

- Maximum expected operating temperature
- Allowance in temperature for instrument error and dead band (+4°F)
- Margin in volume (1.4 percent)
- Allowance in volume for thermal expansion (1.6 percent)
- Margin in core power associated with use of engineered safeguards design rating (ESDR)
- Allowance for calorimetric error (2 percent of ESDR)
- Conservatively modified coefficients of heat transfer

- Allowance in core stored energy for effect of fuel densification
- Margin in core stored energy (+20 percent)

REFILL - The calculations in this period have been minimized by making the conservative assumption that the bottom of core recovery occurs immediately after the end of blowdown.

14C.1.1 Description of the Core Re-flooding Model

The SATAN calculations are performed until the completion of blowdown. In this context the end of blowdown is defined as the time at which zero break flow is first computed. At this time the normal blowdown transient calculations are terminated and the re-flooding calculations are performed.

The re-flooding calculations are done in the following two steps:

1. Calculate the core inlet mass flow rate and the fraction of the inlet mass flow rate that leaves the top of the core. This hydraulic calculation yields core flooding rate and entrainment fraction.
2. Calculate the core exit conditions due to the addition of various energy sources. Also perform calculations of the thermal conditions on the primary and secondary side of the steam generator. This step is an energy balance calculation.

14C.1.2 Hydraulic Model

The hydraulic model represents the downcomer region and the active core region with two volumes. The core communicates with the downcomer via a non-resistive flow path representing the lower plenum region. The core and the downcomer communicate with the containment via flow paths with resistances, which represent the broken loop and the intact loop. The model is shown in Figure 14C-3. The resistances used to calculate the loop pressure drop are based on a loop area of 4.5 ft². Standard losses from Crane (Reference 7) were used to model area changes and losses due to fittings. Frictional losses were calculated assuming typical re-flood conditions, and then calculating friction factors based on homogeneous fluid assumptions. The losses in the core and the hot leg were increased by 30 percent to allow for the effect of higher-pressure drops for two-phase flow conditions. The components of the loop losses as illustrated in Figure 14C-3 are summarized in Figure 14C-4.

The core-flooding rate is limited by the pressure in the core caused by the generation of steam when the re-flood water is heated up by the hot fuel rods. Any steam generated in the core region must be vented through the intact and broken loops via the resistive paths shown in Figure 14C-3.

Steam, which flows through the intact steam generator must encounter the injected water in the cold legs of the broken and intact loops. During the accumulator injection phase an equilibrium calculation indicates that the amount of water available is sufficient to condense this

steam, thus reducing the flow to the Containment. Moreover, preliminary results from steam-water mixing experiments performed by Westinghouse indicate that the heat transfer between the steam and injected liquid is quite high, and justify an equilibrium calculation. This benefit was not included in the present calculations.

The steam-water experiments also indicate an increase in resistance in this section of pipe over the steam flow only resistance considered in the present analysis. This increase in resistance would provide some reduction in flooding rate, an effect which is conservatively omitted in the present analysis.

The pressure drops along the two paths in these calculations were calculated with the associated loss coefficients and with fluid density conservatively evaluated at maximum core pressure during the hydraulic transient. In actuality, the fluid density varies around the loop, becoming smaller as the local pressure decreases from core pressure to containment pressure. Again, the reduction in flooding rate due to this effect has not been included in the present analysis. This phenomenon results in less flow for a given pressure drop and hence reduced energy flow to the Containment. The pressure drop across the pump is calculated by assuming that the rotor is free spinning. However, a sensitivity study was performed to compare free spinning assumptions to locked assumptions on the rotor for calculation of pressure drop across the pump. This study showed a slightly higher flooding rate for the locked rotor case with an associated increase in energy release over re-flood of about $0.6E+6$ Btu. The increased flooding rate for locked rotor assumption vis-a-vis the free spinning assumption is true to the pump suction and not the cold-leg break. The core exit quality in the hydraulic calculation is based on lower value of heat flux as compared to the total contribution of remaining core stored energy, hot metal energy, and decay heat. This results in a larger value of core exit density and hence a slightly (about 7 percent) higher flooding rate. This is conservative for containment pressure calculations. The fraction of calculated core flooding rates that is vaporized and entrained is calculated using the Westinghouse entrainment correlation obtained from the FLECHT results. The resulting transient values of core flooding rate and the entrainment fraction is utilized in the energy balance model to calculate mass and energy release rates to the containment for calculation of the containment pressure transient.

14C.1.3 Energy Balance Model

The energy balance model consists of three reference elements which represent the core, the steam generator in the broken loop, and the steam generator in the intact loop. Figure 14C-4 presents a diagram of the model where the variables shown are defined as follows:

m = Mass flow rate into the core (lbm/sec)

$(mh)_{in}$ = Energy flow rate into the core (Btu/sec)

$(mh)_{exit}$ = Energy flow rate out of the core (Btu/sec)

m_1 = Mass flow rate to the broken loop steam generator (lbm/sec)

m_2 = Mass flow rate to the intact loop steam generator (lbm/sec)

$m_1 h_{out_1}$ = Energy flow rate from broken loop steam generator out into containment (Btu/sec)

$m_2 h_{out_2}$ = Energy flow rate from intact loop steam generator out into containment (Btu/sec)

q_{heat} = Sum of heat sources to the core fluid (Btu/sec)

h_f = Saturated liquid enthalpy (Btu/lbm)

q_{SG1} = Heat flow rate from the broken loop steam generator (Btu/sec)

q_{SG2} = Heat flow rate from the intact loop steam generator (Btu/sec)

An energy balance is performed on the fluid entering and leaving the core in order to determine core exit conditions:

$$(mh)_{in} + q_{heat} = (mh)_{exit} + (m_{in} - m_{exit})h_f$$

The mass flow rate of fluid entering the core is identical to the calculated flooding rate times the product of the core area and liquid density. This fluid is taken to be at injection conditions. The heat source term is added to the fluid in the core and is the sum of the following:

- Decay heat
- Thick metal (reactor vessel) heat
- Core stored energy left at end of blowdown
- Thin metal energy remaining at end of blowdown

Decay heat is calculated using the Westinghouse standard decay heat curve and evaluated at 102 percent of Engineered Safeguards Design Rating. The core stored and thin metal energy, that are remaining at end of blowdown, are brought out at a constant rate over the period between the bottom of core recovery (end of blowdown) and the quench of the 8-foot elevation in the core. The thick metal decays exponentially with a time constant of 0.0032^{-1} seconds.

This treatment of energy release may result in core exit temperatures, which are higher than the steam generator temperature for the period where the exit mass flow is small. However, the effect on containment pressure is small because of the short duration of this small core exit mass flow (about two seconds). In particular, for the present analysis the amount of energy transferred to the steam generators was $0.2E+6$ Btu for the double-ended pump suction break and $0.05E+6$ Btu for the 3-ft² break. This energy is not lost but increases the steam generator internal energy and is available to flow back into the Containment.

The mass flow rate leaving the core is equal to the inlet flow rate times the entrainment fraction calculated from the hydraulic model. The difference between inlet and outlet flow represents the fluid, which remains in the core and this is heated to saturated liquid enthalpy.

The above considerations provide sufficient information to determine the core exit enthalpy.

The flow split between the intact loop and the broken loop steam generators is determined in the hydraulic model described earlier. Separate energy balances are performed on the broken loop and intact loop steam generators. Fluid, which enters the primary side of the steam generator is assumed to be heated instantaneously to the shell side temperature. This sets the outlet enthalpy; the steam generator inlet enthalpy is equal to the core exit enthalpy. Hence, the energy addition from the steam generators to the fluid entering the Containment is determined.

This energy flow results in a decrease in internal energy for the shell side of the steam generator. Metal heat on the secondary side is included in the internal energy calculation. The steam generator secondary side fluid mass (and hence, density) is taken as constant and temperature can be found directly from the internal energy. Feedwater addition is not considered in the present analysis; this effect would reduce steam temperature, hence, omission is conservative.

The fluid which leaves the steam generator primary side is assumed to flow directly into the containment. No credit is taken for the quenching effect of the accumulator water, which spills to containment.

For hot leg breaks the flow that leaves the core is subdivided between the direct flow to the containment and that to the intact loop, vessel annulus and broken loop path. Since about 85 percent of the flow goes directly into the Containment, not much energy is extracted from the steam generators and a lower peak containment pressure results. For cold leg breaks, the flooding rates are lower than for the pump suction breaks because of the resistance of the pump in the broken loop. This results in less energy release during re-flood. The pump suction breaks are worse than either the hot or cold leg breaks.

14C.1.4 Results

The results of the analysis described above shows that the 3-ft² pump suction break yields the maximum containment pressure. The mass and energy released to the Containment as a function of time for this break are given in Figure 14C-5 and Figure 14C-6.

For this case the accumulator flow rates to the intact loop and broken loop are given in Figure 14C-7 and Figure 14C-8, also the core inlet velocity as a function of time after bottom of core recovery is given in Figure 14C-9. This results in the containment pressure transient given in Figure 14C-10. The peak pressure for this design case is 43.1 psig.

In addition to the above case, the following cases were considered to determine the sensitivity of the pressure transient to break size and break location. These calculations demonstrate that the worst break is the 3.0-ft² pump suction break.

- Figure 14C-11 gives the Containment Pressure Transient for the Double-Ended Guillotine Pump Suction Break (10.5 ft²).
- Figure 14C-12 is for the 0.6 Double-Ended Guillotine Pump Suction Break (6.3 ft²).
- Figure 14C-13 is for the 4.0-ft² Pump Suction Break.
- Figure 14C-14 is for the 2.0-ft² Pump Suction Break.
- Figure 14C-15 is the Double-Ended Guillotine Cold Leg Break (8.25 ft²).
- Figure 14C-16 is for the Double-Ended Guillotine Hot Leg Break (9.2 ft²).
- Figure 14C-17 is for the 0.6 Double-Ended (5.5-ft²) Guillotine Hot Leg Break.

The blowdown enthalpy, length of blowdown, the blowdown peak pressure and the peak containment pressure for the various cases analyzed are summarized in Table 14C-5.

The contribution of core stored energy, decay heat, thick- and thin-metal heat, and steam generator energy to total re-flood enthalpy for the various cases analyzed are summarized in Table 14C-6.

In addition to the above, the following analyses have been performed to further verify that the peak calculated pressure following a LOCA will not exceed the design pressure.

Case 1: The 3.0 ft² pump suction break has been analyzed with the following assumptions:

- Entrainment during re-flood continues until the quench front reaches the 8-foot level.
- Water in the lower plenum is initially saturated with temperature decreasing during the re-flooding transient to 230°F.
- The core-flooding rate has been analyzed using a more detailed pressure drop calculation and local densities throughout the loop.
- The structural heat sinks given in Table 14C-7 have been used for the containment pressure calculations. The values in Table 14C-7 represent the as-built configuration inside containment.

This case resulted in a peak containment pressure of 39.2 psig.

Case 2: The 3.0-ft² sump suction break has been further analyzed showing a peak pressure of 40.5 psig. The assumptions in this case were the same as those in Case 1 above except that the entrainment during re-flood was arbitrarily extended until the quench front reached the 10-foot level to show additional margin. The mass and energy releases for this case are given in Figure 14C-18.

14C.1.5 Additional Post-Re-flood Energy Release Analysis

Consideration is given here to the possible additional energy release to Containment during the post re-flood phase of the large-break accident. This postulated additional energy would result from the presence of a two-phase mixture in the steam generator tubes. A proper analysis of this phenomena requires a simulation of the RCS behavior that cannot be done at the present time.

FLECHT - SET, PHASE B. will address the post re-flood and re-flood phases of the LOCA. It will determine the two-phase mixture level and the core and steam generator heat release during the post re-flood transient. These results are expected to confirm the conservatism associated with the present containment energy release calculation.

However, to demonstrate the margin associated with the Kewaunee containment design, an upper bound calculation has been performed for additional steam generator heat release following re-flood. For the purpose of the calculation, it is assumed that a two-phase mixture is present in the steam generator tubes following re-flood. This mixture is assumed to remain in the tubes and to boil until all the available secondary side energy has been removed to the containment.

At end of re-flood, 56.2E+6 Btu available secondary side energy remains in the two steam generators. Of this total, 21.6E+6 Btu is contained in the broken loop steam generator and 34.6E+6 Btu in the intact loop steam generator. Froth boiling in the steam generator tubes is the mechanism for removal of this energy. These boiling rates plus the decay heat addition constitute the potential energy release to the Containment.

The rate of froth boil-off in each of the steam generators is calculated by balancing the loop resistance to steam flow against the available driving ΔP . In the intact loop, steam flow results from the density difference between the downcomer and the core. The broken loop steam flow results from a density difference between downcomer and core plus a pressure difference between downcomer and containment due to the pressure drop across the broken loop reactor coolant pump.

The effect of decay heat addition as core steam generation is accounted for in the driving ΔP calculation and the steam flow calculation for each loop.

The effects of SI flow and auxiliary feedwater flow on the containment energy release rate are also considered in the calculation. The addition of injection water to the RCS acts to reduce the energy release rate by the heat required to raise this water to saturation temperature at containment pressure. This reduction is included in the release rate calculation and is supported

by the results of steam/ECCS water mixing tests. Auxiliary feedwater flow to the secondary side of each steam generator does not affect the energy release rate but does reduce the available steam generator energy by the heat required to raise the feedwater to saturation temperature at containment pressure.

The post re-flood containment mass and energy release rate transient generated by the froth calculation is presented in Table 14C-8. The calculation is for the 3-ft² pump suction break and is started at end of 10-foot entrainment time. The decrease in release rates at 500 seconds results from the cooldown of the broken loop steam generator. Intact loop steam generator cooldown occurs at 1040 seconds. At this time all secondary side steam energy has been removed and the froth calculation is terminated.

A recalculation of the containment pressure transient using the data given in Table 14C-8 results in a peak pressure of 43.6 psig.

14C.2 Sensitivity Studies

14C.2.1 Containment Initial Conditions and Active Heat Removal Initiation Times

In addition to the analyses discussed in Section 14.3 and Section 14C.1, an analysis has been performed using a more conservative set of containment initial conditions and analysis input parameters. This analysis was performed using the well-known CONTEMPT-LT/26 computer code. The design basis 3.0 ft² reactor coolant pump suction break was the analyzed event. Three combinations of active heat removal systems were considered including one internal containment spray train with two containment fan coil units, two internal Containment spray trains, and four containment fan coil units.

The Containment initial conditions used in the analysis included the following:

1. Since the KPS Technical Specifications allow a normal operation containment pressure accumulation of up to 2 psig, an initial containment pressure of 16.85 psia was used in the calculation. The 16.85 psia allows for the 2-psig accumulation plus 0.15 psi for instrument tolerance.
2. The active heat removal equipment cooling initiation times were revised from the previously assumed 60 seconds to reflect additional conservatism. The values used for these inputs were 135 seconds for internal containment spray cooling initiation and 85 seconds for Containment fan coil unit cooling initiation.
3. The Containment fan coil unit heat removal rates were revised to account for cooling water temperatures, which may exceed the 66°F originally used in the analysis. A cooling water temperature of 85°F was selected.

4. The passive structural heat sinks have been revised to reflect the as-built configuration of concrete structures. Table 14C-7 and Table 14C-9 were used as the passive heat sinks. Additionally, the effect of paint and other coatings was accounted for in modeling the passive heat sinks.

Using the blowdown and re-flood mass and energy additions shown in Figure 14C-5 and Figure 14C-6, and the post re-flood mass and energy releases shown in Table 14C-8, the predicted maximum peak pressure is 45.2 psig for the case of two internal containment spray trains functioning. With one internal containment spray system and two Containment fan coil units, the peak containment pressure is 45.0 psig, and for the case of four fan coil units, the peak pressure was 44.7 psig. All the calculated peak containment pressures are below the design value of 46 psig. It is noted that the assumption of 2.15 psig initial containment pressure is very conservative and, therefore, there is sufficient margin in existence for the containment peak pressure post-LOCA. The analysis results are plotted on Figure 14C-19.

14C.3 References

1. Dittus, F. W., and L. M. K. Boelter, University of California (Berkeley), Pbls. Eng., 2. 443, 1930
2. Jens, W. H., and P. A. Lottes, "Analyses of Heat Transfer, Burnout, Pressure Drop, and Density Data for High Pressure Water," USAEC Report ANL-4627, 1951
3. Macbeth, R. V., "Burnout Analysis, Pt. 2, The Basis Burn-out Curve," U.K. Report AEEW-R 167, Winfrith (1963). Also Pt. 3, "The Low-Velocity Burnout Regimes," AEEW-R 222 (1963); Pt. 4, "Application of Local Conditions Hypothesis to World Data for Uniformly Heated Round Tubes and Rectangular Channels," AEEW-R 267 (1963)
4. Dougall, R. S., and W. M. Rohsenow, "Film Boiling on the Inside of Vertical Tubes with Upward Flow of Fluid at Low Quantities," MIT Report 9079-26
5. McEligot, D. M., P. M. Magee, and G. Leppert, "Effect of Large Temperature Gradients on Convective Heat Transfer: The Downstream Region," J. of Heat Transfer, Vol. 87, 1965, pp 67-76
6. McAdam, W. H., "Heat Transmission," McGraw-Hill 3rd edition, 1954, p. 172
7. Crane Company, "Flow of Fluids Through Valves, Fittings, and Pipe," Technical Paper, No. 410

Table 14C-1
Summary of Heat Transfer Correlations Used to Calculate
Steam Generator Heat Flow in the SATAN Code

Primary to Secondary Heat Flow	
Primary (Tube Side)	Secondary (Shell Side)
Dittus-Boelter	Jens Lottes
Secondary to Primary Heat Flow	
Primary	Secondary
Jens-Lottes	McAdams
Dougall-Robsenow	
McEligot	

Table 14C-2
Sensitivity of Core Stored Energy to Power Level
Nodes in the Pellet and Fuel Densification

Power (kw/ft)	Number of Radial Nodes in Pellet	Stored Energy (# full power seconds)
I. Instantaneous Isotropic Densification to 96.5% TD		
7.66 ^a	10	6.59
7.66	1 (average pellet)	6.53
15.04	10	6.80
15.04	1	6.69
II. No Densification (92% TD)		
7.66	1	5.78

- a. This value of kw/ft can be considered a typical core average power and was used as a reference value for core stored energy calculations.

Table 14C-3
Available Core Energy During Blowdown
(3.0 ft² Pump Suction)

1. Power = 1755.8 ^a Megawatts Thermal	
2. Initial Core Stored Energy Above Average Coolant Temperature – Equivalent to 7.94 Full Power Seconds	13.32E+6 Btu
3. Initial Core Stored Energy From Average Coolant Temperature to Saturation Temperature of Containment	3.35E+6 Btu
4. Core Power Generation (To End of Blowdown)	4.54E+6 Btu
5. Total Core Energy Available During Blowdown (3.0 ft ²)	21.21E+6 Btu

a. 102% of Engineered Safeguards Design Rating.

Table 14C-4
Resistances Used in Reflood Analysis

Component	Resistance
Core	17.0
Hot Leg	0.83/1.3
Steam Generator and Pump Suction Piping	4.10
Pump	3.83
Cold Leg Piping	0.4
Annulus	0.65

Resistances shown are the values of K used in the equation $\Delta H = K (V^2/2g)$. All velocities are based on a flow area of 4.5 ft² except in the core where an area of 26.9 ft² is used.

Table 14C-5
Summary of Results

Break	Length of Blowdown (sec)	Blowdown Energy Release (E+6 Btu)	Blowdown Peak Pressure (psig)	Peak Containment Pressure (psig)
Double-Ended Pump Suction (10.5 ft ²)	12.8	169.73	38.5	42.8
0.6 Double-Ended Pump Suction (6.3 ft ²)	14.7	169.06	38.2	42.7
4.0 Square Foot Pump Suction	18.0	166.29	37.95	42.66
3.0 ^a Square Foot Pump Suction	22.2	167.29	38.2	43.05
2.0 Square Foot Pump Suction	27.5	160.51	37.45	42.49
Double-Ended Cold Leg (8.25 ft ²)	12.1	170.52	39.4	40.9
Double-Ended Hot Leg (9.2 ft ²)	12.4	166.38	39.7	39.7
0.6 Double-Ended Hot Leg (5.5 ft ²)	14.8	164.87	39.32	39.34

a. Worst Break

Table 14C-6
 Reflood Energy Release (E+6 Btu)

Break	2.0 ft ² Pump Suction		Double-Ended Cold Leg		Double-Ended Hot Leg		0.6 Double-Ended Hot Leg
	Maximum	8.0	Maximum	8.0	Maximum	8.0	Maximum
Safeguards Assumption							
Height in Core Entrainment Is Assumed to Stop (Feet)							
Energy Types:							
1. Core Stored	3.56		8.14		7.11		6.3
2. Decay Heat	10.53		13.52		10.09		9.84
3. Thin Metal (Internals)	5.19		5.19		5.19		5.19
4. Thick Metal (Reactor Vessel Metal)	3.18		3.18		3.18		3.18
5. Steam Generator Energy	24.20		12.36		4.89		6.13
Total Reflood Energy to Containment at End of Entrainment	48.46		44.43		33.88		33.09

Table 14.C-6
 Reflood Energy Release (E+6 Btu)

Break	0.6					
	Double-Ended Pump Suction		Double-Ended Pump Suction		4.0 ft ² Pump Suction	
Safeguards Assumption	Maximum	8.0	Maximum	8.0	Maximum	8.0
Weight in Core Entrainment Is Assumed to Stop (Feet)						
Energy Types:						
1. Core Stored	8.71	8.22	7.93	5.51	5.19	5.19
2. Decay Heat	11.78	11.56	11.22	10.87	10.87	10.87
3. Thin Metal (Internals)	5.19	5.19	5.19	5.19	5.19	5.19
4. Thick Metal (Reactor Vessel Metal)	3.18	3.18	3.18	3.18	3.18	3.18
5. Steam Generator Energy	18.22	18.98	19.44	22.30	22.30	22.30
Total Reflood Energy to Containment at End of Entrainment	49.04	49.13	48.60	49.04	49.04	49.04

Table 14C-7
Structural Heat Sinks

Linings	Material	Exposed Area (ft ²)	Thickness (in.)
Containment Cylinder	Carbon Steel	41,300	1.5
Containment Dome	Carbon Steel	17,300	0.75
Reactor Vessel Liner	Carbon Steel	1260	0.25
	Concrete Backup	1260	12.00
Refueling Canal	Stainless Steel	1100	0.1875
	Concrete Backup	1100	12.0
	Stainless Steel	5500	0.25
	Concrete Backup	5500	12.0

Steel Structures The following items consist of various thicknesses and exposed areas. The cumulative exposed area contribution of all of the identified items are grouped by thickness value.

Steam Generator Supports			
Pressurizer Support		4055	0.336
Reactor Coolant Pump Supports		16,925	0.5
Crane	Carbon Steel	28,500	0.75
Crane Rail		2000	1.5
Seismic Restraints		500	2.0
Hangers			
Handrails	Carbon Steel	1695	0.145
Grating	Carbon Steel	12,400	0.09
Exposed Pipe	(None assumed for calculations)		
Exposed Conduit and Cable Trays	Carbon Steel	2000	0.1
Ductwork	Carbon Steel	18,000	0.07
Accumulators	Carbon Steel	2200	1.44

Note: Concrete structures inside containment not used in the calculation include:

Heavy Walls	40,800 ft ²	12 in. thick
Heavy Floors	25,070 ft ²	6 in. thick
Light Floors	7570 ft ²	3 in. thick

Table 14C-8
Post Reflood Mass and Energy Release

Time	Mass Release Rate (lbm/sec)	Energy Release Rate (Btu/sec)
320.00	149.06	182537.27
340.00	149.92	83604.17
360.00	146.75	179697.39
380.00	145.80	178532.94
400.00	141.81	173694.77
420.00	145.86	178604.19
440.00	141.87	173768.34
460.00	141.00	172693.45
480.00	137.97	168965.83
500.00	137.06	167846.64
520.00	67.34	80708.04
540.00	75.30	90330.07
560.00	74.88	89813.55
580.00	73.02	87611.97
600.00	72.63	87139.44
620.00	72.30	86729.24
640.00	71.97	86335.15
660.00	71.66	85956.08
680.00	71.36	85591.01
700.00	71.07	85239.05
720.00	70.79	84899.37
740.00	70.52	84571.21
760.00	70.26	84253.89
780.00	70.01	83946.78
800.00	69.76	83649.29
820.00	69.55	83393.40

Table 14C-8
Post Reflood Mass and Energy Release

Time	Mass Release Rate (lbm/sec)	Energy Release Rate (Btu/sec)
840.00	69.35	83144.98
860.00	69.15	82903.63
880.00	68.95	82669.03
900.00	68.77	82440.81
920.00	68.58	82218.67
940.00	68.41	82002.32
960.00	68.23	81791.49
980.00	68.06	81585.94
1000.00	67.90	81385.41
1020.00	67.62	81052.62
1040.00	67.36	80728.62

Table 14C-9
Concrete As Passive Heat Sink

Concrete Floors

Total Thickness, Inches	One Side Area, ft ² (one side exposure)
4	1785
6	2156
8	464
10	2405
12	6592
15	880
> 15	6512

Concrete Walls

Total Thickness, Feet	One Side Area, ft ² (one side exposure)
1.0	238
1.167	846
1.667	175
1.75	144
2.0	1842
> 2.0	21,900

Figure 14C-1
3.0 Ft² Pump Suction Break (Split)

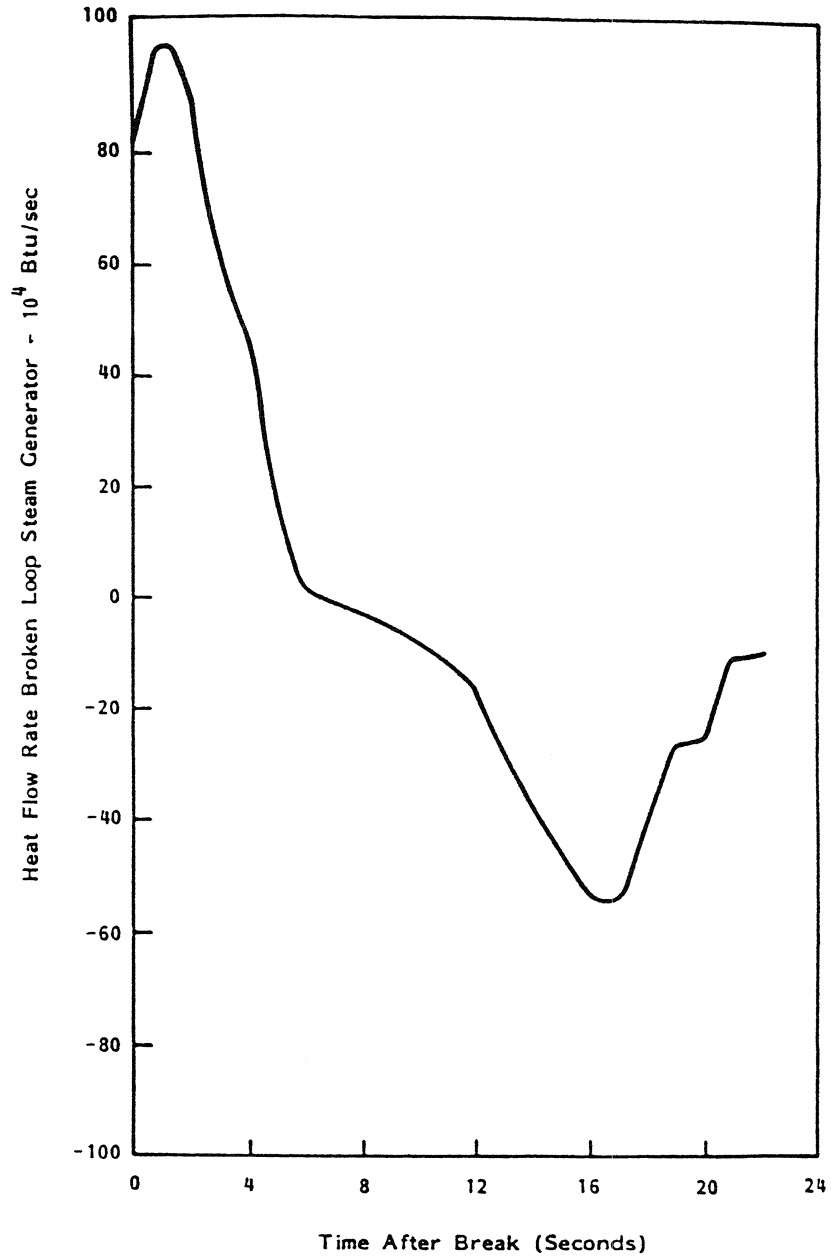


Figure 14C-2
3.0 Ft² Pump Suction Break (Split)

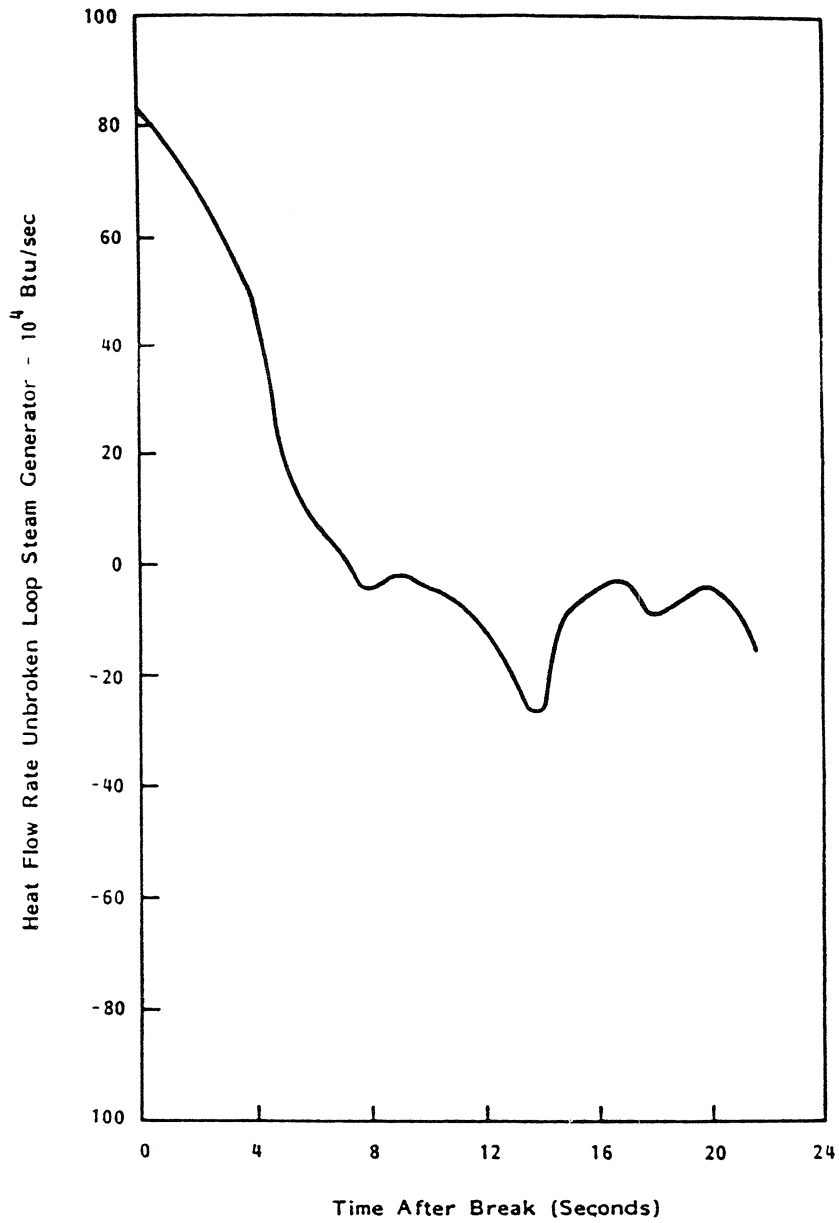


Figure 14C-3
Hydraulic Model for Pump Suction Break

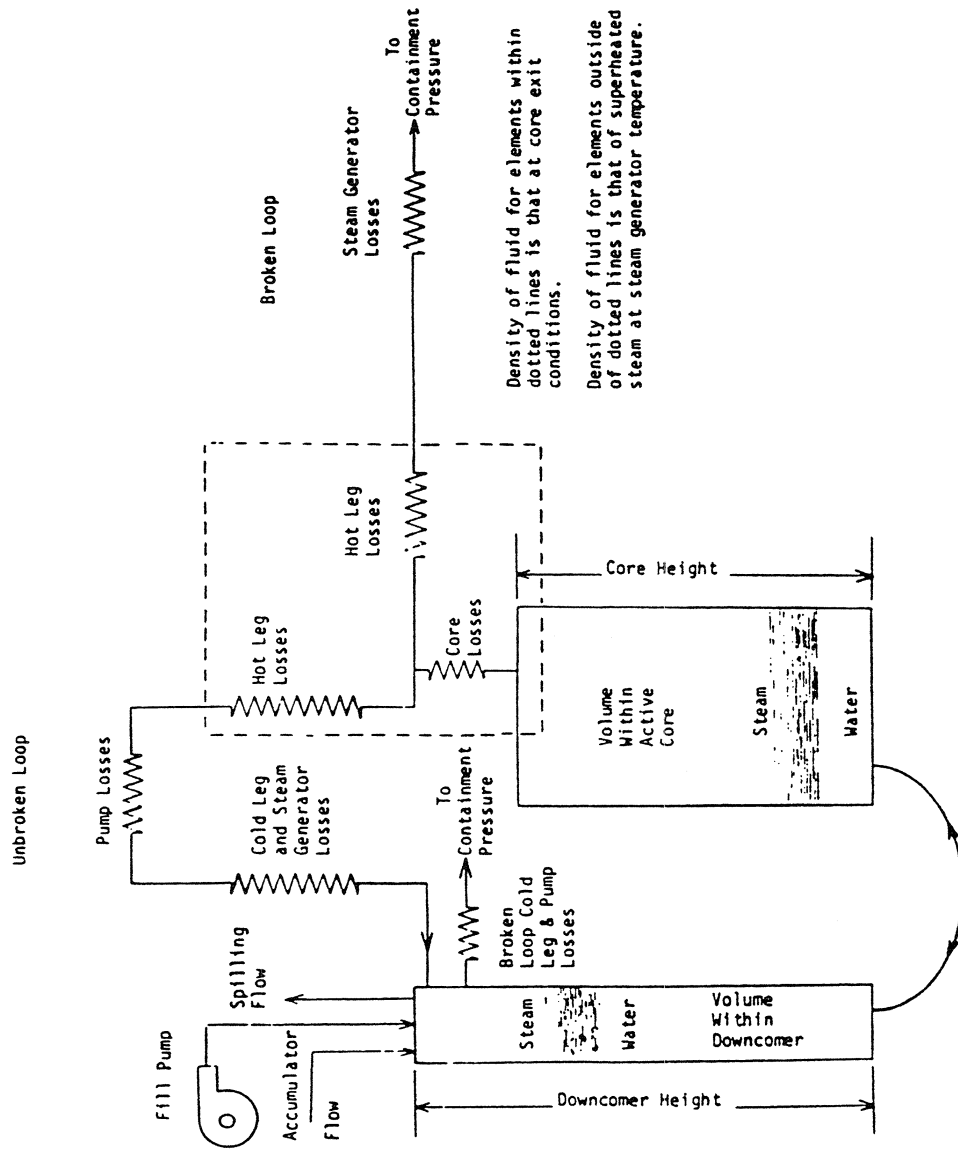


Figure 14C-4
Energy Balance Model

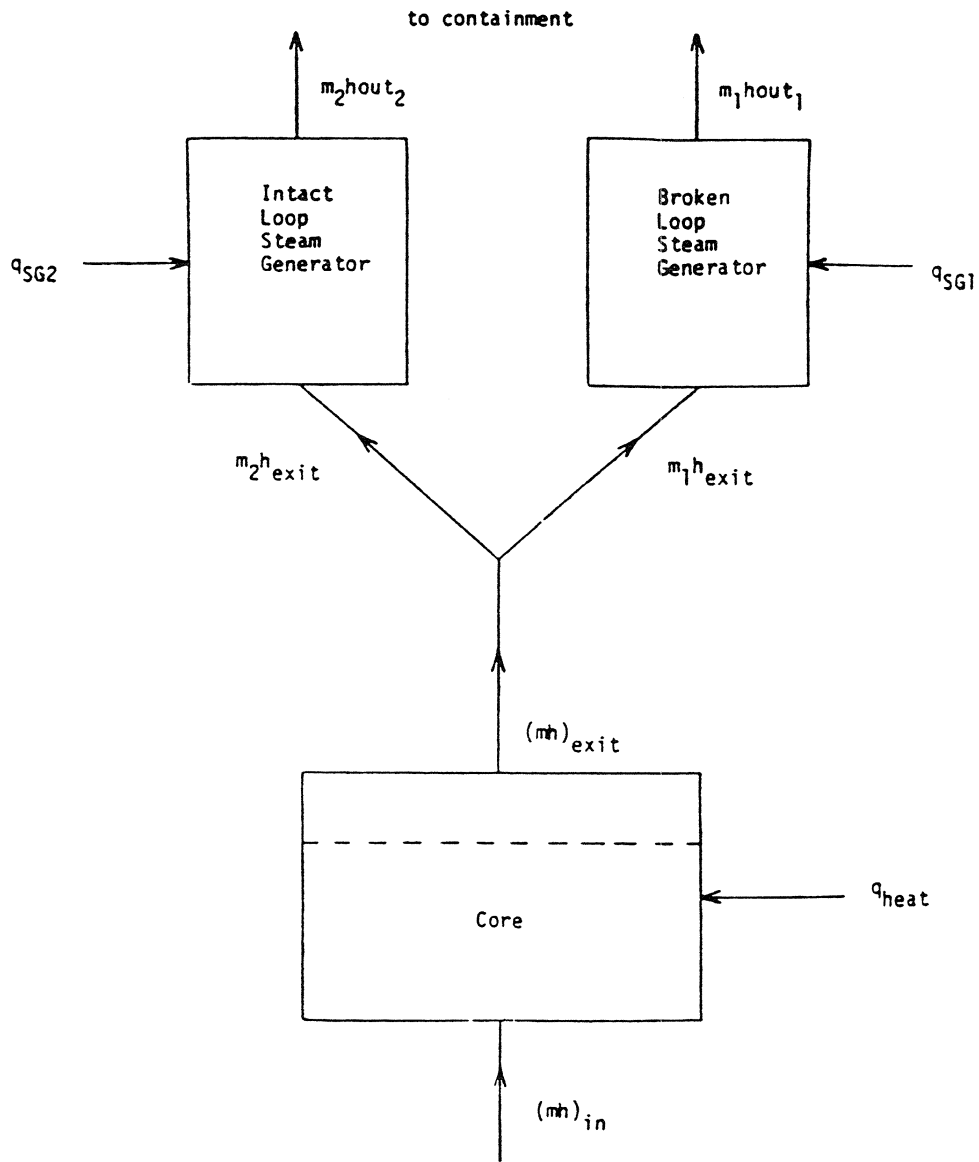


Figure 14C-5
3.0 Ft² Pump Suction Break (Split) Mass and Energy Released During Blowdown

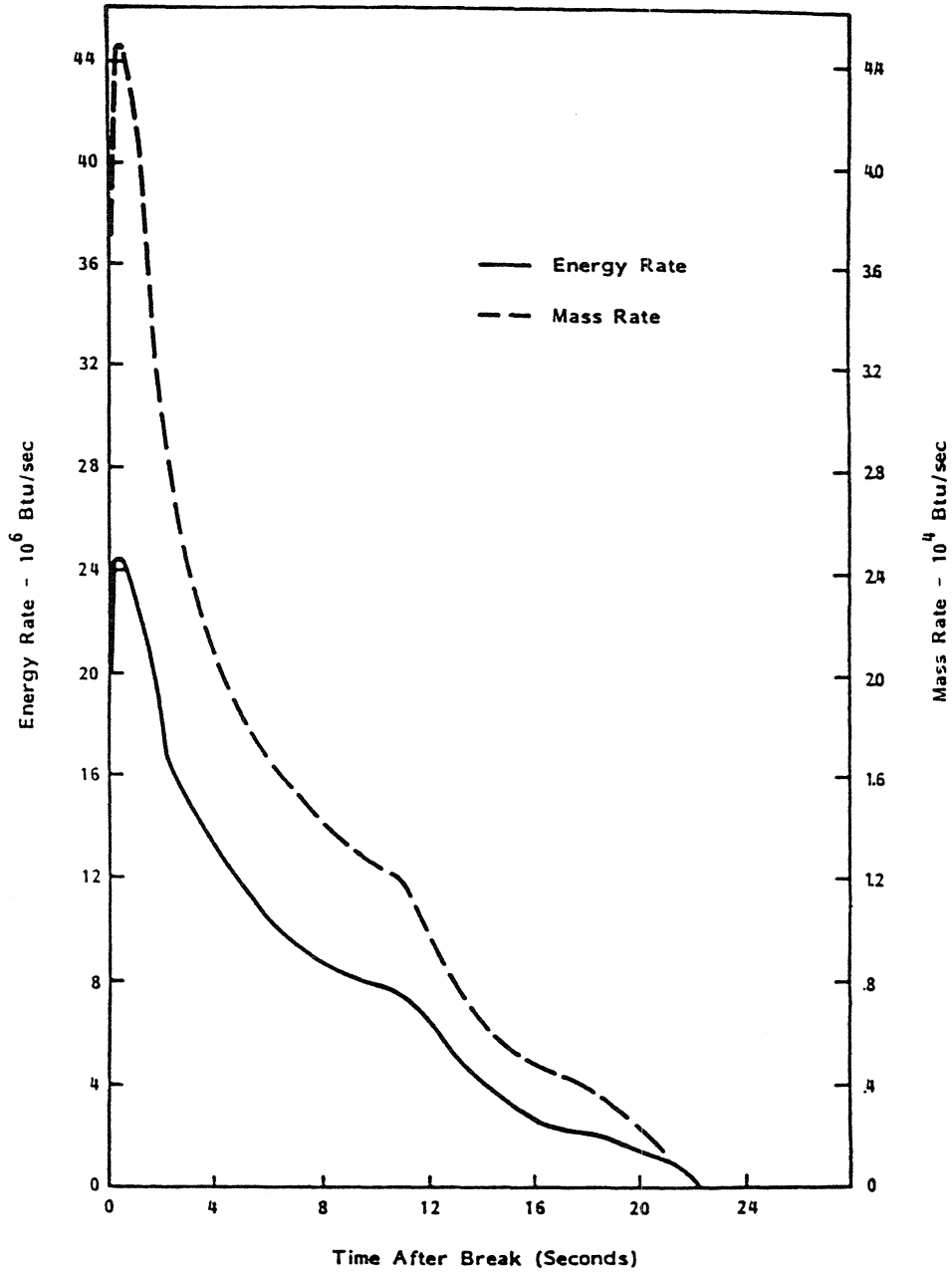


Figure 14C-6
3.0 Ft² Pump Suction Break (Split) Mass and Energy Released During Reflood

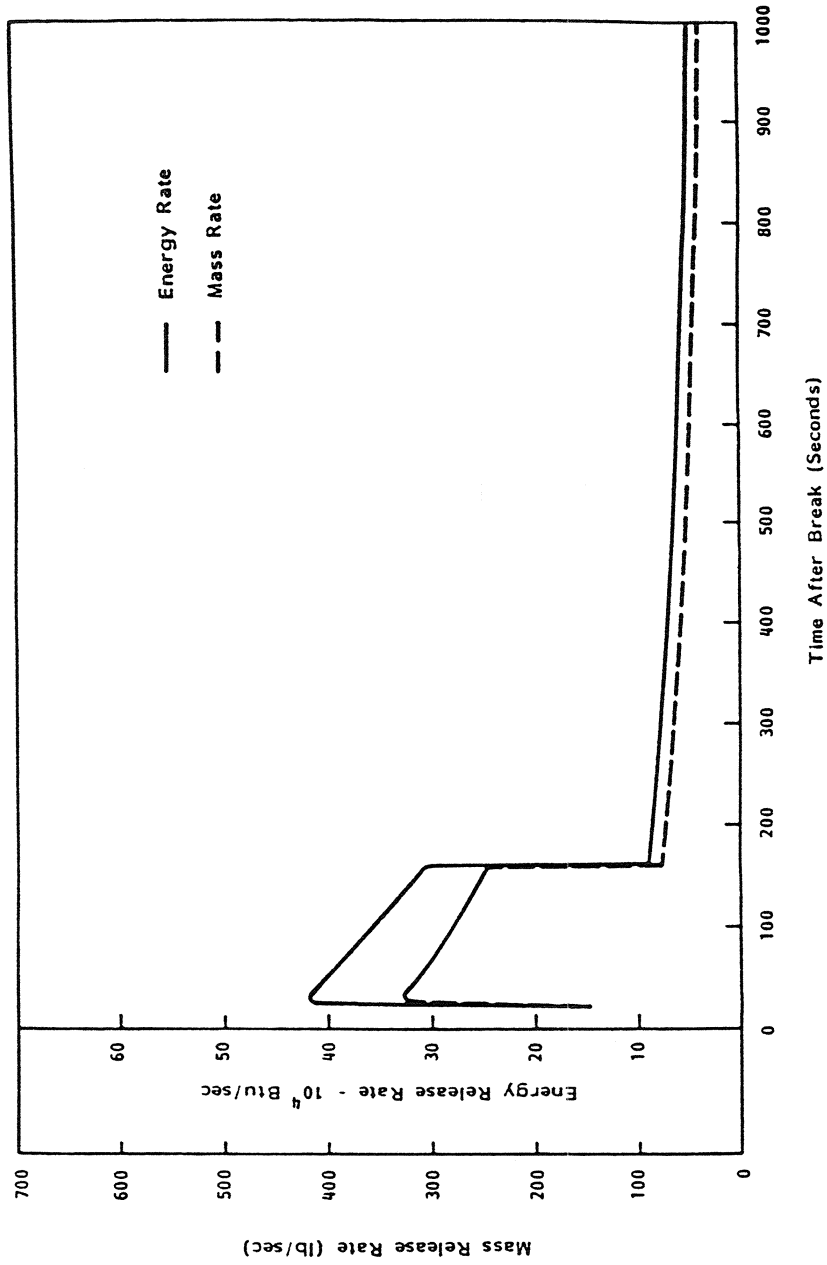


Figure 14C-7
3.0 Ft² Pump Suction Break (Split) Accumulator Flow Rate

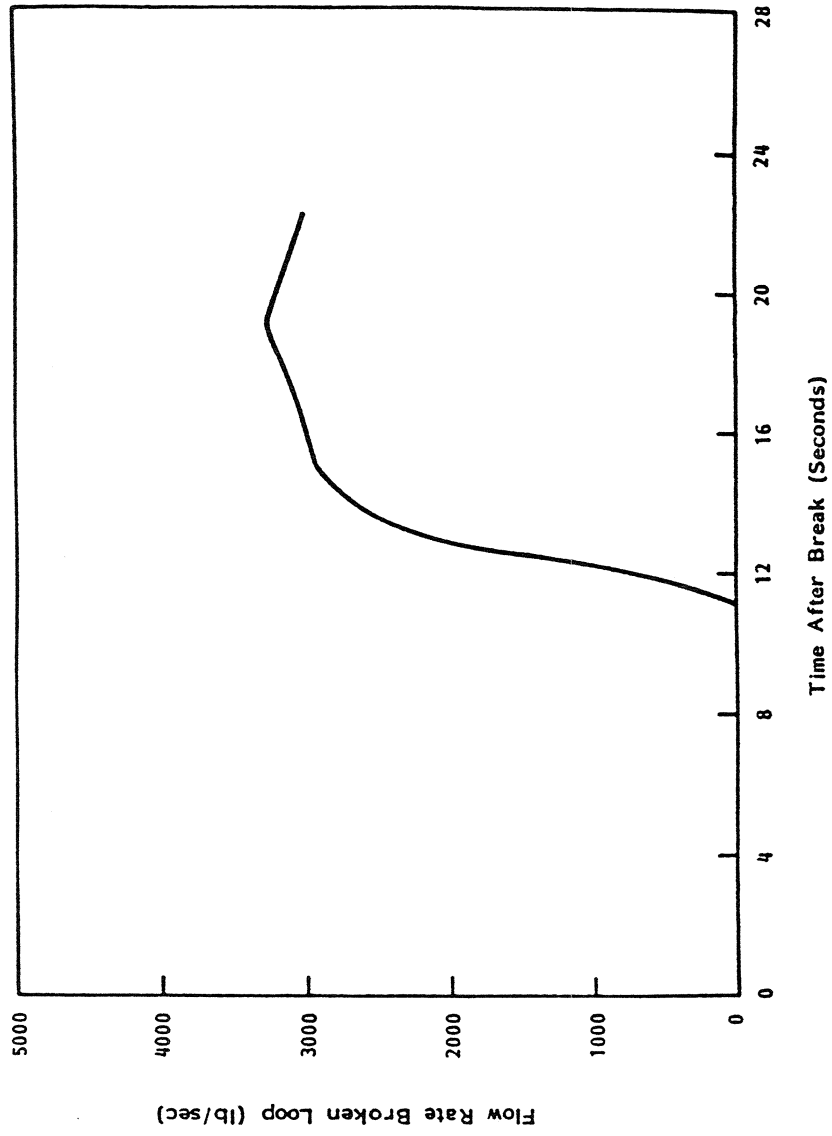


Figure 14C-8
3.0 Ft² Pump Suction Break (Split) Accumulator Flow Rate

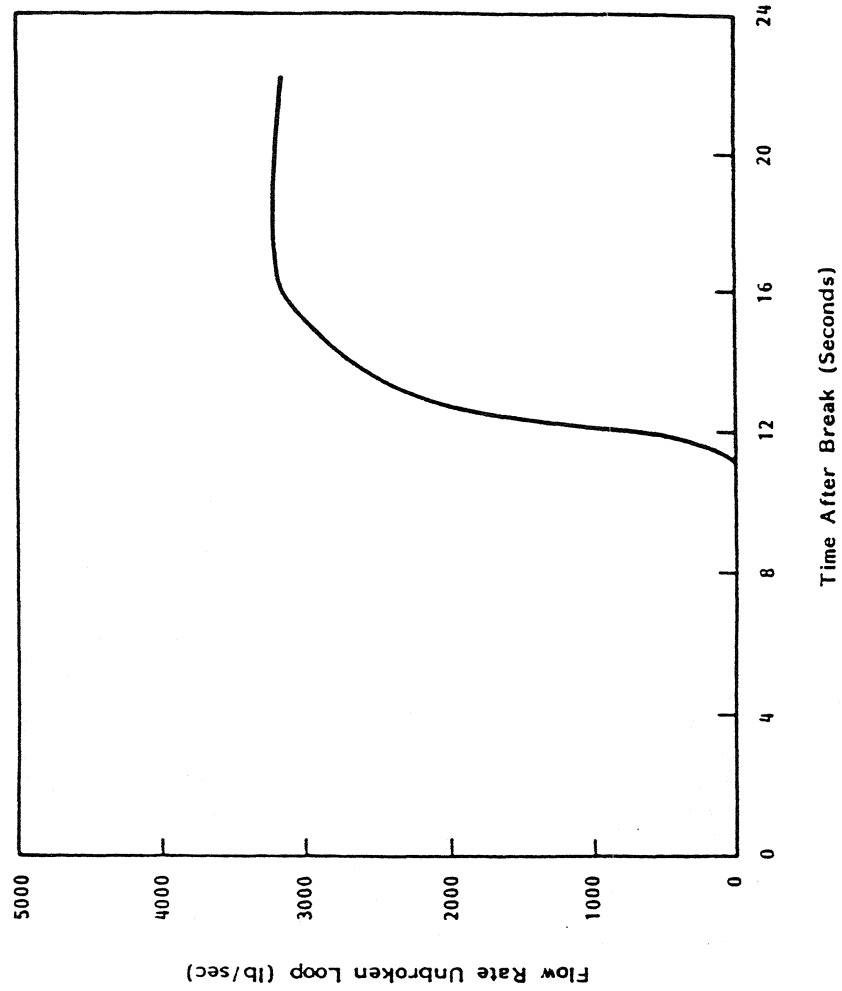


Figure 14C-9
3.0 Ft² Pump Suction Break

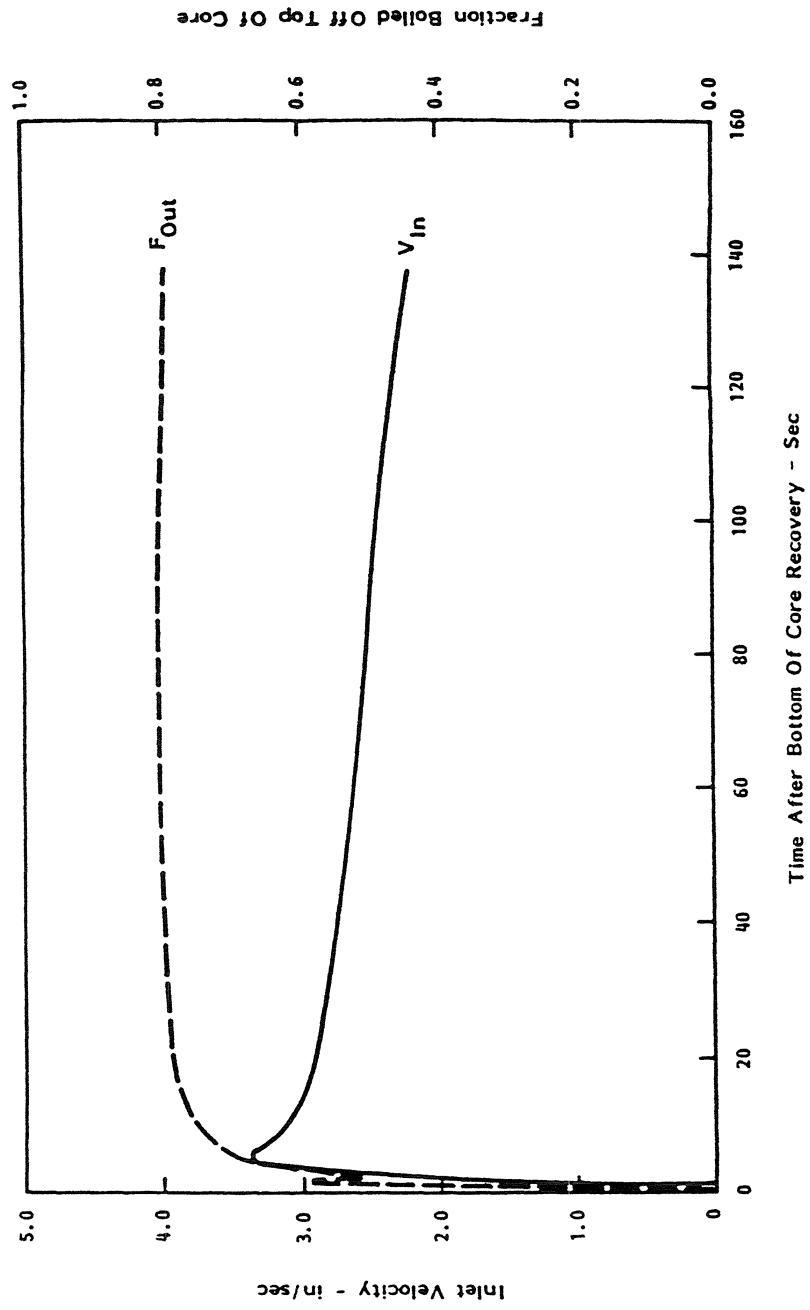


Figure 14C-10
3.0 Ft² Pump Suction Break

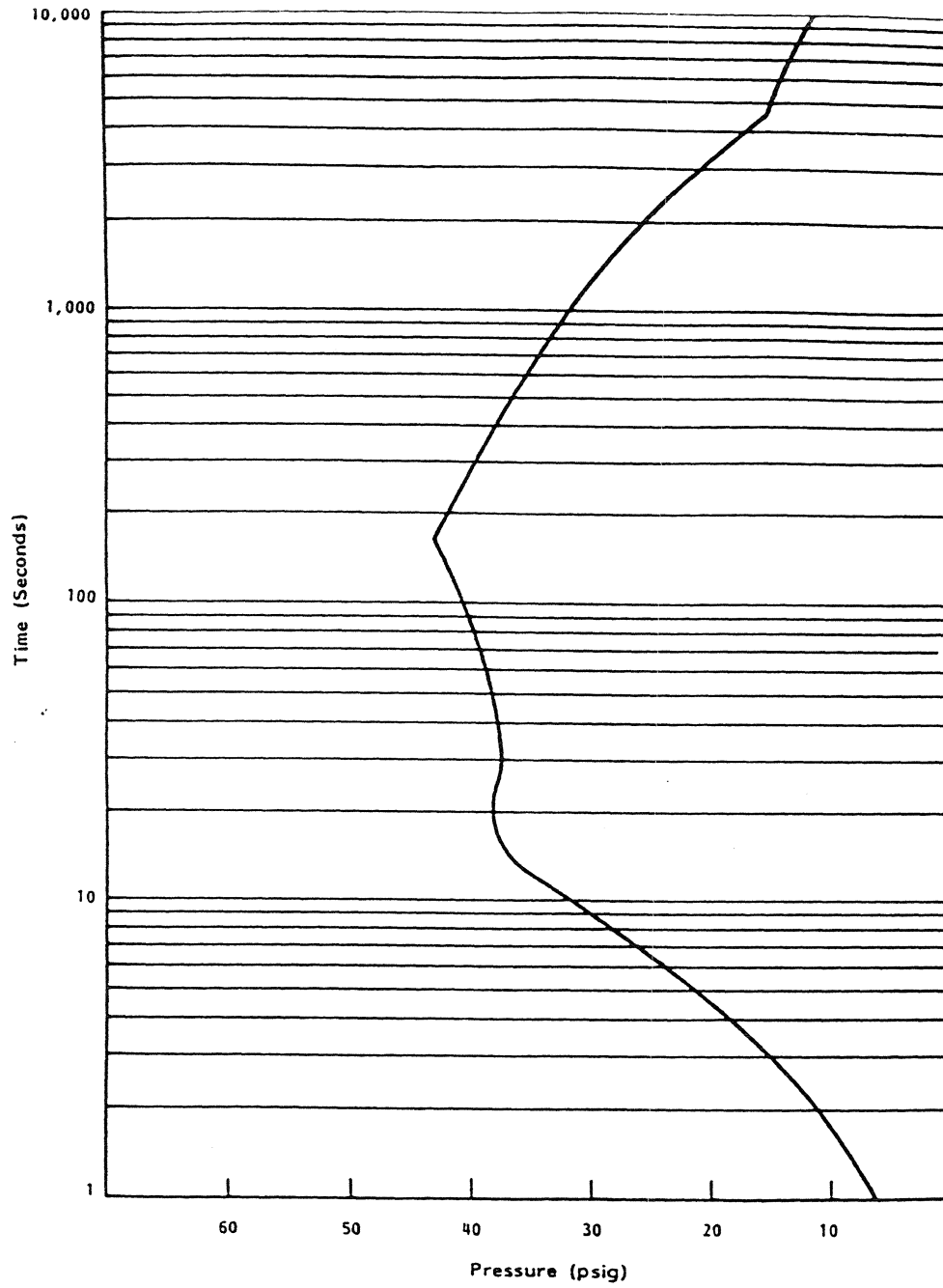


Figure 14C-11
Double Ended Pump Suction Break

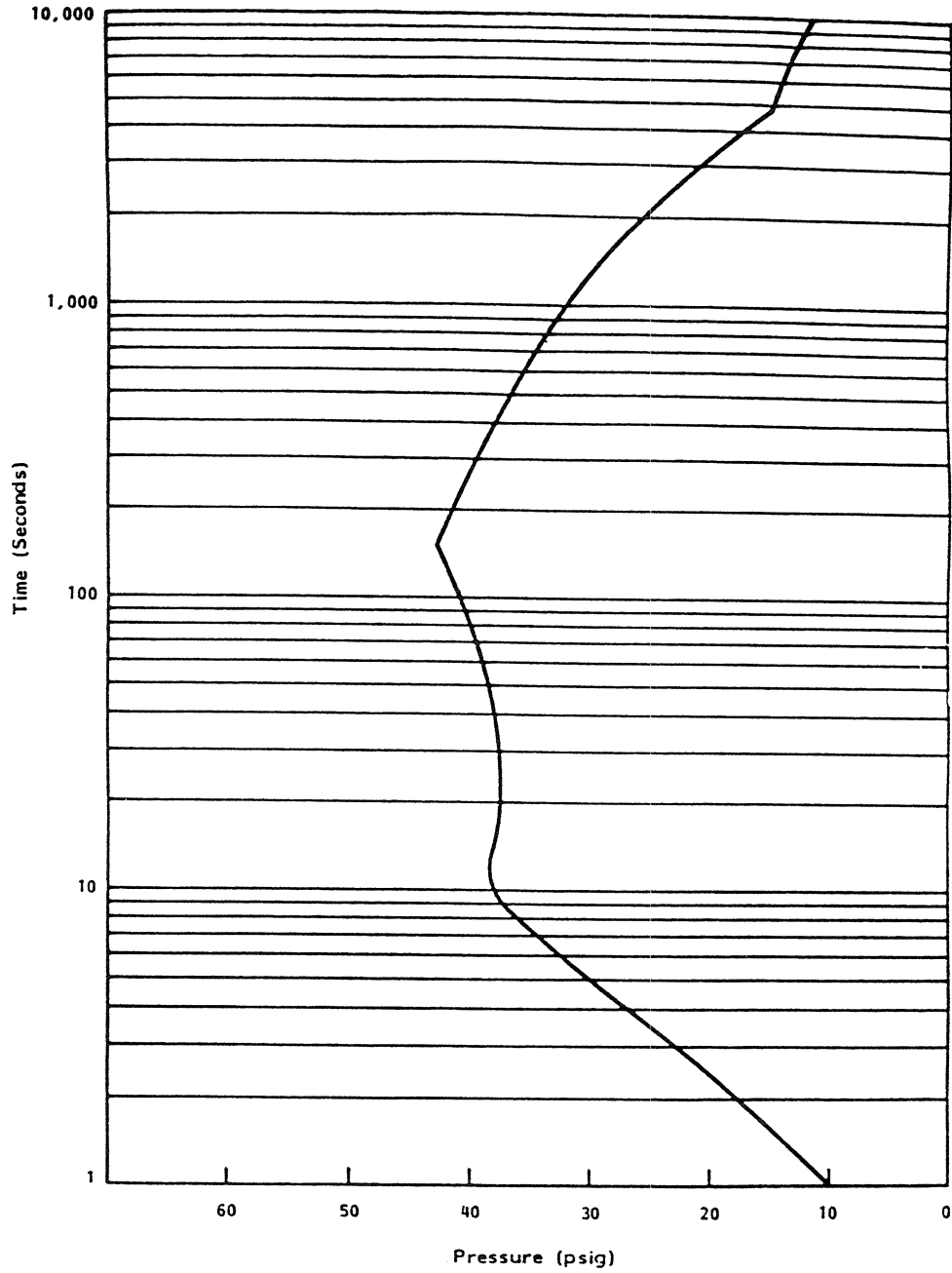


Figure 14C-12
0.6 Double Ended Pump Suction Break

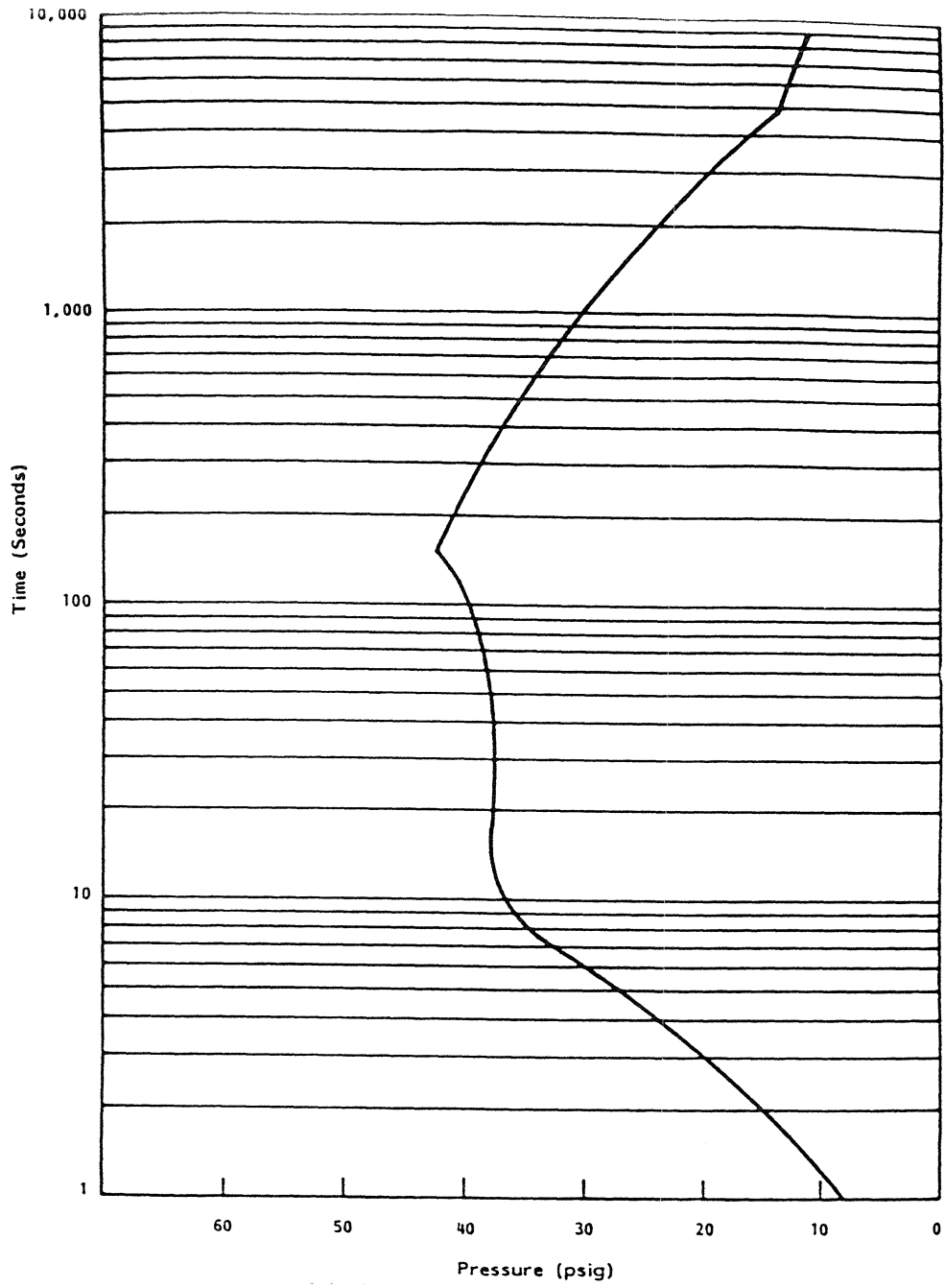


Figure 14C-13
4.0 Ft² Pump Suction Break

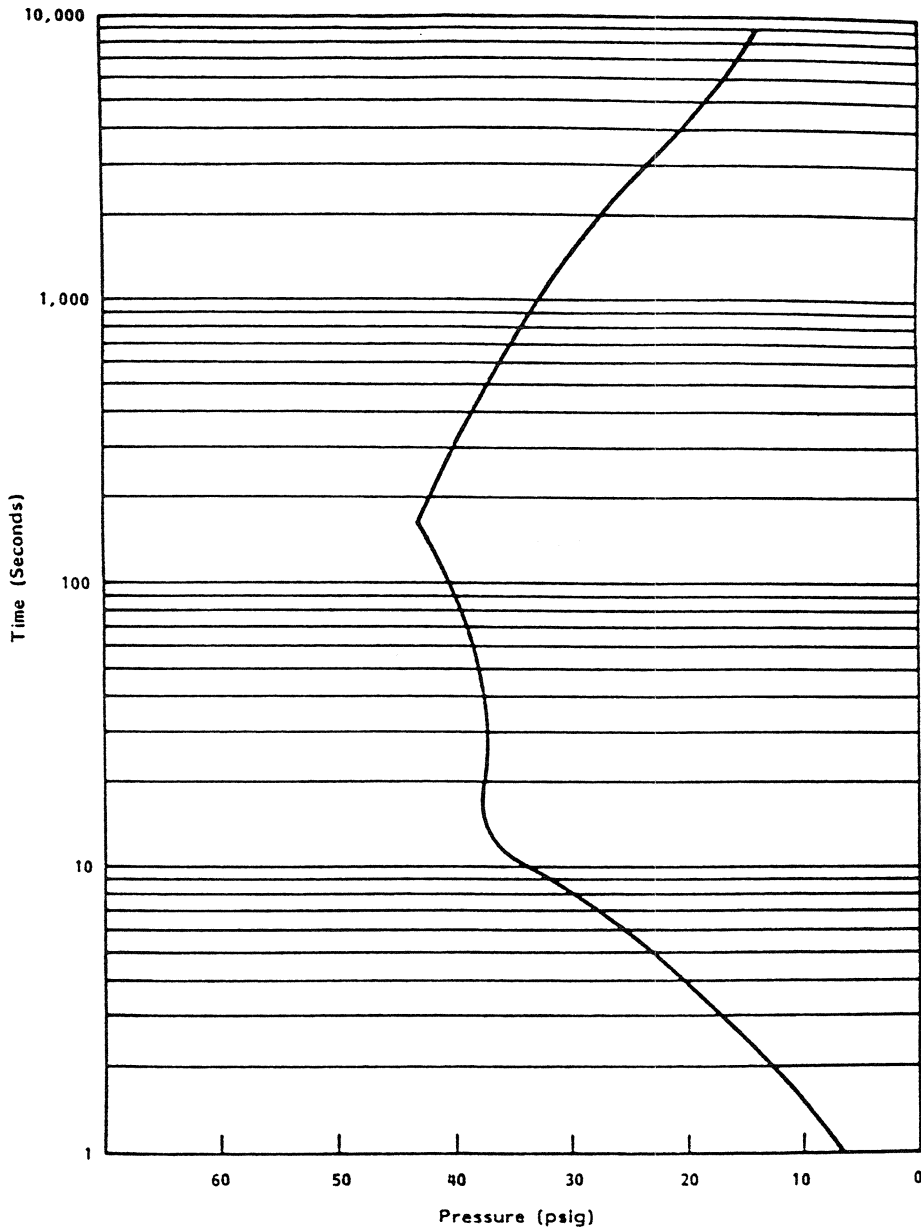


Figure 14C-14
2.0 Ft² Pump Suction Break

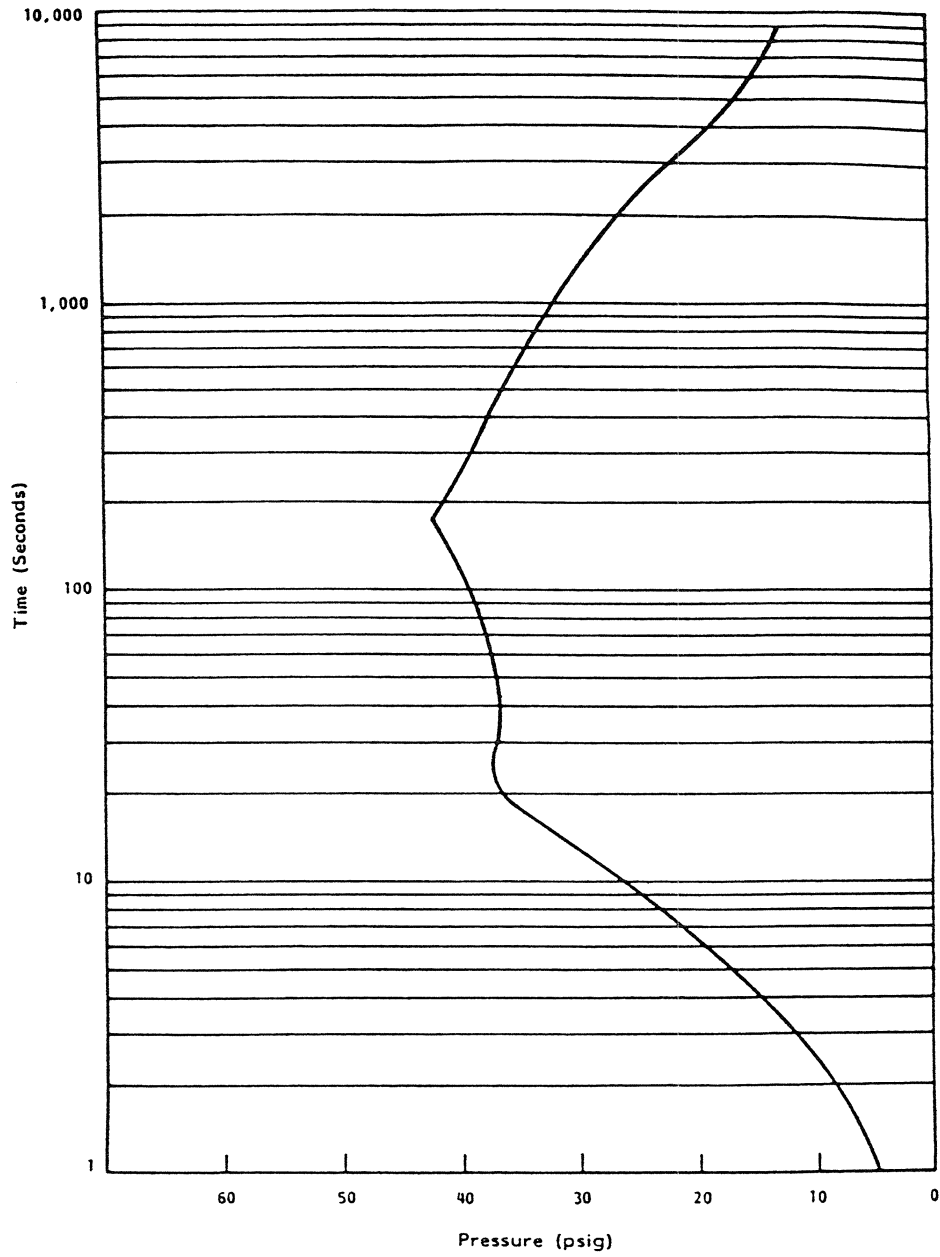


Figure 14C-15
Double-Ended Cold Leg

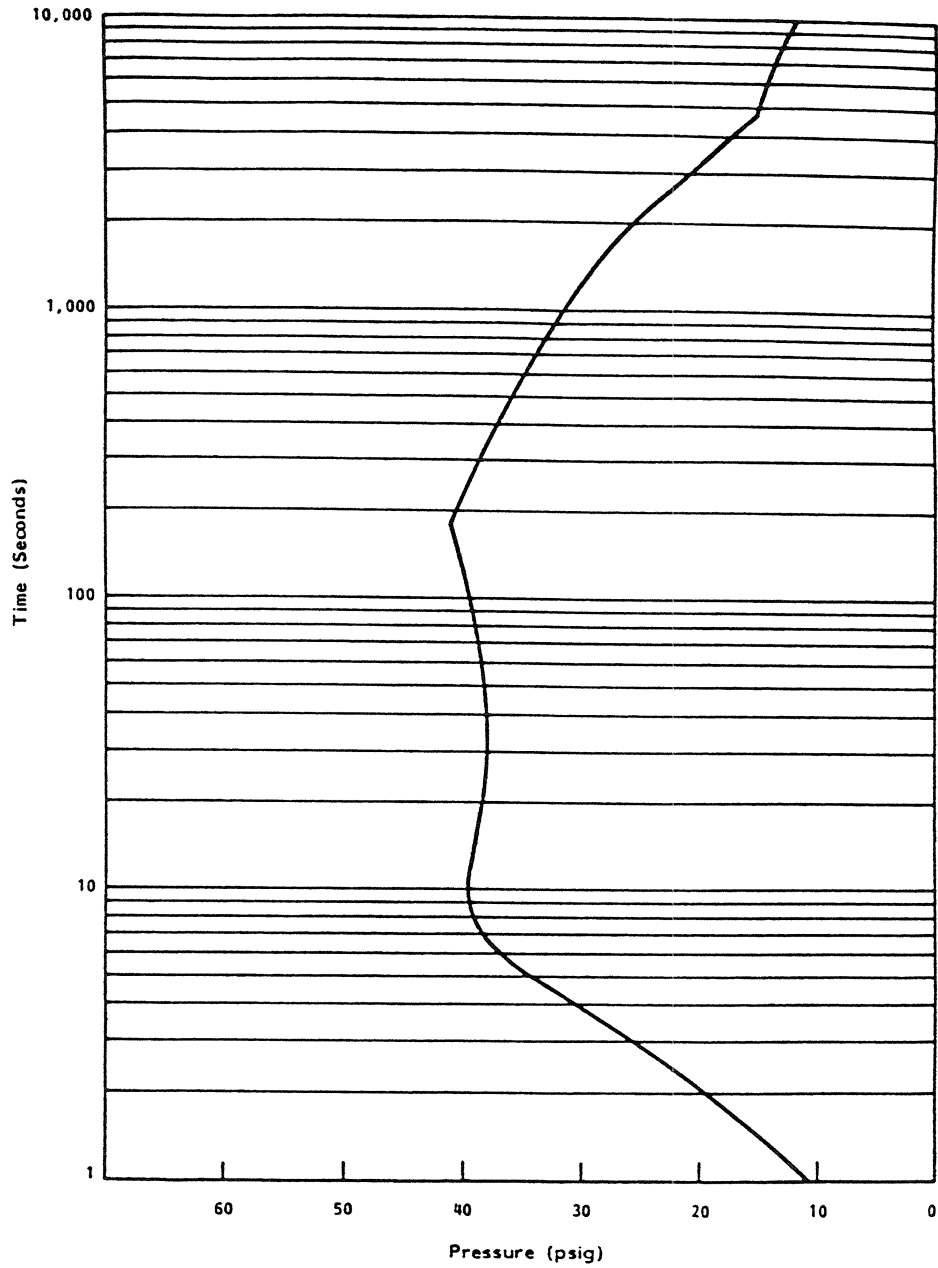


Figure 14C-16
Double-Ended Hot Leg Break

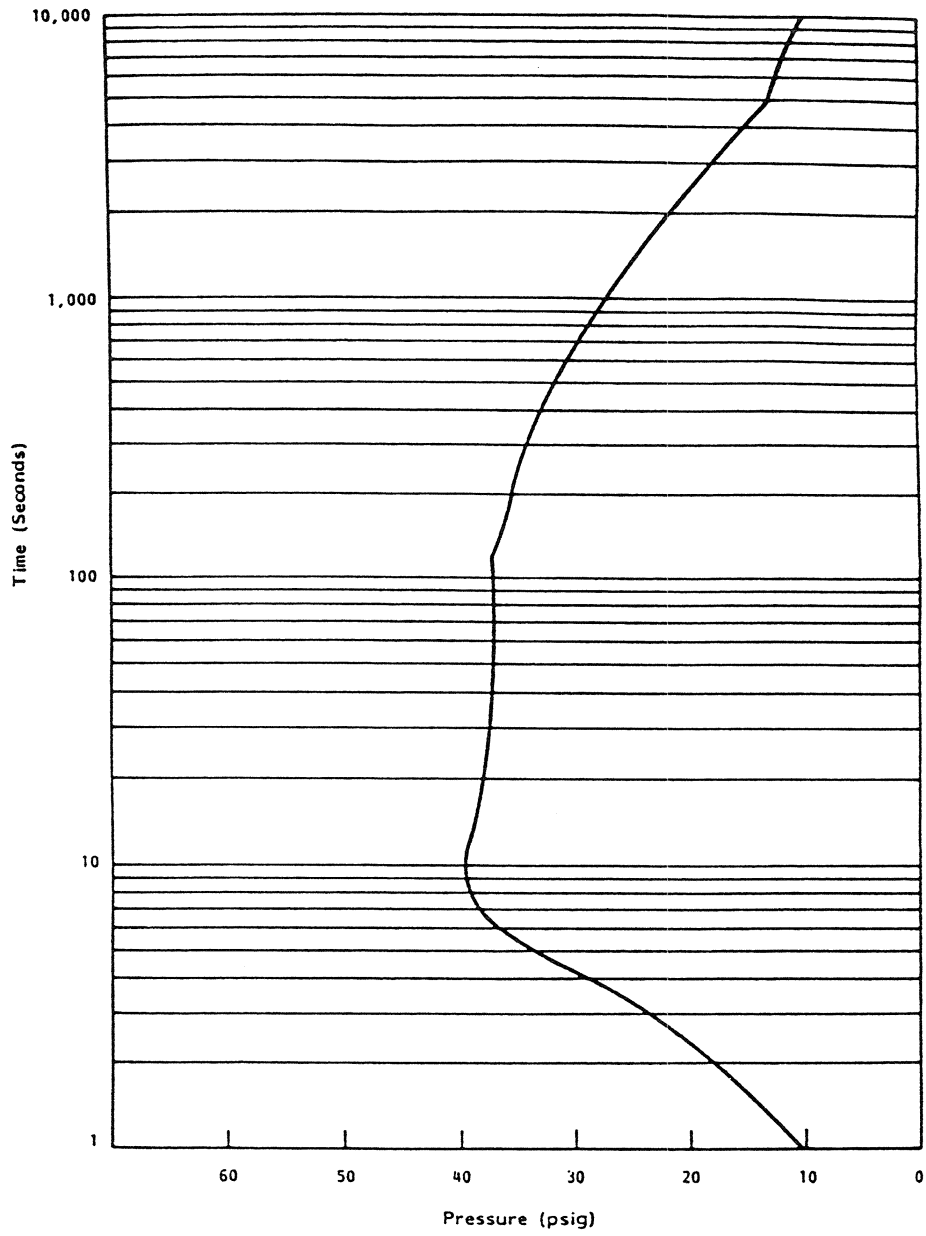


Figure 14C-17
0.6 Double-Ended Hot Leg Break

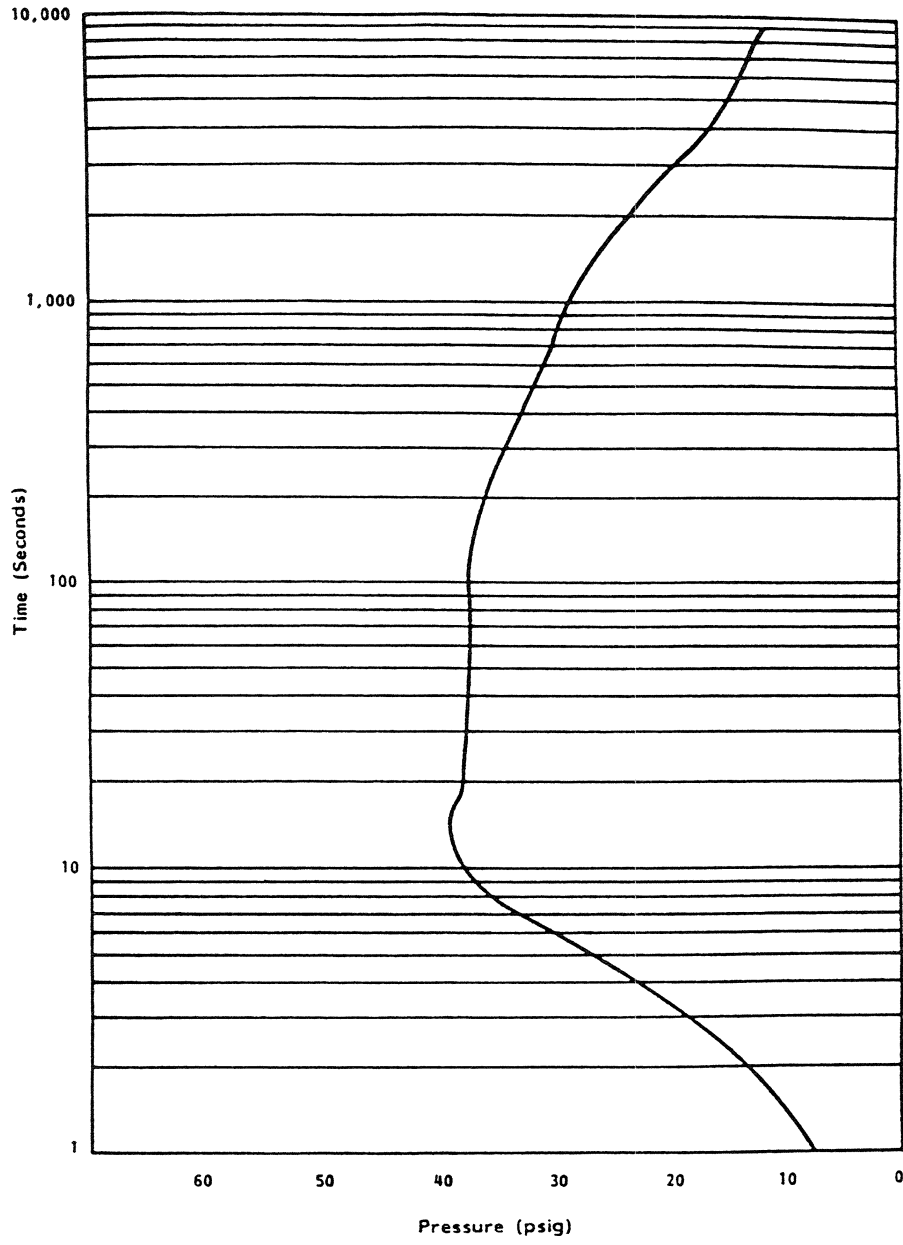


Figure 14C-18
3.0 Ft² Break (Split) Mass and Energy Released

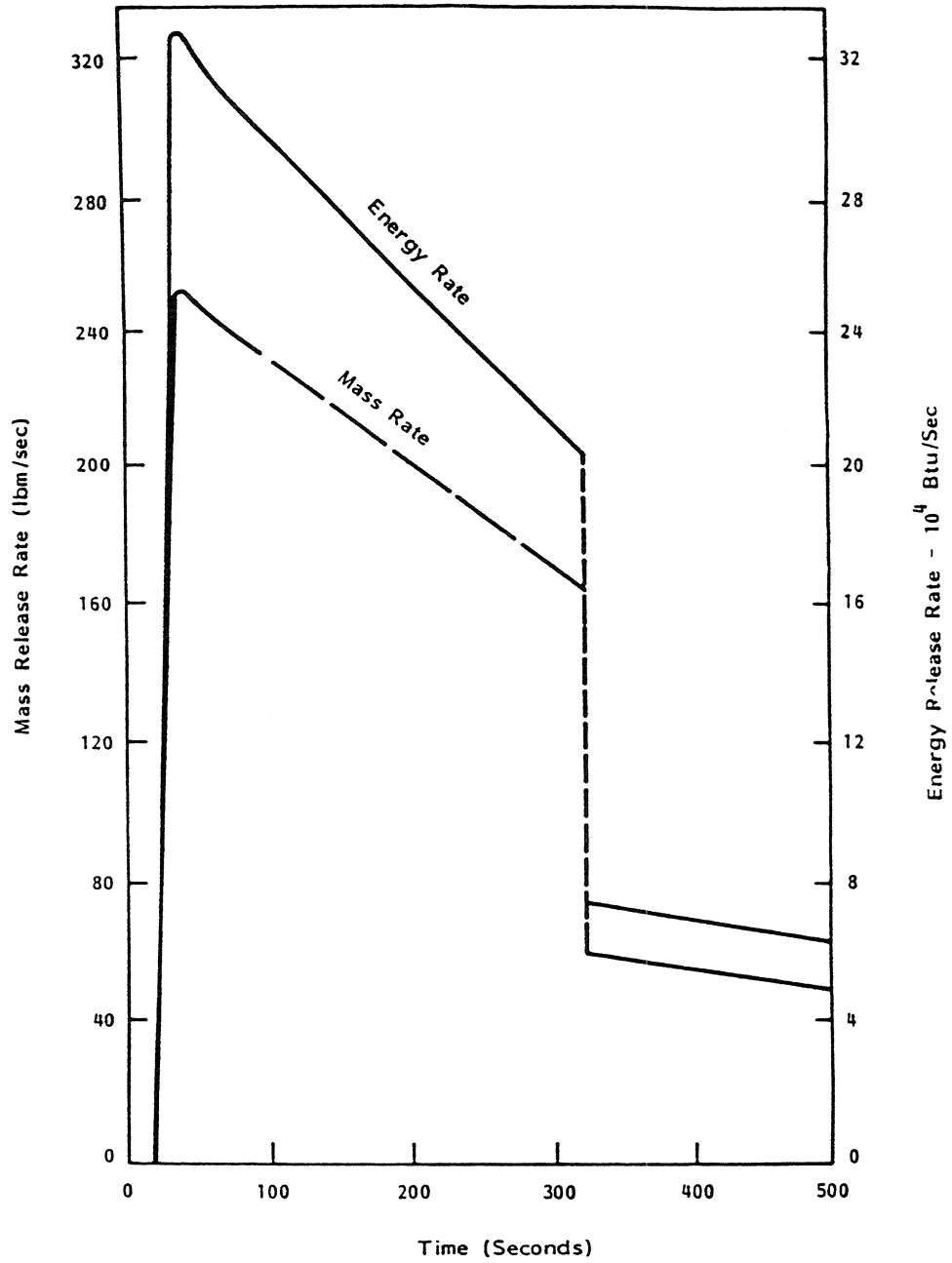
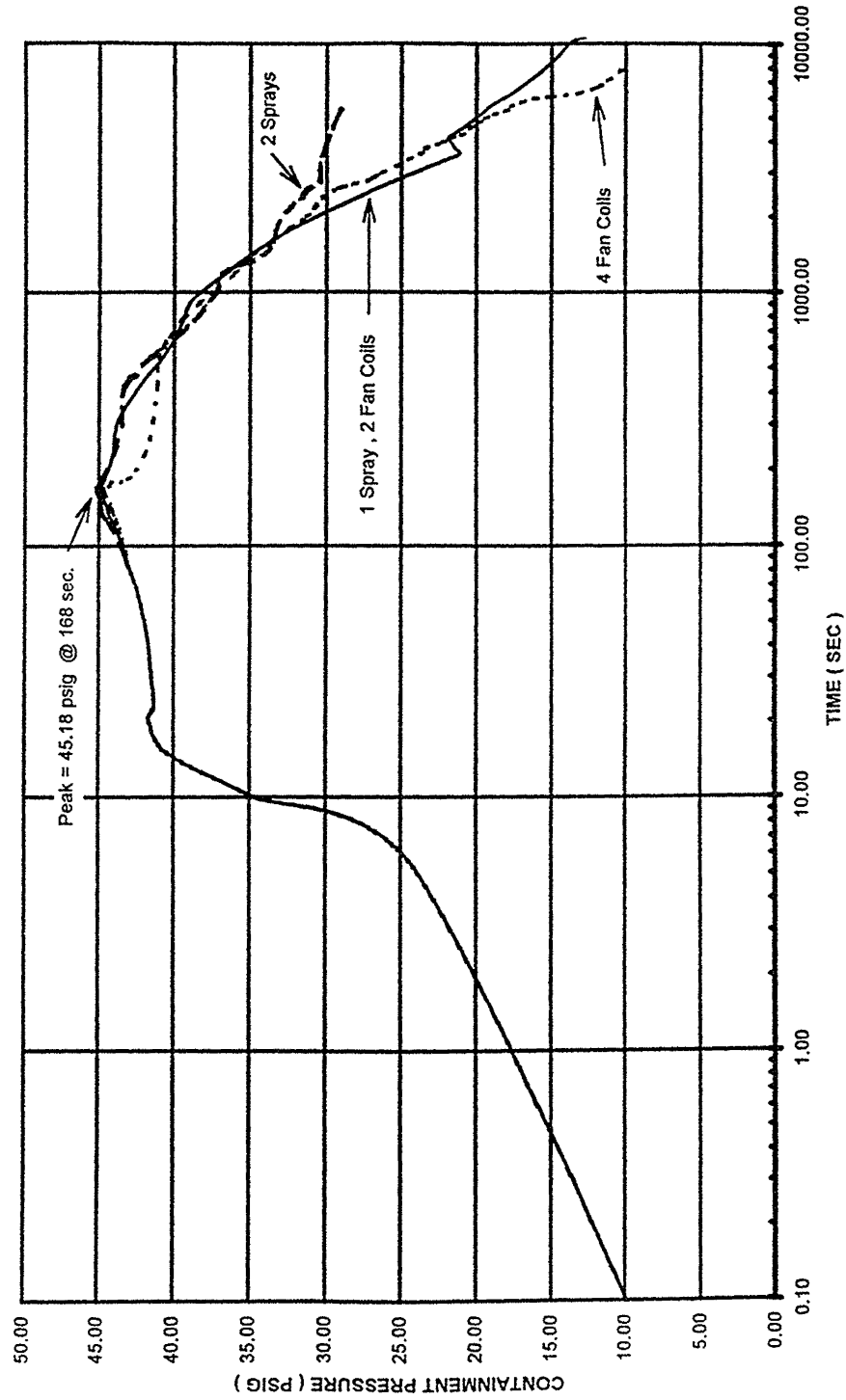


Figure 14C-19
Containment Peak Pressures Sensitivity Study
(Calculation No. SSFI-23-1, Revision 0, 02/03/89)



Intentionally Blank